57th ANNUAL
HIGHWAY GEOLOGY SYMPOSIUM

BRECKENRIDGE, COLORADO
SEPTEMBER 26-29, 2006

PROCEEDINGS

HOSTED BY
The Colorado Geological Survey
The Colorado Department of Transportation

57th ANNUAL HIGHWAY GEOLOGY SYMPOSIUM

BRECKENRIDGE, COLORADO

SEPTEMBER 26-29, 2006

PROCEEDINGS

HOSTED BY

The Colorado Geological Survey

The Colorado Department of Transportation

www.HighwayGeologySymposium.org

PROCEEDINGS OF THE 57TH HIGHWAY GEOLOGY SYMPOSIUM
TABLE OF CONTENTS

Proceedings Papers

(Page Numbers given in Table Of Contents preceeding The Papers, Posters and Index section)

Technical Session I – Landslides/Slope Stability

Landslide Investigation and Mitigation Along US 160 Between Durango And Mancos, Colorado, Using Lightweight Fill, Ground Anchors, and Rockery Buttresses
Ben Arndt, Tom Allen, and Richard Andrew

The 2005 Logan Bluff Landslide Repair.
Nancy C. Dessenberger and Leslie A. Heppler

Non-Structure Alternatives for Incidental Slopes
Donald V. Gaffney and Ryan S. Tinsley

Technical Session II – Landslides/Slope Stability

Recipe For Trouble: Just Add Water
Eugene Vaskov, and Christopher Ruppen

SR48 Landslide Repair
Joseph W. Schultz, Richard B. Schutte, and F. Barry Newman

Widening US 199 over Pine Mountain, Letcher County, Kentucky
Mark A. Litkenhaus

Repair of Small Scale Embankment Failures and Landslides in East Tennessee Using the Railroad Rail Repair Method
Harry Moore, George Sutton, and Len Oliver

Technical Session III – Applied Geophysical and Imaging Techniques

Analysis of Seismic Refraction Data – A Three-Decade Perspective
Alan Rock and Phil Sirles

Subsurface Modeling Using Seismic Refraction Data
Phil Sirles, Alan Rock, and Khamis Y. Haramy

Use of refraction MicroTremor (ReMi) Data For Shear Wave Velocity Determination at an Urban Bridge Rehabilitation Site
Douglas W. Lambert, Glen Adams and Veronica Parker

Dodging Salt Sinkholes: Seismic Reflection and K-61 Near Inman, Kansas
Neil M. Croxton

Digital Outcrop Characterization for 3-D Structural Mapping and Rock Slope Design Along Interstate 90, Snoqualmie Pass, Washington
William C. Haneberg, Norman I. Norrish and David P. Findley

The Use of Ground-based LIDAR for Geotechnical Aspects of Highway Projects
John Kemeny, Justin Henwood and Keith Turner (Abstract only)

Technical Session IV – Geotechnical Applications

Accelerated Investigation, Design, Bidding and Construction to Realign Highway US 191, Upper Chase Creek, Morenci, Arizona
Anthony H. Rice, Nick Priznar, Larry Barela, Teresa Speigl, and James Melvin

Shrink and Swell Estimation: Practices and Procedures
Justin Henwood, Matt DeMarco, and Charlie Martinez

Design of an Innovative Retaining Wall System for Highway Construction in Steep Terrain
K.F. Morrison, F.E. Harrison, J.G. Collin, and Scott Anderson

Replacing the US101 Beverly Beach Bridge, Lincoln County, Oregon
David Higgins, Gary Peterson, Tim Potter, and Daniel Hogan

Design of Rockery Walls on Marginally Stable Talus Slopes; Taylor River road, Gunnison County, Colorado
William Gates, Brendan Fisher, Chad Lukkarila, Kami Deputy, Samantha Sherwood, and Daniel E. Alzamora

Surprising Soil Behavior at Zolezzi Lane
Sherif Elfass, Gary Norris, and Rob Valceschini

Petrography of Coarse Aggregates Used in Design of Stone Matrix Asphalt Pavements in Indiana
Terry West, Brandon J. Celaya and John E. Haddock

Technical Session V – Hazards I

Guess What Dropped in for Breakfast?
Joseph A. Fischer, James G. McWhorter and Andrew Salmaso

NHDOT Response to The Destructive Forces of Nature: Alstead Flood 2005
Richard M Lane and Marc Fish

Case Study: Monteagle Mountain Rockfall Project
Vanessa Bateman and Len Oliver

Karst Vulnerability Considerations in Highway Route Selection, Juneau area, Alaska
N.J.Darigo

I-70 Georgetown Incline Rockfall Mitigation Feasibility Study, Georgetown, Colorado
Ben Arndt, Ty Ortiz, and Richard Andrew

US Highway 6-Clear Creek Canyon Rockslide: Working to Reopen a Major Road Closure
Kent Pease, Minal Parekh, and Ty Ortiz

Technical Session VI – Hazards II and Geology/Geomorphology

Field Testing and Numerical Modeling of Flexible Debris Flow Barriers
C. Wendeler, B.W. McArdell, D. Rickenmann, A. Volkwein, A. Roth, M. Denk and J. Kalejta (presenter)

Rolling Rocks in Peru for Calibration of the CRSP Model
Nancy C. Dessenberger and Michael Skurski

British Columbia Provincial Highway Tsunami Hazard Evaluation
Donald R. Lister, Rowland J. Atkins, Jason McNamee, and Rob Buchanan

How Wide is a River? Bridge Design and Applied Geomorphology
Rowland J Atkins, and Peter W. Morgan (Abstract only)

The Role of Engineering Geology on Rehabilitation of the Likelike Highway Wilson Tunnel, Oahu, Hawaii
Victor S. Romero and Clayton Mimura

POSTER SESSIONS

The Influence of Rock Geometry on the Tangential Coefficient of Restitution in Rockfall Analysis Based on Rigid Body Impact Mechanics
Parham Ashayer and John H. Curran

Improved p-y Curve Response Based on the Strain Wedge Model Analysis
Mohammed Ashour, Gary Norris, and Sherif Elfass

Laterally Loaded Pile/Shaft Response in Liquefying and Lateral Spreading Soil
Mohammed Ashour, Gary Norris and JP Singh

Maple Ridge Wind Farm access road
Martin P. Derby and Patrick O'Rourke (Abstract only)

Landslide Mitigation, Arterial Highway Stabilization with Multi-Agency Interaction; El Toro Road, Mission Viejo, California
William Goodman (Abstract only)

Application of the Block Theory for Rock Slope Stability Analysis at Highway Semenyih-Sg.Long, Selangor State in Malaysia
Hswanto and Rafek A. Ghani (Abstract only)

Overview of 2005 Storm Damage to Lower Mount Wilson Road, San Gabriel Mountains, Los Angeles County, California
J.R. Keaton (Abstract only)

Nightmare on Elm Street – Urban Rockfall Case History
Thomas McArdle, Tom Eliassen, Daniel Journeaux, Jay Smerekanicz, and Peter Ingraham (Abstract only)

Effect of Rock Types on Slope Failures Along Selected Problematic Parts of a Mountain Road, Al-Baha, Saudi Arabia
Bahaaeldin H. Sadagah

Rockfall Hazard Inventory Development and Maintenance – a 20 year Perspective
Michael Vierling, Richard Cross, and Peter Ingraham (Abstract only)

AUTHOR INDEX

Welcome to the 57th Annual Highway Geology Symposium

This year's HGS is hosted by the Colorado Department of Transportation (CDOT) and the Colorado Geological Survey (CGS). The Host Committee has put together what we hope is an interesting, educational, and enjoyable Symposium. Authors will be presenting on practical and engaging topics, including landslides and other hazards, slope stability, and geotechnical applications.

This year's field trip will include dramatic stops with presentations on rockfall, debris flows, landslides, avalanches, highway engineering, and general geology for the historic Breckenridge, Silver Plume, and Georgetown mining areas; Interstate 70 from Georgetown through the Eisenhower Tunnel to Vail Pass; Highway 6 over the Continental Divide at Loveland Pass; and the Dillon Dam and Reservoir.

We hope that you have time to explore and enjoy our beautiful state, and take advantage of the many recreational and cultural opportunities Colorado can offer. So again, welcome, enjoy the Symposium, and we hope your experience is an enjoyable one.

Sincerely,

The Host Committee for the 57th Highway Geology Symposium

Frank Harrison, Golder Associates Inc.
Barry Siel, FHWA
Jonathan White, CGS
Mark Vessely, CDOT

HIGHWAY GEOLOGY SYMPOSIUM

HISTORY, ORGANIZATION AND FUNCTION

Established to foster a better understanding and closer cooperation between geologists and civil engineers in the highway industry, the Highway Geology Symposium (HGS) was organized and held its first meeting on March 14, 1950, in Richmond, Virginia. Attending the inaugural meeting were representatives from state highway departments (as referred to at the time) from Georgia, South Carolina, North Carolina, Virginia, Kentucky, West Virginia, Maryland and Pennsylvania. In addition, a number of federal agencies and universities were represented. A total of nine technical papers were presented.

W.T. Parrott, an engineering geologist with the Virginia Department of Highways, chaired the first meeting. It was Mr. Parrott who originated the Highway Geology Symposium.

It was at the 1956 meeting that future HGS leader, A.C. Dodson, began his active role in participating in the Symposium. Mr. Dodson was the Chief Geologist for the North Carolina State Highway and Public Works Commission, which sponsored the 7th HGS meeting.

Since the initial meeting, 56 consecutive annual meetings have been held in 33 different states. Between 1950 and 1962, the meetings were held east of the Mississippi River, with Virginia, West Virginia, Ohio, Maryland, North Carolina, Pennsylvania, Georgia, Florida and Tennessee serving as host state.

In 1962, the Symposium moved west for the first time to Phoenix, Arizona where the 13th annual HGS meeting was held. Since then it has alternated, for the most part, back and forth, from the east to the west. The Annual Symposium has been held in different locations as follows:

List of Highway Geology Symposium Meetings

No.	Year	HGS Location	No.	Year	HGS Location
1st	**1950**	**Richmond, VA**	**2nd**	**1951**	**Richmond, VA**
3rd	**1952**	**Lexington, VA**	**4th**	**1953**	**Charleston, W VA**
5th	**1954**	**Columbus, OH**	**6th**	**1955**	**Baltimore, MD**
7th	**1956**	**Raleigh, NC**	**8th**	**1957**	**State College, PA**
9th	**1958**	**Charlottesville, VA**	**10th**	**1959**	**Atlanta, GA**
11th	**1960**	**Tallahassee, FL**	**12th**	**1961**	**Knoxville, TN**
13th	**1962**	**Phoenix, AZ**	**14th**	**1963**	**College Station, TX**
15th	**1964**	**Rolla, MO**	**16th**	**1965**	**Lexington, KY**
17th	**1966**	**Ames, IA**	**18th**	**1967**	**Lafayette, IN**
19th	**1968**	**Morgantown, WV**	**20th**	**1969**	**Urbana, IL**

HIGHWAY GEOLOGY SYMPOSIUM

HISTORY, ORGANIZATION AND FUNCTION

21st	**1970**	**Lawrence, KS**	**22nd**	**1971**	**Norman, OK**
23rd	**1972**	**Old Point Comfort, VA**	**24th**	**1973**	**Sheridan, WY**
25th	**1974**	**Raleigh, NC**	**26th**	**1975**	**Coeur d'Alene, ID**
27th	**1976**	**Orlando, FL**	**28th**	**1977**	**Rapid City, SD**
29th	**1978**	**Annapolis, MD**	**30th**	**1979**	**Portland, OR**
31st	**1980**	**Austin, TX**	**32nd**	**1981**	**Gatlinburg, TN**
33rd	**1982**	**Vail, CO**	**34th**	**1983**	**Stone Mountain, GA**
35th	**1984**	**San Jose, CA**	**36th**	**1985**	**Clarksville, IN**
37th	**1986**	**Helena, MT**	**38th**	**1987**	**Pittsburgh, PA**
39th	**1988**	**Park City, UT**	**40th**	**1989**	**Birmingham, AL**
41st	**1990**	**Albuquerque, NM**	**42nd**	**1991**	**Albany, NY**
43rd	**1992**	**Fayetteville, AR**	**44th**	**1993**	**Tampa, FL**
45th	**1994**	**Portland, OR**	**46th**	**1995**	**Charleston, WV**
47th	**1996**	**Cody, WY**	**48th**	**1997**	**Knoxville, TN**
49th	**1998**	**Prescott, AZ**	**50th**	**1999**	**Roanoke, VA**
51st	**2000**	**Seattle, WA**	**52nd**	**2001**	**Cumberland, MD**
53rd	**2002**	**San Luis Obispo, CA**	**54th**	**2003**	**Burlington, VT**
55th	**2004**	**Kansas City, MO**	**56th**	**2005**	**Wilmington, NC**
			57th	**2006**	**Breckenridge, CO**

Unlike most groups and organizations that meet on a regular basis, the Highway Geology Symposium has no central headquarters, no annual dues, and no formal membership requirements. The governing body of the Symposium is a steering committee composed of approximately 20-25 engineering geologists and geotechnical engineers from state and federal agencies, colleges and universities, as well as private service companies and consulting firms throughout the country. Steering committee members are elected for three-year terms, with their elections and re-elections being determined principally by their interests and participation in and contribution to the Symposium. The officers include a chairman, vice chairman, secretary, and treasurer, all of whom are elected for a two-year term. Officers, except for the treasurer, may only succeed themselves for one additional term.

A number of three-member standing committees conduct the affairs of the organization. The lack of rigid requirements, routing, and relatively relaxed overall functioning of the organization is what attracts many of the participants.

Meeting sites are chosen two or four years in advance and are selected by the Steering Committee following presentations made by representatives of potential host states. These presentations are usually made at the steering committee meeting, which is held during the Annual Symposium. Upon selection, the state representative becomes the state chairman and a member pro tem of the Steering Committee.

HIGHWAY GEOLOGY SYMPOSIUM

HISTORY, ORGANIZATION AND FUNCTION

The symposia are generally for two and one-half days, with a day and a half for technical papers and a full day reserved for the field trip. The Symposium usually begins on Wednesday morning. The field trip is usually Thursday, followed by the annual banquet that evening. The final technical session generally ends by noon on Friday. In recent years this schedule has been modified to better accommodate climate conditions and tourism benefits.

The field trip is the focus of the meeting. In most cases, the trips cover approximately from 150 to 200 miles, provide for six to eight scheduled stops, and require about eight hours. Occasionally, cultural stops are scheduled around geological and geotechnical points of interest. To cite a few examples: in Wyoming (1973), the group viewed landslides in the Big Horn Mountains; Florida's trip (1976) included a tour of Cape Canaveral and the NASA space installation; the Idaho and South Dakota trips dealt principally with mining activities; North Carolina provided stops at a quarry site, a dam construction site, and a nuclear generation site; in Maryland, the group visited the Chesapeake Bay hydraulic model and the Goddard Space Center; The Oregon trip included visits to the Columbia River Gorge and Mount Hood; the Central Mineral Region was visited in Texas; and the Tennessee meeting in 1981 provided stops at several repaired landslides in Appalachia regions of East Tennessee.

In Utah (1988) the field trip visited sites in Provo Canyon and stopped at the famous Thistle Landslide, while in New Mexico in 1990 the emphasis was on rockfall treatment in the Rio Grande River canyon and included a stop at the Brugg Wire Rope headquarters in Santa Fe.

Mount St. Helens was visited by the field trip in 1994 when the meeting was in Portland, Oregon, while in 1995 the West Virginia meeting took us to the New River Gorge bridge which has a deck elevation 876 feet above the water.

In Cody, Wyoming the 1996 field trip visited the Chief Joseph Scenic Highway and the Beartooth uplift in northwestern Wyoming. In 1997 the meeting in Tennessee visited the newly constructed future I-26 highway in the Blue Ridge of East Tennessee. The Arizona meeting in 1998 visited Oak Creek Canyon near Sedona and a mining ghost town at Jerome, Arizona. The 2006 field trip features dramatic stops in the core of the Colorado Rocky Mountains including the historic Colorado's historic mining areas; Interstate 70 from Georgetown through the Eisenhower Tunnel to Vail Pass; Highway 6 over the Continental Divide at Loveland Pass; and the Dillon Dam and Reservoir.

At the technical sessions, case histories and state-of-the-art papers are most common; with highly theoretical papers the exception. The papers presented at the technical sessions are published in the annual proceedings. Some of the more recent proceedings may be obtained from the Treasurer of the Symposium.

HIGHWAY GEOLOGY SYMPOSIUM

HISTORY, ORGANIZATION AND FUNCTION

Keynote and Banquet speakers are also a highlight and have been varied through the years. For the 57th Highway Geology Symposium, the keynote “Canyons, Mountains, and Highways--Thirty Years Between a Rock and a Hard Place” by Ralph J. Trapani, P.E., Senior Project Manager at Parsons, will open the symposium. Vincent Matthews, Colorado State Geologist, will speak on Colorado's Colorful Geology or “Messages in Stone” at this year’s banquet.

A Medallion Award was initiated in 1970 to honor those persons who have made significant contributions to the Highway Geology Symposium. The selection was and is currently made from the members of the national steering committee of the HGS.

A number of past members of the national steering committee have been granted Emeritus status. These individuals, usually retired, who have resigned from the HGS Steering Committee or are deceased, have made significant contributions to the Highway Geology Symposium. A total of 20 persons have been granted the Emeritus status. Ten are now deceased.

Several Proceedings volumes have been dedicated to past HGS Steering Committee members who have passed away. The 36th HGS Proceedings were dedicated to David L. Royster (1931-1985, Tennessee) at the Clarksville, Indiana Meeting in 1985. In 1991 the Proceedings of the 42nd HGS meeting held in Albany, New York was dedicated to Burrell S. Whitlow (1929-1990, Virginia).

57th ANNUAL
HIGHWAY GEOLOGY SYMPOSIUM

Breckenridge, Colorado
SEPTEMBER 26-29, 2006

LOCAL HOST COMMITTEE

Frank Harrison – Golder Associates Inc.
Barry Siel – FHWA / CFLHD
Mark Vessely – Colorado Department of Transportation
Jonathan White – Colorado Geological Survey

HIGHWAY GEOLOGY SYMPOSIUM
STEERING COMMITTEE
OFFICERS

Mr. G. Michael Hager, Chairman
Wyoming Department of Transportation
P.O. Box 1708
Cheyenne, WY 82009-1708
PH: 307-777-4205
Email: Mike.Hager@dot.state.wy.us

Mr. Richard Cross, Vice Chairman
Golder Associates
RD 1 Box 183A
Solansville, NY 12160
PH: 518-471-4277
Email: dick_cross@juno.com

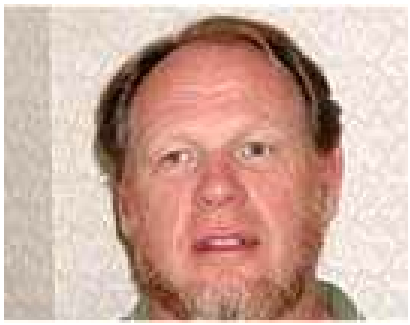

Mr. Jeff Dean, Secretary
Oklahoma DOT
200 NE 21st St.
Oklahoma City, OK 73105
Ph: (405)521-2677 or (405)522-0988
Fax: (405)522-4519
Email: jdean@odot.org

Mr. Russell Glass, Treasurer
North Carolina DOT (Retired)
100 Wolfe Cove Road
Asheville, NC 28804
Email: frgeol@aol.com

2006 HIGHWAY GEOLOGY SYMPOSIUM
NATIONAL STEERING COMMITTEE

NAME/ADDRESS	PHONE/FAX/E-MAIL
Ken Ashton West Virginia Geological Survey P.O. Box 879 Morgantown, WV 26507-0879	PHONE: 304-594-2331 FAX: 304-594-2575 Email: ashton@geosrv.wvnet.edu
John Baldwin West Virginia Div. Of Highways 190 Dry Branch Rd. Charleston, WV 25036	PHONE: 304-558-3084 FAX: 304-558-0253 Email: jbaldwin@mail.dot.state.wv.us
Vernon Bump South Dakota DOT (Retired) Geotech. Engr. Activity 700 E. Broadway Ave. Pierre, SD 575010-2586	PHONE: 605-224-7008 FAX: Email: vernglobump@pie.midco.net
Richard Cross Golder Associates RD 1 Box 183A Solansville, NY 12160	PHONE:518-471-4277 Cell: (603)867-4191 Email: dick_cross@juno.com
Jeff Dean Oklahoma DOT 200 NE 21st St. Oklahoma City, OK 73015	PHONE: 405-522-0988 FAX: 405-522-4519 Email: jdean@odot.org
John Duffy California State Dept. of Transportation 50 Higuera Street San Luis Obispo, CA 93401	PHONE: 805-549-3663 FAX: 805-549-4693 Email: John_Duffy@dot.ca.gov
Tom Eliassen State of Vermont, Agency of Transportation Materials & Research Section National Life Building, Drawer 33 Montpelier, VT 05633	PHONE: 802-828-2561 FAX: 802-828-2792 Email: tom.eliassen@state.vt.us

2006 HIGHWAY GEOLOGY SYMPOSIUM
NATIONAL STEERING COMMITTEE

NAME/ADDRESS	PHONE/FAX/E-MAIL
Russell Glass North Carolina DOT (Retired) 100 Wolfe Cove Rd. Asheville, NC 28804	PHONE: 828-252-2260 FAX: 828-299-1273 Email: frgeol@aol.com
Robert Goddard National Magnetic Field Lab Florida State University 1800 E. Paul Dirac Dr. Tallahassee, FL 32306-4005	PHONE: 850-644-4304 FAX: 850-644-0687 Email: goddard@magnet.fus.edu
G. Michael Hager Wyoming DOT P.O. Box 1708 Cheyenne, WY 82009-1708	PHONE: 307-777-4205 FAX: 307-777-3994 Email: mike.hager@dot.state.wy.us
Bob Henthorne Materials and Research Center 2300 Van Buren Topeka, KS 66611-1195	PHONE: 785-291-3860 FAX: 785-296-2526 Email: roberth@ksdot.org
Richard Humphries Golder Associates PO Box 2059 Squamish BC, Canada V0N 3G0	PHONE: 604-815-0768 FAX: 604-815-0769 Email: rhumphries@Golder.com
A. David Martin Maryland State Highway Administration Office of Materials & Technology 2323 W. Joppa Road Brooklandville, MD 21022	PHONE: 410-321-3107 FAX: 410-321-3099 Email: dmartin@sha.state.md.us
Henry Mathis, PE H.C. Nutting Co. 561 Marblerock Way Lexington, KY 40503	PHONE: 859-296-5664 PHONE: 859-223-8632 Home FAX: 859-296-5664 Email: hmathis@iglou.com
Harry Moore Tennessee DOT 7345 Region Lane Knoxville, TN 37901	PHONE: 865-594-2701 FAX: 865-594-2495 Email: harry.moore@state.tn.us

2006 HIGHWAY GEOLOGY SYMPOSIUM
NATIONAL STEERING COMMITTEE

NAME/ADDRESS	PHONE/FAX/E-MAIL
John Pilipchuk NCDOT Geotechnical Engineering Unit 5253 Z-Max Blvd Harrisburg, NC 28075	PHONE: 704-455-8902 FAX: 704-455-8912 Email: jpilipchuk@dot.state.nc.us
Nick Priznar Arizona DOT 1221 N. 21st Ave. Phoenix, AZ 85009-3740	PHONE: 602-712-8089 FAX: 602-712-8415 Email: NPRIZNAR@dot.state.az.us
Eric Rorem Geobrugg North America, LLC. Geobrugg Protection Systems 551 W. Cordova Road, PMB 730 Santa Fe, NM 87505	PHONE: 505-438-6161 FAX: 505-438-6166 Email: erik.rorem@us.geobrugg.com
Christopher A. Ruppen Michael Baker Jr. Inc. 4301 Dutch Ridge Rd. Beaver, PA 15009-9600	PHONE: 724-495-4079 FAX: 724-495-4017 Email: cruppen@mbakercorp.com
Stephen Senior Ministry of Transportation Room 220, Central Bldg. 1201 Wilson Ave. Downsview, ON M3M 1J6, Canada	PHONE: 416-235-3743 FAX: 416-235-4101 Email: stephen.senior@mto.gov.on.ca
Willard L. Sitz Alabama DOT 1409 Coliseum Blvd. Montgomery, AL 36110-2060	PHONE: 334-206-2279 FAX: 334-264-6263 Email: sitzw@dot.state.al.us
Jim Stroud Vulcan Materials Co. 4401 N. Patterson Ave. P.O. Box 4239 Winston-Salem, NC 27115	PHONE: 336-767-4600 FAX: 336-744-2019 Email: stroudj@vmcmail.com

2006 HIGHWAY GEOLOGY SYMPOSIUM
NATIONAL STEERING COMMITTEE

NAME/ADDRESS	PHONE/FAX/E-MAIL
John Szturo HNTB Corporation 1201 Walnut, Suite 700 Kansas City, MO 64106	PHONE: 816-527-2275 FAX: 816-472-5013 Email: jszturo@hntb.com
Robert Thommen Rotec Enterprises Inc. P.O. Box 31536 Sante Fe, NM 87594-1536	PHONE: 505-753-6586 FAX: 505-753-6590 **Email:** thommen@rotecinternational-usa.com
Sam Thornton 37812 N Highway112 Fayetteville,AR72704	PHONE: FAX: Email:
Michael P. Vierling New York State Thruway Authority 200 Southern Blvd. Albany, NY 12209	PHONE: 518-471-4378 FAX: 518-436-3060 Email: michael_vierling@thruway.state.ny.us
Chester F. "Skip" Watts Radford University Radford, VA 24142	PHONE: 540-831-5652 FAX: 540-831-5732 Email: cwatts@runet.edu
Terry West Earth and Atmospheric Science Dept. Purdue University West Lafayette, IN 47907-1297	PHONE:765-494-3296 FAX: 765-496-1210 Email: trwest@cas.purdue.edu
W.A. Wisner Martin Marietta Aggregates P.O. Box 30013 Raleigh, NC 27622	PHONE: 919-783-4649 FAX: 919-783-4552 Email:

HIGHWAY GEOLOGY SYMPOSIUM

EMERITUS MEMBERS OF THE STEERING COMMITTEE

Emeritus Status is granted by the Steering Committee

R.F. Baker*
David Bingham
Virgil E. Burgat*
Robert G. Charboneau*
Hugh Chase*
A.C. Dodson*
Walter F. Fredericksen
Brandy Gilmore
Joseph Gutierrez
Charles T. Janik
John Lemish
Bill Lovell
George S. Meadors, Jr.*
Willard McCasland
David Mitchell
W.T. Parrot*
Paul Price*
David L. Royster*
Bill Sherman
Mitchell Smith
Steve Sweeney
Sam Thornton
Berke Thompson*
Burrell Whitlow*
Earl Wright
Ed J. Zeigler

*Deceased

HIGHWAY GEOLOGY SYMPOSIUM

MEDALLION AWARD WINNERS

The Medallion Award is presented to individuals who have made significant contributions to the Highway Geology Symposium over many years. The award, instituted in 1969, is a 3.5-inch medallion mounted on a walnut shield and appropriately inscribed. The award is presented during the banquet at the annual Symposium.

Hugh Chase*	**-**	**1970**
Tom Parrott*	**-**	**1970**
Paul Price*	**-**	**1970**
K.B. Woods*	**-**	**1971**
R.J. Edmonson*	**-**	**1972**
C.S. Mullin*	**-**	**1974**
A.C. Dodson*	**-**	**1975**
Burrell Whitlow*	**-**	**1978**
Bill Sherman	**-**	**1980**
Virgil Burgat*	**-**	**1981**
Henry Mathis	**-**	**1982**
David Royster*	**-**	**1982**
Terry West	**-**	**1983**
Dave Bingham	**-**	**1984**
Vernon Bump	**-**	**1986**
C.W. "Bill" Lovell	**-**	**1989**
Joseph A. Gutierrez	**-**	**1990**
Willard McCasland	**-**	**1990**
W.A. "Bill" Wisner	**-**	**1991**
David Mitchell	**-**	**1993**
Harry Moore	**-**	**1996**
Earl Wright	**-**	**1997**
Russell Glass	**-**	**1998**
Harry Ludowise	**-**	**2000**
Sam Thornton	**-**	**2000**
Bob Henthorne	**-**	**2004**
Mike Hager		**2005**

*Deceased

57th HIGHWAY GEOLOGY SYMPOSIUM SPONSORS

The following companies have graciously contributed toward sponsorship of the Symposium. The HGS relies on sponsor contributions for events such as refreshment breaks, field trip lunches and other activities and want these sponsors to know that their contributions are very much appreciated.

AIS Construction Company has been providing professional, cost-effective solutions to the marine and construction industry since 1995. AIS provides particularly steep excavation and dredging services for projects having difficult access, slopes and hard to reach areas. Whether it is excavating the side of a remote mountain or dredging a canal with virtually no access, AIS is committed to quality and efficient service.

The staff of **AIS professionals** has over 100 years of combined dredging, engineering, and marine construction experience. Knowledge innovation, and cost effective solutions for difficult projects is what sets AIS apart. Customers receive the most competitive prices and the highest quality of service available. Over 80% of AIS' contracted work is due to referrals from a long list of satisfied customers.

AIS Construction Offers a Full Range of Services:

- Project engineering and design
- Hydrographic and land surveying
- Mechanical and hydraulic dredging and pile driving and seawall construction
- Soil nails and MSE walls
- Rock drilling and compaction grouting

Contact
Andy Schaefer
President/CEO
AIS Construction
PO Box 239
Carpenteria, CA 93014
Phone
805.684.4344

57th HIGHWAY GEOLOGY SYMPOSIUM SPONSORS

BEAVER RUN
RESORT & CONFERENCE CENTER

Step outside your door and crisp mountain air fills your lungs, blue sky touches the mountain tops and the bright sun warms your heart. You're in Breckenridge, a winter wonderland and a summer escape offering activities and adventures for travelers of all ages**. Beaver Run Resort** boasts the largest conference facility and hotel under one roof in Breckenridge, Colorado. Coupled with a full-time flexible staff, your meeting is sure to be a success.
www.beaverrun.com

Crux Subsurface, Inc. provides specialty drilling services to the engineering and construction industry through geotechnical exploration and construction services. Crux combines innovative drilling systems and equipment with the experience to complete logistically challenging and environmentally sensitive projects.

Founded in the geotechnical exploration industry, Crux has grown to be a leader in exploration drilling for engineering design projects where access, sample recovery and instrumentation are critical. Crux utilizes custom designed and manufactured drills from our in-house fabrication facility allowing for the flexibility to accommodate virtually any project requirement.

Geotechnical Exploration
- **Soil & Rock Core Drilling**
- **Casing Advancing**
- **Deviation Controlled Core Drilling**
- **In situ Testing**
- **Permeability Testing**
- **Specialized Sampling Methods**
- **Instrument Installation**
- **Difficult Formation Recovery**
- **Geophysics OPTV & ATV**

Crux Geotechnical Construction, Inc. combines innovative equipment and drilling systems with the experience to complete logistically challenging and environmentally sensitive projects. Crux designs and constructs specialty foundations for industrial, commercial, residential and utility contractors. Crux provides specialty ground improvement for tunneling contractors, too slope and foundation stabilization for developers.

Geotechnical Construction
- **Micropiles**
- **Permeation Grouting**
- **Compaction Grouting**
- **Rock Bolts & Soil Nails**
- **Tiebacks**
- **Cased River Crossings**
- **Pre-Tunnel Excavation Exploration & Stabilization**

CRUX subsurface, inc.

Geotechnical Exploration | **Geotechnical Construction**
16707 E. Euclid Avenue | Spokane Valley, WA 99216
P 509-892-9409 **|** F 509-892-9408 **|** 866-cruxsub (278-9783)

Scott Tunison | scott@cruxsub.com | www.cruxsub.com

57th HIGHWAY GEOLOGY SYMPOSIUM SPONSORS

Golder Associates
540 North Commercial Street, Suite 250
Manchester, New Hampshire 03101-1146
Phone (603) 668 0880 / Fax (603) 668 1199
www.golder.com/
pingraham@golder.com

Golder Associates is proud to be a part of this year's Host Committee and has been a sponsor of the HGS for more than 15 years

Golder Associates is an international group of science and engineering companies. The employee-owned group of companies provides comprehensive consulting services in support of environmental, industrial, natural resources and civil engineering projects. Founded in 1960, Golder now employs over 4,500 people operating from more than 130 offices located across Africa, Asia, Australia, Europe, North America and South America, and projects in more than 140 countries.

At **Golder Associates** we strive to be the most respected global group specializing in ground engineering and environmental services. With Golder, clients gain the advantage of working with highly skilled engineers and scientists who are committed to helping them succeed. By building strong relationships and meeting the needs of clients, our people have created one of the most trusted professional services firms in the world.

Geobrugg North America, LLC.
Geobrugg Protection Systems
551 W. Cordova Road, PMB 730
Santa Fe, New Mexico 87505
Phone (505) 438 6161 / Fax (505) 438 6166
www.geobrugg.com
info@us.geobrugg.com

Geobrugg helps protect people and infrastructure from the forces of nature. The technologically mature protection systems of steel wire nets developed and produced by us are now used all over the world. Our dynamic and static barrier systems offer proven protection against rock falls, avalanches, mud flows and slope failures.

57th HIGHWAY GEOLOGY SYMPOSIUM SPONSORS

HAYWARD BAKER
Denver Grouting Division

KELLER

Hayward Baker Inc., North America's leader in specialty geotechnical construction, is committed to provide the most economical and technically correct solution for each geotechnical challenge.

Central Region
Denver Area Office
DENVER GROUTING
A Division of Hayward Baker

11575 Wadsworth Blvd.
Broomfield, CO 80020-2752
Toll Free:800-864-4328
Tel: 303-469-1136
Fax: 303-469-3581
Bruce Stover, PG
Project Manager
bkstover@haywardbaker.com

Hayward Baker's Denver office serves the Rocky Mountain Region and offers a large variety of geotechnical services including compaction and cement grouting, commercial and residential foundation remediation, shoring, slope and landslide stabilization, jet grouting, soil nailing, drilling and blasting, and mining services including mine rehabilitation and specialized drilling services.

Since our beginning, we have made numerous advances in geotechnical construction technology and procedures. While we take pride in our innovations, we also recognize that not every problem requires an original solution. We apply our decades of experience to specific problems, giving our clients peace of mind in knowing that we can provide a solution that we have proven, in the field, to be cost effective and efficient. Meeting a project's specialized needs is a hallmark of Hayward Baker's approach to ground improvement.

Whether your site requires Foundation Support and Rehabilitation, Settlement Control, Structural Support, Site Improvement, Soil and Slope Stabilization, Underpinning, Excavation Shoring, Earth Retention, Seismic Stabilization or Ground Water Control, *we are ready and eager to assist you.*

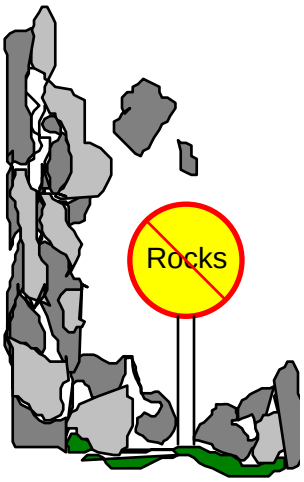

HI-TECH Rockfall Construction, Inc.
2328 Hawthorne Street
P.O. Box 674
Forest Grove, OR 97116-0674
Phone (503) 357-6508
Fax (503) 357-7323
HTRockfall@aol.com
www.HI-TECHRockfall.com

"The Rockfall Specialists"

HI-TECH Rockfall is a General Contractor who, since 1996, has specialized in rockfall mitigation and is considered to be the industry leader in designing and installing rockfall protection systems throughout the United States. **HI-TECH** is licensed/prequalified in 19 states and constructs a vast array of rockfall mitigation systems in a variety of locations such as highways, railroads, dams, quarries, mines, construction sites, commercial and residential properties. **HI-TECH** has installed over 6,877,000 sf of wire mesh drapery, 1,027,000 sf of cable net drapery, 174,597 sf of Tecco mesh, 55,038 lf of rock bolts, dowels and anchors, 56,500 lf of rockfall and debris flow barriers and 10,000 crew hours of scaling.

57th HIGHWAY GEOLOGY SYMPOSIUM SPONSORS

Janod Inc.
34 Beeman Way
P.O. Box 2487
Champlain, NY
12919
Tel: (518) 298-5226
Fax: (450) 424-2614
info@janod.biz

Janod Ltd.
190 VALOIS
Vaudreuil-Dorion
Quebec, CANADA
J7V 1T4
Tel: (450) 455-1223
Fax: (450) 424-2614
info@janod.biz

Janod has specialised in rock stabilization and rock remediation since 1968

Janod was founded in 1968 by Douglas Journeaux, and at that time, soft earth tunneling was the principle part of our operations. In 1970 Janod was introduced to rock slope stabilization when called in by Quebec Cartier Mining Looking towards the future of rock stabilization to perform some emergency work along the railway. **Janod** has since become a specialist in rock stabilization, and employs a combination of innovative mechanized equipment and highly trained rock remediation technicians who have an intimate knowledge of geology and influence of climatic conditions on exposed rock structures.

Janod takes pride in having successfully met many different challenges at numerous and varied worksites throughout North America.

Michael Baker Jr., Inc.
4301 Dutch Ridge Road
Beaver, PA 15009
Phone (724) 495-7711
FAX (724) 495-4017
www.mbakercorp.com
cruppen@mbakercorp.com

Michael Baker Corporation has evolved into one of the leading engineering and energy management firms by consistently solving complex problems for its clients. We view challenges as invitations to innovate.

Baker has been providing geotechnical services since the mid-1950. Professional geotechnical engineers and geologists are supported by a staff of highly trained assistants. Expertise covers most major facets of geotechnical investigation and design, including geologic reconnaissance, subsurface investigations, geotechnical analysis and design, and geotechnical construction phase services.

57th HIGHWAY GEOLOGY SYMPOSIUM SPONSORS

American Mountain Management Inc.
Financial Plaza Building, 1135 Terminal Way, Suite 106
Reno, Nevada, 89502-2145, U.S.A.

Telephone: 1-866-466-7223
Fax: 450-455-8762
http://www.mountainmanagement.biz/

Mountain Management is a new North American distributor and manufacturer of rock fall barrier, erosion control and avalanche systems. Our suppliers have more than 20 years experience in mitigation systems. Our systems are guaranteed and have proven over the years to assemble and install with more ease and less time required. We have the latest in design and technology. Many of our products are patent protected and field tested.

Mountain Management Rock Fall protection systems are capable of handling energies ranging from 50 to 5000 Kilojoules. Submitted to testing, our systems are the outcome of more than 20 years of combined field experience and Rock Fall Simulation Studies.

Wyllie & Norrish Rock Engineers is a specialist engineering company working in the fields of:

- Rock slopes
- Landslides
- Tunnels
- Foundations
- Blasting

Mission Statement

The company principals, Duncan Wyllie and Norm Norrish, have a total of 75 years experience in applied rock mechanics, and aim to bring innovative, timely and economic solutions to projects involving excavations in rock.

Canada
Wyllie Norrish Rock Engineers Ltd.

Suite 200 Viva Tower
1311 Howe Street
Vancouver, BC
V6Z 2P3
Phone:(604) 691-1717
Fax: (604) 669-3688
Email:
dwyllie@wnrockeng.com

United States
Wyllie Norrish Rock Engineers Inc.

17918 NE 27th Street
Redmond, WA
98052
Phone: (425) 861-7327
Cell: (206) 790-3476
Fax: (425) 861-7327
nnorrish@wnrockeng.com

Web: www.wnrockeng.com

57th HIGHWAY GEOLOGYSYMPOSIUM EXHIBITORS

The Host Committee for the 57th Annual Highway Geology Symposium would like to express sincere appreciation to the following exhibitors and sponsors. You are invited to visit their displays at the Symposium, and please be sure to express *your* appreciation.

58th HGS
4301 Dutch Ridge Road
Beaver, PA 15009
Phone (724) 495-7711
FAX (724) 495-4017
CRuppen@mbakercorp.com

AIS Construction Company
6420 Via Real, Suite 6
Carpinteria, CA 93013
Phone (805) 684-4344
Fax (805) 566-6534
www.aisconstruction.com
andy@aisconstruction.com

Anderson Drilling
10303 Channel Road
Lakeside CA92040
Phone (619)443-2891
Fax (619)443-0724
www.andersondrilling.com
dpoland@andersondrilling.com

Association of Civil Engineers (ASCE)
http://sections.asce.org/colorado/index.htm
mparekh@lymanhenn.com

Association of Engineering Geologists (AEG)
http://www.aegweb.org/
broland@aegweb.org

Central Mine Equipment Company
4215 Rider Trail North
Earth City, MO 63045
Phone (800) 325-8827
Fax (314) 291-4880
www.cmeco.com
info@cmeco.com

Colorado Geological Survey (CGS)
http://geosurvey.state.co.us/
Jonathan.White@state.co.us

Contech Construction
4891 independence St. Suite 195
Wheat Ridge, CO 80033
Phone 303/431-8999
Fax (303)431-9839
www.contech-cpi.com
KucinckiB@contech-cpi.com

57th HIGHWAY GEOLOGYSYMPOSIUM EXHIBITORS

CRUX Subsurface
16707 E. Euclid Ave.
Spokane Valley, WA 99216
Phone (509)892-9409
Fax (509)89209408
www.cruxsub.com
scott@cruxsub.com

Diedrich Drill, Inc.
5 Fisher Street
Laporte, IN 46350
Phone (800) 348-8809
Fax (219) 324-5962
www.diedrichdrill.com
dditr@diedrichdrill.com

Durham Geo Slope Indicator
12123 Harbor Reach Drive
Mukilteo, WA 98275
Phone (206) 383-6720
Fax (425) 413-0518
www.slopeindicator.com
jtavares@slope.com

Environmental Drilling Supply & Services, Inc.
5806 Franklin Street
Denver, CO 80216
Phone (303)297-9215
Fax (303)297-8066
environdrill@juno.com

Geobrugg North America, LLC.
Geobrugg Protection Systems
551 W. Cordova Road, PMB 730
Santa Fe, New Mexico 87505
Phone (505) 438-6161
Fax (505) 438-6166
www.geobrugg.com
info@us.geobrugg.com

Geokon, Inc.
48 Spencer Street
Lebanon, NH 03766
Phone (603) 448-1562
Fax (603) 448-3216
www.geokon.com/
chuck@geokon.com

gInt Software
7710 Bell Road
Windsor, CA 95492
Phone (707)383-1271
Fax (707)838-1274
www.gintsoftware.com

Golder Associates
540 North Commercial Street, Suite 250
Manchester, New Hampshire 03101-1146
Phone (603) 668 0880
Fax (603) 668 1199
www.golder.com/
pingraham@golder.com

HDR, Inc.
3 Gateway Center
Pittsburgh, PA 15222-1074
Phone: (412) 497-6045
Fax: (412) 497-6080
www.hdrinc.com
larry.artman@hdrinc.com

Hi-Tech Rockfall Construction, Inc.
P.O. Box 674
Forest Grove, OR 97116
Phone (503) 357-6508
Fax (503) 357-7323
www.hi-techrockfall.com
HTRockfall@aol.com

57th HIGHWAY GEOLOGYSYMPOSIUM EXHIBITORS

Janod Inc.
34 Beeman Way, PO Box 2487
Champlain, NY 12919
Phone (518) 298-5226
Fax (450) 424-2614
www.janod.biz/
info@janod.biz

JJ Drill Company
PO Box 884
Golden, CO 80402
Phone (720) 530-6465
(303) 733-7849
Fax (303) 733-7849
dlnpln@comcast.net

Layne GeoConstruction
22537 Coleman's Mill Road
Ruther Glen, VA 22546
Phone (804) 448-8060
Fax (804) 448-1771
www.laynechristensen.com
dwschriever@laynechristensen.com

Maccaferri, Inc.
10303 Governor Lane Blvd
Williamsport, MD 21795
Phone (301) 223-6910
Fax (301) 223-4590
www.maccaferri-usa.com
gbrunet@maccaferri-usa.com

Michael Baker Jr., Inc.
4301 Dutch Ridge Road
Beaver, PA 15009
Phone (724) 495-7711
FAX (724) 495-4017
www.mbakercorp.com
cruppen@mbakercorp.com

Mirafi (Tencate) Construction Products
365 s. Holland Drive
Prendergrass, GA 30567
Phone (706) 693-2226
Fax (706) 693-1780
www.mirafi.com
b.odgers@tencate.com

Mountain Management Inc.
Financial Plaza Building
1135 Terminal Way, Suite 106
Reno, Nevada, 89502-2145
Phone (866) 466-7223 (toll free US & Canada)
Fax (450) 455-8762
http://www.mountainmanagement.biz/
peter@mountainmanagement.biz

P.E. LaMoreaux & Associates, Inc. (PELA)
106 Administration road, Suite 4
Oak Ridge, TN 37830
Phone (865)483-7483
Fax (865) 483-7639
www.pela-tenn.com
bbeck@pela-tenn.com

PennDrill Manufacturing
500 Thompson Ave
McKees Rocks, PA 15136
Phone (412)771-2110
Fax (412)771-2115
www.penndrill.com
tsturges@penndrill.com

Rotec International, LLC
P. O. Box 31536
Santa Fe, NM 87594-1536
Phone (505) 753-6586
Fax (505) 753-6590
www.rotecinternational-usa.com
thommen@swcp.com

57th HIGHWAY GEOLOGYSYMPOSIUM EXHIBITORS

RST Instruments Ltd.
200-2050 Hartley Ave.
Coquitlam, BC
V3K 6W5, Canada
Phone (604) 540-1100, (800) 665-5599
Fax (604) 540-1005
www.rstinstruments.com/
cbray@rstinstruments.com

Ruen Drilling Inc.
3441 Todd Ct.
Modesto, CA 95350
Phone (209)988-4261
Fax (209)577-3157
www.ruendrilling.com
jmarasovic@aol.com

Simco Drilling Equipment, Inc
802 S. Furnas Drive
Osceola, IA 50213
Phone (800) 338-9925
Fax (641) 342-6764
www.simcodrill.com
info@simcodrill.com

Tensar
8703 Yates Drive, Suite 110
Westminster, CO 80031
Phone (303) 429-9511
Fax (303) 428-6770
www.tensar-international.com
jkerrigan@tensarcorp.com

Terracon
301 N. Howes Street
Fort Collins, CO 80521
Phone (970)484-0359
Fax (970)484-0454
www.terracon.com
djjobe@terracon.com

US Geological Survey
http://landslides.usgs.gov/
highland@usgs.gov

Williams Form Engineering
251 Rooney Road
Golden, CO 80401
Phone (303) 216-9300
Fax (303) 216-9400
www.williamsform.com
tbird@williamsform.com

Wyllie & Norrish
17918 NE 27th St.
Redmond, WA 98052
Phone (425)861-7327
Fax (425)861-7327
www.wnrockeng.com
nnorrish@wnrockeng.com

Zapata Engineering/ Blackhawk
301 Commercial Road, Suite B
Golden, CO 80401
Phone (303) 278-8700
Fax (303)278-0789
www.zapend.com
khanna@zapend.com

57th HIGHWAY GEOLOGY SYMPOSIUM

Future Symposia Schedule and Contact List

Year	State	Host Coordinator	Telephone Number	Email
2007	Pennsylvania	Chris Ruppen	(724) 495-4079	cruppen@mbakercorp.com
2008	New Mexico	Erik Rorem	(505) 438-6161	erik.rorem@geobrugg.com
2009	New York	Mike Vierling	(518) 471-4378	michael_vierling@thruway.state.ny.us

57th HIGHWAY GEOLOGY SYMPOSIUM

Beaver Run Resort
Breckenridge, Colorado
26-29 September, 2006
Meeting Agenda

Tuesday September 26, 2006		
11:00 am - 5:30 pm	*Beaver Run Resort lobby*	HGS Registration
12:00 pm - 5:00 pm	*Peaks 6-10, 2nd Level*	TRB Session
5:30 pm- 7:30 pm	*Colorado Ballroom, 3rd Level*	Welcome reception – *Sponsored by Beaver Run Resort* Sponsor introductions Visit with Exhibitors Poster Sessions
	Colorado Ballroom, 3rd Level	**EXHIBITS OPEN** *Open Tuesday evening and Wednesday and Friday during breaks, Thursday during cocktails*
	Colorado Ballroom Foyer, 3rd Level	**POSTER SESSIONS** *Open Tuesday evening and Wednesday during breaks*

57th HIGHWAY GEOLOGY SYMPOSIUM

Wednesday September 27, 2006		
7:00 am - 9:00 am	*Beaver Run Resort lobby*	HGS Registration
9:00 am - 2:00 pm	*Meet at Beaver Run Resort lobby*	Guest Tour
7:00 am - 6:30 pm	*Colorado Ballroom, 3rd Level*	Exhibits Open cash bar 6:00-7:00?
7:00 am - 8:00 am	*Colorado Ballroom, 3rd Level*	Continental Breakfast *Sponsored by Janod* Exhibits Open
8:00 am	*Breckenridge Ballroom , 1st Level*	**Welcome and Keynote**
9:00 am	*Breckenridge Ballroom , 1st Level*	**Technical Session I – Landslides/Slope Stability**
10:00 am - 10:30 am	*Colorado Ballroom, 3rd Level*	Break *Sponsored by HiTech Rockfall* Exhibits Open Poster Sessions
10:30 am	*Breckenridge Ballroom , 1st Level*	**Technical Session II – Landslides/Slope Stability**
11:50 pm - 1:00 pm	*Peak 5 or Blue River Hall, TBD*	Lunch Buffet
1:00 pm	*Breckenridge Ballroom , 1st Level*	**Technical Session III – Applied Geophysical and Imaging Techniques**
2:50 pm - 3:20 pm	*Colorado Ballroom, 3rd Level*	Break *Sponsored by CRUX Subsurface* Exhibits Open Poster Sessions
3:20 pm	*Breckenridge Ballroom , 1st Level*	**Technical Session IV – Geotechnical Applications**
5:40 pm	*Breckenridge Ballroom , 1st Level*	**Field Trip Announcement**

57th HIGHWAY GEOLOGY SYMPOSIUM

Thursday September 28, 2006		
7:30 am - 4:00 pm	*Meet at Beaver Run Resort lobby* Box Breakfast to be distributed in the parking lot (weather permitting), or lobby. Box Breakfast?	**57th HGS Field Trip** *Morning break sponsored by AIS Construction* *Lunch sponsored by GeoBrugg* *Refreshments sponsored by Golder Associates*
6:00 pm - 7:00 pm	*Colorado Ballroom, 3rd Level*	Social Hour and Exhibits *Sponsored by Hayward Baker*
7:00 pm - 10:00 pm	*Breckenridge Ballroom , 1st Level*	**Annual Banquet**

Friday September 29, 2006		
6:45 am- 8:00 am	*Spencer's Private Dining Room*	Steering Committee Meeting
7:00 am – 8:00 am	*Colorado Ballroom, 3rd Level*	Continental Breakfast *Co-sponsored by Michael Baker, Jr. and Mountain Management* Exhibits Open
8:00 am	*Breckenridge Ballroom , 1st Level*	**Technical Session V – Hazards I**
10:00 am	*Colorado Ballroom, 3rd Level*	Break *Sponsored by Wyllie & Norrish* Exhibits Open
10:20 am	*Breckenridge Ballroom , 1st Level*	**Technical Session VI – Hazards II and Geology/Geomorphology**
12:00 pm	*Breckenridge Ballroom , 1st Level*	**Concluding Remarks – Adjournment**

57th Highway Geology Symposium
TABLE OF CONTENTS

TECHNICAL SESSION I
LANDSLIDES/SLOPE STABILITY

TECHNICAL SESSION II
LANDSLIDE/SLOPE STABILITY, CONTINUED

TECHNICAL SESSION III
APPLIED GEOPHYSICAL AND IMAGING TECHNIQUES

TABLE OF CONTENTS

TECHNICAL SESSION IV
GEOTECHNICAL APPLICATIONS

TECHNICAL SESSION V
HAZARDS

TABLE OF CONTENTS

TECHNICAL SESSION VI
HAZARDS, CONTINUED

POSTERS

TECHNICAL SESSION I
Landslides/Slope Stability

Landslide Investigation and Mitigation along US 160 Between Durango and Mancos, Colorado using Lightweight Fill, Ground Anchors, and a Rockery Buttress

Ben Arndt, P.E., P.G. ***(Presenter/Author)***
Yeh and Associates, Inc.
5700 East Evans Ave
Denver, CO 80222
barndt@yeh1.net

Thomas L. Allen, P.E. ***(Co-Author)***
Yeh and Associates, Inc.
570 Turner Drive, Suite D
Durango, CO 81303
tallen@yeh1.net

Richard Andrew, P.G. ***(Co-Author)***
Yeh and Associates, Inc.
5700 East Evans Ave
Denver, CO 80222
randrew@yeh1.net

ABSTRACT

During the spring of 2004, five landslides developed along US 160 between Durango and Mancos, Colorado. The landslides became active after above average snowfall and rainfall in the area. One of the five landslides appeared to have been unsuccessfully mitigated with sawdust fill in the past and had re-activated. Yeh and Associates, under a task order with the Colorado Department of Transportation (CDOT), provided a geotechnical investigation, landslide evaluation, landslide mitigation alternatives, and final mitigation design for the landslides.

Regional geologic units that underlie the landslide areas are composed of Cretaceous Age Mancos Shale that typically weathers near the surface to form sandy silts and clayey materials with low shear strength and poor slope stability characteristics. The geometry and movement of the active landslides appeared to be controlled by a combination of factors including elevated groundwater levels, highly weathered bedrock surfaces, and inappropriately placed embankment materials. Typically the landslide geometries exhibited classic rotational and shallow planar failures.

Three of the landslides were mitigated by replacing existing embankment fills with lightweight expanded polystyrene (EPS) fill. Lightweight EPS fill reduces the driving forces that act on a slope profile and increase the overall global factor of safety. The density of the EPS is typically between 1 to 1.5 pounds per cubic foot, as compared to 100 to 110 pounds per cubic foot of existing embankment fill. The other two landslides were mitigated by installing a ground anchor tieback system in one of the landslides, and rockery buttress in the other landslide. The paper addresses the geotechnical evaluation, design concepts and constructability issues of the mitigation systems.

INTRODUCTION

During the spring of 2004, five landslides developed along US 160 between Durango and Mancos, Colorado. The landslides became active after above average snowfall and rainfall in the area. The landslides were located between Mile Markers 69.8 and 75.7 along US 160. One of the landslides was located west of the town of Hesperus. The other four landslides were located east of the town of Hesperus and west of the Durango West subdivision.

The landslides were numbered 1 through 5 going from west to east along US 160. Landside #1 was located at approximate mile marker 69.8, Landslide #2 was located at approximate mile marker 74.2, Landslide #3 was located

at approximate mile marker 75.1, Landslide #4 was located at approximate mile marker 75.3, and Landslide #5 was located at approximate mile marker 75.5. See site location map for approximate locations.

Yeh and associates was contracted with the Colorado Department of Transportation (CDOT) to provide a geotechnical investigation which consisted of subsurface drilling, a landslide evaluation of each site, a list of landslide mitigation alternatives and relative associated costs, and final mitigation design for the landslides which included plans and special provisions for construction of the mitigation alternative chosen.

A field exploration program consisting of geologic reconnaissance and exploratory drilling was conducted to obtain information on subsurface conditions in the vicinity of the slope failures. Yeh and Associates sub-contracted a drilling vendor with a Dietrich D-50 rubber track drill rig to conduct the exploratory drilling in the summer of 2004. Material samples obtained during the field exploration were tested in the laboratory to determine the classification and engineering characteristics of the on-site materials.

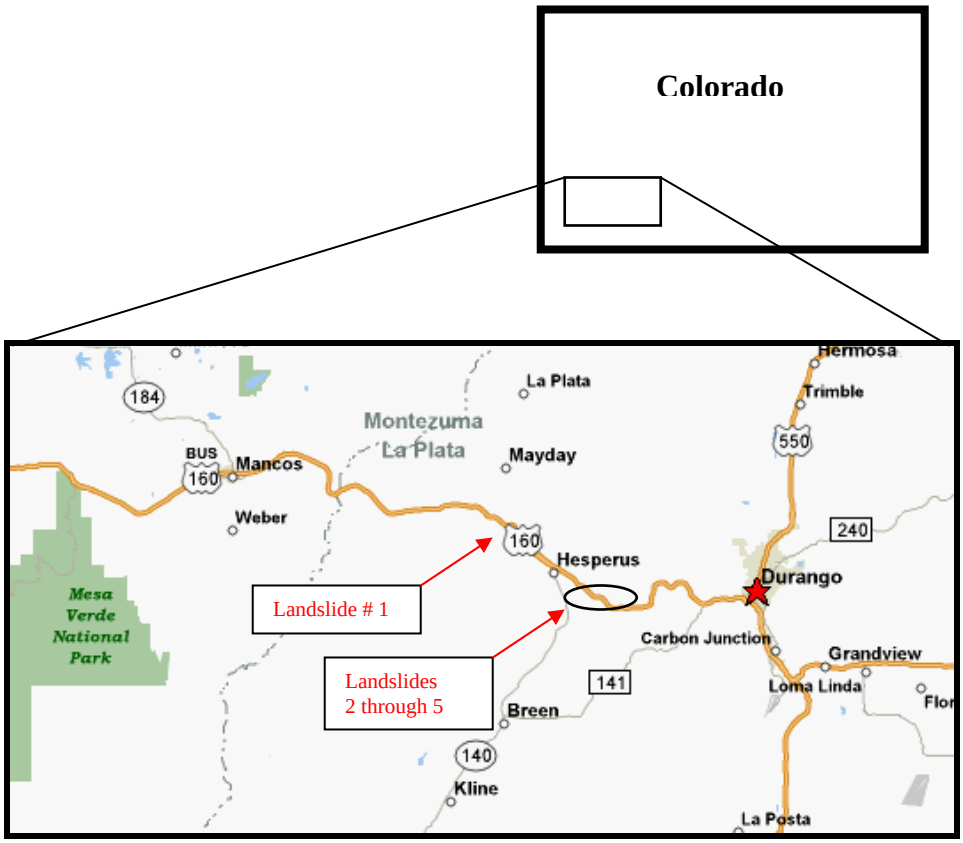

Figure 1. Site Location Map

REGIONAL AND SITE CONDITIONS

The geologic units that underlie the landslides in this area are composed of Cretaceous age sandstones, siltstones, limestones and shales. The geologic units that underlie most of the project area consist of sandstones and shales of the Mesaverde Group. These geologic units form blocky, well-jointed, sandstone cliff faces that underlie Mesa Verde National Park to the southwest. In the immediate project area, the Mesaverde Group is composed of thinner sandstones, silts, and shales. Underlying the Mesaverde Group is the Mancos Shale. The Mancos Shale is a marine deposited geologic unit that is typically known for low shear strength properties. Highway embankments and fills that are constructed with weathered shales and clays from the Mesaverde and Mancos Formations exhibit low shear-strength properties when wetted and are prone to landslides and embankment failures.

Overall the results of the subsurface investigation generally indicated the soil materials underlying US 160 at the subject sites consisted of approximately 15 to 25 feet of low to medium plasticity clays with local areas of sandy silt that are underlain by weathered to unweathered shale/claystone bedrock. The overburden clay materials were generally medium stiff to stiff. The distinction between embankment fill and natural clay materials was not evident from the borings logged by standard sampling methods and sample intervals. It appears from the samples obtained, and the general topography of the site, that both the embankment fill and underlying clays consisted of low plasticity materials that generally have similar strength and material properties. Occasional gravel sized bedrock fragments of local and imported origins were also encountered. The overburden clay materials generally consisted of A-6 to A-7 materials (i.e., CL and CH materials). Moisture contents of the overburden clay materials above the shale/claystone bedrock ranged from 10 % to 25 % throughout the project area. Typically the optimum moisture content for low to medium plasticity clay (CL) material ranges from 12% to 24% for dry unit weights ranging from 95 to 120 pcf.

Based on the investigation, it also appeared that the upper 2 to 5 feet of the shale/claystone bedrock is generally partially to very weathered while the lower shale is less weathered. Blow counts indicated the shear strength of the underlying materials becomes greater with depth. The unweathered claystone also appeared to be dry, indicating likely groundwater movement along the interface of the overburden clays and the top of the claystone bedrock.

Groundwater was observed seeping out of the slope near the toe of many of the slide areas as well as localized areas along the embankment slopes. The locations of these seeps are likely controlled by a variety of factors and subsurface conditions. Standpipe piezometers were installed at several slide locations to allow long-term monitoring of groundwater levels. Horizontal drains were installed at many of the slide locations to lower the groundwater levels and further mitigate the unstable slopes.

LANDSLIDE EVALUATIONS

For the purposes of the project terminology, the failed slopes were referred to as landslides although many of the slope failures could also be termed large-scale embankment fill failures. Global stability of the landslides (i.e., embankment fill failures) was evaluated using several computer programs that use limit equilibrium methods to determine factor of safety of a slope including PCStabl6, GStabl7, and Slope/W.

The stability of the slopes was evaluated using limit equilibrium models based on existing slope geometries, subsurface conditions and previous experience. Representative overall shear strength parameters for each slide area were back calculated assuming a factor of safety near 1.0 and relatively dry conditions. Generally, a factor of safety equal to 1.0 is the point at which a slope failure would occur. The stability analysis indicates the internal friction angle (phi) Φ of the embankment materials ranges between 25^0 to 15^0 and the cohesion ranges between 250 and 50 psf. These values were generally consistent with the results from laboratory tests performed on discrete samples obtained from the exploratory borings.

Landslide #1 (MM 69.8)

Approximately 400 feet of eastbound US 160 experienced excessive lateral and vertical deformations that resulted in an outside lane closure due to failure of the embankment on the south side of the roadway. Tension cracking was evident along the eastbound travel lane and the roadway shoulder and outlined the landslide headscarp. The tension cracks ran parallel to the highway along eastbound lane for approximately 320 feet. The tension cracking then continued down the embankment slope for approximately another 150 feet. At this location US 160 has two eastbound lanes, the right lane in this area had dropped vertically approximately 6 to 8 inches and the measurable vertical depth of the crack was approximately 2 feet. The width of tension cracking ranged from 2 to 12 inches (see Figures 2 and 3).

Throughout the project limits, it appeared that materials used for the roadway embankment consisted primarily of low to medium plastic clays of shale/claystone origin, which characteristically have low shear strength. In many cases it was difficult to distinguish between the native clay and embankment fills because they were composed of the same materials. The clay material, when dry, possesses high cohesive strength, which will typically support embankment slopes up to 2H:1V. However, when the clay becomes wet, the shear strength of the material is reduced and subsequently leads to a slope failure. Subsurface wetting of the embankment had generally been caused by seasonal rises of the groundwater level and/or surface water infiltration. It appeared that failure of the

embankment resulted from placement of low strength clay embankment materials over native clay materials that lost shear strength due to wetting. The stability analysis indicated that elevating the groundwater level would reduce the global factor of safety below 1.0.

Figure 2. Looking west along US 160 at Landslide 1.

Figure 3. Looking east along US 160 at Landslide 1.

Figure 4 depicts a typical slope cross section at or near slope failure of the preexisting slope for Landslide #1. The groundwater level is based on the conditions encountered at the time of drilling.

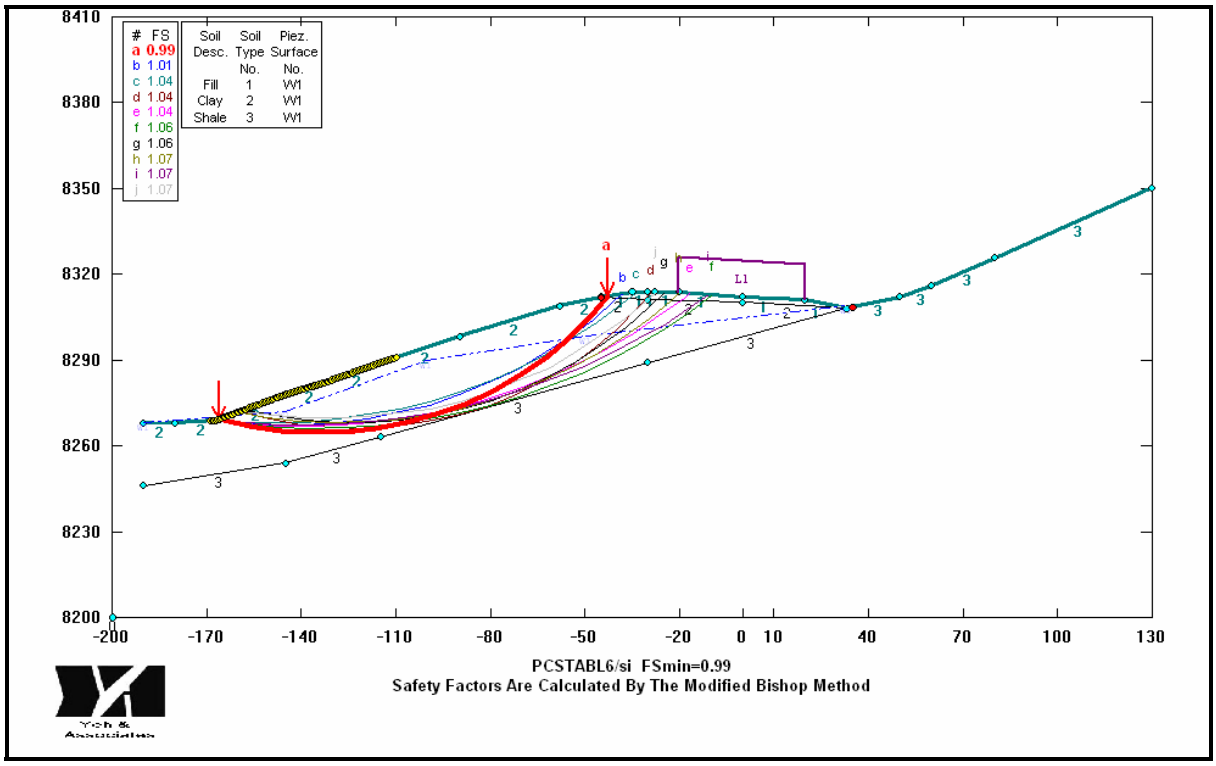

Figure 4. Landslide 1 Pre-failure Slope Stability Model.

After excavation of the landslide section the failure plane became more evident. Figure 5 depicts the outline of the failure plane during mitigation of the landslide.

Figure 5. Outline of failure plane during excavation and mitigation of Landslide 1.

Landslide #2 (MM 74.2)

Landslide 2, located near mile marker 74.2, exhibited a shallow rotational failure feature with a well-defined headscarp and toe. The headscarp ran parallel to US 160 for approximately 275 feet. The area appeared to be deforming as a result of an embankment fill failure on the north side of the roadway. The vertical displacement of the headscarp along the highway ranged from 1 to 6 feet. The toe of the landslide also exhibited an earth flow feature indicative of a rotational failure. The surface topography at the body of the landslide exhibits a hummocky appearance in localized areas. Slope profiles vary, but generally consist of 2H:1V slopes in the vicinity of the slide. Figures 6 and 7 depict sections of the landslide area.

Figure 6 – Looking west along US 160 at Landslide 2
(Utility lines are visible on the surface).

Figure 7 – Looking east along US 160 at Landslide 2.

The landslide is located on an inside curve of US 160. It is likely surface water runoff from the roadway and/or infiltration and migration of ponded water from the south side of US 160 likely contributed to the slope failure. The clays, clayey sands, and underlying shales are very sensitive to groundwater and surface water infiltration. Global stability of the slope failure was evaluated based on a review of the existing site conditions, groundwater conditions, and available subsurface information. It appeared that the materials used for the roadway embankment consisted primarily of low to medium plasticity clays of shale/claystone origin, which characteristically have low shear strength. Figure 8 depicts a typical slope stability model of the pre-failure slope.

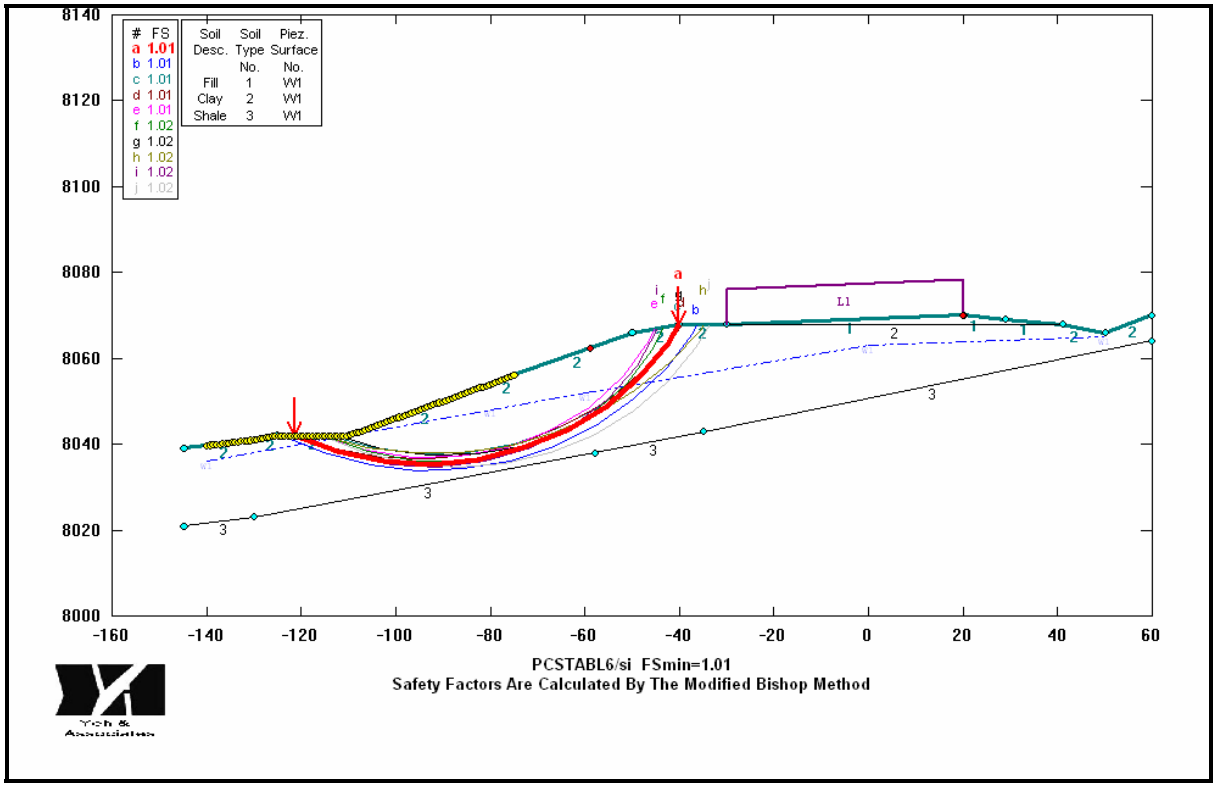

Figure 8. Landslide 2 Pre-failure Slope Stability Model.

Landslide #3 (MM 75.1)

Landslide 3, located near mile marker 75.1 on US 160, failed adjacent to the roadway. This slope failed because of a previously unsuccessful use of sawdust as a lightweight fill mitigation option. It also appeared that piles located approximately 50 feet from the existing shoulder had been driven in an attempt to improve stability of the slope. Both mitigation methods appear to have been ineffective. The landslide was active as evidenced by a well-defined toe that formed an earth flow feature, indicating a rotational slope failure. The sawdust observed during our field investigation was extremely unstable and saturated with water. During drilling operations large tension cracks developed within the surface sawdust materials.

The landslide, as observed during the investigation, exhibited a shallow rotational failure feature with a well-defined headscarp and toe. The headscarp runs parallel to US 160 for approximately 100 feet. The observed movements of the landslide appear to result from extreme deformation of the sawdust and possible movement of the underlying weaker shales and clays. The vertical displacement of the headscarp along the highway ranged from 3 to 8 feet. A cover of sawdust approximately 7 feet thick had been placed over the existing landslide. Figures 9 and 10 depict Landslide 3.

Figure 9 – Landslide 3 - Looking east along US 160.

Figure 10 – Landslide 3 - Looking west along US 160
(Foreground is composed of sawdust fill).

In order to evaluate the current conditions of the slope, a stability analysis was performed based on the likely pre-existing slope and subsurface conditions prior to the sawdust and driven pile mitigation attempts. Generally a factor of safety equal to 1.0 is the point at which a slope failure will occur. The model showed that elevating the groundwater conditions reduces the factor of safety below 1.0. The following figure depicts the existing slope profile for Landslide #3. The groundwater level is based on the conditions encountered at the time of drilling.

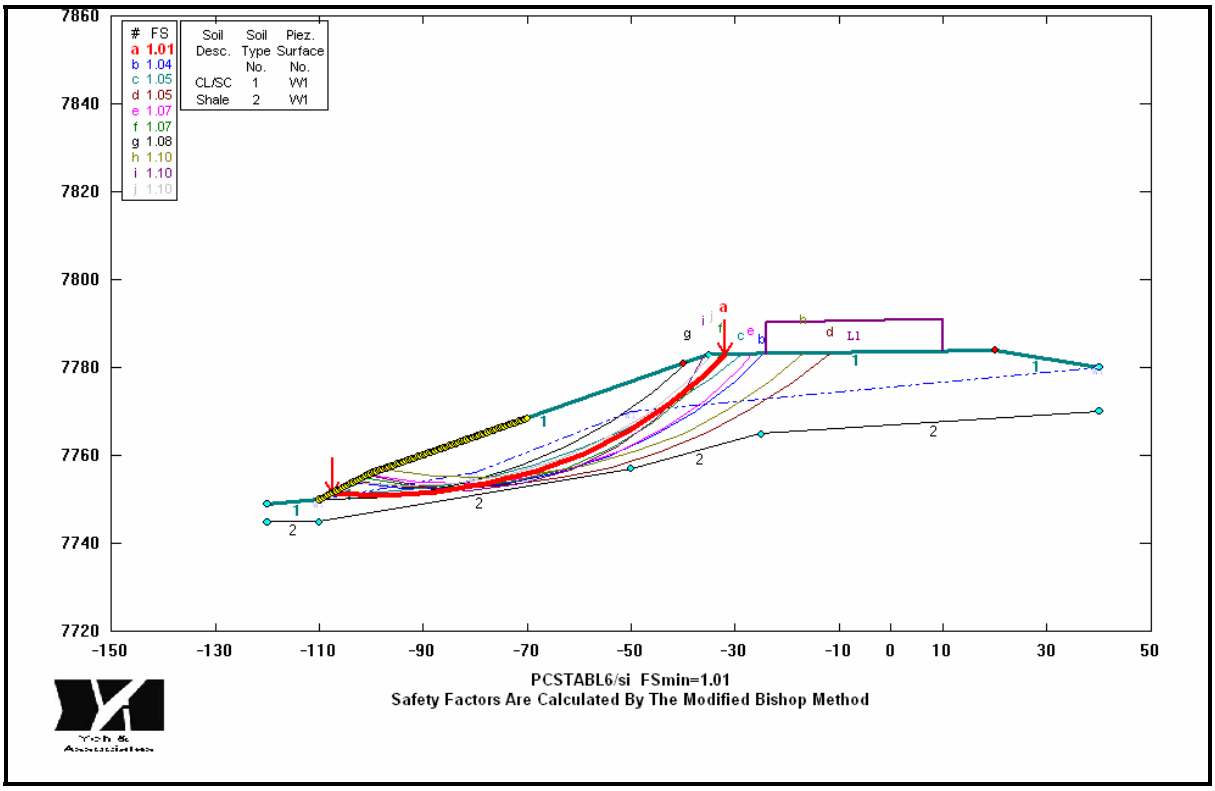

Figure 11. Landslide 3 - Pre-failure Slope Stability Model.

Landslide #4 (MM 75.3)

Landslide 4 was located near Mile Marker 75.3 on US 160. The landslide appeared to be a large deep-seated failure that exhibited a rotational failure feature with a well-defined toe. The landslide extended from 300 to 400 feet along US 160. A well-defined large-scale headscarp was not apparent. However pavement distress was observed in smaller sections where the active portions of the landslide had impacted the pavement section. The landslide was intermittingly active for a number of years and various mitigative alternatives have been attempted that include soil nails and use of flowable fill to replace failed embankments. The activity of the landslide was likely increased by placement of embankment fill on the north side of the roadway during a pavement widening project. The vertical displacement of the headscarp of the landslide was likely in excess of 10 feet based on the thickness of the asphalt and aggregate base course materials beneath the roadway. The surface topography at the body of the landslide exhibited a hummocky appearance in localized areas. Slope profiles varied, but generally consisted of 2H:1V slope in the vicinity of the slide. Figures 12 and 13 show sections of the landslide area.

Figure 12. Landslide 4 Looking east along US 160

Figure 13. Landslide 4 - Looking west along US 160.

Global stability of the slide was evaluated based on a review of the existing site conditions, groundwater conditions, and available subsurface information. Figure 14 depicts a typical slope stability model for the landslide.

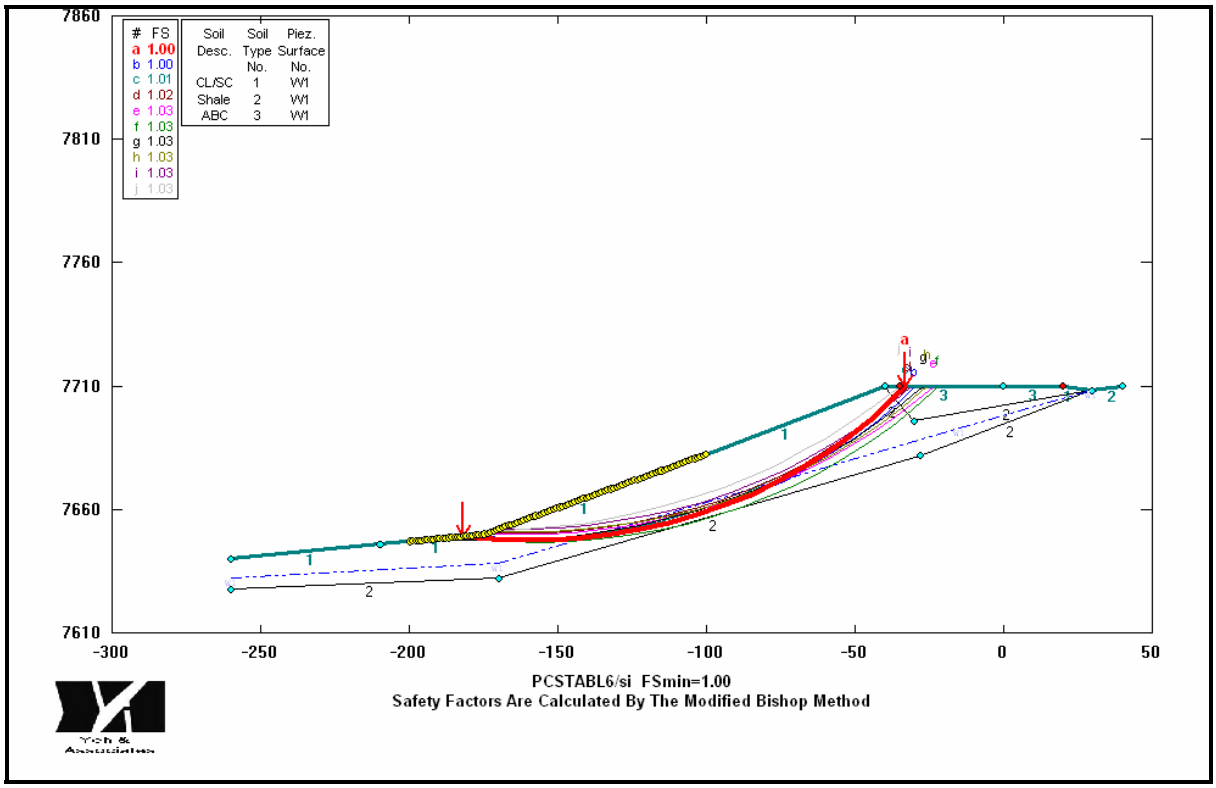

Figure 14. Landslide #4 Pre-failure Slope Stability Model.

Landslide #5 (MM 75.5)

Landslide 5 was located near Mile Marker 75.5 and was approximately 100 to 150 feet in length. This landslide was more characteristically an embankment fill failure on an outside curve of US 160 that did not affected the travel lanes of the roadway. It appears the material was placed at an angle steeper than could be supported by the shear strength of the fill. Surface and/or groundwater infiltration probably contributed to the failure. The embankment fill failure is a shallow slough that occurred on an existing 1.5H:1V slope. The final steepness of the slide approaches 60^0. Figure 15 shows the embankment fill failure area.

Figure 15 – Landslide 5 - Looking west along US 160.

Figure 16 depicts a generalized stability model for the failed slope. It is likely that the existing materials were placed at too steep an angle and the addition of water cause the failure.

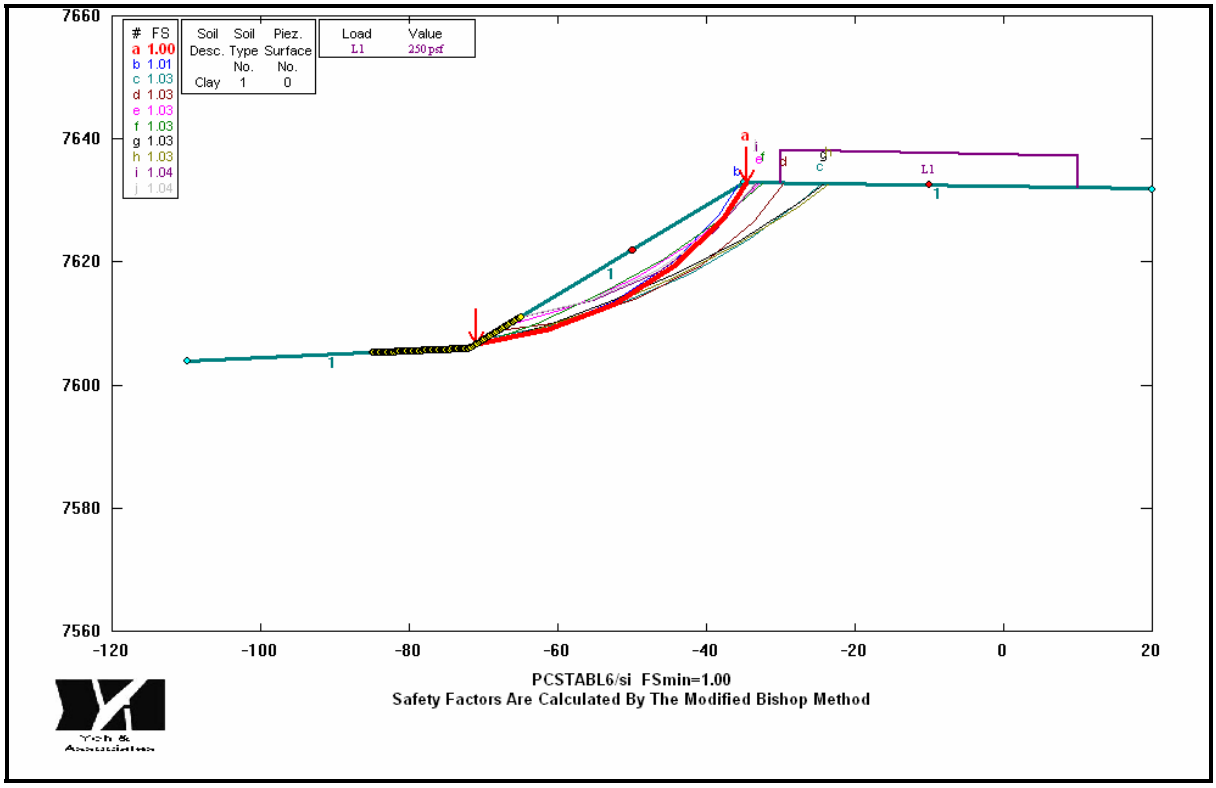

Figure 16. Landslide 5 Pre-failure Slope Stability Model.

MITIGATION ALTERNATIVES AND CONSTRUCTION

Landslides 1 through 3

Based on the results of our geotechnical investigation and our evaluation of the landslides, we recommend that the failed sections for Landslides 1 through 3 be mitigated by replacing a section of the existing failed embankment with lightweight expanded polystyrene (EPS) fill and regrading the slope. Our analysis showed that an acceptable factor of safety against slope failure would be obtained by replacing the existing fill below the roadway with lighter weight material. The use of lightweight fill was the most cost-effective and efficient mitigation method for the conditions at Landslides 1 through 3. Typically, lightweight fill consists of expanded polystyrene (EPS) that has about one percent of the weight of compacted soils. The previous repair of Landslide #3 was an attempt to place lightweight sawdust fill, but because of the site conditions and groundwater levels the sawdust was easily saturated and tended to float and flow down the slope and did not provide an effective mitigation option. The design parameters for the EPS fill replacement were as follows:

- A minimum EPS a density of 1.15 pcf, minimum compressive strength of 5.8 psi and 16.0 psi at 1% and 10% deformation respectively, and a maximum water absorption of 3%.
- The footprint of the excavation was laid-back as a temporary cut prior to EPS placement.
- A concrete cap and/or impervious liner was placed on top and around the EPS to prevent petroleum products, especially diesel fuel from dissolving the EPS material.
- A drainage system was placed behind and underneath the proposed EPS material.
- The EPS was also tapered on both ends of the excavation cut to minimize the potential for differential settlements in the roadway at the boundaries of the replacement.

Design of the EPS system consisted of evaluating the typical retaining wall features such as internal, external and global stability. For internal stability it is necessary to determine how much overburden pressure the EPS system can tolerate without excessive lateral deformation or deflection. The results from unconfined compression creep tests on block-molded EPS were used to determine the total allowable overburden pressure (i.e., roadway, roadway traffic, asphalt, subgrade and other vertical loads). A factor of safety was applied to insure the EPS would not deform or compress over time due to these loads.

It was also necessary to evaluate the shear strength of the EPS for use in global stability analysis. Overall the allowable overburden stress and the thickness of the EPS fill are governed by the deformation and strength characteristics of the EPS materials. Additionally, it is imperative to evaluate the sliding potential of the EPS and either provide passive pressure elements to resist sliding or reduce the active earth pressure that will act to destabilize the EPS system laterally. A subsurface drainage system is essential to reduce the potential effects of excess hydrostatic and buoyant pressures on the fill.

Figures 17 and 18 depict a generalized design of the EPS system and construction of the elements.

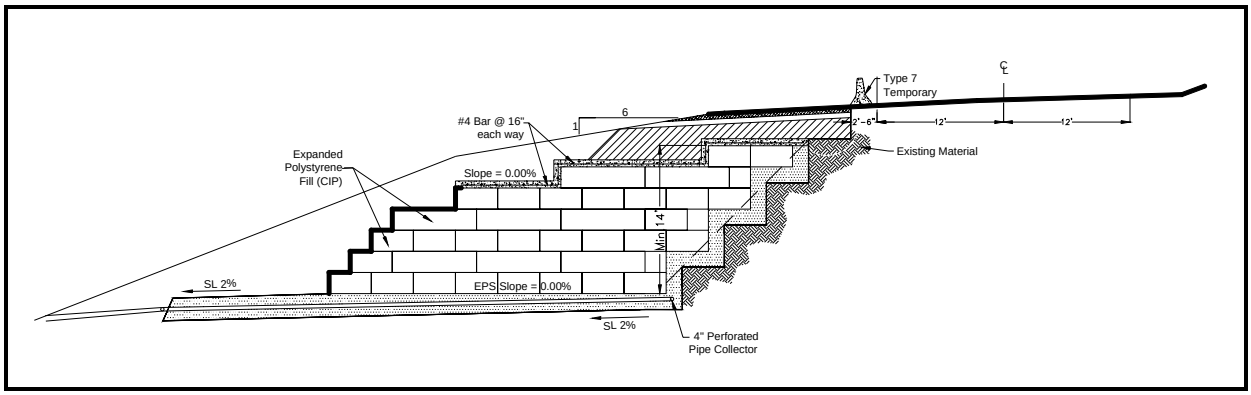

Figure 17. Typical EPS replacement system

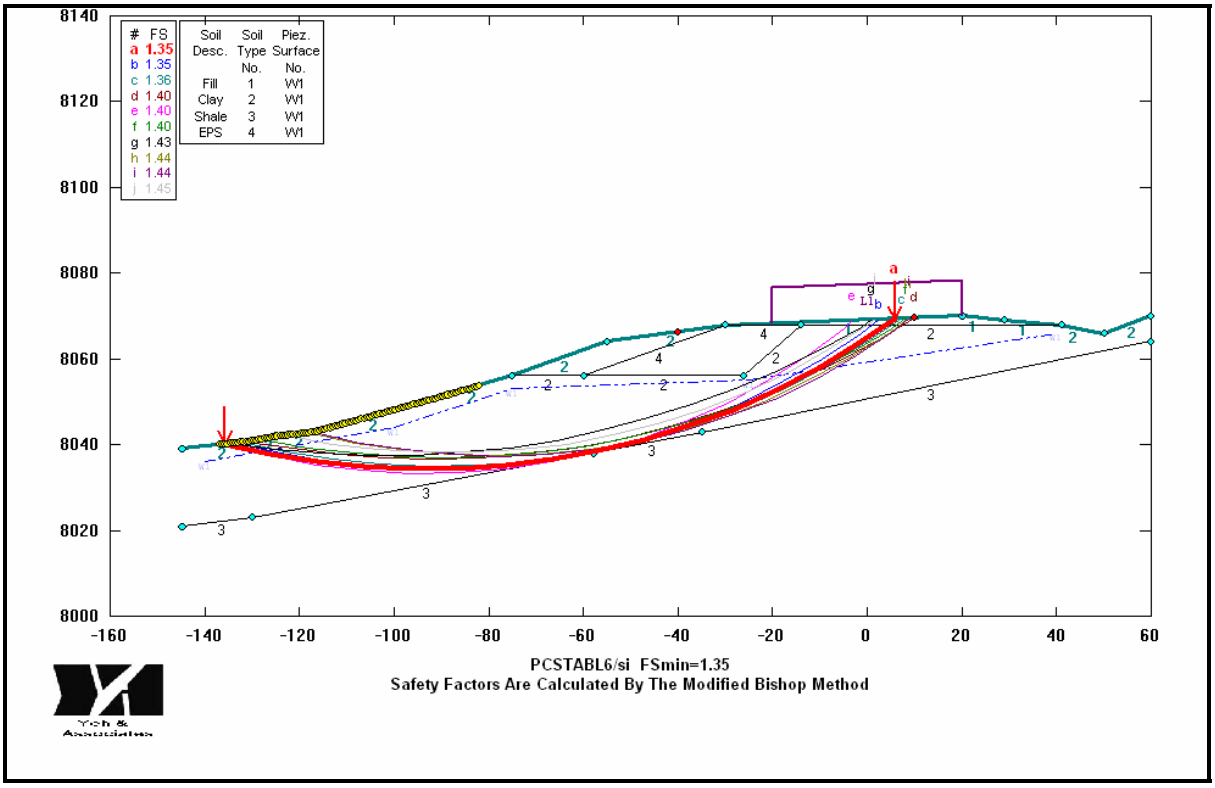

Figure 18. Typical Global Stability Model of EPS system.

Figures 19 and 20 depicts placement of the EPS lightweight fill during construction.

Figure 19. EPS placement in Landside #2.

Figure 20. EPS placement in Landslide #3 (Replacing Sawdust Fill).

Landslide 4

Based on the results of our geotechnical investigation and our evaluation of Landslide #4, we recommend installing ground anchors and tie-back panels as the most cost-effective and efficient mitigation option. Our analysis indicated an acceptable factor of safety against slope failure would be obtained by installing 3 rows of ground anchors at 10-foot spacing. The ground anchors were designed to be a post-tensioned (i.e., pre-stressed) reinforcement element. The design parameters for the ground anchors were as follows:

- The ultimate bond stress is estimated to be 4.5 to 9.0 psi for the native soils and weathered bedrock. The ultimate bond stress for partially weathered and unweathered shale bedrock is estimated between 10 psi and 30 psi depending upon the type of shale bedrock encountered and moisture conditions.
- Ground anchors should be installed with a minimum free length of 15 feet and bond length of at least 15 feet. However, depth to bedrock was anticipated to require a 40-foot free length and shale bedrock was anticipated to require a minimum bond length of 35-foot for an 8-inch diameter hole.
- Ground anchors were sized for a 112 kip design load. The ground anchors were to be locked off at 80% of design load to decrease the potential for localized bearing capacity failures behind the tieback panels.

The ground anchor design was based on global stability analysis of the site and the localized bearing capacity of the tieback panels. Because of the overall low strength of the embankment materials, it was necessary to balance adequate tieback load against the potential for causing bearing capacity failures at the tieback panels. Too much anchor tension would cause the tieback panels to fail into the groundmass.

Figures 21 and 22 depict a typical cross section of the ground anchor tieback layout. Figure 23 depicts the typical global stability analysis for mitigation of Landslide #4 with tieback anchors.

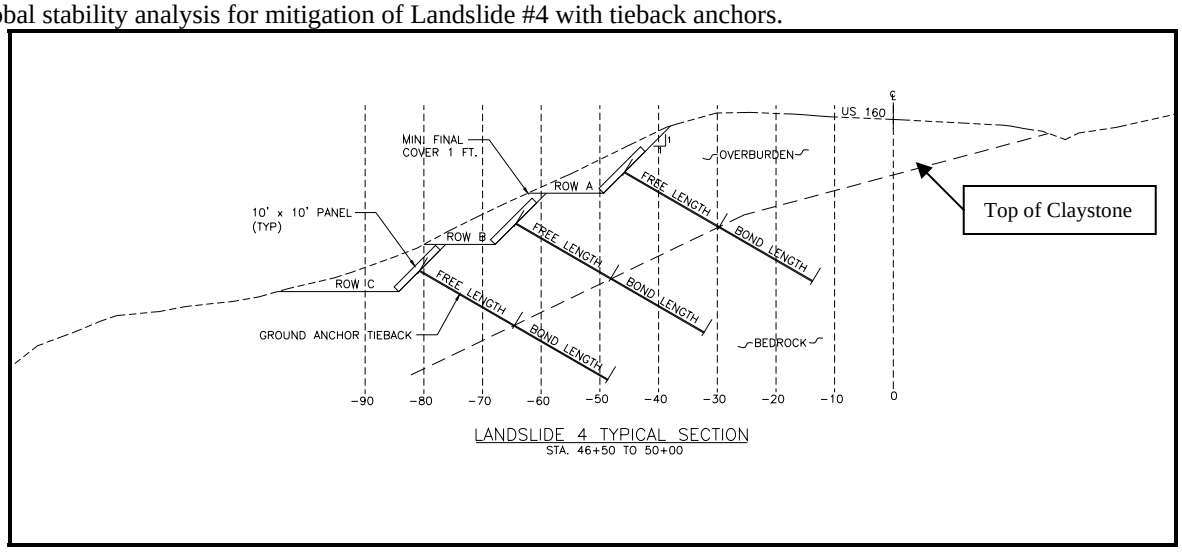

Figure 21. Typical Cross Section of Ground Anchor Tieback System.

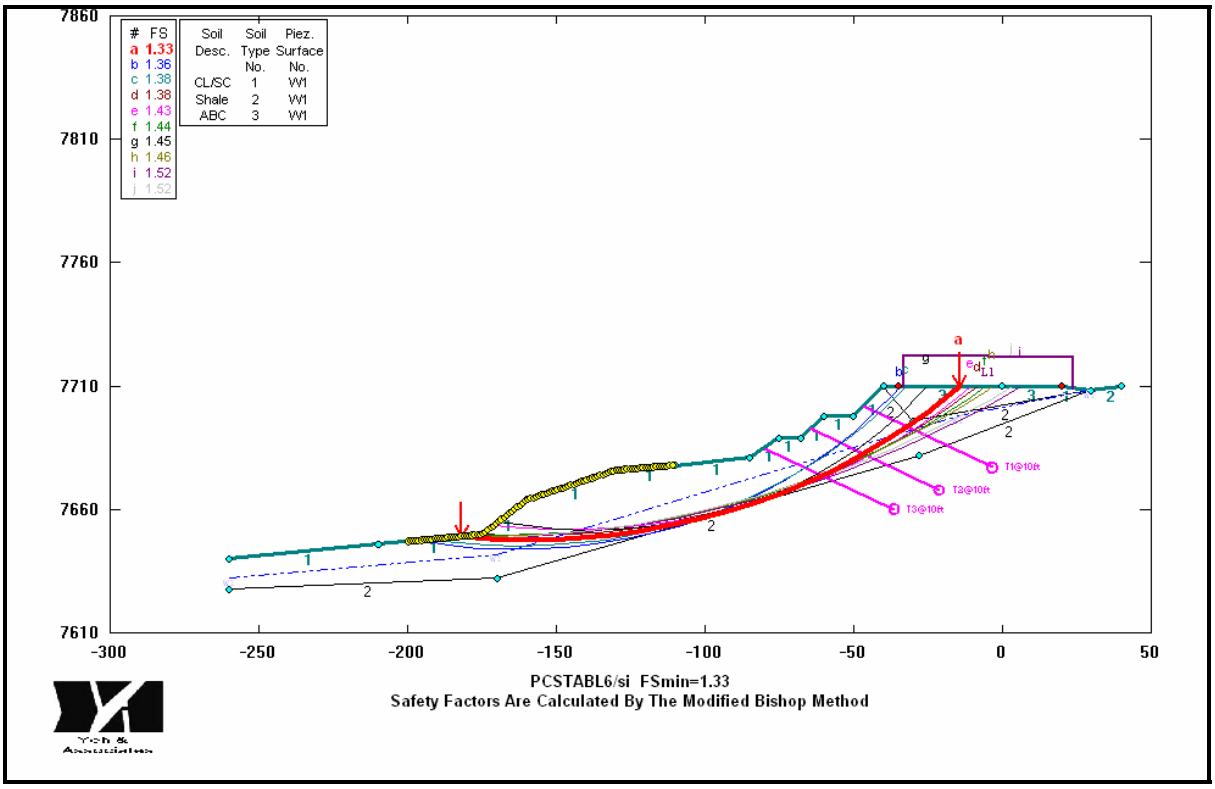

Figure 22. Typical Slope Stability Model of Ground Anchor Tieback System.

Figure 23. Installation of the Tieback Ground Anchors.

Landslide 5

Based on the results of our geotechnical investigation and our evaluation of the landslide, we recommend a large diameter boulder buttress be used to mitigate Landslide 5. From the stability analysis, an acceptable factor of safety against slope failure could be obtained by installing a buttress wall at the base of the slope. The effect of the boulders is that the greater mass would increase the forces resisting movement, thereby improving the stability of the section. The general design parameters for the buttress wall were as follows:

- The design height of the buttress was less than 15 feet with a base width of at least 0.65 of the design height.
- The buttress had to have a minimum of 3 feet of embedment.
- The face inclination of the buttress would not exceed 2V:1H.
- Boulders for the buttress were to have nominal diameter of 36 inches and voids between the boulders were in-filled with aggregate base course. Drainage geotextile was placed around the buttress to prevent the migration of fine grained materials through the in-fill.
- Embankment slopes constructed above the buttress should be reinforced with a geotextile or geogrid if constructed steeper than 3H:1V.

The rockery buttress was evaluated in a similar manner to a retaining wall by reviewing the internal, external and global stability of the system. Figures 24 and 25 depict a generalized cross section of the buttress.

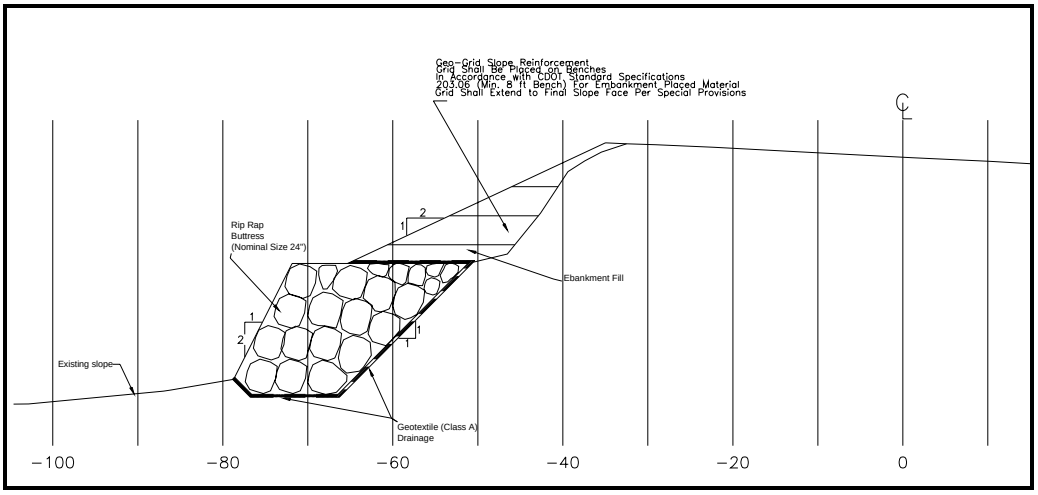

Figure 24. Generalized cross section of the boulder buttress.

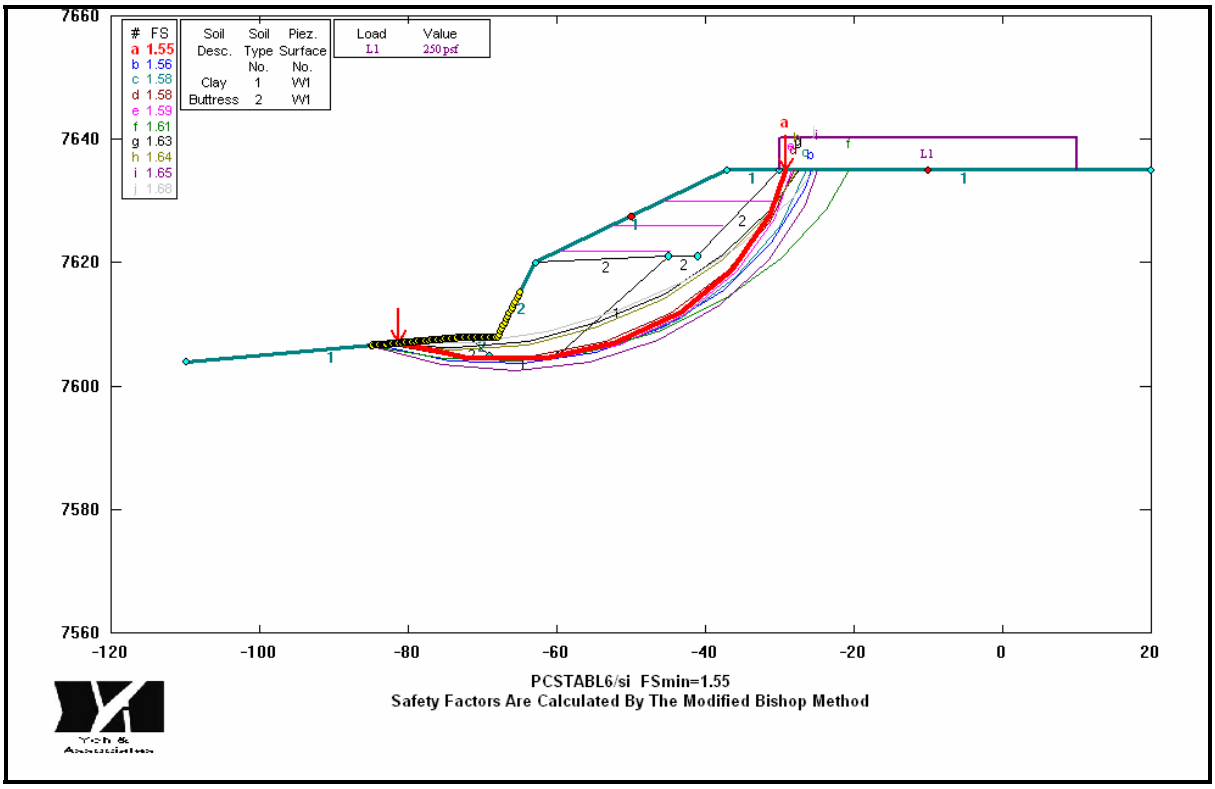

Figure 25. Global Stability Analysis of the Boulder Buttress.

SUMMARY

Overall the use of lightweight EPS fill provided a suitable slope stabilization mitigation alternative for Landslides 1 through 3. The total project cost to mitigate Landslide 1 was approximately $1.3 million. The total project cost to mitigate Landslides 2 through 5 was approximately $3.2 million. The cost of placing the EPS materials ranged from $72 to $82 a cubic yard and generally proceeded quickly and efficiently. The cost of the ground anchor tieback system was $100 per square foot of face.

Although these construction costs may seem high, the costs associated with using conventional mitigation methods such as regarding embankments to create flatter slope angles, would likely have been double when right-of-way costs are included. If tieback anchors were used on the entire project instead of EPS, the cost could easily have tripled.

As with all geotechnical and geotechnical design projects the success of the project is dependant on the designer of record being available throughout the construction process to address construction issues or make modifications to the design. It is important to have close communication between the Owner, Contractor and Designer to provide the best quality product.

REFERENCES

Horvath, John S. *Geofoam Geosynthetic*. Horvath Engineering, P.C., Scarsdale, New York, 1995.

NCHRP – Report 529, Guideline and Recommended Standard for Geofoam Applications in Highway Embankments, TRB 2004.

Recommendations for Prestressed Rock and Soil Anchors, Post Tensioning Institute, 4th Edition, 2006.

The 2005 Logan Bluff Landslide

Nancy C. Dessenberger, P.E., P.G.
Golder Associates Inc.
44 Union Blvd. Suite 300
Lakewood, Colorado 80228
NDessenberger@golder.com

Leslie A. Heppler, P.G.
Utah Department of Transportation
Salt Lake City, Utah

ABSTRACT

Sometime during the night of September 9/10, 2005, the hillside along a portion of Logan Bluff slid into the Logan Northern Canal, causing water and mud to flow onto the lower slope and into the residence below. UDOT maintenance personnel were dispatched to the site on the morning of the 10th, and discovered that over 1200 cubic yards of soil, rock and debris had mobilized from the slope above the canal. Water was flowing from the exposed soils and slide debris, and masses of the over-steepened soils were continuing to collapse into the failed area. Occupants of the residence were advised to evacuate until the situation could be further assessed. Due to the potential human hazard down slope of the slide, and the threat to a parking lot immediately above the area, the situation quickly came into the public eye.

UDOT was deemed "responsible", as owner of the failed ground, which they had acquired through a Right of Way (ROW) land trade in the 1980's to accommodate the interests of Utah State University (USU), located on the opposite side of State Highway 89. USU was particularly concerned about the situation, since the threatened parking lot within the UDOT ROW was reserved for their faculty.

Preliminary investigation into the causes of the slide came to the conclusion that groundwater emerging from the slope was a key factor in causing the landslide. Furthermore, similar conditions conducive to future landslides exist along approximately two miles of Logan Bluff.

As the study proceeded, it raised questions about the sources of the groundwater, which had not significantly abated through the winter of 2005/2006. Local water management practices were discovered to include dry wells feeding urban and university storm runoff directly into the permeable gravels capping the bluff, irrigation ditches above the bluff with large seepage losses, and infiltration-intensive landscape irrigation practices. These findings raised significant questions about the potential role of non-UDOT entities which may be contributing to the problem.

UDOT proceeded with repair of the 2005 landslide area, which included re-grading of the slope and placement of a seepage collection system. UDOT has emphasized that they are only repairing this specific area, and that the entire bluff area may be at risk of similar failures in the future if measures are not taken to control the sources of groundwater. UDOT petitioned the Utah State Legislature to provide funding for studies to determine the sources of the water, perform a risk evaluation, and identify at-risk areas of the Logan Bluff.

LOGAN BLUFF LANDSLIDE HISTORY

The failure occurred on the south-facing slope of Logan Bluff, immediately south of the Utah State University campus, across Highway 89, directly downslope of an existing parking area used by USU. The location of the 2005 Logan Bluff Landslide is shown in Figure 1. The slide initiated on the slope above the Logan Northern Canal, which traverses the bluff about 30 feet above the valley floor. Slide debris filled the canal, causing a mudflow of slide debris and canal water to flow down the slope, breaking through basement level windows and filling the back yard of the private residence below.

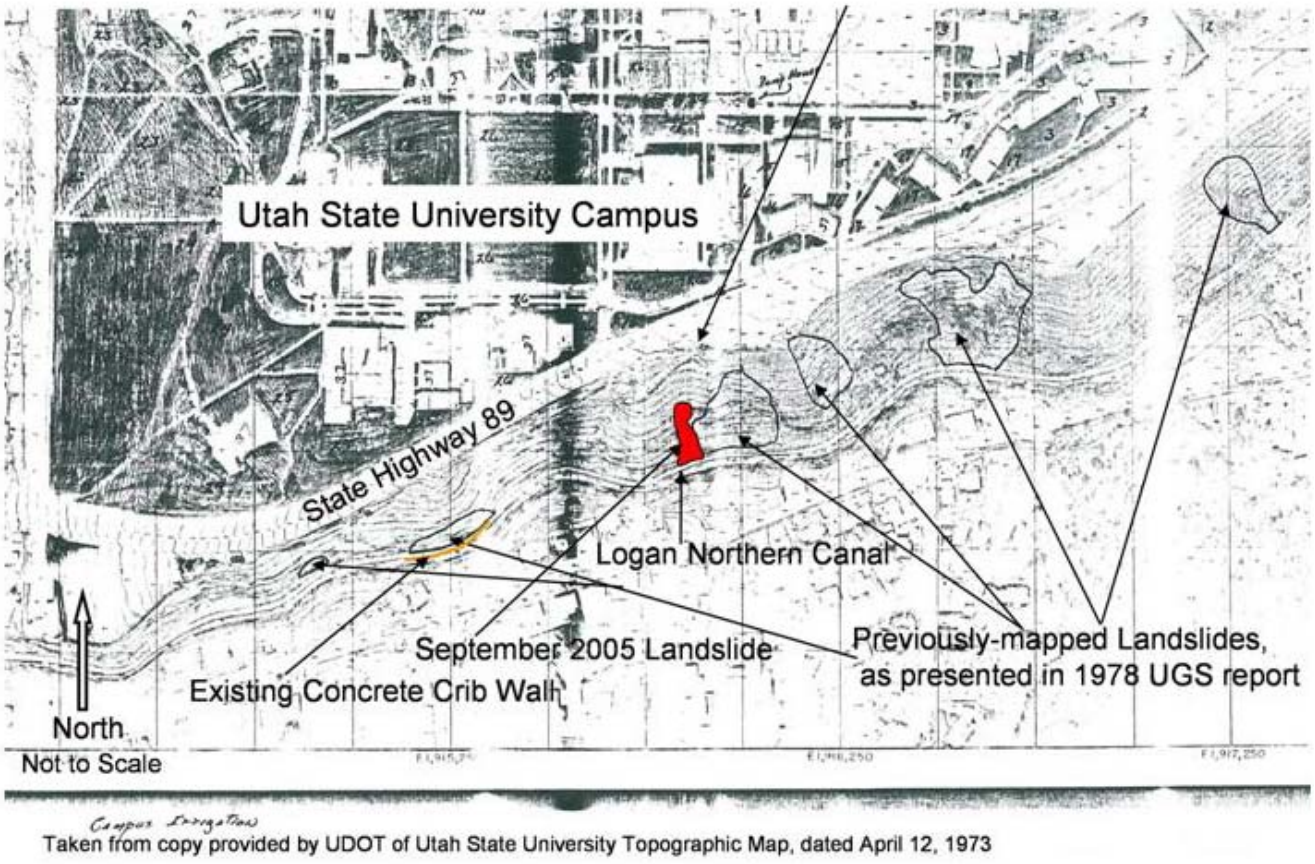

Figure 1: Landslide Area Location Map

Approximately 35 feet of the canal lining was destroyed during the landslide. Culverts were installed in the canal through this 35-foot section of the canal, and flow in the canal was restored on September 23. While the slide scarp continued to ravel and slough, another significant movement of the landslide, sufficient to again fill the north side of the canal and partially plug the culverts, occurred early September 26 or the previous night. Canal flows were then suspended for the rest of the season.

The site area has a history of landslide activity. The primary resource for this history identified at the time of our study is the Utah Geological and Mineral Survey (now UGS) Report of Investigation No. 123, completed in 1978 by Robert Klauk and Bruce Kaliser. The 1978 work describes three previous landslides, documented in the fall seasons of 1976 and 1977, and the spring of 1978. Based on the map included in the 1978 report, and our field observations, it appears that the current landslide has occurred, either partially or entirely, in an area that was previously subject to landslide movements. In addition, there is geomorphic evidence of older slope failures at other locations along the bluff. Aerial photography from 1937 shows numerous landslide features (UGS, 1978).

Previously observed landslides, including the 2005 slide, appear to affect only the slopes above the canal. The 1978 report opines that the "real cause" of the slides is the construction of the canal, and the consequent over-steepening of the slope.

A "brief background and history" of conditions along the bluff was provided with a letter from Utah State University, dated June 15, 1978. This document described that, although seepage has historically been observed in the bluff, "(a)s the areas on the bench above the bluff have developed, the amount of water showing up on the hillside has increased. This development includes the University, residences, some commercial establishments, and a golf course." This supports the hypothesis that increased irrigation associated with development has increased

groundwater seepage along the bluff. Seepage from the slopes above the canal is perennial, based on historical reports, vegetation observed on the lower bluff slopes, and our observations of seepage flows along the bluff during the fall, winter, and spring of 2005/2005.

The property containing the 2005 landslide, and much of the Logan Bluff slope below Highway 89, was previously owned by USU, but was deeded to UDOT in a state-mandated land transfer. At the time of this transfer, slope stability problems on Logan Bluff were known and UDOT protested the land transfer.

INITIAL RESPONSE ON THE 2005 LANDSLIDE

When the initial failure occurred the night of September 9/10, UDOT personnel arrived at the site by 8 AM the next morning. The initial impression expressed among UDOT, USU, the canal company, and Logan City personnel was that the slide was triggered by a broken culinary or irrigation water line (Thurgood, 2005). Crews began clearing mud and debris from the canal on September 20. On the night of September 25/26 the slide moved again, refilling the canal and enlarging the slide scar. Figures 2 and 3 show the slide configuration before and after the second movement (September 26). On September 26, UDOT, the Logan City Emergency Services Coordinator, and the Red Cross coordinated to evacuate the homeowners and renters (living in the basement) of the residence. UDOT confirmed that there was no immediate threat to the parking area above the slide.

Figure 2: The slide configuration before the second movement (September 26).

Figure 3: The slide configuration after the second movement (September 26).

At the time of the slide's occurrence and initial response, both the City of Logan and USU were involved in discussions regarding possible causes for the slide and appropriate responses. The City and USU agreed to check their respective water lines for possible leaks that could have trigger the slide. No leaks were detected/reported, although in the days prior to the slide, a water line break had occurred within the USU campus.

Golder Associates was engaged by UDOT under an emergency contract to give preliminary opinions on the likely causes of the failure and potential options for repairs. Golder visited the site on September 29, and by October 7 provided a report to UDOT which presented a preliminary opinion on the then-current stability condition of the slide, recommendations for immediate actions, and preliminary options for mitigation. Recommendations were also provided for identifying the sources of excess groundwater, although these measures primary included monitoring which would not bear fruit in time to support design of the emergency repair of the current slide area.

This initial report was followed by more complete document issued on October 21, which presented options for emergency mitigation of the landslide, with alternative measures, relative cost comparisons, and recommendations for a site investigation to support the emergency design.

CONTEXT OF THE EMERGENCY MITIGATION DESIGN

The design for repair of the failed area was undertaken as an emergency response action, to be implemented quickly, to allow reoccupation of the residence, restoration of flows to the canal, and preservation of the parking lot facilities. Thus, the work focused on addressing the immediate area of the 2005 slide, to restore that portion of the slope to a condition of greater stability than the existing failed slope, under the constraints of the site.

No UDOT facilities were immediately threatened, although there was concern that further failure could eventually threaten Highway 89. The entities immediately threatened by the failure were:

- The residents of the house below the slide;
- The Logan Northern Canal company and its users;
- USU, due to the threat to the parking facility located above the slide.

Each of these entities had specific requirements or requests which were addressed by UDOT in repairing the landslide. These requirements constrained the design of the repair in some very significant ways.

1. Minimizing disturbance to the residential property below the slide limited the potential for slope flattening to increase stability;
2. Restoration of the canal was needed to provide water by April 2006 irrigation season. Options to pipe canal flows through the slide area were examined, but it was preferred to restore the canal to its previous configuration. This limited the time available for construction, and restricted slope geometry for repairs;
3. The owner of the residence had been using seepage emerging from the pre-slide slope to irrigate their property. Capture of seepage flows from the slide area to provide irrigation to the residence restricted the level of subdrains to lower groundwater pressures in the repaired slope; and
4. Avoiding or minimizing disturbance of the existing parking lot above the slide area, as requested by USU eliminated the potential for slope flattening to increase stability above the slide. Although the parking area is on UDOT ROW, UDOT chose to accommodate USU's concern to preserve the parking area to the extent possible.

UDOT asked the Utah State legislature for emergency funding to assist in covering the cost of the slope repair. Also, in early meetings with UDOT, the City had promised to assist with funding for the slope repairs. However, no funding was actually obtained from the City, partial funding was provided by the legislature, and UDOT was required to pay for a significant amount cost of the repairs.

DESIGN PROCESS

The October 21 report to UDOT included a range of conceptual alternatives for mitigation. The alternatives each included re-grading of the slide area, but some alternatives combined with additional strategies such as dewatering with wells or horizontal drains, or use of mechanically stabilized earth (MSE) or soldier pile retaining walls. The October 21 report included a qualitative comparison of the various strategies and options, including estimated relative costs, effectiveness and performance expectations, and time to construct (Table 1). The report went on to provide a comparison of the effectiveness of several alternative plans developed from these strategies, in terms of their expected effectiveness in the additional criteria of reducing risk to the residence, preserving the parking lot, and restoring canal flows (Table 2).

UDOT selected the alternative which consisted of re-grading of the slope with compacted fill, without the use of MSE or other specialized measures. This alternative was estimated to have the lowest relative cost, but also successfully met the most comparison criteria. The design included cut and fill re-contouring of the failed area, subsurface drainage within the slide footprint, and reconstruction of the damaged portion of the Logan Northern Canal. Figure 4, taken from the construction plans, presents the configuration of the proposed mitigation. The design cross-section was developed by calculating stability to obtain a configuration that would:

- Allow an open canal section of essentially the same configuration as the pre-slide condition;
- Maximize stability in the toe area of the slide, without adding destabilizing loads to the lower portion of the slope below the canal;

- Allow placement of subdrains below the stabilizing fill, but maintaining a minimum elevation that would allow gathering and delivery of seepage flows to the residence below; and
- Flatten the upper slope to a more stable configuration, while minimizing disturbance of the parking lot.

In order to maintain a minimum stable slope angle in the upper slope, it was necessary to modify the corner of the parking area, removing two parking spaces.

The proposed configuration was shown to increase stability as compared to both the existing condition, and the estimated pre-slide configuration. However, resulting calculated factors of safety were on the order of 1.2; less than a value typically accepted in new construction. However, these estimates are based on relatively conservative assumptions. There are many cases, particularly in emergency situations, where mitigation must be designed to attain an achievable increase in stability, but may not meet "standard criteria".

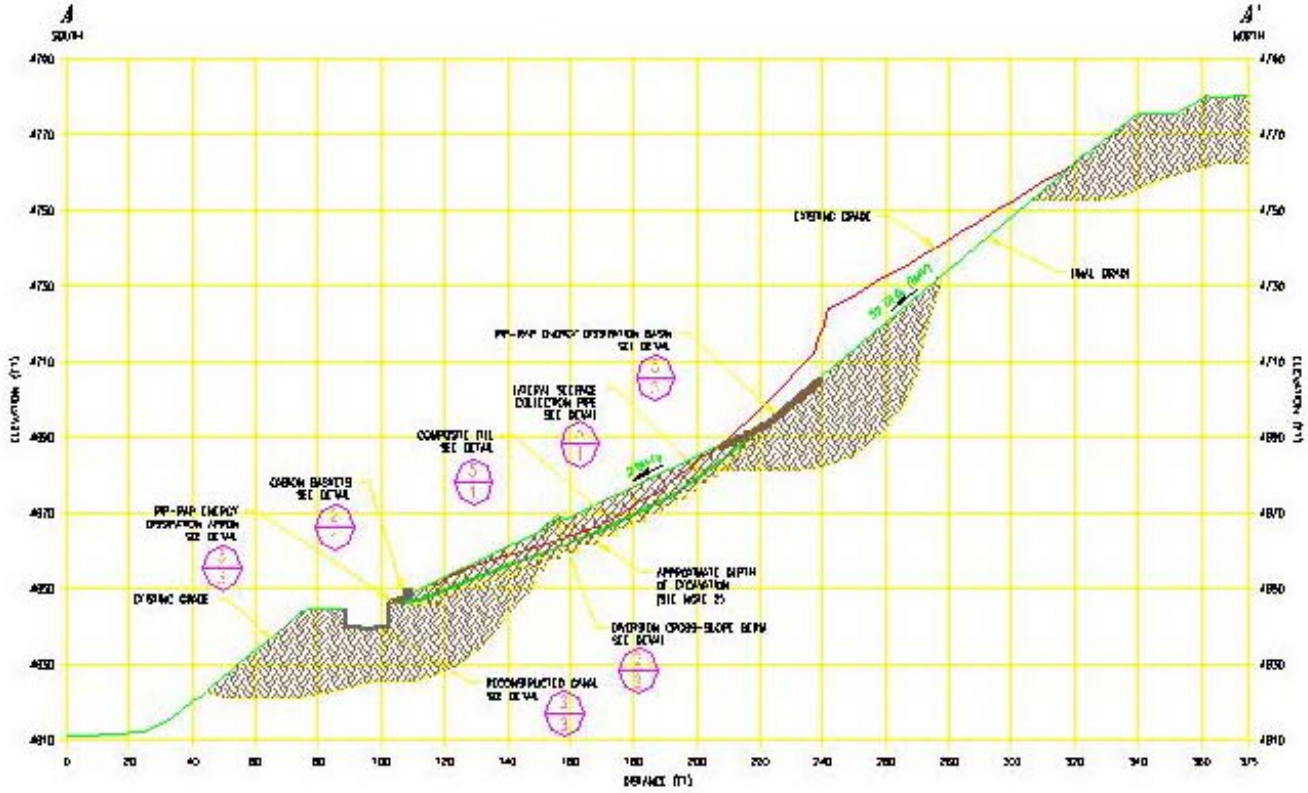

Figure 4: Configuration of the Proposed Mitigation

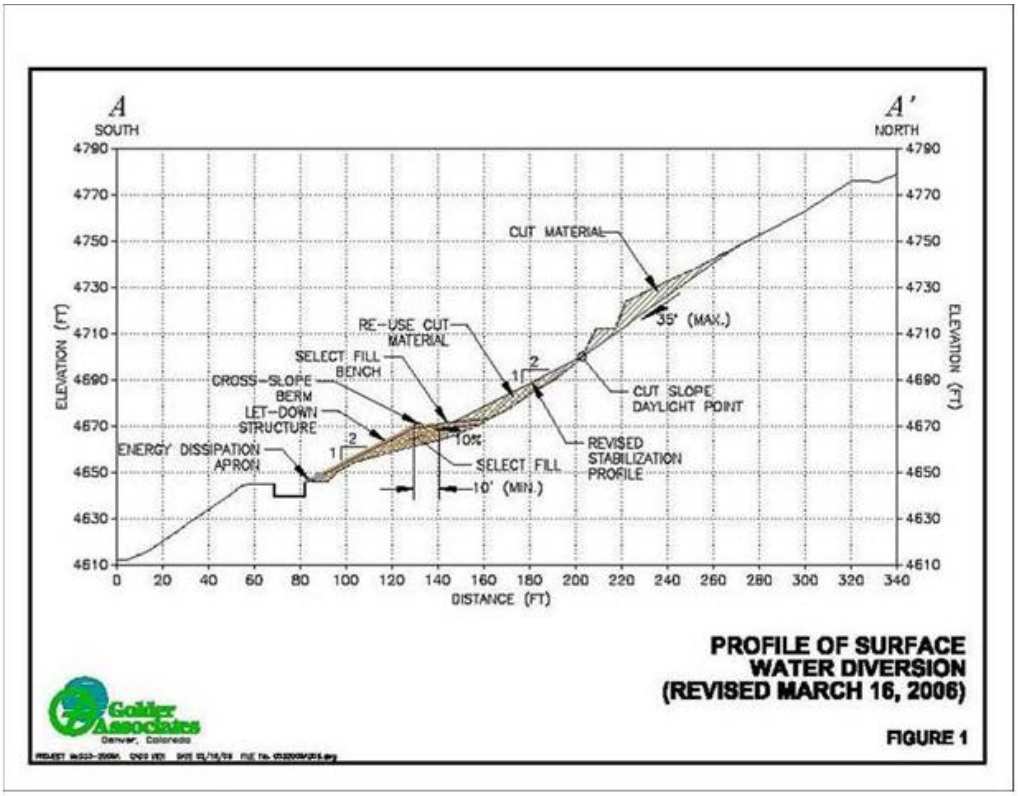

Figure 5: Revised Design

Because of the geometric constraints for the stabilization fill, the design was required to rely on assumed, relatively high strengths for the fill materials. Rather than using readily available, local "pit run" granular materials, it was necessary to import the materials from other sources. Gravel materials in the immediate Logan are composed of rounded alluvial materials. The design specified crushed rock in order to obtain the greatest feasible shear strengths. This resulted in considerable additional costs for imported materials, but was considered a key factor in maximizing the increase in stability under challenging geometric constraints.

CONSTRUCTION

Construction efforts at the site began in early January 2006. Initial dewatering efforts appeared to have minimal effect. It was hoped that seasonal freezing would facilitate construction activities, but in fact continued high seepage from the slide area created "quick" conditions in the loose slide debris soils in the lower portion of the slope.

Open excavation, even to the planned relatively shallow depths of 3 to 4 feet was not working, as any excavation was immediately filled with flowing mud from adjacent areas. The problem was solved by the relatively tedious method of placing a trench box in the slide mass, excavating the loose, wet materials inside, and replacing with compacted granular fill. In many cases the trench box sank or was simply pushed into the soft subgrade. This method was used in "patchwork" over the entire toe area.

Although the method used to excavate and provide stable fill in the lower portion of the slide was a greater effort than expected, it did have significant benefits. Since the toe area below the proposed fill had been excavated to a greater depth, and replaced with competent fill, the toe of the stabilized area was much stronger than was assumed in the initial design. By incorporating assumptions with regard to the changed size and strength of the toe area, Golder was able to reconsider the design of the proposed stabilization fill. This resulted in a revised design (Figure 5), with a steeper lower fill face to add additional stabilizing mass at the toe. This reconfiguration also allowed relocation of the cut in the upper portion of the slope such that it was not necessary to disturb the parking lot. This was managed without increasing the volume of fill required to be imported.

During construction an unexpected geologic constraint came to light that also drove the design of the reconfigured fill section. At the time of initial investigation, the contact between the Bonneville sediments and the overlying gravels was estimated based on the contact location found in the borehole above the slide area, near the parking lot. Since the dip of this contact was estimated to be toward the south west, the inferred elevation of the contact where it would daylight in the designed slope cut was conservatively assumed to be no higher than the elevation indicated by the upper boring. However, as construction proceeded and detailed site surveying was performed, the contact was found to be at a significantly higher elevation than assumed in the initial design. If this contact were to daylight in the cut slope, above the fill, the upper slope would be subject to slaking and erosion from seepage and consequent instability. This situation was remedied in the design by applying a wedge of fill, composed of the sands and gravels excavated from the upper unit, to act as a stabilizing fill to the portion of the slope and as a "weighted filter" for potential seepage.

PROJECT COMPLETION

Construction of the landslide repair was successfully completed in April 2006. The canal is restored and prepared for the 2006 irrigation season. Seepage from the subdrain system is being captured for residential irrigation.

The design and construction of the 2005 slope repair were performed under "emergency conditions". A complete assessment of the causes and long-term expectations for landslides at this location and throughout the bluff are was not included in the scope of this work. There are many questions yet to be answered regarding risk for similar failures in the future.

Unlike most landslide environments, groundwater levels and seepage did not appear to significantly abate over the winter season. Hydraulic conditions along Logan Buff are such that, based on 2006 observations, flows appear to be maintained at relatively constant levels year round. It would be unusual that such conditions would be naturally-occurring. It seems very likely than man-induced conditions, whether through irrigation, storm water handling, or leaking water infrastructure, play a role in the conditions at Logan Bluff.

A close and cooperative relationship between owner, designer, and construction contractor is essential to the successful execution of an "emergency" project such as this, where difficult, unexpected conditions are encountered, and design decisions and changes must be made quickly. As conditions change in the field from initial design assumptions, the project designer should continue to re-evaluate the effects of these changes on the proposed design, looking to mitigate unforeseen problems and to take advantage of unforeseen improvements to maximize the benefits of the final product.

THE FUTURE OF LOGAN BLUFF

The studies related to the emergency design of the repairs for the 2005 Logan Bluff landslide clearly pointed out that the current repair only addressed mitigation at the specific area of the 2005 failure, and that other portions of the bluff were at risk for similar failures. Although the legislature did not provide partial funding for the actual emergency slope repair, they did grant significant funds to USU to perform a risk study for future potential landslides along Logan Bluff. UDOT has essentially no control over the process of this study or its findings, but presumably will be called to the table to address mitigation needs which may be identified by the study.

CONCLUSION

When the 2005 Logan Bluff landslide occurred, UDOT took the initiative in first-response activities to address the hazard, and acted appropriately and without hesitation to protect public safety. As the repair design was developed, UDOT accommodated the various interests of stakeholders, to restore and protect facilities to pre-slide conditions. However, there are questions of "shared responsibility" for this and future failures, where contributors to irrigation, operating the canal, and capture and use of seepage flows could be contributing to potential stability problems. During the course of the emergency design study, a number of potential contributory factors came to light, such as the university's use of dry wells in the alluvium to dispose of surface runoff, an unlined canal upgradient of the site which is reported to have high leakage, and irrigation by USU and private landowners upgradient of the bluff.

When the next failure occurs, and there is every reason to believe one will unless preventative measures are taken, how should UDOT respond?

What options will UDOT have if the USU study identifies that extensive, expensive measures are indicated on UDOT ROW to mitigate for potential future failures?

What avenues does UDOT have to bring "contributing entities" or other stakeholders to the table to deal with future hazards?

REFERENCES

Evans, James P., McCalpin, James P., and David C. Holmes. 1996. Geologic Map of the Logan 7.5' Quadrangle, Cache County, Utah. Utah Geological Survey. Miscellaneous Publication 96-1, 1996.

Klauk, Robert H. and Bruce N. Kaliser. 1978. Report of Investigation No. 123, Utah Geological and Mineral Survey, Slope Stability Evaluation of the Logan River Bluff below Utah State University, Logan, Utah. Utah Geological Survey. May 1978.

Nussbaum, L. Scott. 2005. Notes regarding Island Slide. Utah Department of Transportation. September 29, 2005.

Thurgood, Norton. 2005. Notes regarding Logan 400 North Landslide. Utah Department of Transportation. September 29, 2005.

Utah Geological Survey. 1979. Untitled package of borehole drilling information, on Utah State University property, from UGS files. Utah Geological and Mineral Survey. February 26, 1979.

TABLE 1

COMPARISON MATRIX OF LANDSLIDE MITIGATION MEASURES

Mitigation Component	Expected Effectiveness	Expected Long-term Performance Reliability	Estimated Maintenance Required	Time Frame of Construction
Groundwater	High	High	Low	Short
	Moderate	Moderate	Moderate	Moderate
	High	High	High	Moderate
Stabilization of Existing Landslide	TBD (see Note)	Moderate	Low	Short to Moderate
	TBD (see Note)	High	Low	Short to Moderate
	TBD (see Note)	High	Low	Moderate
	TBD (see Note)	High	Low	Moderate
Stabilization of Existing Scarp	Moderate	Moderate	Low	Short
	High	High	Low to Moderate	Moderate
	Low	Low	Moderate to High	NA
Restoration of Canal	High	High	Low	Short
	High	Moderate	Moderate	Short
Revegetation	Moderate	Moderate	Moderate to High	Short
	High	High	Low to Moderate	Short
	High	High	Low to Moderate	Short

TABLE 2

COMPARISON MATRIX OF ALTERNATIVE MITIGATION PLANS

Alternative Plan	Expected Effectiveness to Restore Canal Flows	Expected Effectiveness to Preserve Parking Lot/Highway	Expected Effectiveness to Minimize Risk to Residential Areas	Expected Long-term Performance Reliability	Estimated Maintenance Required	Time Frame of Construction
1: Cut and Fill	High	Low	TBD	High	Low	Short
1A: Cut and Fill with Sub-horizontal Drains	High	Low	TBD	Moderate	Moderate	Short
2: Compacted Earth Slope	High	Moderate	TBD	High	Low	Short
2A: Compacted Earth Slope with Scarp Retaining Wall	High	High	TBD	High	Moderate	Moderate
3: MSE Wall above Canal	High	Moderate	TBD	High	Low	Moderate
3A: MSE Wall above Canal with Scarp Retaining Wall	High	High	TBD	High	Low to Moderate	Moderate to Long
4: MSE Walls over Canal	High	Moderate	TBD	High	Low	Moderate
4A: MSE Walls over Canal with Scarp Retaining Wall	High	High	TBD	High	Low to Moderate	Moderate to Long

Non-Structure Alternatives for Incidental Slopes

Donald V. Gaffney

Michael Baker Jr., Inc.
4301 Dutch Ridge Road
Beaver, PA 15009
(724)495-4254
dgaffney@mbakercorp.com

Ryan S. Tinsley

Michael Baker Jr., Inc.
4301 Dutch Ridge Road
Beaver, PA 15009
(724)495-4175
rtinsley@mbakercorp.com

ABSTRACT

Often small, overlooked or unforeseen aspects of large projects impact schedules, costs, design, and construction. For example, stable slopes may be designed for excavations and embankments relatively early in the highway design process. Then, during finalization of design, small problem areas are discovered where those slopes won't fit due to site constraints or project conflicts. We call these 'incidental slopes' because their design is a consequence of these constraints and conflicts.

Traditionally, a short wall has been a good answer to the problem of incidental slopes. However, use of a structure carries with it a host of other problems. Besides the additional construction cost, there are policies and procedures that must be met during design of construction items identified as structures. Consequently, adding a structure to a project late in the design phase (or during construction) can be a project manager's nemesis.

In the search for alternatives, engineering geologists and geotechnical engineers are often asked to provide non-structure solutions. Some of these non-structure alternatives include reinforced soil slopes, grouted and ungrouted rock fills, gabions, concrete barriers, and recycled materials used to steepen or retain incidental slopes.

This paper takes a look at non-structure alternatives used to handle incidental slopes on highways throughout Pennsylvania over the past 20 years, including common applications of alternatives, various construction specifications and details, case histories of installations on numerous projects, and lessons learned from their use.

TECHNICAL SESSION II
Landslide/Slope Stability, continued

Recipe for Trouble: Just Add Water

Eugene W. Vaskov, P.G.
Allegheny County Department of Public Works
501 County Office Building
542 Forbes Avenue
Pittsburgh, PA 15219-2904
412-350-5585
gvaskov@county.allegheny.pa.us

Christopher A. Ruppen, P.G.
Michael Baker Jr., Inc.
Box 280
4301 Dutch Ridge Road
Beaver, PA 15009-0280
724-495-4079
cruppen@mbakercorp.com

ABSTRACT

The mention of hurricanes and tropical storms create pictures in our minds of the destruction caused in coastal areas from storms such as Katrina. However, as these storms move north, they often slow down and drop record rainfall in inland areas. Two recent remnant hurricanes/tropical storms had a major impact on the infrastructure of Western Pennsylvania.

Tropical Depressions Francis and Ivan swept through the greater Pittsburgh, Pennsylvania, metropolitan area in September 2004, packing a very potent and destructive one-two punch. Francis, which came through on September 8th, set a single-day precipitation record of 3.6 inches. Nine days later on September 17th, Ivan followed and broke that record with over 5.9 inches of rain in a 24-hour period.

In addition to damage to numerous private homes and businesses, 443 roads and 77 bridges were damaged. oadways were undercut and numerous old retaining walls were impacted,with many failing completely. stormwater scour and landslides triggered in saturated soil were also major problems. As part of emergency response efforts, teams of professional engineers and geologists provided direction for rapid repair of these damaged but vital transportation links. To accomplish this repair the Allegheny County Department of Public Works took a unique approach to procuring contractors which enabled reconstruction to begin almost immediately. The diverse nature of the damage and the remedial action taken provide insight into the geotechnical aspect of the emergency response that was required. Typical situations and solutions illustrate geotechnical emergency response. Suggestions are made to enhance future preparedness.

BRIEF HISTORY OF TROPICAL STORM AND LANDSLIDE OCCURRENCE IN WESTERN PENNSYLVANIA

The events that impacted western Pennsylvania centered on the September 2004 storms and were not isolated one-time events. In fact, there is significant historical data on hurricanes which have impacted the Ohio River Valley. Heavy storm precipitation in western Pennsylvania can be derived from decaying stages of extratropical cyclonic storms entering the Ohio River Basin. Although such storms generally have lost hurricane wind velocities by the time they have entered the Ohio River Basin, they bring with them or cause heavy rain[(1)].

Rainfall is considered excessive when it falls at the rate of 0.25 inch in 5 minutes, 1 inch in 1 hour, or 2.5 inches in 24 hours[2]. FIGURE 1[1] displays the relative tracks of extratropical storms entering the Ohio River Basin for the 100 year interval between 1871 and 1972. Additional hurricane events have occurred since 1972, and this paper will focus on two such events, Hurricanes Francis and Ivan.

FIGURE 1

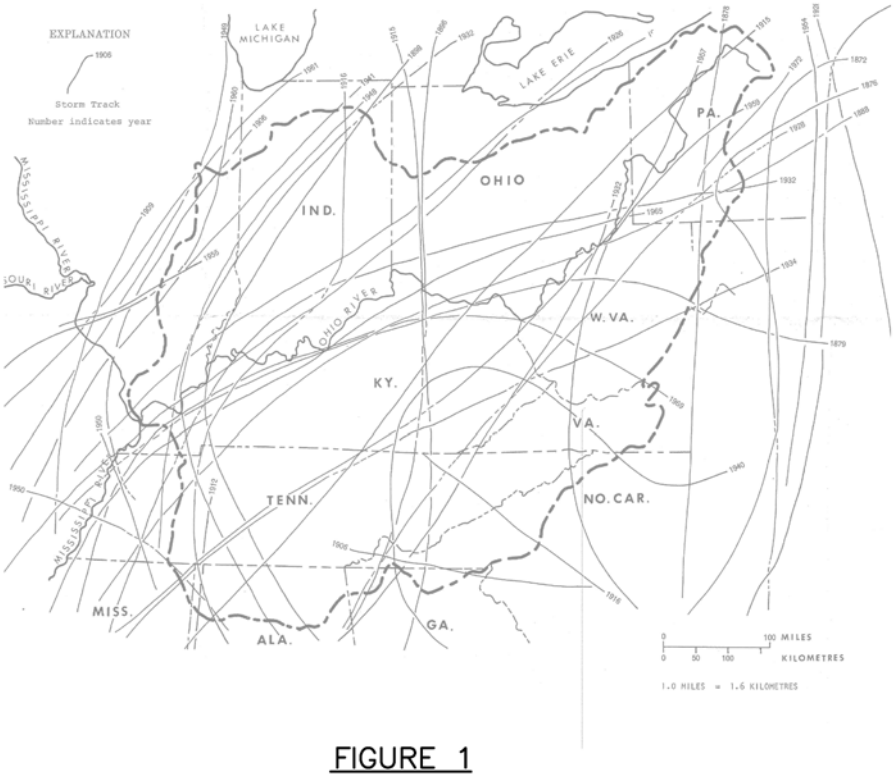

FIGURE 1
TRACKS OF EXTRA TROPICAL STORMS
ENTERING THE OHIO RIVER BASIN, 1871–1972)
(ADOPTED FROM RELYEA, 1969)

TABLE 1 depicts hurricanes which impacted the western Pennsylvania region during the 1871 to 1972 time period and the rainfall amounts recorded.

TABLE 1

DATE	RAINFALL (in.)	DATE		RAINFALL (in.)
1872, October	2.63	1928, September		.88
1876, September	4.89	1932, September		.07
1878, September	4.48	1934, June		1.56
1879, August	3.88	1940, August		.09
1879, September	.07	1941, September		0
1880, September	.06	1948, September		.17
1888, August	6.21	1949, August		.76
1893, October	1.39	1949, October		.82
1896, July	2.02	1950, August		1.14
1898, October	.17	1950, September		.14
1906, September	2.54	1954, October	(Hazel)	3.69
1909, September	.34	1955, August	(Connie)	4.22
1912, September	.20	1957, June	(Audrey)	1.07
01915, August	.30	1959, September	(Gracie)	1.68
1915, September	.09	1961, September	(Carla)	.04
1915, October	1.50	1965, September	(Betsey)	.18
1915, July	1.57	1969, August	(Camille)	1.80
1916, October	2.25	1972, June	(Agnes)	4.20
1926, July/August	.01			
1928, August	.27			

[(1)] Source: Adapted from Relyea – Precipitation Data from National Weather Source

The peak season for these storms in Western Pennsylvania is June to October. Although not all of the storms have a significant or even noticeable impact, it is important to note that based on historical data these events should be anticipated and response mechanisms should be in place to deal with the aftermath.

HURRICANES FRANCIS AND IVAN
Chronology and Meteorological Data

The meteorological history preceding the Hurricane Ivan event played an important part in the magnitude of the storm's impact. As portrayed in the time series plot in FIGURE 2[(3)] below, Western Pennsylvania has averaged approximately 42 inches of rain per year for the period between 1950 and 2000. This is consistent with historical data for the Northeast United States where an average of 41.08 inches of rain per year has been recorded between 1901 and 2000[(1)] (by NOAA).

FIGURE 2

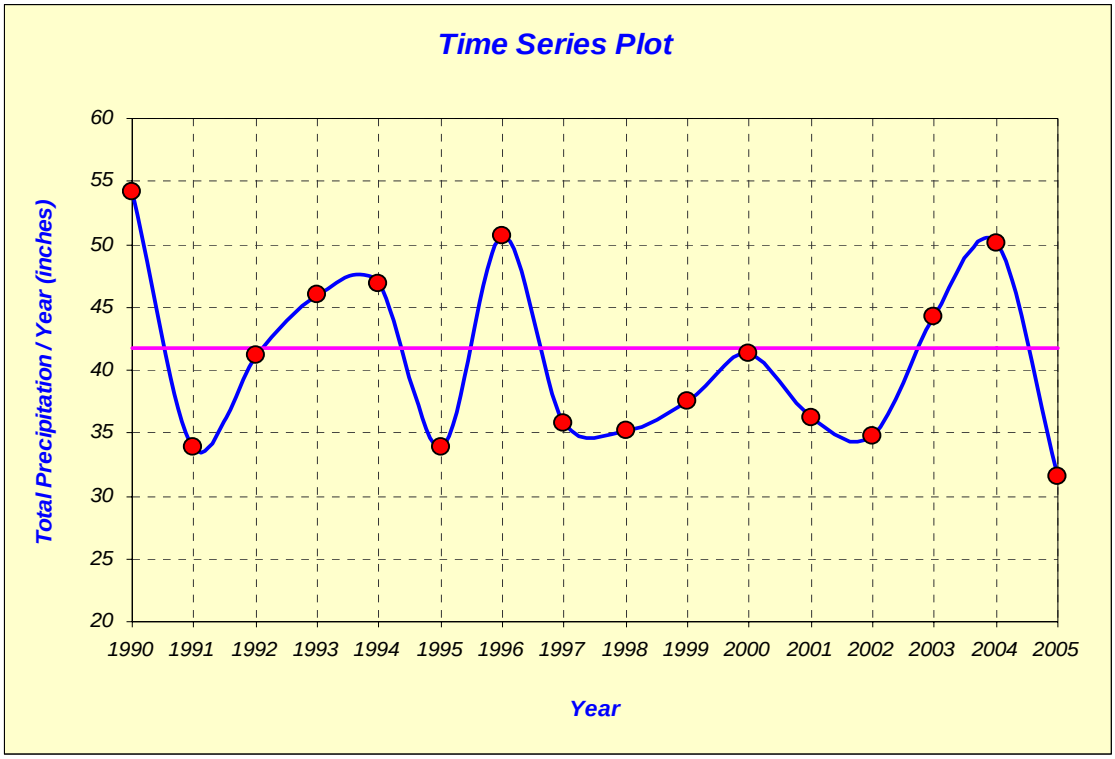

[(3)]Data used from "Pennsylvania State Climatologist" http://www.climate.psu.edu/

In the time period immediately preceding September 2004, the region had essentially experienced a drought in 2002, followed by two years (2003 and 2004) of above average precipitation. This is displayed in FIGURE 3 on the following page.

FIGURE 3

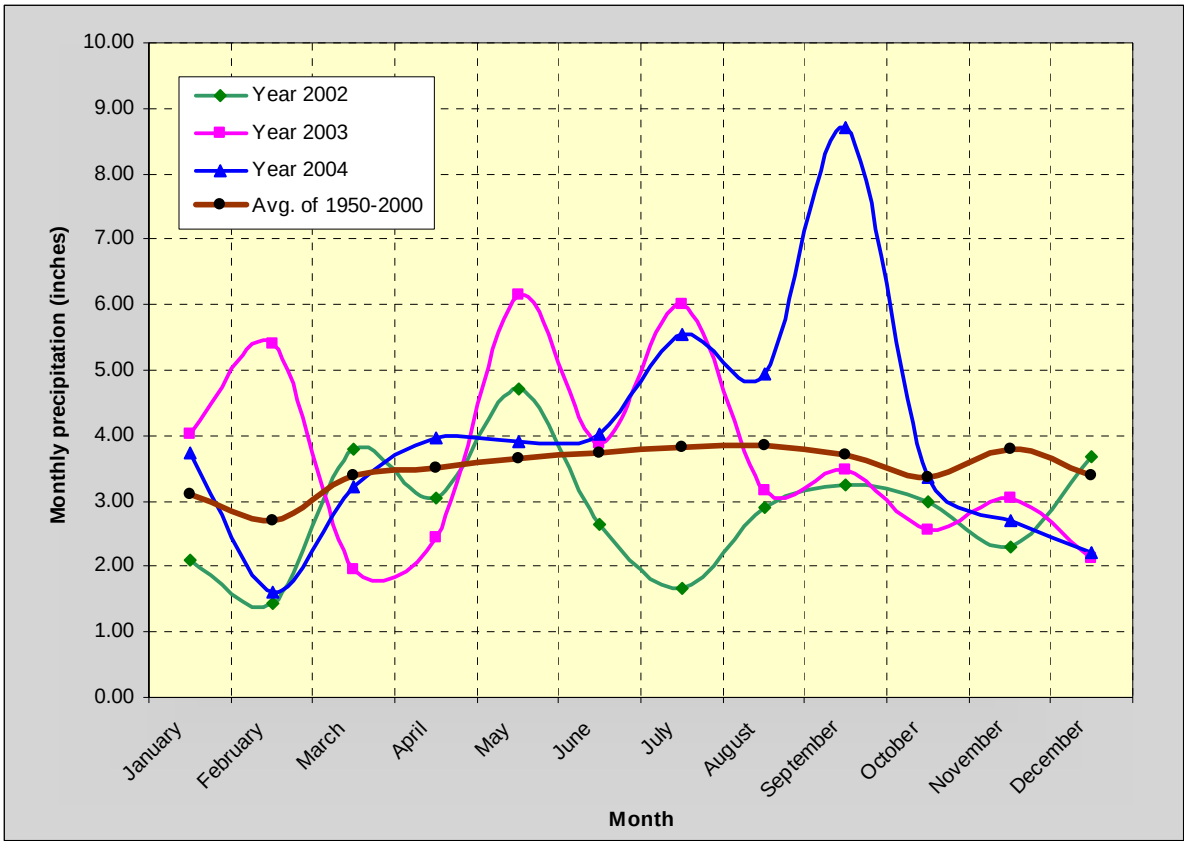

[4]Source:
Average of 1950 to 2000 (Regional Precipitation data of Northeast USA) taken from: Publication of the National Oceanic & Atmospheric Administration (NOAA), http://www.noaa.gov/ [4]. Total precipitation data for year 2002 through 2004, taken from: Data archive of the Pennsylvania State Climatologist, http://www.climate.psu.edu/ [3].

This above average precipitation in 2003 and 2004 played an important role in the activities that followed in September 2004. Due to the above average precipitation, groundwater tables were elevated, soils were nearly saturated and there was little ability for the soils to handle the nearly 10 inches of rain that fell during the 10 day period of September 8 to 17, 2006. Soils became oversaturated, soil strength was lost and many failures occurred.

Allegheny County

Allegheny County, located in southwestern Pennsylvania, has a total area of 745 square miles and a total population of 1,282,000 as of the 2000 census. The County is comprised of 130 individual municipalities (more than any other county in the United States), each with its own governmental structure. The largest municipality is the City of Pittsburgh (56 square miles, population 335,000) and the smallest is Pennsbury Village (0.08 square miles, population 741). (See FIGURE 4).

FIGURE 4

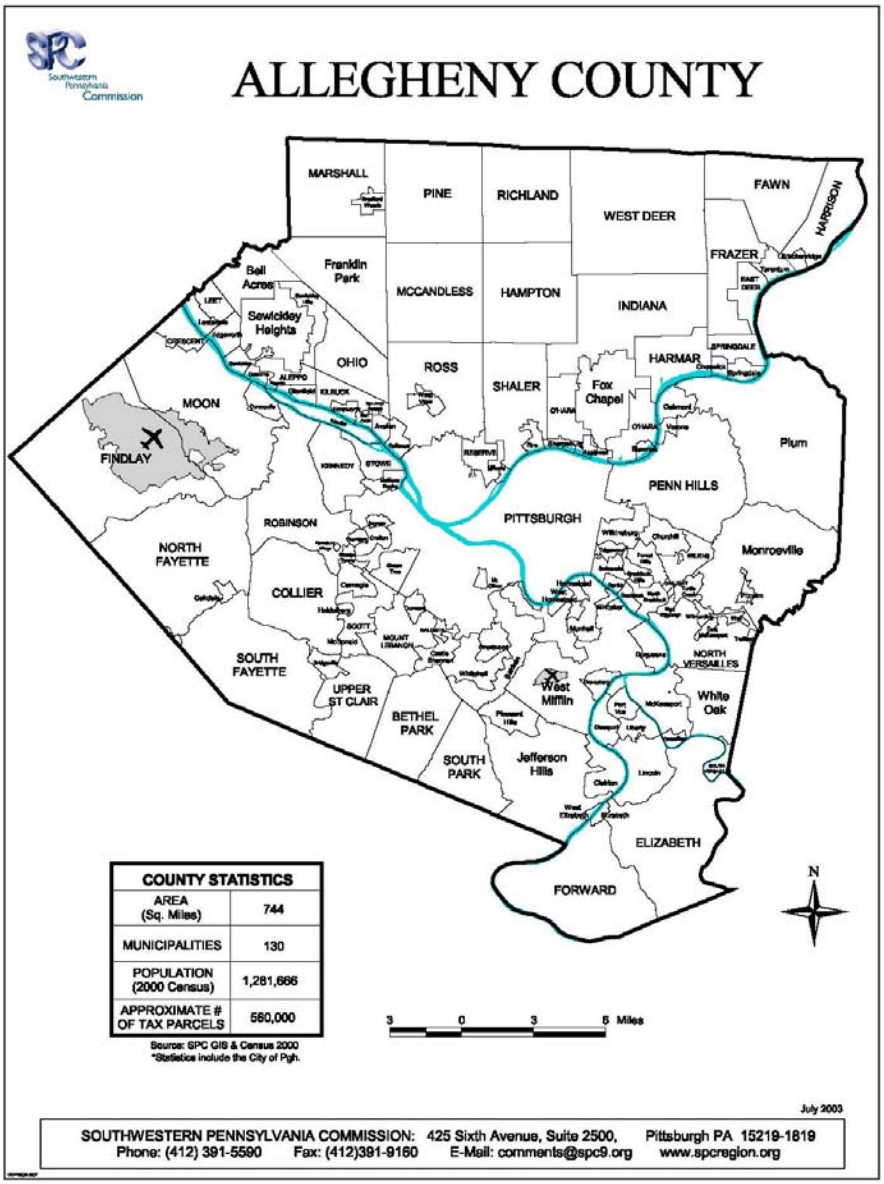

Allegheny County lies within the Appalachian Plateaus Province (see FIGURE 5[5]). The highest elevation is at 1,400 feet above MSL and the lowest is at 680 feet above MSL. The general topography is rolling hills with deep, narrow stream-cut valleys.

FIGURE 5

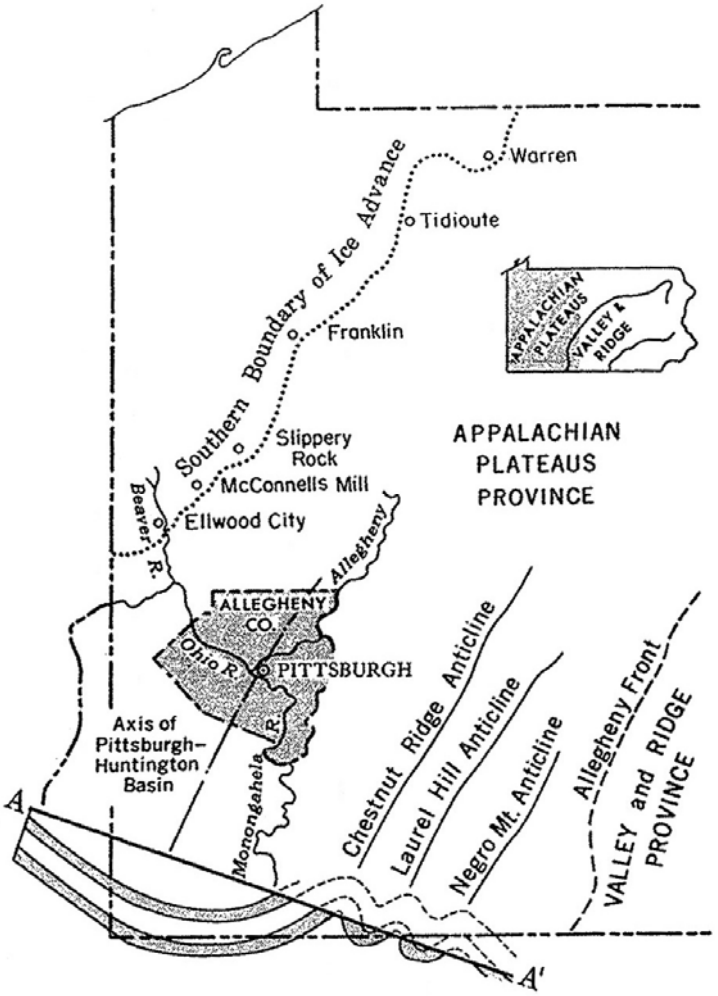

Figure 5. Geologic Setting of Western Pennsylvania

Geology of the Pittsburgh Area, 1970

Since January 1, 2000 Allegheny County has been governed by a Home Rule Charter with an elected Chief Executive Officer, a 15-member Council and an appointed County Manager. The Department of Public Works is responsible for the maintenance of 800 lane miles of roads, 500 bridges and 12,000 acres of parks.

Emergency Operations Center

In preparation for the potential Y2K problems, the County created an Emergency Operations Center (EOC). The EOC, which serves 13 Counties in southwestern Pennsylvania, is a centralized location, equipped with state of the art communication equipment, for all agencies involved in response to an emergency situation. There are individual stations for the County Executive, the Emergency Services Department (Police, Fire, Hazardous Materials), Public Works, Federal Emergency Management Agency (FEMA), Pennsylvania Emergency Management Agency (PEMA) and others. (TABLE 2) These stations are located within one large room and are interconnected by computer to allow for fast and thorough sharing of information.

TABLE 2

Region 13 Emergency Operations Center

During an Emergency the EOC Coordinates the following Services and/or resources:

➢Public Health	➢Media
➢Public Works	➢Transit
➢State Resources PEMA	➢Federal Resources FEMA
➢Fire	➢Police
➢Coast Guard	➢DEP
➢Mental Health	➢Municipal
➢Counties	

5/31/2006 Allegheny County Public Works 7

Although, initial weather reports called for the storm to pass to the south of Allegheny County, rainfall began at 3:00 a.m. on Friday, September 17, 2004 with the rate increasing between 10:00 a.m. and 7:00 p.m., then becoming light and steady between 7:00 p.m. and midnight. The southernmost maintenance district reported flooding on one of the County roads at 2:00 p.m. and by 3:00 p.m. on the 17th . The remaining seven maintenance districts had reported at least some flooding. The EOC was notified of the flooding at 3:00 p.m. and the Center was fully activated at 3:30 p.m.

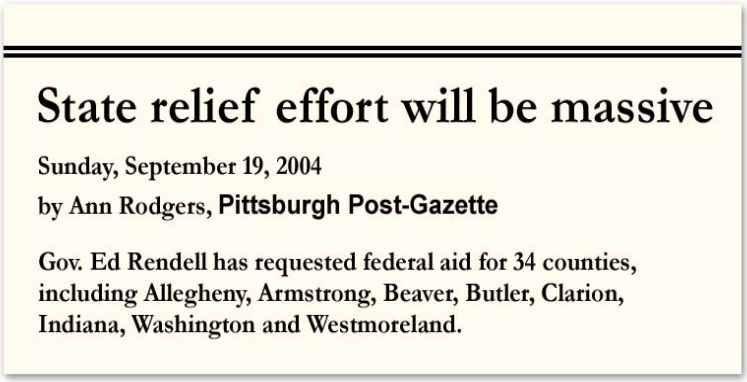

State relief effort will be massive

Sunday, September 19, 2004

by Ann Rodgers, Pittsburgh Post-Gazette

Gov. Ed Rendell has requested federal aid for 34 counties, including Allegheny, Armstrong, Beaver, Butler, Clarion, Indiana, Washington and Westmoreland.

Over the 24-hour period, 89 of the 130 municipalities sustained some degree of damage and 74 municipalities declared a State of Emergency. The extent of damages is indicated on TABLE 3.

TABLE 3

Extent of Damages

Units	*Structures and Infrastructure*
8,919	Single family homes
704	Multi family homes
77	Mobile homes
1,095	Businesses
42	Hospitals
4	Schools
51	Public Buildings
443	Roads
77	Bridges
9	Fire Departments

5/31/2006 Allegheny County Public Works 12

The Department of Public Works was charged with coordinating the equipment and labor needs to clear debris and make the roads and bridges passable. This effort required the cooperation of many government agencies, such as the Pennsylvania Turnpike Commission, the Allegheny County Airport Authority, and many of the municipalities that had not experienced extensive damage. These agencies were very generous in the donation of equipment and operators, despite internal restrictions and/or reservations regarding the use of these resources outside of the normal area of responsibility. A number of private contractors and consultants volunteered equipment and manpower for the initial response. This effort allowed for the immediate response to repair critical locations.

Geotechnical and Engineering Problems

Many of the County-owned roads are older, original road courses that parallel adjacent to the many small meandering streams that transect Allegheny County. Many of these roads are supported by walls constructed in the 1930's under the Works Program Administration (WPA). Common construction techniques during this era included field stone, cut stone and timber crib walls. Over time, these roads have been upgraded to current road and drainage
standards. This has been done by widening roadway widths, providing appropriate width shoulders and updating surface water drainage conveyance structures. As a result of the typical constraints of limited right-of-way, adjacent streets on one side and steep slopes on the other, the County maintains many old retaining structures and a plethora of marginally stable natural and embankment slopes. This is compounded by many culverts and bridges that switch streams from side to side to fit the roadway along the valleys. This combination places many of the county roads in a very precarious position. Regular storm events are easily conveyed and minimal stability issues are typically recorded. However, large rainfall events, especially when combined with the previously discussed meteorological data, can create stability issues for this older infrastructure.

The back-to-back storm events of September 2004 activated many stability, foundation or pipe failures. Many of these failures occurred along these roadways when elevated stream levels scoured and under-cut existing retaining walls, embankment slopes, old landslide prone slopes, bridge foundations and culvert pipe outfalls.

Allegheny County alone responded to 58 different failures impacting County-owned roads and infrastructure. The breakdown of the impacts is as follows:

Damaged or Failed Retaining Walls:	20
Failed Embankments:	25
Damaged Cross Pipes or Culverts	7
Roadway, Shoulder, Guiderail & Inlet Failures	6

Many more maintenance type issues and failures were also field viewed and prioritized. These included landslides, environmental concerns, clogged culverts and bridge openings and utility impacts.

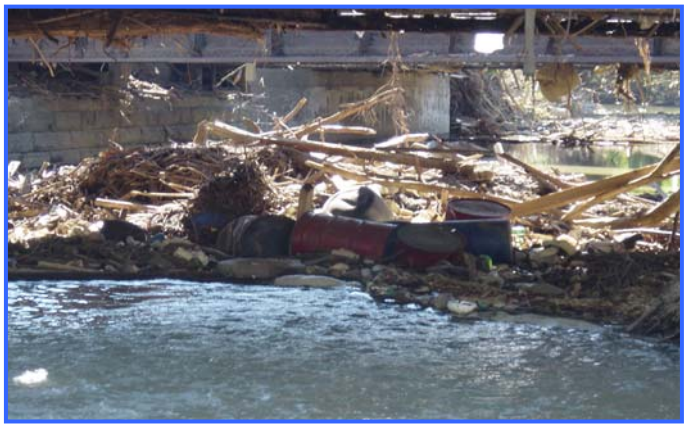

Additionally, County representatives provided assistance to residential and commercial landowners to help align the local, state and federal response assistance. This support of residents and commercial landowners proved to be a major benefit to lessen the blow of the storms and immediately improve the health and safety aspect of the impact.

Public Works Response for County Facilities

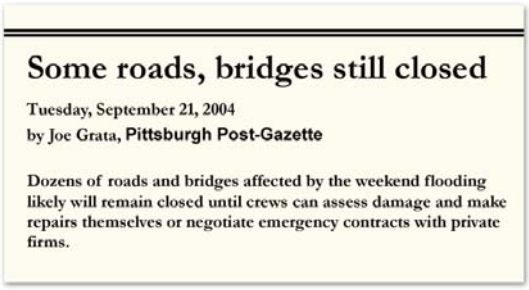

Some roads, bridges still closed

Tuesday, September 21, 2004
by Joe Grata, Pittsburgh Post-Gazette

Dozens of roads and bridges affected by the weekend flooding likely will remain closed until crews can assess damage and make repairs themselves or negotiate emergency contracts with private firms.

The County Executive declared a State of Emergency on Friday September 17, 2004. On Monday, September 20, 2004, after the general clean up was well underway, the Department of Public Works turned its attention to evaluating the damage to County-owned roads, bridges and other facilities. The professional staff was divided into teams of two, with each team assigned to make a field view of County-owned roads and bridges within a different section of the County. Once these field visits were completed and the extent of damage evaluated, a plan of action for each site that needed attention was developed. The plan of action included determining a probable "best fix" and identifying a competent and qualified contractor to perform the work. The contractors were selected from the list of those who had contacted the EOC and from contractors who had previously worked well with the Department. One aspect of the declaration of a State of Emergency was that the requirement to publicly advertise for bids to engage contractor services was rescinded. A field view was scheduled with each contractor and a design/build scope of work was developed. The contractors provided a proposal based on Force Account which includes negotiated prices for Materials, Labor and Equipment with predetermined overhead percentages along with an allowable overhead for subcontractors. This insures that the contractor is fairly compensated for work that could be extremely variable due to unknown factors. The owner must employ tight inspection procedures to avoid unnecessary costs. Once the final contract price was negotiated the contractor was given a Notice to Proceed on his own recognizance while the Contract was executed.

The County learned that the Federal Highway Administration (FHWA) would reimburse the County for the engineering, construction and inspection of the repair to roads that were on the federal highway system. All but one of the sites fell into this category. A field view with representatives from the FHWA was conducted to determine eligibility, verification that the damage was related to the Frances/Ivan event and the development of the amount of reimbursement.

The Pennsylvania Department of Environmental Protection was contacted to request emergency water obstruction permits for the work along and within streams. A verbal approval was obtained and the normal permit application process was followed subsequent to the work beginning.

CASE STUDIES

To expedite the construction, a number of "typical" construction solutions were employed to remediate the slopes and walls. Where possible, walls were eliminated and buttressed slopes were constructed. When walls were needed, precast jumbo block walls were typically used for wall heights less than 12 feet. If wall heights were over 12 feet or if a global stability issue existed, soldier pile and lagging walls were constructed. For landslides, the "remove and replace with a rock toe support embankment process" was the typical constructed solution. The case histories below exhibit a sampling of the typical failures and constructed solutions.

Nadine Road

This is an example of a slope failure caused by the September 2004 storm events. The failure impacted a private residence and utility service lines. The slope was stabilized by excavating the slide below the shear plane and reconstructing the slope with a rock toe and engineered buttressed slope.

Thoms Run Road

An existing "concrete jumbo block" retaining wall failed when the rising stream entered the wall backfill and pushed it over. The footing was reestablished and the wall units reset.

Anderson Road

A "concrete jumbo block" wall was overturned when an upstream storm sewer was overwhelmed and the water flowed down the roadway. In this case it was determined that the retaining wall could be eliminated and a buttressed rock slope was constructed to support the roadway and protect the roadway embankment from future scour.

Wible Run Road

A recent culvert reconstruction had included the installation of a soldier beam and lagging wingwall. A wooden cribwall extended along the stream beyond the limits of the wingwall. The wooden crib wall was destroyed by the flooding and was replaced with a soldier beam and precast concrete lagging wall using the design parameters of the adjacent wall.

Cochran Mill Road

An old 1930's vintage Works Program Administration cut sandstone wall was undercut by the adjacent stream and failed. This failure impacted Cochran Mill Road and threatened an adjacent sanitary sewer line and gasline. A precast jumbo block wall was constructed to buttress the slope and reopen the roadway.

Cliff Mine Road

During the flooding, a 90-degree turn in Cliff Mine Run directed the brunt of the stream force into the slope below Cliff Mine Road, undercutting the roadway and causing it to fail. Due to the slope height, a soldier pile and lagging wall was employed to support the road embankment and to reopen the road.

LESSONS LEARNED

Recipe for Trouble

Take: *Landslide prone soils*
Streams adjacent to roadways
Old retaining walls

Add: *An extended period of above-average precipitation*
A heaping dose of rainfall within a short period of Time.

Mix for short period of time and wait.

The resulting mix is guaranteed to provide disastrous conditions that will keep professional geologists and engineers extremely busy for a long time.

Our experience with the subject "Recipe for Disaster" has provided the following comments and reflections:

- Based on historical data and recent trends, the occurrence of severe storms capable of causing extensive damage is a matter of "When" not "If". Precipitation data should be monitored regularly, especially to track periods of above-average amounts, to serve as predictions for the potential for extensive damage.
- Policies and procedures should be developed for the sharing of services, personnel and equipment among government agencies during an emergency.
- Agreements of Understanding should be developed with regulatory agencies to allow for work to proceed without the delay of the normal permit acquisition process.
- Precast jumbo block walls up to a height of 12 feet performed very well if the wall was constructed on a footing. Blocks bearing on soil or soft rock were typically undercut and failed.
- Policies and procedures should be developed with Federal and State funding agencies to prevent delays in reimbursements.
- Internal policies and procedures regarding the procurement of services should be developed. What does the declaration of an emergency allow us to do?
- An expedited response can be achieved by maintaining a database of contractors and their qualifications.
- The elimination of the usual "red tape" allowed for the completion of an enormous amount of work to be performed within a short period of time. Approximately 50 projects were completed within three months, with the remainder being completed within months from the date of the storm event.

Although this recipe produced a concoction that was not "healthy" for a large number of private individuals, businesses and governments, the cooperation of numerous agencies, the application of a "common sense" approach to develop the repair strategies, and the ability to "do what we were educated and trained for" created a sense of accomplishment and satisfaction. The project teams' accomplishments were also noted by others in that the project was presented the Engineers' Society of Western Pennsylvania "Project of the Year Award".

ACKNOWLEDGEMENTS

The authors would like to thank the Allegheny County Department of Public Works and the Michael Baker Corporation for their support in the development of this paper. The information presented is factual and reflects the understanding of the authors and not necessarily that of the respective organizations.

REFERENCES

(1) Relyea, C.M., 1969, Hurricanes and the Ohio River: New York Academy of Sciences Trans., Ser. II, v.31, n. 1, p 42-55, January

(2) Blair, T.A., 1944, Weather Elements. Prentice Hall, Inc., New York, 404 p. (Revised Edition)

(3) Pennsylvania State Climatologist, http://www.climate.psu.edu

(4) Publication of the National Oceanic & Atmospheric Administration, http://www.noaa.gov/

(5) Wagner, W.R. et al, 1970, General Geology report G59, Geology of the Pittsburgh Area. Pennsylvania Geological Survey, Fourth Series, Harrisburg.

(6) Subitzky, S., 1976, M-G410: Heavy Storm Precipitation and Related Mass Movement: Greater Pittsburgh Region, Land and Water Studies for Environmental analysis. United States Department of the Interior Geological Survey.

SR 48 Landslide Repair

Joseph W. Schultz, PE,
District Geotechnical Engineer, District 11-0
Pennsylvania Department of Transportation
45 Thoms Run Road
Bridgeville, PA 15017
Office Phone 412.429.4923
josschultz@state.pa.us

Richard W. Schutte, PG,
Engineering Geologist, District 11-0
Pennsylvania Department of Transportation
45 Thoms Run Road
Bridgeville, PA 15017
Office Phone 412.429.4922
rischutte@state.pa.us

F. Barry Newman, PE
Geotechnical/Structural Group Manager
GAI Consultants, Inc. Pittsburgh Office
385 East Waterfront Drive
Homestead, PA 15120-5005
Office Phone: 412.476.2000 x 1300
b.newman@gaiconsultants.com

ABSTRACT

A landslide occurred in a side-hill highway embankment along the two-lane SR 48 east of Pittsburgh, PA. The landslide was about 100 feet long immediately adjacent to the road and threatened to progress into the highway. The total length of embankment having signs of instability was about 450 feet. An initial attempt was made to repair the slope by overexcavating a portion of the slide mass and replacing it with compacted backfill. The initial repair failed leading to a geotechnical exploration and analysis of the failure, and evaluation of more extensive options for repair. The explorations determined that embankment was underlain by relatively weak claystone-derived soils. The design of the repair was complicated by right-of-way constraints and the need to maintain traffic during the repair. This paper presents an overview of the problem, the results of the explorations and analyses, the options considered for repair, and the combination buttress and retaining wall solution used to complete the repairs. The difficulties encountered and resolved during construction are presented.

INTRODUCTION

SR 48 is a two-lane north-south highway running through the hilly terrain of Allegheny County in south-western Pennsylvania. A landslide occurred in the east slope of a side-hill fill in 2000 south of the intersection of SR 48 and SR 130 in the area shown in Figure 1 The landslide was repaired by over-excavating the disturbed cohesive embankment soils and replacing them with compacted granular backfill to improve slope strength and drainage. Unfortunately, the landslide reappeared again in the spring of 2001 which necessitated a geotechnical exploration to determine the cause of the slope failure and options for repair.

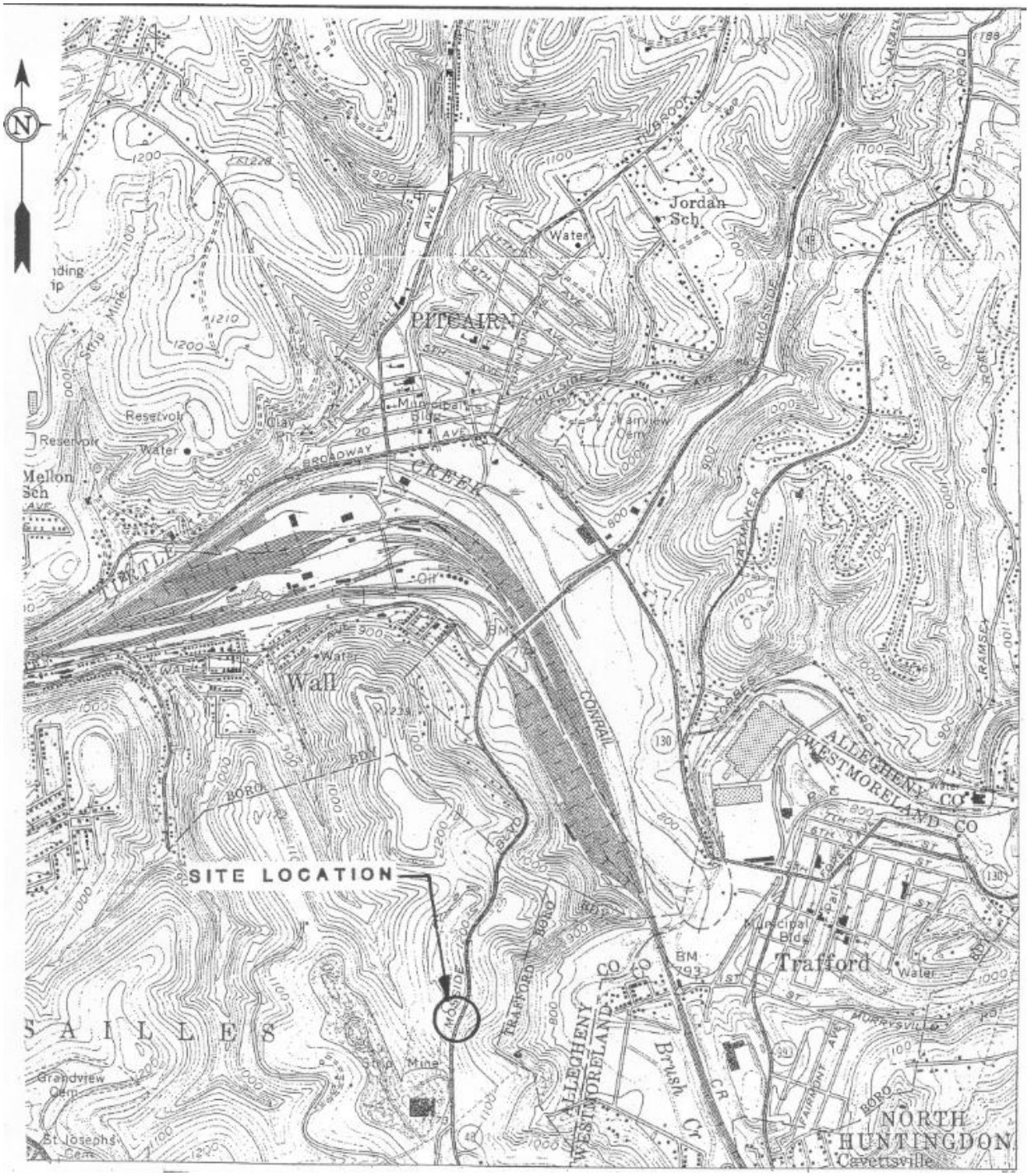

FIGURE 1 - AREA OF LANDSLIDE ON SR 48

DESCRIPTION OF LANDSLIDE

The landslide that reoccurred in the east slope of the highway embankment in the early summer of 2001 was a classic slump. The top width was about 100 feet adjacent to the highway, and the total length of the slide perpendicular to the slope was about 90 feet. . The slide mass moved downward about 10 feet and laterally about 20 to 30 feet. Photograph 1 shows the landslide from the south looking north. Fortunately, the failure did not extend into the highway, and therefore, traffic was not affected. However, the failure had undermined the normal location of the guide-rail, which was re-established in the remaining shoulder closer to the highway, as shown in Photograph 2.

Photograph 1 – SR 48 Landslide Looking from South to North

Photograph 2 – Relocated Guide Rails at Head of SR 48 Landslide

SITE GEOLOGY

The site is located in the upland area of the Appalachian Plateau Physiographic Province. The structural features of this province are predominately a series of northeast-southwest trending ridges and valleys. This upland area has been dissected and eroded by many small branching streams, resulting in rugged, steep forested hillsides with valleys comprised of alluvial material. Surface elevations range from about 1170 feet MSL at the roadway above the landslide to 1080 feet at the lowest portion of the slope below the slide area. The total relief within this slide area was about 90 feet.

The natural soils in the area are residual or colluvial cohesive soils derived from weathering of the underlying rock and are relatively weak and susceptible to landsiding. The embankment soils were derived from local cutting and filling to develop the desired grade of the highway. Some of the embankment consisted of slag from the earlier repair.

The rock strata are members of the upper Casselman Formation of the Pennsylvanian age Conemaugh Group. The Casselman Formation is about 300 feet thick and extends downward from the base of the Pittsburgh coal to the top of the Ames limestone. It consists of a sequence of alternating layers of sandstone, shale, red bed claystones, limestones and thin discontinuous coal seams. These rocks are commonly interbedded and change lithologically over short lateral distances. The Pittsburgh Coal, the dominant coal seam mined in southwestern Pennsylvania, is stratigraphically about 20 to 40 feet above the level of the landslide.

GEOTECHNICAL EXPLORATIONS

A preliminary geotechnical exploration consisting of 10 borings in the slope and embankment was conducted to investigate the unstable soils and the underlying bedrock for evaluation of the cause of the landslide and to develop options for repair. An inclinometer casing was set in boring B-5 along the centerline of the slide mass to determine the rate of slope movement and piezometers were set in the slope to monitor water levels. Ten additional borings were later drilled to determine subsurface conditions and to obtain soil and rock samples for laboratory testing for establishing parameters for final design of the repairs. The plan of borings for both the explorations is shown in Figure 2. Figure 3 shows a typical section through the center of the landslide.

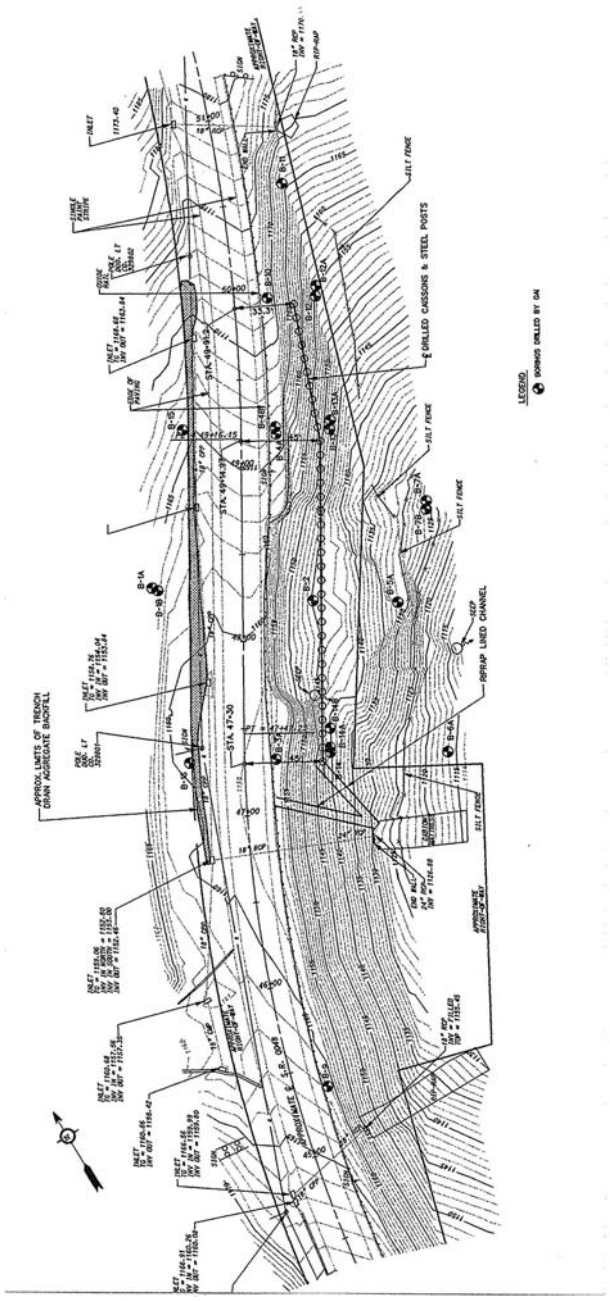

Figure 2 – Plan and Locations for Borings for SR 48 Landslide

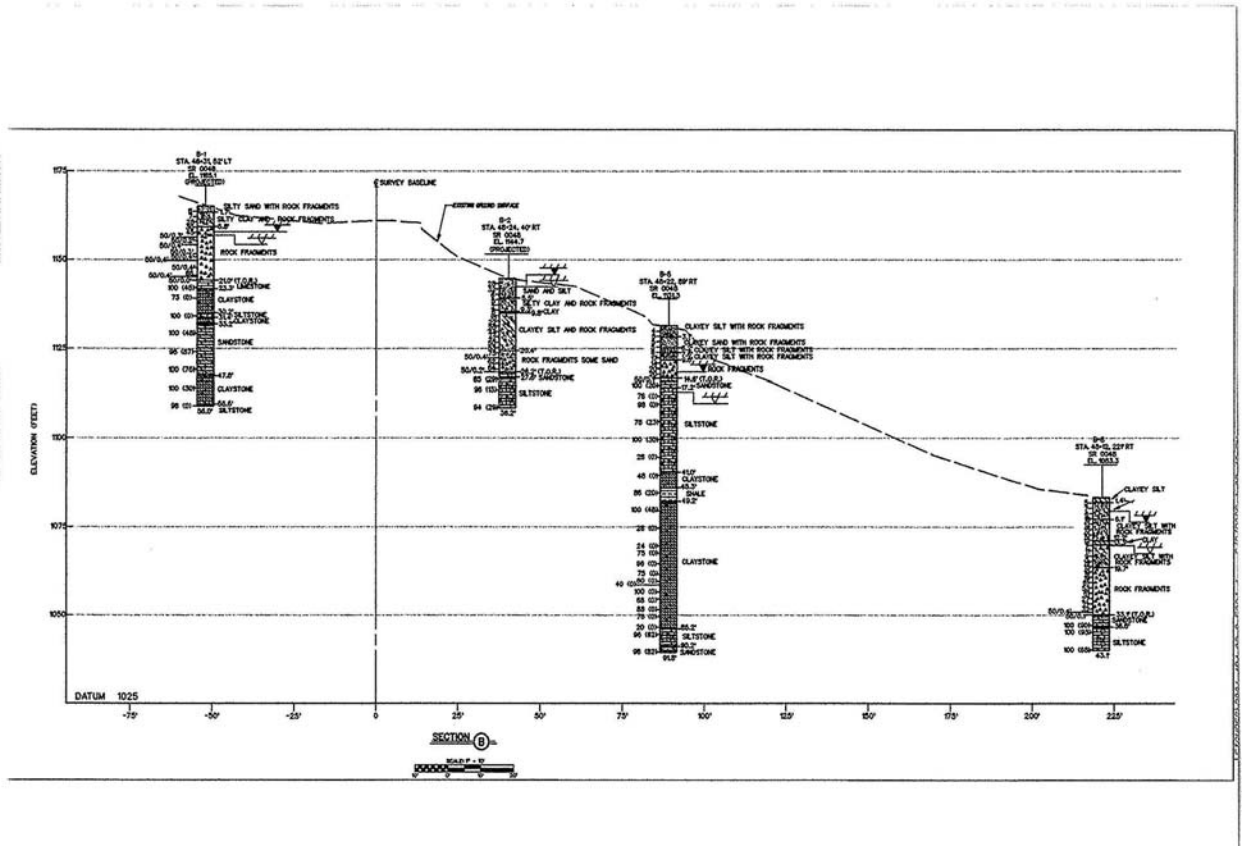

Figure 3 – Geologic Section through the Center of the Landside

The soil along the east edge of the highway embankment was about 25 to 35 feet thick in the area of the landslide. Information from both explorations indicated that embankment soils were underlain by relatively weak cohesive soils and claystone. This limestone was also found near the top of rock in some areas. The inclinometer tube became severed quickly and indicated that the slope movements were in the natural cohesive soil below the fill and above the top of rock.

The data from 8 piezometers indicated that ground water in the rock layers is generally well below the top of rock. Ground water did appear to be present in the thin limestone layer found in some locations near the top of rock. Water also appeared to be perched in some of the more permeable soil zones. However, much of the soil sampled was not saturated, and a well-defined phreatic surface was not found in the soil.

CAUSE OF FAILURE

Stability analyses were conducted to analyze the failure of the slope using the computer software PASTABLM. Results of a direct shear test of the silty clay with rock fragments from below the center of the slide mass indicated a drained angle of shearing resistance of about 20 degrees with little cohesion. The prefailure slope geometry was modeled, and the slope was found to have a safety factor of about 1 at the time of failure using the approximate ground water conditions found in the borings and piezometers. It was concluded that the embankment failed because it was underlain by relatively weak soils, and that ground water may have contributed to the failure. It was also concluded that the first repair was not extended deep enough to remove the weak soils and that future repairs must address this issue.

SELECTION OF REPAIR APPROACH

Options considered for the repair included:

- Construct a buttress to stabilize the toe of the slope and then reconstruct the embankment slope. This approach would have been the lowest cost option; however, it could not be used because the first constraint placed upon the selection of the repair approach was that it must be implemented in the existing right-of-way. The right-of-way was very close to the toe of the highway embankment in the area of the landslide which prohibited the consideration of a buttress.
- Remove the embankment and the underlying weak soils and reconstruction of the embankment using suitable embankment materials. This approach was estimated to be the next least costly. However, the depth of the weak soil that must be overexcavated would require that the overexcavation extend well into the highway embankment, which would require temporary closure of the highway and a 9-mile detour. The small route is heavily traveled and closure of the highway was not an option. That eliminated this approach.
- The third option considered was the installation of an anchored soldier beam and lagging retaining wall in the embankment slope. This approach could be accomplished by constructing a temporary bench across the embankment slope that would permit the installation of drilled pier foundations socketed into rock to support the wall. Rock anchors could also be installed as needed when the face of the wall was exposed by excavating on the downhill side. This approach was selected because it meets the requirements to stabilize the slope, maintain traffic in two lanes, and could be implemented within the right-of-way.

DESIGN OF REPAIRS

The typical section and front view of the wall is shown in Figures 5 and 6. The wall was designed to resist the lateral loads that might be imparted considering the presence of the weak cohesive soils that will remain under the embankment. Lateral earth pressures were computed based on an angle of shearing resistance of 20 degrees and considering the sloping backfill behind the wall. The design included an upper row of rock anchors to be installed with minimal excavation below the wall, to reduce the risk of additional slope movements during construction that could reduce the width of the highway. A second lower row of anchors was included to assure the normal stability of the wall. In addition, the two rows of anchors provided redundancy in the design. In the event that a single anchor fails, the other anchor has sufficient strength to prevent failure of the wall. This was not the case if only a single row of anchors was used. The rock strata found underlying the slope included thin discontinuous layers of hard limestone, thicker layers of sandstone, and layers of soft weak claystone and more competent siltstone. These layers varied in thickness and elevation both laterally and vertically. The locations and elevations of the anchors were selected so that the bond zones were mostly in the more competent rock layers and avoiding the weaker claystone layers. Finally, the failed embankment material that extended across the right-of-way line was to be removed as a part of the repair.

IMMINENT LANDSLIDING IN THE SOUTHERN PORTION OF EMBANKMENT

Near the completion of the design of the repairs, it was noted that the southern portion of the embankment was beginning to fail. Small tension cracks were starting to occur near the top of the embankment, and bulges and cracking were occurring near the base of the embankment. Considering the timing, the Department decided to include an optional request for the contractor to submit a design and a price to improve the stability of the southern portion of the embankment, in conjunction with the construction of the repairs of the northern portion of the embankment.

BIDDING AND MODIFICATIONS TO THE DESIGN

The contractor was awarded the project based on competitive bids and also provided an alternate bid that included refinements to the design and potential cost savings to the Department. The major change was to reduce the number of rows of rock anchors from two to one, and to add horizontal beams to the face of the wall to provide redundancy support of the wall in the event of an anchor failure. Other aspects of the design remained unchanged. The Department accepted the contractors bid using his alternate design. However, when the contractor provided submittals, it was learned that the alternate design was based upon higher soil and rock strength parameters than the original design. The bid documents clearly stated that acceptable alternate designs must be based on the design parameters for the project included in the contract documents. In addition, the contractor proposed to reduce the anchor load testing criteria from a specified test load of 1.5 to 1.3 times the design load. This would have eliminated one strand from each of his proposed anchors. After the alternate design was adjusted to the original design parameters, the cost of construction reverted to the approximate original cost, had the original design been implemented. The schedule was delayed in correcting the alternate design to the original criteria, and the added benefit of having the slope protected against failure during construction by the initial row of anchors was resuced.

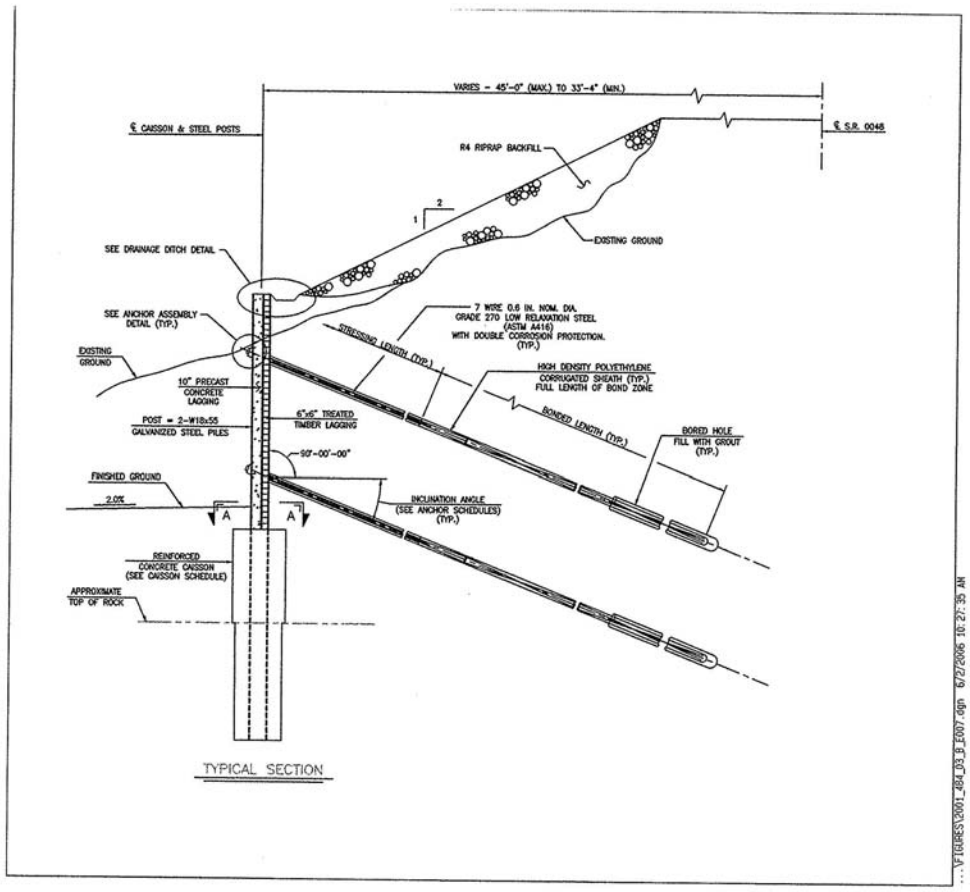

Figure 5 – Section through Retaining Wall Looking South

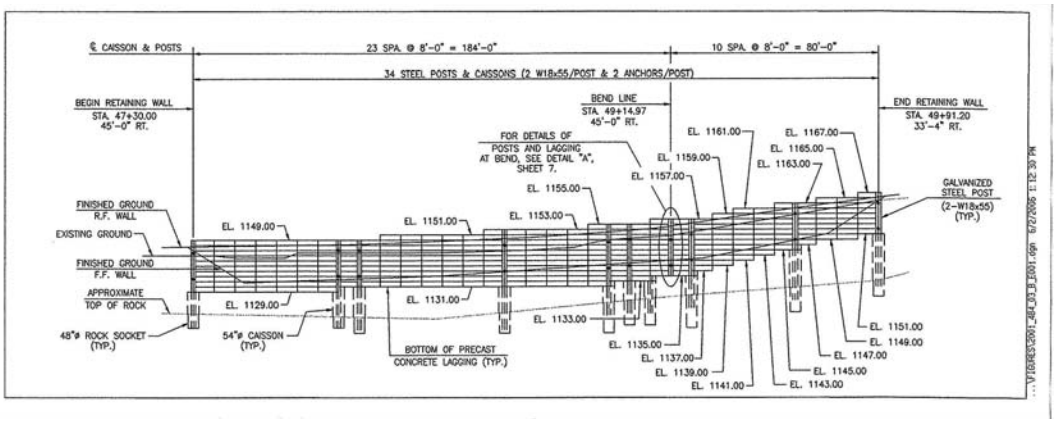

Figure 6 – Front View of Retaining Wall Looking West

The contractor also proposed a rock buttress constructed of R-4 durable riprap to stabilize the southern portion of the embankment. Since the right-of-way was considerably wider at this location, a rock buttress was a feasible option. However, the contractor provided no stability analyses to verify that the size of the rock buttress was adequate to stabilize the slope. The submitted cross section for the proposed buttress was analyzed and found to be inadequate. Subsequent analyses were performed and the size of the buttress was increased and a toe key was added. Taking the existing slope to be marginal with a safety factor of 1.0 against failure, the final sizing of the buttress was established to increase the safety factor to 1.3. The final geometry of the acceptable buttress is shown in Figure 7.

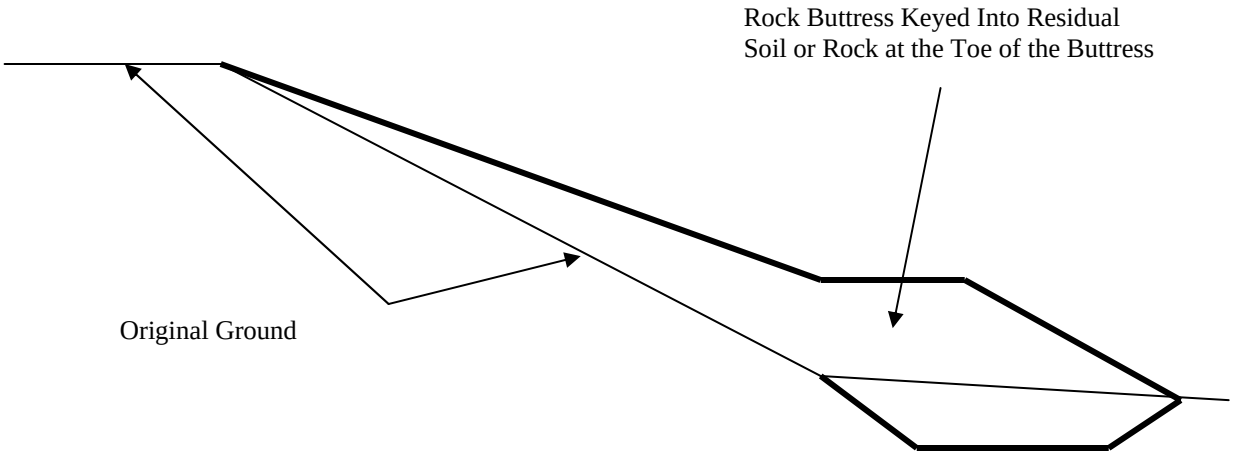

Figure 7 – Section Through Rock Buttress Looking North

OBSERVATIONS DURING CONSTRUCTION

The basic construction sequence was as follows. Erosion and sedimentation control measures were installed. Then, the highway was widened to the west to move traffic farther from the edge of the embankment, in case the slide progressed toward the highway and to provide more room for construction. The installation of the rock buttress for the southern portion of the slope was accomplished next, which also provided access to construct the temporary bench across the northern slope to install the retaining wall. The contractor had difficulty aligning some of the soldier beams; however, drilled shaft construction was accomplished as planned, and the temporary lagging for the wall was installed. The embankment was restored above the wall and then the anchors and permanent lagging were installed. Finally, the horizontal beams were welded to the face of the wall to provide redundancy in the anchor support, and the area was cleaned up.

The major problems occurred during the installation and testing of the rock anchors. During the drilling for the installation of the anchors it became apparent that significant portions of some of the bond zones for the revised locations of the anchors were encountering relatively soft claystone, and not the more competent rock. Longer anchors were ordered and installed to address this issue. There was also drilling water communication (flow) among some of the anchor bond zones. This necessitated consolidation grouting of some the bond zones and re-drilling, so that satisfactory grouting of the anchor installations could be achieved.

During the testing and stressing of the anchors, one of the vertical beams moved inward about 2 inches, and two of the strands in this anchor failed due to contact with the edge of the bearing plate. (This anchor was later replaced.) As a result of the unusual movement, the beam was instrumented with strain gages, retested, and the drilled shaft was exposed. This evaluation determined that the beams could deflect up to two inches without overstress, and this criteria was added to the testing criteria as a movement limitation. The beams at the ends of the walls were limited to 1 inch deflection because they have only half the bearing area. Little additional beam movement was observed, and all of the anchors were successfully grouted and tested to the planned test load of 1.5 times the design load.

Photograph 3 shows the completed installation. The approximate cost of the retaining wall was $800,000 and the approximate cost of the rock buttress was $200,000. These costs do not include the other construction activities needed to complete the repairs.

Photograph 3 – Repaired SR 48 Landslide (Northern Retaining Wall and Southern Rock Buttress) Constructed Within the Limits of the Irregularly Shaped Available Existing Right-of-Way

CONCLUSIONS

The landslide along the northern portion of the SR 48 embankment resulted from the presence of relatively weak claystone-derived cohesive soils below the highway embankment. Ground water may have contributed to the landslide. The first attempted repair of the slope by rebuilding the embankment using more permeable backfill did not totally address the underlying cause of the landslide. The correction of the landslide required increasing the resistance to sliding or removal of the weak soils below the embankment. Right-of-way limitations and the desire to maintain highway traffic precluded the economical use of a buttress or making a deep excavation to remove the weak soils. Thus, an anchored soldier-beam and lagging retaining wall was the technically sound method selected to provide the additional resistance needed to stabilize the slope.

The southern portion of the embankment slope that was beginning to fail was in an area having a significantly larger right-of-way. The economical solution to improving the stability of the slope without affecting traffic and while staying within the right-of-way was a rock buttress. Comparison of the two approaches confirms that the buttress is a much more cost-effective approach, where space is available to implement this approach.

Contractor-designed options can provide economical refinements to existing designs. However, the designs must be compared based on the same design criteria. An alternate design based on differing criteria may not lead to savings, when the alternate design is adjusted to meet the project design criteria.

The repairs implemented along the SR 48 embankment have improved the stability of about 450 lineal feet of highway embankment. The repairs are anticipated to provide a long-term stable highway embankment.

Widening US 119 over Pine Mountain, Letcher County, Kentucky

Mark A. Litkenhus, PE, Associate
Fuller, Mossbarger, Scott and May Engineers, Inc.
1409 North Forbes Road
Lexington, Kentucky 40511
859.422.3000
mlitkenhus@fmsm.com

ABSTRACT

The Kentucky Transportation Cabinet (KYTC) spent 30 years evaluating improvements for US 119 over Pine Mountain from Oven Fork to Whitesburg. In 2001, following a number of accidents and related problems, this portion of US 119 was closed to trucks longer than 30 feet (including tractor-trailers, coal trucks and school buses). Understandably, enhancements were necessary to improve safety and to promote economic development in this area of the state, while maintaining and preserving the pristine nature of Pine Mountain. The geologic conditions within this area are influenced by the Pine Mountain Overthrust Fault and consist of bedrock with considerable folding, faulting and overturning. Building a new roadway was not only a challenge to design but expensive as well.

Design and construction of cut slopes across the mountain included the use of conventional cut slopes (for Kentucky), as well as non-traditional approaches such as slopes excavated along bedding planes, use of enlarged ditch areas with rock catchment fences, excavation of old colluvial materials within drainage features, shot-in-place berms, and construction of cuts with the roadway alignment perpendicular to the strike. Additionally, steep terrain, dipping lithology, and environmental concerns resulted in restricted use of roadway embankments.

This paper presents background information and discusses actual conditions encountered during construction of the multiple and various types of cut slopes.

PROJECT LOCATION AND BACKGROUND INFORMATION

The Kentucky Transportation Cabinet (KYTC) has been evaluating possible improvements to portions of US 119, located within the Pine Mountain area of Letcher County, since the late 1960's. The length of US 119 that was improved as part of the US 119 Design Build Mountain Project consisted of an approximately 7-mile long section of roadway from Oven Fork across Pine Mountain to Whitesburg. This portion of US 119 was a narrow, two-lane roadway exhibiting severe curves and steep grades at many locations. Safe and efficient movement of today's vehicular traffic sizes and volumes was inhibited by the severity of these existing conditions. Figure 1 is a regional map showing the location of US 119 discussed herein.

Figure 1. Regional Location Map

This region of the state is characterized by some of the most rugged mountainous terrain existing in Kentucky. Highly dissected uplands with irregular mountain ridges, steep slopes, and narrow stream valleys display topographic relief on the order of 1000 feet. Pine Mountain itself was formed through seismic activity along a near-by fault line, now known as the Pine Mountain Overthrust Fault. As a result of this seismic activity, bedrock within this region can be severely folded and overturned. Because of these topographic and geologic conditions, any new roadway alternate in this area is expensive to design and build. Use of conventional roadway cut and embankment slope geometries are often not sufficient to provide stability and acceptable long-term performance of a roadway. Unique solutions such as excavating roadway cuts along the bedding plane of the dipping bedrock formations, enlarged ditch areas with rock catchment fences and shot-in-place berms were required to improve stability and performance.

Numerous options considered over the years have included widening of the existing roadway, new alignment locations, and possible construction of a tunnel to carry US 119 through Pine Mountain. In 2001, the KYTC selected the team known as The Mountain Team consisting of Qk4, Mountain Enterprises, Inc., Bizzack, Inc., American Consulting Engineers, PLC, PDR Engineers, Inc. and FMSM to design improvements and construct US 119 under a Design/Build contract approach. FMSM was the geotechnical engineering consultant responsible for field exploration efforts, laboratory testing of recovered samples, engineering analyses to evaluate embankment and cut stability conditions, and overall geotechnical engineering support. Figure 2 is a vicinity map showing the existing US 119 alignment as well as the locations selected for improvements. This paper focuses on the geotechnical conditions encountered at the sites selected, and the design features implemented to address the unique geotechnical aspects of the roadway corridor.

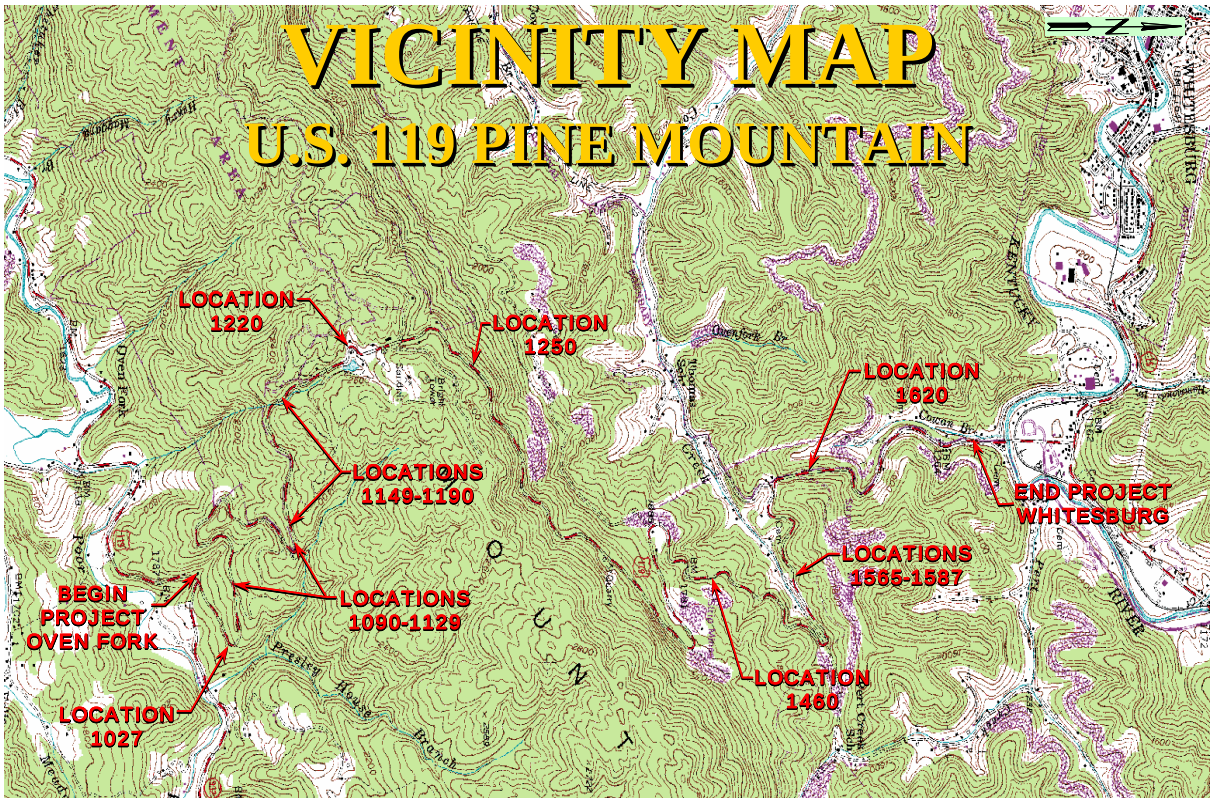

Figure 2. Vicinity Map of US 119 over Pine Mountain.

REGIONAL PYSIOGRAPHIC AND GEOLOGIC SETTING

The project area is located within the Eastern Kentucky Coalfield physiographic region of southeast Kentucky. This region consists of highly dissected uplands with irregular mountains ridges, steep mountain slopes, and narrow stream valleys. Ridges and valleys are generally oriented in a southwest-northwest direction as a result of the past tectonic activity associated with the Pine Mountain Overthrust Fault.

The Whitesburg (1973) USGS quadrangle map (*1*) indicates the region is underlain by bedrock belonging to the Breathitt, Grainger, Newman, Pennington, Lee and Hance Formations. These formations consist of siltstones, shales, sandstones, limestones and coal which were primarily deposited during the Lower and Middle Pennsylvanian geologic periods.

The roadway corridor crosses over the Pine Mountain Overthrust Block which delineates the southeast boundary of the Appalachian physiographic province. The overthrust block contains numerous faults such as the Pine Mountain, Jacksboro, Russell Fork and Hunter's Valley faults (*2*). The Pine Mountain Overthrust fault is described as an up-turned and out-cropping feature in which Silurian age bedrock is present beneath upper Cambrian bedrock. This overthrust block was created during the Appalachian Orogeny in the Pennsylvanian geologic age and has since been inactive. The thrust block of the fault is from the southeast, moving over a slip plane towards the northwest. Considerable folding, faulting and overturning of bedrock along the fault plane have occurred, particularly within the down-thrown block. Figure 3 is an illustration of a geologic section within the area.

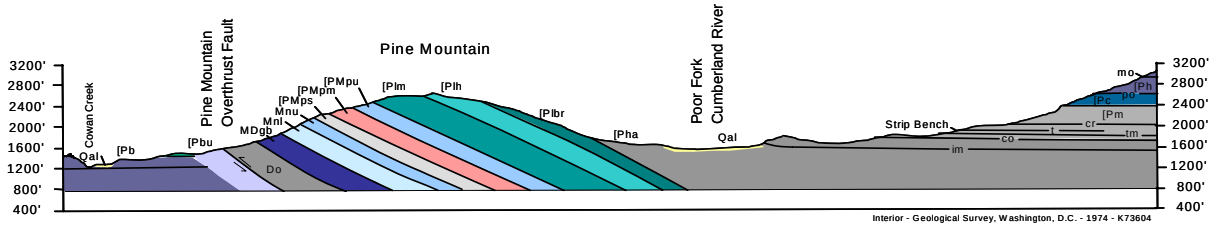

Figure 3. Geologic Section of Pine Mountain. (1)

Pine Mountain is situated on the southeast side of the Pine Mountain Overthrust Fault, between the fault and the Poor Fork of the Cumberland River. A series of hogbacks (sharp-crested ridges formed by the out-cropping edges of steeply inclined resistant rocks, and produced by differential erosion) have formed along the southeastern dip slope on the southeastern flank of Pine Mountain. Based upon bedding measurements compiled from numerous studies in this area, the average strike of bedding is approximately N63°E and the bedrock dips downwardly in a southeasterly direction between 2 and 35 degrees from horizontal.

TRADITIONAL KYTC ROCK CUT SLOPES

The Kentucky Transportation Cabinet's Geotechnical Manual (*3*) provides general guidelines for design of cut slope configurations based upon different rock types. Each cut interval is designed independently with consideration given to lithology as well as joint inclination and continuity. Cut slopes in nondurable shales, as measured by the slake durability index (SDI), are generally constructed on a 1.5H:1V to 2H:1V as shown in Figure 4. The KYTC separates shale into four categories for design purposes, depending upon SDI and Jar Slake values as follows:

Classification	SDI (%)	Typical Jar Slake Category
Durable	≥ 95	6
Nondurable, Class I	80 to 94	4 or 5
Nondurable, Class II	50 to 79	3 or 4
Nondurable, Class III	≤ 49	1 or 2

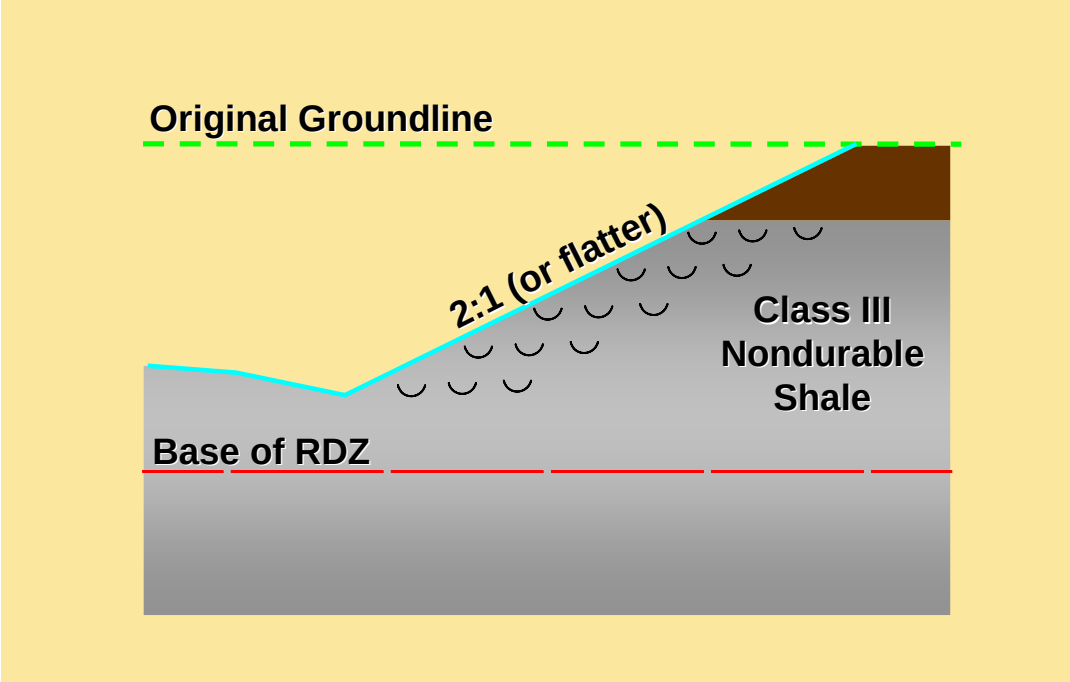

Figure 4. Cut Slopes in Nondurable Shales. (*3*)

For more durable rock lithology, intermediate benches are located at the top of the least resistant lithologic unit within each cut section. Figures 5 and 6 provide examples of the two most common cut slope configurations utilized in this area of Eastern Kentucky.

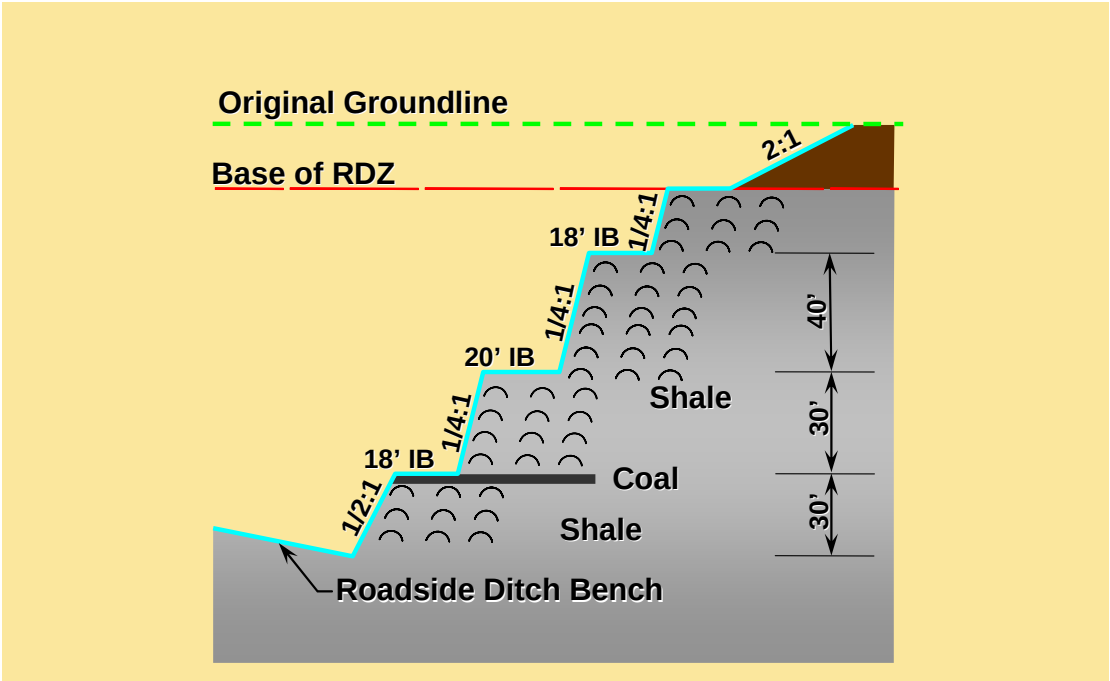

Figure 5. Cut Slopes in Durable Shales. (*3*)

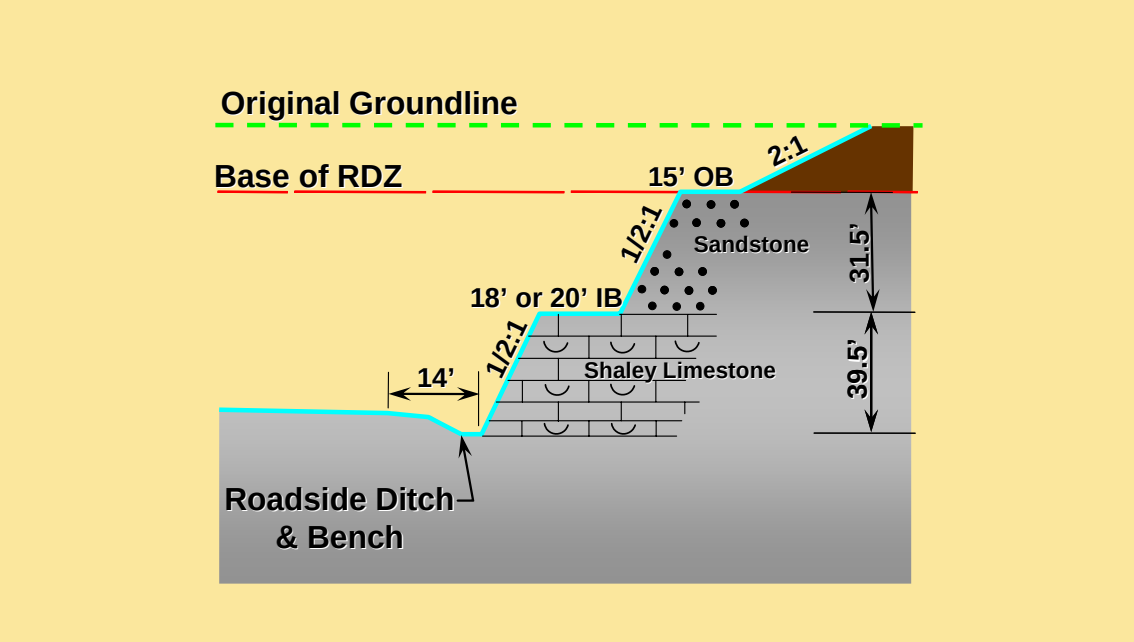

Figure 6. Cut Slopes in Shaley Limestone or Sandstone. (*3*)

Conventional KYTC cut slopes for durable sandstones or shales vary from 1/2H:1V to 1/4H:1V. This material is generally stable using this type of configuration. However, the presence of joints, fractures, solution features, cross-bedding, etc. will also influence the slope geometry. Intermediate benches are typically 18 feet wide for cut heights less than 30 feet and 20 to 25 feet wide for lift heights greater than 30 feet. The benches are generally placed on top of the least resistant material.

US 119 CUT SLOPES ACROSS PINE MOUNTAIN

Because of the considerable folding, faulting and overturning of the bedrock associated with the Pine Mountain Overthrust Fault, the success of conventional cut slopes was considered to be limited. Location 1090 - 1129 was the first area requiring a different type of cut slope design. Bedrock dipped downwardly 18 degrees towards the roadway for portions of this widening. Figure 7 presents a plan view of the area.

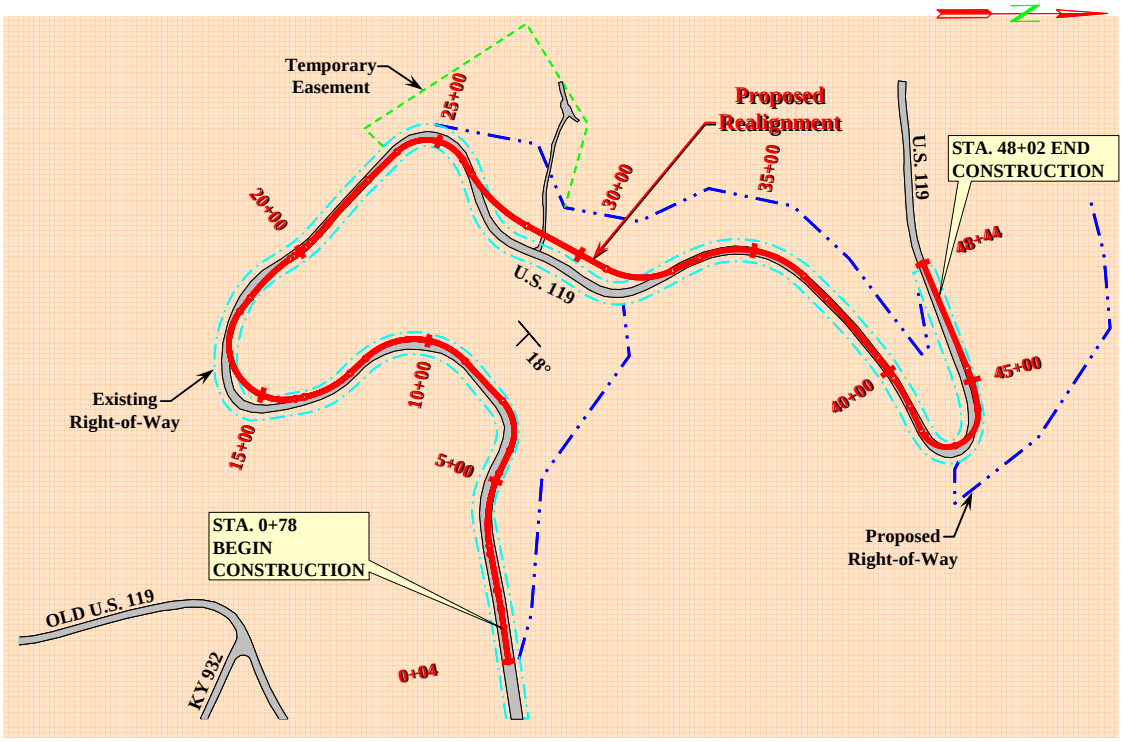

Figure 7. Plan View of Location 1090 - 1129

Therefore, roadway centerlines parallel with strike of bedding and with bedrock dipping downward towards the roadway required 3H:1V slopes (approximate bedding plane angle) with transitions in and out of curves when the roadway turned away from the strike direction. The KYTC Geotechnical Branch had experienced slope failures in the past when the excavation was constructed steeper than the true dip angle. Figure 8 presents a cross section showing the planned roadway and Figures 9 and 10 are photographs showing before and after construction of the slopes.

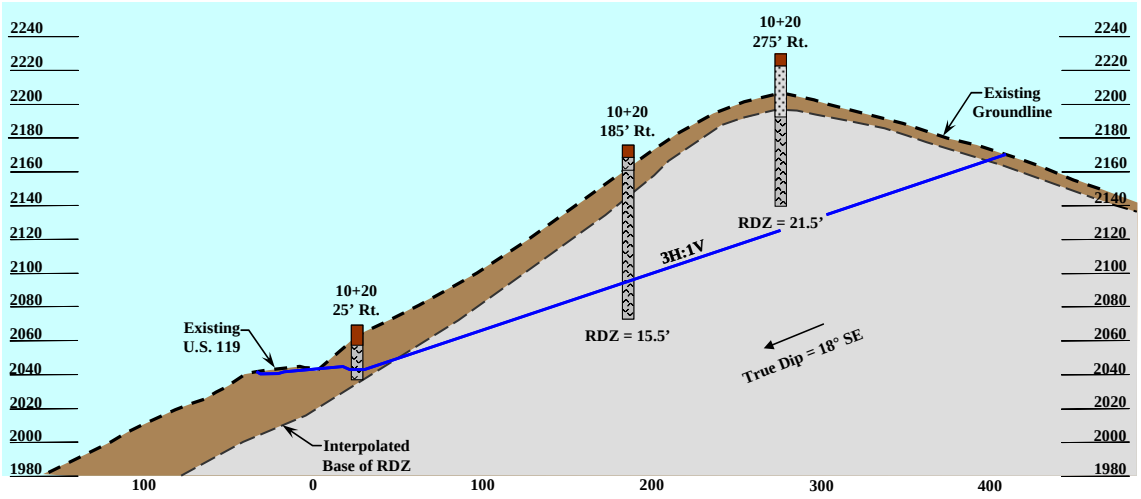

Figure 8. Location 1090 with Centerline Parallel to Strike at Station 7+00

Figure 9. Before Construction

Figure 10. Completed Construction

The alignment between Stations 20+00 and 25+00 was parallel to strike with the bedrock dipping away from the roadway. Therefore the cut could be excavated as a conventional cut slope configuration. Because the bedrock in this area consisted of nondurable shale, these slopes were excavated on a 1.5H:1V grade as shown in Figure 11.

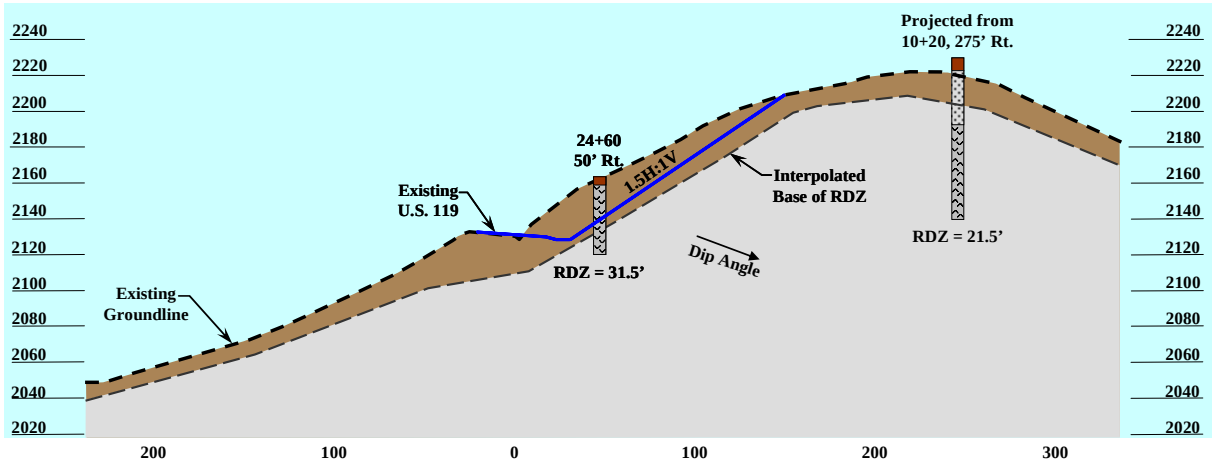

Figure 11. Cross Section at Station 24+00

Location 1149 – 1190 involved similar roadway configurations as described for location 1090 – 1129, with the roadway centerline parallel to the strike, and bedrock dipping towards the roadway. However, this section of US 119 was located adjacent to a wildlife management area. In addition, cut slopes excavated along the dip angle continued up the mountain a considerable distance before the cut could be daylighted. Therefore, the Design Team elected to utilize a "shot-in-place" berm technique. The principal decision behind using this method was to reduce the amount of disturbance that would have been required if the slope was fully excavated along the bedding plane. As shown in Figure 12, a predetermined area was "rubble-ized" by blasting, and then left in place to form the berm. The blasting helped break up any bedding planes that may have served as failure planes. The size of the area was based upon the estimated weight required to resist the driving force of the weight of any material above the shot-in-place zone.

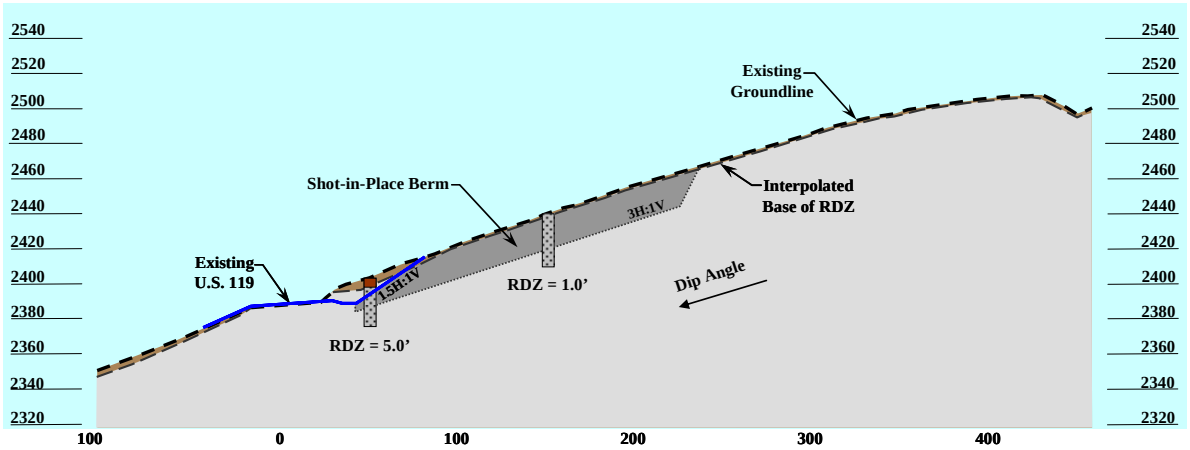

Figure 12. Cross Section of Typical Shot-In-Place Berm

Figure 13 depicts an area during construction that has been rubble-ized. In addition, the 1.5H:1V regrade slope within the blasted area has been excavated. Figure 14 is a photograph in which you can visually see the bedrock bedding planes and how they are dipping towards the roadway.

Figure 13. Shot-In-Place Berm

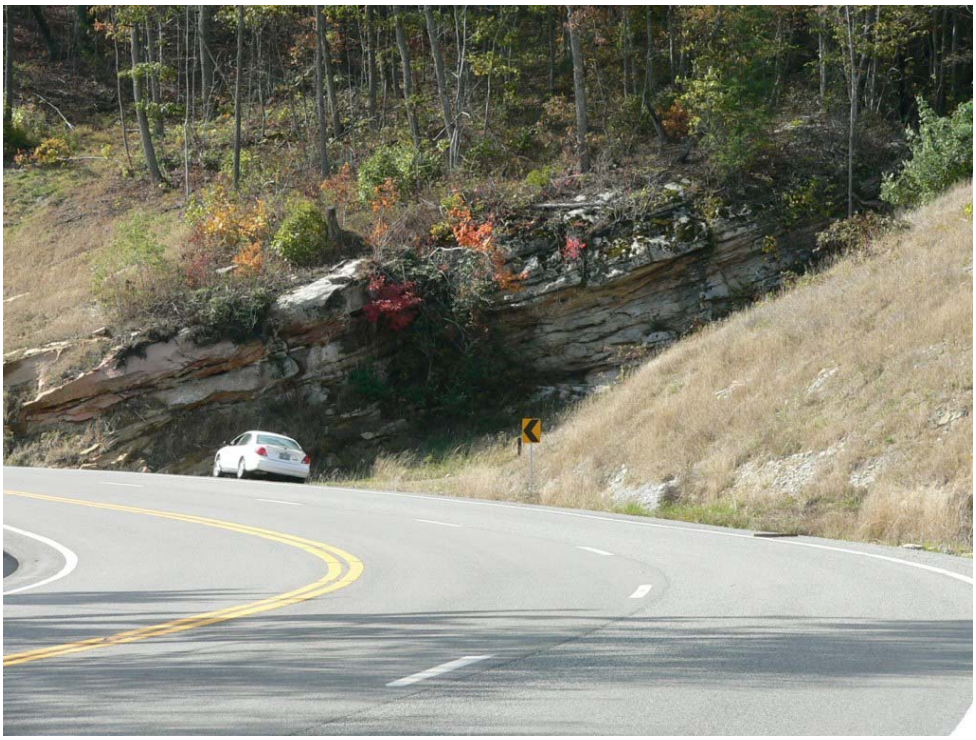

Figure 14. Photograph Showing Bedding Planes of Bedrock.

As US 119 approached the top of Pine Mountain, the orientation of the roadway centerline was such that it was perpendicular to the strike. Figure 15 shows the location of this site. The bedrock within this area consists of durable sandstone and shales. Because of these two conditions, cut slopes were constructed using conventional 1/2H:1V slopes.

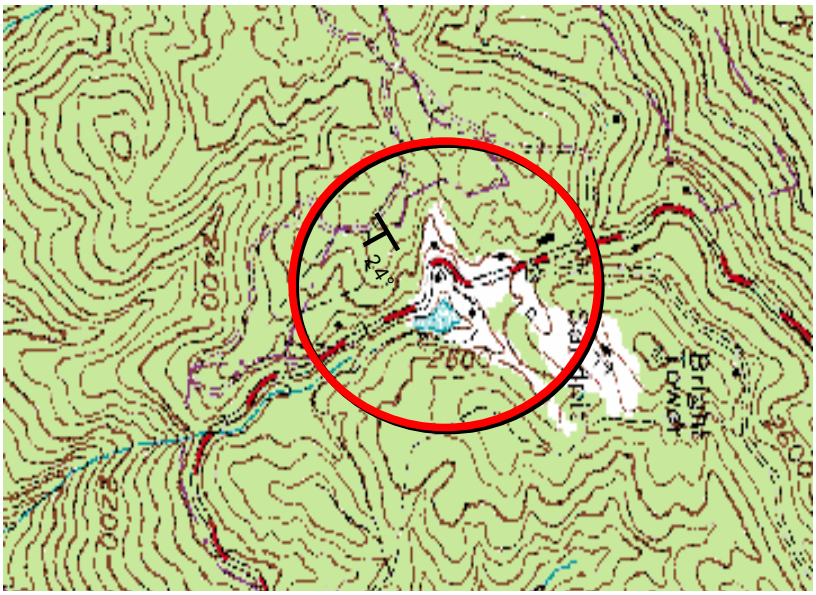

Figure 15. Location 1220

Figure 16 shows the completed cut slopes. Within this area, the roadway alignment also had a couple of sharp curves causing the orientation of centerline relative to the strike of the bedding planes to skew from perpendicular. At such locations, excavation of materials along the bedding plane was required to provide adequate slope stability.

Figure 16. Roadway Centerline Approximately Perpendicular to Strike of Bedding Planes.

Figure 17 shows the roadway alignment turning such that the direction of bedding dip is into the roadway at an approximate angle of 24 degrees, resulting in using approximate 3H:1V slopes for construction. The far right of the photograph shows the centerline turning such that more conventional 1/2H:1V cut slopes could be designed and constructed.

Figure 17. Constructed Cut Slope Involving a Roadway Alignment that is both Parallel and Perpendicular to the Strike of Bedding.

Location 1250 is positioned on the north side of Pine Mountain. At this location the bedrock is dipping into the hillside and away from the roadway. Past roadway improvements in this area allowed FMSM to perform open face logging and collect dip measurements in many areas. In addition, the performance of the existing cut slopes could be evaluated. However, an existing radio tower above this site required 3/4H:1V slopes to be designed with no intermediate benches. The 3/4H:1V was based upon bedding measurements and existing conditions such that the slope angle would be greater than most of the fracture angles measured. Because there was not enough room for multiple intermediate benches, an 18 foot wide ditch bench and rock fall catchment fence were designed to reduce the potential of rock fall into the road. Figure 18 shows this cut configuration.

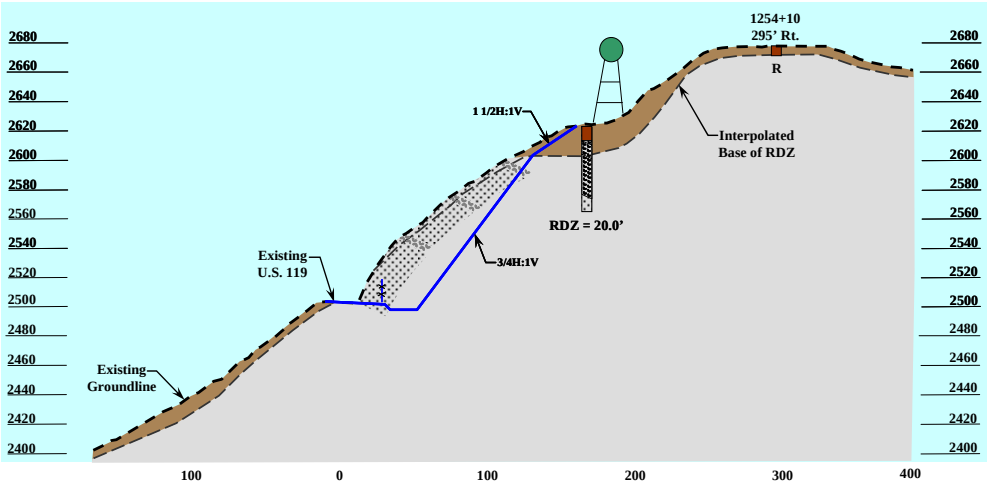

Figure 18. Cut slope with bedrock dipping into hillside.

Figure 19 shows the completed construction at this location. The radio tower building is present in the upper right corner of the photograph.

Figure 19. Completed cut slopes at Location 1250.

One of the more difficult areas encountered was Location 1460. This site contained past mining (above and below ground), deep colluvial deposits, and a lot of water draining/seeping from the hillside. Figure 20 depicts the plan view within this area.

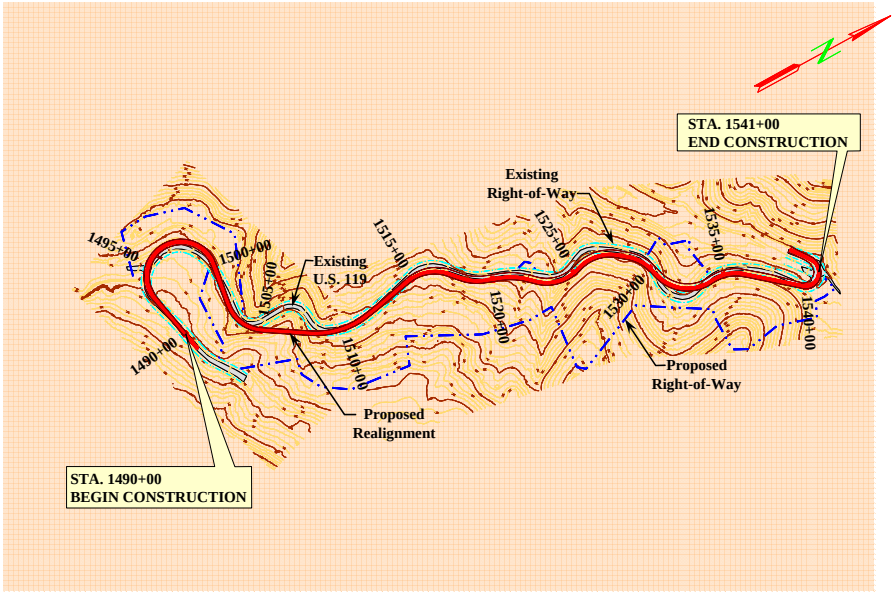

Figure 20. Location 1460.

Deep colluvial soils were present throughout the majority of this area. Extensive stability analyses were performed to evaluate the steepest allowable slope configuration in order to reduce the amount of right-of-way that would be required. In addition, there were remnants of past coal mining highwalls and other surface operations. A 2.5H:1V slope was ultimately designed. Figure 21 illustrates a typical section used for construction.

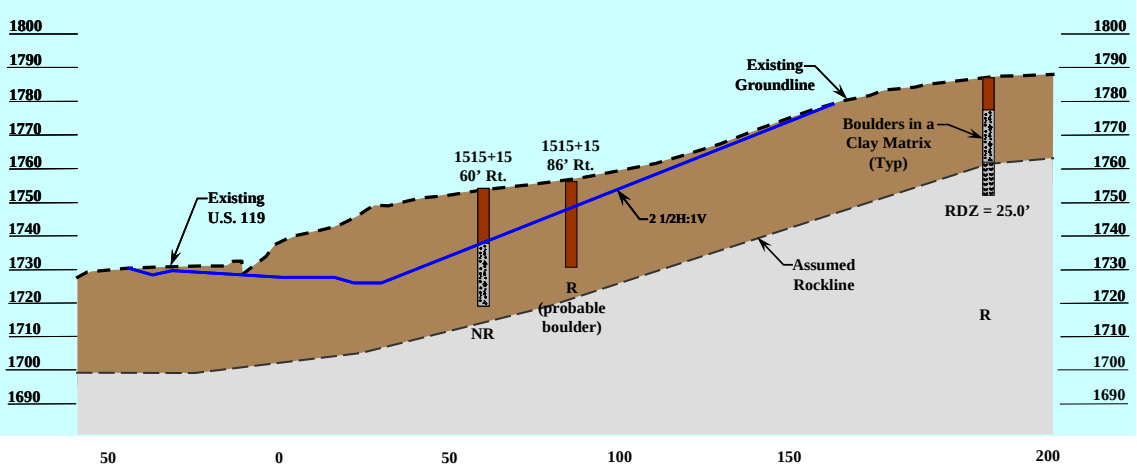

Figure 21. Typical Section through Location 1460.

During construction, an area near Station 1522+00 exhibited a significant amount of water seepage near elevation 1760 feet. It was interpreted that this water was being collected in a large drainage area up-slope from the site, seeping along the top of bedrock, and discharging out of the newly excavated cut slope. The amount of water flowing from the hillside was creating shallow surface failures. In order to reduce the potential for additional slope failures, a collector ditch and rip rap were installed on the slope near the 1760 elevation. Figure 22 shows the completed slope.

Figure 22. Completed cut slope in colluvial deposits.

One of the last areas constructed involved traditional cut slopes within horizontally bedded material. However, this cut included both durable sandstones and nondurable shales. Therefore, the exposed shale zone was isolated using intermediate benches and graded on 1.5H:1V slopes. The sandstone below the shale was relatively massive with

very few joints, allowing the 1/4H:1V slopes. The sandstones above the shale contained several joints and weathered zones requiring the use of slightly flatter 1/2H:1V slopes. Figure 23 depicts the typical section within this area, and Figure 24 is a photograph of the completed cut slope.

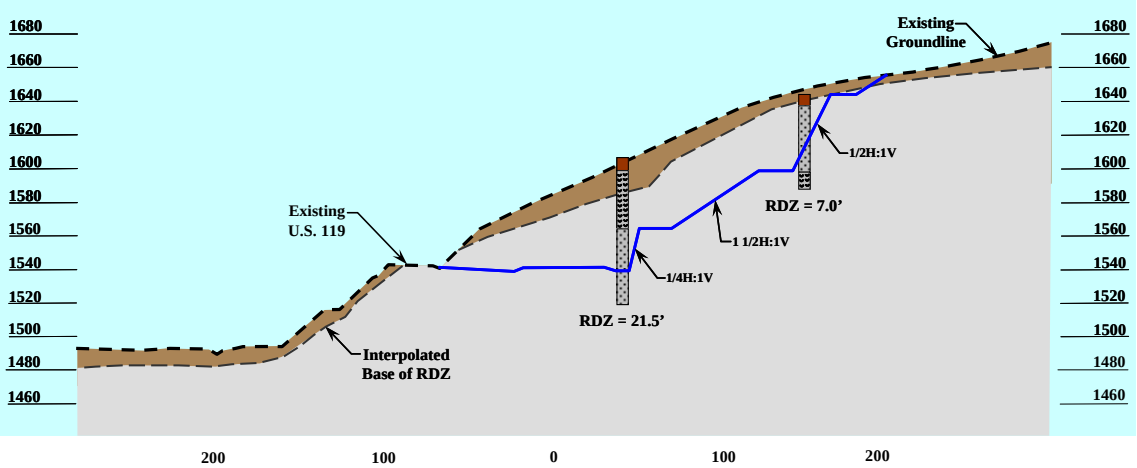

Figure 23. Cut slope in horizontally bedded material.

Figure 24. Completed cut slopes at Location 1565.

SUMMARY

Natural geologic conditions along the US 119 corridor created unique geotechnical challenges to designing and building a safe transportation facility. Dipping lithology, deep colluvial soil deposits, steep terrain, limited right-of-way, and the need to preserve pristine environmental conditions were all successfully addressed to accomplish the Kentucky Transportation Cabinet's goal of improving US 119 and allowing truck traffic to once again travel over the mountain. The task was accomplished through the cooperative efforts of local interest groups, industry, the Kentucky Transportation Cabinet, other governmental agencies, and the Mountain Design Team. The project's successful completion is a tribute to all those involved.

REFERENCES

United States Geological Survey, Geologic Map of the Whitesburg Quadrangle, Kentucky-Virginia, and Part of the Flat Gap Quadrangle Letcher County, Kentucky, 1973.

McFarlan, A. C., "Geology of Kentucky," Kentucky Department of Economic Development; Kentucky Geological Survey, 1961.

Kentucky Transportation Cabinet, Division of Materials, Geotechnical Branch, "Geotechnical Manual," May 1997.

Repair of Small Scale Embankment Failures and Landslides in East Tennessee Using the Railroad Rail Repair Method

Harry Moore
Tennessee Department of Transportation
Geotechnical Engineering Section
7345 Region Lane, Knoxville, TN 37914
865-594-2701
Harry.Moore@state.tn.us

George Sutton
Tennessee Department of Transportation
Geotechnical Engineering Section
7345 Region Lane, Knoxville, TN 37914
865-594-2703,
George.Sutton@state.tn.us

Len Oliver
Tennessee Department of Transportation
Geotechnical Engineering Section
6601 Centennial Blvd., Nashville, TN 37243-0360
615-350-4130
Len.Oliver@state.tn.us

ABSTRACT

In numerous areas of the mountainous terrain of East Tennessee small-scale embankment failures provide a challenge to state maintenance forces. The use of alternative remedial concepts to resolve and remediate geotechnical stability issues is often successful and can lead to dollar savings over conventional methods. The Tennessee Department of Transportation Geotechnical Engineering Section and Region One Maintenance office decided to implement the use of a railroad rail / guardrail retaining system to remediate a small-scale embankment failure on Tennessee State Route 116 in Anderson County.

This concept, developed in Kentucky and used widely by the Kentucky Transportation Cabinet, Department of Highways involves drilling holes along the roadway shoulder, installing the railroad rails and placing the guardrail against the exposed ends of the railroad rails to construct a small retaining wall along the roadway shoulder. This concept is often referred to as the Railroad Rail Landslide Repair Method.

Estimates by the regional FEMA office put the proposed rock buttress/rock fill concept on SR 116 at over three million dollars, mostly due to the extensive undercutting and embankment reconstruction due to the extreme steepness of the natural slope. The project to repair the embankment failure was let to contract in March of 2004 for an estimated price of $280,575.50 to Phillips and Jordan, Inc. The total project cost upon completion was $279,895.45, a total of $680.05 under the bid price. Using the railroad rail/guardrail slide repair concept enabled TDOT to save approximately 2.7 million dollars over the three million dollar estimate by FEMA for using our conventional rock buttress/rock fill remedial approach to fixing roadway embankment failures.

Upon completion of the first bid-letting contract for the use of railroad rail/guardrail slide repair concept, the RR rail method is considered a viable concept as shown by the success of this project. It is highly recommended that this remedial concept be considered for future use in repairing small scale embankment failures and landslides where appropriate to meet design requirements.

INTRODUCTION

In the mountainous terrain of rural East Tennessee, numerous small-scale embankment failures have impacted many State roadways. These small-scale embankment failures provide a challenge to state maintenance forces that often are required to repair the failures with limited funds and manpower. The use of alternative remedial concepts to resolve and remediate geotechnical stability issues is often successful and can lead to dollar savings over conventional methods.

The Tennessee Department of Transportation initially investigated in 1995 the concept and use of railroad rails and lagging to repair small-scale embankment failures. This concept, first developed and implemented by the Kentucky Transportation Cabinet and C&C Drilling Co., Inc. of Stanville, Kentucky, involved the use of used railroad rails and cribbing to stabilize small embankment failures along Kentucky's rural state routes in eastern Kentucky.

Since 1995 the TDOT Region One Maintenance Division has used the railroad rail concept (using a contract with a private company) to repair three state routes containing small embankment failures. These include SR 116 in Anderson County (near Lake City), SR 93 at the Washington – Sullivan County Line (near Fall Branch), and SR 91 in Carter County (on Cross Mountain). All three of these areas have been successfully stabilized using the railroad rail method, and remain so today.

These three sites involved embankments up to ten feet in height and depths to in-place bedrock of eight to twelve feet. Small-scale embankments appeared to be the best candidate for using the RR rail repair method.

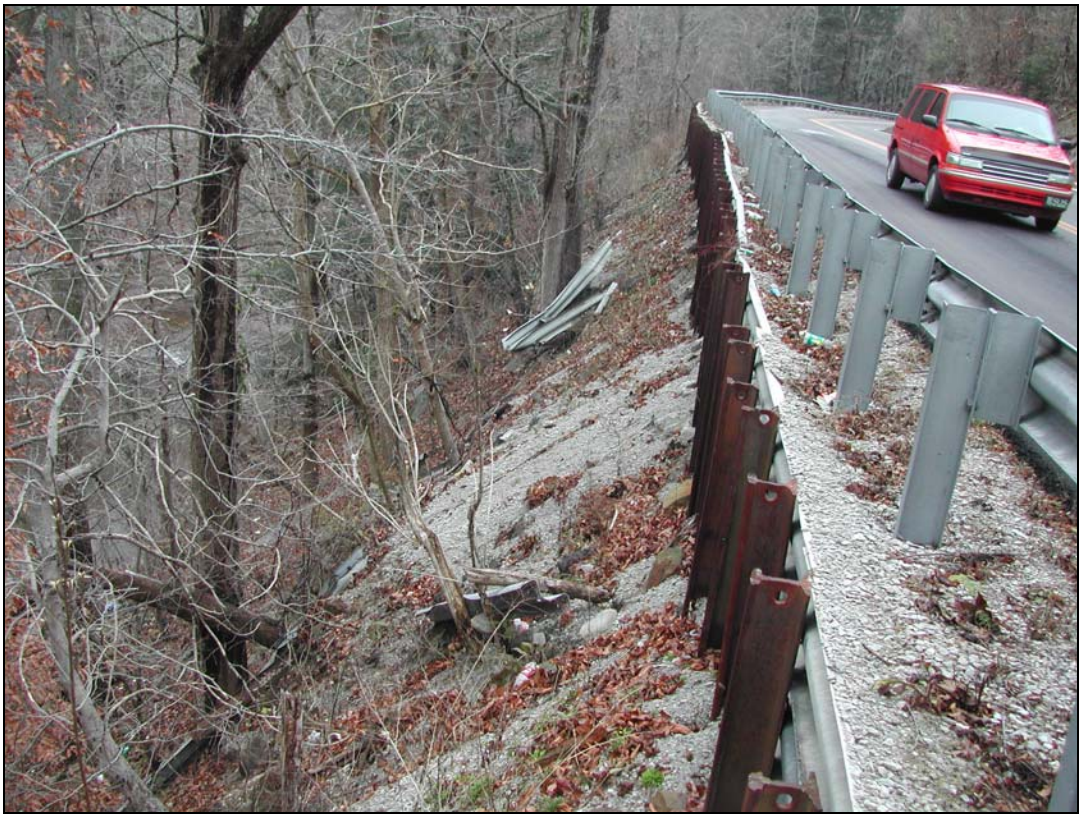

This photo shows one of the earlier trial sites in 1995 using the Railroad Rail concept on SR 116 in Anderson County, near Lake City, Tennessee. At this site only one row of railroad rails was used for stabilization due to the shallow rock depth (six to eight feet).

In November of 2003 Region One TDOT Maintenance forces reported an embankment failure on SR 116 in a rural mountainous coal mining area of Anderson County. This embankment failure provided an opportunity to design and let to competitive bidding a contract to repair a slide using the Railroad Rail repair method.

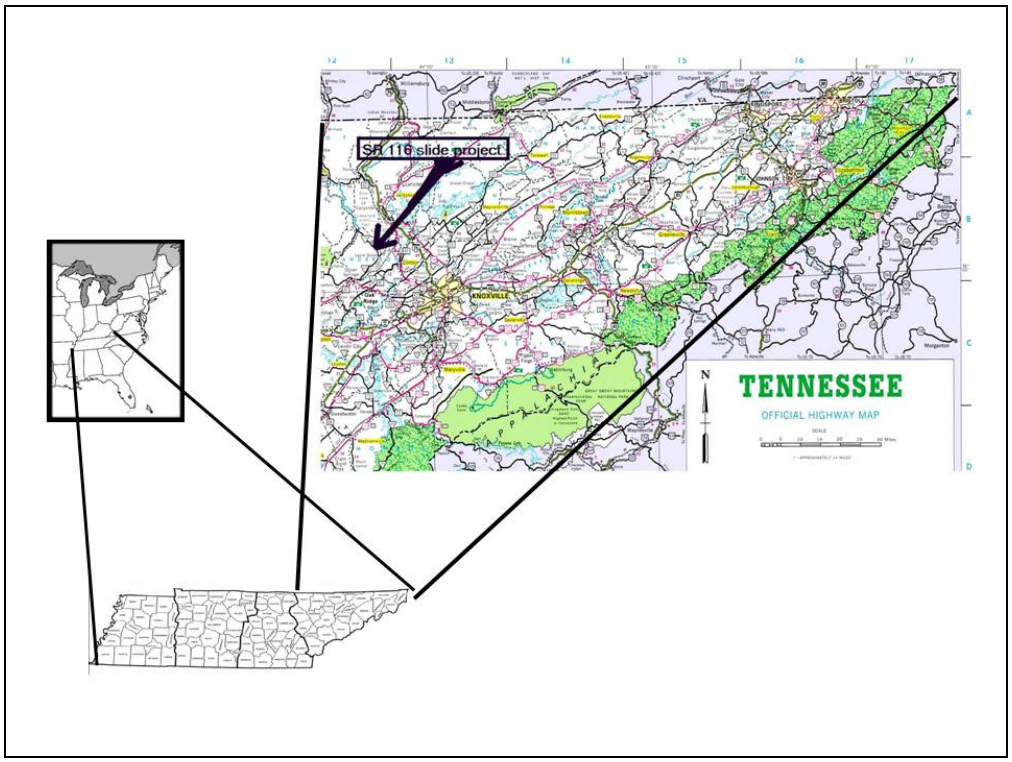

Location of SR 116 Railroad Rail slide repair project in Anderson County, Tennessee.

PROJECT HISTORY

An embankment (fill) failure along a section of SR 116 in Anderson County at LM 9.5 occurred after a period of heavy precipitation in February of 2003. As a result, the roadway stability was compromised and cracking occurred along the traffic lane.

Eventually, the affected embankment failed and the fill material slid down slope resulting in the closing of the outside shoulder area and moving the traffic lane over to the inside. This also resulted in a narrowed traffic lane section approximately 350 feet long, which would not physically permit two large trucks to pass through this section of roadway (coal and timber trucking is common on SR 116).

TDOT Region One Maintenance forces tried to repair the failure by placing large boulders over the failed slope. Due to the steepness of the natural slope beneath the roadway, the material continued to slide down slope, eventually undermining the existing outside traffic lane in one fifty-foot long section. Concrete barriers were then placed along the undermined section which even further restricted the roadway width.

The Geotechnical Engineering Section was contacted by TDOT Maintenance (Region One) for remedial recommendations.

Site Conditions

The subject site is located on a very curvy section of SR 116 as it traverses the side of Little Ridge in the Laurel Grove community in Anderson County. Side-hill cut and fill sections make up the typical roadway cross-section in this area, with very steep natural slopes.

The natural slope below the embankment approximates between a 1:1 to a 1.2:1 ratio and extends over 250 feet down slope to a creek. The existing roadway consists of a cut/fill section where the outside traffic lane is fill material which is resting on a very steep natural slope.

The site is underlain by silty shale strata of the Pennsylvanian Age Slatestone Formation. The strata are horizontally bedded with widely spaced joints. Weathering of the shale has produced a variable thickness of yellowish brown weathered shale and clay soils that sit atop the hard gray silty shale and siltstone units.

This photo shows the subject slide area in November 2003 where undermining of the existing roadway has required the use of portable barrier rails for safety.

Rock drilling was performed by the Geotechnical Engineering Section for subsurface information at the subject slide site in December 2003.

Core drilling along the roadway shoulder was performed by TDOT Geotechnical Engineering personnel in December 2003 to obtain accurate depths of the weathered zone, slide material, and in-place bedrock.

The drilling results indicated that the weathered shale extends to approximately 13 feet beneath the existing ground surface along the roadway. In some places the roadway fill is up to 13 feet in thickness with approximately eight feet of fill being most common. In-place shale and siltstone was found to be from eight feet to about 18 feet beneath the roadway shoulder. The combination of fill material, weathered shale, and in-place shale/ siltstone varies in thickness and depth from the surface, but stable material is generally found approximately 14 to 16 feet beneath the surface.

Remedial Concept

Several options for correcting the embankment failure were considered by the TDOT Geotechnical Engineering office and the TDOT Region One Maintenance office. These included a standard rock buttress/rock fill construction method and a relocation of the road. Discussions with TEMA and FEMA Officials and Jim Phillips (TDOT Region One Maintenance) involved Remedial Repair Concepts for the subject slide. Estimates by the FEMA office put the rock buttress/rock fill concept at over three million dollars, mostly due to the extensive undercutting and embankment reconstruction due to the extreme steepness of the natural slope. In addition, there was environmental concern about the excavation for under-benching and placement of the rock buttress due to the adjacent creek at the toe of the subject slope.

Relocation of the road was also considered and would have required new Right-of-Way and extensive excavation that would have been over 100,000 cubic yards. The excavation would have included removing both shale and siltstone along with the weathered shale material. In addition, locating a suitable waste disposal site was problematic due to very limited available and suitable ground for such purposes.

Considering the conditions at the subject slide area, it was decided to try the Railroad Rail repair method using “used” railroad rails and “used” highway guardrail. This concept, developed in Kentucky and used widely by the Kentucky Transportation Cabinet (as discussed above), involves drilling holes along the roadway shoulder, installing the railroad rails and placing the guardrail against the exposed ends of the railroad rails to construct a small retaining wall along the roadway shoulder. In addition, this would provide an opportunity to “let to contract”

this repair method to see what the actual contracting cost would be. This concept is often referred to as the Railroad Rail Landslide Repair Method.

By using an offset drilling method only one lane of traffic is blocked, permitting the road to remain open to one lane traffic during construction. This method consists of drilling an 8 to 12 inch diameter hole along the roadway shoulder into bedrock or below the failure plane, and then installing a133 to 136 pound-per-linear yard railroad rail section and backfilling the hole with suitable aggregate (flowable fill, grout, or concrete may also be used).

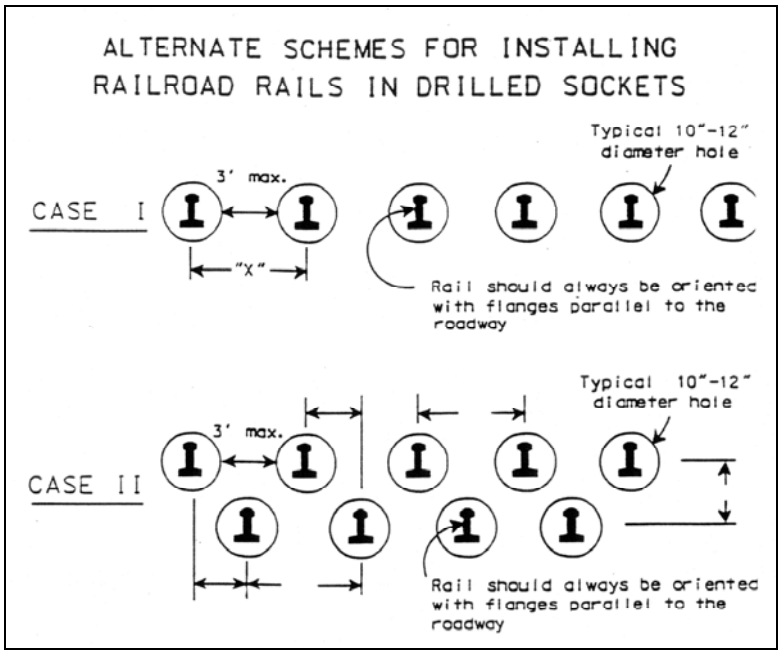

This is a sketch showing a plan view of the two drilling schemes used by TDOT to repair small-scale embankment failures using railroad rails. (From C&C Drilling Manual and Kentucky Transportation Cabinet, Geotechnical Unit)

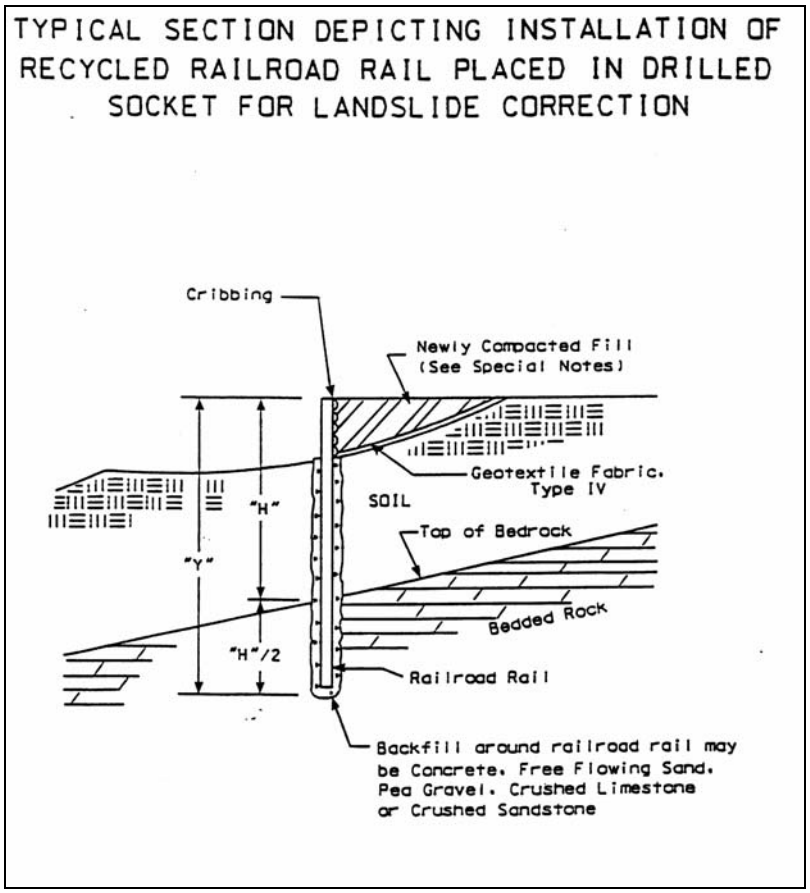

This drawing illustrates the typical section for using the RR rail landslide repair concept. (As developed and used by Kentucky Transportation Cabinet, Dept. of Highways Geotechnical Unit).

As a rule, one-third of the free standing hole is drilled into bedrock or stable material. For example, if the depth to bedrock and stable material is 10 feet, then the total depth of the drilled hole would be 15 feet. This allows for five feet of rail to be placed into stable material, normally referred to as embedment.

In most instances, this method results in a varying length of railroad rail being exposed above the drill hole. This allows for the placement of guardrail members against the exposed railroad rails forming a small retaining wall along the edge of the shoulder. This concept is limited to a maximum depth to stable material of around 22 feet, due to the standard length of railroad rail being around 39 feet.

At the subject site it was determined that the depth to stable material varied from about 14 to 16 feet. The drilling investigation indicated that stable material consisted of both slightly weathered shale and in-place shale. As a result, it was decided to place the stable zone at 20 feet making the total depth of the drilled hole at 30 feet.

Due to the depth of the unstable material it was decided to use a double row of rails, with each rail spaced at 28 inches and each row staggered (following the design guidelines provided by KY Transportation Cabinet , Department of Highways, Geotechnical Engineering office). This places the rails in the second row such that the rails are equidistant between the rails in the first row. The two rows were to be 24 inches apart, with the guardrail lagging placed on the outer most row of railroad rails.

The total length of the slide area was measured to be approximately 350 feet. It was decided to place the outside-most row of railroad rails a minimum of five feet from the edge of the future roadway pavement (after repair). In some instances this was widened a foot or two to accommodate the horizontal curve and the natural ground slope.

Construction

The slide repair project along SR 116 in Anderson County using the railroad rail remedial concept was let to contract in March of 2004. The contract was awarded to Phillips and Jordan, Inc. of Knoxville, Tennessee for an estimated total cost of $280,575.50. Construction began the second week of April, 2004 with a completion time set for on or before May 31, 2004.

The contractor chose to use a 12-inch diameter drill which was attached to a mandrill that was connected to the arm of a large track hoe. This was somewhat different from past experience with the drilling of the holes usually being performed with a large truck-mounted drilling rig that had a swivel tower base for turning to the side to drill the holes for the railroad rails. TDOT Maintenance forces were very interested in this drilling equipment with the possibility of obtaining the same apparatus to repair numerous similar slide situations using TDOT forces.

It was decided to use railroad rails that weighed 130 to 133 pounds per linear yard and backfill material consisting of No. 68 crushed stone. The contractor elected to drill one hole at a time, installing the railroad rail and backfill stone before starting the next hole location. After completion of 40 to 50 railroad rail installations, the contractor began placing the used guardrail sections (horizontally) against the outside row of RR rails for construction of the small retaining wall.

Filter cloth was placed along the exposed portion of ground between the retaining wall and the roadway shoulder then drainage backfill stone (No.6 size stone) was placed atop the filter cloth. After the drainage stone placement was completed, then the remainder of the backfill material, consisting of compacted base stone, was installed.

After completion of the railroad rail and guardrail installation, TDOT maintenance forces provided new guardrail at the shoulder and repaved the roadway section through the project site.

This photo shows the track-hoe mounted drilling apparatus used by Phillips and Jordan, Inc. on the subject slide repair on SR 116 in Anderson County. Note: RR rails in foreground and slide scarp in shoulder stone to the right of the track-hoe.

The holes drilled for placing the railroad rails penetrated weathered shale and in-place gray shale.

This photo shows the installation of railroad rail into the drilled hole. Note the RR rails in the background prior to trimming the tops.

This photo shows the installation of guardrail along the outside row of railroad rails forming the retaining wall to support the stabilized and widened roadway shoulder.

The guardrail was installed in horizontal sections forming small "step-downs" along the top of the retaining wall and shoulder edge.

As the railroad rail installation proceeded ahead, the guardrail portion of the retaining wall was constructed. The stacked rock along the wall base was used by workers to climb up and down the wall during construction.

This view of the construction shows the small compactor (at left along vertical rails) along the RR rails where base stone was being placed. Note the drilling and RR rail installation ahead.

After the guardrail installation and backfill stone placement was completed the RR rails were then trimmed forming the final retaining wall stabilizing the roadway.

This view of the completed RR rail wall shows the highest portion of the wall at 10 feet (near the middle left of photo). Note the new guardrail installed along the roadway shoulder.

This view shows the completed slide repair site with completed railroad rail wall and newly installed roadway guardrail. The previously undermined section of road was located just to the right of the guardrail near the upper-middle portion of the photo.

Here the slide repair work and the final paving is completed, supported by the railroad rail retaining wall.

Shown in this view of the slide repair project is the completed railroad rail/guardrail concept, with new guardrail and paving.

SUMMARY

To summarize, the project to repair the embankment failure was let to contract in March of 2004 for an estimated price of $280,575.50 to Phillips and Jordan, Inc. The total project cost upon completion was $279,895.45, a total of $680.05 under the bid price.

A total of 50 work days were used out of an estimated 56 work days set up in the contract. The amount of railroad rail used totaled 10,213.6 linear feet (almost 2 miles of RR rail) out of a total of 10,500 linear feet set up in the contract. In addition, 2,611 square feet of used guardrail was used out of an estimated contract amount of 3,845 square feet. The used guardrail was furnished by TDOT.

The contract administration was conducted by the construction field office supervised by Mr. Bobby Parks and his staff in LaFollette, TDOT Region One. Additional field technical assistance was provided by the Geotechnical Engineering Section

A special feature of this slide repair concept is recycling used materials to fix a stability problem. The project was able to be constructed with used railroad rails and used guardrail which saved money by not using new steel and new guardrail, and also helped our environment by recycling those items.

Overall, using the railroad rail/guardrail slide repair concept enabled TDOT to save approximately 2.7 million dollars over the three million dollar estimate by FEMA for using our conventional rock buttress/rock fill remedial approach to fixing roadway embankment failures.

Upon completion of the first bid-letting contract for the use of railroad rail/guardrail slide repair concept, the RR rail method is considered a viable concept as shown by the success of this project. It is highly recommended that this remedial concept be considered for future use in repairing small scale embankment failures and landslides where appropriate to meet design requirements.

ACKNOWLEDGEMENT

The writers wish to acknowledge C&C Drilling, Inc. of Stanville, Kentucky, The Kentucky Transportation Cabinet, Department of Highways Geotechnical Unit, and Mr. Henry Mathis (retired with KY Trans. Cabinet) presently with H.C. Nutting, Inc. for their willingness to share this technology with the Tennessee Department of Transportation, Geotechnical Engineering Section. Their help in understanding the design and experiences in using the railroad rail concept provided much needed resources to enable the authors to apply this concept to applicable embankments in Tennessee, and for this we are grateful.

TECHNICAL SESSION III
Applied Geophysical and Imaging Techniques

Analysis of Seismic Refraction Data – A Three-Decade Perspective

Alan Rock
Summit Peak Technologies, LLC
6121 N. Powell Road
Parker, CO 80134
(303) 841-0988
arock@summitpeak.net

Phil Sirles
Zonge Geosciences, Inc.
1990 Garrison Road, Suite 6
Lakewood, CO 80227
(720) 962-4444
phils@zonge.com

ABSTRACT

This paper presents a brief overview of the standard techniques used to process and analyze data acquired using the seismic refraction technique. The generalized reciprocal method (GRM), which has been used since the early 1980's, is discussed as to show its ability to determining velocity and structure beneath a seismic line. The method is very straight-forward and requires only simple line geometry parameters to derive a 2D layered-earth model beneath a seismic line. More recently refraction tomography is gaining acceptance because of the more robust and potentially higher resolution results provided in a cross-sectional view of the subsurface. Both GRM and tomography provide *images* of the subsurface and each can be validated with ground truth data (i.e., geologic or geotechnical data), but both are limited to 2D image results. An advanced numerical modeling method, called GAP, is also presented to demonstrate the next generation of seismic analysis for refraction data. Refraction data can be acquired in 2D or 3D, using a variety of arrays, and processed in full 3D to take into account the effect of variable Fresnel zones caused by lateral and vertical heterogeneities. GAP 3D modeling has been optimized for seismic applications and combines the discrete element method and particle flow code approaches to solving for material properties. The paper is not a treatise on the methods, or a complete discussion of all available software or methods to reduce refraction data. It is designed to show the progression of data analysis, as it relates to refraction seismic testing for engineering applications, over the past two to three decades. Additional value will be placed on results obtained from geophysical investigations, when they can produce 2D or 3D models for further engineering analysis using dynamic or static forces.

GENERAL PRINCIPLES OF REFRACTION

Seismic refraction defines the subsurface in both velocity and structure. Because these two factors are intrinsically related their independent determination is ambiguous. Geologic knowledge reduces the affect of this ambiguity and the refraction method is generally useful in subsurface investigation. The method involves placing a line of sensors or geophones on the surface and measuring the relative arrival time of a seismic wave. Figure 1 is a schematic illustration of refraction ray-paths generated by an impact to the ground. The seismic source can be any well-timed sonic disturbance such as hammer blows or explosive charges. The relative arrivals are used to define a subsurface structure and/or velocity.

The critical ingredients of successful refraction profiling include accurate sensor location, timing of relative arrivals to precisions of less than a few milliseconds, and modeling or calculating the bedrock depths and velocities. The geophone locations are routinely surveyed relative to the shot points to precisions of +/- 0.5 feet. Typical recording instrumentation utilized today allows accurate timing of first arrivals to better than +/- 2 milliseconds.

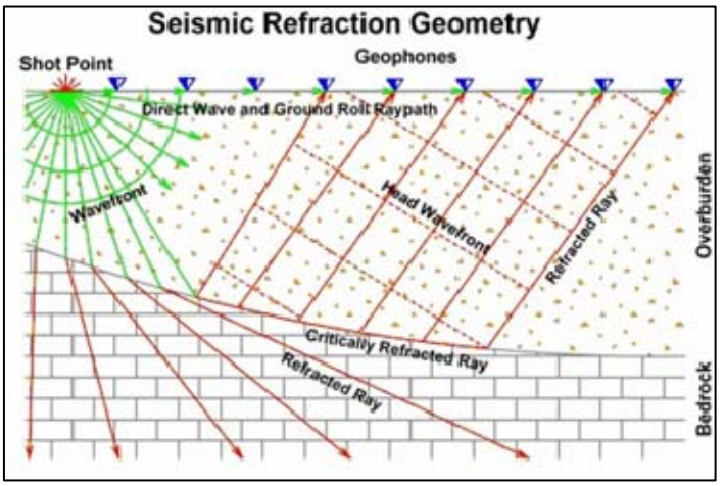

Figure 1. Seismic refraction ray-path geometry *(1)*

A generalized analysis procedure for seismic refraction data is illustrated in Figure 2. The first step in the analysis is to pick the arrival times, then plot the arrival data in a travel-time curve. The seismograms are picked to obtain source-receiver travel times. These travel times along with source-receiver distances are utilized to construct a time-distance plot for each shot point. The velocities inferred from the travel time curves are apparent velocities, and not necessarily true velocities. True velocities are determined from arrival times from shot points at both ends of the sensor line during the modeling procedure. In addition, small variations of individual data points from a true "straight-line" velocity on the time distance curve can indicate either undulations of the subsurface structure or lateral velocity changes. All information obtained from the time-distance plots is used as a basis for further modeling. In some instances shot coupling is not optimum, or sufficient cultural noise is present to make picking of arrival times inaccurate. As a result, some of the stations or shot arrivals may not be used in the analysis.

The refraction method can be implemented with either compressional (P) or shear (S) waves. P-waves are generated with vertical impacts or explosive charges at the surface, whereas S-waves are generated using traction or torsional source mechanisms, also on the ground surface. Obtaining velocity information from both P- and S-waves allows the calculation of elastic material properties such as Poisson's ratio, Bulk and Shear Modulus.

While the waves travel along the bedrock surface, seismic waves continually refract back to the ground surface, which may be detected by geophones placed on the ground surface. An illustration for the most general case of two layered ground, with a completely level layer interface, is shown in Figure 3. Example waveforms with picks are shown in Figure 4. . An illustration of a refraction travel time curve data that would be observed from an earth model with four layers is shown in Figure 5.

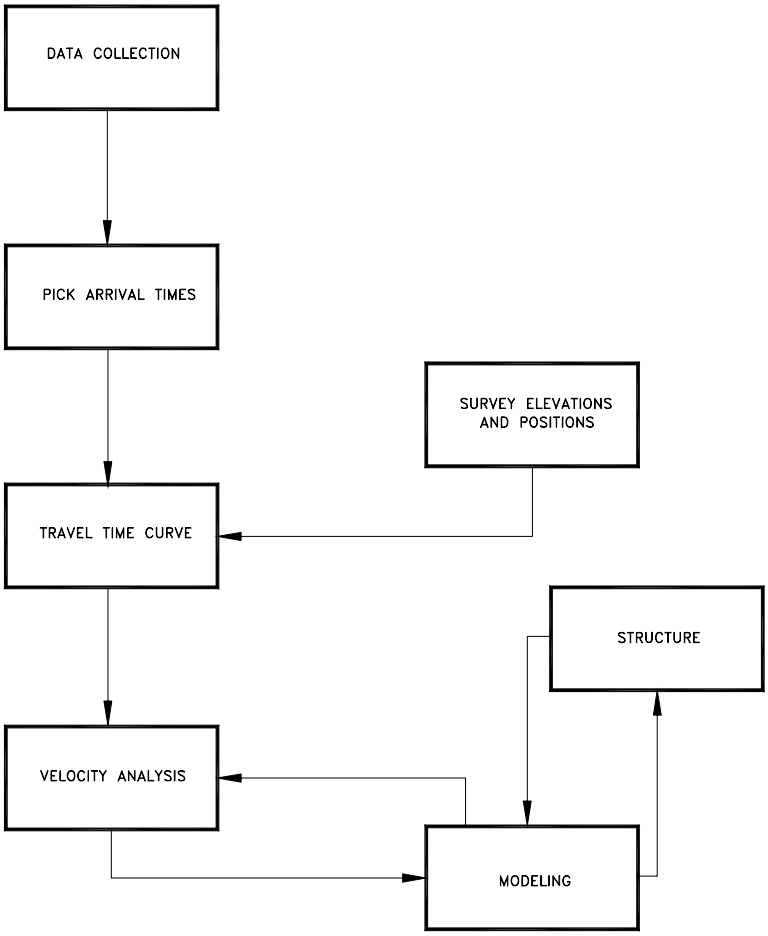

Figure 2. Generalized seismic refraction data analysis procedure *(2)*.

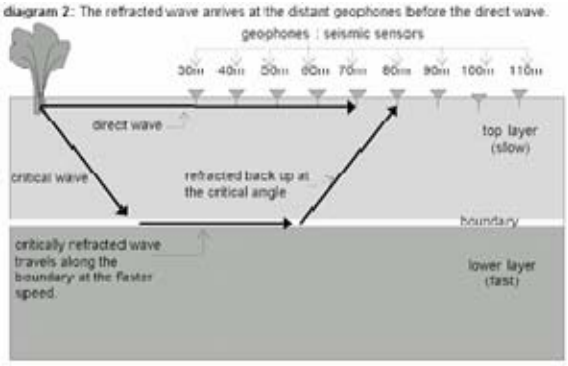

Figure 3. Seismic refraction raypath geometry – two layers beneath level ground *(3)*

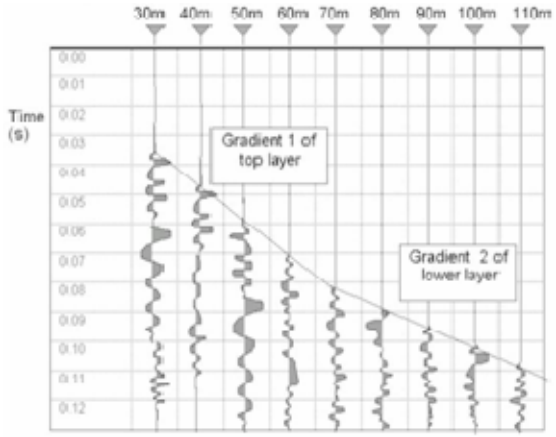

Figure 4. Seismic refraction waveforms (from example in Figure 3) with first arrival picks *(3)*

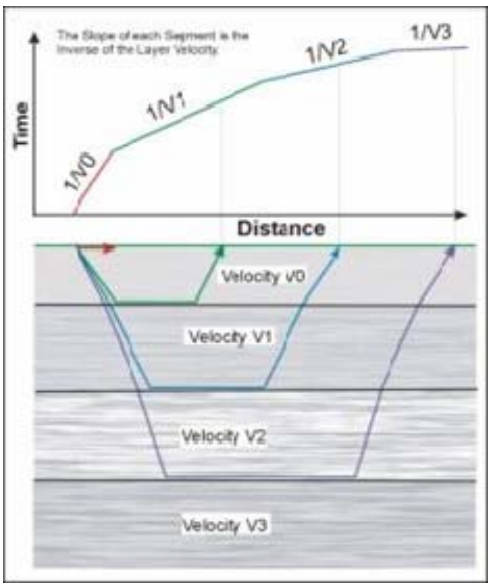

Figure 5. Predicted seismic travel-time curve from a refraction line above four subsurface layers *(4)*

Additional Considerations for Seismic Refraction

Because the two factors of velocity and structure are intrinsically related in refraction theory, their independent determination from refraction surveying alone is impossible. The ambiguity is that structure can be traded for velocity differences over a broad range of velocity-structure pairs.

Additionally, modeling ambiguity can be introduced due to the existence of low-velocity layers. Because there is no refracted information from a buried layer with a velocity less than that of the overlying material, the low-velocity layer will be hidden in the arrival time data. When this situation occurs, calculated depths to deeper refractors can be offset and in error. Boreholes, downhole logs, and geologic information are critical to limiting the range of these uncertainties.

One additional physical principle applies when considering low-velocity zones - Fermat's principle. Fermat stated that "*the energy will take the least-time path from one point to the next*". This principle is the basis for seismic refraction, but it also means that the first arrival energy will go around a low velocity zone. Unless the geometry is favorable (no high velocity path possible) the first arrival information will not reveal a low velocity area.

One should not be discouraged by these potential pitfalls. When accurate subsurface ties to borings and good estimates of the probable geology are available, these problems are minimized and an accurate subsurface image is produced.

DATA ANALYSIS USING THE GENERALIZED RECIPROCAL METHOD (GRM)

Since the 1980's the most common method of refraction interpretation is known as the Generalized Reciprocal Method. Dr. Palmer *(5)* first pioneered an analysis method that permitted calculation of time depths beneath each geophone along the line. This analysis procedure occurs in the "velocity analysis" part of the processing flow (shown in Figure 2). Figure 6 illustrates the simplified reciprocal ray paths and the initial calculation of reciprocal time.

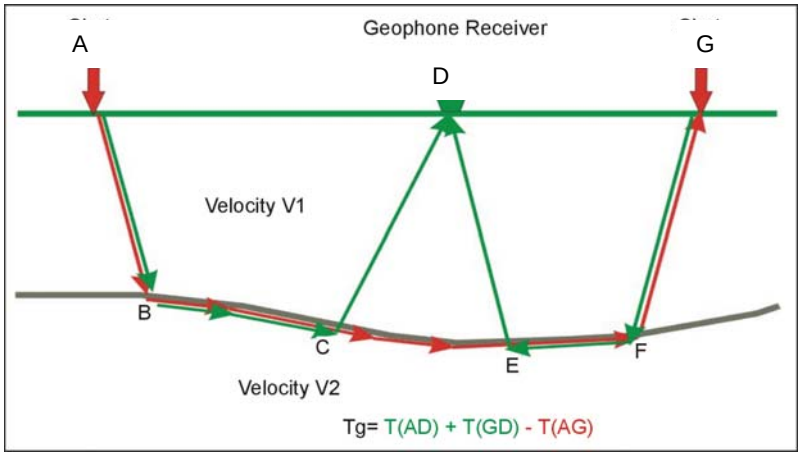

Figure 6. Basic generalized reciprocal method interpretation *(4)*

The objective is to find the depth to the bedrock under the geophone at D (Figure 6). This is done using simple calculations. The travel times from the shots at A and G to the geophone at D are added together (T1). The travel time from the shot at A to the geophone at G is then subtracted from T1.

Figure 7 shows the remaining waves after the above calculations have been performed. These are the travel times from C to D added to the travel times from E to D, subtracting the travel time from C to E. The sum of these travel times is approximately the travel time from the bedrock at H to the geophone at D. Since the velocity of the overburden layer can be found from the time-distance graph, the distance from H to D can be found, giving the bedrock depth. This process is extended to apply to several layers, if the first arrival times support additional higher velocities.

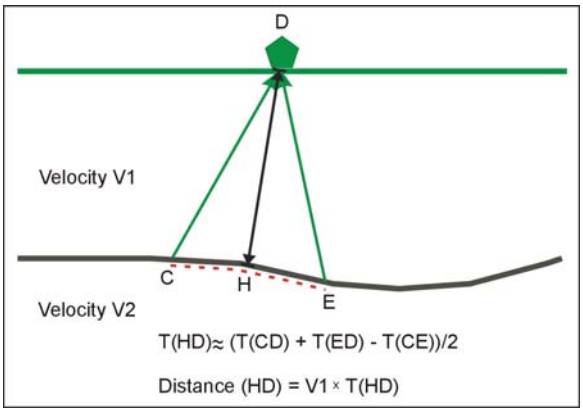

Figure 7. Generalized Reciprocal Method interpretation *(4)*

Once the velocities of the layers are assigned, these should be interpreted to give appropriate geologic layers. Figure 8 displays the typical output from GRM interpretation. The upper plot shows the travel-time curves, the middle plot shows the layer velocities for each layer, and the lower plot shows the resultant layer geometry. For example, a layer with a velocity of 4,920 ft/s (1,500 m/s) suggests a dense soil or soft rock (e.g., glacial outwash or claystone, respectively); whereas, a velocity of 15,000 ft/s (4,570 m/s) indicates hard, competent bedrock (e.g., limestone or granite). Lateral changes in the velocity of the layers can indicate either changes in lithology or changes in the degree of weathering or fracture density. GRM is capable of detecting lateral changes in the layer's velocity, but the analysis procedure is not robust for laterally variable geologic conditions (e.g., volcanics).

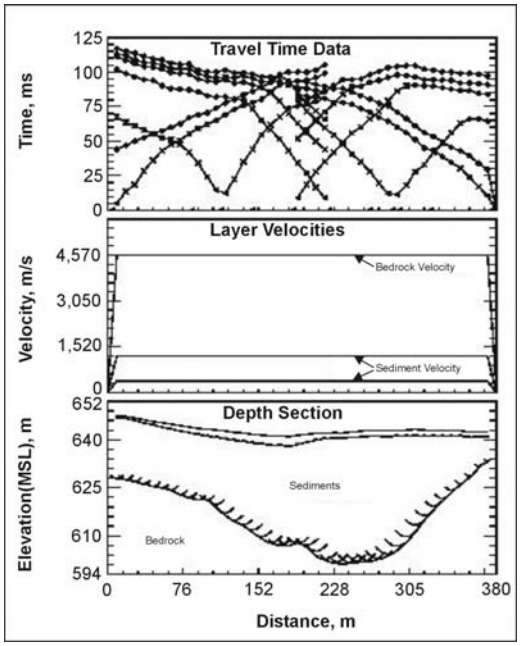

Figure 8. Example final plot from GRM refraction data analysis *(4)*.

SEISMIC REFRACTION TOMOGRAPHY

Two-dimensional refraction tomography is being used for high resolution subsurface imaging, either between boreholes (i.e., crosshole tomography) or on the ground surface (refraction tomography). Not unlike the medical CAT (Computer Automated Tomography) Scan, seismic tomography attempts to place the raypaths between source and receiver pairs into the space between them utilizing as many pairs as possible to obtain a robust image of the media between the source(s) and receiver(s). In doing so, the inversion programs produce a seismic tomography "panel", which is a two-dimensional (2D) cross-section of velocity (or attenuation).

In general, tomography is an inversion procedure that provides two 2D velocity and/or attenuation imaging from observation of transmitted first-arrival seismic energy. The first applications for seismic tomography were cross-hole tomography (XHT), utilizing boreholes for the placement of sources and receivers (Figure 9). Tomography data collection involves scanning the region of interest with many combinations of source and receiver depth locations (for XHT), or source and geophone positions (for refraction tomography) on the ground surface.

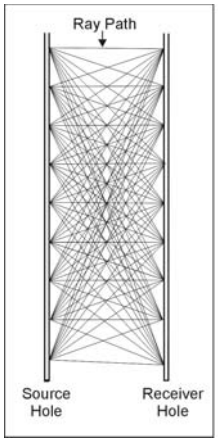

Figure 9. Source and receiver locations for a XHT seismic tomography survey showing dense ray coverage between the borings *(4)*.

The use of tomographic analysis for imaging geological boundaries and velocity variations has become a well established technique in geophysical investigations. It involves imaging the seismic properties from the observation of the transmitted seismic, compressional (P-) or shear (S-), first arrival energy either in time or amplitude. The relationship between the velocity field v (x,y) and travel time t_i is given by the line integral (for a ray i):

$$t_i = \int_{Ri} ds / v(x,y) \qquad (1)$$

where R_i denotes the curve connecting a source receiver pair which yields the least possible travel time according to Fermat's principle. Tomography is an attempt to match calculated travel times (model responses) to the observed data by inversion of these line integrals. Initially, the region of interest is divided into a rectangular grid of constant velocity cells (j) and a discrete approximation of the line integral is assumed as:

$$t_i = \sum_j \Delta S_{ij} \cdot n_j \qquad (2)$$

where ΔS_{ij} is the distance traveled by ray i in cell j, and n_j slowness within cell j. Using a first order Taylor expansion and neglecting residual error, equation (2) can be written in matrix form as:

$$\underline{y} = \mathbf{A}\,\underline{x} \qquad (3)$$

where the vector $\underline{y}$ is defined as the difference between computed travel times (from the model) and the observed travel times, vector $\underline{x}$ as the difference between the true and the modeled slowness, and **A** is the Jacobian matrix. In travel time tomography, equation (3) is solved using matrix inversion techniques.

The seismic wavefield is initially propagated through a presumed theoretical model and a set of travel times are obtained by ray-tracing (forward modeling). The travel time equations are then inverted iteratively in order to reduce the root mean square (RMS) error between the observed and computed travel times. The inversion results can be used for imaging the velocity (travel time tomography) and attenuation (amplitude tomography) distribution between boreholes or beneath the refraction line.

There are several commercially available refraction tomography algorithms each of which have been tested and described in detail *(6)*. This paper is not intended to present the theoretical differences between the major types of tomography code. Sheehan's paper *(6)* is a terrific introduction to the modeling parameters used by commercial code, and the benefits as well as limitations associated with differing tomography techniques. Figure 10 presents a refraction tomography solution (2D cross-section) produced using the RAYFRACT code, which is one of the commercially available codes discussed in Sheehan's paper *(7)*.

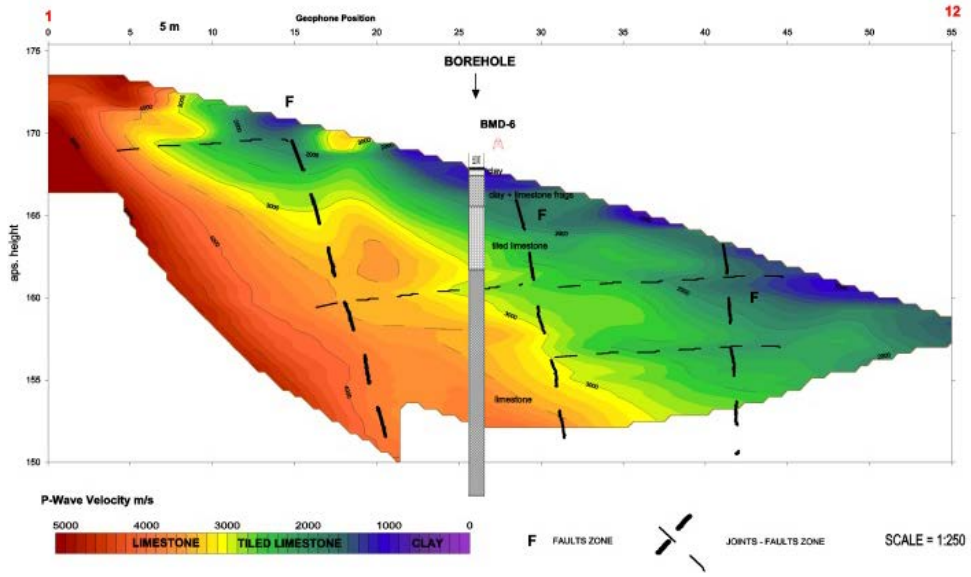

Figure 10. 2D refraction tomography model – RAYFRACT *(8)* output. Colors represent velocities, but the have been interpreted for material type.

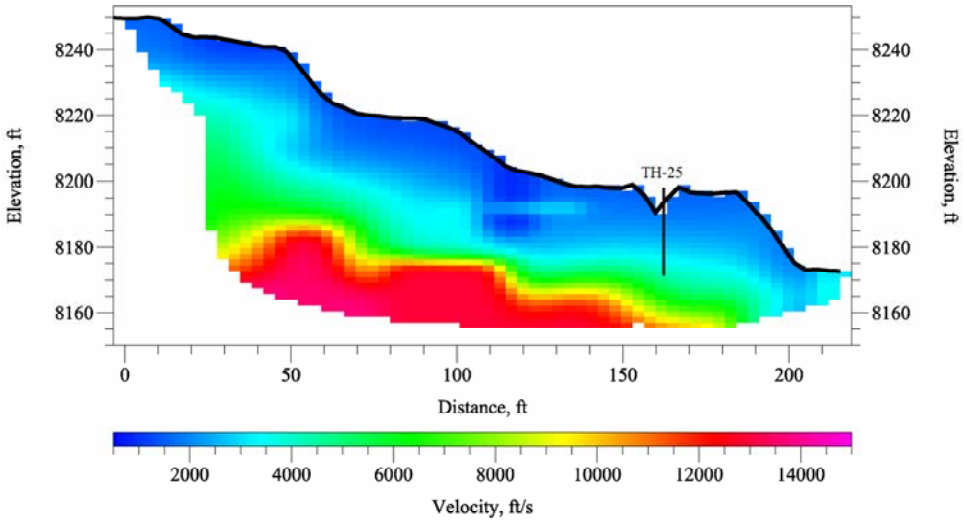

Figure 11. 2D refraction tomography Model – OPTIM *(8)* output. TH represents nearest geotechnical boring that drilled to top of rock, which correlates with a Vp of about 6,300 ft/sec.

Another approach to tomographic inversion, not discussed by Sheehan, is the synthetic annealing approach used by Pullammanappallil *(8)* and Optim *(9)*. An example output using the commercially available Optim software is shown in Figure 11. The lateral changes in velocity within a single layer are evident in the tomogram, and the resolution and variability of Vp within the soil (blue) and weathered bedrock (green) is evident. The hot colors (orange/red) were interpreted as competent bedrock (hard limestone) at this site in Vail, Colorado.

Each tomography algorithm utilizes specific velocity analysis steps (from Figure 2) to arrive at 2D velocity sections representative of the subsurface. None of the codes are applicable all the time, or in all the geologic conditions encountered. The benefit of propagating seismic waves and using wave equation theory to resolve lateral changes, which is a serious limitation of GRM, is the most beneficial attribute of refraction imaging using tomographic procedures. For most engineering applications standard travel-time (i.e., velocity) tomography is sufficient; however, when additional rock properties are required the attenuation tomography may be useful but additional source features are required. It should be noted that the results from the two different tomography approaches shown in Figures 10 and 11 are presented for example purposes only and do not constitute an endorsement by the authors, although we have implemented both (when appropriate) on consulting projects.

REFRACTION ANALYSIS USING THE GEOSTRUCTURAL ANALYSIS PACKAGE (GAP)

The Geostructural Analysis Package (GAP), recently developed by Summit Peak Technologies *(10)*, uses 3D refraction tomography rather than 2D GRM or tomography velocity analysis procedures. Integrating the Discrete Element Method *(10)* (DEM) of numerical modeling with Particle Flow Code *(11)* (PFC) is an approach to discretized earth or man-made material models, deform them in a dynamic mode, and manage the complex interaction of the system. The practical nature of this comprehensive modeling package, called GAP *(12)*, allows the material properties and interlocking mechanisms to interact. The sensible aspect that numerical modeling affords in a 3D geologic world is the unique opportunity to view materials and their interactions in 3D. The result of optimizing DEM and PFC for seismic applications is greater accuracy, faster speed for data processing, less memory requirements for the hardware, higher resolution of subsurface material characteristics, and more functionality for the output results. That is, results of numerical modeling produce a 2D, a 2.5D and/or a 3D model not simply *images*, as seen with GRM and refraction tomography. They are calibrated ground simulations *(13)*. The GAP DEM-PFC code has been used to perform forward or inverse modeling for various geotechnical applications.

Very similar initial steps for data analysis of GRM or tomography solutions occur for GAP velocity analysis also. However, an initial 3D volume with site coordinates, drill hole information, geotechnical data, and other available information (e.g., hydrogeology) is established that will include all the seismic data acquired. The refraction data can be acquired in either standard 2D format, which will produce 2.5D results, or in a full 3D acquisition mode which can be processed and interpreted in 3D.

Traditional arrival time picking is necessary in order to provide 2D and/or 3D analysis. The first step in processing and interpreting (any) refraction seismic data is to pick the arrival times of the signal, called first break picking. A travel time curve is then generated showing the arrival times versus distance between the shot point and geophone (Figure 5). A sample plot of seismic waveforms in the GAP model with arrival picks, is shown in Figure 12, as obtained beneath a receiver-line. The waveforms and travel-time data are entered into a 3D volume (i.e., a cube).

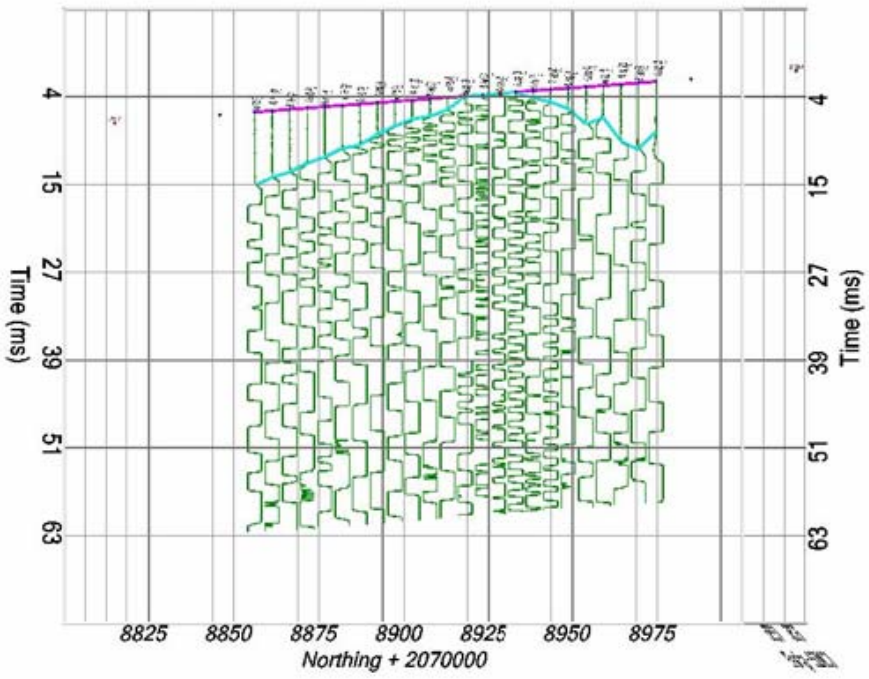

Figure 12. Shot record posted in a 3D GAP volume showing arrival picks (light blue), where the signals have been clipped for display purposes.

The first-arrivals are typically measured manually, or picked using an 'automated picker' algorithm. GAP uses a pattern recognition technique for consistent arrival-time picking across a line or for an entire project (site). The pattern recognition technique is similar to artificial intelligence algorithms.

First arrivals are then used to compute a 3D velocity tomogram (or model) from a uniform, high-velocity starting model as shown in Figure 13. The velocities within the volume are computed so that the arrival times of waves propagated through the 3D tomographic model match the first-break picks measured from the field data. Images from the volume can then be extracted to infer underlying lithology or estimate material volumes. If needed, GAP provides the advantage that additional stress analyses can be performed on the 3D DEM-PFC model for construction / excavation, loading, reinforcement, or slope stability assessment.

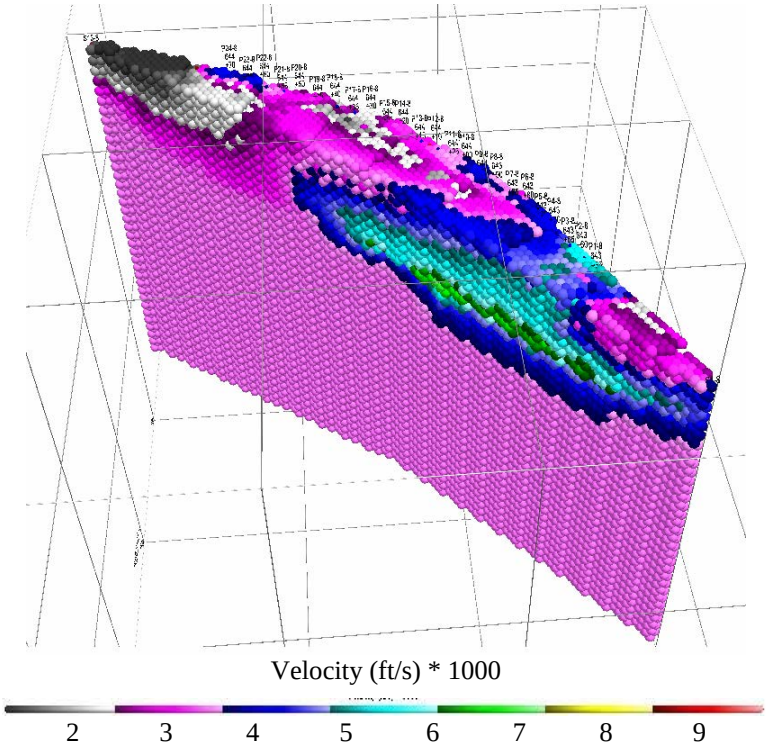

Figure 13. 3D GAP reconstructed velocity volume.

The velocities are determined iteratively using tomographic inversion. First, a seismic wave is propagated through the model for each source, to determine arrival times at each receiver. A plot of arrival times, shown as wavefronts, from a sample source point on the surface of the model is shown in Figure 14. Seismic energy travels faster through regions of higher velocity, resulting in pronounced refraction patterns which can be observed near the surface in the right portion of the image.

The *simulated* arrival times are then compared to the observed first-break picks from the field records. Adjustments to the velocities are required to resolve differences in arrival times. Tomographic inversion is used to determine where and how to change velocities within the GAP model to ultimately reduce differences in arrival times.

The tomographic inversion process used by GAP is simple and straightforward. A ray-path is determined for each source/receiver pair by adding the wavefront arrivals propagated from the corresponding source and receiver locations. Regions in the volume where this sum is close to the first arrival time are assigned a high ray-path probability. This source/receiver pair "ray-path region" is defined as the Fresnel zone. A simple example Fresnel zone, for a single source-receiver pair, is shown in Figure 15. Similar Fresnel zones exist for every source/receiver pair in the volume. A Fresnel zone often corresponds to the traditional ray-path, except that the zone has a larger cross-section in the center, and is narrow at the ends (e.g., shaped like a football). However, there are cases where the Fresnel zone approximates multiple ray-paths, as shown in Figure 16. In this case, the direct wave arrival along the surface (i.e., surface wave) is similar to the refracted arrival. Although the probability of the surface wave affecting the velocity function, if the simulated arrival is less than the first-break pick, the velocity within the entire region must be decreased to reduce the difference.

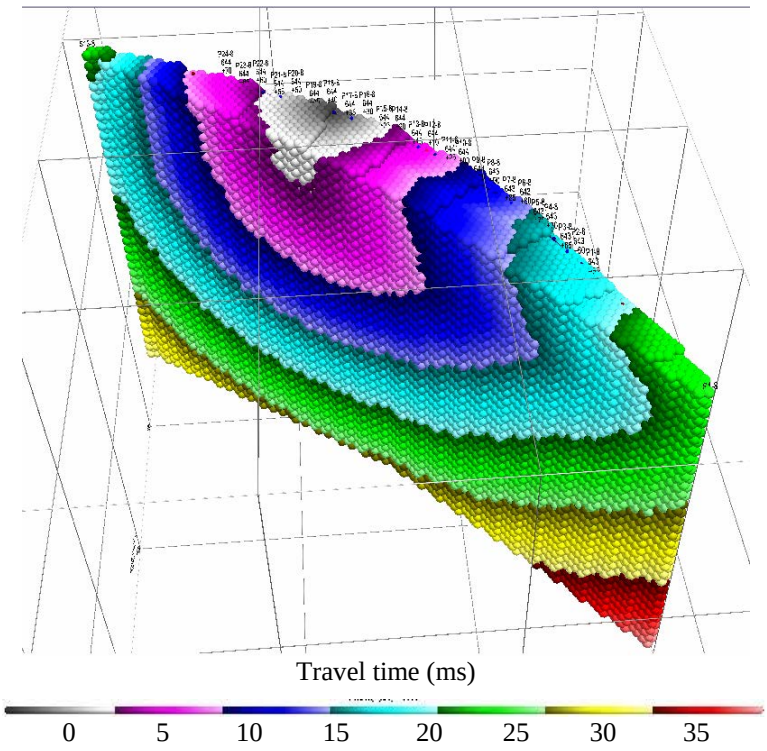

Figure 14. Arrival times as the wavefront propagates through the model from a source point on the surface.

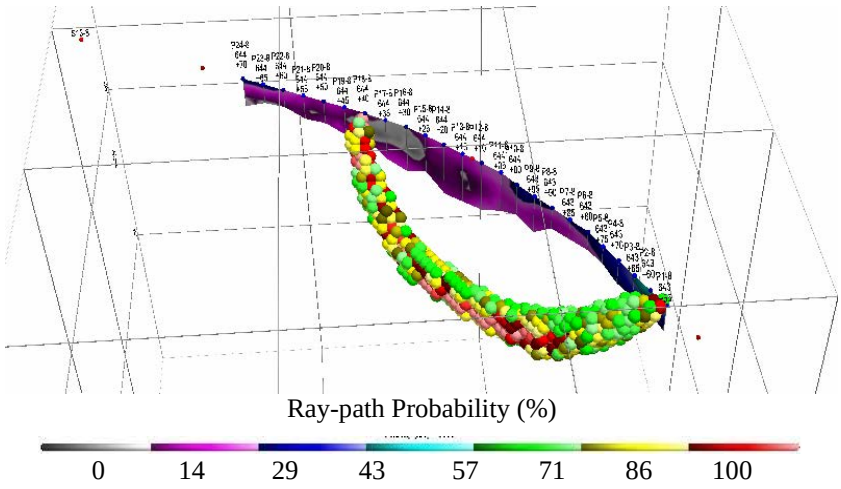

Figure 15. Single ray-path (i.e., Fresnel zone) from a mid-line source to a receiver at the beginning of the line.

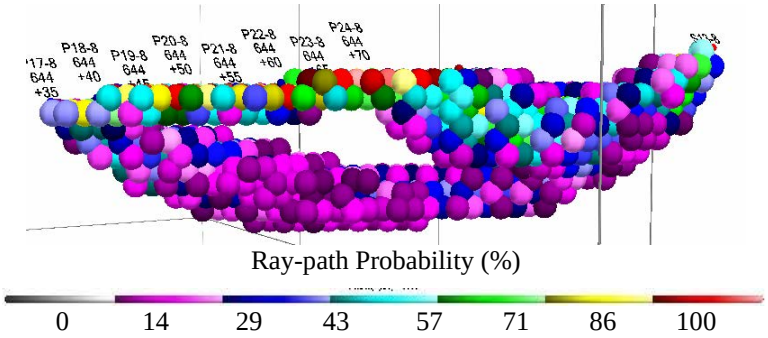

Figure 16. Multiple ray-path Fresnel zone.

The sum of all the individual ray-path regions for each source/receiver pair indicates the ray-path coverage of the survey. Various views of the ray-path coverage along a slightly curved shot-line are shown in Figure 17. Section (a) shows the ray-path coverage along the outside of the curve. This image shows that data is available only in very shallow regions beneath the receivers. Rays typically dive deeper as the separation between the source and receiver increases. The curve in the shot-line laterally displaces these longer ray-paths toward the inside of the curve. This results in shallow coverage, with no deep coverage, in the region along the outside of the curve. Section (b) shows the ray-path coverage along the inside of the curve. This region has deeper coverage, but no shallow coverage, for the same reasons. Section (c) shows that the ray-path coverage is mostly continuous, gradually moving from shallow coverage on the outside of the curve to deeper coverage toward the inside of the curve. This phenomenon would be important to consider when interpreting data using a less robust technique such as GRM, or when producing 2D tomography images below the shot-line.

The velocities within each Fresnel zone are updated proportional to the difference between the simulated arrival time and the first-break pick. Velocity changes for all the source/receiver Fresnel zones are combined according to a weighted average for each iteration. A plot of the reconstructed velocities within the ray-path coverage is shown in Figure 18. Section (a) shows the velocities within the full ray-path coverage. Section (b) is a cross-section showing internal velocities reconstructed on the inside of the curve. The depth of the bedrock at this point can be seen from deeper data on the inside of the curve. Section (c) shows a 2D cross-section of data beneath receivers.

Usually 6 to 8 iterations are required for solution convergence using this technique. Convergence thus requires about 1 to 2 minutes on a typical desktop (Pentium-type) computer, depending on desired resolution. Resolution is discretized by the DEM modeling, and definition of the element size.

Figures 19 and 20 show various views of a GAP 3D survey results from three parallel seismic lines. Future surveys with sources outside the traditional ‘linear array’ seismic line, or with sources and receivers spread out over a larger area, could provide more accurate 3D inversion results.

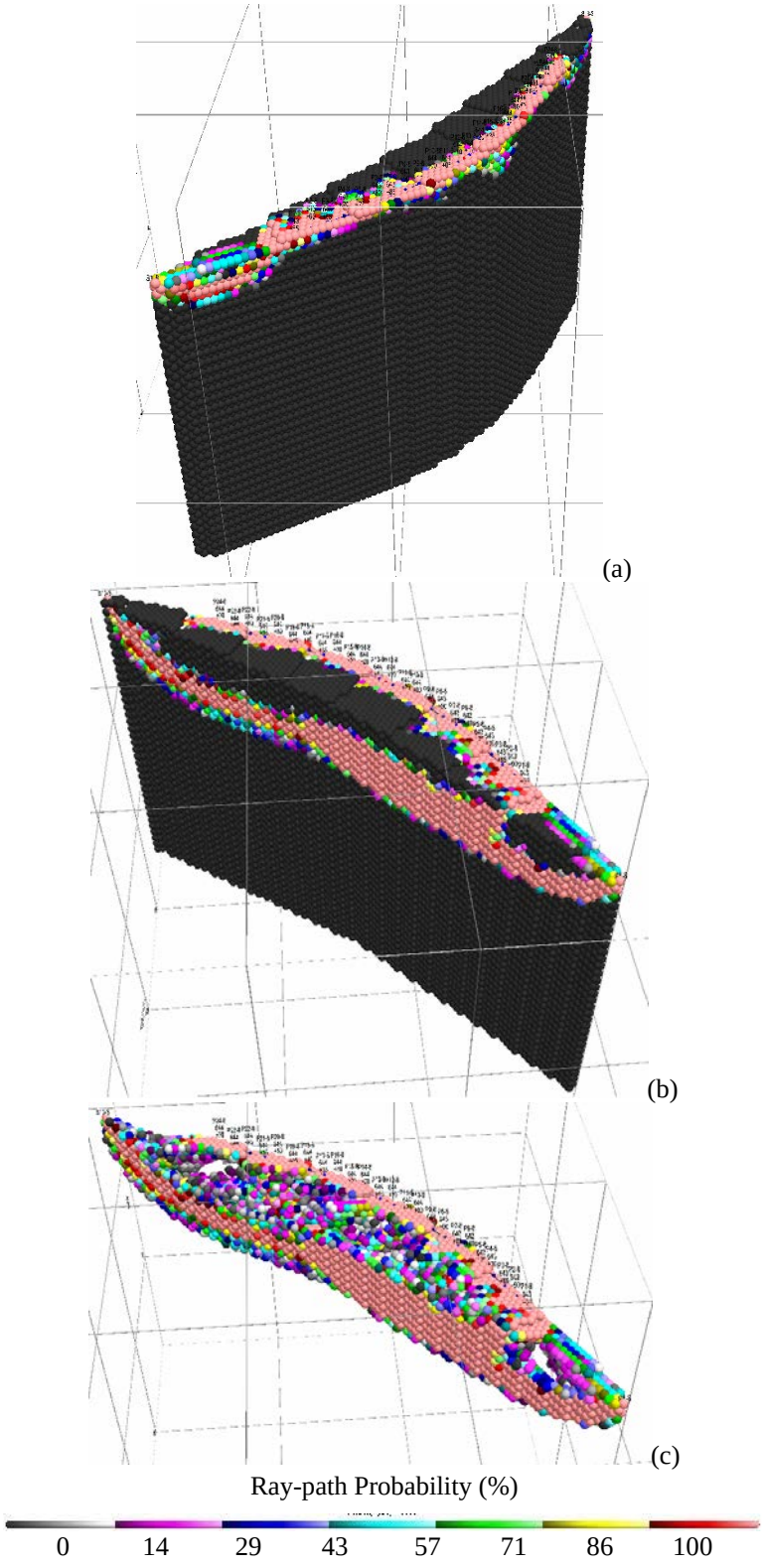

Figure 17. Ray-path coverage. (a) Outside of curve has shallow coverage, (b) inside of curve has deeper coverage, but no shallow coverage, and (c) continuity of coverage.

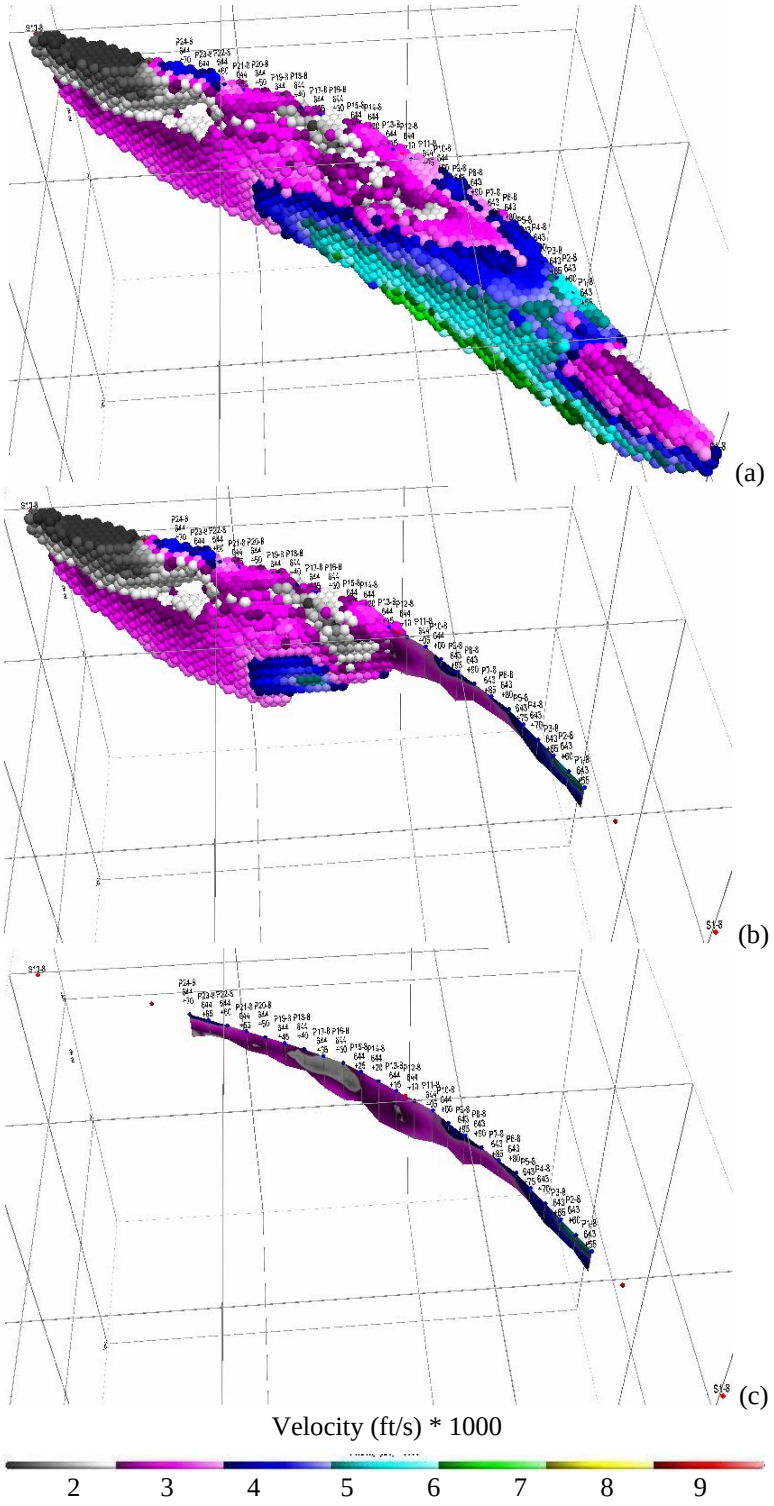

Figure 18. Tomography velocities plotted within 3D ray-path coverage along a curved seismic line. (a) Full ray-path coverage, (b) cross-section, and (c) 2D velocity section beneath the receivers.

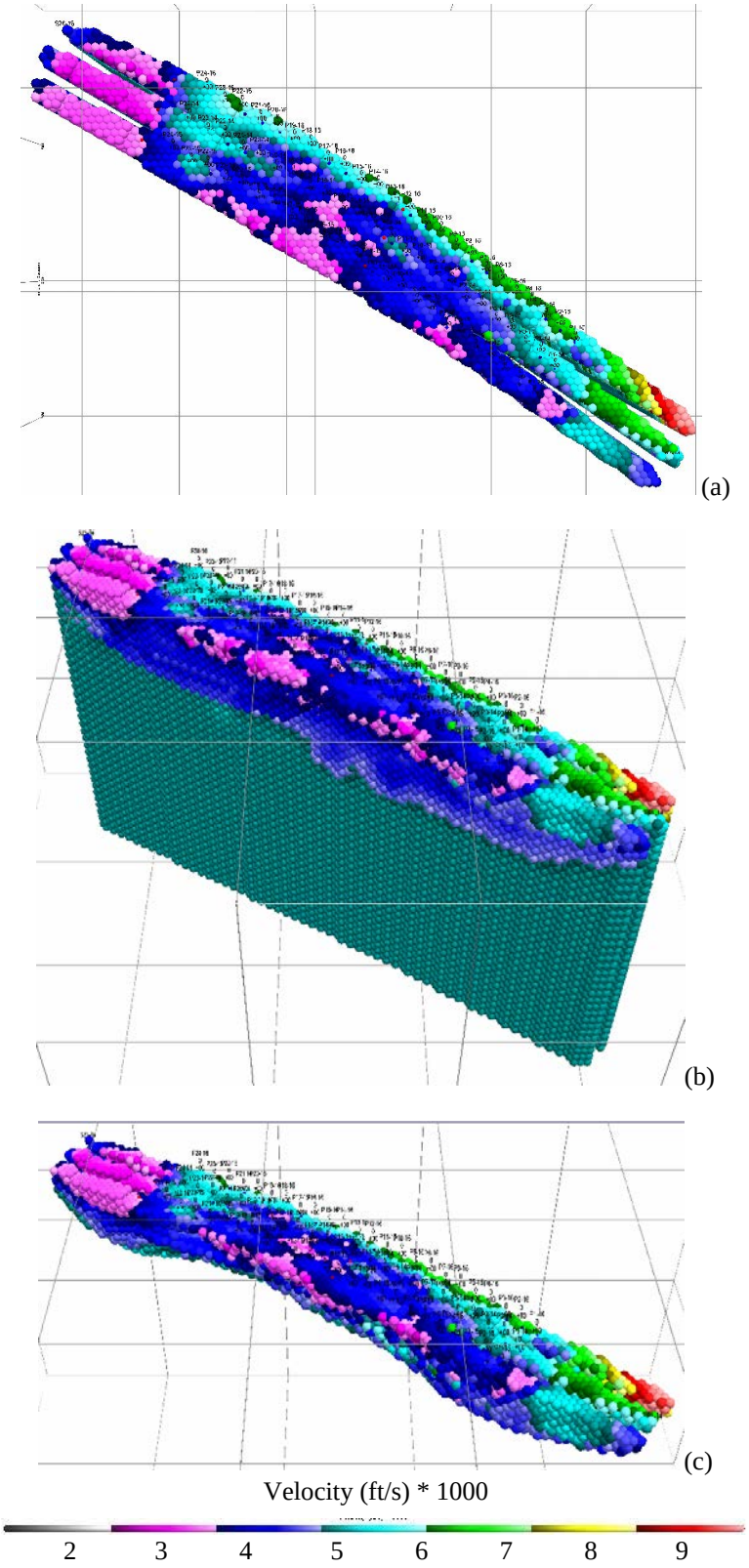

Figure 19. 3D GAP survey data. (a) Plan view, (b) orthogonal view, and (c) ray-path coverage.

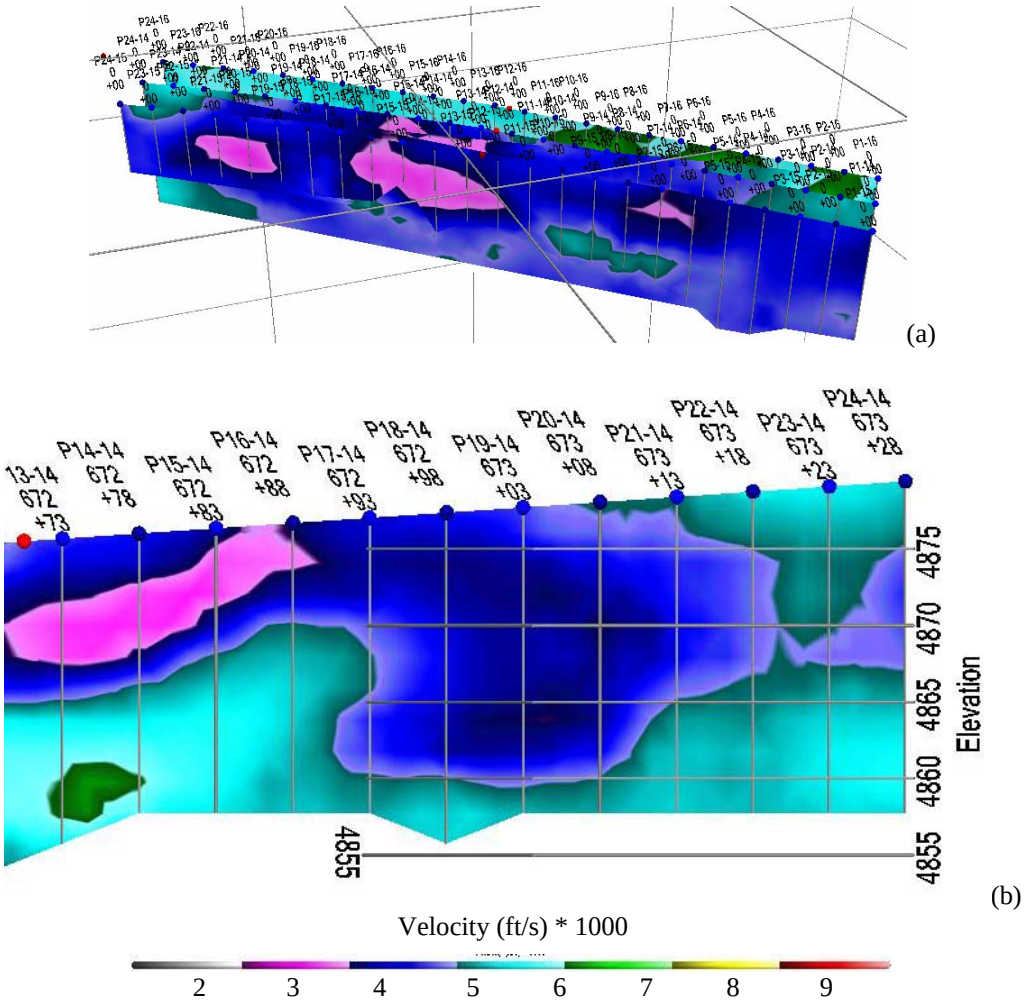

Figure 20. Panel views of (a) 3D survey, and (b) 2D segment extracted from a piece of the central panel.

ACKNOWLEDGEMENTS

The authors would like to thank a few professionals, each of whom have processed data with standard GRM methods, and refraction tomography techniques, as well as contributed to this paper: Dr. David Butler (MicroGeophysics Corp.), Chet Lide (Zonge Geosciences, Inc.), and Khamis Haramy (Central Federal Lands Highway Division – FHWA).

REFERENCES

1. Enviroscan, Inc. , http://www.enviroscan.com/html/seismic_refraction_versus_refl.html . Accessed June 12, 2006.
2. Butler, D., Seismic Refraction Method Appendix, MicroGeophysics Corporation, Wheat Ridge, Colorado.
3. Quake Trackers, Inc. http://www.gns.cri.nz/outreach/qt/quaketrackers/seismo_refract.htm. Accessed June 10, 2006.
4. Federal Highway Administration. *Central Federal Lands Highway Division*. U.S. Department of Transportation. http://www.cflhd.gov/agm/. Accessed June 12, 2006.

5. Palmer D., 1981, An Introduction to the Generalized Reciprocal Method of Seismic Refraction Interpretation, *Geophysics*, Vol. 46, pp. 1508-1518.

6. Sheehan, J.R., W.E. Doll, and W.A. Mandell, 2005, An Evaluation of Methods and Available Software for Seismic Refraction Tomography Analysis, *Jour. Of Environmental and Engineering Geophysics*, Vol. 10, No. 1, pp. 21-34.

7. Intelligent Resources, Inc., RAYFRACT *Seismic Refraction Tomography*, http://rayfract.com/ . Accessed June 10, 2006.

8. Pullammanappallil, S., J.N. Louie, 1994, A generalized simulated-annealing optimization for inversion of first-arrival times, BSSA, Vol. 84, pp. 1397-1409.

9. OPTIM, Inc., 2005, SeisOpt@2d, (Ver. 4.0), www.optimsoftware.com . Seismic Refraction Tomography Software (copyright), University of Nevada, Reno, Nevada.

10. Summit Peak Technologies, LLC., http://www.summitpeak.net/ . Accessed June 10, 2006.

11. Zhang R. and S. Sture, Discrete Element Particles Analysis at Low Stress States, *in Proceedings of the 10th ASCE Engineering Mechanics Specialty Conference.* 1995.

12. Itasca Consulting Group, Inc., 2003, PFC3D (*Particle Flow Code in 3 Dimensions*), Ver. 3.0. 656 pp.

13. Sirles, P., A. Rock and R. Zhang, NDT Technologies and Unknown Foundations, *in Presentations and Notes, FHWA Unknown Foundation Summit*, Lakewood, Colorado, U.S. Department of Transportation. 2005.

14. Rock A. and R. Zhang, 2002, Acoustic model calibration, *in Proceedings of the American Society for Composites 17th Technical Conference.*

Subsurface Modeling Using Seismic Refraction Data

Phil Sirles
Zonge Geosciences, Inc.
1990 Garrison Road, Suite 6
Lakewood, CO 80227
(720) 962-4444
phils@zonge.com

Alan Rock
Summit Peak Technologies, LLC
6121 N. Powell Road
Parker, CO 80134
(303) 841-0988
arock@summitpeak.net

Khamis Haramy
FHWA - Central Federal Lands Highway Division
12300 West Dakota Avenue, Suite 210
Lakewood, CO 80228
(720) 963-3521
Khamis.haramy@fhwa.dot.gov

ABSTRACT

Standard geophysical survey practice using seismic refraction techniques has predominantly produced two-dimensional cross sections of the subsurface. The state-of-the-practice for nearly three decades has been to process refraction data with layer reconstruction techniques using the generalized reciprocal method, time-intercept and other similar techniques. Within the past decade, advancements in the computer technology and the development of tomographic modeling algorithms have greatly increased the ability to detect subsurface anomalous features, increase lateral and vertical resolution, and provide better graphical presentation of the data. Recently, 2D finite-element modeling of seismic data has proven successful to image discrete anomalies such as voids.

This paper presents recent developments in a new approach for processing refraction data, the presentation of subsurface data, and the use of these data after geophysical modeling is complete. The approach adapts numerical modeling using the discrete element method and particle flow code (DEM-PFC). The procedure is termed the *Geostructural Analysis Package (GAP)* which, in its initial stages of development has been optimized for geotechnical applications, such as 2D and 3D seismic refraction data processing and presentation on engineering projects. Although GAP has not been primarily created for seismic refraction, this paper will illustrate significant advancement in refraction data processing. Currently, using GAP for seismic applications represents an innovative approach that includes improved data analysis processes and produces more functional result for the end users. For the application illustrated in this paper the end users are typically civil or geotechnical engineers. The value of using this approach for seismic applications is its ability to produce 2D, 2.5D and 3D models to assist engineers or geologists extract additional information from the geophysical data (e.g., material properties), or perform static and dynamic stress analysis. This paper makes the point that mapping the top of bedrock may be the *objective* of a geophysical survey, but it is not the engineering *purpose* for the site investigation (e.g., construction of a critical facility, design of a foundation for a structure, etc.). With high-quality calibrated 2D, 2.5D and 3D DEM-PFC *models*, not geophysical *images*, engineers are more likely to use the seismic results by incorporating them directly into their engineering analyses.

Results from two case histories are presented showing the benefit of assessing seismic refraction data using the DEM-PFC numerical modeling approach. In the first example, standard 2D refraction data were analyzed and the interpolated results were presented as a 3D model. The second example is a 3D surface tomography reconstruction of four slightly offset 2D refraction shot lines.

INTRODUCTION

Conventional seismic refraction *'first-arrival time'* data have been processed and presented utilizing a number of methods for a very long time. Palmer's *(1)* approach using the generalized reciprocal method (GRM) has been the industry standard for assessing a layered earth using first (refracted) arrival times of body wave energy to produce images of the subsurface. It has been effective, proven, and incredibly valuable as a method to analyze refraction data. Similarly, over the past decade multiple refraction tomography algorithms have been developed as the 'next generation tool' for data analysis, presentation and visualization of refraction data. These newer, more complex mathematical approaches, all termed tomography, vary to some degree in their analysis, but the image results are generally comparable *(2).* In either case, GRM or tomography, the analyses produce two dimensional (2D) images of the subsurface. These 2D images represent the geophysical results provided to the engineers (for example) for the next phase of site investigation or design. More recently, 2D finite difference modeling of wave propagation has successfully demonstrated the strength of using numerical modeling as an approach to analyze elastic wave propagation and deformation *(3, 4).* Gelis *(5)* was particularly successful applying finite difference modeling as a means of using surface–wave energy to detect shallow cavities and create 2D models.

The purpose of this paper is to introduce a new approach to analyze seismic refraction data. Clearly, GRM, refraction tomography, and 2D finite difference models each have their value, strengths, and weaknesses (like all geophysical data analysis methods). The goal is to continue promulgating surface seismic investigations using refraction field techniques, and additionally offer alternative means to fully address the purpose of the engineering or environmental application. Not all field programs need advanced numerical modeling to process seismic data, but when complex geologic environments or engineering problems carry high risk associated with the results, more sophisticated and robust approaches may be required.

Numerical modeling using discrete element method (DEM) code is not new as it has been applied by Zhang and others *(6; 7, and 8).* However, optimizing the advantages offered by the numerical modeling codes (either FEM or DEM) to create a more comprehensive modeling package is a significant advancement. The advantage of FEM over DEM is its ability to efficiently work with continuum under static conditions. The advantages gained though the use of DEM analysis is its ability to deal with discontinuities and manage element interactions in dynamic models. FEM and DEM techniques can each support these separate capabilities, although rather inefficiently and with significant limitations.

Integrating DEM numerical modeling with particle flow code (PFC) is an approach to discretize earth or man-made material models, deform them in a dynamic mode, and manage the complex interaction of the system. The practical nature of this comprehensive modeling package, called GAP *(9)* allows the material properties and interlocking mechanisms to interact. The sensible aspect that numerical modeling affords in a 3D geologic world is the unique opportunity to view materials and their interactions in 3D. The result of optimizing DEM and PFC for seismic applications is greater accuracy, faster speed for data processing, less memory requirements for the hardware, higher resolution of subsurface material characteristics, and more functionality for the output results. That is, results of numerical modeling produce 2D, 2.5D and 3D model not simply *images*. They are calibrated ground simulations *(10).*

The GAP DEM-PFC code has been used to perform forward or inverse modeling for various geotechnical applications. Through two case histories presented herein, the approach and value of producing results in models (versus images) will be shown. The Micro Model Method is similar in some ways to what was developed by Itasca *(11, 12)* in the approach they call particle flow code. GAP and PFC use the same fundamental element interaction equations used in DEM. Therefore, the mathematical approach uses well established numerical modeling techniques. The current version of GAP has been optimized for seismic wave propagation, for both forward and inverse modeling. It supports tomographic and holographic inversion, and soon will support full-waveform seismic inversion. The full-waveform inversion module is currently under development. The package, in its current form, includes a wide range of built-in digital signal processing capabilities, such as filtering, automatic first arrival-time picking, and common source/receiver comparison in 3D geometry. The modeling uses a rapid consolidation algorithm developed by Dr Runing Zhang *(8).* This modeling package can model geotechnical materials such as rock, soil, dry or wet sand, construction materials such as wood, steel, and concrete, or fluids. It can model the interaction between different materials, including solids and fluids, friction, and other interlocking mechanical systems. The ability to model discontinuities such as cracks, distinct layers, and blocks of arbitrary shape, including dynamic crack propagation is a distinct advancement. It is efficient for both static load analysis and dynamic simulation. Modeling very small-strain deformations such as seismic wave energy, up to large deformations such as mine subsidence or slope failure can also be performed.

The GAP code is the most comprehensive numerical modeling and seismic analysis program, which was developed over the past year, for practical near-surface engineering and environmental applications. Because GAP is not a refraction *imaging* package, the following paragraphs were included to shed light on the breadth this technology has beyond the refraction application presented here. That is, the code is being used to model chemical processes, and supports modeling cement hydration in concrete *(13)*. This includes modeling the thermodynamics of heat flow from the heat of hydration generated during the concrete curing process, and heat transfer to the surrounding environment. The DEM-PFC technology is being developed further to model ground water flow, membranes for geosynthetics, MSE-type retaining walls, and thin supports systems such as soil nails, roof bolts, and rebar (Rock, *in progress*).

Using numerical modeling, this approach can support numerous boundary conditions for stress analysis, including static and dynamic vertical and lateral loads. Similarly, dynamic constraints for seismic analysis are supported and static and dynamic simulations can also be easily generated. Extensive front-end user interface for model initialization has been developed allowing complex geological formations and structures to be quickly constructed (in 2D or 3D). Geologic features such as faults, voids, cracks, layers, karstic bedrock, radical ground surface topography, lakes, and rivers can be integrated into the model. Man-made structures can be quickly generated, including reinforced concrete, rockery walls, piles, shafts, and tunnels for other geotechnical applications. In the seismic application, a distinct advantage of the DEM-PFC method is the ability to process as many source/receiver positions as necessary to meet the project objectives. Source and receiver arrays can be either on the ground surface or in a crosshole configuration. Positional accuracy of sources and receivers is very important to produce calibrated earth models.

The back-end data visualization and reporting capabilities are very useful for the end users of the data. Various material properties such as velocity, stress, compression, acceleration, displacement, material density, and cracking, can be displayed. This is accomplished by using different palettes, contouring, slicing (not just horizontal or vertical slices); and of course, rotating, translating, or enlarging the resultant model volume. Any combination of materials, velocity ranges, stress ranges, etc, can be hidden or displayed. Output into animated slide presentations (e.g., Microsoft PowerPoint), AVI movie files, or complete MS Word documents (reports with figures, captions, and text) have been automatically generated through the GAP process.

Several seismic techniques have implemented the GAP process such as crosshole tomography, crosshole sonic logging, and surface refraction. Applications vary from bedrock mapping, determining layer thickness and stiffness, volume calculations, geotechnical boring interpolation, driven pile assessment, rockery walls with wedge-type failure, assessment of drilled shaft integrity, concrete curing, slope stability, rock fall barrier evaluation, and avalanche modeling. The two geotechnical case histories illustrated in this paper are fully integrated field programs implementing parts of the GAP numerical modeling process.

APPROACH

The approach to using the DEM-PFC technique can best be illustrated through a series of diagrams or models. The model is made up of what can be thought of as a system of *elements* and *links*. The discrete elements can be described as a set of spherical elements, or balls. Each ball has it own property (e.g., velocity), and the *links* between each element represent a series of spring-and-dashpot resistant forces. Both the elements and connective forces (links) are initially set in the model, but they are both iteratively varied to produce an earth model with the same seismic response as measured by seismic data collected in the field. Survey objectives and required definition for a particular application dictate the model size and resolution.

Figures 1a through 1h, described in the following paragraphs, illustrate the capability of DEM-PFC type modeling. Sources and receivers can be placed at any position in a model. The model is a 10-foot by 10-foot 2D grid representation. Figure 1a presents the model that includes surface topography, has a resolution of 0.5 feet (i.e., 2 elements per foot), and shows move-out of a seismic wavefront in a homogeneous medium. Arrows indicate wavefront direction from a point source. GAP models use a tight tetrahedral node packing instead of a cubic grid. Figure 1b represents the same model at a resolution of 0.1 feet. The wavefront should be a perfect circle for a model with zero error (very close for initial model). With only a slight modification the model can now simulate a layer of soil overlying a competent bedrock rock interface (Figure 1c). Figure 1d shows a plot of the initial model velocities. The velocities of the elements are only shown for reference. The actual velocities are carried in the links, and allow for anisotropic inversion.

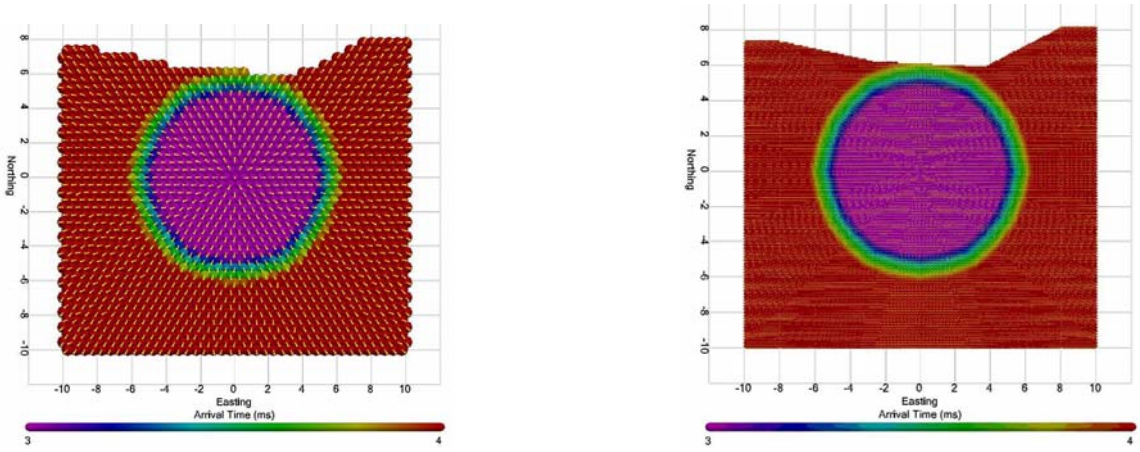

(a) (b)

Figures 1a & b. Wavefront arrival times in a homogeneous DEM model with a point source at 0,0; different resolutions (0.5 feet in a. and 0.1 feet in b) represent 2 and 10 elements per foot, respectively.

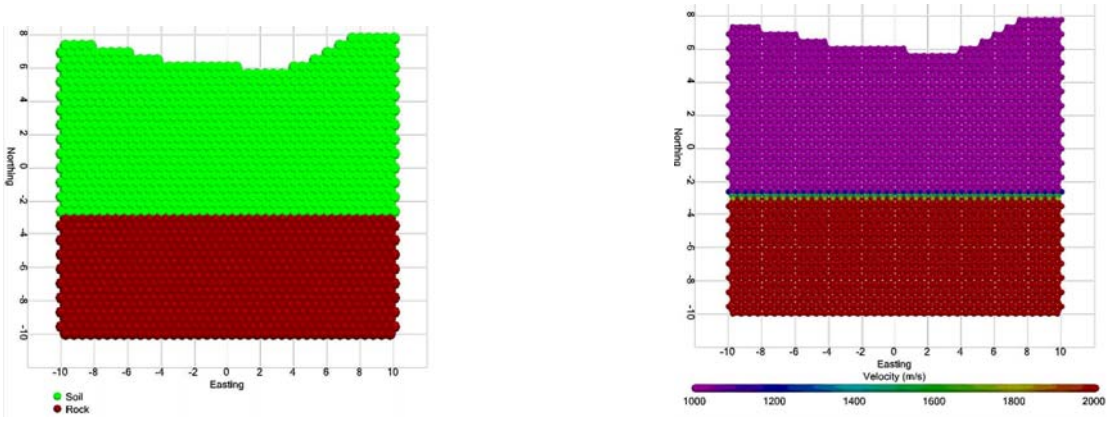

(c) (d)

Figure 1c & d.Initial earth model with soil overlying rock (c) and initial model velocities (d).

Figure 1e shows move out of the wavefront for a source originating at grid coordinate 0E,0N in the earth model (easting coordinates given first in GAP model space). As anticipated, the wavefront expands faster in the higher velocity rock. Yellow wavefront direction arrows are shown in the elements, where direct and refracted energy can be observed.

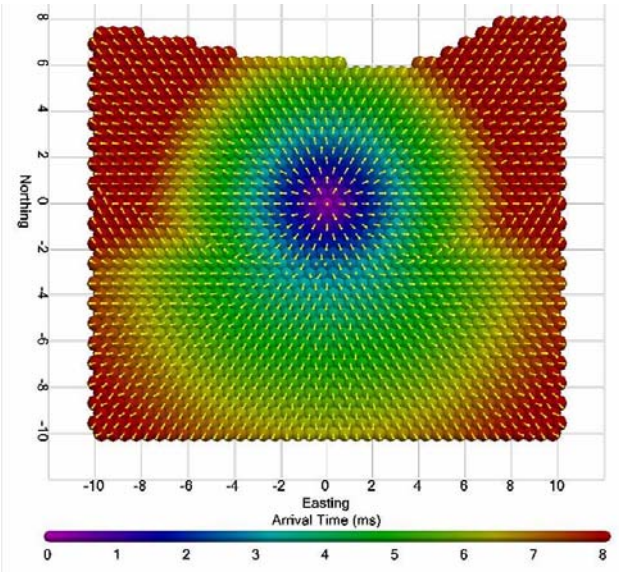

(e)

Figure 1e. Wavefront from a point source moving through the earth model.

A "*straight ray-path*" simulation with a source at (-8,1) and a single receiver at (8,6) is shown in Figure 1f. Seismic waves do not travel in straight ray-paths through anisotropic earth materials. The elliptical region corresponds to the area most likely to affect measured arrival times, and is used for model inversion,. Figure 1g shows a "*curved ray-path*" with a source at (-8,1) and a receiver at (8,-7). The ray-path area is wider in the higher velocity (rock) portion of the model. Note the sharp bend at the soil/rock interface.

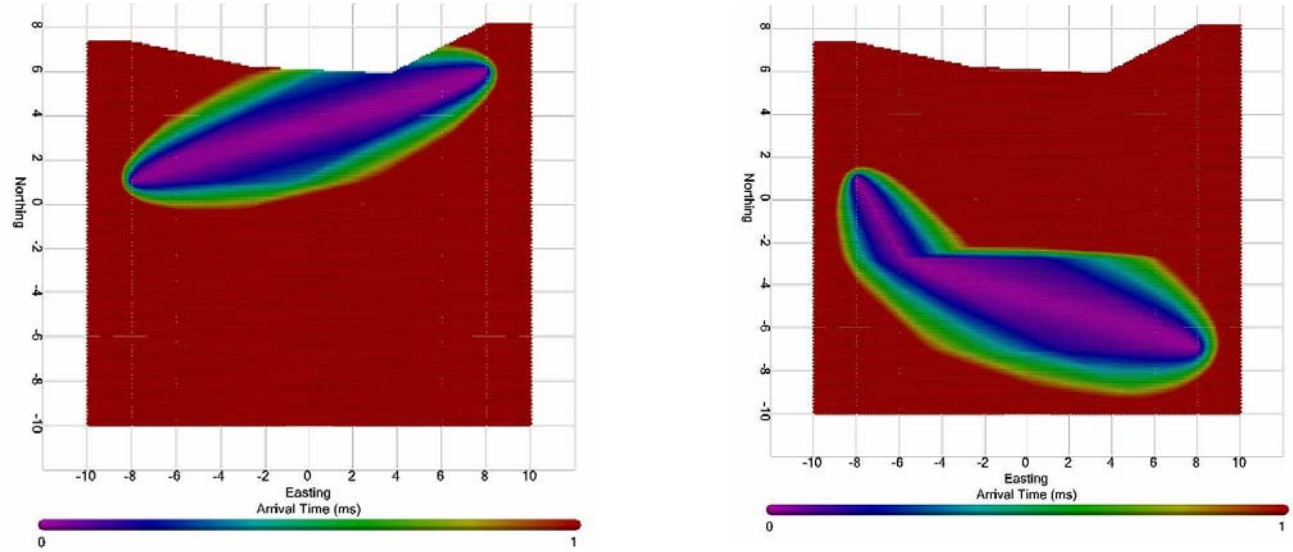

(f) (g)

Figure 1f & g. Straight ray path arrival time models in the soil layer (f), and curved ray path arrival times starting in the soil and propagating across the soil/rock interface (g) – the arrival time scale is normalized to 1.

To illustrate the DEM-PFC capability, Figure 1h presents a "*multiple ray-path*" waveform move out simulation with a source at (-8,1) and a receiver at (8,3). One region corresponds to part of the wave traveling directly through the soil layer, and the other region corresponds to refracted wave energy propagating through the rock layer.

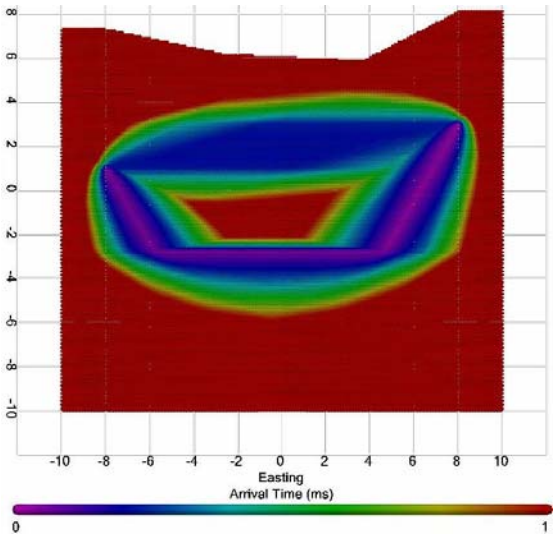

(h)

Figure 1h. Multiple ray-path wavefront moving through the earth model – the arrival time scale is normalized to 1.

This modeling approach cannot only model forward modeling simulations (as shown in Figures 1a-1h), but also can to produce refraction tomograms from inverse modeling of field data. The procedure is complete with pilot signal correlation (for chirp signals), digital signal filtering, automated first-arrival time picking, and supports borehole deviation surveys, all in either 2D and 3D.

CASE HISTORIES

The following two sections present case histories where geophysical testing, using standard 2D seismic refraction field techniques, were conducted for geotechnical investigations. For legal reasons, in both instances, at the client's request site details and project-specific data are not included because (at the time of this publication) they have not yet been released. Both projects are currently active and the geotechnical exploration programs have not been completed. Where geologic and/or geotechnical data are available (and permission granted to present) they are shown, and were incorporated into the GAP modeling.

Condominium Development, Vail, Colorado

In the spring of 2005 geotechnical borings were placed in accessible areas of a proposed multi-level condominium complex located adjacent to a ski slope at Vail, Colorado. The geotechnical exploration program was limited by thick forest vegetation and steep slopes – a black diamond ski slope. In mid-summer Zonge Geosciences began a seismic refraction investigation to supplement the geotechnical data. The objectives were: to map the top of bedrock; determine thickness of overburden soil; and, to evaluate the variability the soil and competency of the bedrock.

The geophysical survey area dimensions were roughly 350 feet north-south and 500 feet east-west. Figure 2 shows a site map, identifying locations of nearby buildings, geotechnical borings, and the seven seismic refraction lines. The area of investigation rises steeply to the south with a slope varying from 20° to 40°. Site geology generally consists of colluvial soils over a weathered bedrock contact, that grades to competent bedrock. Overburden soils predominantly consist of loose, unconsolidated coarse-grained materials (sands, gravels, cobbles and boulders) that range from saturated to unsaturated, depending on the season. The bedrock consists of the sandstone, limestone, and shale of the Minturn Formation. Geotechnical data indicate the soils thickness in the geophysical survey area ranges from 0 feet (i.e., a rock outcrop on the north end of Line 2) to about 50 feet in the southwestern portion of the survey area. Based on blow counts obtained in the soils the relative density varies considerably; and, rock quality also varies dramatically based on core samples and RQD.

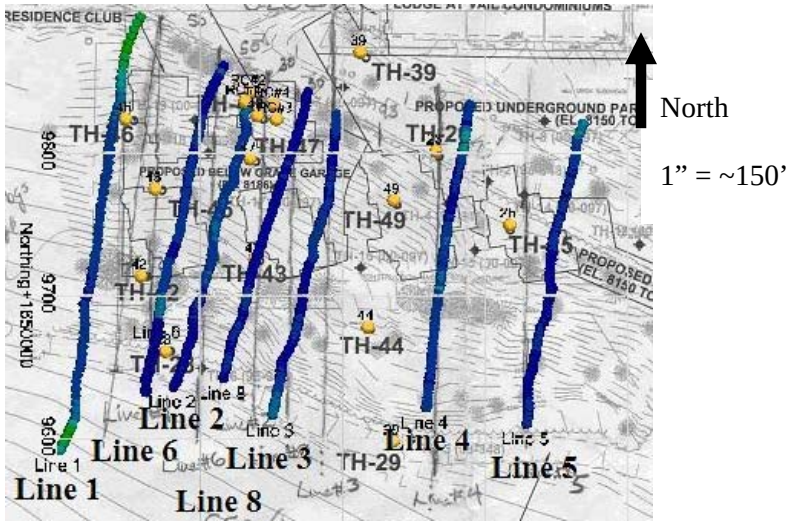

Figure 2. Geophysical survey area showing seismic lines (blue), and geotechnical borehole locations (yellow). The base map shows a proposed layout for six new condo buildings.

GPS coordinates were acquired for most of the geophone and shot locations, however a few positions were interpolated due to poor quality GPS data obtained in the trees. Seismic refraction data were acquired with the following field parameters: a 24-bit seismograph, 24 8-Hz vertical phones, 10 foot receiver spacing (except Line 1 which used 15-foot spacing); hammer and plate source; a minimum of nine shot points per line; 0.25 millisecond sample rate SEG2 records; and a 500 msec record length.

The 2D GAP refraction data processing package had not been fully completed to analyze the data from this project. Therefore, initially data processing involved tomographic inversion using a synthetic annealing algorithm developed by Pullammanappallil and Louie (14). Tomographic analysis was performed using SeisOpt@2D™, a commercially available 2D refraction tomography imaging package through Optim Software (15).

All seven lines were processed with the same parameters in SeisOpt@2D, and results from 3 lines are presented here. Tomograms from Lines 5, 6, and 8 are presented in Figures 3a, b and c, respectively. The 2D images show the velocity distribution below the refraction line. Interpretation of the P-wave velocities obtained indicate: 1) low-velocity materials interpreted as the overburden colluvial soils (shaded in blues / cool colors); 2) moderate-velocity materials interpreted as weathered bedrock (shaded in greens); and, 3) high-velocity materials interpreted as competent bedrock (shown in yellow and red / hot colors). Data quality was very good for all lines and showed consistent interpretations.

Borehole information, including elevation for top of bedrock, was provided by the geotechnical engineers. These borehole data (labeled TH for test holes in Figures 3a-c) were projected onto the nearest velocity line. Test hole projection was done 'along the elevation contour', as recommended by the geotechnical engineer. By mathematically comparing the top of bedrock encountered in all the borings to the velocity data produced with tomography, it was determined that the break over from overburden soil to bedrock occurs at an average P-wave velocity of 6,300 feet/second (light green). There is a gradational boundary between the overburden and bedrock, probably caused by variable degree of weathering on the bedrock interface, as documented in the test hole logs. Competent bedrock was detected beneath each line (yellow-red). Although, the depth to- and the amount of- hard bedrock appears to be quite variable between each of the seven lines. This layer interpreted as competent limestone bedrock was not encountered during test hole drilling.

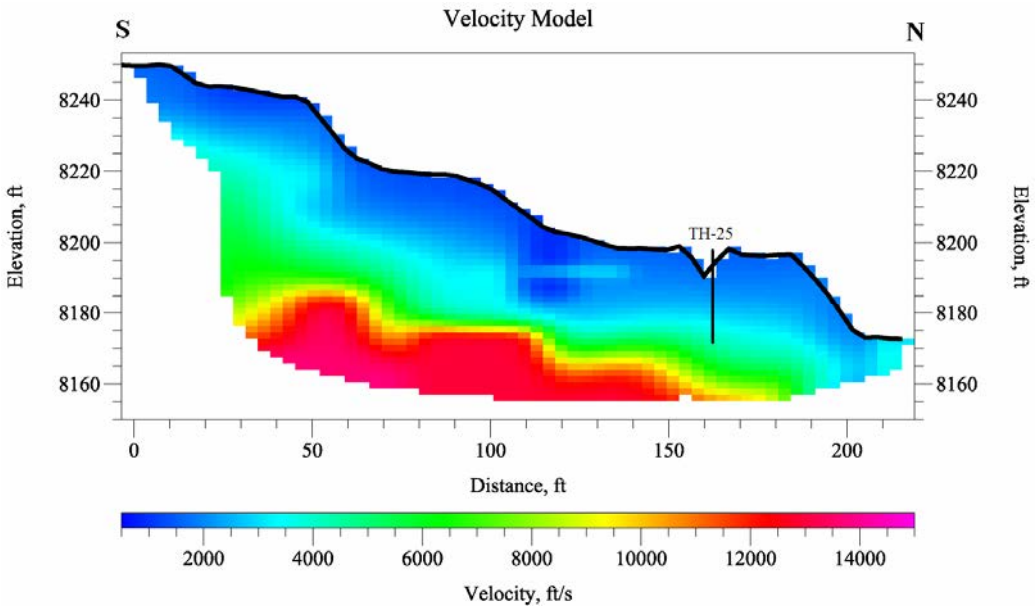
Velocity Model
S
N
TH-25
Elevation, ft
8240
8220
8200
8180
8160
0
50
100
150
200
Distance, ft
2000
4000
6000
8000
10000
12000
14000
Velocity, ft/s

(a)

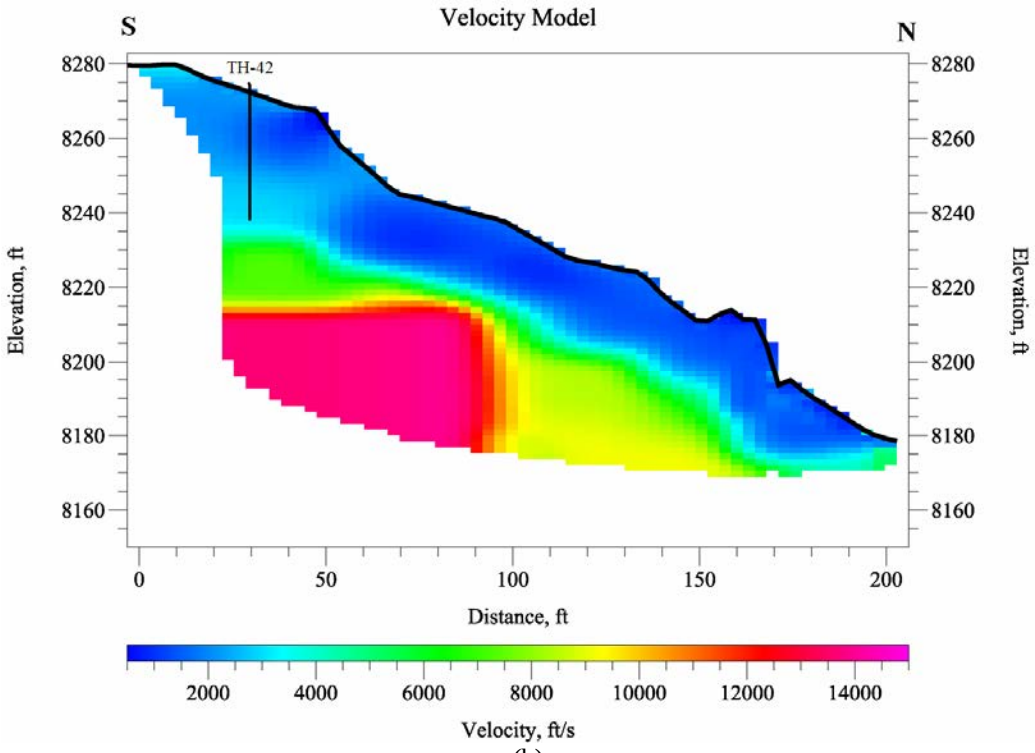
Velocity Model
S
N
TH-42
Elevation, ft
8280
8260
8240
8220
8200
8180
8160
0
50
100
150
200
Distance, ft
2000
4000
6000
8000
10000
12000
14000
Velocity, ft/s

(b)

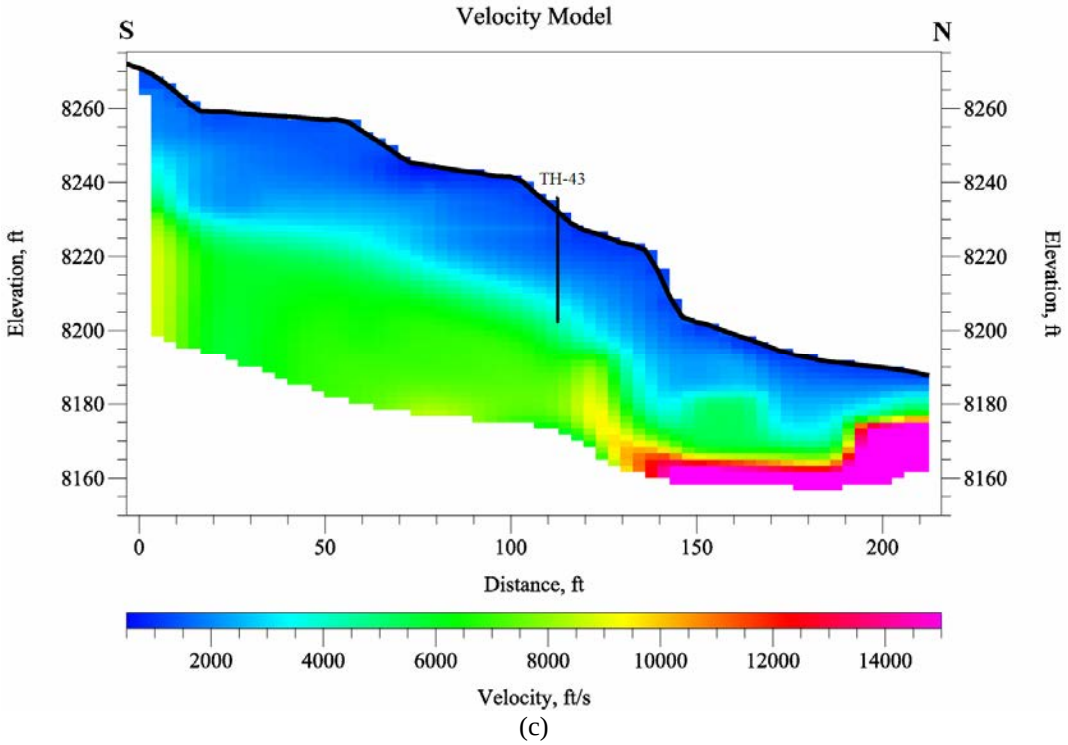

(c)

Figure 3. 2D Refraction tomograms for Line 5 (a), Line 6 (b), and Line 8 (c). TH represents nearest geotechnical boring and the line represents the soil thickness as measured in the TH (i.e., top of rock).

Advanced 3D modeling was requested by the client to gain a greater understand the irregular bedrock surface for design, excavation, and construction of the condominiums. With the 2D velocity tomography results, and good borehole control a calibrated GAP 3D velocity model could be constructed for the survey area. Contoured isosurfaces were generated with both the velocity and the borehole data using a B-spline interpolation with non-symmetric linear Voronoi Basis functions. This technique was used for all the elevation data and for combining the 2D velocity profiles with the geotechnical borehole information to provide a calibrated 3D model. Each individual velocity profile (as shown in Figure 3) was used to assess competency of the rock. However by calibrating the velocities using borehole data, the GAP models provided: "3D soil thickness (isopach)" (Figure 4); and "3D top of weathered bedrock" (Figure 5) as well as "3D top of competent bedrock" (Figure 6) isosurfaces. These 3D models show only one perspective view (generally looking south towards the mountain). Of course the 3D model can be rotated for any perspective, and different velocity slicing produces unique isosurfaces. The 3D model will be used to evaluate the thickness of the overburden soil deposits, the relief of the weathered bedrock and the extent of competent bedrock and how it affects foundation design and construction of a 5-story underground garage. Figure 7 shows a plan (2D) depth to bedrock map produced through the GAP DEM-PFC analysis which incorporated the geotechnical borehole and the geophysical seismic data.

The seismic data for this project were acquired in 2D. The mathematical interpolation between lines created 2.5D images of the subsurface, but the models shown in Figures 4, 5 and 6, are not just images. The represent a 'snap shot' of the GAP model that will be used for the next phase of work – design and construction of structures. This is the value added, or the advancement that DEM-PFC modeling of seismic data brings our industry. Whether the GAP data are presented in 2D, 2.5D or 3D they are calibrated models, not images, to be used by the engineers.

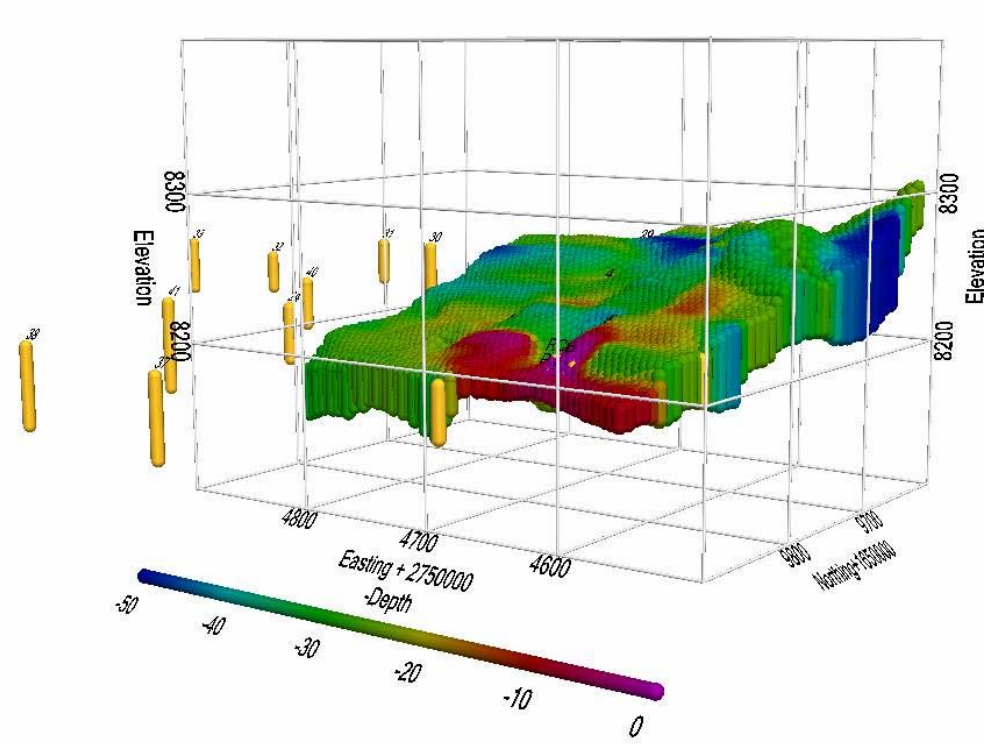

Figure 4. 3D model isopach of soil overburden (units in feet) - perspective view to the southeast. Yellow 'bars' are the location (and number) of geotechnical borings, where the length represents depth to weathered bedrock.

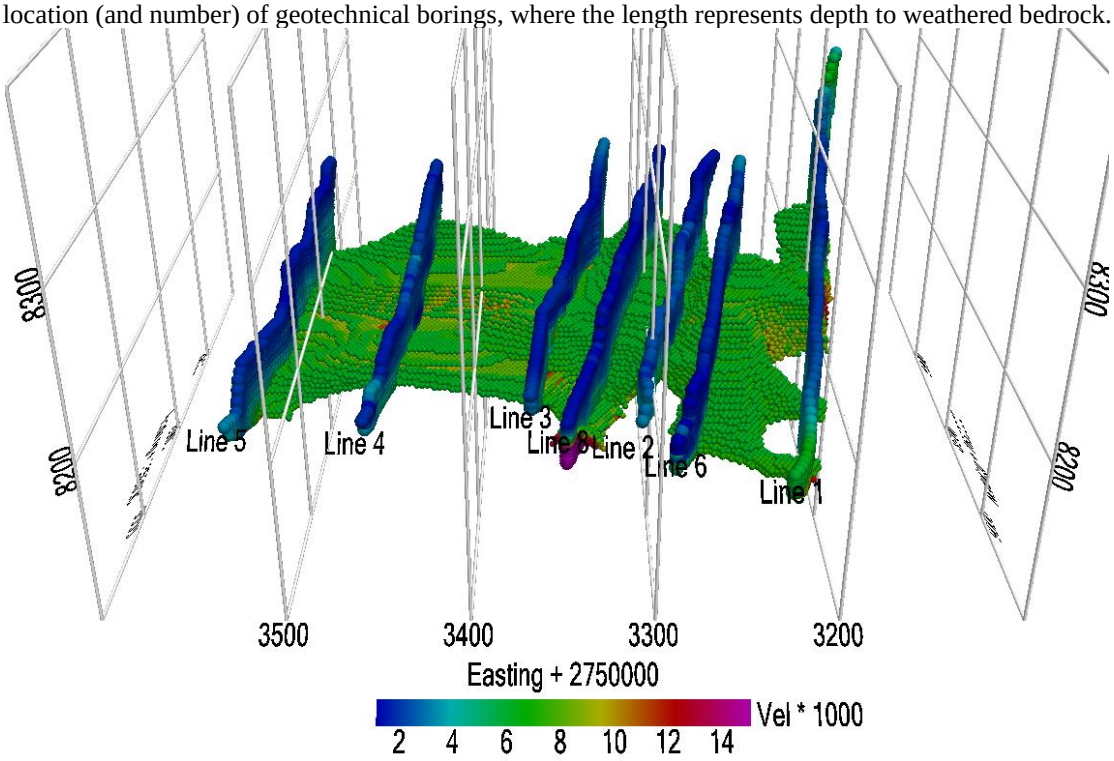

Figure 5. 3D model top of *weathered* bedrock based on a velocity isosurface (slice) at 6,300 ft/sec (units in feet & ft/sec) - perspective view to the south. Top of the refraction lines is the ground surface.

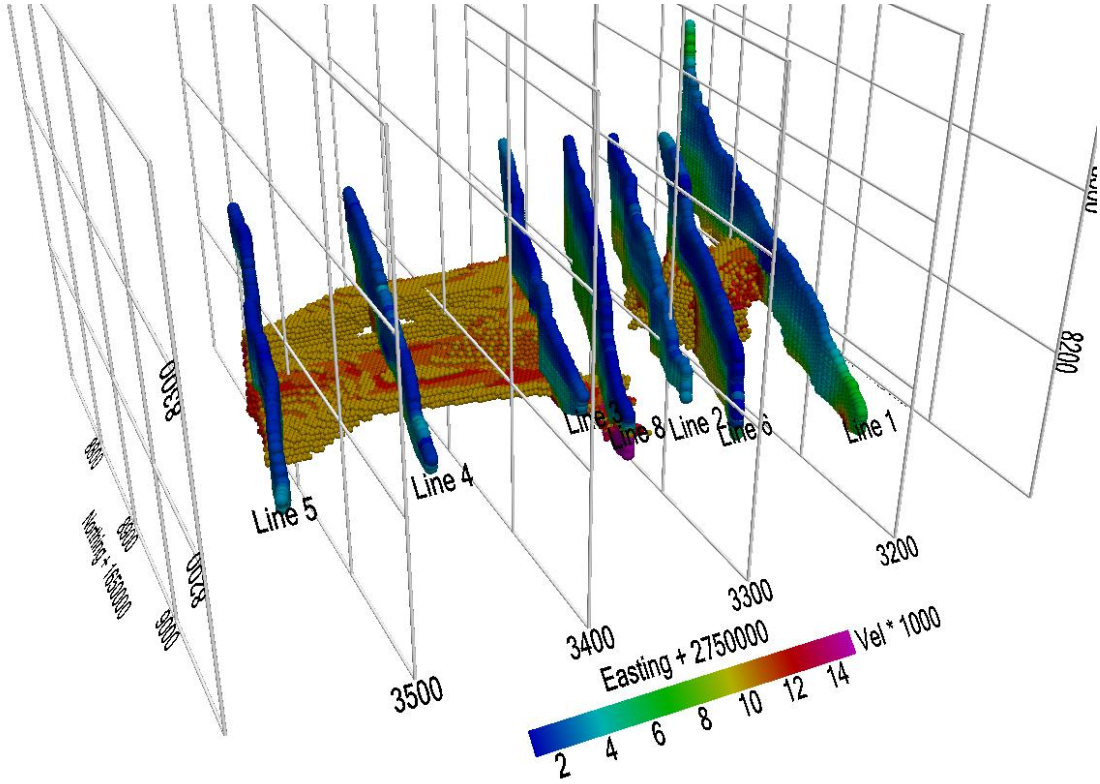

Figure 6. 3D top of competent bedrock based on a velocity isosurface of 11,000 ft/sec (units in feet & ft/sec) - perspective view to the southwest.

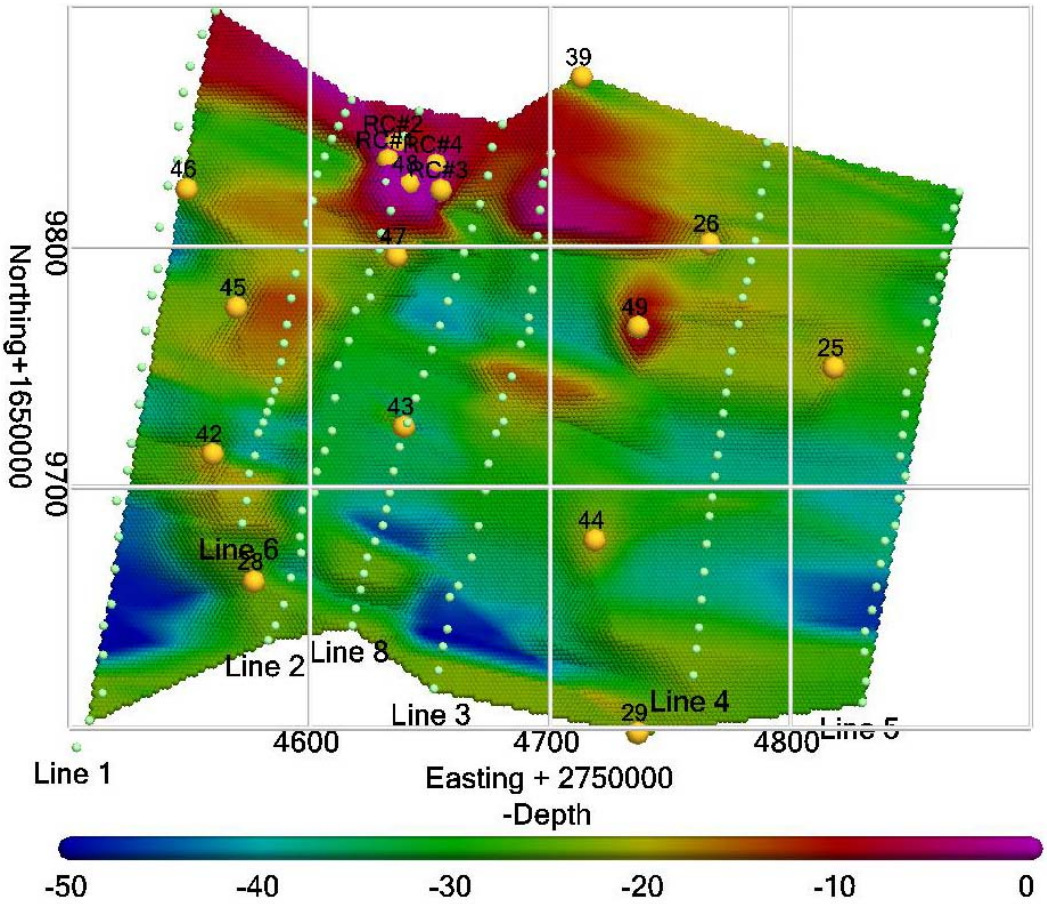

Figure 7. 2D plan map of depth to bedrock - green dots are geophone positions and yellow dots are borehole positions with TH number. Note zero thickness at the rock outcrop (RC) at north end of Line 2 which is the base of the hill. All units in feet, north is to the top.

Blue Ridge Landslide, Sterling, North Carolina

Modeling of 2D seismic refraction data was performed for the Eastern Federal Lands Highway Division (EFLHD) of the Federal Highway Administration. The geophysical survey consisted of investigating a landslide that is currently active; as such, details regarding the geotechnical analysis cannot be provided. The model results were provided by EFLHD personnel, as analyzed using the GAP processing approach. Seismic data were acquired by EFLHD staff and processed by Summit Peak Technologies. The following is a brief description of the project provided by EFLHD, and example 3D seismic plots.

Based on review of highway plans and previous geotechnical investigations, the landslide is through a large hillside of soil. This is a natural landslide area consisting of colluvial soil (landslide debris) deposits, overlying residual soils, and ultimately bedrock at depth. The colluvium consists of boulders with sand and silt and the residual soils consist of micaceous silty sands and sandy silts formed by in-place weathering of the parent mica gneiss and schist bedrock. At this point, it is not certain what caused a reactivation of movement, however, it is believed the slide may be occurring at the interface between colluvial deposits and residual soils and is exaggerated by a rise in the static water table (*personal communication with Khalid Mohamed geotechnical engineer at EFLHD*).

A GAP model space was generated based on the survey coordinate data provided from EFLHD. Data were acquired along 4 lines, using 12-channels with geophones spaced 10-feet apart and 11 shots per line. A hammer and plate were used as the source. Signals were combined for the common-shot and common-receiver positions, and are analyzed beneath the corresponding locations. Figure 8 shows the common-shot record for Survey Line 1, shot position S-5. The signals are all plotted and clipped at the same amplitude levels. Arrival-times were then picked for each SEG2 shot record using an auto-picker (a module in the processing package) then authenticated manually. The manual picks were used to train the automatic

picker. The automated picker discarded signals with low confidence picks. All arrival-time picks were cross-examined in both common-shot and common-receiver plots.

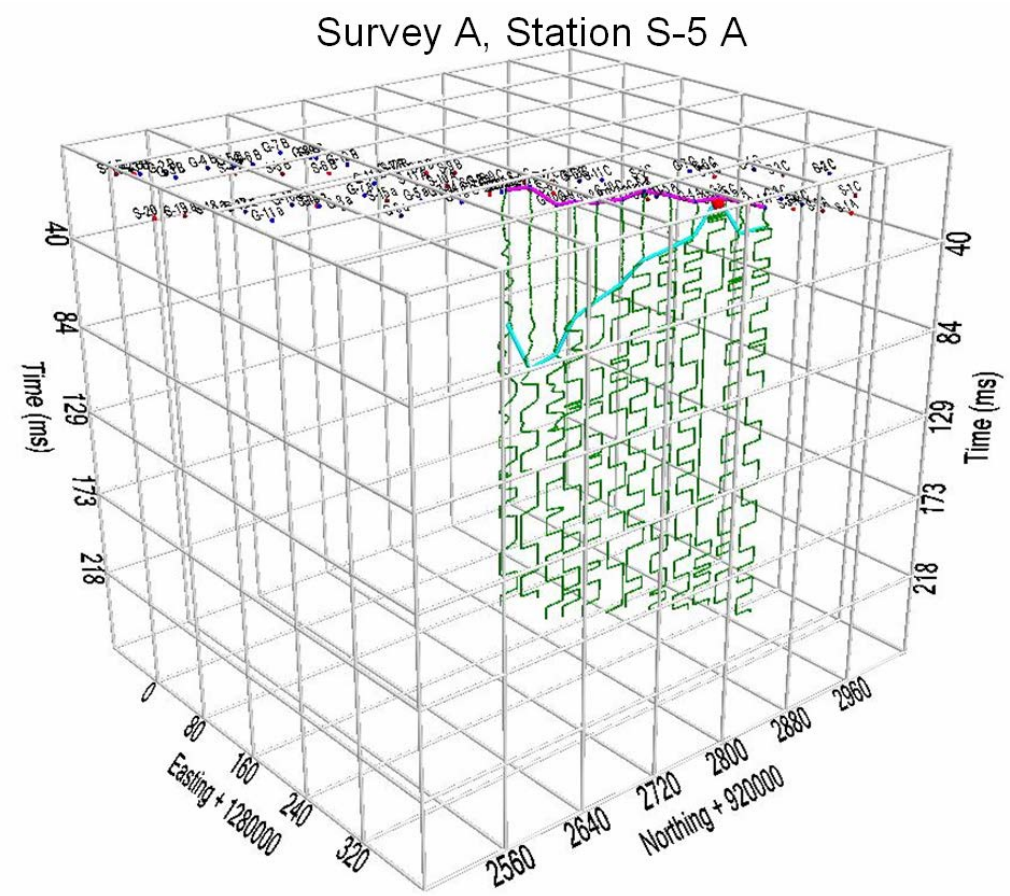

Figure 8. Common shot signals with picks (shown in light blue).

Two iterations were computed at 32-, 16-, 8-, and 4-foot resolutions. This technique allows 2D tomographic reconstruction at higher resolution with reduced distortion. The resulting 3D velocity model, obtained by using borehole (1D) and velocity (2D) images is shown in Figure 9. The 2D refraction tomogram in Figure 9 was computed in 8 iterations using GAP starting from a homogenous velocity model.

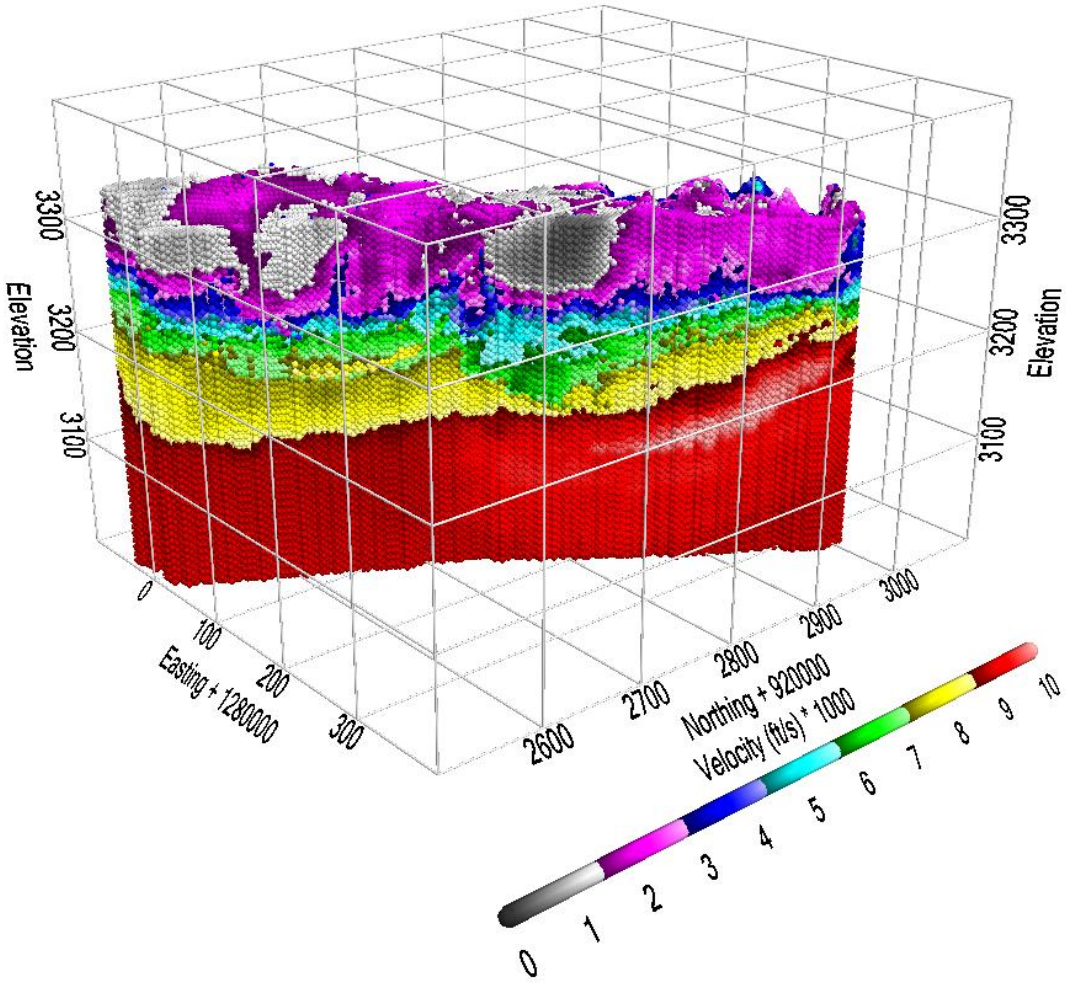

Figure 9. Refraction tomography velocity model using 4-foot resolution.

Using boring logs from the geotechnical investigation seismic velocities were mapped to match geologic materials. The resultant 3D model, presented in Figure 10, identifies the material types and their distribution in the model, as defined by seismic velocities. An advantage of using refraction tomography reconstruction is that it has much better capability of mapping both vertical and lateral velocity variations. A GAP 3D plot of the velocity variation *within* each geologic layer is shown in Figure 11.

The ray-path coverage for all rays in the model is shown in Figure 12. A ray is a region in the model that has the highest contribution to the first arrival time, and typically descends from the source at the ground surface to higher velocity layers before ascending to the surface receiver(s). From the ray-path coverage model, it is clear that the rays descended approximately 150 feet below the surface. Velocity data shown below this depth (in Figures 9, 10, or 11) are not constrained by the model parameters, as first-arrival seismic energy was not transmitted through these deeper portions of the DEM-PFC model.

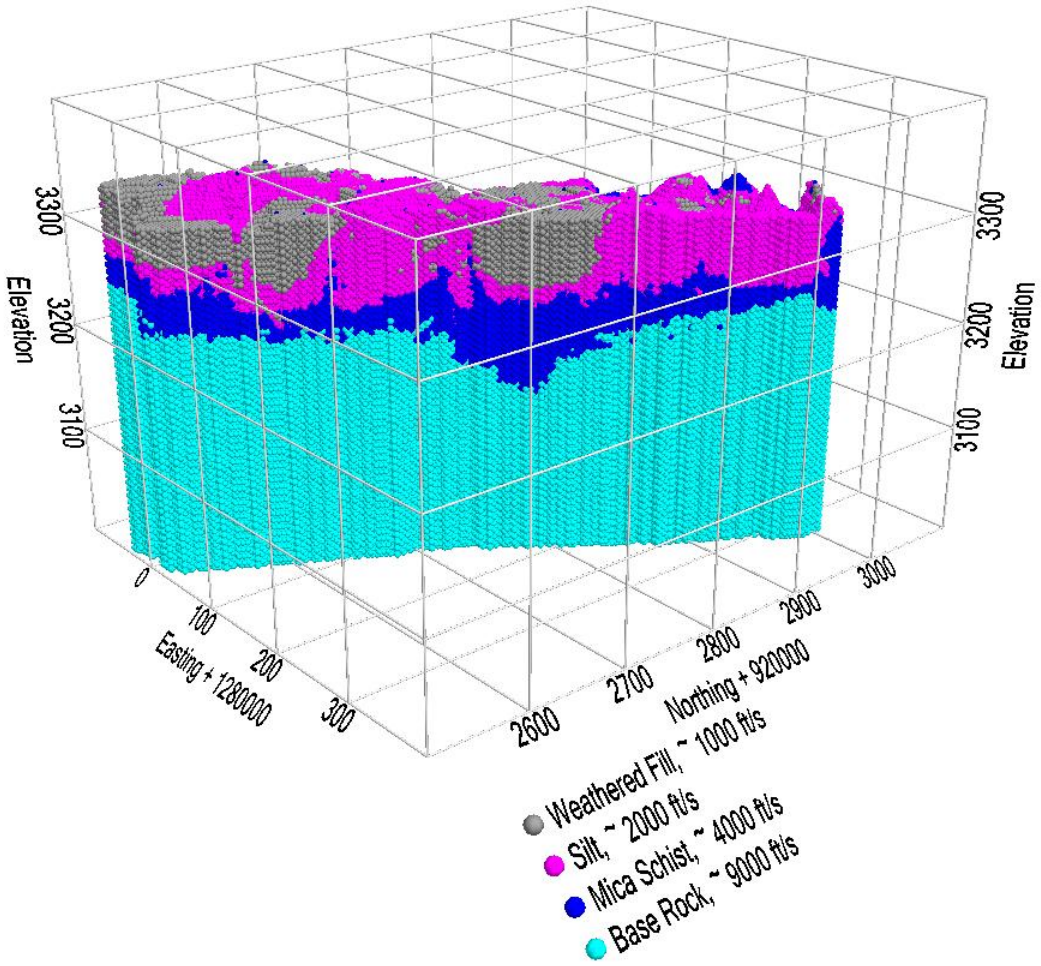

Figure 10. Refraction tomography *material* model as derived from geologic boring logs.

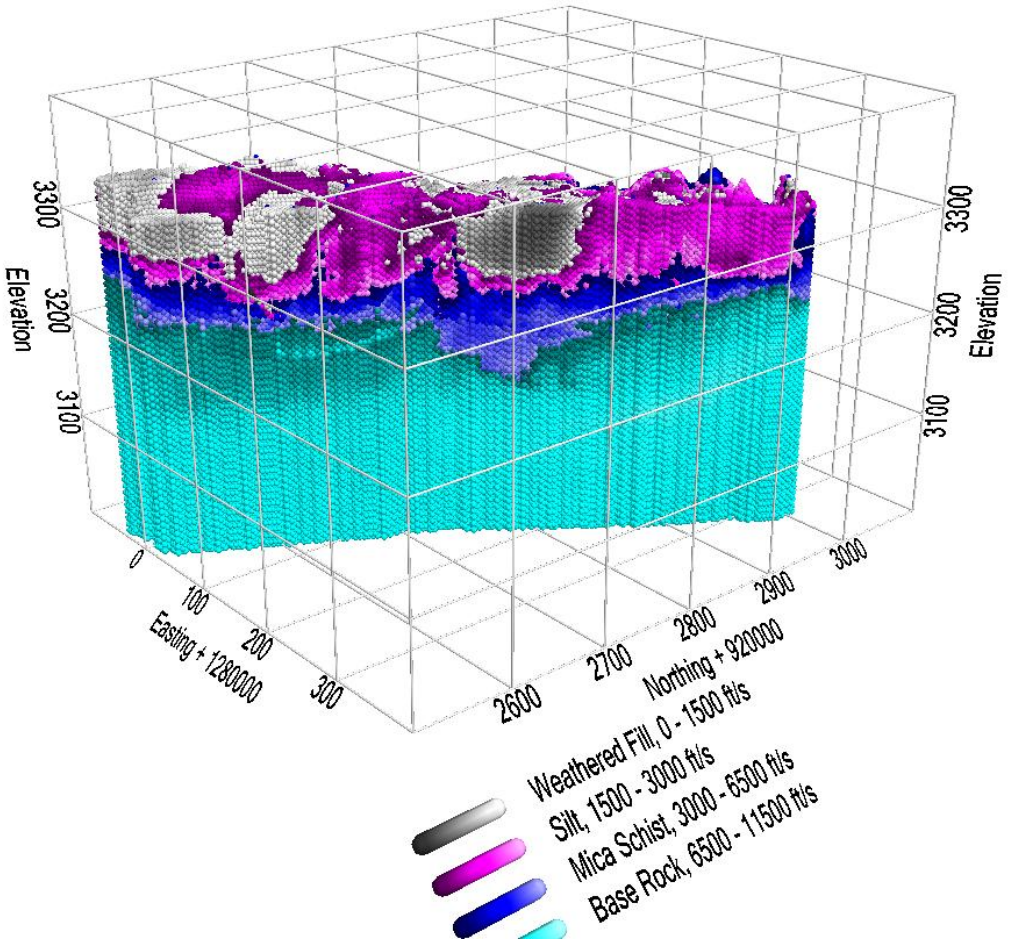

Figure 11. Refraction tomography model showing the velocity variation within each of the material layers (color scales shown in legend).

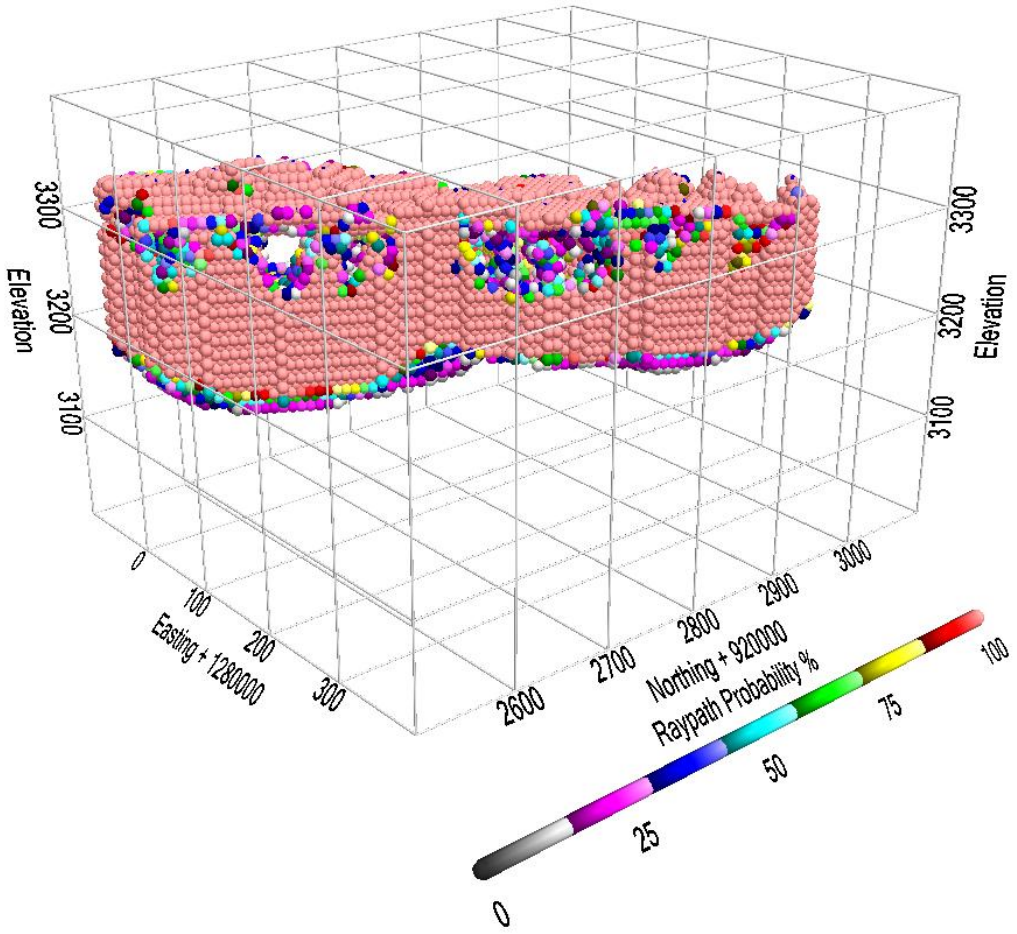

Figure 12. 3D model of ray coverage using probability (%).

CONCLUSIONS

Applying a more comprehensive numerical modeling approach to process and present seismic refraction data using the Geostructural Analysis Package (GAP) is described in this paper. GAP is a robust discrete element particle flow modeling technique that can produce high-resolution 2D and 3D models through forward modeling (simulations) as well as inverse modeling of standard seismic refraction data. The models are generated such that seismic wave arrival times simulated in the model match arrival times measured in the field. The same technique is used to modify the material properties in the model to reduce differences between the model waveforms and the field waveforms.

The name refraction tomography may perhaps be misleading for what GAP performs. GAP is optimized for seismic wave propagation, as shown here, but its purpose is much broader in scope to model chemical, thermodynamic, and hydrologic processes as well. In its current form it supports tomographic and holographic inversion. The algorithm includes a wide range of built-in signal processing capabilities, such as automatic arrival time picking and digital filtering. It can efficiently image low velocity regions in the subsurface because it increases resolution with each iteration and reduces arrival time errors using Fresnel volumes, or curved ray-path regions. The GAP technique of matching arrival times will be extended to match the full waveforms, and will then be termed *surface holography inversion.*

This modeling approach is gaining acceptance within the engineering community because of its added value to produce a 2D or 3D model. Two case histories with complex geologic settings and site conditions show the value of integrating geological and geotechnical data into the GAP modeling process. Each case history used standard 2D refraction field procedures, data were processed using 2D tomography inversion, and then calibrated 3D models were generated through interpolation. The models could be considered 2.5D based on the procedures used, but the model is 3D. These volume

models can be velocity sliced to strip away materials, or geologic layers, calibrated to have a particular velocity or range of velocities.

Perhaps the most important advancement using discrete element particle flow code is the models can be used in the next step of engineering analyses. As refraction data can be acquired in 3D, and field appropriate field parameters are used, GAP can support full 3D processing of these data to produce calibrated models which incorporate geologic, geotechnical, and geophysical data. After the geophysics is done, the models can then be used for engineering analyses. For example, they can undergo large-strain deformation such as cracking, subsidence, or slope failure modes; and, low-strain static and dynamic loading. Clearly, this is an advantage over producing 2D, 2.5D or 3D images of the subsurface for geotechnical applications. As the capabilities increase for GAP to model other processes such as chemical, thermodynamics of heat flow, or groundwater flow it will become a very powerful and useful tool for applications other than geotechnical engineering.

ACKNOWLEDGMENTS

The authors would like to thank Mr. Dan Feeney of Vail Resorts Development Company and Mr. Khalid Mohamed Eastern Federal Lands Highway Division of the FHWA for granting permission to include GAP seismic data from the two case histories referenced in this paper. Also we appreciate Mr. W. Koechlein, of Koechlein Consulting Engineers, for engineering input and support on the Vail project.

REFERENCES

1. Palmer, D., 1981, An introduction to the generalized reciprocal method of seismic refraction interpretation, Geophysics, Vol. 46, pp. 1508-1518.
2. Sheehan, J.R., W.E. Doll, and W.A. Mandell, 2005, An evaluation of methods and available software for seismic refraction tomography analysis, JEEG, V. 10, No. 1, pp. 21-34.
3. Saenger, E.H., Gold, N., and Shapiro, S.A., 2000, Modeling the propagation of elastic waves using a modified finite difference grid: Wave Motion, Vol. 31, pp. 77-92.
4. Saenger, E.H., and Bohlen, T., 2004, Finite Difference Modeling of viscoelastic and anisotropic wave propagation using the rotated grid: Geophysics, Vol. 69, No. 2, pp. 583-591.
5. Gelis, C., D. Leparoux, J. Virieux, A. Bitri, S. Operto, and G. Grandjean, 2005, Numerical modeling of surface waves over shallow cavities, Jour. Of Environmental & Engineering Geophysics, Vol. 20, No. 2, pp. 111-121.
6. Zhang R. and S. Sture, 1995, Discrete Element Particles Analysis at Low Stress States, in Proceedings of the 10th ASCE Engineering Mechanics Specialty Conference.
7. Zhang, R. and S. Sture, 1996, Flexible Boundary for Discrete Element Simulation of Granular Assemblies, in Proceedings of the 11th Engineering Mechanics Conference.
8. Zhang, R., 1996, Discrete Element Modeling of Granular Materials Under Biaxial Conditions, Ph.D. dissertation submitted to the Faculty of the Graduate School of the University of Colorado
9. Sirles, P., A. Rock and R. Zhang, 2005, NDT technologies and unknown foundations, *in* Presentations and Notes, FHWA Unknown Foundation Summit, Lakewood, Colorado, U.S. Department of Transportation
10. Rock A. and R. Zhang, 2002, Acoustic model calibration, *in* Proceedings of the American Society for Composites 17th Technical Conference.
11. Itasca Consulting Group, 1999, PFC2D Users' Guide, Command Reference, FISH Reference, and Theory and Background, Minneapolis.
12. Itasca Consulting Group, Inc., 2003, PFC3D (Particle Flow Code in 3 Dimensions), Ver. 3.0. 656 pp.
13. Rock, A., D. Wilkinson, and R. Zhang, 2005, Velocity variations in Drilled Shaft CSL Surveys, Report to Federal Highway Administration, Publication No. FHWA-CFL/TD-04-001.
14. Pullammanappallil, S., J.N. Louie, 1994, A generalized simulated-annealing optimization for inversion of first-arrival times, BSSA, Vol. 84, pp. 1397-1409.
15. Optim, Inc., 2005, SeisOpt@2d, (Ver. 4.0), Seismic Refraction Tomography software copyright University of Nevada, Reno, Nevada.

Use of Refraction Microtremor (ReMi) Data for Shear Wave Velocity Determination at an Urban Bridge Rehabilitation Site

Douglas W. Lambert, R.G., Sr. Project Manager
Geotechnology, Inc. St. Louis, Missouri
2258 Grissom Drive
St. Louis, Missouri 63146
D_lambert@geotechnology.com

Glen Adams, R.G., Senior Geophysicist
Geotechology, Inc., St. Louis, Missouri

Veronica Parker, Staff Geophysicist
Geotechnology, Inc., St. Louis, Missouri

ABSTRACT

A refraction microtremor (ReMi) survey was conducted to determine site specific shear wave velocities for seismic hazard evaluation at a bridge rehabilitation site in St. Louis, Missouri. The bridge, located within a highly urbanized area, is approximately 1,200 feet long with fourteen spans and three driving lanes in each direction. The rehabilitation will include widening of the existing abutments, superstructure and deck, replacement of various foundations, and seismic retrofit of the existing piers and superstructure. The bridge is situated within approximately 70 feet of fill, clay and clayey gravel, underlain by limestone bedrock.

The ReMi survey methodology, developed by John Louie of the University of Nevada, Reno, is a quick, non-intrusive method for determining a one-dimensional shear wave velocity profile by recording and analyzing surface waves. ReMi data were collected by a two-person crew in one day at two different locations, one at each end of the bridge. The surveys were conducted by establishing a 24-geophone spread along a straight line at each location and recording random surface wave energy. The random energy was primarily provided by street and railroad traffic; an artificial seismic source was not required. The data were processed and modeled using SeisOpt ReMi software (Optim LLC).

The shear wave velocity profiles were constrained using drill data which provided depth to bedrock and standard penetration test results at each of the survey locations. The results were used to identify the AASHTO soil profile type and establish seismic design parameters in accordance with AASHTO guidelines.

Notable benefits in using the ReMi method included the ability to collect data quickly with a two-person crew and the ability to collect the seismic data in a noisy urban environment.

INTRODUCTION

The Grand Avenue Bridge, located in a highly developed area of south central St. Louis, Missouri, is currently planned for rehabilitation by the City of St. Louis. The rehabilitation will include widening the structure and replacing various foundations. The bridge is located in a topographically low-lying area known as old Mill Creek valley and overlies significant thicknesses of fill and alluvial deposits. Shear wave data is desired to assist in evaluating seismic effects on the design of the new structural elements.

Shear wave data may be obtained indirectly or directly using a variety of methods. Shear wave velocities may be estimated indirectly using standard penetration tests (N) or cone penetrometer results, but these results may be less reliable and provide less depth of exploration as compared to results obtained by measuring seismic energy directly (*1, 2)*. Direct shear wave measurements obtained performing a crosshole seismic survey, or downhole seismic survey, require the use of cased boreholes that add time and expense to a project. Shear wave velocity profiles can be modeled from the direct measurement of surface waves using the methods known as Spectral Analysis of Surface Waves

(SASW), Multi-Spectral Analysis of Surface Waves (MASW), and Refraction MicroTremor (ReMi). SASW requires specialized equipment and, along with MASW, normally requires the use of an artificial source which can sometimes result in lower quality data when collected in an area with significant background noise. The ReMi method involves recording surface waves generated by surrounding background "noise" using typical seismic refraction equipment. The method has been successfully used for mapping coarse-grained deposits, characterization of bedrock, characterization of fill, and detection of low-velocity zones (3, *4, and 5*). Without adding significant time or expense to the Grand Avenue Bridge project, we used the ReMi method to develop shear wave velocity profiles. This geophysical survey was conducted in addition to performing geotechnical borings, laboratory testing, and engineering analyses for the project. The subsurface drilling data was used to help refine the shear wave velocities.

PROJECT DESCRIPTION

Figure 1. Grand Avenue Bridge project area.

The project includes rehabilitation of the Grand Avenue Bridge located between Chouteau Avenue to the south and Interstate 64 to the north in St. Louis, Missouri. The site location is shown in Figure 1. The central part of the bridge crosses various sets of railroad tracks used by Missouri-Pacific Railroad, Burlington Northern–Santa Fe Railroad and the MetroLink public transportation system. MetroLink operates a passenger station directly beneath the bridge with pedestrian access to the bridge deck (Figure 2). In addition, the bridge crosses Bernard and Scott Streets on the north end and Gratiot and Papin Streets towards the south end. Areas beneath and adjacent to the southern end of the bridge are used for storage by various industrial entities.

Figure 2. View towards the west beneath Grand Avenue Bridge showing the MetroLink passenger station.

The existing bridge is approximately 1,200 feet in length, includes fourteen spans and has three driving lanes in each direction. The general site topography slopes downward from the abutments towards the central, east-west trending valley of Mill Creek. The creek has been piped underground and the valley was filled to form the rail yard. Maximum relief is approximately 50 feet, between Elevation 510 msl near Chouteau Avenue and Elevation 460 msl in the rail yard. Grade is about El 490 near the Interstate 64 off-ramp.

General features of the bridge rehabilitation include widening of the existing north and south abutments, widening of ten piers, replacement of various foundations, widening of portions of the superstructure and deck, seismic retrofitting of existing piers and superstructure, and installing various amenities and aesthetic features.

GEOLOGIC SETTING

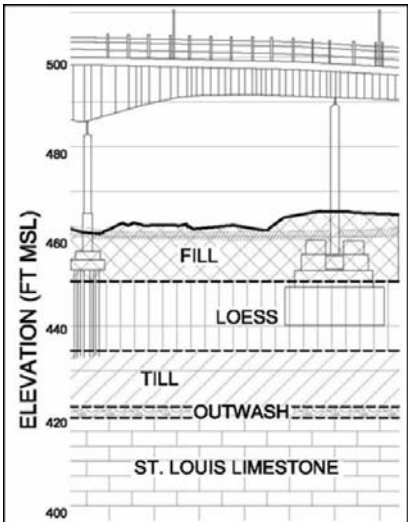

Figure 3. Typical geologic profile for the Grand Avenue Bridge area.

The near surface geology in the vicinity of the site is dominated by sediments related to Pleistocene glaciation. Glacially-derived soils in the region consist of till and outwash deposits overlain by modified loess (post-glacial windblown sediments comprised of silt and clay). At the subject site, surficial fill is present in most areas, as a result of previous grading in the Mill Creek valley. The underlying soil deposits include, from younger to older, Pleistocene-age loess, glacial till, and glacial outwash. Bedrock is generally Mississippian age carbonates. A typical geologic profile for the subject site is shown in Figure 3.

At the bridge site, fill extends to depths of 8 to 18 feet and typically consists of lean and fat clay with sand, gravel, and variable amounts of cinders, brick fragments, concrete, and glass. Loess deposits occur below the fill and extend to depths of 18 to 28 feet. The loess has been modified by weathering and consists of brown to gray, lean and fat clay. Glacial till and outwash deposits occur below the loess and extend to bedrock at depths of 33 to 77 feet. The till and outwash deposits are comprised of fat and lean clay with sand and silt layers, underlain by silt and/or clayey sand and gravel.

Bedrock in the area is Mississippian-age limestone of the Meramecian Series. The bedrock generally dips to the northeast away from the Ozark uplift centered in southeastern Missouri (i.e., St. Francois Mountains) and towards the Illinois Basin centered in east-central Illinois. Bedrock at the subject site is St. Louis Limestone which is composed of gray to brown, lithographic to finely crystalline, medium-bedded to massive limestone. Blue and bluish-gray shale seams occur throughout the formation. The St. Louis Limestone is about 180 feet thick in the St. Louis area; however, at the project site, much of the formation has been removed by erosion. Karst features are prevalent in the formation, with solution voids and pinnacles that may penetrate 20 feet or more into the rock. Experience indicates weathering is typically in the range of 3 to 7 feet. Underlying the St Louis Limestone is the Salem Formation which is a 100- to 160-foot thick, bluish-gray to gray, argillaceous, oolitic limestone. The Salem is conformable with and difficult to differentiate from the overlying St. Louis Limestone.

REFRACTION MICROTREMOR METHOD

A refraction microtremor (ReMi) survey was performed to determine site specific shear wave velocities at the bridge location. The ReMi method utilizes the dispersive property of surface waves (*5*). ReMi data are collected by passively recording background surface wave "noise" such as the vibrations generated by passing vehicles, airplanes or trains, as well as added noise created by initiating impacts (via sledgehammer) at the ground surface. The surface waves are recorded using a seismic system comprised of geophones, cables and a seismograph. Shear wave velocity profiles are constructed by analyzing surface wave phase velocities and frequencies, and performing inversion modeling.

REMI DATA COLLECTION

Figure 4. View along ReMi Line 1 showing 20-foot geophone spacings.

ReMi surveys were conducted by a two-person crew on November 21, 2005, using a Seistronix RAS24 engineering seismograph and 4.5-Hz vertical geophones. ReMi data were collected along one east-west trending line parallel to the Metrolink tracks (ReMi Line 1), and one north-south trending line parallel to the eastern edge of the bridge in an industrial storage lot (ReMi Line 2). ReMi survey locations are shown in Figure 1. ReMi Line 1 extended 460 feet, and ReMi Line 2 extended 440 feet. A 20-foot geophone spacing was used for each line (Figure 4). To assist in geophone coupling on ReMi Line 2, ¼-inch diameter holes were hammer-drilled into the asphalt pavement and the geophones spikes were securely seated into each hole (Figure 5). The ReMi data were acquired by collecting approximately 20 background microtremor "noise" recordings using a time window (sampling length) of 30 seconds each. The "noise" recordings were supplemented with sledge hammer blows on a metal plate at the end of each line.

Figure 5. View of typical geophone secured into pavement prior to surveying.

REMI DATA PROCESSING

The data were processed and modeled using SeisOpt ReMi software developed by Optim LLC. Plots of inverse velocity (slowness) versus frequency were plotted for each line as shown in Figures 6 and 7.

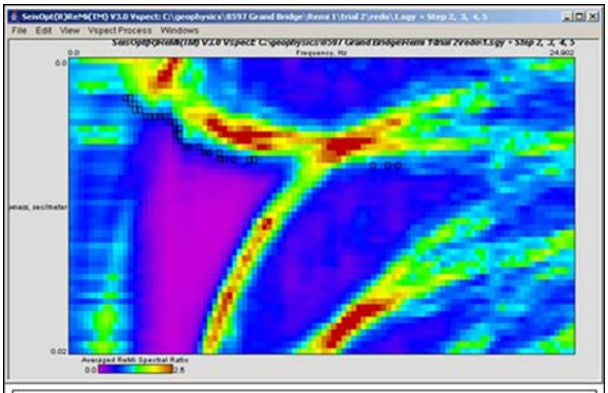

Figure 6. Dispersion curve (slowness versus frequency) of data recorded along ReMi Line 1.

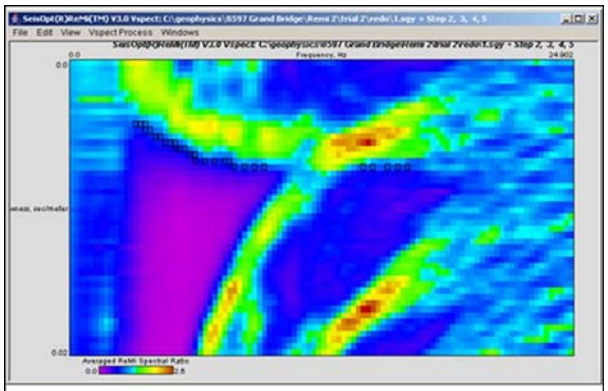

Figure 7. Dispersion curve (slowness versus frequency) of data recorded along ReMi Line2.

The surface wave energy is easily identified as the high amplitude data trending from the upper left corner (high velocity and low frequency) towards the lower right corner (lower velocity and higher frequency). The lower edge of this data package was picked and used to develop a graph of phase velocity versus period (inverse frequency). The graphed data for each ReMi line is shown in Figures 8 and 9.

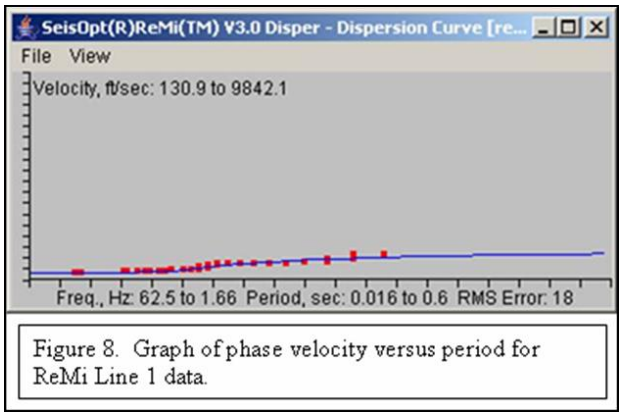

Figure 8. Graph of phase velocity versus period for ReMi Line 1 data.

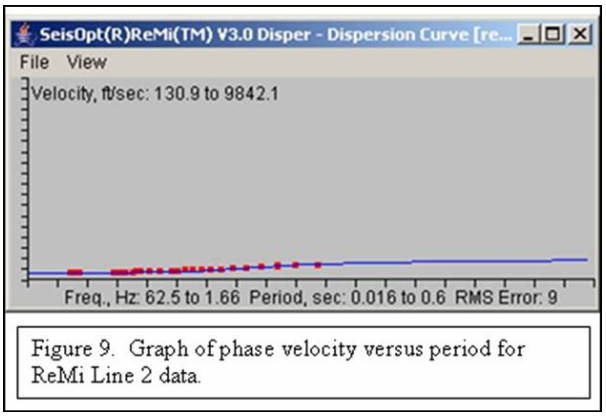

Figure 9. Graph of phase velocity versus period for ReMi Line 2 data.

These graphed data were used to develop models of shear wave velocity profiles centered at the location of each ReMi line. The models are developed by adjusting values of shear wave velocity and unit thicknesses with depth. Boring data available from the geotechnical exploration were used to help refine the shear wave velocity modeling results. Distinct layers of fill, loess, granular outwash, and limestone bedrock, identified during drilling, were used to constrain the thicknesses of the subsurface layers, and the velocities were adjusted to provide the best fit with the recorded and graphed data.

SHEAR WAVE VELOCITY PROFILES

The one-dimensional shear wave velocity profiles derived from ReMi Lines 1 and 2 are presented in Figures 10 and 11, respectively. The horizontal scale is shear wave velocity in feet per second and the vertical scale is depth in feet.

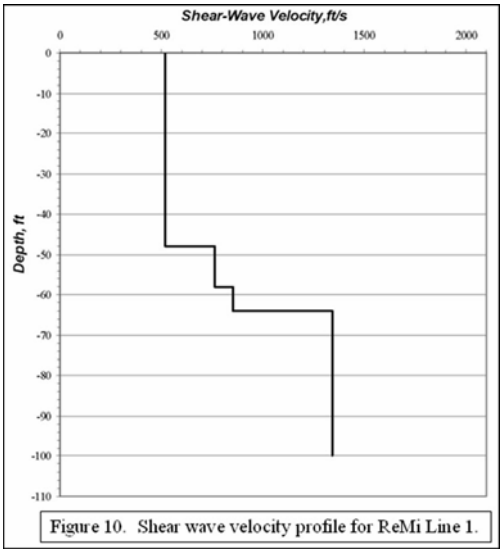

Figure 10. Shear wave velocity profile for ReMi Line 1.

Along ReMi Line 1, top of bedrock was interpreted to occur at an approximate depth of 62 feet and the shear wave velocity of bedrock was interpreted to be approximately 1,630 ft/sec. This line revealed a low shear wave velocity layer, approximately 476 ft/sec, extending from the surface to a depth of approximately 28 feet, which corresponds to the surficial fill and underlying loess. Data from two borings located on ReMi Line 1, generally agree with the interpretation. The average shear wave velocity for the top 100 feet is approximately 810 ft/sec, which corresponds to a stiff soil profile.

Along ReMi Line 2, bedrock was interpreted to occur at an approximate depth of 64 feet and the shear wave velocity of bedrock was interpreted to be approximately 1,340 ft/sec. This line also revealed a layer with low shear wave velocity, approximately 518 ft/sec, extending from the surface to a depth of approximately 48 feet, which corresponds to the surficial fill and underlying loess. Data from a boring located on ReMi Line 2, generally agrees with the interpretation. The average shear wave velocity for the top 100 feet is approximately 720 ft/sec, which corresponds to a stiff soil profile.

Based on the boring data and ReMi results, the AASHTO soil profile may be considered Type I and the corresponding site coefficient, S, is 1.0.

CONCLUSIONS

Based on these results, the ReMi method appears to be a viable and low-cost method for developing shear wave velocity profiles in highly developed urban environments. ReMi data were collected at two locations within an area of high industrial and vehicular activity. A primary requirement for collecting ReMi data is the ability to extend survey lines approximately 400+ feet in the vicinity of the area of interest. Although not required, boring data collected in the vicinity of the ReMi survey assists in constraining the shear wave velocity model.

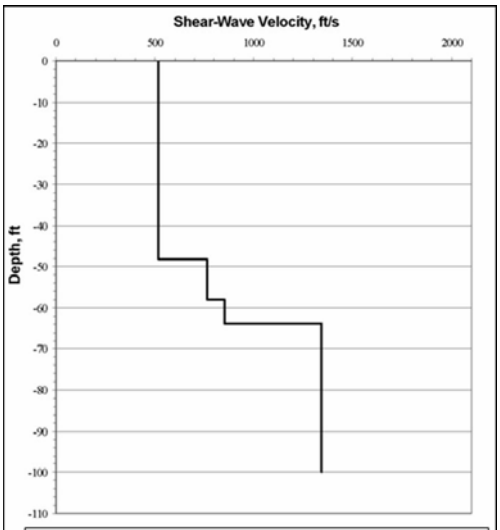

Figure 11. Shear wave velocity profile for ReMi Line 2.

REFERENCES

1. Malovichko, A. M., D. A. Malovichko, D. Y. Shylakov, P.G. Butirin, and N.L. Anderson. *Estimation of Near-Surface Shear-Wave Velocities by SASW Method in Southeast Missouri.* Mining Institute, Ural Branch, Russian Academy of Sciences and Department of Geology and Geophysics, University of Missouri-Rolla.

2. Anderson, N. and T. Fennessey. *Comprehensive Shear-Wave Velocity Study in the Poplar Bluff Area, Southeast Missouri.* Department of Geology and Geophysics, University of Missouri-Rolla and Missouri Department of Transportation, Research Development and Technology, 2005.

3. Rucker, M. L. *Applying the Refraction Microtremor (ReMI) Shear Wave Technique to Geotechnical Characterization*. AMEC Earth & Environmental, Inc.

4. Rucker, M. L. *Characterizing Potential 'Bridging Ground' Conditions using the Ref4raction Microtremor (ReMi) Surface Seismic Technique.* AMEC Earth & Environmental, Inc.

5. Louis, J. N. *Faster, Better: Shear-Wave Velocity to 100 meters Depth from Refraction Microtremor Arrays.* Seismological Laboratory and Department of Geological Sciences, Mackay School of Mines, The University of Nevada, Reno, Nevada, 2001.

Dodging Salt Sinkholes: Seismic Reflection and K-61 Near Inman Kansas

Neil M. Croxton, P.G., CPG
Regional Geologist,
North-Central and Northwest Region
Kansas DOT
neilc@ksdot.org
(785) 827-3964

ABSTRACT

The Kansas Department of Transportation is designing a 4-lane expressway to replace the existing K-61 between the south-central towns of McPherson and Hutchinson. This highway corridor crosses the dissolution front of the Hutchinson Salt Member, the portion of its outcrop belt where groundwater is removing salt.

Overpass bridges will need to be constructed at two locations near the town of Inman, which is within the dissolution front of the salt. KDOT geologists were concerned about aligning the $188 million improvement over active or developing sinkholes which could damage the bridges or threaten large-scale settlement of the roadway. Local opposition to the new alignment, particularly near Hutchinson and Inman, encouraged us to evaluate the geology carefully. Expensive repairs after construction would be disastrous for already-strained public relations.

In the summer of 2005, we contracted with the seismic reflection crew at the Kansas Geologic Survey, under Dr. Rick Miller. The plan was to run a seismic survey across the Inman bypass, and a local paved road that serves the town. In September of last year, the survey was completed. KDOT and Geologic Survey crews had to contend with high heat and humidity, large thunderstorms and the ensuing mud, irate landowners, and dangerous traffic.

As a result of Dr. Miller's analysis, KDOT designers in the State Road Office decided to completely relocate the county road north of Inman. This allowed a proposed overpass bridge to be moved out of a settlement zone without changing the alignment of the expressway. Had a seismic survey not been performed, the new bridge might have been plagued by expensive and embarrassing repairs.

INTRODUCTION

The Kansas Department of Transportation is designing a 4-lane expressway to replace the existing K-61 between the south-central cities of McPherson and Hutchinson. This corridor runs southwest to northeast and is nearly 23 miles long. Total cost of the new highway is expected to exceed 130 million dollars. In addition to the usual design problems of such a large project, the K-61 corridor has a special concern: the highway crosses the dissolution front of the Hutchinson Salt Member.

GEOLOGY OF THE PROJECT

The Hutchinson Salt is a member of the Permian Wellington Formation. This unit is 300 feet thick where unweathered in the project area; its top is approximately 400 feet below the surface. The overlying Permian rocks consist primarily of weak shale. Bedrock along the highway corridor is covered by 10 to 40 feet of sandy alluvium known as the "Equus Beds". There is a regional dip of strata to the west, the result of uplift along the Nemaha Anticline, 40 miles to the east. Consequently, there is a buried outcrop belt of the Hutchinson Salt Member where the overlying shale beds have been partially removed by weathering, and where groundwater is removing salt. This narrow, irregular belt of active salt dissolution results in sinkholes that appear at random locations. Most of the sinkholes are shallow depressions that are difficult to notice unless a house or barn has been built over it. A very few sinkholes are quite large, however, leaving features named "Dirks Lake", "Lake Inman", and "Big Sinkhole Lake" to the east of the project area. The new, 130 million-dollar K-61 must cross this dissolution front.

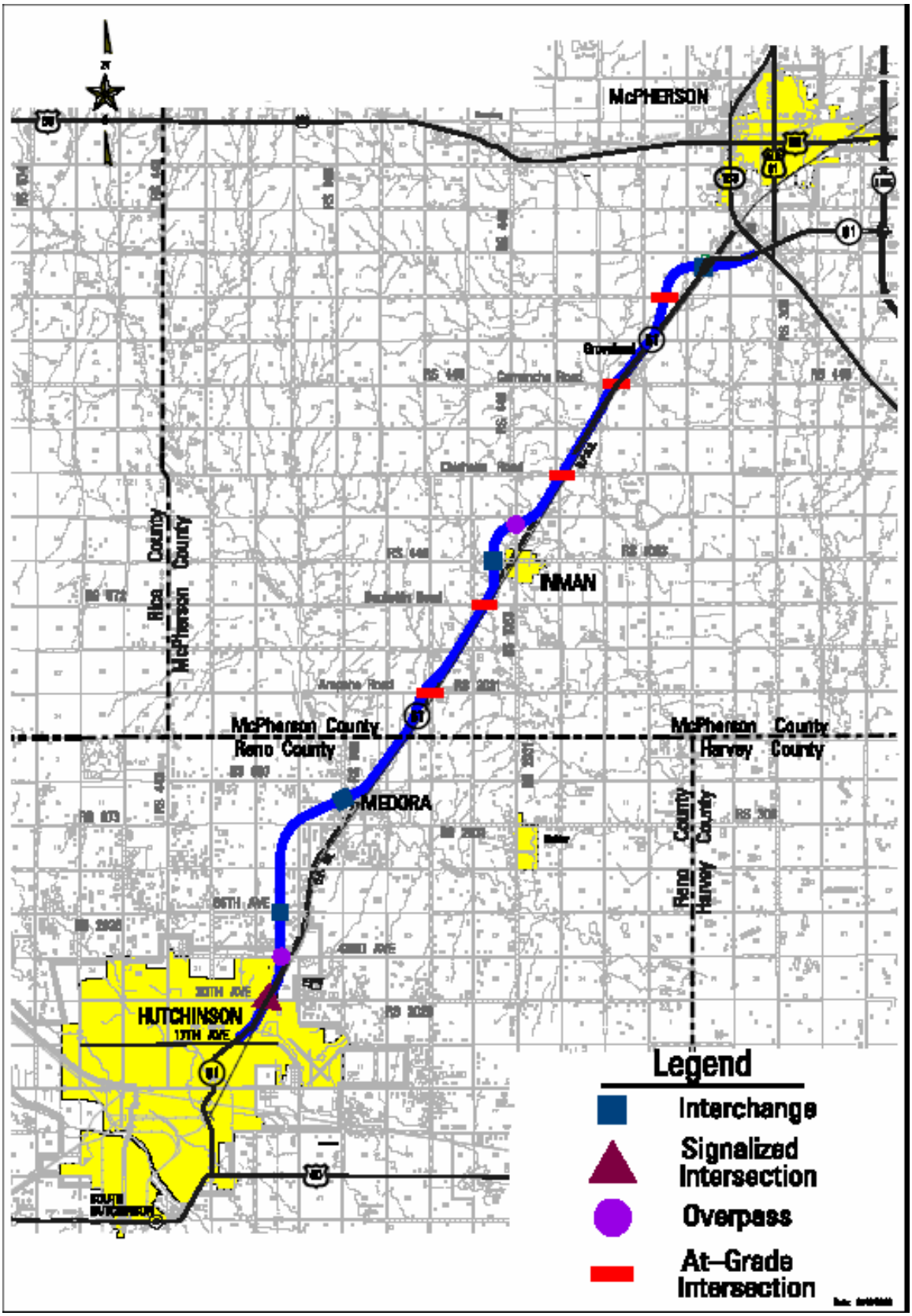

Figure 1: K-61 Project Alignment

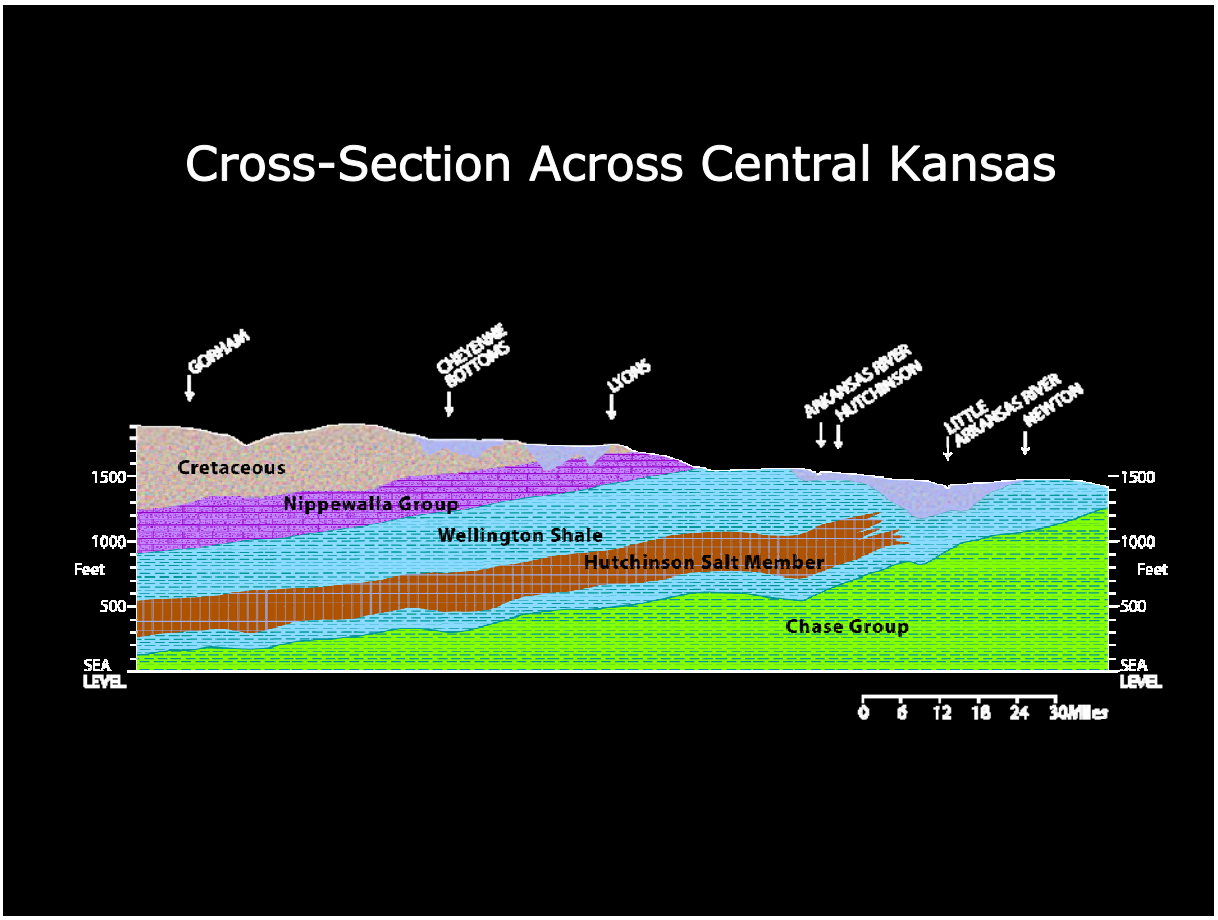

Figure 2: General Geology of the Project Area

DANGEROUS TRAFFIC, HOSTILE NATIVES, AND THAT SALT BED

Hutchinson and McPherson are undergoing high population growth, and the traffic along K-61 has increased dramatically in the last 15 years. A traffic count in January, 2006 found that up to 7500 vehicles use K-61 daily, including over 700 trucks. In 2005, there were 59 vehicle accidents on this road, including 23 injuries. Previous years have seen fatalities. The highway crosses through land farmed by people who resent and fear the dangerous traffic, but who are equally upset about KDOT's plans to create an expressway. In 2005, McPherson County was named by a national farm magazine as the best place in the country for agriculture. The population growth of the nearby cities and the proposed 4-lane highway will permanently change this area, and the long-time residents know it. There was strong resentment about the whole idea of rebuilding K-61 before the Geology Section began its work.

As part of the reconstruction, the State Road Office decided to bypass the small town of Inman, which is south of the Burlington Northern-Santa Fe tracks and near the midway point of the corridor. The bypass is to swing around to the northwest and include a full, separated-grade interchange with the county road entering Inman from the west. A single bridge will carry traffic over the expressway on the paved county road that enters town from the north. KDOT's Chief Geologist, Robert Henthorne, studied the alignment and compared it to a salt isopach map of the area prepared by the state geological survey. The proposed Inman bypass appeared to cross the dissolution front of the salt bed.

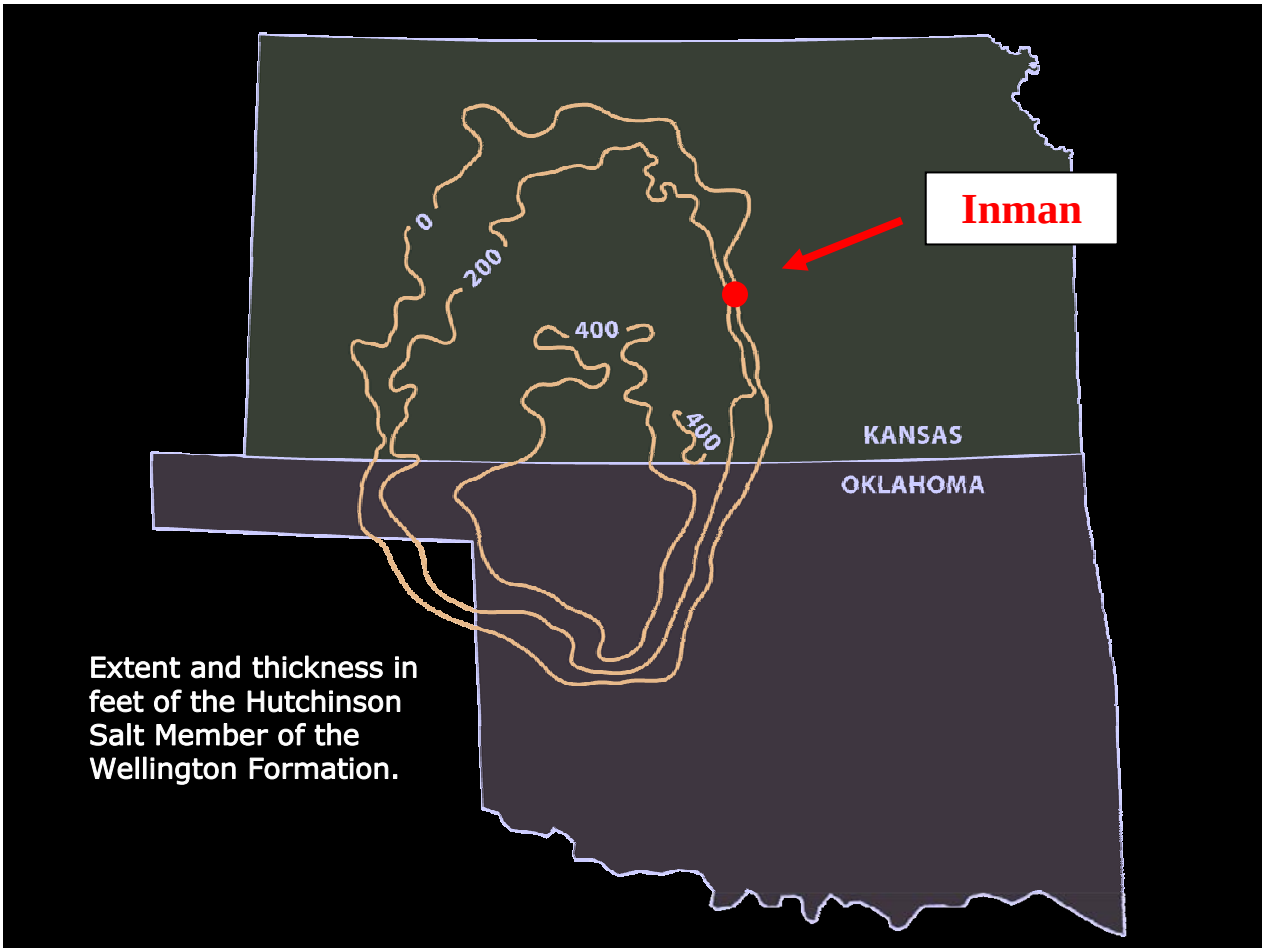

Figure 3: Project Location in Relation to the Extent of the Hutchinson Salt Member

Salt subsidence is a way of life for the maintenance crews in this part of the state. Roads will begin to settle, albeit slowly, and nothing can be done except to add fill. Because of the overlying soft Permian shales and Pleistocene Equus Beds, the collapse of a subterranean salt cavern does not create a catastrophic collapse on the surface, but instead fills with overlying material and shows up as a gentle depression. Most of these subsidence areas are minor, posing only a nuisance threat to a highway. Protecting the entire length of the proposed expressway from such settlement seemed unrealistic, considering the geology. But there were two things about the alignment that concerned KDOT Geology. The first was the possibility of a large sinkhole forming directly under the roadbed of the 4-lane highway: a potential "Lake K-61". The other worry, one far more likely, was the chance of building one or more bridges over an area with only moderate surface settlement. Given the local resentment of the project, having expensive bridge repairs shortly after construction would be a public relations disaster.

Mr. Henthorne decided to use Dr. Rick Miller and the seismic reflection crew at the Kansas Geologic Survey for an investigation along and south of the bypass of Inman. Dr. Miller has developed a type of survey that utilizes close spacing of points for very high resolution of deep beds. A custom-made source truck, the "MiniVibe" sends signals in a range of wavelengths into the ground. Up to 240 pairs of geophones collect the reflected signals, allowing geophysicists to develop a cross-section of the deep subsurface. Past reflection surveys in the Hutchinson area have detected beds 3000 feet below the surface. It is a time-consuming process that would be prohibitively costly were we to hire a consultant; KDOT's contract with Dr. Miller essentially pays only for the crew's expenses. The KGS seismic reflection crew has worked for us before, looking for potential salt subsidence south and east of Hutchinson on the right-of-way of US 50, as well as checking the status of known sinkholes. This project would be somewhat different, however, as the most vulnerable portion of the alignment is currently private land. Although we at KDOT Geology are relatively comfortable with the technology used by Dr. Rick Miller and his staff, the logistics of obtaining the data was daunting.

PREPARING FOR THE SURVEY

The first step in the seismic investigation was simply obtaining permission from landowners to cross their properties with the equipment. To do this, we began by using public information meetings organized by the Bureau of Design in early February of last year with affected residents. These one-on-one meetings were held in Inman, and served to give each landowner a chance to ask questions. At these meetings, Mr. Henthorne and the author took the opportunity to explain the seismic survey we were planning. We detailed our idea for cutting a shallow trench across cultivated fields so that the geophones would "couple" with the ground, and we showed photos of the equipment that would be used. Then, in late July, our office began calling and meeting with the landowners and renters to tell them that work was imminent and to obtain permission to trespass. In all, over 30 families were contacted, including several landowners who initially refused our request. After nearly two weeks of calls and meetings, permission was finally secured all across the proposed bypass alignment.

Meanwhile, our office staff was walking the proposed centerline, trying to find survey marks. Many wooden stakes had been removed, and some rudimentary surveying had to be done at the last moment. Also, cuts had to be made through two hedgerows of Osage-orange trees so that the seismic line could be laid out without interruption. By now, the heat and humidity of July on the Central Plains was a factor, as it would continue to be throughout the survey.

The next step was to cut the shallow "V" trench across cultivated fields for the placement of geophones. A KDOT Maintenance motor grader was used, and the trench was in place in less than four hours. The seismic survey could now begin.

GATHERING THE DATA: A LONG AUGUST

On August 2, 2005, the KGS crew arrived and began by surveying a north-south line along the county road that runs north from Inman. Personnel from both the Salina and El Dorado geology offices assisted with traffic control and in placing geophones. The geophone spacing for our survey was eight feet, with two phones per location for redundancy. Placing and removing geophones is backbreaking work that the KGS workers knew to dread and KDOT helpers learned to dread. The seismic crew works from dawn to dark, and the first day was quite a change for the KDOT staff that had never been around Rick Miller and his crew. We were out in the heat flagging and moving geophones and cables until after 9:00 that evening. The temperature during the afternoon went over one hundred degrees. The north-south line was completed; nearly three-quarters of a mile of data was gathered that first day.

Figure 4: Placing geophones on the first day of the survey

Figure 5: Collecting data in a milo field using a 240-channel seismograph and the custom-made "MiniVibe"

Early the next morning, work started along centerline of the new bypass itself. A week had passed since the trench was cut for the geophones, and 2 farmers had already disked over it. So the motor grader was again brought out; the trench would eventually have to be cut a total of 3 times in some locations.

On the third day of work, data collecting had to stop because of lightning in the area. As Rick Miller put it, "We've essentially strung out a giant antenna along the ground and hooked it up to hundreds of thousands of dollars of equipment." This was the first time storms interfered with the Inman seismic survey, but certainly not the last. Lines of heavy thunderstorms repeatedly pounded the Inman area, delaying the survey for over a week. Work resumed on August 17, only to be interrupted by a large overnight storm the following Monday that dumped over two inches on the area. More storms were predicted. Geophones were in the ground, ready to shoot, but it was too muddy for the "vibe" truck to move around. Both KGS and KDOT crews earned their wages that day, pulling the muddy phones and cables back to the trucks.

The survey finished on August 30, four weeks after it began. The bypass survey covered over five miles, for approximately 3500 receiver stations. Including the initial survey along the county road, the KGS and KDOT crews placed pairs of geophones at over 4,000 locations to collect the data.

ANALYSIS: MOVE THAT OVERPASS

Dr. Miller's final report will not be finished for several months yet, but in November he provided us the critical information regarding the bridges. The seismic images revealed that the salt is intact south and west of the intersection of the bypass and the north-south county road. The interchange west of Inman was therefore safe. At the proposed overpass north of town, however, there was a problem. The location of Pier 1 was underlain by 300 feet of salt, which is most of its thickness. But at Pier 2, only 150 feet of salt remained, with the difference being filled by collapse material. In plan view it appears that a "bull's-eye" of salt remains beneath the proposed bridge location. No voids were detected at the bridge site that might warn of a sudden collapse, but the threat of gradual settlement is very high.

The bridge location had to be moved. The best option was to relocate the county road to the west, and build the overpass in the area where salt dissolution has not yet begun. This, however, would affect property owners to the south, within the Inman city limits. During public information meetings several months before, KDOT had assured these landowners that their properties would not be affected. The road designers understandably did not enjoy the thought of going back on their word and facing angry landowners once more. We finally decided to move the county road to the east, across an area of relatively uniform salt thickness. The proposed overpass across the expressway was therefore relocated 1130 feet to the northeast, where about 150 feet of salt remains across the entire length of the structure. The alignment of K-61 was not changed at all.

CONCLUSION AND LESSONS LEARNED

The seismic geophysicists at the Kansas Geological Survey have once more assisted KDOT in making important decisions regarding a major highway. In this case, a preliminary investigation allowed us to change the location of a bridge that would have otherwise been at risk. This is the first time that the Kansas Department of Transportation has changed the design of a project based on geophysical information. Seismic reflection technology is quite advanced; KDOT is very fortunate to have the services of leading scientists at KGS.

Although we are very pleased with the survey's results, this project clearly showed the need to allow flexibility in the design phase of a critical project. Designers were reluctant to change the location of a county road, even though the geology section had months before warned of the possibility of finding a salt-related feature that threatened the alignment of the expressway itself. Preliminary geophysics will be used more and more on highway projects, both at KDOT and across the country. The project schedule must contain enough time and flexibility to make optimum use of the information so gathered.

ACKNOWLEDGMENTS

The author would like to thank the following individuals for their assistance with this paper: Mr. Robert Henthorne, P.G., KDOT Chief Geologist, Mr. Robert Hirt, P.E., KDOT Road Office, Dr. Rick Miller, Section Chief, Kansas Geological Survey, and Dr. Lynn Watney, Executive Director, Kansas Geological Survey Energy Center. Cathy Johannes of KDOT's support services drew the diagrams.

REFERENCES

Walters, Robert F., *Land Subsidence in Central Kansas Related to Salt Dissolution*. Kansas Geological Survey Bulletin 214, Lawrence, KS, 1978.

Watney, W. Lynn; Nissen, S.E.; Bhattacharya, Saibal.; and Young, David, *Evaluation of the Role of Evaporite Karst in the Hutchinson, Kansas Gas Explosions, January 17 and 18, 2001*, in Johnson, K.S.; and Neal, J.T. (eds.), *Evaporite Karst and Engineering/Environmental Problems in the United States*. Oklahoma Geological Survey Circular 109, Norman, OK, 2003.

Digital Outcrop Characterization for 3-D Structural Mapping and Rock Slope Design Along Interstate 90 Near Snoqualmie Pass, Washington

William C. Haneberg
Haneberg Geoscience
10208 39th Avenue SW, Seattle WA 98146
bill@haneberg.com, (206) 935-0846

Norman I. Norrish
Wyllie & Norrish Rock Engineers
17918 NE 27th Street, Redmond WA 98052
nnorrish@wnrockeng.com, (425) 861-7327

David P. Findley
Golder Associates
18300 NE Union Hill Road, Suite 200, Redmond WA 98052-3333
dfindley@golder.com, (425) 883-0777

ABSTRACT

We used digital outcrop characterization in a rock slope remediation project along Interstate 90 approximately 66 miles east of Seattle. Forty-three photo pairs of rock exposures over a distance of 1600 feet were combined with surveyed camera and control point positions to create 3-D digital outcrop models that can be rotated, panned, and zoomed. The photogrammetry and much of the structural mapping were performed using software created for surface mining applications. Each 3-D model consists of a rectified digital photograph integrated with a cloud of several hundred thousand x-y-z points, with estimated positional errors typically on the order of millimeters to centimeters. Discontinuity orientations are determined by fitting planes to user-selected surfaces or their traces, and the fitted planes can be added to the 3-D model to facilitate visualization of the outcrop-scale structural geology. Discontinuity orientations can be exported and plotted on stereo or equal area nets, and the software calculates surface areas of planes and lengths of traces to characterize discontinuity persistence and spacing. Profiles can be extracted for outcrop-scale joint roughness coefficient (JRC) estimates. We also projected the 3-D models onto a large screen that allowed collaborative structural mapping and interaction among the project team members. The structural data obtained from the digital outcrop characterization were verified with conventional mapping from accessible areas near highway grade. The potential uses of the digital data for slope mitigation projects include kinematic analyses for structurally controlled failure mechanisms, roughness profiles for rockfall simulations, remediation design, and quantity takeoffs for trim blasting and scaling.

INTRODUCTION

Two rockslides along the westbound lanes of Interstate 90 near Snoqualmie Pass, approximately 60 miles east of Seattle, in September and November 2005 prompted a re-evaluation of slope stabilization projects that had previously been deferred in light of anticipated capital improvements to the highway. The September rockslide killed three motorists and the November rockslide caused a short but complete closure and an extended partial closure of the highway while repairs were made. As a result of the re-evaluation process, three rock slopes along a portion of Interstate 90 from milepost 66.00 to milepost 66.58 were slated for immediate remediation on the basis of high rankings in the Washington State Department of Transportation (WSDOT) Unstable Slope Management System.

Bad weather, snow and ice covered surfaces, winter traffic hazards, and a short time frame for remedial design required an expedited approach to rock slope characterization for this project. There were no known existing surface

or subsurface geotechnical data for the project area beyond the information collected for the Unstable Slopes Management System review process. To help meet project deadlines, we used 3-D digital outcrop models for office-based structural mapping of rock mass discontinuities and extraction of rock slope profiles. This technique, using commercially available software supplemented by custom in-house routines, employs high-resolution digital photogrammetry to create detailed 3-D representations of complicated rock exposures. The digital modeling was supplemented by limited field mapping for verification of the digital results and an aerial man lift survey to allow additional observations of the rock slopes.

GEOLOGIC SETTING

The milepost 66 project site lies along Interstate 90 east of Snoqualmie Pass in the Cascade Range of Washington State and traverses the western slope of Anabilis Mountain, a topographic extension of Keechelus Ridge (Figure 1). The summit of Anabilis Mountain lies at an elevation of 4,554 feet and Interstate 90 lies at an elevation of about 2,535 feet.

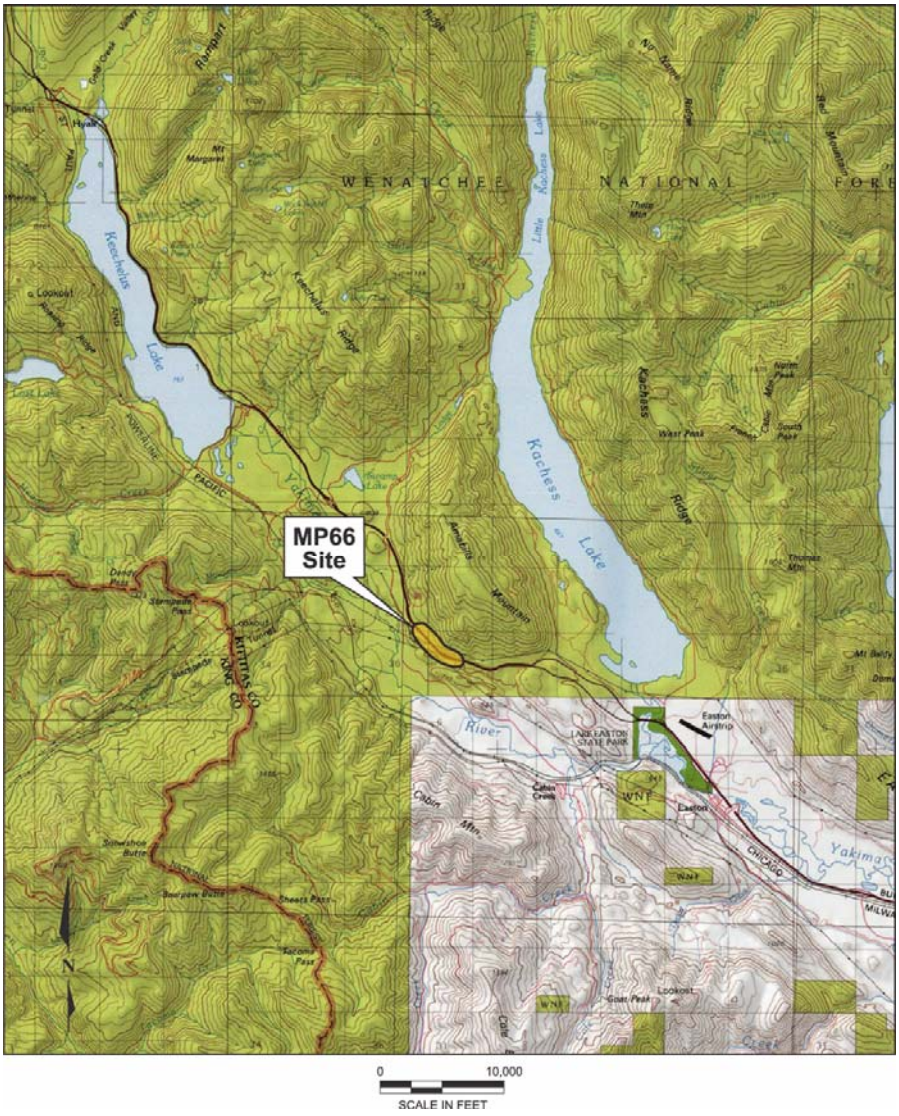

Figure 1. Index map showing the project area in relation to local topography and features. Location is 66 miles east of downtown Seattle.

Bedrock exposed in cuts along the westbound lanes consists of early Oligocene to middle Eocene Naches Formation rhyolite, andesite, and basalt, tuff, and breccia with lesser amounts of sandstone, argillite, and laminated siltstone interbeds (*1*). Bedding generally strikes north-northwest and dips to the west-southwest at 50° to 75°, with anomalies near faults. There is evidence for at least three major alpine glacial advances in the vicinity of the site during the Pleistocene (*1*). Glacial deposits at and near the site, including moraines near the south end of Keechelus Lake and Kachess Lake, range from till on upland and valley margin surfaces to sand and gravel outwash deposits in lowland areas. Lake Keechelus, which is located approximately three miles from the project, is a moraine-dammed lake raised in the early twentieth century by a man-made dam. Kachess Lake, two miles east of the project site, is a natural lake on which an outlet structure was constructed in 1905 to provide flood control and irrigation storage for the Yakima River project. Holocene material at the site consists of mass wasting, colluvium, and minor fluvial deposits of sand and gravel in nearby drainages.

DIGITAL PHOTOGRAMMETRY, MODELING, AND MAPPING

Fieldwork

Digital photographs for the project were taken on the morning of January 24, 2006, with weather ranging from cloudy to partly sunny. Temperatures were at or near freezing, and ice on parts of the eastbound shoulder made it difficult to walk and mark camera locations. The right eastbound lane of the interstate was closed by WSDOT for safety.

Forty-three pairs of 6.1-megapixel photographs were obtained using a Nikon D70 digital SLR with a Nikkor AF-D 24 mm f2.8 lens. The camera was mounted on a standard camera tripod with a pan head. A plumb bob and a retractable steel tape used to mark each camera station and measure the camera height. Although an infrared remote control was available for the camera, it was not used for most of the photographs because its slight time lag made it difficult to ensure that photographs were taken between passing trucks. The files were saved as native Nikon NEF (also known as RAW) files to allow for greater flexibility if exposure or white balance adjustments were needed and to ensure lossless conversion to the tiff format required by the photogrammetry software.

The approach used in this project requires two surveyed camera positions and one surveyed control point location for each photo pair. Alternative approaches can be used for other situations, for example making use of three or more surveyed control points in cases where it is not feasible to accurately determine the camera location (as would be the case if photographs were taken from a helicopter or boat). Camera stations were marked on the shoulder of the eastbound lane using spray paint and PK nails, and control points were marked on the rock face using spray paint. In the case of the camera stations, the letters A and B were used to denote the eastern and western points in each pair (photography proceeded from east to west). The locations of both the camera stations and control points were later surveyed by WSDOT and the coordinates provided in an Excel spreadsheet. The approximate distance between the camera stations and the outcrop, which is required to establish an appropriate baseline length of 1/6 to 1/8 of the distance to the outcrop, was estimated using a pocket laser distance finder to measure the distance to the median barrier. That distance was doubled and 10 feet were added (to account for the distance between the outcrop and shoulder) to establish the approximate distance to the outcrop. The result divided by 6 to calculate the approximate baseline length of 1/6 the distance between the camera locations and the base of the outcrop. As shown in Figures 2 and 3, the photographs covered three cuts, the easternmost of which consisted of five smaller components.

The WSDOT survey coordinates were based on an arbitrary datum assuming camera station 6A to have (east, north, elevation) values of (10000, 10000, 10000) feet. The WSDOT coordinate system further assumes that the vector from camera station 16A to camera station 6A is aligned due east (090°). Office inspection of plans after the 3-D models had been processed showed that the vector from 16A to 6A has an azimuth of 110°. Therefore, a 20° correction was added to dip directions calculated from the 3-D models.

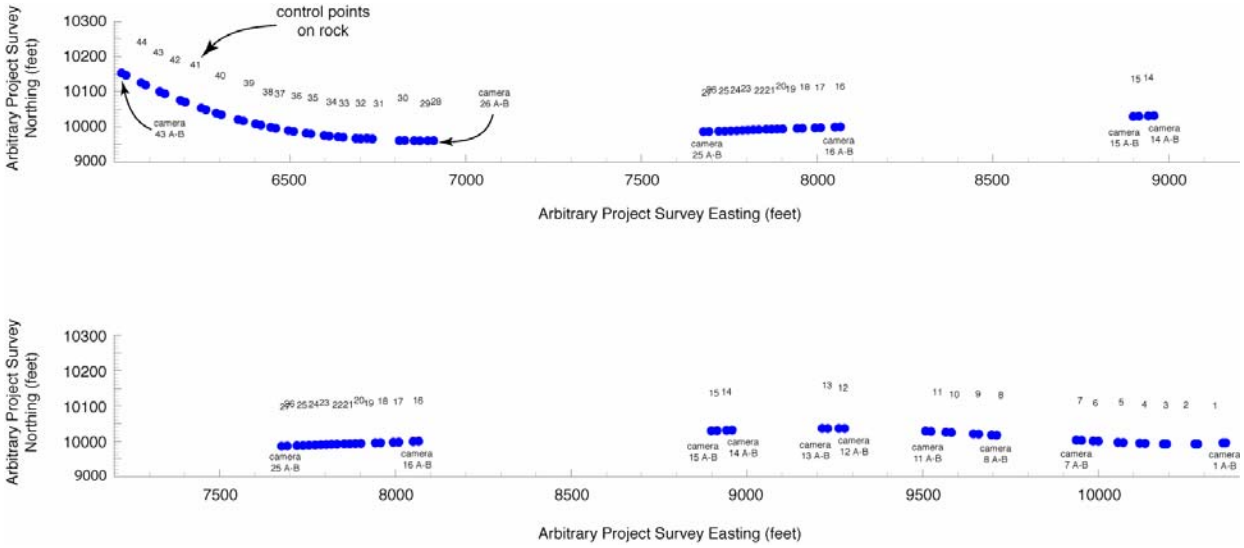

Figure 2. Camera and control point layout. Easting and northing measures are given in arbitrary project coordinates supplied by WSDOT with camera location 6A assumed to have a value of (10000 feet, 10000 feet), and the project easting has a true azimuth of approximately 110°. Upper and lower figures overlap each other.

Image Processing and 3-D Model Creation

Sirovision software (version 3.1) from the Australian Commonwealth Scientific and Industrial Research Organization (CSIRO) was used to create the 3-D outcrop models (*2*). The software consists of two programs: Siro3D for 3-D model creation and Sirojoint for structural mapping and analysis. Although the software was originally developed for surface mining applications, it has proven useful for non-mining geotechnical and hydrogeologic rock mass characterization. Additional information about the software is available at www.sirovision.com.

The photograph files were downloaded from the camera to a computer and converted from NEF to tiff format. Each photograph was then corrected to remove lens distortion using the default Sirovision parameters for the lens, which is among the list of those supported by the software, and each pair was combined with the WSDOT survey results to set up the 3-D orientation for the pair. This processes uses the camera station, camera height, and control point locations for each model and requires that the surveyed control point and three other common (but not surveyed) points be identified in each photograph. A 3-D model area was then defined for each pair, using as much of the overlap area as was practical in each case. Irregular topography, trees, and snow along the tops of the road cuts complicated this task and, as a consequence, some of the models are either truncated along their top edge or contain irregularities near the trees and snow. Finally, 3-D models were generated using block matching (the recommended Sirovision option for structurally or geometrically complicated outcrops). Each 3 by 3 block of pixels in the defined overlap area yielded one spatial data point on the outcrop face, which yielded models consisting of approximately 200,000 to 500,000 xyz points each. This process took approximately 30 minutes per photo pair.

Figure 4 illustrates the progression from a photo pair to a rectified orthophoto and then a 3-D outcrop model for outcrop model 18. Figure 5 shows the 3-D geometric framework of outcrop model 18 using both a point cloud and a triangular faceted surface. This outcrop model is typical of the results obtained in this project and contains an interesting variety of structures. It is used as an example throughout the paper.

Once a 3-D model is created, it can be manipulated within Siro3D or saved for further analysis. Outcrop model 18 consists of 425,523 xyz points in the project coordinate system and covers approximately 8,000 square feet of outcrop surface, giving an average linear xyz point spacing of about 1.6 inches. Denser xyz point spacing can be obtained with higher resolution cameras. A 12-megapixel camera, for example, would have produced more than

800,000 points with an average linear spacing of about 1.2 inches. The estimated root-mean-square (RMS) error of the xyz points comprising outcrop model 18, which is calculated by the Siro3D software, was ±0.75 inches.

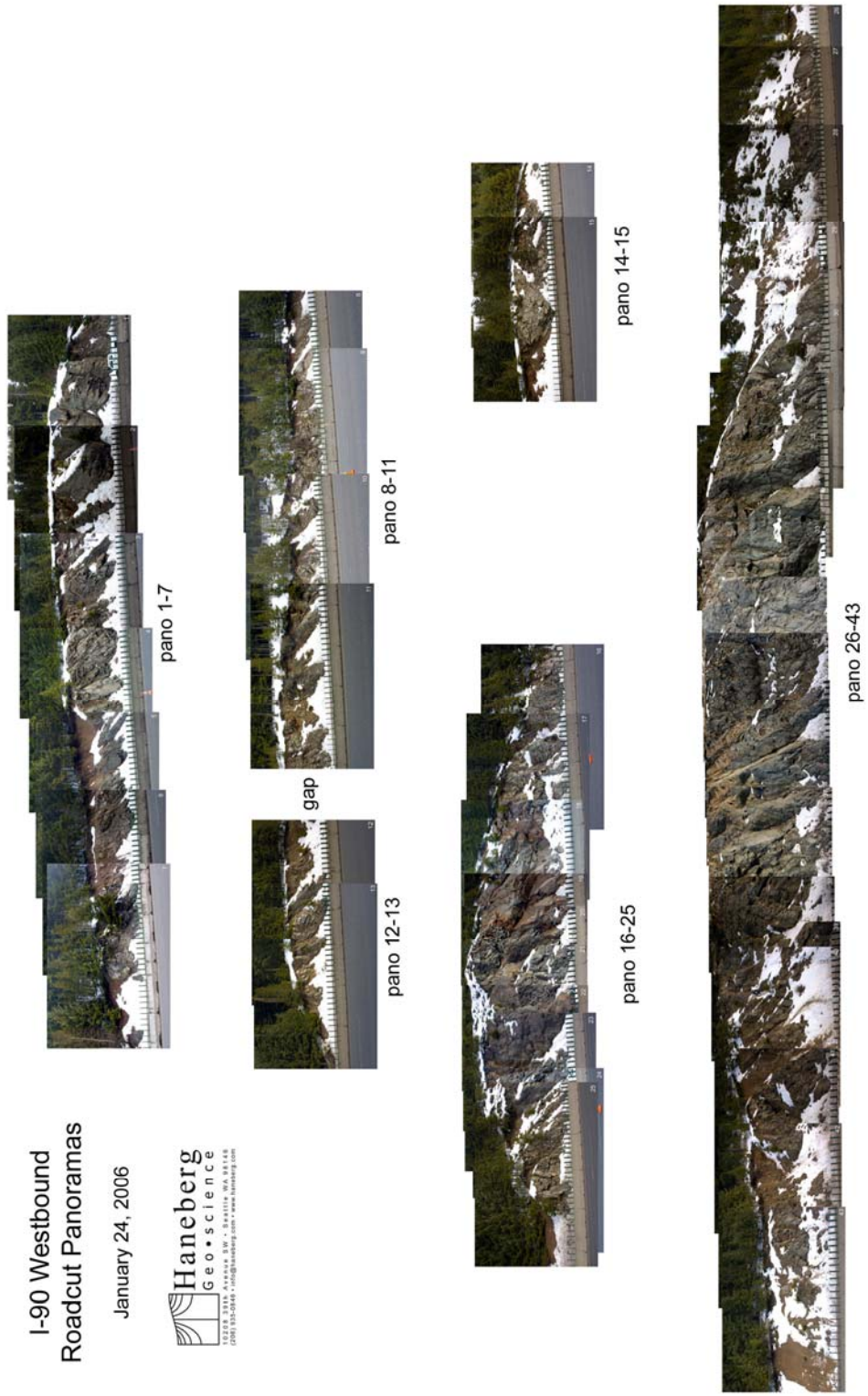

Figure 3. Unrectified photo panoramas of the outcrops modeled in this project. The left image of each photo pair was used to construct the panoramas, and the panorama numbers refer to the photos used.

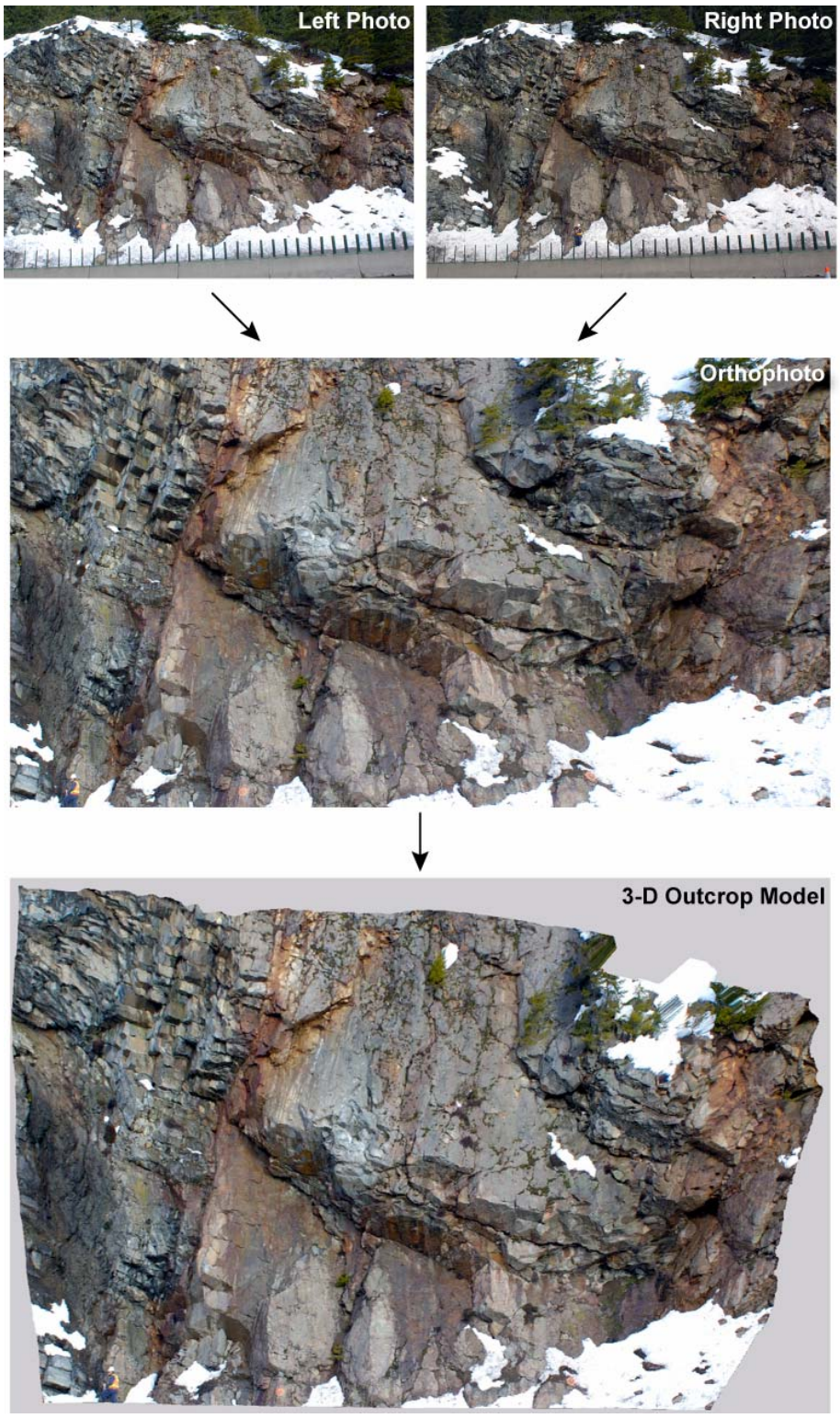

Figure 4. Results for outcrop model 18 showing progression from the individual left and right photos to the rectified orthophoto and finally the 3-D outcrop model saved in a proprietary enhanced tiff format. The 3-D outcrop model consists of 3.8 million color pixels draped over 425,523 xyz points.

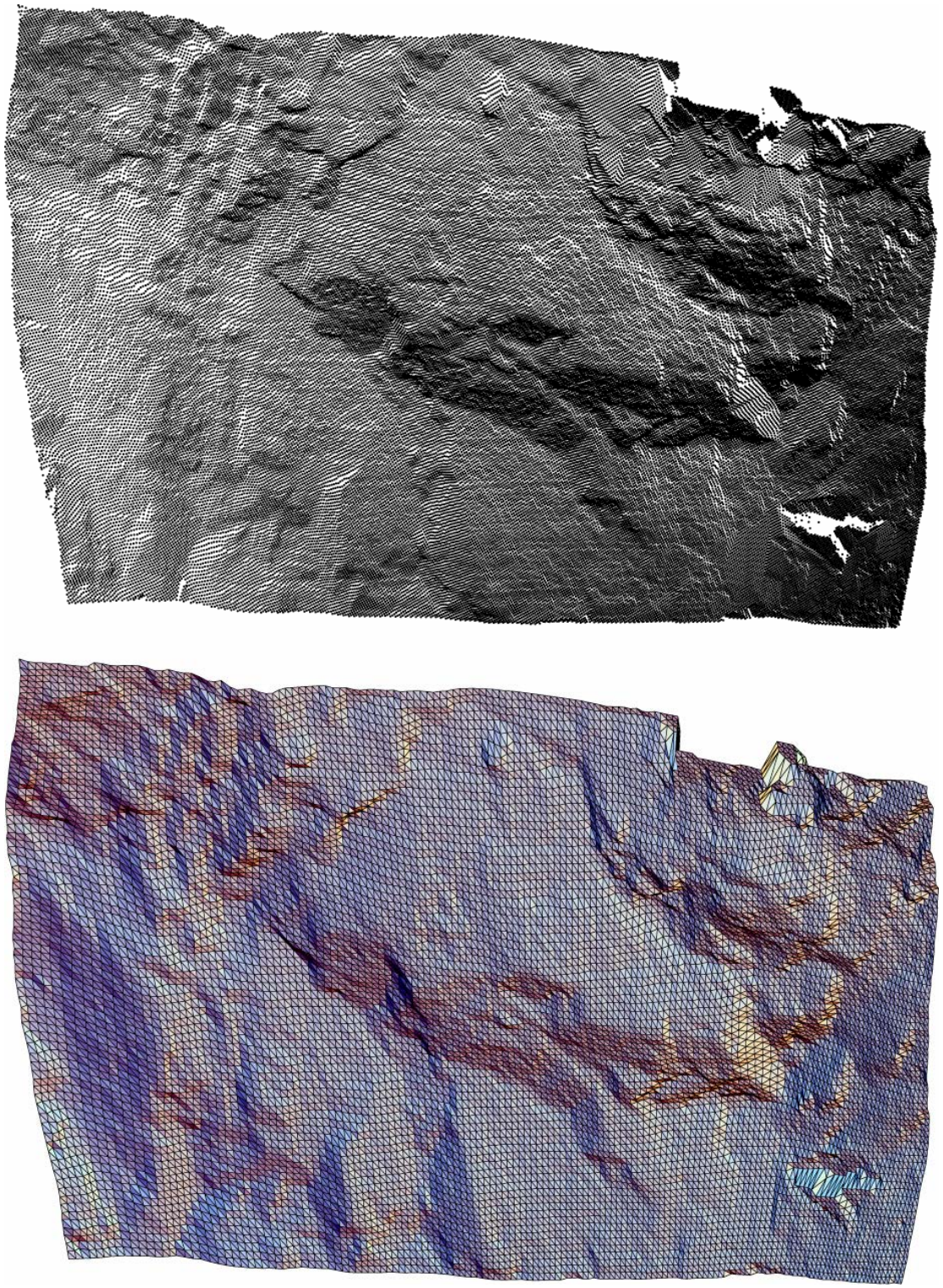

Figure 5. Reduced point cloud and reduced triangular mesh surface for outcrop model 18. Every fifth point was plotted in the point cloud so that individual points can be seen. Note the correspondence between flat facets and snow and trees visible in Figure 4. The mesh was reduced to 23,360 triangular facets for ease of manipulation. Plots were produced by importing Sirovision output into Mathematica and using in-house visualization routines.

As long as a common coordinate system is used for all of the models, two or more models can be combined into a 3-D panorama. Experience has shown, however, that real-time manipulation of the models and structural mapping become slow for models consisting of millions of xyz points. Therefore, the most efficient approach is to use each outcrop model separately.

The models were saved in two formats: special Sirovision rectified tiff files containing 3-D information and an ASCII xyz matrix format for use in profile extraction and visualization. Point density in the ASCII matrices was reduced by factors of 3 to 7 to produce meshes with 20,000 to 25,000 points each. The 3-D meshes can also be exported as ASCII xyz point cloud or dxf files with or without mesh reduction.

INTERPRETATION AND ANALYSIS

Structural Mapping

Digital structural mapping based on the 3-D models was performed at the Golder Associates office. A laptop computer running the Sirojoint component of Sirovision was connected to an LCD projector and used to display the models on a conference room white board, which allowed for collaborative mapping of significant structures by the project team. Sirojoint structural models were created for 3-D outcrop models 1, 2, 3, 4, 5, 11, 13, 18, 20, 24, 27, 30, 32, 36, and 40. Each model includes joint surfaces identified during collaborative mapping, the orientations of which were exported and delivered electronically to Wyllie & Norrish and Golder Associates for further plotting, analysis, and incorporation into slope designs.

Sirojoint allows users to map discontinuities by drawing either polygons, outlining visible discontinuity surfaces, or 3-D lines, that represent the traces of discontinuities intersecting the outcrop face at high angles. The drawing can be done on either the 2-D rectified photograph or the 3-D model, and the latter can be rotated to better expose unfavorably oriented discontinuities. For each discontinuity that is mapped, the software calculates the orientation of a best-fit plane defined by the points within the polygon or comprising the 3-D line. As each orientation is calculated, it can be added to an automatically updated equal area net (with or without contours) or rose diagram. Figure 6 is a screen capture of a Sirojoint session for outcrop model 18, showing the 3-D model, several discontinuities that were mapped as polygons, the planar projection of a fault that was mapped as a three dimensional line, and a contoured equal area net showing poles to the selected planes.

A limited program of field-based manual structural mapping was undertaken to verify and calibrate rock mass discontinuity measurements obtained from the 3-D digital models. Discontinuity orientations were measured at selected locations accessible from the highway shoulder and a limited number of locations accessible with an aerial man basket. The data were collected in general accordance with Golder Associates technical procedures and International Society of Rock Mechanics guidelines, then plotted using the commercial computer program Dips. With the exception of the 20° strike bias arising as a consequence of the WSDOT coordinate system alignment, the manual and digital orientations were in excellent agreement (Figure 7).

Once discontinuity orientations are calculated, they can be displayed within Sirojoint or exported for further visualization and analysis using such computer programs as Mathematica and OpenDX (*2-4*). Although Sirojoint has some advanced visualization and analysis capabilities, we prefer the flexibility offered by our own in-house visualization routines and commercial stereo-net software. As an example of alternative visualization methods, Figure 8 shows thirteen best-fit planes superimposed on both filled and wire mesh representations of outcrop model 18.

If an outcrop mesh is composed of triangular facets, as in Figure 8, the vertices of each facet can be used to solve a three-point problem that gives the orientation of the facet. The facet orientations can then be assigned to sets using statistical techniques such as cluster analysis or based upon professional interpretation of a smaller number of manually measured orientations (*4-6*). Each triangular facet in Figure 9 is colored according to its affiliation with the three discontinuity sets shown in the inset stereo net, allowing for visualization of planar features that may not have been identified during the manual measurement phase. A facet was classified as a member of a discontinuity set if its dip direction and dip angle were both within ±20° of the average values for the set. The continuity of each

colored patch in Figure 8 reflects the roughness or irregularity of discontinuity surfaces. The blue release plane surfaces shown in Figure 8, for example, are much rougher and less continuous than the yellow wedge left surfaces. Although we did not do so in this project, directional roughness profiles and joint roughness coefficients (*7*) can be calculated by exporting the portions of the 3-D model corresponding to specific discontinuity surfaces (*8*).

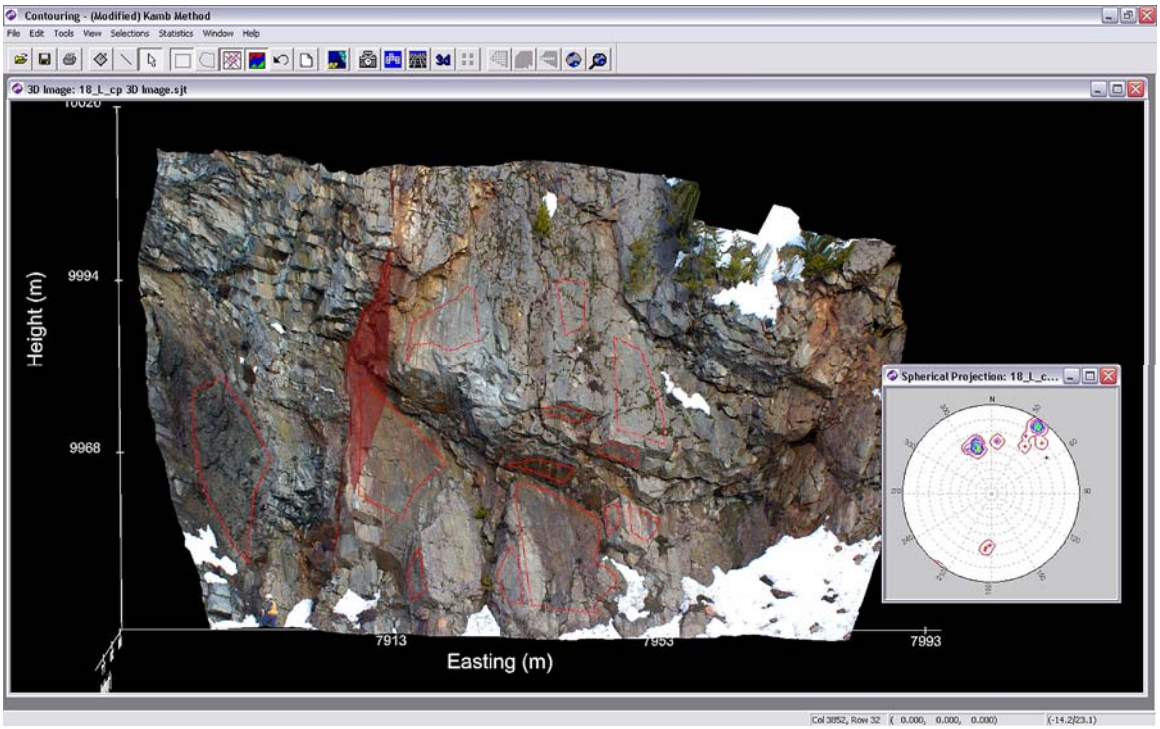

Figure 6. Screenshot of the Sirojoint model of outcrop 18 illustrating the capability to measure orientations and sizes of selected discontinuities. Areas outlined in red were mapped as planar polygons. The translucent red plane is the projection of a fault trace mapped as a 3-D line. The inset shows a Kamb-contoured equal area plot of the poles to the mapped planes. Distances are in feet, not meters as shown (this cannot be changed in the Sirovision software).

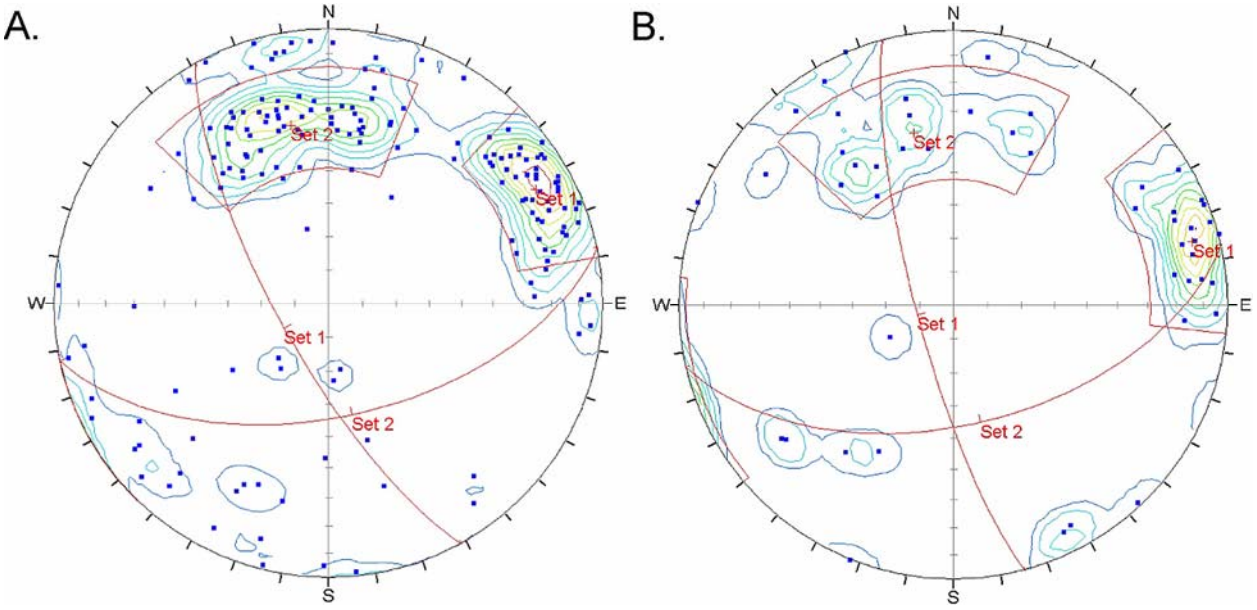

Figure 7. A) Poles and planes calculated using Sirojoint (n = 171). B) Poles and planes measured manually (n = 49). Sirojoint orientations have been adjusted by 20° to account for the survey coordinate system. Results are from all outcrops modeled for this project.

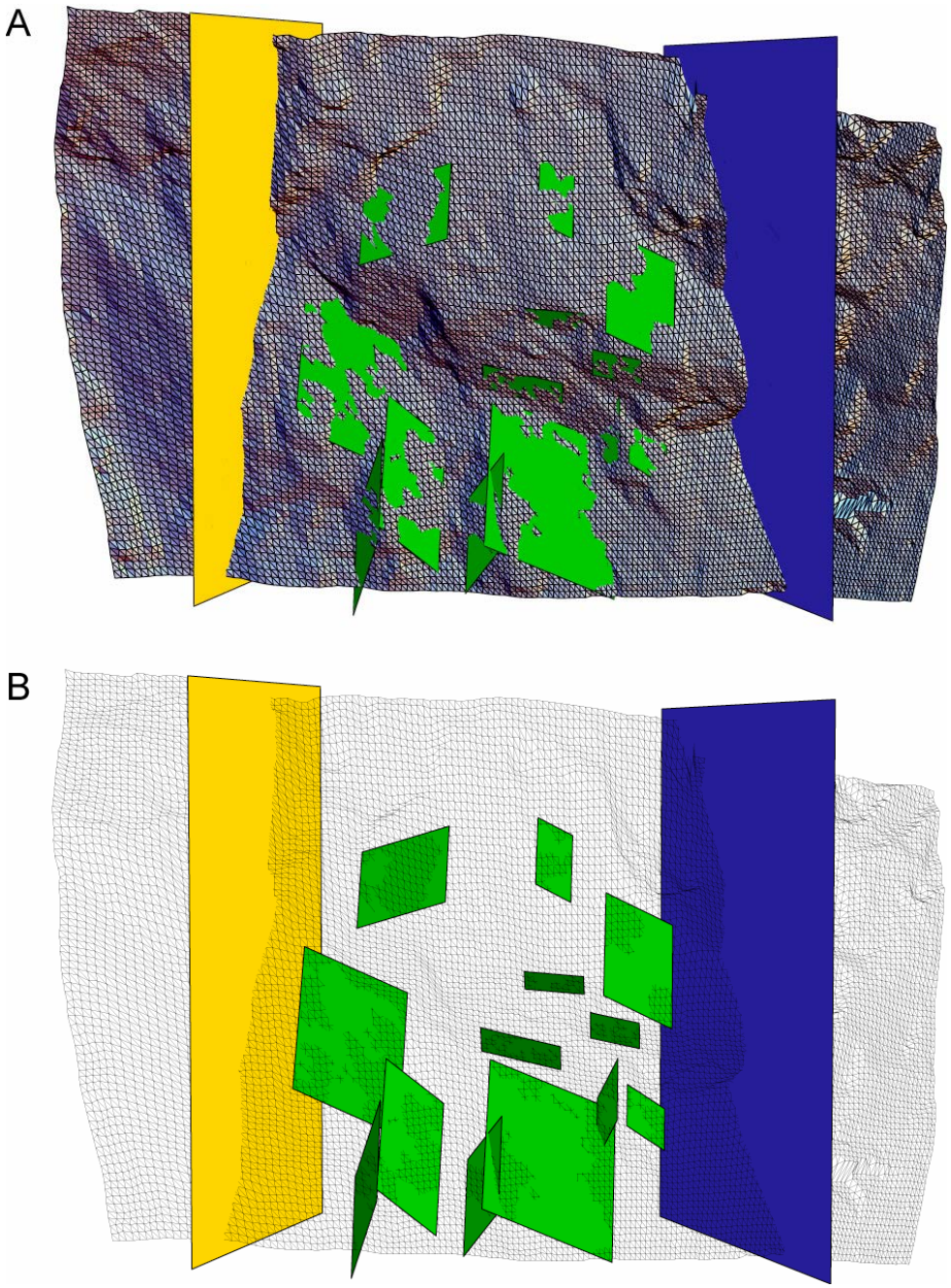

Figure 8. Reduced mesh for outcrop model 18 showing best-fit planes for selected discontinuities and two vertical cutting planes of the type used for profile extraction. These plots were produced by importing Sirovision results into Mathematica and using in-house visualization routines. A) Shaded surface. B) Wire mesh surface.

Profile Extraction

Vertical profiles of each outcrop model were extracted from the reduced meshes and used in the remedial design. Except for three profiles that were moved to avoid trees, profiles were created by slicing the 3-D mesh with a north-south vertical plane passing through each surveyed control point. Profile extraction was accomplished using in-house Mathematica functions that calculate the intersection of a vertical plane with arbitrary strike and the triangular facets comprising outcrop model surface. Figure 8 includes two examples of profiles created by the intersection of arbitrarily striking vertical planes with the outcrop mesh.

Each profile was exported converted to an Excel spreadsheet that included the coordinates of the relevant control point and also converted to dxf format as a five foot wide 3-D strip for easier visualization in Golder's CAD software. A series of annotated jpeg images showing the profiles and control points superimposed on the 3-D mesh was also provided to help visualize the profile locations.

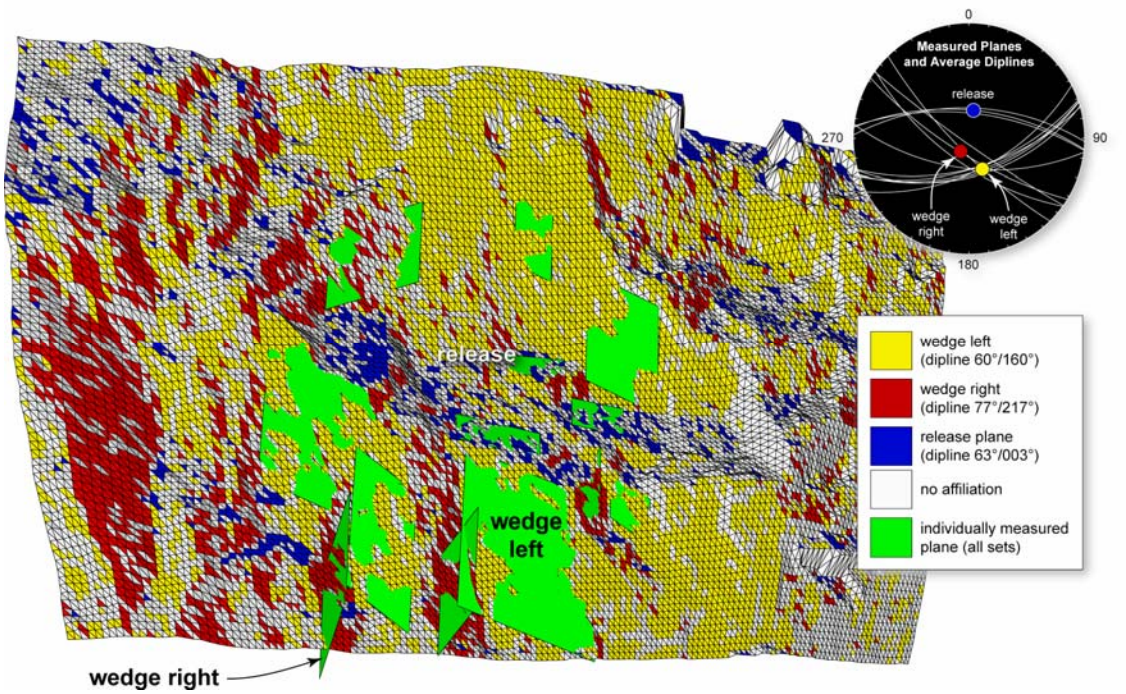

Figure 9. Reduced mesh for outcrop model 18 colored according to discontinuity set affiliation. Individually measured discontinuities are shown in green as in Figure 5B. Orientations shown on the stereo net have not been corrected and azimuths therefore differ from those in Figure 7 by 20°.

REMEDIAL DESIGN

Geologic aspects relevant to remedial design of the rock slope covered by outcrop model 18 include:

- A potentially unstable planar slab of rock near the top of the model. The slab is more than 10 feet thick and rests on a joint surface dipping 50°+ towards the highway.
- Blocky volcanic rock with a colonnade structure in the upper left hand corner of outcrop model 18. Significant joint apertures and rock mass dilation were noted during fieldwork.

- Zones of weathered and highly fractured rock with random discontinuity orientations and limited persistence. These zones will not be amenable to rock bolting or long term stabilization using only scaling.

Remedial measures for the slope consisted of a combination of hand and mechanical scaling and debris removal, top-down installation of 60 kip tensioned rock bolts and 60 kip non-tensioned rock dowels, placement of fiber-reinforced shotcrete, installation of horizontal drains, and installation of cable netting. The particulars for the area covered in part by outcrop model 18 are shown in Figure 10. Sirovision data were used to obtain discontinuity data used in a plane analysis of the large slab, to estimate slab thickness, and to provide vertical profiles such as the one inset into Figure 10.

Figure 10. Rock slope design for the area covered by outcrop model 18, consisting of a combination of scaling, rock bolts and rock dowels, horizontal drains, shotcrete, and cable rockfall nets. Section S18 (inset figure) illustrates typical rock bolt placement and was based on a vertical profile extracted from a Sirovision 3-D mesh.

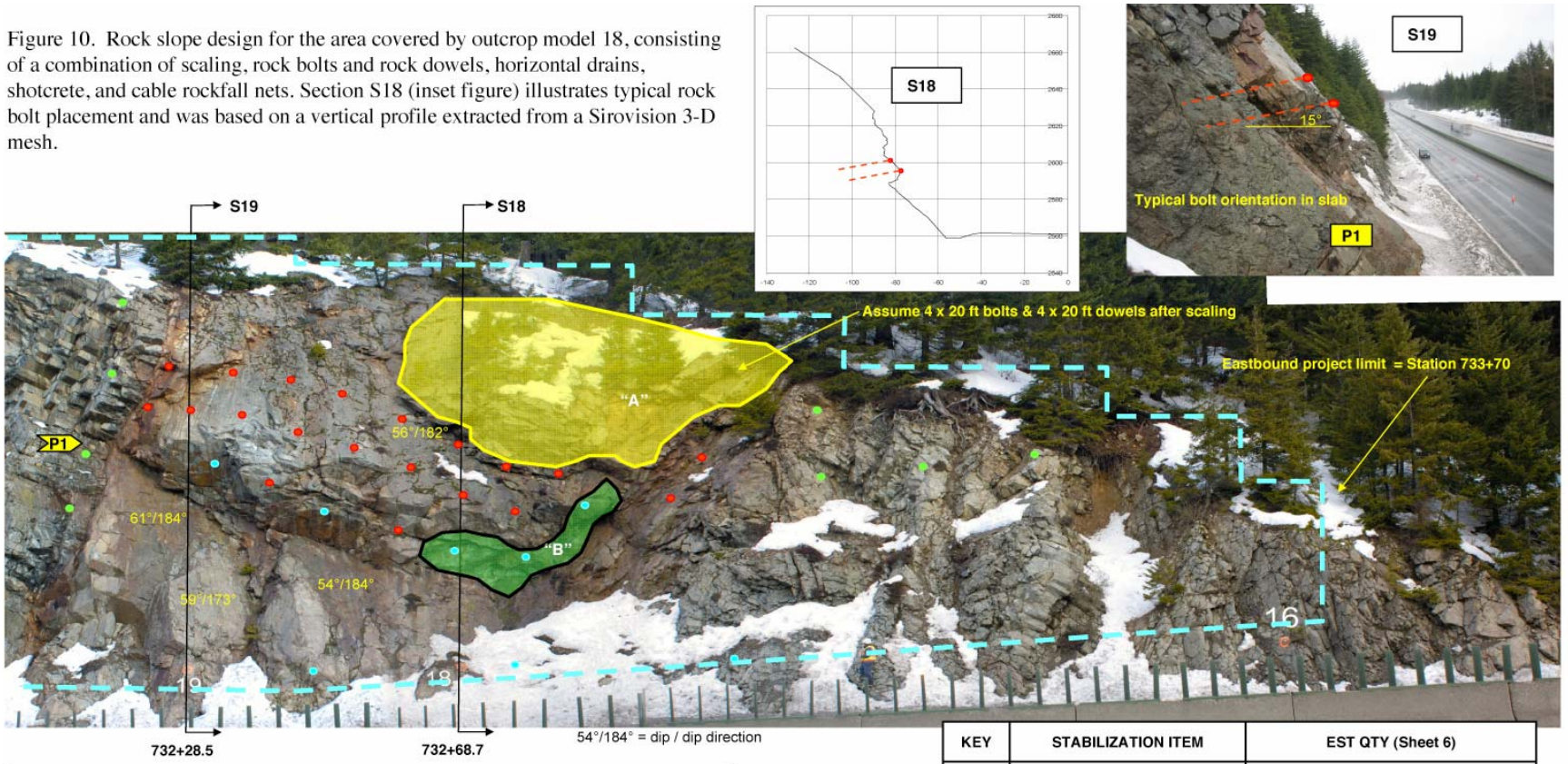

Stabilization Sequence:

- Remove rock slab at location "A" using mechanical scaling.
- Intensive hand scaling with selective mechanical scaling of entire slope including tree removal from face and 15 ft beyond crest to clearing limit.
- Install rock bolts or dowels from **top down** at specified locations and as directed by the Engineer.
- Apply 4-inch minimum thickness fiber reinforced shotcrete at location "B".
- Install horizontal drains at locations shown (upper row = 5 @ 30 ft, lower row = 3 @ 40 ft)
- Install 12" x 12" cable net with double-twist wire mesh to limits shown (12 ft +/- 2 ft above ditch).

KEY	STABILIZATION ITEM	EST QTY (Sheet 6)
	60 kip tensioned rock bolt	24 x 20 ft = 480 ft
	60 kip untensioned rock dowel	12 x 20 ft = 240 ft
	Horizontal drain	3 x 40 ft + 5 x 30 ft = 270 ft
	Scaling / Debris removal	40 crew hr & 2 machine day / 2000 cy
	Shotcrete	40 ft x 10 ft x 4 in = 5 cy
	Cable Net Slope Protection	140 ft x 70 ft avg = 9800 sf

wyllie & norrish ROCK ENGINEERS

I 90 MP 66.27 – 66.31 (Left) WB

Golder Associates

CONCLUSIONS

High-resolution digital photogrammetry provided a fast, safe, and economical characterization alternative for a fast-track rock slope remediation design project conducted under challenging conditions. Field photography was completed within a day of verbal authorization to proceed and the photographs necessary to characterize 1600 feet of rock slopes were obtained in about four hours. Subsequent processing took about 30 minutes for each of the 43 digital outcrop models, and office-based collaborative structural mapping using 15 of the 43 outcrop models was accomplished in less than one day. Additional time was required for file format translation, data management, graphical output, and report writing. The accuracy of the digital structural data was verified against manually collected discontinuity orientation data, and both the orientation data and outcrop surface profiles provided important information for the remedial design.

Advantages of structural mapping using digital photogrammetry and Sirovision software include:

- Equipment portability. The necessary equipment can be carried in a daypack.
- Complete integration of high-resolution digital photographs with 3-D models.
- The ability to select and measure the orientation of individual discontinuities selected on the basis of professional experience and geological insight (*i.e.*, virtual fieldwork).
- The ability to export results in a variety of formats of direct interest to engineering geologists and amenable to quantitative methods such as cluster analysis or eigenvalue fabric analysis.
- 3-D models can be created using photographs taken from a moving aircraft or watercraft.
- Low cost of readily available cameras and software compared to terrestrial laser scanners.

Complete integration of high-resolution color photographs with the 3-D models, in particular, is extremely useful for geologic interpretation because it can convey information about non-geometric attributes such as the distribution of alteration or weathering, locations of seeps, and some variations in rock type. The result is a virtual outcrop that provides more information for geologic interpretation than an unadorned point cloud or mesh.

Disadvantages associated with digital photogrammetry and Sirovision software include:

- Dependence upon proprietary and single-source software for critical parts of the work.
- A steep learning curve for novice users.
- In common with laser scanners, depicts only those features in the direct line of sight.
- Also in common with laser scanners, an inability to extract information about variables such as joint filling, joint aperture size, small-scale joint roughness, and field-based estimates of rock material strength such as those in the ISRM system (*9*).

The density of photogrammetric point clouds tends to be less than that for laser scanners, but in practical applications clouds consisting of hundreds of thousands of points provide useful models. Thus, it is not a significant disadvantage. Although it is possible to estimate large-scale directional joint roughness (feet to tens of feet), the data we describe in this paper are inadequate for the estimation of fine-scale roughness (inches to tens of inches). Future improvements may, however, make fine-scale roughness calculation possible.

Our experience has been that structural mapping using digital photogrammetry and 3-D modeling represents a significant advancement in rock slope characterization for engineering purposes by:

- Greatly reducing the need for high-angle rope belay access to slopes.
- Improving the efficiency and reducing the cost of structural mapping,
- Providing a greatly increased number of data points that help to reduce the uncertainty of stability and kinematic analyses.

Regardless of the advantages that digital photogrammetry presents to the rock slope practitioner, and in contrast to claims that technology will alleviate the need for compasses and measuring tapes (*10*), there will always be a need for trained geotechnical eyes in the field and field-based reality checks to validate digital results.

REFERENCES

1. Tabor, R.W., V. Frizzell, D.B. Booth, and R.B. Waitt. *Geologic Map of the Snoqualmie Pass 30 x 60 Minute Quadrangle, Washington*. United States Geological Survey Map I-2538, 2000.
2. Poropat, G.V. New methods for mapping the structure of rock masses. In *Proceedings, Explo 2001*, Hunter Valley, New South Wales, 28-31 October 2001, pp. 253-260.
3. Haneberg, W.C., *Computational Geosciences with Mathematica*. Springer-Verlag. 2004.
4. Haneberg, W.C. 3-D digital rock mass characterization using high-resolution photogrammetric or laser scanner point clouds. *Geological Society of America Abstracts with Programs*, v.37, 2005, p. 245.
5. Slob, S., H.R.G.K Hack, B. van Knapen, and J. Kemeny. Automated identification and characterization of discontinuity sets in outcropping rock masses using 3-D terrestrial laser scan survey techniques. In *Proceedings of the ISRM Regional Symposium EUROCK 2004 & 53rd Geomechanics Colloquy*, Salzburg, 2004, pp. 439-443.
6. Slob, S., H.R.G.K. Hack, B. van Knapen, K. Turner, and J. Kemeny. A method for automated discontinuity analysis of rock slopes with 3D laser scanning. In: *Proceedings of the Transportation Research Board 84th Annual Meeting*, January 9-13, 2005. Washington, D.C. 2005.
7. Barton, N.R., 1973, Review of new shear strength criteria for rock joints. *Engineering Geology*, v. 7, p. 189-236.
8. Haneberg, W.C. Measurement and visualization of directional rock surface profiles using three-dimensional photogrammetric or laser point clouds. *International Journal of Rock Mechanics and Mining Sciences*, submitted.
9. International Society for Rock Mechanics. Suggested Methods for the Quantitative Description of Discontinuities in Rock Masses. Pergamon Press. 1981.
10. Slob, S. and B. van Knapen. Rock mass characterization with 3D laser scanning: Never again struggling with geologic compass and measuring tape? *Ingeokring Newsletter*, v. 12, no. 1, 2005, pp. 4-9.

The Use of Ground-based LIDAR for Geotechnical Aspects of Highway Projects

John Kemeny
Department of Mining and Geological Engineering
University of Arizona, Tucson, AZ
520-621-4448 (phone)
520-621-8330 (fax)
kemeny@u.arizona.edu

Justin Henwood
Central Federal Lands Highway Division
Lakewood, CO 80228
720-963-3362
Justin.Henwood@fhwa.dot.gov

Keith Turner
Dept. of Geology and Geological Engineering
Colorado School of Mines
Golden, CO
303-273-3802
kturner@mines.edu

ABSTRACT
This paper discusses the use of Ground-based LIDAR for geotechnical applications associated with highway projects. This is part of a one-year project being conducted at the University of Arizona and funded by the Federal Highway Administration. Ground-based LIDAR (also referred to as laser scanning) consists of a compact instrument that rapidly sends out laser pulses and calculates the three dimensional position of reflected objects. A typical scan takes 5-15 minutes and results in a three-dimensional point cloud containing 1 – 1.5 million points. Laser scanners have a range of up to 1 km and an accuracy of ± 3-10 mm. There are two important applications of ground-based LIDAR in geotechnical site investigation, and in the construction and maintenance of highways. First of all, three-dimensional information from a LIDAR survey can be used to estimate dimensions and volumes at a site. This dimensional information can be used, for instance, to accurately estimate the amount material that must be scaled or excavated at a site. Before and after LIDAR surveys can also be used to determine the amount and location of rockfall that has occurred at a site, thus providing direct input for rockfall remediation. Secondly, LIDAR surveys can be used for rock mass site characterization. This can reduce or eliminate access issues and safety concerns, and potentially reduce the time and costs associated with conventional site characterization methods. The paper will describe results of the one-year project, including field case studies in Arizona and Colorado, and recommendations on best-practices and standards related to field scanning, data processing and management.

TECHNICAL SESSION IV
Geotechnical Applications

Accelerated Investigation, Design, Bidding and Construction to Realign Highway US 191, Upper Chase Creek, Morenci, Arizona

Anthony H. Rice, P.E. Geotechnical Engineer,
formerly of MWH Americas, Inc., Tempe, AZ
Golder Associates Inc.
18300 NE Union Hill Road, Suite 200, Redmond, WA 98052
Tel: (425) 883-0777 e-Mail: trice@golder.com

Nick Priznar, Engineering Geologist
Arizona Department of Transportation
1221 N. 21st Avenue Mail Drop 068R, Phoenix, AZ 85009
Tel: (602) 712-8089 e-Mail: npriznar@azdot.gov

Larry Barela, P.E. Highway Design Engineer,
AMEC Infrastructure
3295 West Ina Road, Suite 200
Tucson, AZ 85741
Tel: (520) 219-4998 e-Mail: larry.barela@amec.com

Teresa Speigl, Project Manager
Phelps Dodge Morenci, Inc.
4521 U.S. Highway 191
Morenci, AZ 85540
Tel: (928) 865-6352 e-Mail: tspeigl@phelpsdodge.com

James Melvin, Construction Engineer
Nielsons Skanska, Inc.
22419 Country Road "G", Cortez, CO 81321
Tel: (970) 565-8000 e-Mail: james.melvin@nielsonsskanska.com

ABSTRACT

In late-2005 part of US 191 was realigned through mountainous terrain approximately 11-miles north of Morenci, Arizona. Historically numbered US 666, it is reportedly the least traveled roadway in the Federal Highway System. The realignment facilitated building a new rockfill stormwater diversion dam that would inundate old US 666. The new dam replaces an existing downstream dam that would be excavated by mid-2006 for nearby open-pit mine expansion. The realignment parallels the regionally extensive Chase Creek Fault on the steep west valley wall at approximate elevation 5280-ft.and traverses variable geologic and geotechnical conditions. Soil and rock cut slopes up to 150-ft. high required; drilling investigations, geologic mapping, kinematic analysis and rockfall catch ditch design. Fill slopes to 60-ft. high along the new impoundment shoreline required seismic hazard evaluation and stability analyses. Although planning and feasibility work was completed in mid-2000, a 5-year process to acquire a COE 404 permit necessitated an accelerated 8-month schedule for investigation, design, bidding and construction. Complex geologic structure, limited time for the work, adherence to State highway design standards, constraints imposed by environmental permits and limited right-of-way led to a partnering process between Agency, Owner, Designers, and Contractor. The accelerated partnering process is presented as a case study highlighting lessons learned about minimizing and equitably distributing risk associated with limited geotechnical data, a winter construction period and the need to satisfy multiple stakeholders. Project completion to all stakeholders' satisfaction was partly due to participation by geotechnical, highway design and construction professionals throughout the project.

INTRODUCTION

On January 20, 2006 Phelps Dodge Mining Inc. (PDMI) handed the Arizona Department of Transportation (ADOT) access to a newly constructed 0.8 mile section of Highway US 191 in the Upper Chase Creek Valley approximately 11 miles north of Morenci, Arizona (see Figure 1). Simultaneously ADOT diverted traffic from the old alignment, historically numbered US 666, allowing PDMI and contractor Nielsons Skanska, Inc. (NSI) to commence construction of a new stormwater diversion dam. This culminated an eight month long accelerated investigation, design, bidding and construction process for the highway that had to meet the expectations of multiple stakeholders. Even though the planning for this project commenced some ten years earlier and the permitting process started in 2000, the construction had to be compressed into a three month window to allow at least six months to construct the new dam. In July 2006 an existing downstream stormwater diversion dam was consumed by open-pit excavation as part of PDMI's copper mine expansion and the new dam and highway were fully operational.

The project area features complex fault controlled geology, steep topography, restricted right-of-way, challenging vertical and horizontal alignment constraints, intense rainfall design events, several steep gradient mountain stream crossings and complications associated with the subsequent construction and operation of the new stormwater diversion dam. This paper discusses the above technical aspects of the project and highlights the successful partnering process between Agencies ADOT, Bureau of Land Management – BLM, US Army Corps of Engineers – USACE, Arizona Department of Water Resources – ADWR, State Historical Preservation Office – SHPO, Owner PDMI, Designers MWH Americas, Inc. – MWH, AMEC Infrastructure – AMEC and Contractor NSI.

The paper presents a background discussion of the highway history, project need, timeline and permits. It describes the physical setting in terms of regional physiography, local geology, and hydrology, outlines the site charactererizaton work including geologic mapping, seismic evaluation and subsurface investigations, documents the geometric design in terms of design standards used, design features implemented and agency interaction and approvals, documents the geotechnical design in terms of analyses used, materials required and residual uncertainties, and outlines the contract preparation, estimating and bidding process highlighting owner and contractor approaches to dealing with variations in quantities, escalating fuel and material costs and the isolation of the site. The paper also, summarizes the experiences during construction including schedule and quality control, cost management and equipment and methods used. The paper closes with a summary of lessons learned.

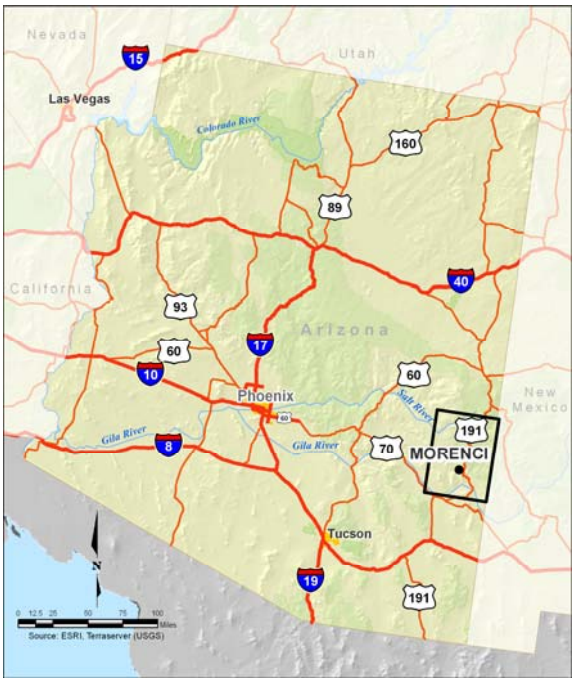

Figure 1 – Project vicinity map showing Arizona Federal Highways and location of major rivers.

BACKGROUND

Highway History

The project alignment was originally part of a wagon road constructed in the late 1800's and early 1900's to access the forest lands for fuel and construction materials to support the rapidly developing mining communities of Morenci, Metcalf, and Clifton in Southeastern Arizona. The years 1919 - 1925 witnessed multiple heroic road building efforts, overseen by Greenlee County, Apache County and the Bureau of Pubic Roads, to overcome the mountainous Apache National Forest and connect the communities of Clifton to Springerville, some 100 miles to the north. When finally completed the route became one of the first public highways financed and constructed in Arizona under the Federal Road Act of 1916. The route officially became a part of the State Highway system in 1928 as Arizona Highway 81 and was incorporated into the Federal Highway system in the 1930's as US Highway 666.

Originally constructed as a ten foot wide single lane unimproved dirt road the alignment evolved, in the 1930's into a 24 ft wide improved gravel surfaced, two lane roadway with intermittent to no shoulders. The route has gone through many episodes of reconstruction and realignment; however the section of road within the project limits had remained very much in the same location and had the same general configuration as the first wagon road.

Today US 191 is classified as rural major collector route that connects communities from the Mexico border (at the port of entry in Douglas, Arizona) north to the Arizona/Utah State line. However, the steep mountainous grades and tight hair pin curves severely limit commercial traffic from traveling north of the project limits. In fact all vehicles over 40 ft. long are restricted from traveling on US 191 for a distance of 75 miles north to the community of Alpine, Arizona. Recently the route between the project and the community of Alpine has been designated as a scenic highway and further highway widening is not contemplated.

Project Need

PDMI operates a large open-pit copper mine within the watershed of Chase Creek, a tributary of the San Francisco River, in the vicinity of Morenci Arizona (see Figure 2). The open-pit complex intercepts the creek bed of Chase Creek, dividing the stream into three reaches. The upper reach (Upper Chase Creek) is located upstream of current mining operations. The middle reach is encompassed by the open-pit complex and related mining operations. The lower reach (Lower Chase Creek) stretches from the downstream limit of the open-pit complex to Chase Creek's confluence with the San Francisco River. The San Francisco River generally flows north to south in the area and is located to the east of the mine. The San Francisco River is an important tributary to the Gila River, which flows northwestward across Arizona towards Phoenix and then southwestward to the Gila River's confluence with the Colorado River near Yuma, Arizona.

The presence of the open-pit complex prevents natural conveyance of flows from the Upper Chase Creek to the San Francisco River. However PDMI is obligated to deliver this water, un-impacted by mine activities, for downstream use. PDMI has operated a pumped diversion facility located above the existing Upper Chase Creek dam for many years. For many years this facility intercepted and pumped all flows within Chase Creek around the mine to a discharge point located in Lower Chase Creek. PDMI mining operations expansion northward along the Chase Creek valley required that the existing stormwater diversion dam be moved to a point farther north in Upper Chase Creek.

The purpose and need for the relocation of the Upper Chase Creek Diversion is to route the un-impacted waters of Chase Creek around the existing and planned mine development activities at the Morenci Mine to protect downstream aquatic resources while providing for the economic utilization of the mineral resources within the Garfield Pit. This diversion will enable full utilization of the mineral resources within the Pit.

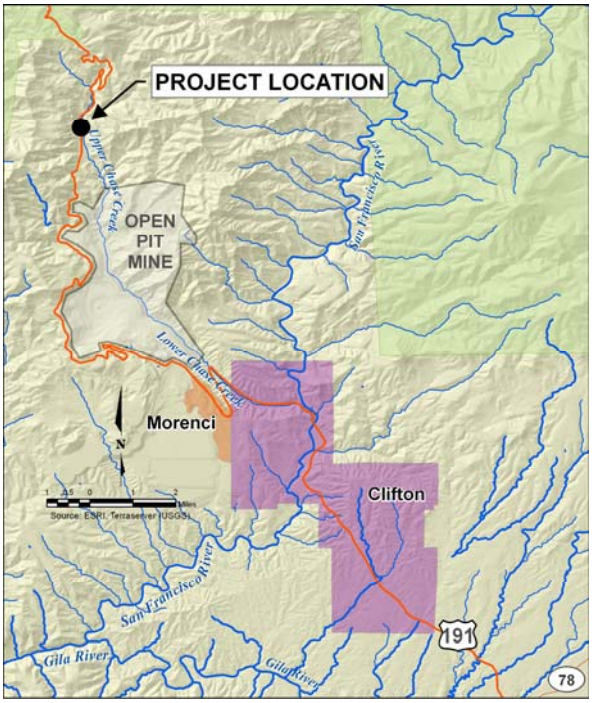

Figure 2 – Project location map showing PDMI open pit operations, Morenci townsite, and US 191.

Project Timeline and Permits

In 1996 PDMI contracted Dames & Moore to perform an Alternative Analysis study of stormwater diversion options in the Upper Chase Creek watershed. This study included a geological, geotechnical, and hydrologic engineering investigations and analysis for the new diversion structure. Three potential dam sites designated as North, Central and South were evaluated along the upper reaches of Chase Creek. Each site was identified on the bases of topographic and geologic characteristics. The Central dam site was selected as the preferred site to the north and south locations because of the storage capacity for given dam height, foundation conditions and lower construction costs (see Photograph 1). The construction of the dam at the Central site would require the relocation

of U.S. Highway 191. Re-routing the Highway along the west side of the valley was determined to be the best alternative. The Alternative Analysis Study was completed in early 1999.

In April 2000 an engineering consulting team consisting of Golder Associates, Inc. (Golder), Parsons Transportation Group (PTG) and Parsons Engineering Science (PES) performed a Preliminary/ Feasibility Design for the Upper Chase Creek (UCC) Dam, Diversion and Highway 191 Relocation in support of the Environmental permitting efforts for the new dam, highway and pipeline (see Reference 8). Their scope included a geotechnical and geologic field and laboratory investigation, geotechnical and seismic parameter review, watershed hydrology assessment, spillway design, analysis of alternative dam types and analysis of highway alignment alternatives.

During this preliminary stage, PTG evaluated three options for the new highway alignment including: first, balanced earthwork considering only the highway alignment; second, minimized impact to the flood pool and minimized waste; and, third, generation of enough suitable cut to construct the highway and provide fill material for the dam. It was determined during this study that the new highway would impact approximately 1.6 acres Bureau of Land Management (BLM) property in order to stay above the maximum flood pool elevation of the new UCC Dam.

In mid 2000, PDMI began the environmental permitting for the UCC Dam and Highway Project. They contracted with Westland (Westland) Resources, Inc. and SWCA, Inc. to implement the environmental permitting process (see Reference 18, 19 and 20). The first steps to the permitting process included developing a 404 Application to be submitted to the USACE as required by the Clean Water Act (CWA). Section 404 of the CWA regulates the discharge of dredged or fill material into waters of the United States. The Application was required to build the dam and contained several studies/documents including an Alternative Analysis, Clean Water Act Section 401 Certification, Cultural Resources Memorandum of Agreement, Jurisdictional Waters Delineation, Mitigation Options for Unavoidable Impacts to Waters of the United States and a Habitat Mitigation and Monitoring Plan.

Photograph 1 – Aerial photograph of Central Upper Chase Creek Dam site on existing Highway US 191.

The National Environmental Policy Act (NEPA) Program required an Environmental Assessment of the Project. Baseline Studies were performed by SWCA, and included an Archeological Evaluation, Biological Evaluation, Land Ownership and Land Use Study. The final 404 application was submitted to the USACE in February 2005 and was approved in June 2005 (see Reference 4).

PDMI applied for an Exception for the new UCC Dam from the ADWR jurisdiction. The Exception was granted to PDMI based on the premise that the storage capacity of the dam would be contained within the property that PDMI owns, operates, controls, maintains, or manages and that is not open to the public. PDMI will also maintain downstream containment structures or sites with sufficient containment for the storage capacity of the dam throughout the useful life of the dam.

In March 2005, PDMI bid the final engineering design to four consulting firms. Each consulting firm was pre-qualified for designing the dam, pipeline and highway. MWH (with AMEC as a sub-consultant for the Highway design) was selected to do the work and started the final engineering in late April 2005. The engineering scope included developing a Basis of Final Design Report for the Dam, Pipeline and Highway, Geologic and Geotechnical Characterization, Dam Design, U.S. Highway 191 Relocation Design, Traffic Engineering Design, Pipeline Diversion Design and a Riparian Flow Collection and Pumping System Design. The deliverables for the design included a Final Design Report, Geotechnical Report, Hydrologic Report for the Dam, Drainage Report for the Highway, drawings, specifications, engineer's cost estimate, and construction bid package.

When the highway design commenced, boring locations were restricted until the 404 Permit was issued in mid-June 2005. This limited the availability of geotechnical data early in the design and required significant assumptions.

Once the Permit was issued, the required borings were drilled in and around the Upper Chase Creek area. The results of the geotechnical investigation were then used in the final design for the dam and highway.

PHYSICAL SETTING

Physiography

The project is located in Greenlee County approximately 11 miles north of the mining community of Morenci Arizona, along US Highway 191, between mileposts 173 and 174. This area is wholly contained in the watersheds of Chase Creek and Chesser Gulch at an approximate elevation of 5280 feet.

The project is located near the eastern border of Arizona on the southeastern flank of a central highland region, commonly referred to as the Transition Zone. The Transition Zone divides the state into two major physiographic provinces, the Colorado Plateau to the north and the Basin and Range to the south.

Photograph 2 – Preconstruction view looking north along US 191 towards the location of the new Upper Chase Creek Dam.

Structural Geology

The new alignment was relocated approximately 200 feet west and uphill of the existing route on the western side of a V-shaped valley created by a regionally extensive north trending high angle normal fault (see Photograph 2). Referred to as the Chase Creek Fault Zone (CCFZ) this structure places Precambrian Granite in contact with Tertiary volcanics and in close proximity with outcrops of Paleozoic sediments. This structure has an apparent dip slip displacement of 950 feet at an approximate inclination of 60 degrees.

Regionally the fault is reported to exhibit a 10 –13 feet wide clay gouge, which can be surrounded with a zone of breccia approximately 100 foot wide as described by Walker, 1995 (see Reference 17). Locally the fault zone approaches 200 feet in width and may represent several, discontinues, sub-parallel discontinuity planes. Sections of the fault zone are clearly revealed in the cuts for the new alignment and display slickensides with a down to the east orientation which control highway cut slope geometry. The CCFZ is not known to be a source of recent seismic activity.

Local Geology

The geologic units in the vicinity of the dam are discussed below in sequence from oldest to youngest. The basement rock in the vicinity of the project is Precambrian Granite. Several small outcrops of Paleozoic rocks were identified within the project limits during the field mapping process and in the exploratory borings. However a considerable thickness of Paleozoic lithologies outcrops on the west side of Chase Creek approximately 1000 feet above the highway. Two suites of Tertiary volcanic rocks are exposed within the project limits. The older being an Oligocene to Miocene assemblage of mafic, basaltic andesite lava. The younger formation consists of a rhyolite dome and tuff complex associated with the Enebro Mountain Formation (EMF). Both these lithologies dominate the east side of Chase Creek and Chesser canyon. They appear to occupy unconformable, and fault contact positions with the Precambrian Granite and the Paleozoic rock units. These Tertiary units dip to the northwest at about 10 to 20 degrees. A generalized geologic cross section of the Upper Chase Creek Valley is presented in Figure 3.

Within the project area the lowest western slopes of Chase Creek are generally mantled with an unconsolidated sandy to clayey granite boulder colluvium. These materials also are presumed to underlay the Quaternary Alluvium that occupies the narrow flood plain of Chase Creek. A dissected alluvial fan is also exposed on the west side of the valley and has been credited as the source of large displaced granitic boulders from local flood events.

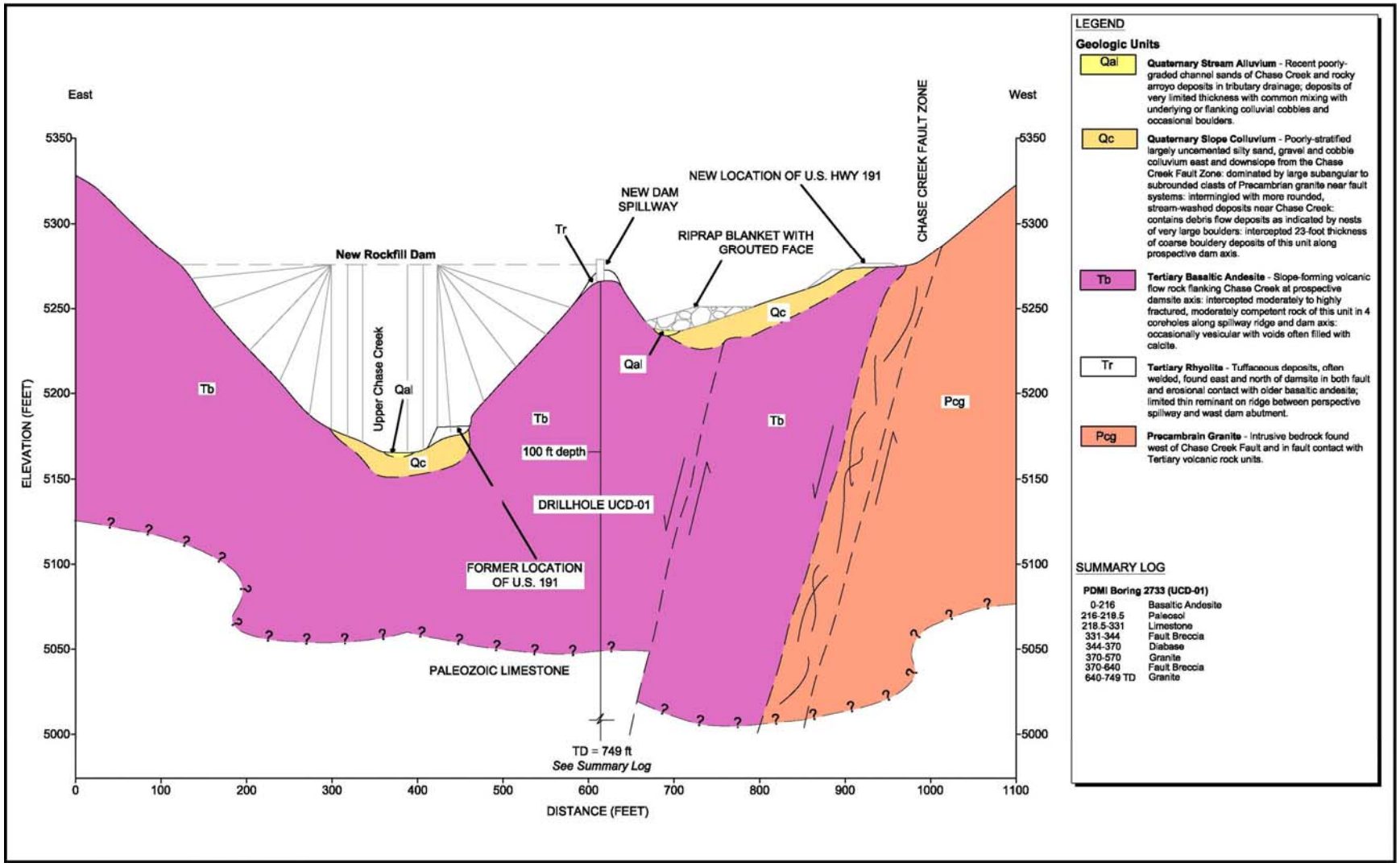

Figure 3 – Generalized Geologic Cross Section – Realigned US 191 and New Rockfill Dam – Looking Downstream (Reference 8).

Granite (Early or Middle Proterozoic) "Red Granite"

Precambrian Granite locally referred to as the "Red Granite", has been described as a fine to medium grained pinkish red granite porphyry. Regionally, Ferguson & Enders, 2000 (see Reference 7) described this material as "coarse-grained, equgranular granite, typically yellowish-red to deep brownish-red in unaltered areas, and light tan to light grey where altered to a quartz-sericite-pyrite assemblage". It is "prominently jointed and exfoliation sheeted in a northeast to north direction. The joints stand almost vertically and separate the rocks into thick ribs, benches, and angular outcrops". The top of the granite is sub-aerially weathered and marks the position of a profound regionally extensive erosional unconformity, that separates the Precambrian rocks from the younger Paleozoic lithologies in most of central and southwestern Arizona (see Photograph 3).

Photograph 3 – Preconstruction view looking south along Upper Chase Creek towards area of US 191 realignment showing Granite with structure paralleling the Chase Creek Fault orientation.

Longfellow Formation (Ordovician)

This unit was originally described by Lindgren, 1905a,b (see References 9 and 10). "It consists of a light tan to brownish grey, medium- to thin-bedded limestone, cherty limestone, and dolomite. The upper 150 feet typically forms a cliff of massive and amalgamated limestone and the lower 250 feet contain shale strata and forms slopes leading to the underlying Coronado Quartzite".

Coronado Quartzite (Cambrian)

This unit was also originally described by Lindgren. It consists of a "medium- to thick-bedded, brown, pink, and maroon quartzite, feldspathic quartzite, and minor arkose. The upper portion of the unit typically forms precipitous cliffs. The lower portion typically consists of quartz pebble to cobble conglomerate that is up to 50 feet thick" as described by Ferguson & Enders.

Basaltic andesite (Oligocene – Miocene)

This unit as described by Ferguson & Enders (2000), consists of a "complex sequence of mafic lavas characterized by abundant plagioclase phenocrysts and variable amounts of pyroxene, with hornblende and biotite. The lavas display typical flow textures and variations in flow morphology (from) massive to brecciated flows that can range from 3 to 35 feet in thickness. In the project area, Golder & Associates 2001 (see Reference 8), reported highly fractured, moderately competent flow rock with a lithologic thickness in excess of 200 feet.

Enebro Mountain Formation (Miocene)

This unit (EMF) as described by Ferguson & Enders (2000), consists of a "crystal-poor to aphyric, high-silica rhyolite lava interbedded with nonwelded tuff and locally intruded by hypabyssal rhyolite. The lava unit includes all varieties of flow type, from vitric or devitrified flow-banded to vitric or devitrified autobreccia, and clast-supported block and ash-flow deposits. Hypabyssal bodies occur as dikes, plugs and sills in, Chesser Gulch". The highway alignment intercepts an outcrop of EMF at highway grade as it deviates northeast away from the CKFZ, to rejoin the old highway corridor. Construction activity within a drainage tributary has exposed a zone of white rhyolite tuff surrounding an opaque (black) flow–banded vitrophyre.

Hydrology

Photograph 4 – Construction view of triple 36 inch culvert inlet on new US 191 alignment near north end of project.

Most of the Upper Chase Creek watershed is located within relatively undisturbed areas that are used for light cattle grazing and recreational activities. In the project area, Upper Chase Creek is a south flowing drainage cut deep in a V-shaped valley. The area is characterized by steep to very steep hills and mountains with numerous drainages and four major side canyons on the west valley wall above the new alignment. US 191 crosses Upper Chase Creek on an existing 40 ft. long hybrid box culvert structure just north of the site but the project did not require any new crossings of Upper Chase Creek. Cross drainage from the four canyons on the west valley wall and general side hill drainage was conveyed across the existing roadway at eight separate locations. There were two sets of dual 36 in corrugated metal pipe (CMP) culverts, one single 24 in CMP culvert, three single 36 in CMP culverts, and one set of dual 42 in wide by 29 in high arch CMP culverts. All but two of these culvert locations were maintained and/or extended to provide drainage under the existing roadway except for one single 36 in. CMP culvert and one set of dual 36 in. CMP culverts at the south tie in of the project. Six new culvert locations were added to allow cross drainage to pass under the new roadway. This included two sets of triple 54 in CMP culverts, one single 36 in CMP culvert, one set of dual 54 in CMP culverts, and one 10 ft wide by 6 ft high reinforced concrete box culvert.

Hydraulic data for the area is limited. For drainage design purposes, AMEC considered this section of U.S. 191 a Class III facility. For this class of roadway, cross drainage is normally designed for a 25-year storm frequency per Table 603.2A of the ADOT *Roadway Design Guidelines* RDG, 1996 (see Reference 2). Hydrologic design followed the procedures outlined in ADOT's *Highway Drainage Design Manual Hydrology, 1994 (see Reference 12)*.

The new culverts were generally designed to operate under inlet control conditions. However the pond behind the new dam will develop a water level during the 25-year event that will result in outlet control at one of the new culverts so this had to be considered in design.

Channel velocities are closely correlated with slope inclination. The new alignment traverses topography generally steeper than that traversed by the existing roadway. Experience with similar topographies in southeastern Arizona led the designers to select higher minimum culvert discharge velocities stipulated in Section 600 of the ADOT RDG for erosion protection and energy dissipation. The RDG allows for dumped stone rip rap or wire-tied gabion baskets to meet the requirements of Section 600. For discharge velocities in excess of 15 fps drop structures, impact basins or other types of energy dissipation can be required. A drop structure was incorporated into the outlet works for the large box culvert.

SITE CHARACTERIZATION

Photograph 5 – Bedrock outcrop above new US 191 alignment near middle of project. Note unfavorably dipping rock structure.

The site characterization work included field reconnaissance, geologic mapping (see Photograph 5), inspection of exposed cut slopes and supervised the completion of ten drill holes. This work supplemented that carried out for the preliminary feasibility study and is described below.

Geologic Mapping

Geologic and geotechnical site reconnaissance was carried out to confirm the geologic information available from the Preliminary / Feasibility Design study, to expand the available data set and to extrapolate the subsurface conditions beyond and interpolate the subsurface conditions between widely spaced drillholes. Exposed rock cuts along the existing highway and rock outcrops above the new alignment were mapped using Brunton and Clar compasses to develop geologic structure data sets. The lithology and surface outcrop of major contacts and structures such as the CCFZ were identified. Potential borrow sources and a potential rip rap quarry in the vicinity of the site were inspected and samples of material were obtained for durability testing. Evidence of geologic hazards such as rockfall and debris flow deposits were noted.

Much of the terrain that was traversed above the highway was very steep, covered by thick vegetation and there was a considerable amount of loose rock in the ground surface. A thick colluvial blanket was noted across the southern part of the site, shallow granitic rock with unfavorably dipping joint structure was noted across the middle of the site and a thick alluvial/colluvial blanket and debris flow deposits were noted across the north end of the site. These conditions were critical in the selection of the highway alignment, the cut-fill balance and the slope design.

Seismic Evaluations

The CCFZ that is exposed in some of the new highway cuts is not known to be a source of recent seismic activity. As part of the evaluation of the dam, seismic evaluation was carried out on portions of a feature described by Pearthree, 1988 (see Reference 13) as the Clifton Fault System located southeast of the town of Clifton (some 15 to 30 miles southeast of the project). At the time the feasibility study was prepared portions of the Clifton Fault System known as the Ward Canyon and Maverick Hill Faults were considered to be potentially active. Aerial photograph interpretation, additional literature review, ground mapping and consultation with staff from the Arizona Geological Survey confirmed that the most recent movement along the Clifton Fault System occurred in the early to mid Quaternary. The fault does not appear to have been active in Holocene or Recent geologic time. The design seismic acceleration chosen for project was 0.15 g associated with a Maximum Credible Earthquake of Richter Magnitude 7.0 along the Safford Fault System some 40 to 70 miles southwest of the project. This acceleration was used in pseudo- static analysis of the stability of the cut slopes and highway embankment in the reservoir. The critical design condition for the embankment was during drawdown conditions when, following the 100 year storm event and reservoir full conditions, the pond level would drop approximately 60 feet over a 30 day period. Though not really a rapid drawdown condition, this would result in locally elevated pore pressures. Fortunately the coincidence of the design seismic event with the drawdown condition was not considered sufficiently likely to require the two events to be superimposed in the analysis.

Subsurface Investigations

Subsurface drilling was carried out at 10 locations along or within 75 ft. of the proposed new highway alignment centerline in conjunction with an investigation of the proposed spillway and dam site (see Photograph 6). The drillholes were advanced to depths of between 20 and 60 ft. The purpose of this drilling was to characterize the material overlying bedrock, define the depth and type of bedrock, and to perform bedrock characterization. Standard Penetration Tests (ASTM D-1586) were carried out in overburden material and Rock Quality Designation (RQD) was determined using the ISRM method.

CRUX Subsurface, Inc of Spokane Valley, Washington completed the subsurface drilling using a Burley 4000 track-mounted drill rig. Their crew included 1 lead driller and 2 helpers. Work was carried out on a schedule of 10-days on, 4-days off, and 10-days on in June 2005. The geotechnical drilling was completed by the beginning of July 2005. Access construction for the drilling program required that an old access route that had been established for drilling the right dam abutment during the 2000 feasibility study be redeveloped. This access route was pushed south and north. Construction of this access route also allowed for easy walking which assisted design, regulatory and bidding contractor personnel to conduct inspections.

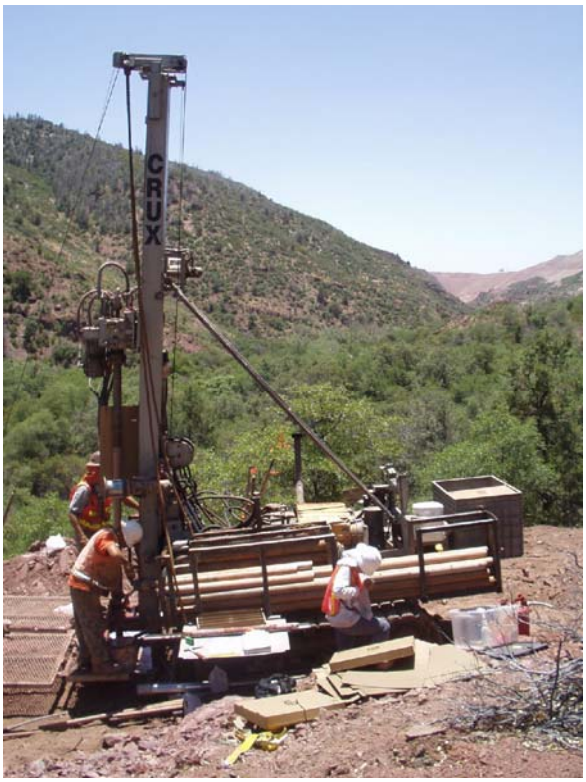

Photograph 6 – Geotechnical Exploratory Drilling along new alignment of US 191 above new Upper Chase Creek Dam.

GEOMETRIC DESIGN

Stakeholders

PDMI both initiated and funded the project but the project had to be turned over to ADOT on completion. AMEC took a lead role in designing the new roadway. ADOT assumed a review role ensuring adherence to established design guidelines and procedures. PDMI led the environmental effort by securing the necessary environmental permits during the project's study process. PDMI also coordinated with the BLM to obtain a highway right-of-way easement for ADOT. AMEC served as the lead coordinator to facilitate communications and meetings with ADOT.

Design Standards

An early study title *Preliminary Feasibility Design for Upper Chase Creek Diversion (see Reference 8)* determined the preliminary location and design for both the highway and dam. Phelps Dodge initiated contact with the BLM, ADWR, and ADEQ during this phase to establish the right-of-way limitations for the highway, determine the design requirements for the dam, and prepare the necessary environmental documents: *MSGP-2000 Storm Water Pollution Prevention Plan Revision 4* (see Reference 18*), MSGP-2000 SWPPP Best Management Practices Plan Revision 1* (see Reference 19*), Environmental Assessment* (see Reference 20*),* and *404 Permit* (see Reference 4).

Although most of U.S. 191 is part of the Federal Highway System, this particular is part of the Arizona State Highway System. Consequently, ADOT, not FHWA standards governed the design criteria for reconstruction. All aspects of the roadway design meet applicable design standards or have an approved design exception/variance. Design criteria not conforming to the requirements found in the *Roadway Design Guidelines* (see Reference 2) call for design exception or variance. Below is a list of additional standards and guidelines used for the design of the roadway:

- *Standard Specifications for Road and Bridge Construction* (see Reference).
- *Manual on Uniform Traffic Control Devices* (see Reference 16).
- *Traffic Engineering Policies, Guides, and Procedures* (see Reference 3).

Design Features

The classification for U.S. 191 in Greenlee County is a rural major collector roadway. The minimum design speed recommended by ADOT for this type of roadway is 60 mph. However, ADOT allowed a 30 mph design speed to accommodate the extreme mountainous terrain, which better matched the existing posted speed limit of 25 mph on the adjacent sections of roadway. This segment of roadway currently has very low traffic use with 600 vehicles average daily traffic (ADT). The projected value used for design is 900 vehicles ADT. Design speed, traffic data, hydrologic analysis, and geotechnical investigations governed the highway design.

The following is a list of the major design features (see Photograph 7):

- 2 – 12 Foot Travel Lanes
- 2 Foot Shoulders
- 4H : 1V Shoulder Wedge
- 2H : 1V Maximum Embankment Slopes
- 0.9V to 1V Maximum Rock Cut Slopes
- 1.5H : 1V Maximum Overburden Cut Slopes
- 25-Year Storm Event
- 2% Normal Crown Slope
- 8% Maximum Superelevation
- 10 Foot Flat Bottom Ditch
- 20 Foot 4 to 1 Ditch Foreslope (At Select Locations for Rock)
- 8% Maximum Grades
- 5 Inches Pavement
- 10 Inches Aggregate Base
- Up to 400 Foot New Right-of-Way Width

Photograph 7 – Newly constructed alignment of US 191 above new Upper Chase Creek Dam with completed pavement.

Agency Interaction

A high level of coordination with ADOT roadway reviewers was required throughout the design phase of the project. An "over the shoulder" review process was used to maintain the design schedule. A project kickoff and four progress/comment resolution meetings kept all members of the design team informed of the project status and development. Three construction document evaluations at the 30%, 60%, and 95% design levels were performed by ADOT reviewers and by members of the design team at two-month intervals, and incorporated two-week review periods. ADOT roadway projects normally require five separate reviews. Therefore, eliminating two of these reviews significantly decreased the amount of time required to complete the project design and remain on the desired schedule.

Due to the small amount of time between reviews and the decreased number of reviews, close coordination with ADOT roadway, traffic, right-of-way, and drainage reviewers were required to minimize reworking designs while holding schedule. This interaction with ADOT allowed for the approval of a number of request, for design exceptions and variances. The project's mountainous terrain, right-of-way limitations, dam flood pool requirements, and existing bridge structure necessitated the design variations.

GEOTECHNICAL DESIGN

Major Issues

The new alignment of US 191 parallels the regionally extensive CCFZ on the steep west valley wall at approximate elevation 5280-ft.and traverses variable geologic and geotechnical conditions. Road surface elevation north of the dam along the impoundment shoreline was constrained by an anticipated full pond elevation of 5,277-ft. following the 100-yr event. Soil and rock cut slopes to 150-ft. high were required with adequate rockfall catch ditches. Fill slopes to 60-ft. high along the new impoundment shoreline required seismic hazard evaluation and stability analyses under drawdown conditions. The subsurface conditions on the southern portion of the project consisted of dense colluvial soils over bedrock. The subsurface conditions in the middle portion of the project consisted of steep shallow bedrock slopes with unfavorably dipping joint structure and loose debris. The subsurface conditions on the northern portion of the project consisted of compact alluvial / colluvial soils over bedrock. Constraints imposed by limited right-of-way above the new alignment over the northern half of the project where the BLM controlled land is located, limited the space available to construct cutslopes. This combined with the loose to compact condition and steep inclination of the alluvial / colluvial soils were the major drivers in the design.

It was determined that excavations of only limited extent could be considered along the northern portion of the new alignment. The compact alluvial / colluvial soils were at, or close to, angle of repose in their existing configuration above the highway. Significant excavations into the toe of these slopes would result in day-lighting well above the top of the limited width easement agreed with BLM. This meant that much of the grade along the northern portion of the alignment would be constructed on fill and that a significant south to north haul of material would be required to achieve project mass balance.

The steep compact condition of the alluvial / colluvial soil along the northern portion of the site caused concern that cutslopes would be eroded by concentrated flow from several gullies upslope of the alignment. The installation of brow or crown ditches in this area was not feasible. Therefore rip rap slope protection had to be incorporated into the cutslopes at critical locations (see Photograph 8). The dense condition of the colluvial soil along the southern portion of the project caused less concern about erosion but brow or crest ditches were installed where slope inclination made it feasible to do so.

The unfavorably dipping joint structure in the middle of the project was dictated that either flattened cut slopes or extensive rock support be utilized. The need for fill material on the northern portion of the project led to the decision to design flattened cut slopes to eliminate potential kinematically viable plane and wedge failures.

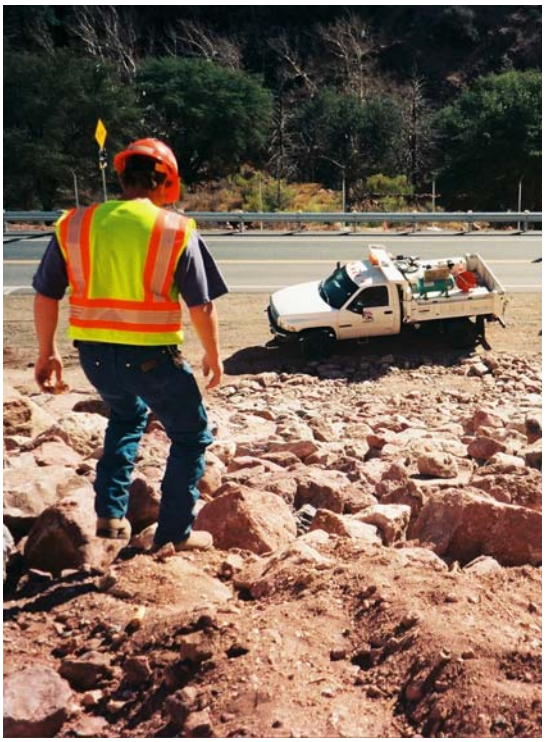

Photograph 8 – Rip rap erosion protection on steep alluvial / colluvial slope above US 191.

Analyses

Structural data from the mapping program was entered into and manipulated by the commercially available computer program DIPS to develop stereonet projections of joint orientation for the design of slope angles. Analysis of this data indicated that the rock structure in the granite bedrock west of the new alignment is strongly influenced by the orientation of the CCFZ. A prominent set of joints dips eastward towards the roadway at approximately 60 degrees. Associated joint sets result in the occurrence of potential wedge failures with plunge angles of 48 degrees. The geometry of the rock slopes was selected to minimize the potential for the occurrence of

wedge failures without the use of artificial support (bolts or dowels) by selecting a rock slope design inclination of 0.9H to 1.0 V. This inclination resulted in stable rock slopes and generated fill material required for construction of the highway over the northern half of the project.

Global stability of the rock mass was not an issue. With selected bedrock strength parameters of phi = 55 degrees, c = 10,000 psf and a unit weight = 145 pcf, the analyses indicated that the controlling factor in slope design was the inclination of the joint structure.

The stability of embankment slopes was carried out using the limit equilibrium method of slices approach with the commercially available computer program SLOPEW. A minimum factor of safety of 1.5 under long term dry static conditions and a minimum factor of safety of 1.3 under short term static drawdown conditions was achieved with selected strength parameters of phi = 35 degrees and c = 0 psf.

Material Requirements

The excavated colluvial, alluvial and bedrock materials were considered suitable for use as highway fill provided adequate moisture conditioning and compaction was applied. The soils across the project exhibited surprisingly high plasticity and fines content and surprisingly low R-values (low subgrade moduli). Potential aggregate from a nearby limestone quarry exhibited poor durability. Consequently subbase and base materials were imported from a commercial gravel pit located near Safford 78, approximately 60 miles from the site. Asphalt material was imported from a commercial hot mix plant also near Safford, Arizona. The limestone quarry material and oversize granitic material from slope excavations was used for rip rap.

CONTRACT PREPARATION, ESTIMATING AND BIDDING

Contract Preparation

In August 2005, PDMI requested MWH and AMEC to evaluate the possibility of an accelerated design and construction schedule in order to finish construction of the entire project by July 2006. It was realized that the conventional design and construction bidding process would not allow the project to meet this schedule. Therefore MWH and AMEC worked with PDMI to bid the Highway portion of the project before the final design was complete and approved by ADOT. A bid package was compiled, including drawings and specifications at a 60% design level, and submitted to several qualifying contractors. The bid package was updated to a 95% design level at the time of the bid walk and submitted to the contractors. PDMI, MWH and AMEC evaluated the bids and selected NSI as the contractor for the Highway construction. NSI began the Highway construction in October 2005 and the new Highway was opened to public traffic as planned in January 2006. With the new alignment in place, the existing, or "old" section of Highway was demolished as the dam contractor (also NSI) started the construction of the Upper Chase Creek Dam. NSI completed the construction of the Dam on schedule in July 2006.

Photograph 9 – Brow or crown ditch installation at south end of new US 191 alignment.

Estimating Uncertainties

It was difficult to develop an accurate cost estimate for the project because of rapidly increasing construction costs associated with global demand for materials, natural disasters in the United States and the rising price of oil. In 2005 increasing construction costs were being

experienced across the United States on similar roadway projects and on most other types of construction projects as well. ADOT has a very thorough and detailed cost database for highway work in Arizona and design firms usually rely on this database to develop their project cost estimates. However, that database underwent significant revision during the course of this project. Even though the design team applied what were thought to be reasonable percentage escalation estimates to unit costs, the final bid price still overran the engineers estimate. The major items that overran the unit price estimate, including the corresponding percentage increase, were:

- Roadway Excavation, + 50%
- Drainage Excavation, + 200%
- Aggregate Base, + 150%
- Asphalt Concrete, + 80%
- Temporary Concrete Barrier, + 250%
- Rock Mulch, + 833%

Photograph 10 – Preparatory work by NSI to establish Grade at south end of new highway

Another reason for uncertainties was the fast tracked schedule. It was difficult to anticipate the contingency that a contractor might add to his bid to account for the accelerated construction schedule. Unfortunately accelerated projects have a tendency to be designed without all the specific details being thoroughly defined and without time for full constructability reviews. This issue arose on this project with regard to the use of crown or brow ditches extensively along the alignment (see Photograph 9). Brow or crown ditches were incorporated into the plans during the late stage of design review and were priced by the contractors in the bid. Subsequently the constructability of the brow or crown ditches came into question, and in some of the locations where they were proposed the ground conditions were such that they were not actually necessary. This resulted in some redesign work at the beginning of the construction schedule, and required the contractor to re-sequence his work. The redesign was complicated somewhat by limited ground survey and had to be based on aerial photograph based contours. The contractor's need to include some contingency for factors such as this can be readily understood.

Bidding

Developing accurate quantities and properties of materials is essential to estimating any project. PDMI understood this need and provided the electronic project drawings to aid in the bidding process. The AutoCAD drawings facilitated rapid and accurate development of quantities and summaries such as mass haul diagrams. Extensive geotechnical information was provided by MWH that allowed both rock locations and strengths to be added to the digital terrain models. The ability to run multiple scenarios and explore options during bidding allowed development of innovative approaches.

Developing a cost estimate for the accelerated realignment of US 191 could not be approached in the same manner as a typical highway construction project. Acceleration required that all resources such as subcontractors, equipment, and permanent materials be readily available to prevent delays during their acquisition. Having all resources standing by on site added extra cost to the project that need to be considered during cost estimating.

The crew method for estimating (using detailed man and equipment hour projections) was considered to be the only appropriate manner to capture these costs. Parametric and unit cost estimates were not appropriate for this type of project. Collaboration with subcontractors and vendors during the bidding process was also critical to ensure that all parties had "buy-in" to the project approach and schedule.

The length of the US 191 project and limited space for equipment and crews was a factor. The project schedule had to be carefully weighed against crew productivity and the required area to operate safely without undue congestion (see Photographs 10 and 11). This balance led to the equipment and methodology chosen for the project and dictated the final bid.

EXPERIENCES DURING CONSTRUCTION

Innovative Approaches

Photograph 11 – Indication of tight working conditions at base of large rock cut in middle of project.

Contractor NSI undertook some innovative construction approaches to meet the schedule constraints placed on the project team. Construction of the new Upper Chase Creek Dam was dependent on completion of the Highway realignment and the expansion of the PDMI Garfield Pit was in turn contingent on completion of the dam. To ensure that the mine expansion progressed to meet PDMI's production targets in a strong copper market, realignment of US 191 had to be completed by January 20, 2006 - just 102 days following project award to NSI on October 10, 2005.

The earthwork portion of the project presented the biggest opportunity to accelerate construction. The mass haul diagram prepared by NSI as shown in Figure 4 illustrates the accumulation of excavated material if earthwork was started at the beginning of the project (BOP), and is the standard method of planning earthwork for highway projects. Conventional earthwork methodology would have indicated moving more than 60,000 cubic yards of material to embankment between station 196+75 and station 218+20. NSI's project planning team quickly realized that the large volume of rock at the BOP would require drilling and blasting and that beginning earthwork at the end of the project (EOP) would allow this shot material to be hauled to stockpile for use in the turnouts for the project at a later time. By commencing earthwork at the EOP, NSI avoided being delayed by the blasting at the other end of the project. The mass diagram shown in Figure 5 is based on starting earthwork at the EOP and working back to the BOP.

To enable the preferred earthwork haul, construction of a concrete box culvert at station 210+50 would have to be completed and backfilled early in the project. In order to build the concrete box culvert and perform the earthwork between station 196+75 and station 218+20 simultaneously, the project team amended the project's Traffic Control Plan to allow haul traffic down the portion of existing US 191 that was to be abandoned. Due to the limited traffic on US 191, the roadway was closed for thirty minute intervals, allowing the haul units to travel safely over the highway with minimal impact to the traveling public.

This approach to the earthwork enabled simultaneous drilling and blasting, hauling, and box culvert construction to take place, in contrast to the end-to-end approach used in typical highway construction.

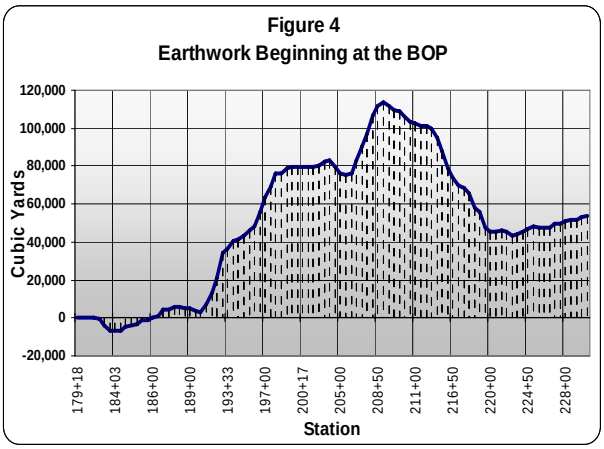

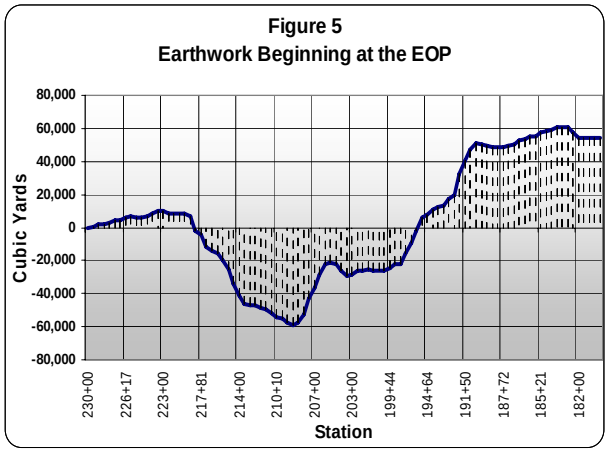

Schedule Control

NSI approached the schedule for bidding with focus on practicality and a commitment to share schedule results with PDMI through the proposal process. Partnering with the owner to avoid unnecessary contingencies in the proposal, such as provision for liquidated damages, was the ultimate goal. Developing a schedule using the critical path method (CPM) during the project bidding process was vital for NSI to evaluate schedule risk.

The CPM schedule (see Figure 6) assisted in identifying activities that posed risk so that the risks could be evaluated and procedures implemented to mitigate the risk. Through this analysis, milestones were created that identified key elements to completing the project on time. The required project finish date led to a schedule with little float and no room for schedule contingency. NSI based its schedule on working six days per week with a ten hour day shift and an eight hour night shift. The project was shut down on Sundays in attempt to prevent "burn-out" among the crew which could negatively impact safety. Paving was planned for five days per week, during warmer hours, with the more expensive weekend days as an opportunity to regain time if needed.

As previously discussed, acquisition and availability of resources is essential to maintaining the schedule. With the ever changing market for construction materials such as cement and steel, PDMI was able to mitigate a portion of the supply and cost risk by purchasing materials through their Global Supply Chain (PDMI's on-line procurement system). PDMI also was able to provide concrete to the project from their batch plant in Morenci. NSI and subcontractors scheduled equipment, personnel and supplies to arrive on site in advance. Production of riprap from the project cuts reduced the need for materials being imported from off the project site.

Contract Administration

MWH led the contract administration team utilizing AMEC for the roadway Resident Engineer position, specific roadway inspections, and material quality assurances. This joint effort was required because of the large amount of common work performed for both the roadway and dam, and because of ADOT's expectation that a Resident Engineer familiar with roadway construction would be utilized.

One unusual aspect on this project was that PDMI requested that it provide certain construction materials that it normally provides within the mine limits to its contractors. This included grout for riprap, concrete, guardrail, guardrail end terminals, water, corrugated metal pipes, chain link fence, and barbed wire fence. Though PDMI incurred savings in cost of material acquisition through bulk buying, avoided contractor markup, and reduced supply risk, this process increased the amount of coordination effort within the contract administration team. Since some of PDMI's suppliers were different than those known to ADOT, additional materials approvals were required from ADOT, additional coordination was required with NSI to schedule requirements for material delivery, and additional time was required for PDMI to receive three quotes from suppliers, and then order the material from suppliers.

Equipment and Methods

Earthwork was accomplished with two Caterpillar D-10 dozers, one Caterpillar D-8 dozer, one Caterpillar 988 loader, seven 40-ton articulated all wheel drive haul trucks, two Caterpillar 815 pad foot compactors, one Caterpillar 320 excavator, one Caterpillar 14 motor grader and two water trucks.

The D-10's were selected to doze the large quantity of excavation to embankment within dozer push range indicated on the mass haul diagram. A D-10 is capable of ripping with approximately 30% more force than a D-9 model. This allowed larger volumes of rock to be ripped, preventing additional delays associated with drilling and blasting. The D-10 dozers pushed overburden and rock from the rock cuts to fills while establishing access for blasting operations. Based on NSI experience on other projects with limited room and very rough, terrain, the use of the articulated, all wheel drive haul trucks was the clear choice.

Dynamic Rock Solutions (DRS) from Peoria, AZ was chosen by NSI to drill and blast all the rock on the project. DRS used three hydraulic rock drills to maintain the accelerated pace. Drilling and blasting was done seven days per week, with shots scheduled at 12:00 pm and 5:00 pm daily. Coordination between DRS and onsite supervisors was essential to maintain access to work areas for DRS while allowing other work activities to progress safely. Following blasting, the 988 loader was used to load material into each of the seven 40-ton haul trucks for transport

to fills. Seven haul trucks were not necessary at all times, as the production capacity of the 988 loader was limited. On shorter hauls, the trucks completed a cycle more quickly and thereby hauled more cubic yards per hour. The 320 excavator was used to scale slopes as excavation progressed. The D-8 dozer was used to spread and smooth the dumped material for access by the 815 compactors. The 815 compactors and the water trucks were used to maintain density and moisture requirements. A Caterpillar 14 motor grader, a smooth drum roller and a water truck were used to prepare subgrade for aggregate base course.

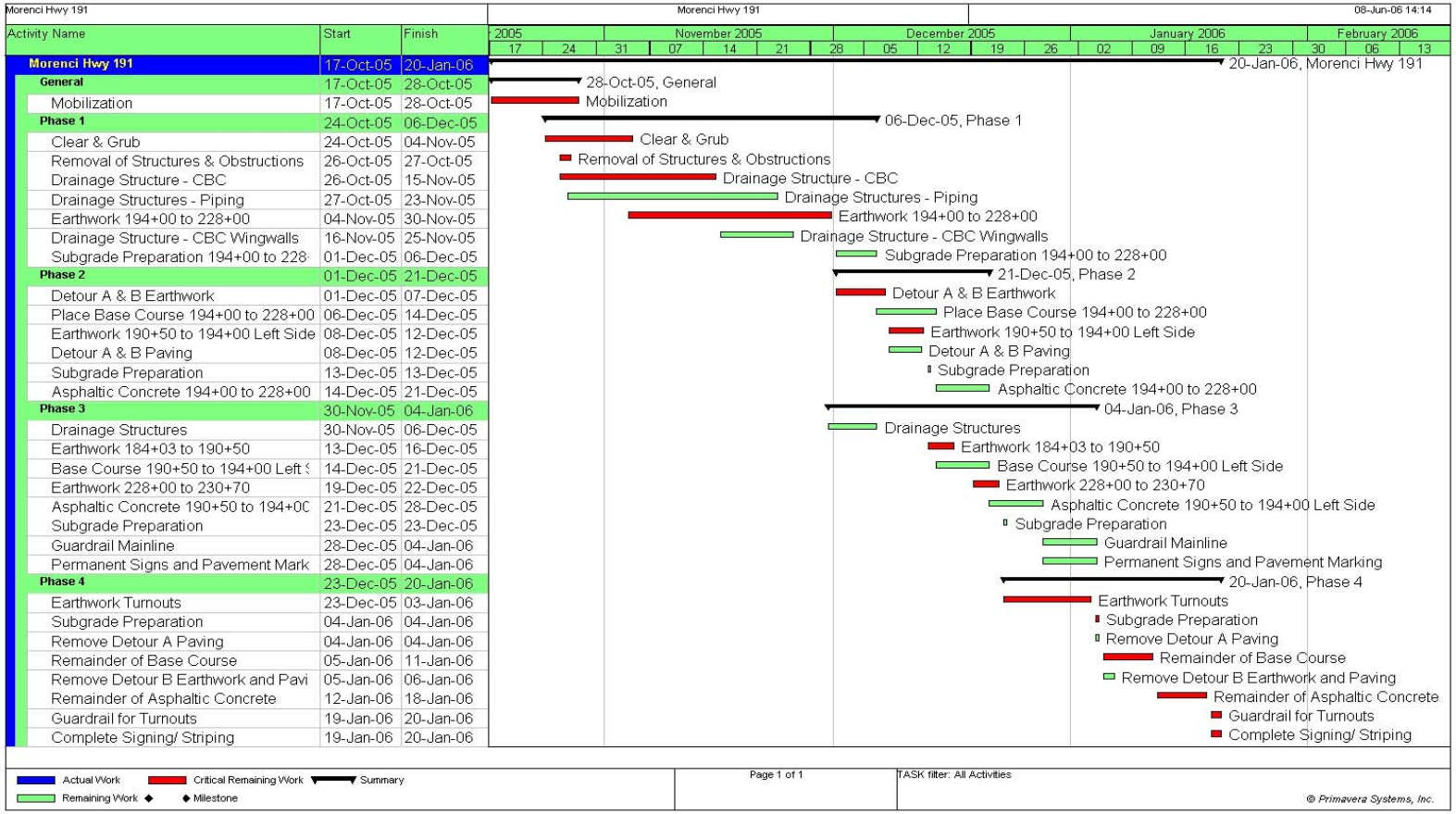

Figure 6 – NSI project schedule for US 191.

Aggregate base course and asphalt mix were obtained from Tri County Materials, Inc. at their pit and plant near Safford, Arizona. NSI subcontracted trucks to haul aggregate base course and asphalt from Safford to the project. Twenty trucks each made an average of two round trips each per day during surfacing, traveling 60 miles one way. Any issues with availability of the material or trucks would have created delays with the surfacing operation, but onsite supervisors were able to work closely with Tri-County and trucking subcontractors to finish on schedule.

NSI used one of its own highway paving crews to place and compact the asphalt material. This approach helped to mitigate the challenges involved in wintertime paving at a remote location. The crew used a large lay down machine and mainline highway paving compaction equipment. The capacity of the laydown spread and expertise of the crew ensured that paving material was laid and compacted on schedule and to specification

LESSONS LEARNED

The primary lesson learned from the realignment of US 191 in Upper Chase Creek is that successful delivery of a project in rugged terrain with a very aggressive schedule requires the stakeholders to come together with a common goal. Extensive technical support from all parties is required to quickly identify issues and resolve them onsite. The stakeholders must also commit the resources needed to support intensive construction activity.

PDMI, MWH, AMEC and NSI worked together through the construction phase to promptly and equitably resolve project issues with timely completion in mind. ADOT also cooperated with the project team. Following substantial completion of construction, traffic was moved to the new alignment on January 20, 2006. Achieving this milestone enabled PDMI to proceed on schedule with the next stage in its expansion project, construction of the Upper Chase Creek Diversion Dam. The Dam topped out May 15, 2006 facilitating the commencement of mining on June 8, 2006. In July 2006 the existing downstream stormwater detention dam was consumed by open-pit excavation and the new dam and highway were fully operational.

The partnering process implemented on this project minimized and equitably distributing risk associated with limited survey, hydraulic and geotechnical data, a winter construction period and the need to satisfy multiple stakeholders. Frequent interaction and detailed communication between PDMI, the designers, MWH and AMEC, the contractor NSI and the major stakeholder ADOT were critical factors in this success. This allowed for potential problems to be anticipated, options to resolve these problems to be discussed among the affected parties and the most effective solutions to be selected without hindering the progress of the work, detracting from the quality of the project or accumulating costs without multiparty concurrence. Project completion to all stakeholders' satisfaction was also in part due to participation by geotechnical and highway design and construction professionals throughout the project.

These were generally positive lessons. One negative lesson related to owner supplied materials. Experience on this project indicates that on future projects of this type it might be better to give the responsibility of material acquisition to the contractor in spite of some cost and delivery uncertainty associated with this approach.

REFERENCES

1. ADOT Contract and Specifications Group. *Standard Specifications for Road and Bridge Construction.* 2000 Edition & Updates. Arizona Department of Transportation, Phoenix, Arizona, 2000 with Updates.

2. ADOT Roadway Engineering Group. *Roadway Design Guidelines*. Arizona Department of Transportation, Phoenix, Arizona, May 1996 With Updates.

3. ADOT Traffic Engineering Group. *Traffic Engineering Policies, Guides, and Procedures.* Arizona Department of Transportation, Phoenix, Arizona, 2001 with Updates.

4. David J. Castanon. *404 Permit*. Permit #2000-00559-MB. Army Corps of Engineers, May 24, 2005.

5. Diehl, A C., Doelle, W.D., 2006, A Cultural Resource Survey Report of U.S. Highway 191 Between Mileposts 175 and 186, Near Morenci, Greenlee County, Arizona, prepared by: Desert Archaeology Inc., Tucson Arizona, prepared for: Arizona Department of Transportation, Environmental and Enhancement Group

6. Enders, M.S., 2000, The evolution of Supergene Enrichment in the Morenci Porphyry deposit, Greenlee County, Arizona: unpublished Ph.D. dissertation, University of Arizona, Tucson

7. Ferguson, C.A., Enders, S.M., Peters, L., McIntosh, W.C., 2000, Mid-Tertiary Geology and Geochronology of the Clifton-Morenci area, Greenlee and Graham Counties, Arizona, and adjacent New Mexico, Arizona Geological Survey Open-file Report 00-07, with Arizona Geological Survey, Digital Geologic Map 1 (DGM01)

8. Golder Associates and Parsons Transportation Group. *Preliminary Feasibility Design for Upper Chase Creek Diversion Volumes I to IV*. Phelps Dodge Morenci, Incorporated. March 2001.

9. Lindgren, W., 1905a, The copper deposits of the Clifton-Morenci district, Arizona; U.S. Geological survey, Professional Paper No. 43

10. Lindgren, W., 1905b, Description of the Clifton Quadrangle: U.S. Geological Survey, Clifton Folio

11. Lock, T., 1999, Geologic map of the Cheesier Gulch area north of Morenci, Greenlee County, Arizona: unpublished Part II Field Project map, Department of Earth sciences, University of Cambridge, Cambridge, UK

12. NBS/Lowry Engineers & Planners, Inc. and George V. Sabol Consulting Engineers, Inc. *Highway Drainage Design Manual Hydrology*. Report No.: FHWA-AZ93-281. Arizona Department of Transportation, Phoenix, Arizona, March 1993, Revised August 11, 1994.

13. Pearthree, P. A., 1988, Quaternary fault data and map of Arizona: Arizona Geological Survey, Open-file Report

14. Schroeder, T. J., 1996, Geologic map of the Enebo Mountain Rhyolite: Arizona Geological Survey, Contributed Map: CM-96-A

15. Schroeder, T. J., 1996, Physical Volcanology of the Enebro Mountain Rhyolite, unpublished, MS Thesis, NAU

16. U.S. Department of Transportation. *Manual on Uniform Traffic Control Devices.* 2003 Edition. Federal Highway Administration, 2003.

17. Walker, M.A., 1995, Structural interpretation of the Morenci Mining district, Greenlee County: unpublished M.S. thesis, New Mexico Institute of Mining and Technology

18. Westland Resources, Incorporated. *MSGP-2000 Storm Water Pollution Prevention Plan Revision 4* Phelps Dodge Morenci, Incorporated. July 2005.

19. Westland Resources, Incorporated. *MSGP-2000 SWPPP Best Management Practices Plan Revision 1*. Phelps Dodge Morenci, Incorporated. June 2002.

20. Westland Resources, Incorporated. *Environmental Assessment*. Permit #2000-00559-MB, Phelps Dodge Morenci, Incorporated.

Shrink and Swell Estimation: Practices and Procedures

Justin Henwood
Central Federal Lands Highway Division
12300 West Dakota Avenue
Lakewood, CO 80228
(720) 963-3362
justin.henwood@fhwa.dot.gov

Matthew DeMarco
Central Federal Lands Highway Division
12300 West Dakota Avenue
Lakewood, CO 80228
(720) 963-3520
matthew.demarco@fhwa.dot.gov

Charlie Martinez
Central Federal Lands Highway Division
12300 West Dakota Avenue
Lakewood, CO 80228
(720) 963-3523
charlie.martinez@fhwa.dot.gov

ABSTRACT

Inaccurate estimates of material shrink/swell, and/or mistakes in earthwork calculations, are costly construction errors, often resulting in significant construction modifications, claims, or poor cost estimates for earthwork projects. While the material properties of the soil/rock contribute significantly to the final "apparent" shrink/swell factor for the constructed project, there are a number of other project elements that contribute to final earthwork balances, including type and size of construction equipment, haul losses, over-excavation, survey errors, highly variable topography, variations within material types, poor estimates of materials types and quantities, and inaccurately designed earthwork volumes.

Within the Federal Lands Highway program, a wide range of soil and rock conditions are encountered on partner agency roadway construction projects. Frequently, these projects are constructed in challenging, mountainous terrain within geologic units possessing complicated shrink/swell characteristics, namely: decomposed granite, volcanic rocks, karstic limestone, and soil masses containing a large percentage of boulders.

This paper presents an effort to tighten geotechnical procedures for estimating shrink/swell factors and sort through the various design and construction related issues that influence these factors. A synopsis of the shrink/swell practices and procedures of various State DOT's in the western region of the United States is also presented.

INTRODUCTION

The Federal Lands Highway Division (FLH) of the Federal Highway Administration (FHWA) is principally responsible for rehabilitating, repairing, resurfacing and constructing roadways for federal land management agencies throughout the U.S., including the National Park Service, U.S. Forest Service, U.S. Fish and Wildlife Service, and similar resource agencies. Construction projects within these lands typically involve low-volume roads within environmentally sensitive regions, and are commonly constrained by budget, environmental impact limitations, restricted construction seasons, and local/regional socioeconomic considerations. Working within these constraints, FLH seeks to develop context sensitive solutions to roadway design – promoting a "Light on the Land" roadway philosophy that is well-aligned with partner agency goals and land management initiatives.

In support of this philosophy, FLH roadway projects routinely attempt to minimize earthwork impacts on projects by attempting to exclusively use on-site materials and balance cut and fill quantities – minimizing roadway footprints,

total excavation, and the need for off-site borrow or wasting. In particularly sensitive, pristine regions, including most National Parks, earthwork balancing is generally required since borrow sources and waste sites are often not located within the region or Park boundaries. Failure to accurately balance materials on such jobs during design not only results in potentially adverse environmental and resource impacts during construction, but can also greatly add to project material costs and create unacceptable schedule delays.

In recent years, the Central Federal Lands Highway Division office (CFLHD), located in Denver, CO, has experienced several notable earthwork busts on projects thought to be balanced – all of which resulted in substantial cost overruns paid through both contract modifications and claims. In many cases, the cause of excessive borrow and/or waste on a project has been blamed on inaccurate representation of shrink/swell factors in the original earthwork estimation – values that are commonly estimated (as opposed to being measured) for various soil and rock types, and which may be significantly in error job-to-job. Upon further review of this all-to-often recurring problem at CFLHD, it has been discovered that a host of error sources potentially influence final earthwork quantities, resulting in "apparent" project shrink/swell values which may or may not be significantly tied to inaccurate material characterization. "Apparent" shrink/swell for the project may include, and be substantially influenced by non-geotechnical items such as inaccurate earthwork calculation in the design package, poor project surveys and volume estimation, poor construction volume management, failures to account for substantial incidental site construction, etc.

Recognizing that the impacts of these sources of error are cumulative throughout the project, and are very difficult to uncover through back-analysis of earthwork processes on past projects, CFLHD has undertaken an in-house effort to begin researching methods for improved earthwork estimation and management. To this end, this paper presents **(1)** an overview of geotechnical and non-geotechnical sources of error thought to potentially be impacting CFLHD projects within its very geotechnically diverse 14-state region, **(2)** a review of earthwork estimation and management practices at several state DOT's representative of CFLHD road construction settings, and **(3)** the preliminary development of recommendations for improvements in earthwork estimation and management processes at CFLHD.

PROBLEM GEOTECHNICAL SETTINGS

While constructing roadway projects within a 14 state region, the CFLHD Geotechnical Group has encountered a wide range of geologic settings that are particularly problematic when estimating material shrink/swell properties. In some cases, these problem settings can generate errors approaching +/- 30%, resulting in significant under- and over-runs on highly constrained projects. The following highlights some of the more problematic ground conditions:

- **Bouldery Ground**: When boulders are common to the excavation ground mass over a substantial area of the project, various difficulties arise in accurately estimating boulder quantities and managing their apparent shrink/swell impact on constructed roadway features. Visual surface estimates may grossly underestimate boulder quantities, and borings and test pits provide only limited site characterization. The ability to reuse boulders in large fills, along with fines placement in the intervening fill voids, can mitigate boulder impacts to overall quantity errors on a project; however, when crushing boulders for project aggregate, or stripping boulders from shallow subgrade excavations (generating an unquantifiable fill item), significant errors may be introduced into project earthwork estimates.

- **Volcanic Materials**: Volcanic soil and rock units are particularly problematic due to the extreme ranges in shrink/swell material properties that may be present within a given excavation or material source deposit (40-50% shrink to 30-40% swell), coupled with the potential of unsuitable materials present in the excavated unit. Problems stem from the nature of volcanic deposits – often extremely complex and laterally discontinuous layers of volcanic ash, scoria, clinker, and widely ranging densities of basalt lava flows. Within a typical stratigraphic column representing several flow cycles, specific gravities for volcanic materials can range from less than 1.0 (entrained gas pockets) to well over 3.0. Volcanic ash deposits, commonly present atop and within lava flows, may be wholly unsuitable for construction due to high clay/silt contents and/or adverse soil chemistries, and may need to be wasted in designated areas. Comprehensive site characterization, selective

material mining and segregation, and heightened material testing and placement inspection are all required to minimize the potential for substantial project impacts to earthwork quantities.

- **Decomposed Granite**: The degree of weathering within a rock mass greatly impacts shrink/swell estimation, and is a rock mass characteristic difficult to accurately characterize or quantify in the field. As rock weathers to soil, material swell percentages steadily decrease, eventually transitioning to shrinking soils (when placed and compacted). Decomposed granites, found throughout the CFLHD mountain states regions, are particularly difficult to characterize as the percent of rock structure and density remaining, depth, degree, and distribution of weathering, and mineral components are difficult to field quantify over large areas. Sampling can be difficult, with a natural bias toward more intact portions of the weathered rock mass, resulting in skewed shrink/swell estimates. This material type is commonly responsible for pushing balanced jobs into borrow jobs – estimating material swells (5-10% standard swell estimation) for weathered rock units where shrinks are more appropriate (5-10% actual shrink).
- **Dense Glacial Tills**: Glacial tills are often encountered on mountain roads projects, and couple problems associated with boulders and unsuitable materials (clays and silt deposits) with ground mass over-consolidation – resulting in significant swells when excavated and placed in constructed fills. Aside from the aforementioned issues associated with managing boulders, glacial tills can be difficult to characterize due to limited subsurface exploration and difficulties in sampling. In addition, density variations with depth (loose at the surface to highly compacted at modest depth) are often overlooked by field investigations, resulting in material overruns (and problems associated with boulder handling/disposal/crushing).
- **High Void Ratio Materials**: Highly jointed and weathered rock masses, rock units containing gas or dissolution created voids (e.g., lava flows or karstic limestone units), and collapsible soils (e.g., loess or overbank silts) are all problematic materials due to structural characteristics of the rock/soil fabric. Estimating rock/soil mass shrinkage on a project subject to large subsurface voids is complicated, and often comes down to engineering judgment based on limited subsurface information. Highly jointed and fractured rock masses exhibiting substantial weathering (open discontinuities) can also be extremely difficult to characterize, and may actually shrink upon final fill placement. Collapsible soils (voids present in the undisturbed deposit) and dispersible soils (voids created by dissolution following fill placement) are much easier to quantify, but require skill at identifying occurrence and extent of deposits in the field.
- **Variable Bedrock**: Substantial variation in bedrock depth within an excavation is difficult to determine from conventional geotechnical subsurface investigations, yet may greatly impact final material quantities. Although this problem often impacts shallow roadway subgrade excavations, it is most notably a problem on large side-slope excavations for retaining wall construction. Side-cast material from previous roadway construction atop original slopes can complicate estimation of bedrock depths based on one or two borings, resulting in gross misrepresentation of the subsurface conditions in these settings. Such errors not only impact excavation and haul quantities, but may greatly impact availability of suitable wall fill material, requiring off-site hauls on previously balanced projects.
- **"Block-in-Matrix" Materials**: BIM materials are perhaps best described as a complex mix of variably-sized rock blocks in a soil and/or highly worked/reworked rock unit matrix. A common example of such a material impacting CFLHD projects is the notoriously complex Franciscan mélange, a chaotic mixture of variably strong rock materials encased in a clay, shale, serpentinite soft ground matrix (to name a few of the possible matrix constituents). Due to the sheer size of some of the rock blocks in this formation, it is not uncommon to mistake large blocks as actual bedrock outcrops on projects – only to discover later that the excavation includes a large percentage of shrinking soils and weak, highly disturbed sedimentary materials. This particular formation is prevalent within much of the western coastal ranges, though similar BIM units are not uncommon in the central mountain regions.
- **Variable Topsoil**: The accurate characterization of topsoil, duff, and vegetation, is critical to minimizing eventual fill placement volume errors, but is often given only minimal attention. Inaccurately estimating duff clearing depths, stumpage and brush clearing quantities (root mass volume , topsoil depths, and then allowing overstripping of those soils to be conserved beneath eventual fills), can result in substantial shrinkage errors, pushing 1-3% on large fills (equating to several thousand cubic yards of material overrun in some cases).

Management of topsoil stripping, particularly in areas where topsoil depths vary greatly along the project and topsoil replacement requirements drive the potential for overstripping, is central to minimizing shrinkage errors on CFLHD projects (particularly impacting mountain projects where topsoil is commonly in short supply).

Although poor characterization of rock and soil types has significant impacts, project quantities and distribution can affect any project setting, these particular settings have been found especially problematic on CFLHD projects in recent years.

"APPARENT" SHRINK/SWELL SOURCES OF ERROR

Aside from the material property problems discussed in the previous section, site investigation, design and construction processes greatly affect earthwork estimation, final earthwork pay quantities, and "apparent" shrink/swell on the project. The following describes some of the more common sources of geotechnical and non-geotechnical errors when estimating and managing earthwork volumes, and underscores the complexity of accurately estimating project material quantities and avoiding substantial earthwork busts.

Geotechnical Sources of Error

It is the responsibility of the Geotechnical Engineer to provide design and construction efforts with specific materials information related to **(1)** the types and distribution of rock and soil materials on the project, **(2)** the suitability of materials for specific construction purposes (e.g., unclassified borrow, general aggregate, riprap, pavement aggregate, etc.), **(3)** the presence of unsuitable construction materials that must be removed from the project, **(4)** the availability of suitable borrow sources, **(5)** any special excavation techniques required on the project, **(6)** the compacted properties of site materials, and required methods to attain these compaction standards, and **(7)** a measure of the uncertainty (risk) involved in using site materials for construction. Geotechnical-related earthwork estimation errors typically fall under one or more of these categories, and may include one or more of the following more specific failings:

- Poor in-place materials characterization and soil/rock classification stemming from insufficient mapping, subsurface exploration, sampling, and testing programs during project design phases (poor site investigation planning and implementation).
- Lack of in-place density testing comparisons to lab-determined optimum moisture density testing results, and poor assessment of risk involved in reporting these relationships.
- Improper reporting of shrink/swell value definitions – neglecting to note additional shrink or swell that may be due to design and construction activities.
- Poor identification and/or incomplete delineation of subexcavation areas requiring wasting of unsuitable materials.
- Failure to consider variable ground conditions and material in-place densities with depth, particularly as depth relates to consolidation, weathering, and changing depositional and stratigraphic settings.
- Limited measurement and inaccurate estimation of shrinkage associated with stumpage and duff (and clearing losses associated with both), variable topsoil depths, and the compressible nature of loose near-surface soils impacted by high fills.
- Poor estimation of boulder-bearing ground and a lack of consideration for how boulder materials may be generated and used on a project.
- Failure to account for soil and rock settings that may contribute to over-excavation – particularly highly jointed rock masses subject to substantial overbreak and excessive scaling requirements.
- Failure to adequately quantify residual soil/decomposed rock zones within projects.
- Failure to relate uncertainties and geotechnical risk to the Designer, particularly where materials may barely meet minimum aggregate standards on a project, where specific material quantities needs may be difficult to

meet, or where on-site aggregate manufacturing methods may greatly impact resultant quantities and/or qualities of specified materials from any given source.

- Failure to revisit/investigate the site following substantial design and/or alignment changes.
- Failure to clearly identify materials that should be wasted from a project when limited material quantities create pressures to use all available excavation.
- Improper accounting of materials when wasting and in-filling large boulders in the bottom of large fills.
- Failure to recognize collapsible or dispersible soils on a project which may lead to immediate or long-term volume losses.
- Failure to adequately characterize cut/fill transition zones so Designers may properly account for soil/rock volumes.
- Inadequate verification of materials quantities and qualities during construction operations.

Other Sources of Error

In addition to common earthwork estimation errors stemming from purely geotechnical-related sources, substantial errors can be introduced throughout design and construction by failing to define and capture construction quantities comprehensively, as well as through problems with construction execution. More specifically, the following type of problems and oversights can introduce apparent shrink/swell errors well in excess of standard geotechnical-related margins of error:

Design-Related Errors

- Inaccurate design quantities of manufactured aggregate or borrow related to over- and under-estimation of roadway base and sub-base aggregates, subexcavation backfills, utility line and culvert excavation and fill, pioneered road construction, parking areas, temporary drainage paths/ditches, etc. (or failure to consider altogether).
- Employing shrink/swell factors in mass haul estimations that only consider material properties (as reported in the geotechnical report), ignoring construction practices that substantially impact the apparent shrink/swell on the job (may actually double apparent shrink on many jobs).
- Basing final quantities estimates on remote LIDAR surveys, rather than on more accurate ground surveys, and then carrying out volume estimates beyond the limits justified by field data.
- Failing to correct volumes for roadway horizontal and vertical curves, particularly when a section has a cut on one side and/or a fill on the other.
- Improperly accounting for the excavation volume related to removed/placed structures.
- Improperly measuring quantities associated with roadway obliteration operations (and failing to characterize these materials during geotechnical investigations).
- Improperly including constructed earthwork items in the design that cannot or will not actually be built (e.g., sliver cuts and fills).
- Succumbing to pressures to balance jobs, ultimately influencing shrink/swell factor selection, and the failure to consider factor uncertainty in design (significantly impacting potential waste/borrow quantities).
- Failing to recognize that larger fills may have higher overall apparent shrinks than anticipated due to less control on volume/slope, greater compaction within the fill and subgrade, greater toe losses, greater overall haulage losses, etc.
- Failure to recognize that small fills may incur greater overall shrinks due to the sensitivity of being a few inches off in stripping, subexcavation, and course construction.
- Inaccurate estimation of special materials required for site restoration, including landscape aggregate, boulders, and/or treatment aggregates (e.g., limestone).

- Inaccurate estimation of subex requirements at cut-to-fill transitions and/or within thru-cuts transitioning from surface soils to bedrock.
- Unaccounted quantities related to "undercutting" to remove bedrock in the subgrade immediate to the finish grade line.

Construction-Related Errors

- Allowing overstripping of topsoil beneath planned fills (just a few inches can add 5-10% to the apparent shrinkage error per fill).
- Allowing variations in compactive effort within a given fill, compacting the wrong lift thickness per the specified applied effort, not thoroughly compacting all lifts, and not measuring fill densities regularly.
- Not regularly surveying both excavation and fill construction to manage over-excavation and improper fill quantities, or surveying late in construction when errors cannot be mitigated.
- Failure to minimize haulage/handling waste.
- Placing the wrong materials in the wrong places on the job.
- Failure to require the contractor to effectively manage overbreak during blasting or mechanical excavation.
- Unanticipated changes or variations in aggregate manufacturing processes that result in excess waste products (e.g., fines development).
- Over-building sub-base and base courses on roadways.
- Over-use/under-estimation of required construction site maintenance materials (temporary embankment control aggregate, temporary toppings, construction/crane pads, pioneered roads, etc.).
- Over-benching during fill construction on steep side slopes.
- Poor sliver fill and sliver cut management on the project (when required).

Considering the long list of potential error sources contributing to substantial variations in "apparent" earthwork shrink/swell (upwards of +/-30% on some jobs), it's no small wonder more projects are not notably over or under on quantity estimation. In most cases, small waste overruns can be hidden in fattened fills, slightly elevated roadway grades, oversteepened cuts, etc., while small underruns can be consumed by lowering grades, flattening or widening cuts, or steepening fills. However, significant earthwork busts cannot often be managed easily through the course of construction with on-site materials or waste areas, requiring expensive, long hauls through environmentally sensitive areas to unfavorable/costly borrow/waste pits. Substantial contract modifications and/or claims often result, bringing high-profile attention to this pervasive problem.

To address these unforeseen situations, CFLHD sought the experience and advice of state DOT's around the U.S., covering the variety of geotechnical settings encountered across CFLHD's western states region. The next section describes the methods and procedures common to our neighboring states, and develops some solid recommendations for improving earthwork estimation and construction on CFLHD forest highway projects.

COMMON SHRINK/SWELL PRACTICES

In an effort to characterize the shrink/swell state of practice, the internal procedures for estimating earthwork quantities within CFLHD were investigated and are based on recent attempts to develop guidance and standardize proper earthwork representation. Several state DOT's from around the U.S. were also surveyed on their best management practices regarding estimation of shrink/swell factors. The following represents a compilation of these efforts.

CFLHD Earthwork Estimation Practices

Currently, the standard of practice within CFLHD is to develop a Grading Summary and Mass Haul Diagram through detailed earthwork quantity calculations. Both of these items are included in the construction contract documents. The grading summary is generally divided into several station ranges within which detailed calculations of earthwork quantities are made.

Roadway Excavation quantities are calculated directly by roadway design software using prismatic methods, and also include the excavation required to construct approach roads, allowing the mass haul diagram to better reflect the anticipated haul of material. Adjustments to Excavation quantities allow material unsuitable for embankment construction (topsoil, pavement, etc.) to be removed from the Roadway Excavation quantities. Adjustments can also be used to add material that is available for embankment construction, but is not included in Roadway Excavation (structure excavation, subexcavation, etc.). The adjusted Roadway Excavation quantity (excavation available for fills) is then subject to the shrink/swell factor. Generally, the shrink/swell factor is provided in the geotechnical report – a value representing the simple ratio of placed to in-place density, and not considerate of other non-geotechnical factors.

Roadway Embankment quantities are again calculated directly by roadway design software using prismatic methods and are subject to several adjustments, including: backfill quantities, topsoil replacement quantities, and subexcavation quantities. Mass Haul quantities are also included in the grading summary and are simply the total Roadway Embankment quantities subtracted from the total Roadway Embankment quantities. A Mass Ordinate column is provided and represents the cumulative mass differential as the project moves from the start through the end. The Mass Ordinate quantities are used to develop the Mass Haul diagram.

In lieu of these efforts, earthwork operations continue to represent an area of substantial risk to contractors. In CFLHD contracts, this risk is typically associated with one to four pay items, with Roadway Excavation being the primary item. Within this pay item, the contractor must anticipate and price the work associated with excavation, haul, embankment, benching, adding or subtracting moisture from fills, finishing and other associated activities. Estimating costs is further complicated by the type and variation in the materials to be excavated; if blasting is required and how much; the type of equipment to be used in excavating and hauling material; if the haul is primarily uphill or downhill; coordination of earthwork operations with other installations (culverts, underdrains, etc.); weather considerations and impacts of materials testing.

As mentioned previously, there has been a general trend within CFLHD to balance earthwork projects. In environmentally sensitive, pristine regions, including most National Parks and Forest Service lands, earthwork balancing is generally required since borrow sources and waste sites are often not located within the region or project boundaries. Failure to accurately balance materials on such jobs during design not only results in potentially adverse environmental and resource impacts during construction, but can also greatly add to the project materials costs and create unacceptable schedule delays. In general, within CFLHD projects, roadway designers have been leaning towards creating waste jobs if the overall project earthwork quantities cannot be balanced. Small waste overruns can generally be managed through construction and used to fatten fill slopes, slightly elevate road grades, etc. In general, waste overruns are handled more efficiently than borrow overruns within CFLHD earthwork projects. Often, borrow sites must be environmentally cleared prior to construction, and the cost of locating, opening, and clearing a borrow site during construction can be significant.

In many cases, within CFLHD, the cause of excessive borrow or waste on a project has been blamed on inaccurate representation of shrink/swell factors in the original earthwork estimation, as contained in the Grading Summary. These factors are typically estimated and based on geotechnical values and do not include consideration of the likely construction process or grading equipment to be used. Shrink/swell estimations are based on published, tabulated shrink/swell factor data for various material types, recently collected data, past project experience, engineering judgment, and rarely, lab-field density correlations. Currently, there is no shrink/swell factor multiplier for the non-material related items (survey errors, inaccurate calculation of earthwork quantities, poor construction volume management, etc.) that play a role in the development of “apparent” shrink/swell factors. In recent years, it has not been uncommon for one “average” shrink/swell factor to be used for the entire length of the job, without regard to the various geologic units and different soil types the project may cross.

Methods Used By Selected State DOT's

Recently the CFLHD Geotechnical Unit undertook an effort to canvass several neighboring state DOT's and discuss their standard of practice with regards to shrink/swell estimation and development of earthwork quantities. Selected state DOT's were asked to fill out a brief questionnaire about their current processes and procedures, as well as problem areas encountered, for earthwork quantity estimation. A follow up teleconference was then conducted to gather more information and clarify selected responses. The surveyed states represent a small sampling of the entire state DOT program, but their geographic and geologic conditions were thought to closely represent those within CFLHD's region.

During this process it quickly became apparent that a standardized approach for shrink/swell estimation does not exist, and there is a general lack of uniformity within regions and states concerning shrink/swell practices and procedures. Many state DOT's commented that their current in-house procedures seem to be working, but that they were not comfortable with their approach and would like further guidance on this matter. To follow is a summary of state DOT responses.

There appear to be a variety of methods employed by State DOT's to estimate shrink/swell factors for roadway projects involving substantial earthwork quantities. In some cases, shrink/swell factors are estimated by design or materials personnel, and do not include material specific information from geotechnical or geological personnel. Generally in these cases, the soil survey is done well in advance of any finalized earthwork delineations. Also, some roadway design software packages have the ability to calculate earthwork quantities that incorporate shrink/swell factors, but are only able to assign one default shrink value for soil and one default swell value for rock.

Historical Approach

Several state DOT's rely heavily on historical shrink/swell values calculated upon completion of a project (though the level of back-analysis was not quantified – in-depth tracking of materials vs. final "apparent" shrink/swell for the entire project). These historical values are used for projects in design that are likely to encounter similar subsurface materials from within the same geographic and geologic area, with no accounting for similar types of required construction. In addition, several State DOT's have developed and/or used regional empirical tables correlating shrink/swell factors with various soil and rock types. Due to gross generalizations and resulting inaccurate factors for various soils, these tables are not commonly relied upon. However, some states still rely on the developed empirical tables and other published data to determine swell estimates of rock.

Institutional Knowledge and Experience

Oftentimes, State DOT project personnel, which may include representatives from Design, Construction, and Materials, gather for a roundtable discussion on various project aspects, one of which being shrink/swell factors. Using local knowledge and experience, coupled with historical project data, shrink/swell factors are established for the project and agreed upon by all present.

Geometric Properties

A few states have found that the cross sectional properties of an embankment may provide more information on shrink values than the material properties themselves. This method assumes that embankments with a small cross sectional area have more of a tendency to contribute to shrink values than larger embankments. Small errors in earthwork factors and estimation can be compounded greatly as a total percentage of small fill embankments. The states that use this method have developed tables to estimate the shrink percentage of an embankment, based on average cross-sectional area of the subject embankment.

Field and Laboratory Testing

It appears that very few states perform regular field or laboratory testing to determine shrink/swell characteristics of materials to be used in roadway construction. The most standard laboratory test conducted to determine densities of in-place embankment materials appears to be the Proctor test. The Proctor test is sometimes coupled with a field

sand cone density test or nuclear gage reading to make a determination of bank density to be used in shrink factor calculations. Swell factors continue to primarily be based on published, empirical data or local knowledge, as there has not been a testing method developed to properly characterize swell properties of rock.

Earthwork Estimation Management

Management of earthwork estimates in contract documents also appears to differ significantly between the surveyed states. Generally, management of earthwork estimates range from including grading summaries and mass haul diagrams in the contract documents, and using grading summaries for estimating purposes only, to only paying for in-place excavation or embankment. Most states appear to be in transition between these two methods. Paying for in-place excavation or embankment places more of the risk, with regard to shrink/swell estimation, on the contractor, possibly resulting in a higher bid price for items encompassing excavation and embankment construction, than if traditional grading summaries and mass haul diagrams were used. In using grading summaries and mass haul diagrams, there is potential for earthwork estimates to be imprecise, allowing the contractor to be paid through contract modifications and claims. As such, neither method appears to be preferable over the other and seems to be a matter of historical or institutional preference. Some states mentioned that in moving between more traditional earthwork quantity management to payment for in-place quantities, contractors were initially reluctant to take on the associated risk. Clearly, this practice is more amenable to contractors comfortable with working in local settings, or in areas where waste/borrow sources are readily available. Table 1 provides a summary of earthwork management practices from surveyed states. Table 2 provides a typical range of shrink/swell factors recommended by various states.

TABLE 1. Summary of Earthwork Management Practices

		STATE															
		Arkansas	Colorado	California	Florida	Georgia	Idaho	Kansas	Kentucky	Montana	New Mexico	Oregon	South Dakota	Texas	Utah	Washington	Wyoming
Method of earthwork estimation	Shrink/Swell[1]		X	X	X	X		X		X			X			X	X
	In-place[2]	X	X	X			X		X		X	X		X	X		

[1] Shrink/Swell factors recommended in geotechnical report.
[2] Embankment quantities are estimated as in-place. Shrink/swell factors may be used for estimation purposes only.

TABLE 2. Summary of Typical Shrink-Swell Recommendations

	STATE							
	Colorado	Florida	Georgia	Idaho	Oregon	South Dakota	Washington	Wyoming
State-wide range of recommended shrink factors	10-25	15-20	15-30	10-15	5-10	35	5-25	20
State-wide range of recommended swell factors	15-30	25	5-35	25-40	NP	NP	10-30	10-25

NP. Data not provided.

Inaccurate Earthwork Estimation

Each of the states surveyed suggested they had experienced a limited number of problems in construction with inaccurate earthwork estimates that were handled either by change orders or by the project engineer during construction (raising/lowering grade, fattening/reducing fill slopes, etc.). It was suggested that many of these inaccuracies were due to various project deficiencies other than shrink/swell factor estimation. Project deficiencies cited include: inaccurate original or final survey, contractor tendency to overbuild embankment slopes, and variation in types and age of equipment used in roadway construction.

Summary of State Methods for Handling Earthwork Quantities

While the procedures and practices surrounding earthwork quantity estimation vary significantly between states, all indicated that they had not experienced or were not aware of cases in which their estimations were significantly in error, such that they could not be handled by project personnel during the course of a roadway construction project.

As has been mentioned, CFLHD roadway projects are often constrained by right-of-way or environmental issues. In an effort to "lay lightly on the land" wasting or borrowing large quantities of material along a roadway project is often not possible. The issues surrounding earthwork quantity estimation have been made much more apparent within CFLHD because of the pristine, environmentally sensitive areas in which roadways are constructed. In most cases, states are not bound by the same stringent right-of-way and environmental constraints and can handle an excess or shortage of embankment materials with greater ease.

States often do not have the manpower or budget to collect the number of soil samples required for accurate and detailed shrink/swell analysis throughout the length of a project. In lieu of sample testing, states often rely on historical data, empirical tables, and the knowledge of project engineers familiar with the geographic and geologic conditions. CFLHD is under many of the same constraints with respect to collecting and testing a large number of soil samples. However, more testing can and should be done with the intent of developing specific shrink/swell factors. It appears that recently within CFLHD, historical data or the knowledge of construction personnel has not been considered when developing shrink/swell recommendations. Empirical tables used to develop shrink/swell recommendations will continue to be used, but should only be used by or after consultation with a trained geologist or geotechnical engineer.

FUTURE IMPROVEMENTS AT CFLHD

Within CFLHD, proper representation of earthwork quantities is constrained by the multi-state region in which projects are constructed and the various geologic settings in which these projects lie, many of which are problematic in estimating material shrink/swell properties. Further constraints surround the construction of low-volume roads within environmentally sensitive areas that are further limited by budget, environmental impacts, restricted construction seasons, and local/regional socioeconomic considerations. As CFLHD attempts to develop context sensitive solutions to roadway design, roadway projects routinely attempt to minimize earthwork impacts by attempting to use on-site materials and balance cut and fill quantities, thus minimizing roadway footprints, total excavation, and need for off-site borrow.

Due to the constraints placed on roadway construction projects for partner, land management agencies, CFLHD will continue to develop balanced projects by estimating earthwork quantities for bidding and developing mass haul diagrams. As part of this process, shrink/swell factors will continue to be an integral part of the overall development of accurate earthwork quantities. However, much can be done to improve the current practice within CFLHD to more effectively develop earthwork quantities and provide contractors and construction personnel with the resources necessary to properly manage earthwork quantities in the field.

All phases of a roadway project, from initial design to construction, influence the overall accuracy of developed earthwork quantities, and ultimately the costs associated with roadway excavation and embankment construction. On a Division-wide basis, in both design and construction, there must be an improved awareness of "apparent" shrink/swell sources of error and the cumulative impacts of small errors in fill placement, material shrink/swell estimations, and variations in material properties. Improvements can be made in design guidance for developing

constructible roadway and structure designs, coupled with a sense of appropriate and practical construction methods and equipment types. Improvements can also be made in accurately accounting for quantities throughout the project design, particularly noting difficult terrain issues (vertical and horizontal curves in areas of cuts and fills), as well as the different geologic units and soil types, with their associated engineering properties, that a project may traverse. In an effort to improve risk identification and estimation, it may become necessary to determine when it may be appropriate to develop back-up grading plans to accommodate changes in construction quantities. Efforts should be made to acquire better survey control during design, allowing better volume estimates, and during construction, to track and manage earthwork volumes more accurately.

Historic earthwork information can provide a wealth of knowledge in "apparent" shrink/swell trends for a route and assist in more accurately representing shrink/swell factors. Efforts should be made to track "apparent" shrink/swell on current and past projects, and trend results to material types and types of job elements (rock cuts, large fills, wall excavations, balance requirements, stumpage/duff volumes, problem soil/rock, etc.).

Construction personnel should be included in the design review process as early as possible. Their understanding of constructability issues and knowledge of regional geologic conditions can greatly enhance the accuracy of earthwork estimations. Regular consultation with construction personnel during project design will substantially limit design flaws, namely earthwork quantity estimation errors, from being carried into construction.

With regard to geotechnical reporting of shrink/swell factors, it must be understood that these values are defined as material characteristics related to specific lab preparation methods or empirical data, and do not reflect the apparent shrink/swell factors that might be better used to characterize earthwork volumes during construction. To more accurately define shrink/swell factors it is recommended that routine lab testing, including in-place density and Proctor testing, be used to supplement shrink/swell estimations, when applicable. For various types of geologic materials, namely rock, estimates from published data will be the standard for developing shrink/swell factors. Several attempts have been made to develop field and laboratory tests to determine the swell potential of in-place rock, and all have been met with limited success. Renewed efforts in properly characterizing surface and subsurface materials, and their respective quantities, by station range along the length of a route will greatly increase the accuracy of earthwork estimation.

By recognizing the difficulties inherent in earthwork estimation and development of shrink/swell factors, and by implementing the recommendations discussed herein, estimating earthwork quantities within CFLHD has the potential to become much more accurate, leading to a reduced number of contract modifications and claims associated with earthwork quantities.

SELECTED REFERENCES

The following references proved to be very helpful in providing methods for estimating excavation and embankment quantities, as well as recommending procedures for using shrink-swell factors:

Burch, Deryl. *Estimating Excavation.* Craftsman Book Company, Carlsbad, CA, 1997.

Church. Per *Project Development and Design Manual*. U.S. Department of Transportation Western Federal Lands Highway Division. www.wfl.fha.dot.gov/design/manual/Section_06-1.pdf. Accessed July 3, 2006.

Nichols, Herbert L. *Moving the Earth*. McGraw-Hill Publishing Company, New York, NY, 1976.

Design of an Innovative Retaining Wall System for Highway Construction in Steep Terrain

Kimberly Finke Morrison, P.E., R.G.
Golder Associates Inc., 44 Union Boulevard, Suite 300, Lakewood, CO 80228;
PH (303) 980-0540; email: kmorrison@golder.com

Francis E. Harrison, P.E.
Golder Associates Inc., 44 Union Boulevard, Suite 300, Lakewood, CO 80228;
PH (303) 980-0540; email: fharrison@golder.com

James G. Collin, Ph.D., P.E.
The Collin Group Ltd., 7445 Arlington Road, Bethesda, MD 20814;
PH (301) 907-9501; email: jim@thecollingroup.com

Scott A. Anderson, Ph.D., P.E.
Federal Lands Highway, FHWA, 12300 West Dakota Avenue, Lakewood, CO 80228
PH (720) 963-3519; email:Scott.Anderson@fhwa.dot.gov

ABSTRACT

In steep terrain, mechanically stabilized earth (MSE) walls are frequently constructed to accommodate widening of existing roads or construction of new roadways. However, substantial excavation must be performed to establish a flat bench upon which to construct the wall, and unshored construction may not be practical, particularly if traffic must be maintained during construction. Shoring, often in the form of soil nailing, is therefore employed to stabilize the backslope with an MSE wall being designed and constructed in front of it. Existing public sector guidelines suggest a minimum bench width and MSE reinforcement length equivalent to seventy percent of the design height of the MSE wall (i.e., 0.7*H*). Where the two wall types are appropriate to use together, termed a shored mechanically stabilized earth (SMSE) wall system, a design procedure has been developed that considers both the stabilizing effect of the shoring wall with regard to reduction of lateral loads acting on the MSE wall mass as well as contributions to global stability. Based on the results of centrifuge modeling, field-scale testing and numerical modeling research, a minimum reinforcement length equivalent to 30 percent of the wall height (0.3*H*), as measured from the top of the leveling pad, is recommended for design of the MSE wall component of an SMSE wall system. This paper summarizes the methodology for internal design of this innovative wall technology.

INTRODUCTION

Design and construction of roadways in rugged, mountainous terrain poses several challenges. Where terrain is steep, retaining walls are often constructed to accommodate widening of existing roadways, or construction of new roadways. Mechanically stabilized earth (MSE) walls have proven to be reliable and cost effective for highway projects. However, in steep terrain, excavation is required to establish a flat bench on which to construct the MSE wall. In some cases, the excavation requirements for MSE wall construction become substantial, and unshored excavation for wall construction is not practical, especially if traffic must be maintained during construction of the MSE wall.

When the backslope excavation is supported by a permanent shoring wall, former design methodologies do not allow for a reduction in reinforcement length of MSE walls shorter than 60 percent of the wall height (0.6H) for the private sector (*1*) or 70 percent of the wall height (0.7H) for the public sector (*2*,*3*). A new design methodology has been developed by the Federal Lands Highway Division of the Federal Highway Administration (FHWA) for shored mechanically stabilized earth (SMSE) wall systems (*4*) which allows a potential reduction in the MSE reinforcement length to as little as 30 percent of the wall height (0.3H). Figure 1 conceptually illustrates the MSE component of an

SMSE wall system. This paper summarizes the proposed methodology for internal design of the MSE wall component of an SMSE wall system.

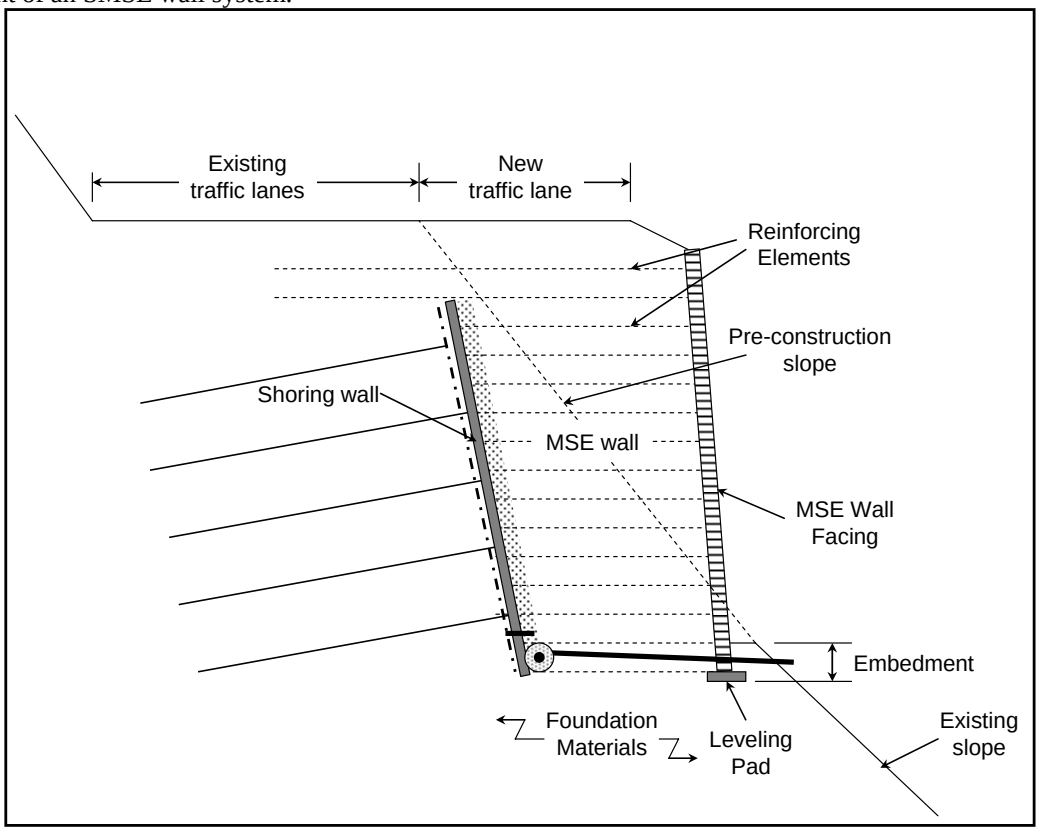

Figure 2. Illustration of a typical SMSE wall system (*4*).

Failure Modes

Design of an SMSE wall system must consider failure modes associated with conventional MSE walls and shoring walls, in addition to internal failure modes specific to the compound nature of the SMSE wall system. Figure 2 illustrates the various failure modes of the compound SMSE wall system (*4*).

When a failure surface passes behind and underneath all elements of the SMSE wall system, global failure (mode 1) occurs. Stability against global failure is dependent on the foundation and slope conditions behind and below the wall system, and is essentially independent of the SMSE wall system strength and structural characteristics. Compound failure of the shoring system and foundation (mode 2) occurs when the shear surface intersects the shoring wall, and continues through the foundation below the MSE wall.

Failure across the shoring wall/MSE wall interface (mode 3) is a failure mode specific to an SMSE wall system. A structurally sound permanent shoring wall facing will generally preclude such failures. In many cases, this failure mode may be excluded from the analysis at the discretion of the engineer. One case where such an analysis may be valid is a tie-back shoring wall with discrete facing panels.

Interface shear failure (mode 4) is a failure which occurs along the interface between the MSE wall and the shoring wall. If MSE reinforcements are connected to the shoring wall, this mode of failure includes failure of the connections. Similar to mode 3, this failure mode is specific to an SMSE wall system.

When the shear failure intersects the MSE wall and the foundation, compound failure of the MSE wall and foundation occurs (mode 5). This failure mode is generally representative of the bearing capacity of the foundation materials.

Internal failure of the MSE component (mode 6) generally occurs due to rupture of reinforcements, or pullout of reinforcements. This failure mode is addressed with appropriate backfill materials, suitable reinforcement vertical spacing, and adequate reinforcement strength and lengths. This paper addresses design of the MSE wall component to resist against failure mode 6.

The reader is referred to Morrison et al. (*4*) for design of the SMSE wall system for failure modes 1 through 5. These failure modes may generally be addressed using limit equilibrium software which includes elements to model the various MSE and shoring wall components, such as Slide 5.0 (*5*).

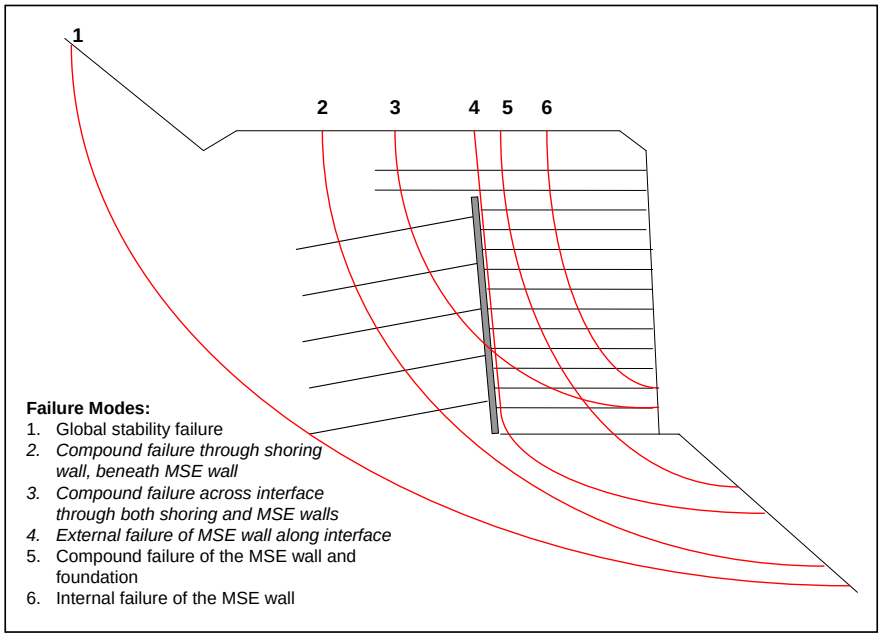

Figure 2. Failure modes of an SMSE wall system (*4*).

Safety Factors

The recommended minimum factors of safety (*FS*) for internal design of the SMSE wall system are provided below:

- Rupture of reinforcements, FS_r:1.5
- Pullout of reinforcements, FS_p:1.5 to 2.0 (range of FS to allow the wall designer to account for potential reduction in vertical stress in the resistant zone due to arching at the shoring wall/foundation interface)

The premise of the SMSE wall design methodology presented herein is that lateral pressures within the MSE mass are self-induced because the shoring wall effectively eliminates external loading. These self-induced pressures would not realistically induce failure modes such as sliding, overturning, or eccentricity within reinforced soil because they would diminish with even minor displacement. Therefore, factors of safety are not provided for these failure modes as they are not considered valid for SMSE walls. This paper focuses on the internal design of the MSE wall component of an SMSE wall. The reader is referred to Morrison et al. (*4*) for design to account for other SMSE wall failure modes and to AASHTO (*2*) for a discussion of global failure mechanisms acting outside the SMSE wall system.

Internal Stability Design

The methodology for design of the MSE wall component of an SMSE wall system evolved from traditional MSE wall design. Similar to a traditional MSE wall, the MSE component of an SMSE wall addresses the internal failure mechanisms which include rupture of soil reinforcements (i.e., elongation or breakage of the reinforcements), and soil reinforcement pullout. The step-by-step process for internal design of the MSE wall component is summarized as follows:

- Select the reinforcement type (inextensible or extensible reinforcements) and trial geometry for the MSE wall.
- Estimate the location of the critical failure surface.
- Calculate the maximum tensile force at each reinforcement level for evaluation of internal stability with regard to reinforcement rupture.
- Calculate the required total tensile capacity of reinforcements in the resistant zone.
- Calculate the pullout capacity at each reinforcement level within the resistant zone.

The MSE wall system type, including facing, must be selected to complete the design. The vertical reinforcement spacing selected should be consistent with the type of MSE facing intended for the application. As evidenced by centrifuge testing conducted on an SMSE wall system (*4*), closer reinforcement spacing increases internal stability. A maximum vertical reinforcement spacing of 600 millimeters (mm) is recommended for the MSE wall component of an SMSE wall system (*4*).

The critical failure surface can be approximated using Rankine's active earth pressure theory within the reinforced soil mass, assuming the remaining portion lies along the shoring/MSE interface. Use of the theoretical active failure surface is consistent with current practice for design of MSE walls with extensible reinforcements, and is considered sufficiently conservative for design of SMSE wall systems. Figure 3A illustrates the conceptualized failure surface for extensible reinforcements. Design for inextensible reinforcements should be conducted using the failure surface illustrated in Figure 3B, consistent with current design practice (*2*,*3*). As shown in both the extensible and inextensible reinforcement cases, the critical failure surface has been assumed to be bilinear with the lower point passing through the toe of the wall.

Reinforcement Rupture

Consistent with current design practice (*3*), internal design of the MSE wall component of an SMSE wall system requires calculation of lateral stresses mobilized in the MSE wall component, which are considered to be a function of reinforcement type (inextensible versus extensible). In the case of an SMSE wall system where the shoring wall already provides the lateral support, lateral loading acting on the MSE wall component is considered minimal so that any lateral pressures generated are essentially the result of reaction against the shoring wall, and thus internal to the MSE mass.

For internal design of the MSE wall component of an SMSE wall system, active earth pressures are conservatively assumed to apply and the maximum tensile forces acting on each reinforcement layer are calculated using the simplified coherent gravity method (*2*). The procedure for reinforcement rupture design is identical to that presented in Elias et al. (*3*) for traditional MSE walls, and has not been reproduced herein.

Pullout Capacity

Internal design of the MSE wall component of an SMSE wall system differs from design of a conventional MSE wall with regard to pullout of the reinforcements. Conventional MSE wall design requires that each layer of reinforcement resist pullout by extending a nominal distance beyond the estimated failure surface (*3*). In the case of an SMSE wall system, only the lower reinforcement layers (i.e., those that extend into the resistant zone) are designed to resist pullout for the entire "active" MSE mass.

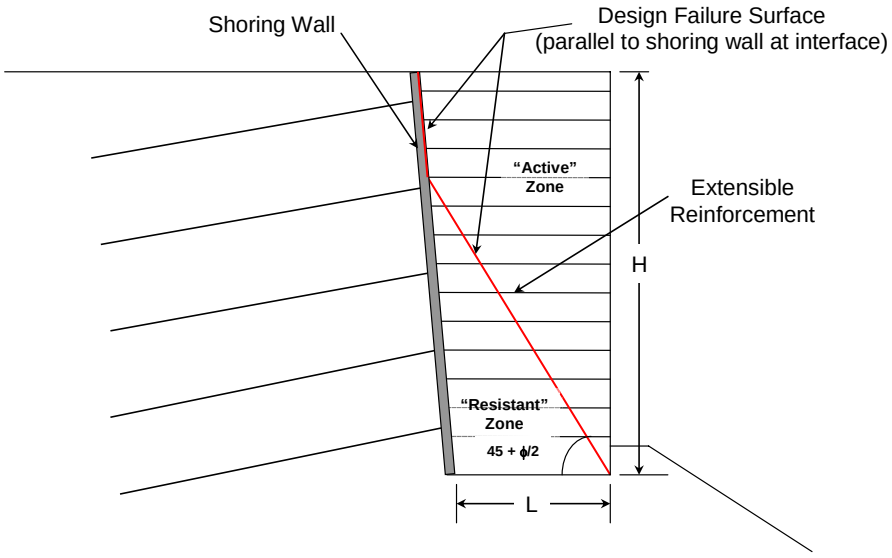

1. Extensible Reinforcements

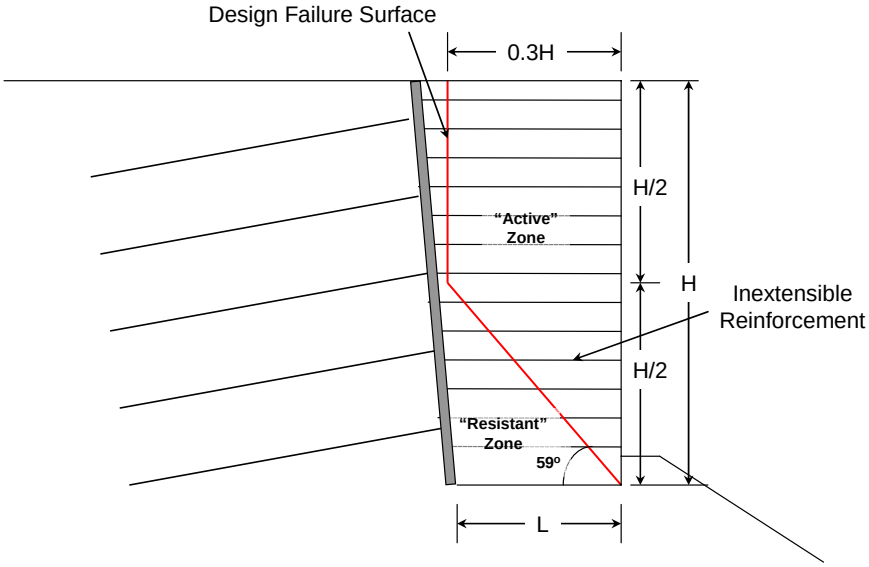

B. Inextensible Reinforcements

Figure 3. Location of potential failure surfaces for internal stability design (*4*).

Required Resistance

The required pullout resistance (T_{max}) of the MSE reinforcements within the resistant zone is calculated as the pullout force derived using the simplified free-body diagram presented in Figure 4. Figure 4 presents the typical case where the grade above the MSE wall is level and is subjected to a traffic surcharge, *q* (force per unit length units).

Regardless of whether or not the shoring wall is battered, the wall designer should assume development of a tension crack at the MSE/shoring interface and that the upper wedge (shown in gray in Figure 4) is in equilibrium.

Therefore, the forces N_2 and S_2 are neglected. Where the upper layers of MSE reinforcement are extended over the shoring interface as recommended by Morrison et al. (*4*), this analysis conservatively excludes the resistance provided from these longer reinforcements. For simplicity, the remainder of the parameters should be assumed the same as shown in Figure 4. Concentrated vertical and horizontal loads (F_V and F_H, respectively) are assumed to apply at the centroid of the truncated active failure wedge.

The weight of the upper wedge is insignificant and may also be ignored in the pullout calculation. Therefore, the weight of the active wedge, *W*, can be calculated as:

$$W = L_W H\gamma - \frac{1}{2} L_W^2 \tan\psi$$

where *H* is the height of the MSE wall, *g* is the unit weight of the reinforced fill, is the angle defined in Figure 4, and L_W is the maximum length of the truncated failure wedge, i.e., reinforced length at the intersection of the shoring wall and active wedge. Assuming that the MSE wall facing is near-vertical, L_W may be estimated as follows:

$$L_W = \frac{L_B v}{v - \tan\psi}$$

where L_B is the width of the MSE wall at the base and *v* is the vertical component of the shoring wall batter (i.e., 1H:*v*V (horizontal:vertical)).

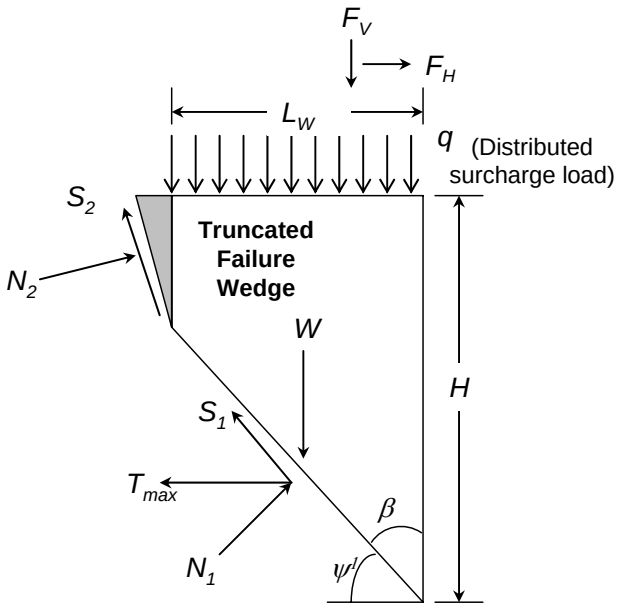

Notes:
1. For extensible reinforcements, $\psi = 45+\phi/2$; for inextensible reinforcements, $\psi = 59$ degrees.
2. Assume tension crack development and neglect forces N_2 and S_2.
3. Assume upper wedge (shown as gray) is in equilibrium.

Figure 4. Free-body diagram for calculation of required tensile capacity in the resistant zone (*4*).

Summing force components perpendicular and parallel to the failure surface results in the following equations:

$$N_1 = W\sin\beta + qL\sin\beta + F_V\sin\beta + T\cos\beta - F_H\cos\beta$$

and

$$S_1 = W\cos\beta + qL\cos\beta + F_V\cos\beta - T\sin\beta + F_H\sin\beta$$

where W is the weight of the active wedge, N_1 represents the reaction force perpendicular to the failure surface, S_1 represents the shear resistance along the failure surface, L is the reinforcement length, T is the resultant pullout force mobilized by the reinforcement in the resistant zone, and β is the angle as defined in Figure 4. At failure, the Mohr-Coulomb failure state defined by:

$$\frac{S_1}{N_1} = \tan\phi'$$

is applied to the reinforced soil, where ϕ' is the effective friction angle for the reinforced soil. When L is less than $H\tan\beta$, the weight of the truncated "active" wedge is given by:

$$W = LH\gamma - \frac{\gamma L^2}{2\tan\beta}$$

where γ is the unit weight of the reinforced soil and H is the height of the MSE wall. Substitution of the expressions for S_1, N_1, and W and performing some algebraic manipulations leads to the following expression for T:

$$T = \frac{L\left(\gamma\left(H - \frac{L}{2\tan\beta}\right) + q\right) + F_V}{\tan(\phi'+\beta)} + F_H \quad \text{for } L \le H\tan\beta$$

For the case where $L \ge H\tan\beta$, the full active wedge would develop whereby the forces S_2 and N_2 are in fact zero. In this case, the weight of the "active" wedge is given by:

$$W = \frac{1}{2}\gamma H^2\tan\beta$$

and the expression for T is given by:

$$T = \frac{H\tan\beta(\gamma H + 2q) + 2F_V}{2\tan(\phi'+\beta)} \text{ for } L \ge H\tan\beta$$

The total required pullout resistance is then calculated by applying a factor of safety to the calculated pullout force, as follows:

$$T_{max} = FS_p T$$

Calculated Resistance

As mentioned previously, a factor of safety against reinforcement pullout (FS_p) of 1.5 to 2.0 is recommended for SMSE wall design. A higher factor of safety should be used where the anticipated wall aspect ratio is less than or equal to 0.4. This increase in factor of safety accounts for arching which may occur near the base of the MSE wall at the shoring interface as evidenced by numerical modeling and field-scale testing of an SMSE wall employing aspect ratios on the order of 0.25 (*4*).

Based on the reinforcement spacing selected, calculate the length of embedment (L_{ei}) of each reinforcement layer within the resistant zone, as follows:

$$L_{ei} = L - \frac{H - z}{\tan \psi}$$

where L is the base length of the MSE wall (equal to 0.3H or greater), z is the depth to the reinforcement layer from the top of the wall, and ψ is the angle defined in Figure 4.

At each reinforcement layer within the resistant zone, calculate the pullout resistance, F_{PO}, as follows:

$$F_{PO} = \frac{1}{FS_p} F^* \sigma_{vi} L_{ei} C R_c \alpha \le T_{allowable}$$

where F^* is the pullout resistance factor, C is the reinforcement effective unit perimeter (i.e., 2 for strips, grids, and sheets), α is the scale effect correction factor to account for a non-linear stress reduction over the embedded length of highly extensible reinforcements, R_c is the coverage ratio (i.e., one for full coverage), σ_{vi} is the overburden pressure at the ith reinforcement level (including distributed dead load surcharges, but neglecting traffic loads), and L_{ei} is the length of embedment in the resisting zone at the ith reinforcement level. It should be noted that the calculated pullout resistance cannot be greater than the allowable strength ($T_{allowable}$) of the specified MSE reinforcement.

The pullout resistance factor (F^*) can be estimated using the following general equation, or from laboratory pullout tests:

$$F^* = \left(F_q \cdot \alpha_\beta\right) + \tan \rho$$

where F_q is an embedment bearing capacity factor, α_β is a bearing factor for passive resistance based on the thickness per unit width of the bearing member, and ρ is the soil-reinforcement interaction friction angle. Refer to Elias et al. (*3*) for more information regarding evaluation of F^*.

The pullout resistance of the MSE wall component of an SMSE wall system is considered adequate if:

$$T_{\max} \le \sum F_{PO}$$

where T_{max} is calculated as presented above.

CONCLUSIONS

This paper presents an innovative method for internal design of shored MSE (SMSE) walls that rationally considers the stabilizing benefits provided by the shoring wall constructed to support the backslope of the excavation in steep or otherwise constrained environments (i.e., limited site access or easements). Internal design of an SMSE wall with regard to reinforcement rupture has not been modified from existing methodologies (*2*,*3*). However, new equations for design of the reinforcements with regard to pullout capacity are proposed, provided herein. This design methodology allows for a potential reduction in the MSE reinforcement length to as little as 30 percent of the wall height (0.3H), provided that the minimum reinforcement length is 1.5 m or greater. The complete design guideline for SMSE walls (*4*) is available for download on the Central Federal Lands Highway Division (CFLHD) of the FHWA website at: http://www.cflhd.gov/techDevelopment/completed_projects/.

ACKNOWLEDGEMENTS

The authors would like to extend their thanks to the Central Federal Lands Highway Division of the Federal Highway Administration for their support in development of these design guidelines for SMSE wall systems and for allowing us to publish this paper.

REFERENCES

1. National Concrete Masonry Association (NCMA). *Design Manual for Segmental Retaining Walls*. Second Edition. J.G. Collin (ed.), 2002.

2. American Association of State Highway and Transportation Officials (AASHTO). *Standard Specifications for Highway Bridges.* Seventeenth Edition, 2002.

3. Elias, V., Christopher, B.R., and Berg, R.R. *Mechanically Stabilized Earth Walls and Reinforced Soil Slopes, Design & Construction Guidelines*. Report No. FHWA-NHI-00-043. Federal Highway Administration, 2001.

4. Morrison, K.F., Harrison, F.E., Collin, J.G., Dodds, A. and Arndt, B. *Shored Mechanically Stabilized Earth (SMSE) Wall Systems Design Guidelines*. Report No. FHWA-CFL/TD-06-001. Federal Highway Administration, 2006.

5. Rocscience. *Slide 5.0* [software], 2003.

Replacing the US101 Beverly Beach Bridge, Lincoln County, Oregon

David Higgins, CEG, Senior Engineering Geologist
Shannon & Wilson, Inc.
2255 SW Canyon Road
Portland, Oregon 97201
Phone (503) 223-6147
djh@shanwil.com

Gary Peterson, CEG, Vice President
Shannon & Wilson, Inc.
2255 SW Canyon Road
Portland, Oregon 97201
Phone (503) 223-6147
glp@shanwil.com

Tim Potter, PE, Bridge/Geo-Hydro Manager
Oregon Department of Transportation, Region 2 Technical Center
455 Airport Road SE, Bldg A
Salem, Oregon 97301-5397
Phone (503) 986-2990
Fax (503) 986-2839
james.t.potter@odot.state.or.us

Daniel Hogan, PE, Senior Engineer
Shannon & Wilson, Inc.
2255 SW Canyon Road
Portland, Oregon 97201
Phone (503) 223-6147
deh@shanwil.com

ABSTRACT

A new US101 bridge will be built in 2007 at Beverly Beach State Park on the central Oregon coast. The bridge is the pedestrian gateway between one of the busiest Oregon State Parks and its popular, scenic beach. An extended public involvement process (NEPA) evaluated realignments and selected an arch bridge design for the site. The new bridge is being designed by ODOT and HW Lochner, Inc., with Shannon & Wilson, Inc. as geotechnical consultant. Geologic hazards and adverse soil conditions abound at the site. Seismic threats are driven by the nearby Cascadia Subduction Zone. Loose liquefiable sediments with layers of wood debris underlie the site and overlie soft siltstone and sandstone bedrock. Poor quality bridge approach embankments exhibit chronic settlement and require improvement to meet seismic design standards.

Wave action is aggressively eroding adjacent bluffs. The bridge's beach exposure allows direct impact of large (30+ foot) ocean waves. Roadway realignment will allow for approximately 50 feet of additional bluff retreat adjacent to the bridge. A creative revetment design was incorporated to prevent erosion and scour and to comply with statewide goals that require avoiding beachfront hardening. Robust erosion protection is incorporated in the foundation systems.

The classic arch bridges of the Oregon Coast drove selection of an arch design for this highly visible bridge. However, an arched structure posed substantial design challenges considering the poor subsurface conditions, seismic threats, and erosion and scour potential. Foundations considered included battered piles and groups of drilled shafts. Deadman anchor systems in the abutments provide additional lateral restraint. Revetments included

various combinations of sheet pile, stone columns, riprap, and gabion systems. Embankments require stone columns to mitigate post liquefaction failures.

INTRODUCTION

The new Spencer Creek Bridge to be built in 2007 is located on US101 at Beverly Beach State Park on the central Oregon coast, 6 miles north of Newport. The Project Vicinity Map, Figure 1, shows the location of the bridge. Spencer Creek is a westerly-draining creek that flows out of the Coast Range directly onto the beach adjacent to the new bridge, then across the broad beach into the Pacific Ocean. The new bridge will be an arch structure and will be a highly visible feature at the state park. A pathway leading beneath the bridge will provide the only direct beach access from the campground and day use parking area, making the arch the pedestrian gateway between one of the busiest Oregon State Parks and its popular scenic beach.

An arched structure at the site posed substantial design challenges considering the poor subsurface conditions, seismic threats from the active Cascadia Subduction Zone (CSZ) where a magnitude 8.5 to 9.0 earthquake is possible, and erosion and scour potential from direct impact of large ocean waves. However, selection of an arched structure on the chosen alignment was the result of an 8 year NEPA public involvement process. The needs and opinions of multiple stakeholders and Oregon statewide planning goals confined the location of the bridge to a poor quality bridge site. The selected bridge type is not conducive to site conditions. This resulted in several delays encountered during the design phase and construction costs will be more than what had originally been anticipated.

Considering the visibility from the park, and the visual frame created by the structure over the beach interface, Oregon State Parks believes this bridge is one of the most photographed in the state. The unique direct interface between the beach and the Beverly Beach State Park, drove concerns that the new bridge should compliment the landscape and serve as a photogenic ambassador of the beautiful Oregon Coast. Photo 1, shows the existing bridge with a sketched overlay of the conceptual new arch bridge. The new bridge is being designed by the Oregon Department of Transportation (ODOT) and HW Lochner, Inc., with Shannon & Wilson, Inc. as the geotechnical consultant. As of this writing, design is complete and the project bidding will occur this summer, leading to construction beginning in 2007.

The new bridge will replace both the abandoned Spencer Creek Bridge and a temporary bypass bridge constructed immediately west of the abandoned bridge. The original bridge was constructed in 1946. By 1999, it had deteriorated to the point of being considered unsafe. A temporary oceanside bypass structure that partially crosses the beach was constructed in 1999 and the original bridge was abandoned. The temporary structure had a design life of 5 to 8 years, and has been in service for 7 years. The salt air and ocean exposure has taken a toll on the bypass structure and it is nearing the end of its useful life.

ODOT had originally thought the replacement of the abandoned bridge would be a simple and routine process. However, due to aggressive sea cliff erosion directly encroaching on US101, stakeholders concerns, and potential conflicts with statewide planning goals, significant challenges were raised, making the replacement of the Spencer Creek Bridge anything but routine.

The active ocean bluff erosion, particularly on the south approach, will soon require realignment of the US101 roadway. Inland realignment of US101 was considered, but any inland alignment would encroach into private and public forest lands and traverse potential landslide areas. Rebuilding on the existing alignment would likely require visible armoring of beach elements. Both encroachment into forest lands and visible revetment protection (beachfront hardening) would conflict with statewide planning goals. These challenges led to an extended public involvement process evaluating realignments and bridge options. Ultimately through this process, the high visibility of the site and the classic arch bridge of the Oregon Coast drove the selection of an arch design for the new bridge, on an alignment 50 feet east of the abandoned bridge.

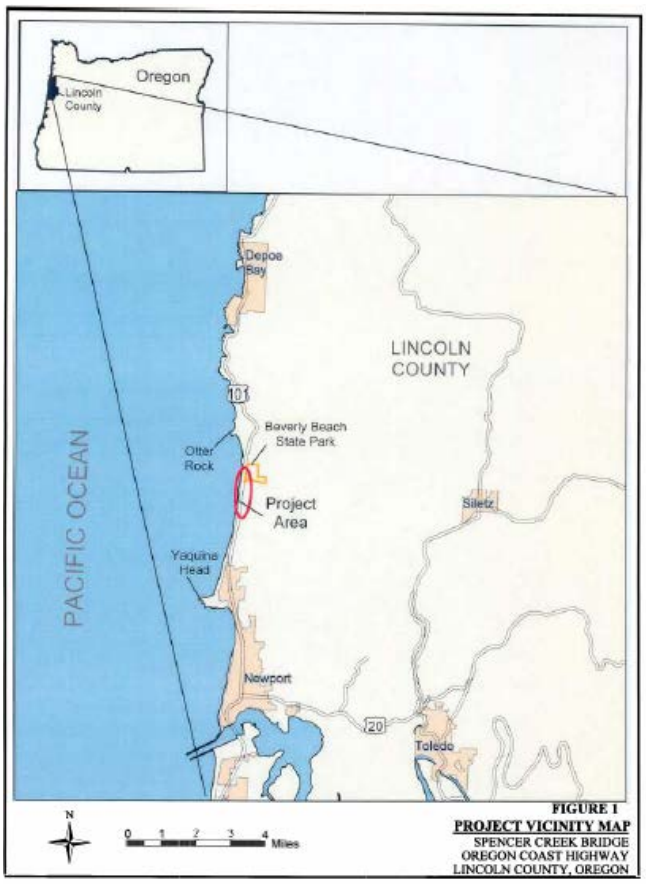

From ODOT 2004 Alternative F Justification

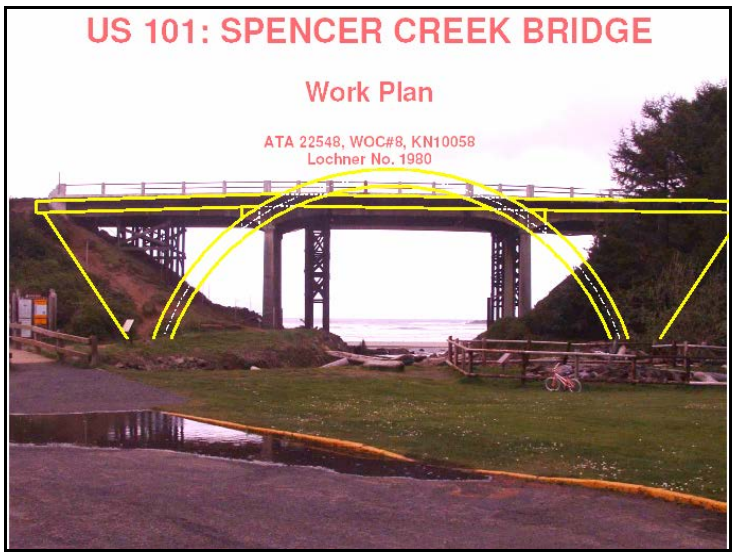

PHOTO 1: From HW Lochner Undated Work Plan
Photo taken from day use parking lot

SITE DESCRIPTION

The Beverly Beach State Park campground and day use parking area is located east of US101 as shown in the aerial photograph, Photo 2. Spencer Creek flows through the campground prior to crossing below US101 and was approximately 20 feet wide and 1 to 3 feet deep beneath the abandoned bridge at the time of the Shannon & Wilson geotechnical investigation. Large riprap constrains the channel beneath the bridge. Large driftwood logs are often present in the stream channel and the streambed consists of gravel and large cobbles. During major storms, sea waves directly impact the stream channel beneath the bridge causing erosion.

US101 sits on 30 to 40 foot high embankments that extend 400 to 500 feet north and south, transitioning from natural ocean bluffs to the original bridge. The approach embankment side slopes are inclined at about 1.5 horizontal to 1 vertical (1.5H: 1V) to 1.7H: 1V, with localized areas being at about 1.2H: 1V. East of the bridge site, the topography is a relatively flat-bottomed drainage basin that encompasses Spencer Creek and the State Park Campgrounds. Historically, the basin was separated from the beach forming a small estuary. West of the bridge site, beach topography gently slopes toward the ocean. Westward-dipping sedimentary rocks, many with impressive fossil assemblages, are locally exposed in the bluffs. More resistant layers crop out through the beach sands and further offshore in the surf zone. The original bridge and its approach embankments are located at the transition from the Spencer Creek flood plain and infilled estuary to the ocean beach. Consequently, variable subsurface conditions are present. The embankment consist of variable fill materials that overlie terrace deposits, beach sand, alluvium, estuary deposits, and at depth, siltstone and sandstone bedrock similar to that exposed in beach front bluffs north and south of the site.

PHOTO 2: From ODOT 2003 Reconnaissance Study Report
Note: 1999 Aerial Photo
Prior to Temporary Detour Structure

BRIDGE REPLACEMENT

In 1998 ODOT realized that the original Spencer Creek Bridge, built in 1947, was rapidly falling victim to the ravages of time, wear, and the corrosive atmosphere of the Oregon coast. Salt spray from the ocean had penetrated the concrete, causing the steel rebar to rust and expand, which placed pressure on the surrounding concrete causing it to spall. The spalling became so accelerated that a net had to be placed below the bridge to protect passing pedestrians from falling concrete. ODOT engineers evaluated the bridge's load-carrying capacity and were shocked to learn that the bridge was carrying heavier loads than it could safely handle. ODOT imposed a 40 ton load restriction on the structure and installed temporary shoring. As an emergency measure, ODOT engineers designed a temporary detour bridge for use until an alignment for a new permanent Spencer Creek Bridge could be selected and the new bridge designed and constructed. The temporary detour bridge was built on the ocean side of the original bridge between June and September 1999 and was intended to remain in use for 5 to 8 years. The temporary detour structure as well as the shoring placed under the original bridge is shown below in Photo 3.

Ocean waves were eroding the cliffs below the highway, particularly south of the bridge, at an alarming rate, threatening to undermine and destroy the bridge approaches. The U.S. Army Corps of Engineers calculated that the sea cliffs were receding at an average of 9 inches per year in the area of Spencer Creek. Parking pull-offs and much of the highway shoulder had already fallen down onto the beach as can be seen above in Photo 2. With the rapid rate of erosion pushing the roadway inland, the original bridge could not be replaced on the same alignment without armoring the bluff. Any new armoring of the beach or bluffs directly conflicts with the Oregon Department of Land Conservation and Development (DLCD) statewide goals (Goal 18). However, moving the alignment inland directly conflicts with another of the Oregon DLCD statewide goals (Goal 4) that prohibits impacts on Forest Lands (http://www.lcd.state.or.us/LCD/goals.shtml).

In 1973 Oregon adopted 19 statewide planning goals. These goals express the state's policies on land use and have been strongly maintained. With respect to structures, an exemption exists for replacing structures built before 1977, where statewide planning goals may not apply. During the very early initial scoping phase for bridge replacement, ODOT believed that beach and sea cliff hardening, such as riprap placement to protect the replacement bridge, would not require a goal exception because the bridge and highway existed before 1977. However, the planning goal exemption does not acknowledge highways or bridges as structures with any specific exemption.

Realignment of the highway approaches and beachfront hardening would both conflict with Oregon's strong statewide planning goals, as well as significantly impact both the human and natural environment. The significant environmental impact, as well as the potential need for exceptions to planning goals, mandate that a National Environmental Policy Act (NEPA) Environmental Impact Statement (EIS) be performed to explore bridge options and alternatives.

PHOTO 3: From ODOT 2002 Conceptual Alternatives Report
Photo from beach

NATIONAL ENVIRONMENTAL POLICY ACT

The National Environmental Policy Act of 1969 (NEPA) established a national policy for the environment and provided for the establishment of a Council on Environmental Quality. The purpose of the Act is detailed in Sec. 2 [42 USC 4321] of the Act and reads as follows:

The purposes of this Act are: To declare a national policy which will encourage productive and enjoyable harmony between man and his environment; to promote efforts which will prevent or eliminate damage to the environment and biosphere and stimulate the health and welfare of man; to enrich the understanding of the ecological systems and natural resources important to the Nation; and to establish a Council on Environmental Quality (CEQ).

In short, NEPA is the basic national charter for the protection of the environment. NEPA establishes policy, sets goals, provides means for carrying out the policy, and contains "action-forcing" provisions to ensure that federal agencies act according to the letter and spirit of the Act. The NEPA regulations inform federal agencies what they must do to comply with NEPA procedures and achieve the goals of the Act. The procedures ensure that environmental information is available to public and agency officials and citizens before decisions are made and before actions are taken. The process is intended to help public officials make informed decisions that include an understanding of environmental consequences, and pursue solutions that meet the project need while protecting, restoring, and enhancing the environment. Although NEPA applies to major federal actions it has been ODOT's practice to apply the NEPA process to all projects that have the potential to impact the environment, even if the project is not a major federal action (http://oregon.gov/ODOT/HWY/GEOENVIRONMENTAL/nepa.shtml).

NEPA policy and practice has three main categories of compliance: Categorical Exclusion Reviews (CERs), Environmental Assessments (EAs), and Environmental Impact Statements (EISs). CERs are the briefest form of NEPA review. The purpose of a CER is simply to verify that neither an EA nor an EIS is needed prior to making a decision on the activity being considered for approval. Categorical Exclusion determinations are issued solely for projects that clearly have no significant impacts and for which an EA or EIS is not necessary. EAs are prepared to analyze the environmental effects of a proposed activity to determine the significance of potential impacts. If no significant or potential impacts are identified by the EA, no further action is necessary. EISs are prepared for any project or process that will significantly impact the environment. EIS regulations are issued by the CEQ and include procedures for preparing EISs. The EIS process for the Spencer Creek Bridge took 8 years to complete and included public involvement and working with multiple stakeholders as an integral element. The process has several elements including but not limited to scoping, analytical scenarios, impact analysis, Draft EIS, public review, and Final EIS. Scoping for the Spencer Creek Bridge, although an integral part of the entire process generally included early scoping phases and general concept development. Analytical scenarios included more specific conceptual alternatives development and impact analysis. Both a Draft EIS and Final EIS were issued and public review was performed after each element of the NEPA process.

In 1998, ODOT engineers performed several borings as part of the geotechnical investigation for the temporary detour bridge and alignment. Based on this investigation, ODOT engineers determined that the Classic Arch Bridge of the Oregon Coast would be a feasible bridge type for an alignment near the original bridge. The arch was adopted and introduced to the public as the new Spencer Creek Bridge. The arch bridge then became the only bridge type considered in the EIS process, even though, several bridge alignment options had been considered.

PUBLIC INVOLVEMENT

The primary public involvement in the NEPA EIS process is for scoping. Scoping is the process used to determine the appropriate contents of an EIS. It begins before any analysis of impacts is done and continues until the Final EIS is initiated. The key role of the public in scoping is to help identify alternatives to be considered in the project and then to reduce those alternatives down to one alternative for the Final EIS. Any alternatives likely to solve the problem, have few environmental impacts, and conform to regulatory compliance were advanced for consideration in later phases. The public is first involved in scoping when it is announced by a Federal Register notice and by press release announcing that an EIS will be prepared and to ask for comments about what should be included. In

this stage, public workshops, meetings, and a public open house were held at the bridge site as well as in surrounding communities to identify an adequate range of reasonable alternatives.

From the initial early scoping phase in 1998, eight alternative concepts were identified. At this time, prior to construction of the temporary detour structure, it was believed that beachfront armoring was a viable option. However, further research disclosed that the existing bridge and highway alignment was not exempt from statewide planning goals and those alternatives requiring armoring were deleted. With this understanding, a second early scoping phase examined very general concepts and many new alternatives were identified. These alternatives were reduced to 23 alternatives considered in a Conceptual Alternatives Report. These were further reduced to 9 alternatives considered in a Reconnaissance Study Report. The nine 9 alternatives were designated as Alternatives A through H plus a No-Build option that was not given a letter designation. The lettered alternatives included many different revetment and alignment options and a No-Build Alternative that would leave US 101 in place, in its existing condition with only routine maintenance and continued repairs and shoring of the temporary bridge. Two lettered alternatives plus the No-Build alternative were considered in the Draft EIS report and a single alternative was selected and included in the Final EIS. Press releases were issued and new public meetings held after each report was issued.

A series of public meetings were organized by the Federal Highway Administration (FHWA), the lead agency for preparing the EIS. In addition to FHWA, the US Army Corp of Engineers (COE) was a cooperating agency. Under section 103 of the 1962 River and Harbor Act, the COE has approved funding for planning, engineering and environmental investigations for shoreline stabilization options that would protect US 101 highway facilities along the beach. The COE considered revetment design options such as an off shore breakwater, sea cliff armoring, terracing the sea cliff, and beach nourishment. Although, sea cliff armoring and terracing were quickly abandoned, the COE continued to evaluate solutions for the shoreline protection problems.

Other regulatory agencies with interests in the project and taking part in public meetings were ODOT, Lincoln County, Oregon DLCD, and Oregon Parks and Recreation Department. The public generally included citizens who live, work, or play in the area as well as various public interest groups. There are a few vocal public interest groups on the Oregon Coast who would like to see all costal highways, including US 101, either completely abandoned or moved several miles inland as to not have a visual or audible impact on the coast. The local business and tourism community as well as most tourists and coastal residents strongly disagree with this opinion.

After the initial scoping phases, where many alternatives were identified, subsequent rounds of public involvement reduced the number of alternatives to be included in a Draft EIS to three. The three alternatives included in this widely distributed document were the two “build alternatives” F and G, as well as the “No-Build” alternative. By CEQ regulation, all Draft EISs must include an alternative where nothing is done; a No-Build alternative to explore potential impacts of inaction and to provide a basis of comparison with the build options. Alternative F would shift the highway alignment 50 feet to the east, avoiding sea cliff erosion for “at least” 50 years. Alternative G would shift the highway alignment inland bisecting the community of Beverly Beach and cross Spencer Creek within Beverly Beach State Park. After the Draft EIS was written and the three alternatives thoroughly analyzed, an additional round of public involvement completed the final phase of scoping when the public reconvened and helped to select Alternative F for the Final EIS.

ENVIRONMENTAL IMPACT STATEMENT

The NEPA process for the new Spencer Creek Bridge began in late 1998 with selection of the Arch Bridge type and the initial scoping phases identifying alternatives. Initial scoping phases ended with a Conceptual Alternatives Report, dated July 2002, evaluating nine different roadway alignments, five sea cliff stabilization options, and nine shoreline erosion protection options. These options were then narrowed to five roadway alignments, three shoreline erosion protection options, and several sea cliff stabilization options included in the Reconnaissance Study Report dated June 2003. Public meetings held after the Reconnaissance Study Report finally narrowed alternatives to three Alternatives: F, G, and the No-Build Alternative, which were all included in the Draft EIS published in July 2004. A public hearing on the findings in the Draft EIS was held in September 2004. After taking into consideration

comments made at the public hearing and further regulatory agency input, Alternative F was ultimately selected for advancement in the Final EIS. The Final EIS was completed and published March 2006.

Although this project had a more extensive pre Draft EIS project development process than would be considered typical, the above timeline details the long time frames required for completing the EIS process. The reason for this was the number of complexities involved due to the adverse and sensitive environment as well as the numbers of technical experts and agency representatives required to fully analyze the project scope. The Spencer Creek EIS had a project management team and a steering committee both made up of officials from different regulatory agencies. A third group also made up of members from different regulatory agencies, the Collaborative Environmental and Transportation Agreement for Streamlining (CETAS) Management Team, participated in the development of the EIS. Additionally, the ODOT Technical Design Group reviewed the alternatives and made recommendations. Prior to initiating the Final EIS, the public, the Steering Committee, the Project Management Team, CETAS, and the ODOT Technical Design Group all recommended support for Alternative F.

The Project Management Team and the Steering Committee had a similar goal, which was to move the NEPA EIS project forward. Regulatory agencies with representation on the Project Management Team and the Steering Committee included ODOT, FHWA, COE, Oregon Parks and Recreation, Lincoln County, and the Oregon DLCD and Development. The role of the Project Management Team was to organize and manage the NEPA EIS process and to make recommendations on which alternatives would be advanced into subsequent phases. The Steering Committee was a higher echelon of management making higher-level management decisions regarding the overall goals of the process and reviewed and considered the recommendations of the Project Management Team. If the Steering Committee had questions, concerns, or objections to the recommendations, they were to be addressed by the Project Management Team before proceeding.

The CETAS Management Team is intended to establish a working relationship between ten state and federal transportation, natural resource, cultural resource, and land use planning agencies to implement a streamlined coordinated review process for highway construction projects. The CETAS Management Team is made up of members from ODOT, Oregon DLCD, Environmental Protection Agency (EPA), FHWA, National Marine Fisheries Service (NMFS), Oregon Department of Environmental Quality (ODEQ), Oregon Department of Fish and Wildlife Service (UDFW), Oregon State Historic Preservation Office, Oregon Division of State Lands (ODSL), COE, and US Fish and Wildlife Service (USFWS). The intention is for CETAS to be a clearinghouse for environmental and planning issues where, if an issue clears CETAS, it should clear any other associated agency. ODOT is currently using the CETAS Management Team to review all highway project EAs and EISs.

Of the three alternatives submitted in the Draft EIS, only Alternatives F and G were considered for the Final EIS. The No-Build Alternative was not considered feasible because it assumed the 1999 temporary detour bridge, with a design life expected to expire in 2007, would remain in service for an indeterminate time. Also, without sea cliff or shoreline protection mitigation, the cliffs would continue to erode, swallowing the highway. Alternative G, which would move the alignment east into the State Park and the community of Beverly Beach, was rejected because it would require Statewide goal exceptions, take land away from the State Park and the community of Beverly Beach, add intersections, and result in more natural resource impacts including filling of wetlands. Alternative F requires no Statewide Planning Goal exceptions, causes the least impact to natural resources, requires less land for new roadway and right of way, and would be the least expensive of the two options.

PROPOSED BRIDGE AND RELATED ELEMENTS

HW Lochner was tasked with the design of the arch bridge. The new bridge will be a three-span arch structure 210 feet in length with a 46-foot wide roadway, which is longer and wider than the original bridge. Two arch supporting foundations form the interior bents. Rebuilt embankments, retained by MSE walls provide the bridge approaches. A 432 foot long sound wall will be located north of the proposed north bridge abutment along the east side of the highway. The new bridge and related elements are shown on the Site Plan, Figure 2.

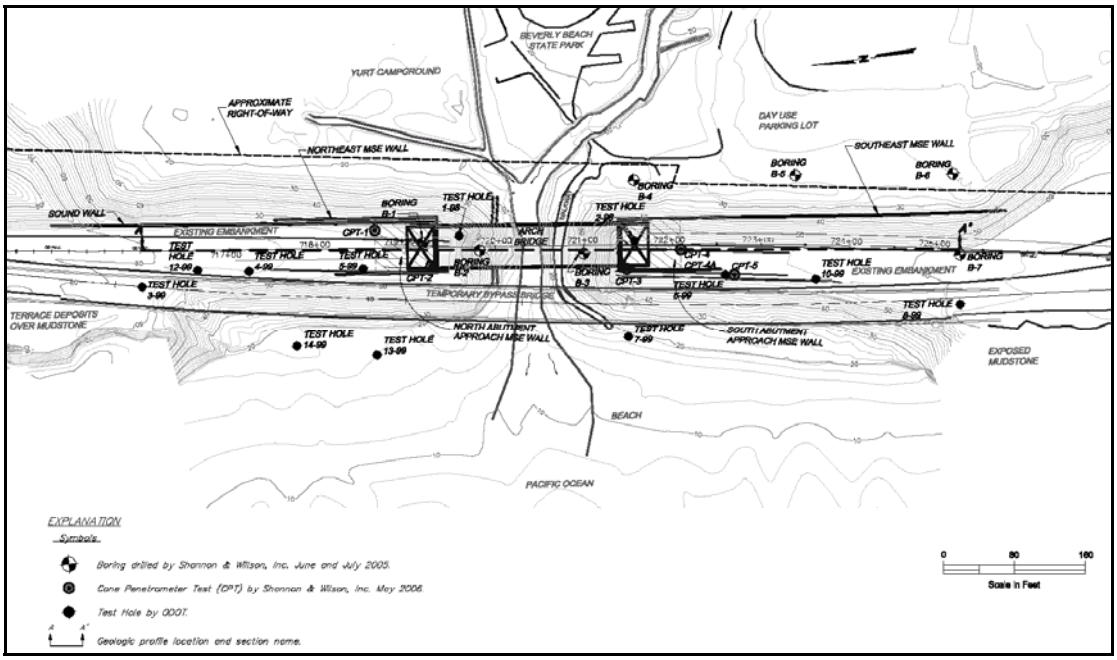

FIGURE 2: From Shannon & Wilson 2006 Geotechnical Investigation

Significant design issues for the bridge include high static lateral loads from the arch configuration, high seismic design load criteria, potential seismic induced liquefaction of soils underlying the bridge and approaches, tall retaining walls at the bridge approaches, stream scour and ocean erosion. These loading conditions would need to be met on a site underlain by relatively thick, soft sediments – not a typical setting for an arch bridge.

The new bridge will be designed for both static and seismic loading conditions as follows. For static conditions, the bridge foundation is designed to resist the 100-year and 500-year flood scour depths. Seismic design criteria adopted by ODOT require that the bridge structure be designed for no collapse during the 1,000-year return event and for serviceability during the 500-year return earthquake event.

MSE retaining walls will be constructed to support the bridge approaches from the north and south. For the north approach, the MSE wall will wrap around the abutment and extend about 357 feet north on the east side and extend about 111 feet north on the west side. For the south approach, the MSE wall will wrap around the abutment and extend about 458 feet south on the east side and extend about 110 feet south on the west side.

Scour depths for Spencer Creek Bridge have been developed by ODOT. The complex site setting provides the potential threat of erosion from stream and ocean flooding, episodic beach erosion, and from direct ocean wave attack. A Hydraulics Report dated October 12, 2005, by ODOT discusses the revetment design criteria in greater detail. Based on the Hydraulics Report, the Ordinary High Water (OHW) elevation is +21.3 feet at the bridge opening, about 6 feet below the surface of the pedestrian pathway. The scour depth criterion is set at elevation +8 feet, considering a sheet pile system as the primary revetment approach. Foundation systems were evaluated based on the ODOT provided scour depth and revetment design.

GEOLOGIC SETTING

The Spencer Creek Bridge site is located along the western margin of the Oregon Coast Range Physiographic province. US Highway 101 generally lies on an uplifted and wave cut terrace that is experiencing rapid ocean erosion. Differential erosion has variably removed the terrace deposits, particularly in the Spencer Creek Drainage.

Geologic mapping by Niem & Niem, (1985), shows that local bedrock consists of Miocene age Astoria formation and is comprised of siltstone, fine sandstone, mudstone and tuffaceous claystone. This extensive geologic formation

is exposed in numerous ocean bluffs from Astoria to south of Newport. The Astoria Formation, estimated at several hundred feet in thickness, was deposited in a shallow sea environment. As exposed in cliff faces near the site, the formation consists of thick to massive beds of variable lithology and color. Generally, the beds can be described as very low strength, fine- to medium-grained micaceous, carbonaceous, fossiliferous marine sandstone and sandy siltstones. Prominent fossil beds are a well recognized feature of Beverly Beach adjacent to the bridge site. The structural dip measurements of the Astoria Formation at the site are 15 to 20 degrees to the west. However, beach front exposures suggest local dips on the order of 5 degrees or less. Strength, weathering and discontinuity spacing varies with the individual beds.

During periods of sea level regression, Spencer Creek had incised a wide canyon into the terrace deposits and that area is now occupied by Beverly Beach State Park. This flat bottomed canyon is likely filled with a complexly layered system comprised of stream alluvium and low energy, estuary deposits. Filling of the estuary occurred as sea level rose over the past 12,000 years, since retreat of the Pleistocene age glaciation.

Seismicity

Spencer Creek Bridge is located adjacent to the active Cascadia Subduction Zone (CSZ), where a magnitude 8.5 to 9.0 earthquake is possible. Structural deformation, local faulting, regional uplift and compelling evidence of very large episodic earthquakes are attributed to the CSZ. Fold axes generally trend toward the northeast and crustal faults typically trend west and northwest. A number of local faults cut Tertiary marine sedimentary rocks near the site, as shown on the US Geological Survey's Fault and Fold Database for the United States (http://gldims.cr.usgs.gov). Off-shore faults identified by geophysical studies (Personius, 2002) often appear to have higher slip rates, with higher associated potential seismicity. Onshore faults, some appearing to be extensions of offshore faults, typically have lower slip rates. In the project area, several faults with apparent activity during the Quaternary period include the Siletz Bay Faults, Cape Foulweather Fault, and Yaquina Faults. These are located within about a 25 km radius of the Spencer Creek Bridge site. It is unknown whether these faults are capable of producing seismic events of their own, or whether displacements on these structures would be related to megathrust earthquakes on the Cascadia Subduction Zone (Personius, 2002).

FIELD EXPLORATIONS

No geotechnical data was available for the original bridge. More detailed explorations, albeit for a close but adjacent alignment, were accomplished to design the emergency detour bridge in June 1999. For this structure, driven pile supports penetrate ocean bluffs, embankments, and beach sand where the alignment crosses the mouth of Spencer Creek. ODOT's 12 exploratory bore holes for the emergency bypass bridge provided limited geotechnical design information for the new structure and were supplemented by 7 borings made to develop geotechnical design recommendations for the permanent replacement. These borings were drilled by Shannon & Wilson, in June and July 2005, to sample and characterize subsurface conditions beneath the bridge site. Mud-rotary drilling was used in combination with carbide tipped coring of mudstone bedrock.

Geophysical Investigations

The field explorations included geophysical explorations performed in July 2005. A seismic shear wave velocity profile was developed in a selected boring to determine the compressional and shear wave velocities for the site soils.

In addition to the downhole survey, three shear wave profiles were developed using refraction micrometer methods (ReMi) deployed from the ground surface. The ReMi profiles were made along the northern and southern approach embankments. Comparative studies of these methods were made to evaluate the relatively new ReMi method in evaluating site response.

Cone Penetrometer Investigation

To supply additional data for contractor bidding, six Cone Penetrometer Tests (CPTs) were made in May 2006. The CPT tests were accomplished to gain additional information within the stone column ground improvement zone (discussed latter in this paper) to provide additional information for contractor bidding, and to reduce the risk of potential construction claims due to variable subsurface conditions.

SOIL and ROCK UNITS

Soil and rock units underlying the bridge site were grouped into three (3) primary soil and rock units as follows:

- Fill – Fill materials form the approach embankments and locally underlie the bridge
- Alluvial / Estuarine Silt and Clay – Soft to medium stiff, clayey silt completely interbedded with loose to medium dense, sandy silt to sand, all with varying amounts of organic material and cobbles and gravel
- Siltstone and Sandstone – Very low to low strength siltstone and sandstone

The interpretive relationships between the units are illustrated on the Geologic Profile, Figure 3. The location and orientation of the interpretive profile is along the proposed centerline of the new bridge.

Fill

Fill materials form both approach embankments and locally underlie the bridge site. In general, fill material consists of loose to medium dense, slightly silty sand, silty sand, and clayey silt. Siltstone fragments are commonly observed in the fill materials that range from gravel to cobble size. Fill thickness ranged from 22 to 45 feet in the north approach embankment, and between about 11.5 to 43 feet in the south approach embankment. The Standard Penetration Test blow count (SPT N-Values) ranged between 3 and 40 blows per foot in the north embankment, and between 2 and 17 blows per foot in the south embankment.

Alluvium & Estuary Deposits

Alluvium and Estuary deposits consist of two phases, a fine grained clay and silt phase and a sandy phase. The soft to medium stiff, clayey silt phase is variably interbedded with the loose to medium dense, sandy silt to sand phase, all with varying amounts of organic material. Organic materials appear to range from disseminated fine organics to large woody debris and potentially logs.

A few late phase explorations (south abutment CPTs) indicate a uniform elevation of cobble and gravel beach deposit with possible woody debris near an abandoned stream / beach interface. The cobble and gravel layer appears to be of limited lateral extent (not found in ODOT borings) beneath the existing south embankment and may form a stringer at a given elevation band.

Fine Grained (Clay & Silt) Phase

Cohesive silt and clay deposits were formed in a low energy estuary environment with sediments supplied by Spencer Creek. These deposits were encountered beneath the fill at the bridge site. Depositional conditions appear to have ranged from silty overbank stream flood deposits to clayey estuary deposits with substantial organics and localized woody debris, including numerous encounters with sticks and wood fragments, and occasional indications of logs. The cohesive, plastic alluvial/estuary deposits primarily consist of soft to medium stiff clayey silt, clayey sandy silt, organic clayey silt, and organic clayey sandy silt.

Based upon the borings done by Shannon & Wilson and ODOT, the clay and silt beneath the existing embankment is stiffer than the organic clay and silt located outside of the embankment footprint. For the clay and silt underneath the existing embankment, the SPT N-values ranged from 3 to 13 blows per foot in the Shannon & Wilson borings

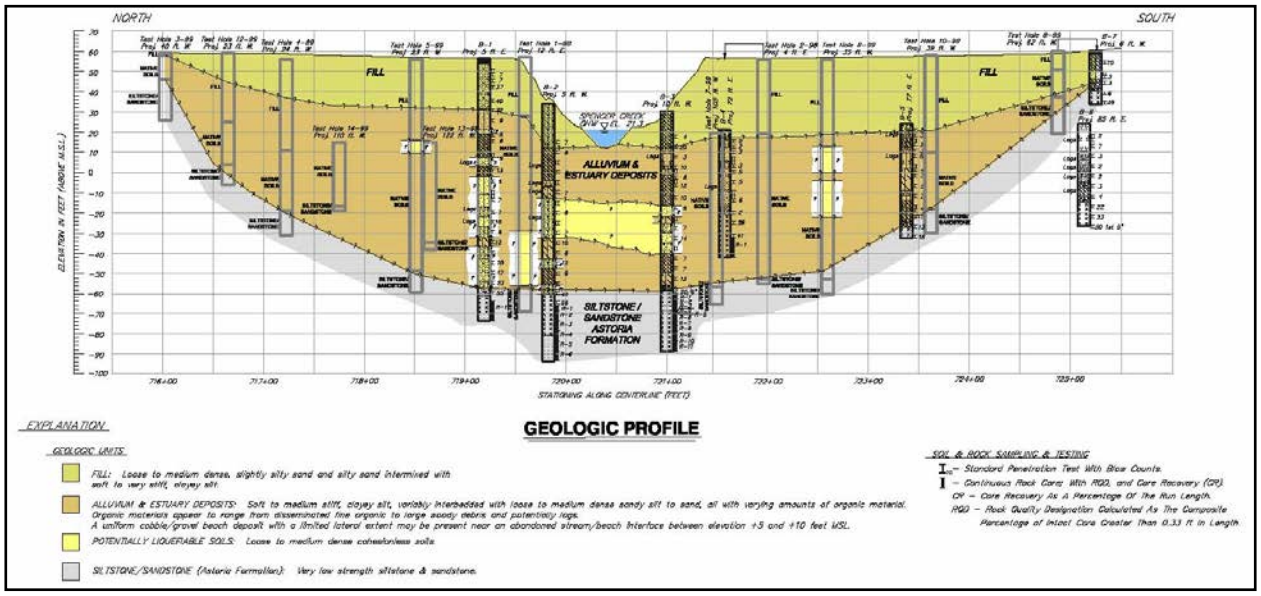

GEOLOGIC PROFILE

FIGURE 3: From Shannon & Wilson 2006 Geotechnical Investigation

and from 3 to 26 blows per foot in the ODOT test holes. Moisture contents ranged approximately from 50 to 256 percent based upon the Shannon & Wilson borings. Atterberg limits tests indicated that the plasticity index varies between 15 and 51. The soils are classified as medium to high plastic clayey silt to silty clay.

The organic silt located outside of the embankment footprint, discovered by Shannon & Wilson borings, is defined as very soft to soft clayey silt. The SPT N-values ranged from 2 to 7 blows per foot in the Shannon & Wilson borings. Moisture contents ranged from approximately 40 to 255 percent. Atterberg limits tests indicated that the plasticity index varies between 32 and 91. The organic content laboratory tests indicated that organic contents range from 25 to 50 percent. The soils are classified as high plastic organic clayey silt.

Alluvium & Estuary Deposits, Sandy Phase

Sand and silty sand layers and lenses were encountered beneath the fill, interlayered with the cohesive, plastic clay and silt phase described above. These sandy phase deposits are likely alluvium, deposited by an active Spencer Creek that maintained a dynamic, meandering stream channel through the estuary environment as sea level rose from an elevation much lower than the present level. Consequently, discontinuous lenses and stringers of alluvial sand may be present erratically within the cohesive estuary deposits. The sandy phase alluvium deposits primarily consist of loose to medium dense, sand, silty sand, and sandy silt. SPT N-values ranged from 2 to 22 blows per foot in the Shannon & Wilson borings and from 1 to 16 in the ODOT test holes. Moisture content ranged approximately from 25 to 50 percent. Local organic materials, including sticks and logs, were noted in the borings.

Siltstone and Sandstone (Astoria Formation)

Along the ocean bluffs and underlying the bridge site and embankments are bedded sedimentary deposits of the Miocene age Astoria Formation. Regionally, this unit contains siltstone, fine sandstone, mudstone and tuffaceous claystone. In the adjacent bluffs, the unit is comprised of relatively thick prominent beds (10 to 30 feet or more thick) each with distinct internal bedding, jointing, weathering, color and fossil content.

Beneath the proposed bridge and embankments, the materials encountered in the borings consist of siltstone and sandstone subunits of the Astoria formation. The top of bedrock elevations ranged from -61.5 feet MSL to +40.5 feet above mean sea level. The siltstone to sandstone sedimentary bedrock is typically of very low strength (R1). Four unconfined compressive strength tests demonstrated that all samples tested ranged from about 120 to 550 psi.

Near the rock surface these soft rock units are variably decomposed and weathered but are typically visually fresh a few feet into the unit. Extensive weathering permeates along joint systems. Bedding within the subunits ranges from thin to thick, being predominately medium bedded, and the joint spacing ranges from very close to wide, being predominately moderately close.

SITE-SPECIFIC SEISMIC EVALUATION

General

The 2004 ODOT Bridge Foundation Design Practice and Procedures (October 2004) manual recommends evaluation of the response and performance of the bridge and foundation materials under both 500 and 1,000 year return seismic events. The performance design criteria for the bridge and the approach fill embankments should meet or exceed the following:

- 500 year event (10% exceedance in 50 years) – The bridge, including its approach embankments, should be serviceable for emergency traffic immediately following this event. ODOT indicates that 12-inches of deformation in the roadway represents a guideline for serviceability.

- 1,000-year event (5% exceedance in 50 years) – The ground motion should not result in total collapse of any part of the bridge. The embankments (approach fills) may experience large amounts of displacement as long as the displacements do not result in the collapse of any part of the structure.

Design Earthquake

The Cascadia Subduction Zone (CSZ) earthquake is the predominant earthquake threat for the bridge site and governed seismic design of the bridge foundations and related structures for both the 500 and 1000 year events. The magnitudes of earthquakes originating on the CSZ for the 500 year and 1000 year return periods were obtained from the USGS web site, Probabilistic Seismic Hazard Deaggregation, based upon the project site location (Longitude = -124.058, and Latitude = 44.730). The magnitude of the model earthquake for both 500-year and 1000-year events is M8.3. The distance (R) of the earthquake source to the project site is 17.3 kilometers.

ODOT recommends that peak ground acceleration (PGA) and other seismic ground motion be obtained from the 2002 U.S. Geological Survey (USGS) Seismic Hazard Maps for the Pacific Northwest Region. The 2002 USGS Seismic Hazard Maps provide probabilistic PGAs on bedrock of 0.30g and 0.45g for the 500-year and 1000-year return events, respectively.

AASHTO Soil Profile

The project site should be classified as an AASHTO TYPE III soil profile type with a Site Coefficient (S) of 1.5. These factors should be used to develop the standard AASHTO site ground response spectra. This conclusion is consistent with the 2004 American Association of State Highway and Transportation Officials (AASHTO) Load Resistance Factor Design (LRFD) Bridge Design Specifications manual (3rd Edition) and is based on the subsurface conditions identified in the borings and the measured shear wave velocity profile obtained in the geophysical investigation.

Site-Specific Response Analysis

Because the proposed bridge is located in a high seismic hazard area, and underlain by a relatively deep, variable soil profile, a site-specific site response analysis was performed. To develop the site response analysis, an equivalent-linear one dimensional method was used with the aid of the computer programs Shake 91 and Shake 2000 (SHAKE). A total of seven input ground motions from a variety of earthquakes were selected to represent the

500-year and 1000-year events. All the ground motion records were then scaled to the design PGA events, 0.30g and 0.45g.

According to the ODOT Seismic Foundation Design Practice Manual (October 2005), the response spectra developed using SHAKE should not be less than 2/3 of the AASHTO spectra. Based on the AASHTO standard spectra and the SHAKE output spectra, the recommended response spectra for the peak ground accelerations are 0.25g and 0.30g for the 500-and 1000-year events, respectively. The reduction in the PGA values at the ground surface from the bedrock values (0.30g and 0.45g) is due to soil damping of the relatively thick, soft soil profile.

Seismic Site Hazards

The seismic hazards were evaluated based on the 2004 ODOT Bridge Foundation Design Practices and Procedures (October 2004), the Liquefaction Mitigation Procedures presented in the ODOT Bridge Design and Drafting Manual (2004 Section 1.1.10.6), and ODOT Seismic Foundation Design Practice (October 2005).

Seismic hazards include strong ground motions, liquefaction of the subsurface beneath the bridge and approaches with associated settlement and potential lateral spreading, post-liquefaction slope instability, seismic deformations that may be either localized or related to regional crustal subsidence, and tsunamis.

Liquefaction Potential Analysis

Soils classified as loose, saturated, cohesionless, sandy, or silty are susceptible to liquefaction. Liquefaction is defined as a decrease in shearing resistance of a cohesionless soil due to the build-up of excess pore pressures that can result from strong ground shaking. During liquefaction, the soils experience a temporary transformation into a viscous fluid. Liquefaction can result in variable ground settlement, foundation bearing capacity failure, lateral spreading, and slope instability.

SPT N-values from borings were used and corrected in accordance with the method described by T. Leslie Youd, 1998 (Technical Report MCEER-98-0005, Screening Guide for Rapid Assessment of Liquefaction Hazard at Highway Bridge Sites, June 1998). The liquefaction potential analysis indicated that all saturated cohesionless soils (sand, silty sand, and non-plastic or low plasticity silt) would likely experience liquefaction for both the 500-year and 1000-year events. The yellow zones on Figure 3 identify the saturated cohesionless soils considered to be liquefiable.

Liquefaction-Induced Settlement

The liquefaction-induced settlement of the northern approach embankment is estimated to be about 6 to 13 inches for the 500-year event, and 8 to 15 inches in a 1,000-year return event. For the southern approach embankment, the estimated settlements are about 7 to 9 inches for both 500-year and 1,000-year return events. Consequently damage to the bridge approach embankments (pavement failures and embankment deformations) may occur as a result of the settlement. Also, the liquefaction-induced settlement may develop negative skin friction along the piles supporting the bridge foundations. Nonetheless, these estimated magnitudes are generally less than to slightly higher than the 500-year serviceability guideline.

Lateral Spreading

Liquefaction induced reduction in shear strength can result in deep seated shear and lateral displacement (lateral spreading). As a result, the embankment and MSE walls may move laterally towards either Spencer Creek or the ocean beach. Shannon & Wilson estimated the magnitude of the potential lateral spreading of the embankment using the simplified approach presented by T. Leslie Youd (1998). The estimated lateral spreading for both the northern and the southern approach embankments is on the order of 15 to 20 feet during both 500 year and 1,000 year return events. This result indicates deficient seismic performance of the site.

Post Liquefaction Slope Stability

Deep seated slope instability was considered as the third mode of seismic impact on the bridge approach embankments. The analysis of risk included a post-liquefaction slope stability analysis focused on the approach embankment slope, utilizing SLOPE/W software.

The slope stability analyses performed for the approach embankment slopes resulted in calculated Factors of Safety (FS) ranging from FS=0.81 to FS=1.03 for both the 500-year and 1000-year events, dependent on slope geometry. Typically, a minimum FS=1.1 is considered acceptable for the design seismic event. The embankment would develop large scale flow failures following the design seismic event. The potential impacts of the embankment slope failures include loss of access to the bridge, and damage to abutment pile foundations. Both impacts indicate deficient seismic performance of the site.

Tsunami Hazards

Spencer Creek is located within a recognized tsunami hazard zone. When an extreme (magnitude 8.0 or greater) earthquake is accompanied by subsidence of a portion of the coast or ocean floor, a tsunami, or seismic sea wave, is generated. Either local or distant earthquakes can generate tsunamis. Tsunami hazard mapping by Priest (1994) indicates that the floodwater resulting from a magnitude 8.8 undersea earthquake could reach an elevation 40 feet above mean sea level. Although not high enough to reach Highway 101, such a wave would pass beneath the Spencer Creek Bridge and run up Spencer Creek nearly one mile above its mouth. Stream channels act as a conduit for the large waves to move a lot of seawater inland, which then rushes back out to sea along the same path caring large amounts of debris. Design criteria for tsunamis hazards have not been developed by ODOT, and this hazard was not considered as part of the design criteria.

DESIGN RECOMMENDATIONS

Arch Bridge

Localized zones within the soil underlying the site are anticipated to liquefy with resulting settlement, potential lateral spreading, and slope instability.

Based upon the FHWA Geotechnical Earthquake Engineering Reference Manual (FHWA HI-99-012, 1998), estimated seismic vertical and/or lateral deformations on the order of 6 to 12 inches are generally deemed to be acceptable in current practice for embankments. The seismic induced deformation of the new bridge approach embankments will exceed the tolerable deformations, primarily due to slope instability. Based on the 2004 ODOT Bridge Foundation Design Practice and Procedures (October 2004) manual, the bridge approach embankment will need to be mitigated seismically.

The primary geotechnical engineering considerations for the Spencer Creek Bridge project were to select appropriate foundations to support the high lateral loads from the arch bridge under static and seismic conditions, develop ground improvement solutions for the MSE wall bridge approaches, and reduce settlement of new embankments and MSE walls. A profile of the arch bridge and preferred foundation elements selected for the design are shown below on the Arch Bridge Elevation, Figure 4.

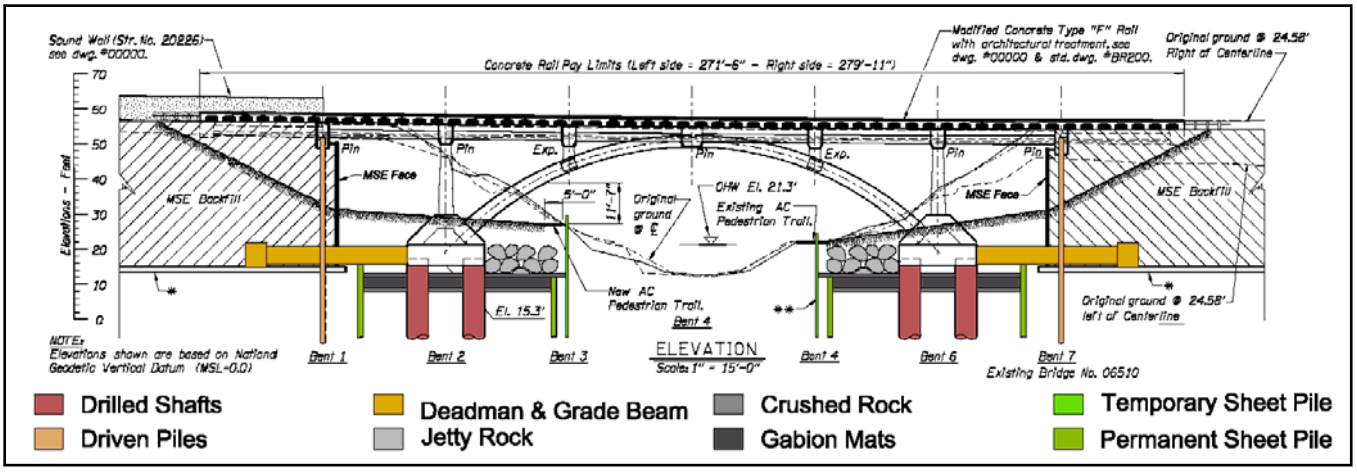

Engineering Challenges

After girders, arch bridges are the second oldest type of bridge. Traditionally, arch bridges were constructed at locations where the arch could be founded on solid ground. These early arches where supported by footings founded on bedrock or dense gravels. This was required due to the high lateral forces that are transferred to the arch from dead and live loads. Early arch bridges were generally built of stone, often without the use of mortar, using keystones. Typically, arch bridges were utilized to span canyons, valleys, or coastal headlands.

Due to planning and right-of-way limitations, it is not always possible to choose the optimum location for a bridge. Also, with the growing understanding of seismicity and unprecedented live loads imposed on bridges, demands on foundation systems have grown.

At the Spencer Creek Bridge site, the subsurface soils are not favorable for an arch bridge. There are about 70 or more feet of soft soils that overlay the bedrock at the Spencer Creek bridge site. Thus a deep foundation system is required to support the bridge. The flat arch that was chosen for this site results in high vertical, lateral, and bending forces on the bridge bents that support the arch. These forces increase with live loads such as traffic and seismic events. The soft soils provide minimal lateral support. The lateral support is further decreased during deep scour events. The limited lateral deflections that the bridge can tolerate coupled with the minimal lateral support that the subgrade soils provide require that the foundation system be stiff. Thus, a more robust deep foundation system is required compared to what would be required for a conventional girder bridge structure at this site. This results in a vast increase in costs for both the design and the construction of the bridge. Generally for structure costs alone, not including foundations, an arch bridge is three times the cost of a traditional girder bridge.

Bridge Foundation Alternatives

The selection of an appropriate foundation system for the proposed arch bridge structure is dependent upon several factors, including foundation capacities, tolerance to total and differential settlement resulting from static loads (including flooding and scour), the risk of structural damage during a design earthquake, and construction considerations.

Shannon & Wilson evaluated several foundation alternatives for the bridge foundations including conventional vertical pipe piles, drilled shafts, and battered piles. The following discussions provide Shannon & Wilson's rational and approach to selecting a preferred foundation alternative that will support the above described design loads, and provide the desired level of performance under the anticipated conditions as well as reasonable construction costs.

Bridge Abutment Foundation Alternatives

Steel pipe piles and drilled shaft foundations were considered to support the northern abutment and the southern abutment.

Due to the relatively high cost of drilled shaft foundations, Shannon & Wilson recommend that steel pipe piles be used to support the proposed bridge abutments. However, due to the presence of ocean salt water and corrosive site soils, the piles need to be sized to compensate for high corrosion rates.

Bridge Interior Bent Foundation Alternative

Selection of an appropriate foundation alternative to support the high lateral loads imposed on the interior bents by the arch bridge structure under static and seismic conditions was a primary consideration. In addition, the relationship of the foundation and revetment design was considered. For interior arch bents, where the arches are founded, Shannon & Wilson evaluated a group of conventional vertical piles, a group of drilled shafts, and a group of battered piles.

The conventional vertical pile groupings were evaluated. To develop sufficient lateral loads to meet the design criteria, the number of the piles required for the traditional vertical pile group was large, and considered unacceptable for the project.

A group of large-diameter drilled shafts (six shafts of 5 to 6 ft diameter) was also evaluated. The initial evaluations disclosed that the large diameter drilled shaft alternative provided sufficient vertical compressive capacity. However, analyses of deflections anticipated for the static lateral loads indicated deficient lateral load capacity. The predicted lateral deflection slightly exceeded stated deflection criteria (1/2-inch). Also, construction of the group of drilled shafts was considered more expensive than other foundation alternatives. However, according to HW Lochner, use of the drilled shaft group would reduce the cost of revetment construction, designed by ODOT.

A third alternative, a group of battered piles was considered. Due to reports of poor performance of batter pile foundations in past earthquakes, the use of batter piles to resist lateral loads under bridge piers is on the decline. In addition, it was determined that revetment construction cost for a battered pile group would be higher than that of the drilled shaft group.

Considering the above alternatives, and based on the specific issues for this project site, ODOT selected the drilled shaft group to support the proposed arch bents, although the lateral load resistance of the drilled shaft group alone was deficient.

Drilled Shaft Foundations

The maximum allowable lateral movement of the drilled shaft group governs the diameter and number of drilled shafts. Based upon Shannon & Wilson's three dimensional lateral load analysis completed using "GROUP" (Version 6.0), the drilled shaft group solution consisted of six, 6-foot diameter shafts. The drilled shafts were evaluated following the FHWA drilled shaft design requirements and the 2004 ODOT Bridge Foundation Design Practice and Procedures to support the interior bents under both static and seismic loading conditions.

Deadman Block Additional Lateral Resistance

Due to the weak soils and high static lateral loads, the drilled shaft group does not provide sufficient lateral resistance to maintain the tight deflection tolerance required by the arch bridge system. Consequently, additional lateral support for static load is being provided by a deadman block designed within the abutment MSE wall. The deadman block is connected with the drilled shaft group cap by three large grade beams.

Static settlement of the MSE wall will cause the deadman block to settle 3 to 4 inches. Shannon & Wilson determined that in order to reduce the impact of static settlement on the connection between the grade beams and the drilled shaft cap, the grade beam connection to the drilled shaft cap should be postponed for at least 30 days after completion of the MSE wall construction.

Embankment Foundations

The existing bridge approach embankment will be mitigated against seismic induced failure. The minimum mitigation limit zone is about 70 feet behind the proposed bridge abutment MSE wall facing.

Seismic Mitigation Ground Improvement Alternatives

Based upon the site subsurface conditions, six different seismic mitigation ground improvement alternatives were identified. These alternatives include:

- Soil mixing column cells;
- Stone columns with wick drains;
- Soil mixing columns with earthquake drains;
- Soil mixing columns with wick drains;
- Earthquake drains with sheet piles;
- Soil mixing columns secant wall along the MSE wall perimeter.

ODOT and Shannon & Wilson agreed that the stone column ground improvement is preferred as a reliable and cost effective alternative for the proposed approach MSE wall foundation ground improvement.

Stone Column Ground Improvement Conceptual Design

The Stone Column treatment area is approximately 80 feet by 80 feet at each abutment (the edges of the stone column treatment area are located approximately 8 to 10 feet outside the MSEW footprint). The stone column treatment depth will extend to a depth of 50 feet below the construction grade elevation. Wick drains will be installed equidistant between the stone columns. A 3-foot thick layer of geogrid-reinforced, compacted crushed drain rock will be placed between the MSE wall and the top of stone columns. The stone columns located outside the MSE wall footprint should be constructed as cemented stone columns or concrete columns to prevent potential local instability of the stone columns during the design seismic event. Alternatively, a double row of stone columns could replace cemented stone columns or concrete columns.

For post improvement static settlement the above conceptual design should reduce the estimated unimproved ground settlement by approximately 50 percent; from about 6 to 8-inches unimproved to 3 or 4-inches improved. Differential settlement beneath the MSE wall should then be less than one percent over most practical distances. For post improvement seismic settlement the current conceptual design may result in seismic settlement of 4 inches within the 50-foot deep treatment zone. This estimated settlement could manifest itself as differential settlement localized between adjacent stone columns or might occur over large areas within the improvement zone. This magnitude of differential settlement in close proximity might violate the current FHWA design guidance for no damage to the MSE wall. However, ODOT seismic criteria and current opinion allows MSE wall damage during the 500-year design seismic event, so long as the serviceability criterion is met.

Mechanically Stabilized Walls

Geotechnical Recommendations for North MSE Wall

The north MSE wall wraps around the north abutment and will be located along the east and west side of US Hwy 101. The proposed MSE wall is to be constructed on and along the edge of the top of the existing embankment slope. Based upon the proposed MSE wall design Shannon & Wilson performed static slope stability analyses to evaluate global stability of the proposed MSE wall and to determine minimum required reinforcement lengths.

The analyses indicated that the factor of safety for the static global stability is greater than the FHWA recommended minimum factor of safety of 1.5.

Geotechnical Recommendations for South MSE Wall

The south MSE wall wraps around the south abutment and will be located along the east and west side of US Hwy 101. Based on observations in borings, very soft organic silt underlies the MSE wall site. Principal engineering concerns for constructing the MSE wall on this soil include static global stability, total and differential consolidation settlement, and the time required for consolidation settlement to occur. To address these concerns, Shannon & Wilson recommend preloading the proposed MSE wall footprint.

Sound Walls

The sound wall will be located north of the proposed north bridge abutment along the east side of US Hwy 101. The sound wall is about 432 feet long. H.W. Lochner will design the sound wall using the ODOT standard design approach.

Revetment Design

The revetment design was provided by ODOT to prevent scour from adversely impacting the bridge foundation elements. This design required the use of an extensive permanent sheet pile enclosures, capped by gabion mats, and jetty rock, as shown in Figure 4. The sheet pile walls will protect the flanks of soil surrounding the pile and drilled shaft foundations and gabion mats and jetty rock will protect the surface. If the soils surrounding the foundations systems are scoured out, the foundation system alone will not be able to restrain the lateral loads of the arch structure. Shannon & Wilson evaluated the geotechnical aspects of the sheet pile walls. The purpose of the evaluation was to provide geotechnical design parameters, including soil properties and estimated sheet pile embedment depths.

Three types of sheet pile walls were included in the ODOT revetment design: Work Containment Sheet Pile walls around the perimeter of the work area, Toe Protection Sheet Pile walls around the bridge foundation perimeter, and Secondary Sheet Pile Wall in front of the MSE wall. The Toe Protection Sheet Pile wall and Secondary Sheet Pile wall are permanent sheet pile walls designed by the design team, and the Work Containment Sheet pile wall is a temporary sheet pile wall that will be designed and constructed by the contractor.

Based upon the ODOT defined scour elevations and the ODOT revetment design, Shannon & Wilson developed geotechnical analytical models for the Toe Protection Sheet Pile Wall and the Secondary Sheet Pile Wall. In the analytical models, the following assumptions were made for the Toe Protection Sheet Pile Wall:

- Jetty rock will remain behind the sheet pile, and will apply 1000 psf surcharge to the sheet piles.
- The water level behind the sheet pile is at elevation +12 feet MSL, assuming that water is trapped behind wall.

- The water level in front of the wall is at the elevation +8 feet MSL assuming that water level is the same as the scour elevation.

For the Secondary Sheet Pile the following assumptions were made:

- The water level behind the sheet pile is at the elevation +21.3 feet MSL, assuming that water is trapped behind wall.

- The water level in front of the wall is at the elevation +12 feet MSL, assuming that water level is the same as the scour elevation.

The sheet pile design analysis indicated that for the Toe Protection Sheet Pile Wall, the minimum embedment (below ODOT scour elevation) with a factor of factor of safety equal to 1.3 is about 32.5 feet. This results in a total estimated finished sheet pile length of about 36.5 feet. For the Secondary Sheet Pile, the minimum embedment (below ODOT scour elevation) with a factor of safety equal to 1.3 is about 28.6 feet. This resulted in a total estimated finished sheet pile length of about 38 feet.

CONCLUSION

The design of the new Spencer Creek Bridge was entirely driven by the NEPA process and was in response to the opinions of multiple stakeholders and compliance with statewide planning goals. The NEPA driven design took nearly 8 years to complete and the resulting arch bridge will likely cost three times as much to build as a comparable girder bridge, which would be more favorable for site conditions on the chosen alignment. The arch bridge structure alone will cost $350 per square foot compared to approximately $150 per square foot for a conventional girder bridge structure. Additionally, the foundation system of a girder bridge is generally about 20 to 30 percent of the total bridge cost, where the foundation system of the new Spencer Creek Arch Bridge will cost more than the entire arch structure. Because the arch bridge was not the preferable engineering solution for the site, the resulting engineering was both expensive and challenging. With so much time invested into the NEPA EIS process, it would not have been practical to change elements of the NEPA design, which would have surely resulted in additional project delays.

From a non-engineering viewpoint, the NEPA driven design is the perfect bridge for the site. The arch bridge will be aesthetically complimenting to the scenic, highly visible site and was chosen by the public for the public. It will be a proud new addition to a number of prestigious Oregon coastal bridges. The public involvement process also decreases the possibility for public objections and limits the potential for legal battles.

Politically and publicly driven designs are becoming more common. It is not for the engineering community to decide if this is the appropriate design approach. The engineering community needs to embrace this trend and understand the demands, limitations, and complications before entering into the design process. This makes it even more important to know your client's needs and expectations because they may not be met by simply the best engineering solution.

REFERENCES

AASHTO, 2004. LRFD Standard Specifications for Highway Bridges, 3rd Edition.

FHWA, December 1998, Geotechnical Earthquake Engineering Reference Manual, Publication No. FHWA HI-99-012.

FHWA and ODOT, – Spencer Creek Bridge US Highway 101 Draft Environmental Impact Statement and Draft Section 4(f) Evaluation, July 2004.

FHWA and ODOT, – Spencer Creek Bridge US Highway 101 Final Environmental Impact Statement and Final Section 4(f)/6(f) Evaluation, March 2006.

HW Lochner, – US 101: Spencer Creek Bridge, Work Plan, Contract ATA 22548, Work Order #8, Key #10058, Lochner No 1980, undated.

Niem, A.R. and Niem, W.A., 1985, Geologic map of the Astoria basin, Clatsop and northernmost Tillamook counties, northwest Oregon: Oregon Department of Geology and Mineral Industries Oil and Gas Investigation 14, scale 1:100,000.

ODOT, – Bridge Design and Drafting Manual 2004.

ODOT, – Bridge Foundation Design Practices and Procedures 2005.

ODOT, – Hydraulics Report for Spencer Creek Bridge #20198, October 12, 2005.

ODOT, – Spencer Creek Bridge Project, Build Alternative F selection, 2004.

ODOT, – Spencer Creek Bridge Project, Conceptual Alternatives Report, July 2002.

ODOT, – Spencer Creek Bridge Project, Reconnaissance Study Report, June 2003.

Personius, S.F., compiler, 2003, Quaternary fault and fold database of the United States, ver 1.0: U.S. Geological Survey Open-File Report 03-417, http://qfaults.cr.usgs.gov.

Priest, G.R., 1994, Chronic Geologic Hazard Maps of Coastal Lincoln County, Oregon: Oregon Department of Geology and Mineral Industries Open-file Report O-94-12.

Shannon & Wilson, – Geotechnical Investigation US 101: Spencer Creek Bridge, Lincoln County, Oregon, May 12, 2006.

US Congress, – The National Environmental Policy Act 1969, (Pub. L. 91-190, 42 U.S.C. 4321-4347, January 1, 1970, as amended by Pub. L. 94-52, July 3, 1975, Pub. L. 94-83, August 9, 1975, and Pub. L. 97-258, § 4(b), Sept. 13, 1982).

USGS, – Interpolated Probabilistic Ground Motion, by Latitude Longitude, 2002. earthquake.usgs.gov/research/hazmaps/products_data/2002/wus2002.php

USGS, – National Seismic Hazard Maps, Pacific Northwest Maps, 2002. earthquake.usgs.gov/research/hazmaps/products_data/2002/wus2002.php

Youd, T.L., 1998, (Technical Report MCEER-98-0005, Screening Guide for Rapid Assessment of Liquefaction Hazard at Highway Bridge Sites, June 1998).

Design of Rockery Walls on Marginally Stable Talus Slopes Taylor River Road, Gunnison County, Colorado

William C.B. Gates
Kleinfelder, 2405 140th Ave NE, Suite A101, Bellevue, WA 98005, 425-562-4200 bgates@kleinfelder.com

Brendan Fisher
Kleinfelder, 2405 140th Ave NE, Suite A101, Bellevue, WA 98005, 425-562-4200 bfisher@kleinfelder.com

Chad Lukkarila
Kleinfelder, 2405 140th Ave NE, Suite A101, Bellevue, WA 98005, 425-562-4200 clukkarila@kleinfelder.com

Kami Deputy,
Kleinfelder, 2405 140th Ave NE, Suite A101, Bellevue, WA 98005, 425-562-4200 kdeputy@kleinfelder.com

Samantha Sherwood
Kleinfelder, 611 Corporate Circle, Suite C, Golden, CO, 80401, 303-237-6601
ssherwood@kleinfelder.com

Daniel E. Alzamora
FHWA, CFLD, 12300 West Dakota Ave., Suite 210, Lakewood, CO 80228, 720-963-3518
daniel.alzamora@fhwa.dot.gov

ABSTRACT

Rockery walls are gravity walls that consist of uncemented, interlocking rows of large rocks that are not tied together and have a low tolerance for movement. The rocks are naturally shaped quarry stone or boulders. Typically, they are only constructed on slopes that are relatively stable. They are not structural walls and are usually employed for erosion control.

The Federal Highway Administration Central Federal Lands is currently considering realigning 22km (14 miles) of road along the Taylor River in the Gunnison National Forrest in Colorado. Major proposed improvements include straightening and realigning curves, design of 35 substantial rock and soil cuts and 23 rockery walls to stabilize the toe of talus slopes.

Talus aprons paralleling the proposed alignment are composed of both granitic and metamorphic rock colluvium ranging from small cobbles to very large boulders 5m (16 feet) in diameter. Existing talus slopes are inclined at the angle of repose. Therefore these deposits are at equilibrium, exhibit a factor of safety of unity and are marginally stable. Excavation of the toe may cause the deposits to slough off towards the roadway.

During the project, the authors were faced with the following design challenges:

- Designing rockery walls as structural walls composed of talus rock with the dual purpose of providing erosion control and to retain marginally stable slopes.

- Estimating critical stable height/base ratios for the rockery walls considering overturning, sliding, and bearing capacity of the walls.

INTRODUCTION

Rockery walls are gravity walls that consist of uncemented, interlocking rows of large rocks that are not tied together and have a low tolerance for movement. The rocks are natural shaped quarry stone or boulders. Typically, they are only constructed on slopes that are relatively stable. They are not structural walls but can be employed for erosion control. Many rockery walls are only single tier, however, if designed properly they may be multitiered as displayed on Figure 1.

Figure 1: Multitiered rockery wall near Reno, Nevada.

Talus slopes are colluvial deposits that have been deposited by some means of mass wasting. The face of the talus deposits rest at the angle of repose, which by definition is at a factor of safety of unity (1) or just at equilibrium. Typically, the angle of repose for talus is in the range of 37 to about 42 degrees depending on the textural gradation of the deposits (Figure 2). Coarse deposits with large blocks may stand steeper. Oversteepening the toe of the talus deposit may affect the marginal stability and cause the deposit to reestablish equilibrium by sliding. In the past, rockery walls have been employed by the Federal Highway Administration (FHWA) to stabilize the toes of talus slopes along the road in the Taylor River Canyon (Figure 3).

Figure 2: Talus slope with a 38° angle of repose, Taylor River Road, Colorado.

This paper presents the results of our geotechnical investigation for the proposed rockery walls that will be required as part of the rehabilitation and realigning of 22 kilometers (14 miles) of road along the Taylor River in the Gunnison National Forest in Central Colorado (Kleinfelder, 2006). Proposed improvements include straightening and realigning curves, construction of substantial cuts and fills, stabilization of talus slope toes, excavation of at least 35 new rock cuts and soil cuts, and construction of at least 23 rockery walls. The proposed rockery walls will average about 3.5 meters high and about 55m long, for a total length approaching 1.3km. Ten rockery walls have been designed for two tiers because the height of a single wall would exceed 3.5m (11.5 feet).

Figure 3: Rockery wall constructed at the toe of a talus slope along Taylor River Road, Colorado.

LOCATION AND ALIGNMENT DESCRIPTION

Taylor River Road starts at Almont, Colorado and follows the river through Taylor River Canyon to the Taylor River Dam and Reservoir (Figure 4). The 22 kilometers (14 miles) of roadway being investigated consists of a two-lane roadway with narrow shoulders. Rehabilitation plans include straightening the road that will require significant cut and fill sections. Cuts will traverse the toe of marginally stable talus slopes, glacial and terrace deposits. Two 3.3m (11 foot) lanes are planned with shoulders that will vary from about 0.3m to 1.5m (1 to 5 foot) in width.

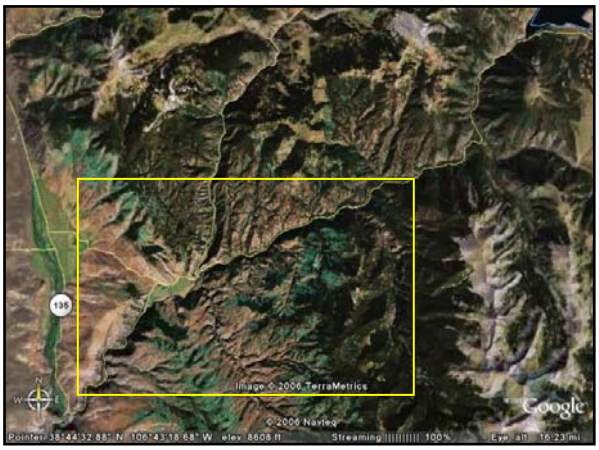

Figure 4: Project Area, Taylor River Road, Colorado (Google Earth, 2006)

The roadway is lined in various locations with existing soils in talus, glacial and terrace deposits and rock cut slopes. The soil slopes consist primarily of rock talus, sandy gravel (GP), clayey gravel and sand (GC/SC), poorly graded sand, (SP) silty sand (SM), and sandy clay with clayey sand (SC/CL). The existing soil slopes range in height from less than one meter to approximately six meters (3 to 20 feet) and have slope inclinations ranging from 25- to 50-degrees. The rock slopes vary from fresh and very strong granites, gneisses, and quartzites to highly weathered and very weak metamorphic rock including schist. The existing rock slopes range in height from approximately 2 to 20 meters (6 to 65 feet) and have slope inclinations ranging from 45- to 90-degrees.

Regional Geology and Seismic Conditions

Taylor River is located on the western flank of the Sawatch Mountains in the Rocky Mountains of Colorado. The river has cut a deep gorge through Precambrian metamorphic rock on the northeast and southwest end of the alignment and granitic rock near the middle of the alignment. During the Laramide Orogeny, the area was subjected to uplift, folding, and thrust faulting. Renewed movement, probably during the Miocene period, dissected the area with a series of high angle normal faults. The last major process to affect the area was glaciation, which modified the preexisting erosional valleys by additionally carving or infilling with debris. The majority of surface exposures in which cuts will be involved along the alignment consist of igneous granitic and metamorphic rocks (consisting of quartzite, gneiss and schist) or talus and soil cover with frequent granitic boulders up to several meters in diameter. According to the United States Geological Survey website http://eqint.cr.usgs.gov/eq-men/cgi-bin/zipcode-06.cgi the estimated probabilistic peak ground acceleration (PGA) with 10% probability of exceedance in 50 years is equal to 0.077g.

Field and Subsurface Investigation

During the summer and fall of October 2005, the authors visited Taylor River Road to observe the geology and geometrics of the road, conduct field mapping at rock outcrops and investigate the talus and soil slopes. We completed thirty (30) test pits at the locations where FHWA had proposed either soil excavations or rockery walls. The test pits were logged in the field and the relative density or consistency of the soil was recorded. Soil samples from the talus matrix were collected from each test pit for index and direct shear testing.

ROCKERY WALL DESIGN METHODOLOGY

It is important to note that similar walls were constructed north of the project area by FHWA. The geometry of the constructed walls was considered during design of the walls described herein.

The chart on Figure 5 was used to facilitate design of the rockery walls along Taylor River Road. The rockery walls planned along Taylor River were designed according to methods developed by Hendron (1960), Gifford and Kirkland (1978), Associated Rockery Contractors (1991), Gray and Sotir (1996), and FHWA (2005). The results of each methodology were considered while estimating the width of the base of the rockery walls planned for the Taylor River Road. The authors established the minimum width of the walls to be equal to one half of the wall height and used the design calculations by Gray and Sotir (1996) to check this assumption. The maximum wall height was checked against the chart developed by Hendron (1960), which considers moment equilibrium only. Figure 5 is a similar chart developed for the rockery walls on Taylor River road with modifications for the site-specific soil and rock engineering properties.

The active earth pressure coefficient is not factored in this chart (Figure 5), which means that there is no safety factor on the wall design. The chart shows the critical H/B ratio given a horizontal backfill with soil that has a friction angle of 35 or 40 degrees. The backfill has a unit weight of about 2,080 kg/m^3 (130 pcf) and the wall has a unit weight of about 2,400 kg/m^3 (150 pcf). To read the chart, first estimate the required height of the wall. Then, given a specific wall angle, the engineer can back out the width at the base of the wall. Because the chart is based solely on moment equilibrium, sliding, and bearing capacity is not considered and should be evaluated separately.

For each of the rockery wall geometries considered for the Taylor River Road project, the back slope behind the wall was assumed to slightly less than angle of repose of talus slopes observed along the Taylor River Roadway. Although the back slopes will be at the angle of repose, the Rankine and Coulomb equations for active earth pressures become meaningless when the friction angle of the soil is equal to the back slope inclination. The angle of repose of the talus was conservatively chosen as the backfill friction angle because the backfill will consist of compacted and crushed talus. In addition, during our calculations and assessment, we assumed that the walls would be constructed vertically, which is a conservative assumption.

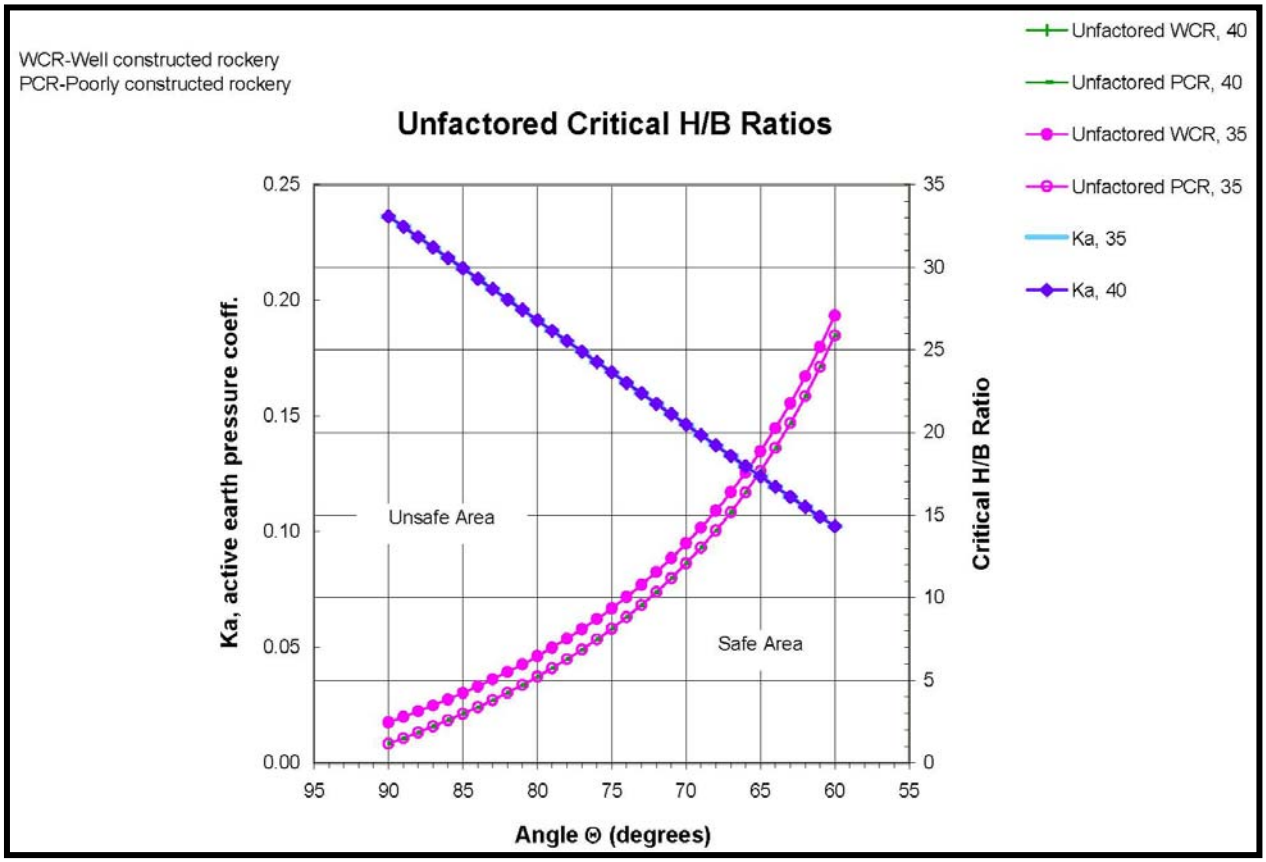

Read the chart as follows:
1. PCW is a Poorly-constructed wall
2. WCW is a Well-constructed wall
3. θ is the inclination of the wall face measured from the horizontal.
4. Ka is active earth pressure coefficient. The drained friction angle of the backfill is assumed to be 35 or 40 degrees.
5. H/B is the height to base width ratio
6. Wall unit weight is 150 pcf
7. Backfill is 130 pcf
8. Backfill is horizontal

Figure 5: Unfactored critical H/B ratios used for rockery wall designs on Taylor River Road (Modified from Hendron, 1960).

The friction factor for sliding between the rock of the wall and the foundation soil (μ) was found by taking the tangent of the friction angle, multiplying by 0.75 and dividing by the desired factor of safety (FS) as suggested by FHWA (2005). This relationship is outlined in the equation below.

$$\mu = \frac{\tan\phi * 0.75}{FS}$$

Passive resistance in front of the walls was neglected, because it is hard to verify uniform compaction at the toe of a rockery wall without full-time construction observation and testing. Further, it is anticipated that the base of the walls will be constructed above the frost line and therefore, soil in front of the wall will deteriorate over time.

The overturning and sliding stability of the rockeries was estimated under seismic loading. As discussed above, the peak ground acceleration (PGA) at Gunnison, CO was found to be 0.077g for a 10% probability of exceedance in 50 years. K_h (horizontal component of acceleration) was assumed equal to one half the peak ground acceleration and K_v (vertical component of acceleration) was assumed to be zero for the seismic case. Since K_h was calculated from the PGA, a tolerable displacement was not estimated or used in the calculations. The factor of safety against seismic failure was calculated using a modified procedure from Pile Buck, Inc (1992). Pseudo-static stability did not govern the design of the rockery walls.

Global slope stability analyses were performed for both the single tier and multitiered rockery walls. Studies showed that the global minimum factors of safety were satisfied for both the static and psuedo-static cases when sliding is assumed to occur beneath the walls. The walls could not be designed to mitigate shallow sloughing behind the walls because the talus will remain at the angle of repose. Re-grading the talus backslopes to remove loose material can reduce the potential for shallow sloughing.

General Rockery Wall Design Guidlines

Over the past years there has been a variety of design guideline suggestions on rockery walls provided by organizations and agencies. For instance, the Associated Rockery Contractors (ARC) published Rock Wall Construction Guidelines circa 1992 attendant to construction of rock walls. In addition, FHWA Central Federal Lands (CFL) has been working on a draft document for Rockery Design and Construction Guidelines (FHWA-CFL, 2005). The following is a summary of the guidelines as they relate to the Taylor River Road project, however, they are also appropriate for other similar construction projects.

The rockery wall will act as a protective system, which retards the weathering and erosion process acting on the cuts in the talus and soils. The degree of retention achieved is a function of the mass of the rock selected for the rockery wall and the height of the rockery wall. Based on our research, the maximum height of a given rockery wall should be limited to 3.5m (11.5 feet) unless the retained soil behind the wall is reinforced as a Mechanically Stabilized Earth wall reinforced with geogrids or geotextiles. (Note: Some local jurisdictions have proposed 2.5m (8 feet) as the limit for an unreinforced rockery wall (Draft Southern Nevada Local Standard, 2005)). With our research in mind, we established that the minimum base width of the walls should be equal to one half the wall height. Where higher walls are required, we recommended FHWA consider using a tiered wall system. The lower wall would be constructed at the roadway grade with subsequent walls placed a distance equal to height of the lower wall behind and above the lower wall to decrease the likelihood of applying additional surcharge on the lower wall. All walls must be keyed into a basal keyway trench. Figure 6 displays typical design and specification requirements for the rockery walls designed for Taylor River Road. The following are guidelines for rockery wall design and construction with narrative comment and examples.

Geotechnical Engineer

Typically, rockery walls that equal or exceed a height of 1.2m (4 feet) should require engineering analysis and a geotechnical report. In these cases the project owner should retain a qualified geotechnical engineer to provide the engineering analysis and provide necessary supplemental rockery wall guidelines during construction. The engineer selected should demonstrate experience in being in responsible charge of a project, including experience with fill construction and stability and rockery wall construction.

Temporary slopes behind the walls that would be excavated by the contractor should always be the responsibility of the contractor. Moreover, the temporary slopes need also to be constructible. During the geotechnical investigation for Taylor River Road, temporary cuts within the talus were observed to stand for a short period. This was attributed to 3-D effects and arching behind the temporary cuts. Therefore, the back walls are constructible, but will require careful construction procedures.

Monitoring

Throughout the project, it is paramount that the geotechnical engineer periodically monitor all rockery walls constructed against cuts or fills exceeding 1.2m (4 feet) in height. It is important for the engineer to verify that the construction and materials meet the original geotechnical recommendations and specifications. The geotechnical engineer should also develop a monitoring plan for visiting the site. For instance, ARC (1991) recommends for a single tiered rockery wall that is less than 15m (50 feet) in length should require a minimum of at least one visit along with daily inspections by a project engineer. For multitiered rockery walls, the geotechnical engineer should visit the site at least once for each stage of the wall. The geotechnical engineer must maintain records of the nature and condition of the wall under observation.

In addition, the engineer should verify the soundness of the rocks selected for the rockery wall by striking the selected rocks with a geology hammer. A loud ring suggests strong competent rock. Conversely, a dull thud will suggest poor rock not fit for a rockery wall.

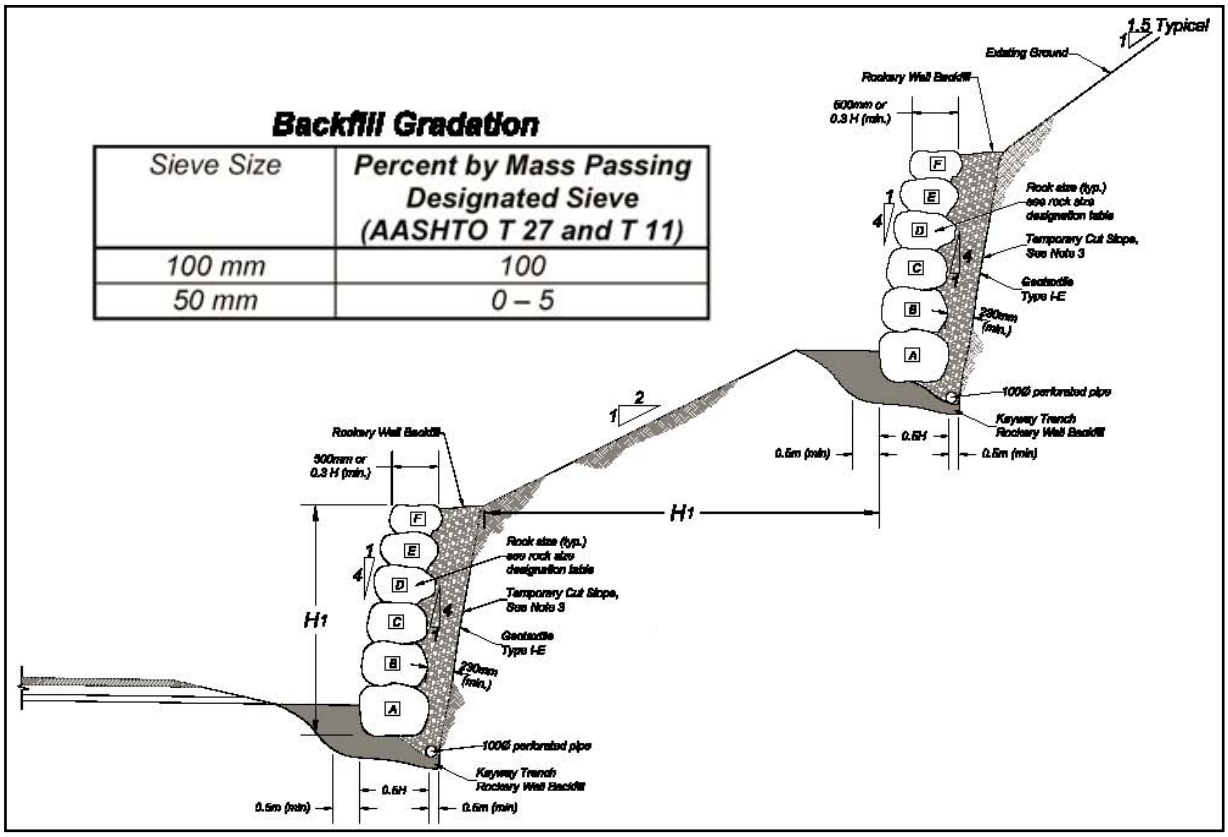

Backfill Gradation

Sieve Size	Percent by Mass Passing Designated Sieve (AASHTO T 27 and T 11)
100 mm	100
50 mm	0 – 5

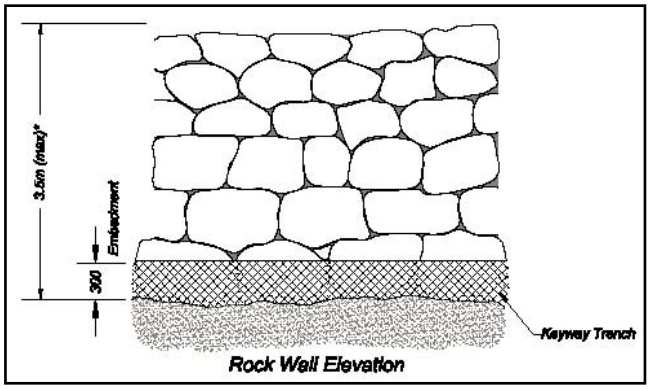

Rock Size

Rock Size (person)	Rock Weight (kilogram)	Average Dimension (meter)
1	20 to 90	0.300 to 0.450
2	90 to 300	0.450 to 0.710
3	300 to 900	0.710 to 0.900
4	900 to 1,800	0.900 to 1.200
5	1,800 to 2,700	1.200 to 1.350
6	2,700 to 3,600	1.350 to 1.500

Rock Size Designation

Wall Height (H)	A	B	C	D	E	F
1	3	2	-	-	-	-
2	4	3	2	-	-	-
3	6	5	4	3	-	-
3.5	6+	6	5	4	3	2

Figure 6: Rockery wall design schematic used for Taylor River Road.

Figure 7 displays an example of a rockery wall failing because weak unsound rock was selected for the wall rock.

Figure 7: Example of rockery wall failing because of placement and use of weak rock for wall rock.

Fill Materials and Compaction

On the Taylor River Road project, the rockery walls will be constructed in front of fill that has been placed in front of the temporary back slopes. Typically, the fill must be composed of 100 to 200 mm (4 to 8 in) rock. The fill must be placed and then tamped with a rod to compact the voids. The fill material must be clean and free of organics and debris. There should be no more than 5% fines passing the number 200 sieve. Fill should be placed in thin lifts not exceeding 250mm (10in) loose thickness.

General Excavation

Prior to construction of the rockery wall the site for the footprint must be prepared. All loose rock, soil and debris must be excavated down to firm subgrade with a bearing strength of at least 97 KPa (2000 psf). Firm subgrade would be material that is relatively difficult to probe with a 13mm (0.5in) steel probe up to 150mm (6in). Soft material would be material that the engineer could probe beyond 150mm (6in). The base should be leveled. This may require excavation of large protruding rocks. Adding a layer of tamped coarse quarry spalls may firm up the soft subgrade. The backslope must be cut in sections of manageable lengths such that the rockery wall can be constructed in one workday. Temporary cut slopes (backwalls) should not be left open overnight because of the potential for collapse.

Rockery Wall Keyway

The first step in the rockery wall construction after general excavation is to construct a keyway trench. The keyway should be designed to contain the basal rock for the rockery wall. Figure 6 displays a typical design for the keyway beneath the rockery wall. Design the keyway as a shallow trench of not less than 300mm (12in) in depth. Extend the keyway the full length of the rockery wall. The width of the keyway should be as wide as the basal rock plus the drain rock layer. The keyway must be excavated in sections of manageable lengths such that the rockery wall can be constructed during one daylong shift. The keyway should be excavated into firm subgrade (see General Excavation). If soft material exists, strengthen and make the soil more firm placing base material meeting the gradation requirements outlined on Figure 6. Where the rockery wall supports a lateral load, a 150mm (6in) layer of base material should be installed. The base material will increase the friction between the subgrade and the base of the rockery wall.

Rockery Wall Keyway Drainage

Along Taylor River Road, the rockery walls constructed in the talus deposits (free of a fine-grained matrix) typically do not require keyway drainage because typically the talus deposits are very course and free draining (Figure 8). Conversely the terrace and glacial deposits and talus with a soil matrix require drainage. Increased water pressure behind the rockery wall may lead to piping of the fines through the wall and ultimate failure of the wall. Figure 9 is an example of a rockery wall collapse related to poor drainage exacerbated by use and placement of poor unsuitable rock for the rock wall.

Figure 8: Rockery wall along Taylor River Road.

Upon completion of the keyway excavation, a 100mm (4in) minimum diameter perforated or slotted PVC drainpipe should be installed at the rear of the keyway behind the basal rock. Figure 6 is a typical schematic, which displays drainage design requirements.

Figure 9: Failure of rockery wall from poor drainage exacerbated by poor rock selection and placement, Reno, Nevada.

Rockery Wall Thickness

Figure 6 displays general rock wall thickness guidelines. Typically the individual rock wall thickness will equal the width of the recommended rock plus the thickness of the drain rock behind. The rockery wall will act as a retaining structure therefore it is critical that the size and mass of the rock be adequate to resist the applied loads.

Figure 10: Rockery wall failing because of poor placement of rock and weak unsound rock.

Rock Selection

During construction, the constructor should insure that there is sufficient space to stockpile several selections of rock for the rockery. Along Taylor River, we expect that the constructor will be able to use good rock excavated from the talus, terrace and glacial deposits. Shapes of the rocks are important. The rocks must be cubical, tabular or rectangular so that they can rest upon each other in the wall. In addition, the rocks must be hard and strong and ring when struck with a geology hammer. Furthermore, the rocks must be free of major weak zones such as cracks, seams and foliation. Spalling from repeated freezing and thawing activity might tend to break the rocks down. Therefore, if there is doubt, we recommend testing selected rock samples

by ASTM C682 for Freeze-Thaw characteristics. Figure 10 is a photo of very weak rock that was selected for a rockery wall in the Reno, Nevada area. The rockery wall is failing not only because of the shape of the rocks but because the weathered weak rock is disintegrating and spalling around stronger core stones.

Rock Placement

Figure 6 displays placement of the rocks in the rockery wall. In general, the first layer of rock should be placed on firm unyielding soil or on the previously installed layer of quarry spalls. The basal rock should fully contact the subsoil or prepared quarry spalls. This may require further shaping of the basal material or dropping or pounding the rock into the base so it conforms to the material. The bottom of the first course of rock should be a minimum of 300mm (12in) below the lowest adjacent site grade. As the wall is constructed, the rocks should be placed so that there are no continuous joint seams in the lateral as well as vertical. The rocks should be placed so that there are at least two rocks below it. In addition, the rock should be placed with the long axis into the slope. The rock should be placed so that it is bearing on the rock below. The rocks should be set such that there are no sloping faces out of the rock wall, which would create a plane of weakness for failure. Figures 3 and 8 display the FHWA walls constructed by FHWA. The rocks are tabular with good rock-to-rock contact and bear squarely upon each other forming a stable rockery wall. Conversely, Figures 7 and 10 display wall rock that is sub-round reducing the rock-to-rock bearing contact, which has jeopardized the stability of the rockery wall.

Face Inclination

Figure 6 displays the inclination of the face of the rockery wall. Some jurisdictions may establish steeper battering of the wall face (Draft Southern Nevada Local Standard, 2005). Conservatively, the authors recommend as does FHWA (2005) battering the wall face to a ratio 4V:1H inclination measured at the exposed face of the rockery wall.

Voids

Because of the shape of the rocks used in the rockery wall, there will be voids created between individual rocks, especially the larger rocks. Voids should be minimized for long-term stability. Where voids exceed 150mm (6in) in diameter, the engineer should visually examine if the void continues through the width of the wall. If it is established that the void is surficial and there is rock-to-rock contact at depth, no further action is required. On the other hand if the void is through going, the void must be chinked with a smaller rock. Because of the potential for the chinking rock to fall out with subsequent loss of drain rock or soil behind the rockery wall, the void must be chinked from the inside of the wall if possible. In this way the lateral pressure will force the chink rock into the void. However, if it is impracticable to chink the voids from the inside face and the constructor elects to chink the void from the outside face, the chinking rocks should be hammered in to insure a tight fit. Chinking rocks must be of the same quality as that for the large rocks. The photo in Figure 10 displays chinking rock that failed and fell out of the voids between large rocks in a rockery walls in the Reno, Nevada area. Rock that was selected for this wall was unsuitable for rockery walls. The rock was very weak (hand samples could be broken with difficulty by hand pressure), fractured and appeared to disintegrate rapidly when exposed to the elements.

Construction Concerns

During the this investigation the authors identified the following construction concerns attendant to the rockery walls:

1) Stability of the temporary backwall behind the rockery wall will be a major issue because of the marginal stability of the talus deposits and possibly the glacial and terrace deposits depending on the textural gradation.

2) Work site safety because of the marginally stable temporary backwall behind the rockery wall. The contractor will be responsible to insure the safety of the workers when excavating the temporary backwall. In addition, the contractor should insure that temporary excavations are not left open for extended periods.

3) Precipitation in the form or snow and rain leading to drainage problems behind the rockery wall. The constructor must insure that there is adequate drainage to account for the annual precipitation and runoff in the area. In addition, the drainage should be captured and diverted to a culvert or depression such that it does not flow over or impact the road.

4) Freezing and thawing cycles may lead to spalling of the individual rocks within the wall. Therefore, rocks selected for the rockery wall must be sound, strong and free of joints and fractures.

5) Ice and snow may cause excessive loads on the rockery wall. The top of the wall and the fill behind should be graded to reduce the snow and ice loads.

Conclusions

During the project, the authors were faced with the following design challenges:

- Designing rockery walls as structural walls composed of talus rock with the dual purpose of providing erosion control and to retain marginally stable slopes

- Designing temporary steeper cuts at the toe of the marginally stable talus slope

- Estimating critical stable height/base ratios for the rockery walls considering overturning, sliding, and bearing capacity of the walls

Rockery walls are typically designed as erosion protection for slopes that are considered stable without reinforcement. A number of procedures have been proposed in this paper for considering the rockeries as structural walls. These procedures are based on published references and were the basis for our design, and summarized here for the convenience of the reader.

There is precedent for designing and constructing rockeries as structural reinforcing elements. FHWA's constructed a series of walls to retain talus slopes north of the current Taylor River Road project area without incident. The talus would not be considered stable at such steep inclinations without reinforcement.

Construction quality control is paramount when specifying rockery walls as reinforcing walls. Hendron (1960) noted this when he produced the design charts modified as part of this paper. We have described a number of practical examples where the integrity of rockeries was compromised because of poor construction procedures. Important aspects of construction that require monitoring include the excavation of a keyway, gradation and compaction of the wall backfill, selection of good strong rock for the wall, "chinking" rock selected for the voids, and proper drainage.

References

Associated Rock Wall Contractors (ARC), *Rock Wall Construction Guidelines*, Woodinville, Washington, 1992.

Federal Highway Administration, *Rockery Design and Construction Guidelines*, Interim Report No. 2 – Rockery Design, Publication No. FHWA-CFL/TD-05-00x, 2005, 35 p.

Gifford, A.B. and Kirkland, T.E., *Uses and Abuses of Rockeries.* Proceedings of the Annual Engineering Geology and Soils Engineering Symposium No 16, 1978, pp. 55-68

Gray, D. H. and R. B./ Sotir, *Biotechnical and Soil Bioengineering Slope Stabilization*. John Wiley & Sons, New York, 1996.

Hendron, A. J., Jr., *Stability Analysis of a Rockery*, In-house report, Shannon & Wilson, Inc., 1960.

Kleinfelder, Inc, *Geotechnical Investigation Report Taylor River Road CO*, PFH 59-1(4) Gunnison County, Colorado IDIQ Contract Number: DTFH68-02-D00002 Task Order No. DTFH68-00-D-00002/T-05-021, 2006.

Pile Buck, Inc., *Earth Support Systems & Retaining Structures*, Pile Buck, Inc® Jupiter, FL., 1992, pp 23-28.

Southern Nevada Local Standard, *Rockery Wall Construction, Southern Nevada Local Standard*: Developed by SNBO Structural Committee, Draft: February 14, 2005.

Surprising Soil Behavior at Zolezzi Lane

Sherif Elfass, Research Assistant Professor
Dept. of Civil and Environmental Engineering, MS258
University of Nevada
Reno, NV, 89557
Phone: (775) 784-6195, elfass@unr.edu

Gary Norris, Professor
Dept. of Civil Engineering, MS258
University of Nevada
Reno, NV, 89557
Phone: (775) 784-6835, norris@unr.edu

Rob Valceschini, Engineering Manager,
Applied Soil Water Technologies, LLC
Sparks, NV, 89431
Phone (775) 331-2375, rvalceschini@appliedsoilwater.com

ABSTRACT

A project to assess possible compression of near surface soils beneath a constructed embankment and the likely reduction in regional (horizontal) flow through this depth of soil yielded quite surprising behavior. This silty sand (with non- to slightly plastic fines) yielded lower SPT blow counts and was, in fact, characterized by the commonly employed CPT tip and sleeve correlation program as fine-grained (silt-clay) soil. However, piezocone readings showed negative pore pressures during field penetration, while triaxial tests on "undisturbed" and reconstituted samples showed drained volumetric expansion or negative undrained pore pressures during shear. Furthermore, in situ void ratios based on water contents in relation to lab established maximum and minimum void ratios indicated medium to very dense in situ conditions, different from the loose to medium conditions established from commonly employed SPT blow count correlation. Low field and laboratory permeability test results indicated the likely development and dissipation of excess pore pressures due to end of construction conditions. However, this did not prepare the investigators for the water level changes recorded in piezometers located beneath versus adjacent to the 30-foot high fill constructed at the Zolezzi Lane site.

INTRODUCTION

The construction of the four miles of the elevated US 395 extension from South Meadows Parkway to Mount Rose Highway in Reno, Nevada took from 1994 to 1996 to complete. This six to eight lane highway embankment is 25 to 30 feet from original ground to roadway surface. A major concern at the time was that this fill might compress the near surface soil beneath it causing a loss of groundwater flow over this depth to agricultural lands on the east side of this north-south freeway. Zolezzi Lane, when extended, crosses beneath the 395 extension as shown in Fig. 1 and was chosen as the site of a study area to address this issue (*1*).

The soils that comprise the meadows of this part of Reno are Quaternary alluvial bajada sediments (Qa) as shown on the Mount Rose Northeast geologic quadrangle map (*2*) and part of the Rose Creek soil unit of the Soil Conservation Service (SCS) Washoe County South Part soils report (*3*). Tables1a and 1b provide the SCS characterizations of the site soils (to a depth of 60 inches), which in retrospect turned out to be very informative. As indicated by Gates and Watters (*4*) regional groundwater flow is from the Carson Range (on the west) northeast across the valley toward the Virginia Range.

PIEZOMETERS

Zolezzi Lane was chosen as the study site because of its easy access and relative privacy. As shown in Fig. 1, the Nevada Department of Transportation (NDOT) had already obtained borings at the location of the bridge. Eight piezometer locations were chosen in an east-west line, as shown in Fig. 1, at some distance from the bridge

abutment so they would fall beneath and adjacent to the embankment, once built. Figure 2 shows the piezometer depths and locations in relation to the embankment to be built (dashed line). Note that the piezometer designated Pz 4D is in a controlling silty gravel with sand (GM) artesian layer that is fed by springtime snowmelt from the Carson Range while the other piezometers are in the compressible near surface soils that lie above this artesian layer. Figure 3a shows the characterization of soil layers adopted for use relative to the finite element mesh of the near surface soil and embankment as shown in Fig. 3b. Figure 4 shows NDOT's boring logs for boreholes B1 and B2 (as indicated on Fig. 1).

The piezometers were installed seven months prior to construction in order to gain data on seasonal fluctuations, and readings were continued a total of two years, one year after completion of the fill at this location. Figure 5 shows the variation in readings for Pz 1, the furthest piezometer "downstream" and the piezometer exhibiting the lowest seasonal water level. The readings from Pz 4D were to be the control since this piezometer is located in the artesian layer beneath the near surface compressible soil. It was also expected that the readings from Pz 1 would be largely unaffected by the fill given its horizontal distance from the toe of planned embankment and the relative proximity of it to the underlying artesian layer. In fact, the Pz 1 readings mirrored those of Pz 4D and the two taken together served as the bounds of upper and lower seasonal water levels over the time span of the investigation.
It was expected, given the high fines content in the near surface compressible soils (see borings B1 and B2 and data from SCS), that the piezometers falling beneath the constructed fill would exhibit a rise (in feet) well above these seasonal values due to an induced excess porewater pressure. This rise might well equal the unit weight of the fill times its height divided by the unit weight of water, or say 60 ft. There is discussion of the different or surprising response that actually occurred in a later section.

SOIL CHARACTERIZATION

The high fines content of the near surface soils given in borings B1 and B2 (despite their classification by the Unified Soil Classification System as a coarse-grained SM or silty sand) indicates a fine-grained silt-clay soil (A4) by the AASHTO classification system. Accordingly, one would expect lower permeabilities and, hence, excess porewater pressure generation, followed by consolidation settlement due to fill loading. In fact, part of the research study program undertaken was to perform lab and field permeability tests, with the intent that the stress path triaxial tests would reflect changing permeability due to the changing stress state and the ensuing consolidation. Therefore, in addition to hollow stem auger borings with standard penetration test (SPT) split spoon sampling (in the holes in which the piezometers were to be placed), Shelby and clear tube samples were also taken. In addition, four piezocone soundings with pore pressure dissipations were made adjacent to Pz 3, 4, 5 and 6, and two wells drilled adjacent to Pz 3. (Actually, piezometers at Pz 3, 4 and 5 are themselves in multiple holes as indicated in Fig. 2.)

Figure 6 gives the cone penetration test (CPT) sounding adjacent to Pz 4 with the piezometer locations superposed on the (penetration) pore pressure record for reference. Table 2 is the corresponding data interpretation every quarter-meter of depth according to Robertson and Campanella (*5*). One thing to notice is the much finer grained soil characterization the classification would suggest. This was true of the other CPT soundings as well. By contrast, Table 3 provides data from SPT and Shelby tube samples assessed in the lab. Note that the in situ void ratio (e), then the dry and saturated unit weights were calculated based on the assessed water content (w) and specific gravity (G_s) for the assumed degree of saturation (S) of unity for samples from below the water table, i.e. $e = w\ G_s / S$; $\gamma_d = Gs\ \ w / (1 + e)$; $\gamma = (G_s + Se); \gamma_w / (1 + e)$. Note the correlation between the water content (and, hence, void ratio) and fines content data of Table 3 plotted as Fig. 7. Superposed are lines for average maximum (Modified ASSHTO) and minimum (spooned loose into a compaction mold) density and liquid limit performed on bulk samples of mixed SPT and Shelby tube samples (fines contents of 24 and 38%, respectively).

From Table 3 and Fig.7, the reader will note that the fines contents for all depths and locations ranges from approximately 20% to 45% with only a few exceptions. (The fines are nonplastic to only slightly plastic, i.e. PI < 6.) However, this fines content encompasses the range of 35 to 50% in which a soil is considered a coarse-grained soil by the Unified Soil Classification system and a silt-clay (hence, fine-grained) soil by the AASHTO system. It would appear that the CPT descriptions (e.g. Table 2) after Robertson and Campanella (*5*) at Pz 3, 4, 5 and 6 locations are more in keeping with the AASHTO system. Accordingly, the CPT data interpretation program (*6*) yields undrained shear strength (S_u) rather that relative density (D_r) and drained friction angle (ϕ) for the soils it considers fine-grained as opposed to coarse-grained (see Table 2).

However, such CPT data interpretation is in contrast to its own piezocone log (e.g. Fig. 6) which indicates negative porewater pressures generated during cone advancement, a characteristic of dilative materials which are cohesionless. Of course, the CPT interpretations of Table 2 are based on a cross plot of just the cone's tip and sleeve resistances (actually normalized sleeve resistance or "friction ratio", i.e. sleeve resistance divided by tip resistance); the penetration pore pressures are extra information obtained only with the more sophisticated piezocone.

The question of the soil's character, fine- or coarse-grained, might also be considered based on its permeability. Many measurements of permeability were attempted, both lab and field: horizontal and vertical flow in a flexible wall permeability or triaxial test (under both isotropic and during stress path loading), from the standard consolidation test, from CPT dissipations, and from field slug and bailing tests. However, the results from these many tests ranged from 10^{-4} to 10^{-7} cm/sec. The triaxial test using reconstituted samples yielded the best comparison with the field bailing and slug tests (probably the best indicator of in situ permeability under prevailing horizontal flow conditions), while the values from CPT dissipations and the more sophisticated undisturbed triaxial test samples were decidedly lower. If one uses the Army Corps of Engineer's (*7*) distinction of soils that should be analyzed for both unconsolidated undrained (UU) end of construction and consolidated drained (CD) long term stability conditions, they set a permeability of 10^{-3} cm/sec as the value below which both should be considered. On that basis, the near surface soils at Zolezzi Lane are fine-grained for which one should expect construction induced excess pore pressures. Of course, soils in this range of fines content might very well be expected to behave as fine-grained relative to one condition (permeability, excess pore pressure generation, dissipation and time rate of settlement) and coarse-grained for another (magnitude of settlement and post construction static slope stability). Surely the permeability of $<10^{-4}$ cm/sec indicates likely fine grain soil excess pore pressures (at least during construction). However, the corresponding compression index (C_c) of approximately 0.04 to 0.05 (for the 100 to 200 kPa pressure range) from triaxial k_o consolidation (and smaller values from the standard consolidation test) indicates a stiffer coarse grain or cohesionless material behavior (smaller settlements).

While SPT tests yielded split spoon samples that classified as silty sand (SM), the clear tube samples, when carefully logged, indicated fairly complex layering of materials of ever changing character (hence, the highly varying permeability). At the same time such samples also revealed small root holes (discernable only when the samples were left to air dry) even at depths up to 6 m (20 ft).

Taken as cohesionless material, the SPT blow counts (N) were used to evaluate relative density (D_r) and drained friction angle (ϕ) using both the Peck, Hanson and Thornburn (PH&T) and the NAVFAC DM-7 correlations (*8,9*). Table 4 provides a comparison of the data obtained based on the two approaches. Note that the PH&T procedure uses a correction (C_N) for effective overburden pressure (σ_{vo}) by which one obtains the corrected value (N_1) at a reference pressure of 1.0 ton/square ft (i.e. $N_1 = C_N N$); D_r and ϕ are a function of N_1 (*8*, Fig. 19.5).
By contrast, the DM-7 procedure uses a correlation of the recorded blow count (N) at the effective overburden pressure to assess D_r (see Fig. 8a), and then based on D_r and the Unified Soil Classification, the drained friction angle (ϕ) and the corresponding void ratio (e) and dry unit weight at $G_s = 2.68$ are obtained (see Fig. 8b). It should be noted that an SM (and an SP) soil falls within a range and so Table 4 gives this range of values for the associated value of D_r. Also shown on Fig. 8b is a superposed line of the supposed friction angle versus void ratio using average lab assessed values of e_{max} and e_{min}. As seen, the lower end of this line tends to an e_{max} more characteristic of low plasticity silt (ML), while the upper end falls at the limit of the designated SM range. The line designated "From Fig. 9" reflects the variation actually assessed from triaxial tests on "undisturbed" and reconstituted samples of the material.

In considering the relatively good agreement in Table 4 of the PH&T and the DM-7 relative density (D_r) and drained friction angle (ϕ) values, one would expect that this silty sand (SM) would be of low to medium density (D_r = 25 to 65%) and low(er) friction angle. Certainly, the lower blow count values reinforce this general conception and suggest a material that would likely be susceptible to liquefaction (at fines contents less than, say, 35%). Such materials would not be expected to be dilative in nature. (Peck suggests that only for N values greater than 15 should one consider correcting the recorded value obtained below the ground water table for negative excess pore pressures generated during SPT driving.) However, this is not to be the case; and it suggests that the commonly used correlations such as the PH&T (*8*) and DM-7 (*9*) are more conservative than commonly understood.

That the material is, in fact, dilative and not likely to be catastrophically liquefiable is suggested by the negative pore pressures from the piezocone logs (see Fig. 6). Of course, the CPT data interpretation program typically regards the material as fine-grained, see Table 2, in contradiction to its own piezo log. However, at those few depths (see Table 2) where it does recognize the material as coarse-grained, it gives higher D_r and drained friction angle (ϕ) values (reflective of a dilative material) than from SPT correlations. This is further corroborated by the D_r values calculated from the lab void ratios (see Table 3) and the previously mentioned e_{max} and e_{min} values. Accordingly, the silty sand has D_r values that range, for the most part, from 45 to 90% (rather than SPT assessed values ranging from 25 to 65%). See Fig. 7.

Another interesting point gleaned from the piezo logs is the relatively high negative pore pressures attained. Note that the magnitude of these values equal or in some logs exceed –100 kPa (-14.5 psi) at which cavitation of the porewater occurs in (clean) sands. Such large negative pore pressures were also observed in undrained triaxial tests. This dilative behavior is certainly more likely to occur in medium to very dense (D_r from 45 to 90%) sands rather than loose to medium dense (D_r from 25 to 65%) sands.

Drained and undrained triaxial tests on both "undisturbed" and reconstituted samples yielded the drained/effective stress friction angle variation (with void ratio, e) shown in Fig. 9 (that was superposed on Fig. 8b). This same variation compares with that of other fluvial materials when superposed on a Lambe and Whitman (*10*, p. 146) figure.

Even more interesting, however, was the much higher undrained than drained strengths of this silty sand, in lab tests at the same consolidation pressure.

FIELD PIEZOMETER READINGS

As mentioned earlier, Pz 1 and 4D (see Fig. 2) reflect the trend in seasonal pore pressure variation unaffected by the construction of the embankment. In a similar fashion, piezometers outside the line enclosing those under the central portion of the fill, showed a variation paralleling that of Pz 1 and 4D, i.e. with no particular influence from fill placement. On the other hand, the expected jump in water levels in the piezometers within the central area beneath the constructed embankment (Fig. 2) did not occur; the piezometers actually showed a drop of 1 to 2 ft. See the circled areas of Fig. 10 characterizing drops in Pz 3A and 4A in particular. This was completely unexpected at the time if one considers the material as either fine-grained soil or loose, compressive coarse-grained soil.

Note from Skempton's undrained pore pressure equation (*11*), $u = B\,\Delta\sigma_3 + A\,\Delta\sigma_d$, where B will be a positive value due to fill placement, implies that A must be negative (dilative) to give a net negative pore pressure drop of 1 to 2 ft. This was confirmed in undrained stress path triaxial test loading in the lab, but also foretold by the piezocone readings. As can be judged from Fig. 10, the negative pore pressures dissipated in less than three weeks. Further, as assessed in the triaxial tests, there was no significant associated volumetric compression with the dissipation of the undrained pore pressures; it was either negligible or slightly expansive. Therefore, what would occur in the field would be similar, i.e. no compression of the near surface soils beneath the embankment and, therefore, no significant effect of embankment construction on the near surface ground water flow beneath the fill.

CONCLUSIONS

The surprising soil behavior at the Zolezzi Lane site was the generation of a negative excess porewater pressure in the near surface soil beneath the central portion of a 30-foot high embankment constructed there. The commonly used CPT interpretation program after Robertson and Campanella (*6*) classified this soil, for the most part, as fine-grained. The AASHTO classification would also suggest that a good portion of it should be fine-grained (material with >35% fines of the 20-45% fines common at the site). According to the Army Corps of Engineers, assessed permeability values ranging from 10^{-4} to 10^{-7} cm/sec (i.e.$< 10^{-3}$) would require that such material's strength be characterized by its short term unconsolidated undrained strength (S_u) as well as long term drained strength (based on D_r).

On the other hand, SPT split spoon and Shelby tube samples yielded materials that would be classified as a coarse-grained soil, i.e. silty sand (SM), of little plasticity (PI from 0 to 6 maximum). However, using commonly employed correlations (*8,9*), the associated blow counts would infer that such materials should be of low to medium density (D_r = 25 to 65%) and low(er) drained friction angle. By contrast, void ratios calculated from water contents of

samples from below the water table, in conjunction with e_{max} and e_{min} values assessed from mixed bulk samples yield much higher densities (D_r = 45 to 90%). Triaxial tests on "undisturbed" and reconstituted samples yielded a much higher drained (CD) / effective stress (CU) friction angle (i.e. its variation with void ratio) than implied from commonly employed SPT blow count correlations (PH&T and DM-7). In fact, consolidated drained tests (CD) yielded dilative volume changes while consolidated undrained (CU) tests yielded negative porewater pressures during shear. The magnitude of the negative pore pressures at failure for the lower void ratio samples was greater than the 100 kPa suction at which geotechnical engineers consider that water in (clean) sands will cavitate. Such undrained test, shear induced, pore pressures are in relative agreement with the negative values from the CPT piezocone logs.

As important as the establishment of the variation in friction angle with density state, the much more interesting response was the much higher strengths of the silty sand from undrained tests (CU) than drained (CD), at the same or even lower effective consolidation pressures in the undrained versus drained tests. This was true of both "undisturbed" and reconstituted samples. Strangely enough, the high soil suction of the material allowed extrusion of relatively intact "undisturbed" Shelby tube samples, different than what one would expect of (cleaner) sands. In fact, given the high negative porewater pressures generated during CPT penetration, one should question the accuracy of any CPT assessed drained friction angle, given that effective stress is not appropriately assessed in such evaluation.

The 1 to 2 ft foot drop of water levels in piezometers in the near surface soil beneath the central portion of the embankment is actually a net negative value due, in part, to a positive pore pressure, the result of the confining pressure increase ($\Delta\sigma_3$), that was overcome by an even larger negative pore pressure due to the deviatoric component of stress change (σ_d). This was unexpected given the CPT classification of the soil and the lower SPT blow counts that would suggest a compressive (not a dilative) material based on commonly employed correlations. However, the fact that this response should not have been considered unusual is supported by the higher density established from lab-determined e and D_r values, the triaxial test response and the piezocone logs.

The lessons learned by the authors from this case study are numerous:

1. Make sure that samples are used to confirm CPT soil classifications.
2. Commonly used SPT blow count correlations may be very conservative.
3. Use whatever additional data or evidence that is available (SCS data, water content data, lab assessed e_{max} and e_{min} values, piezocone logs, shear test volume change or pore pressure data) to get a more complete understanding of the likely material behavior.
4. Things are not always what they seem. Don't stick to preconceived notions of material behavior based on soil classification. Learn from what you record/discover and update your personal database to be better prepared for your next encounter with "surprising" or seemingly conflicting data.

In the present situation, the soil exhibited both fine- and coarse-grained behavior. The soil had the permeability of a finer-grained soil and generated excess pore pressures that persisted through the time of embankment construction. Therefore, undrained as well as drained strength stability analyses should be considered. However, such material exhibited dilative shear behavior and the net volume change that occurred was minimally compressive, if not expansive; this despite traditional CPT and SPT blow count evidence that would suggest otherwise. In essence, the material behaved like a stiffer/denser nonplastic silt, i.e. it had sufficient fines to cause its time dependent behavior, but high enough density to be dilative and, therefore, be governed by its lower drained than undrained strength. (Normally, one assumes that long term or drained strength would be greater than short term undrained strength under loading conditions.)

In retrospect, one might conclude that the near surface soil at Zolezzi Lane behaved like a "cohesionless" material, which includes all coarse-grained soil and nonplastic fine-grained soil, as opposed to a "cohesive" soil (i.e. a plastic fine-grained soil). Such distinction and what it translates to in terms of behavior makes the observed response less "surprising".

References

1. Norris, G., Elfass, S. and Valceschini, R. *Permeability Changes in Soil Due to Fill Loading and Its Effect on the Groundwater Flow Regime.* Department of Civil and Environmental Engineering, University of Nevada, Reno, May 1997.
2. Bonham Jr., H.F. and Rogers, D.K. *Mt. Rose NE Quad Geologic Map*. Nevada Bureau of Mines & Geology, 1983.
3. Soil Conservation Service. *Soil Survey of Washoe County*, Nevada, South Part, 1980.
4. Gates, W.B. and Watters, R. J. Geology of Reno and Truckee Meadows, Nevada, United States of America. *Bulletin of the Association of Engineering Geologists*, Vol. XXIX, No. 3, 1992, pp 229-298.
5. Robertson, P.K. and Campanella, R.G. Interpretation of Cone Penetration Tests: Parts 1 and 2. *Canadian Geotechnical Journal*. Vol. 20, 1983, pp. 718-745.
6. Robertson, P.K. and Campanella, R.G. Guidelines for the Use & Interpretation for the Electronic Cone Penetration Test. Hogentogler & Co., Second Edition, 1984.
7. Dept. of the Army, Corps of Engineers. EM 1110-2-2502, *Engineering and Design: Retaining and Flood Walls*, 1989, p. 4-5.
8. Peck, R. B., Hanson, W. E., and Thornburn, T. H. *Foundation Engineering*, Second Edition, John Wiley and Sons, New York, 1974.
9. U. S. Navy, NAVFAC DM 7.1. *Design Manual: Foundations and Earth Structures*, 1982, pp. 234-241.
10. Lambe, T.W. and Whitman, R.V., 1969, *Soil Mechanics*, Wiley, New York, NY.
11. Skempton, A.W. The Pore Pressure Coefficients A and B. *Geotechnique*, Vol. 4, 1954, pp. 143-147.

TABLE 1 A) DESCRIPTION FROM SCS WASHOE COUNTY, NEVADA, SOUTH PART, P. 264

Engineering Index and Physical and chemical Properties of the Rose Creek Series, Washoe County, Nevada, South Part, p. 513

a) Rose Creek Series

The Rose Creek series consists of very deep, poorly drained soils on flood plains. Drainage has been altered. These soils formed in alluvium from mixed rock sources. Slopes are 0 to 2 percent.

Typical pedon of Rose Creek fine sandy loam, 2,000 feet west and 1,600 feet south of the northeast corner of sec. 17, T. 19 N., R. 20 E.

Ap1p—0 to 8 inches; grayish brown (10YR 5/2) fine sandy loam, very dark grayish brown (10YR 3/2) moist; moderate fine subangular blocky structure; slightly hard, friable, slightly sticky and slightly plastic; many very fine to medium roots; common very fine to medium pores; 10 percent pebbles; effervescent; moderately alkaline; clear smooth boundary.

A12—8 to 16 inches; grayish brown (10YR 5/2) sandy loam, very dark grayish brown (10YR 3/2) moist; common medium prominent strong brown (7.5YR 5/6) mottles; massive; slightly hard, friable, slightly sticky and slightly plastic; many fine to medium roots; common very fine to medium pores; 10 percent pebbles; effervescent; moderately alkaline; clear smooth boundary.

C1—16 to 60 inches; light brownish gray (10YR 6/2) stratified very fine sandy loam, gravelly loamy sand, sandy loam, dark grayish brown (10YR 4/2) moist; common medium prominent strong brown (7.5YR 5/6) mottles; massive; slightly hard, friable, slightly sticky and slightly plastic; common very fine to medium roots; few very fine to medium pores; effervescent; moderately alkaline.

The soil profile is deeper than 60 inches. The mollic epipedon is 10 to 18 inches deep. Reaction throughout the profile ranges from mildly alkaline to moderately alkaline. The control section is stratified and has texture of sandy loam, fine sandy loam, very fine sandy loam, or loam. It is more than 15 percent fine or coarse sand and 5 to 18 percent clay. In pedons where texture is the coarser part of the range, the control section is 0 to 20 percent gravel.

Mottles are common below the upper part of the A horizon. The lower part of the C horizon is highly mottled or gleyed.

b)

Soil name and map symbol	Depth	USDA texture	Classification		Frag-ments > 3 inches	Percentage passing sieve number--				Liquid limit	Plas-ticity index
			Unified	AASHTO		4	10	40	200		
	In				Pct					Pct	
810---------- Rose Creek	0-16	Fine sandy loam	SM, ML	A-4	0-5	90-100	80-95	65-80	45-55	25-30	NP-5
	16-60	Stratified gravelly sand to silt loam.	SM	A-2, A-4	0-5	85-100	70-95	50-70	30-40	20-25	NP-5

Soil name and map symbol	Depth	Clay	Permeability	Available water capacity	Soil reaction	Salinity	Shrink-swell potential	Erosion factors		Wind erodibility group
								K	T	
	In	Pct	In/hr	In/in	pH	Mmhos/cm				
810---------- Rose Creek	0-16	10-15	0.6-6.0	0.10-0.13	7.4-8.4	<4	Low----------	0.32	5	4
	16-60	10-18	2.0-6.0	0.10-0.13	7.9-9.0	2-4	Low----------	0.28		

TABLE 2 CPT Program Output Adjacent to Pz 4

Engineer U.N.R. CPT Date :12/22/93 12:32
On Site Loc:CPT-P4 Cone Used :465
Job No. :U.N.R. Water table (meters) : 3*
Tot. Unit Wt. (avg) : 115 pcf

DEPTH (meters)	DEPTH (feet)	Qc (avg) (tsf)	Fs (avg) (tsf)	Rf (avg) (%)	SIGV' (tsf)	SOIL BEHAVIOUR TYPE	Eq - Dr (%)	PHI deg.	SPT N	Su tsf
0.25	0.82	22.38	0.35	1.57	0.02	sandy silt to clayey silt	UNDFND	UNDFD	9	1.4
0.50	1.64	18.02	0.10	0.58	0.07	sandy silt to clayey silt	UNDFND	UNDFD	7	1.1
0.75	2.46	10.02	0.00	0.04	0.12	sensitive fine grained	UNDFND	UNDFD	5	.6
1.00	3.28	16.46	0.10	0.58	0.17	sandy silt to clayey silt	UNDFND	UNDFD	6	1.0
1.25	4.10	30.22	0.32	1.05	0.21	silty sand to sandy silt	50-60	42-44	10	UNDEFINED
1.50	4.92	70.06	1.17	1.67	0.26	silty sand to sandy silt	70-80	44-46	22	UNDEFINED
1.75	5.74	24.92	0.27	1.07	0.31	sandy silt to clayey silt	UNDFND	UNDFD	10	1.6
2.00	6.56	17.08	0.44	2.59	0.35	clayey silt to silty clay	UNDFND	UNDFD	8	1.1
2.25	7.38	14.88	0.26	1.76	0.40	clayey silt to silty clay	UNDFND	UNDFD	7	.9
2.50	8.20	39.68	0.66	1.66	0.45	sandy silt to clayey silt	UNDFND	UNDFD	15	2.6
2.75	9.02	87.22	0.74	0.84	0.50	sand to silty sand	70-80	42-44	21	UNDEFINED
3.00	9.84	56.46	0.79	1.40	0.54	silty sand to sandy silt	50-60	40-42	18	UNDEFINED
3.25	10.66	65.54	0.53	0.80	0.58	sand to silty sand	60-70	40-42	16	UNDEFINED
3.50	11.48	46.38	0.99	2.13	0.60	sandy silt to clayey silt	UNDFND	UNDFD	18	3.0
3.75	12.30	31.22	0.82	2.64	0.62	sandy silt to clayey silt	UNDFND	UNDFD	12	2.0
4.00	13.12	22.94	0.40	1.73	0.64	sandy silt to clayey silt	UNDFND	UNDFD	9	1.4
4.25	13.94	14.02	0.05	0.37	0.66	sandy silt to clayey silt	UNDFND	UNDFD	5	.8
4.50	14.76	19.50	0.51	2.59	0.68	clayey silt to silty clay	UNDFND	UNDFD	9	1.2
4.75	15.58	31.32	0.69	2.19	0.71	sandy silt to clayey silt	UNDFND	UNDFD	12	2.0
5.00	16.40	34.16	0.92	2.68	0.73	sandy silt to clayey silt	UNDFND	UNDFD	13	2.2
5.25	17.22	92.52	1.75	1.89	0.75	silty sand to sandy silt	60-70	40-42	30	UNDEFINED
5.50	18.04	84.94	2.08	2.45	0.77	sandy silt to clayey silt	UNDFND	UNDFD	33	5.5
5.75	18.86	97.68	1.16	1.18	0.79	sand to silty sand	60-70	40-42	23	UNDEFINED
6.00	19.69	64.82	1.31	2.02	0.81	silty sand to sandy silt	50-60	40-42	21	UNDEFINED
6.25	20.51	116.50	3.52	3.02	0.84	sandy silt to clayey silt	UNDFND	UNDFD	45	7.6
6.50	21.33	149.26	3.41	2.29	0.86	silty sand to sandy silt	80-90	42-44	48	UNDEFINED

Dr - All sands (Jamiolkowski et al. 1985) PHI - Robertson and Campanella 1983 Su: Nk= 15

**** Note: For interpretation purposes the PLOTTED CPT PROFILE should be used with the TABULATED OUTPUT from CPTINTR1 (v 3.04) ****

*** Assumed for the analysis, actual water level was at 2 ft**

TABLE 3 Summary of Soil Properties from SPT Split Spoon and Shelby Tube Samples

Loacation	Depth from	Depth to	w %	Gs	e	γ_d pcf	γ pcf	– #200 %	C_u	D_{50}
Pz 2	7'-6"		33.2	2.65	0.874	88.2	117.5	20.3	6	0.12
	9'-6"		24.6	2.65	0.647	100.4	125.1	20.3		
	9'-11"		21.2	2.65	0.559	106.1	128.6	20.3		
	10'-6"		25.1	2.63	0.661	98.9	123.7	29.9		
Pz 3	1'-6"	2'-6"	15.9	2.67	0.424	117.1	135.7	21.7		
	8'-6"		18.4	2.70	0.496	112.5	133.2	19.4	7	0.26
	9'-6"		16.1	2.70	0.435	117.3	136.3	20.3	12	0.30
	10'-2"		18.4	2.69	0.495	112.3	132.9	29.8	10	0.02
	13'-0"		12.1	2.69	0.325	126.7	142.0			
Well 1	4'-6"	5'-0"	28.6	2.61	0.746	93.3	119.9	44.3	14	0.10
Well 2	2'-0"			2.63				9.0	8	0.43
	4'-0"			2.68				22.1	10	0.23
	9'-6"		24.6	2.68	0.647	101.7	126.7	28.7		
	9'-11"		21.2	2.68	0.559	107.4	130.2	28.7	13	0.16
	12'-8"			2.61				33.6	11	0.16
Pz 4	7'-0"	7'-6"	22.7	2.60	0.592	102.0	125.2			
	11'-0"	12'-6"	22.4	2.66	0.595	104.0	127.2	20.2	11	0.28
	14'-6"		20.8	2.71	0.562	108.0	130.5	27.0	10	0.20
	17'-6"		22.7	2.73	0.619	105.3	129.2	36.8	6	0.11
	21'-0"	22'-0"	24.8	2.64	0.655	99.6	124.2	34.8	10	0.13
Pz 5	4'-0"	4'-6"	24.4	2.65	0.646	100.5	124.9	33.5		
	8'-6"		22.1	2.65	0.585	104.3	127.4	33.5		
	9'-0"	10'-6"	26.1	2.65	0.691	97.8	123.3	33.5		
Pz 7	3'-5"	4'-0"	23.5	2.65	0.621	101.9	125.8	33.5		
	8'-2"	8'-8"	47.2	2.65	1.249	73.5	108.1	62.6		
	9'-0"	9'-6"	31.9	2.61	0.832	88.9	117.3	32.4		
	9'-6"	10'-0"	29.6	2.64	0.782	92.4	119.8	52.1	8	0.18
Pz 8	9'-9"			2.65				27.5		
B1	3'-7"		21.0	2.68	0.563	107.0	129.5	37.0		
	8'-6"							24.0		
	11'-7"		25.0	2.68	0.670	100.0	125.0	42.0		
	18'-8"		20.1	2.68	0.539	109.0	130.5	29.0		
B2	4'-8"							46.0		
	8'-9"							32.0		
	13'-6"							31.0		
	18'-9"							46.0		

All samples from below water table

TABLE 4 Correlations from SPT Blow Counts

Piez. No.	Depth *(ft.)*	N	σ'_{vo} *(psf)*	PH&T				DM-7		
				C_N	N_1	D_r (%)	ϕ (°)	D_r *(%)*	ϕ (°)***	γ_d *(pcf)* ***
Pz3	4 - 5.5	8*	538	1.5	12	37	30.5	35	30.5 - 31.5	95 - 108
	8.5 - 10	12	828	1.3	16	45	32	50	32 - 33.5	97 - 112
	13.5 - 15	11	1022	1.2	13	40	31	50	32 - 33.5	97 - 112
Pz4	6 - 7.5	6	497	1.5	9	30	29.5	25	29 - 30	92 - 106
	11 - 12.5	12	785	1.3	16	45	32	50	32 - 33.5	97 - 112
	18 - 19	12	1219	1.17	14	42	31.5	50	32 -33.5	97 - 112
	19 - 19.5	22	1219	1.17	26	60	35	65 **	33.5 - 36	100 - 115
Pz5	4 - 5.5	6	567	1.45	9	30	29.5	25	29 - 30	92 - 106
	9 - 10.5	11	826	1.3	14	42	31.5	50	32 - 33.5	97 - 112
	16 - 17	12	1042	1.2	19	55	34	55	32.5 - 34	98 - 113
	17 - 17.5	26	1042	1.2	31	67	36.5	70 **	34 - 36.5	100 - 116

* SPT through 8-in OD hollow stem auger, hammer ER=60%, no corrections applied
** Used right side axis of Fig 8a for sand with fine to medium gravel
*** Range for SM soil in Fig 8b

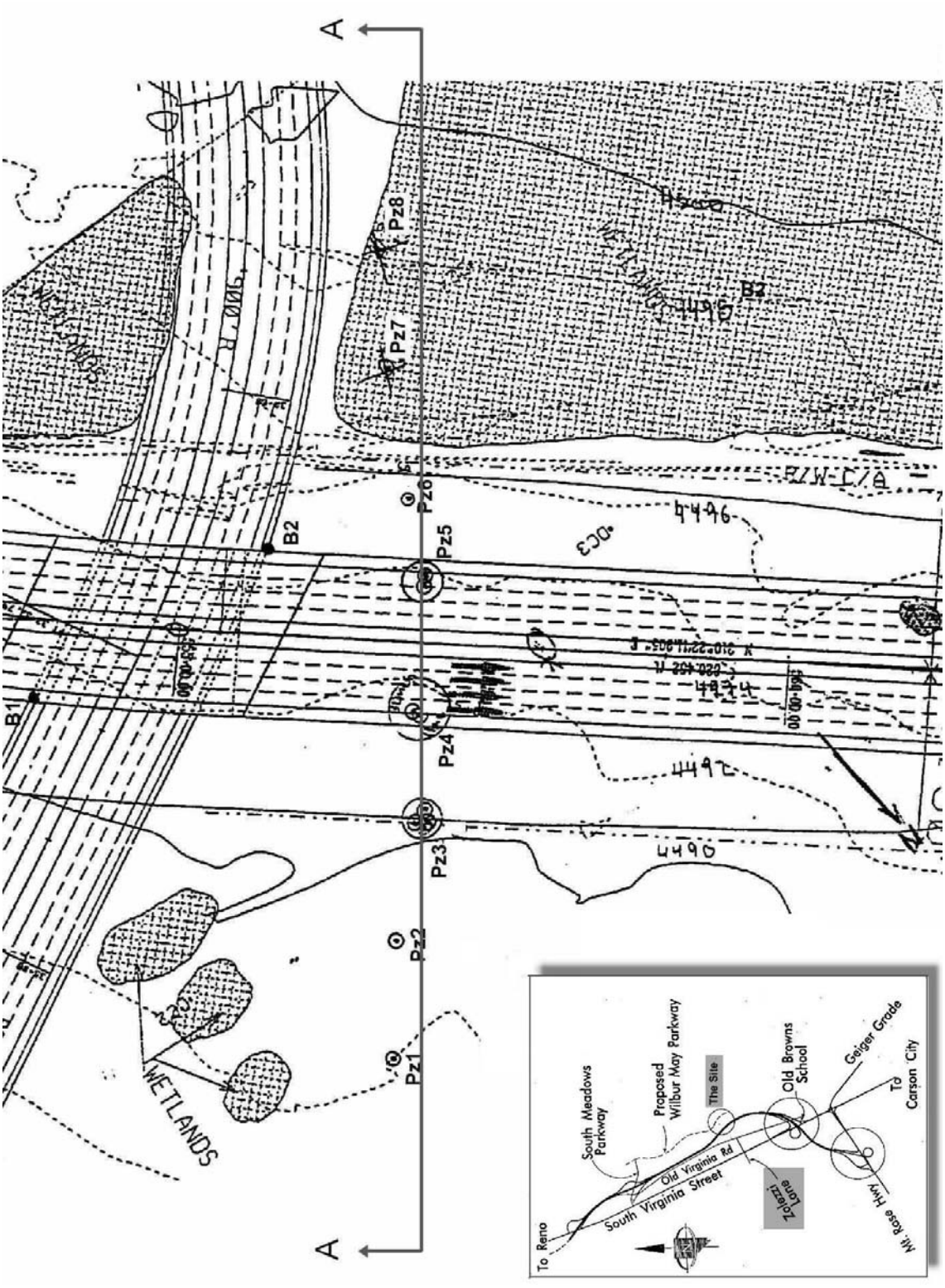

FIGURE 1 ZOLEZZI LANE MAP FROM NDOT PLANS.

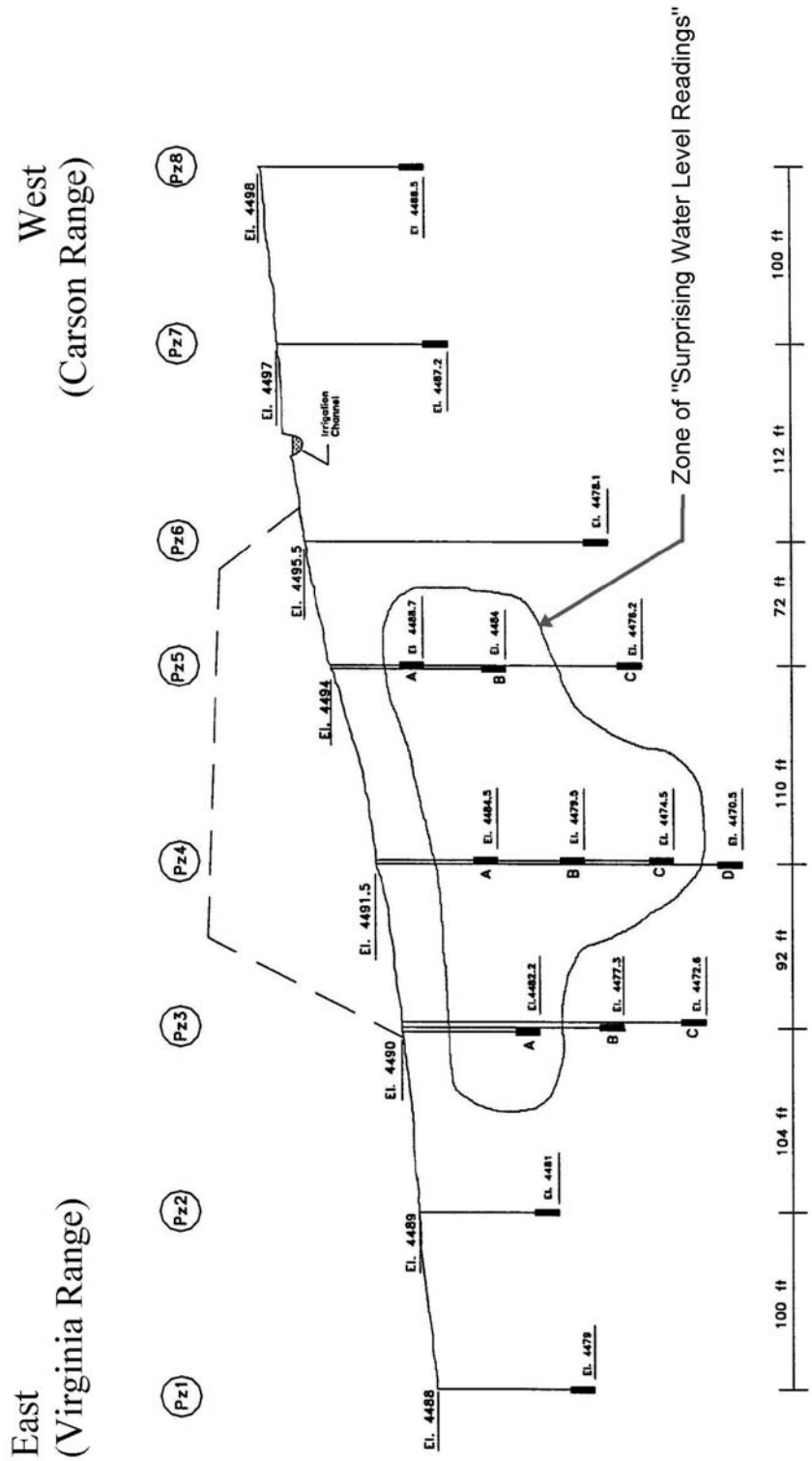

FIGURE 2 Layout of Pneumatic Piezometers (Section A-A from Fig. 1).

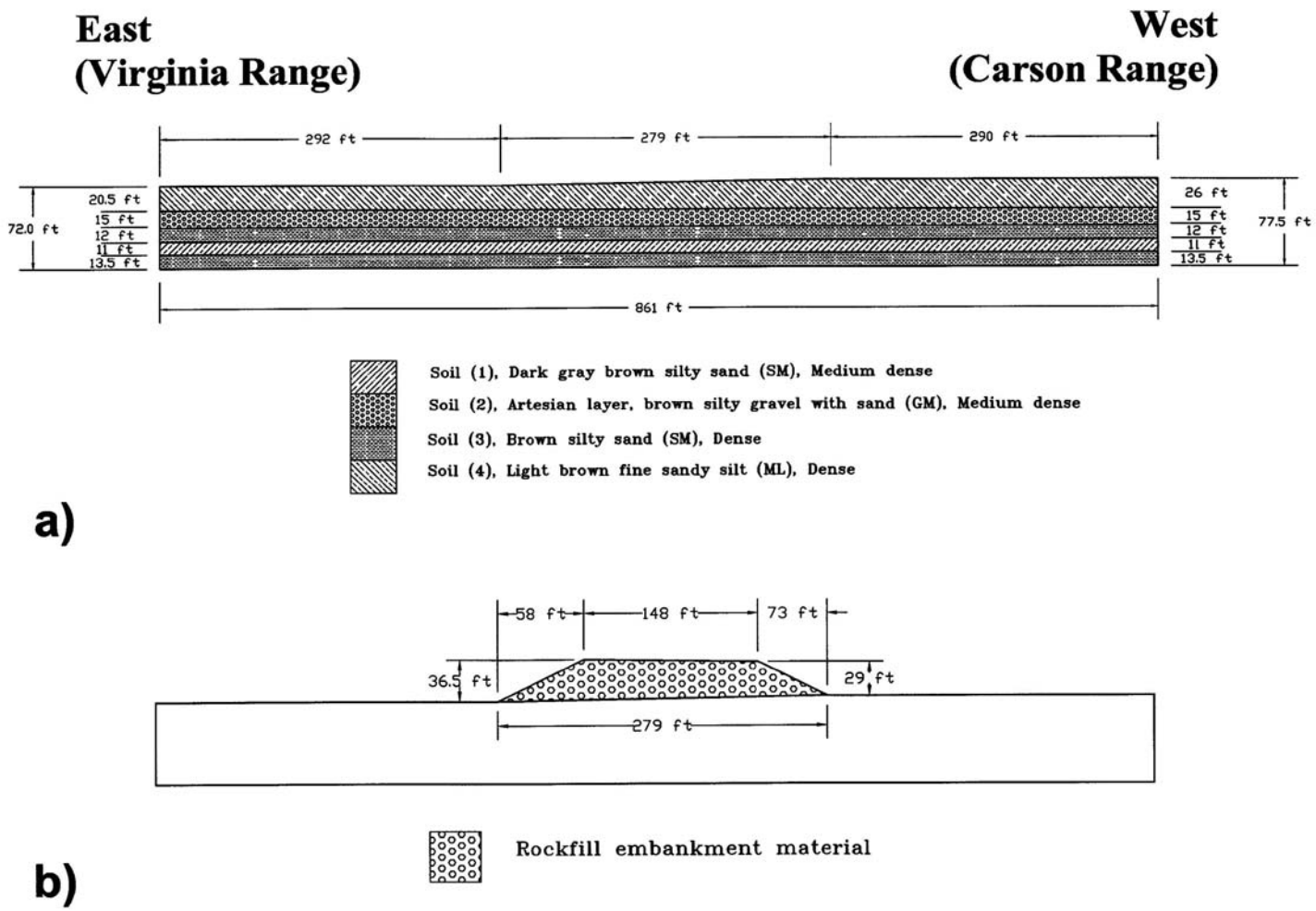

FIGURE 3 a) Layering for Finite Element Analysis and b) Embankment Cross-Section.

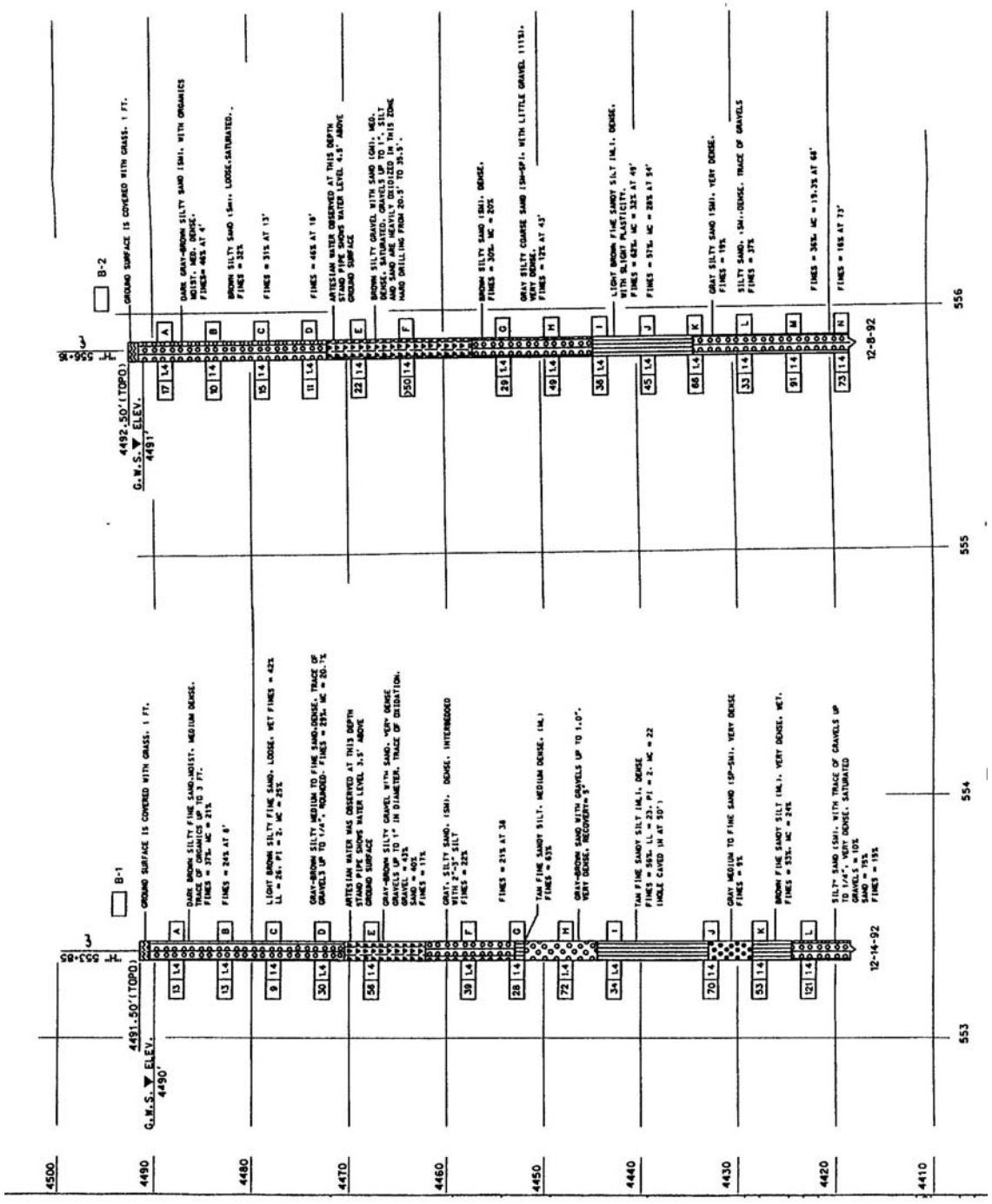

FIGURE 4 NDOT BORING LOGS

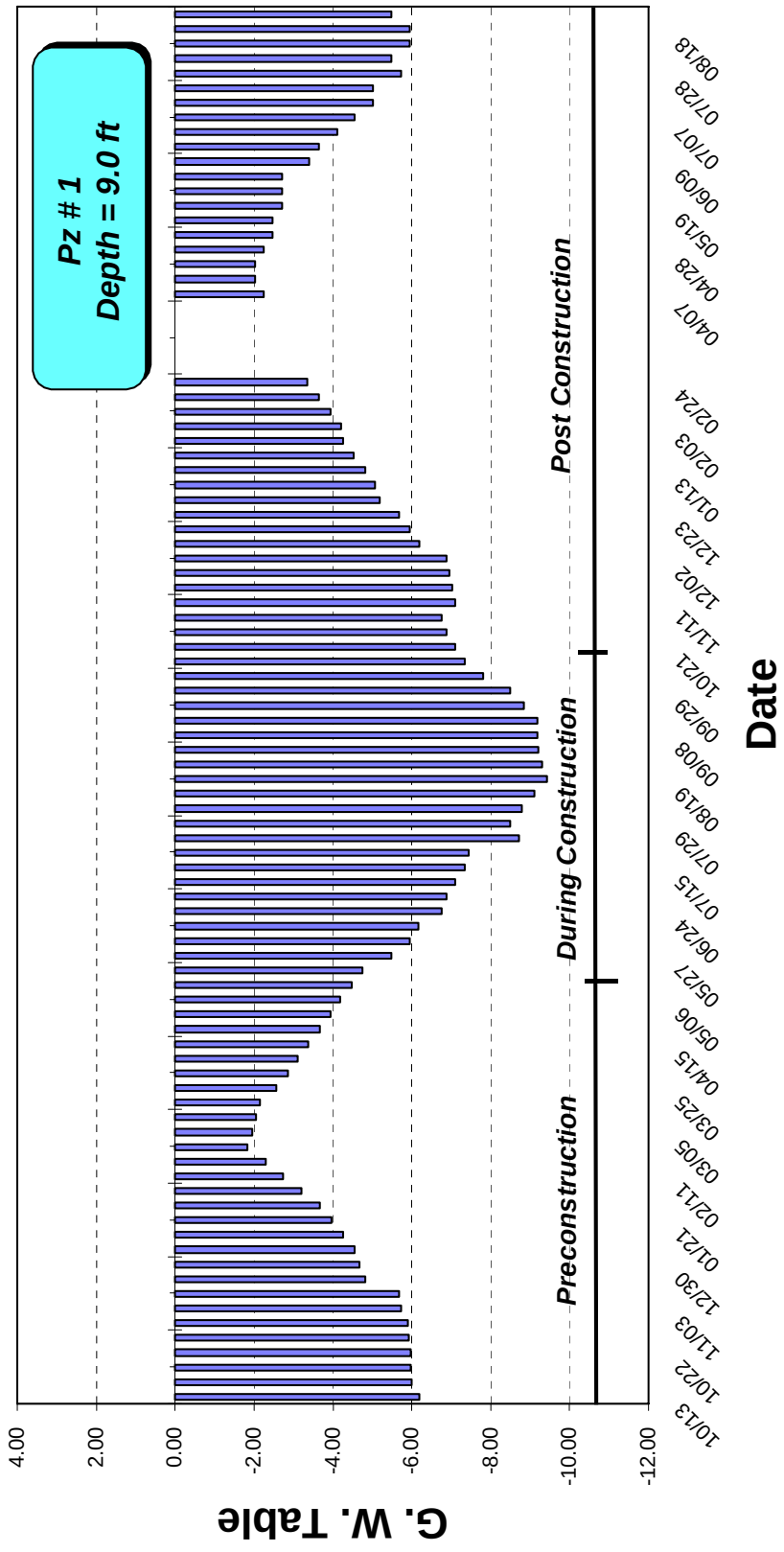

FIGURE 5 Pz1 Readings Expressed as Water Levels (Note break in record when pneumatic readout box was sent for repair and calibration).

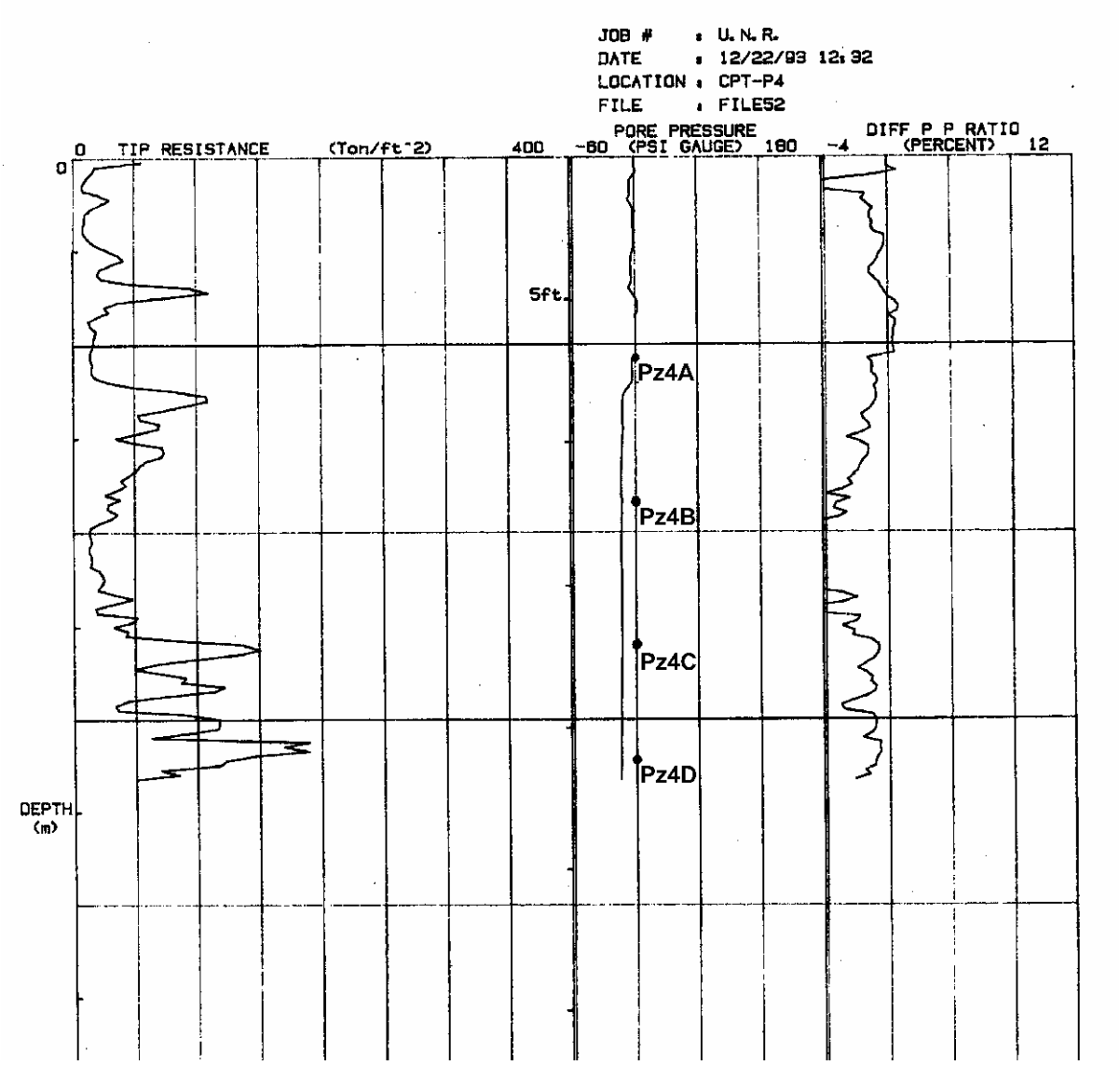

FIGURE 6 Piezo Cone Plots at Pz4.

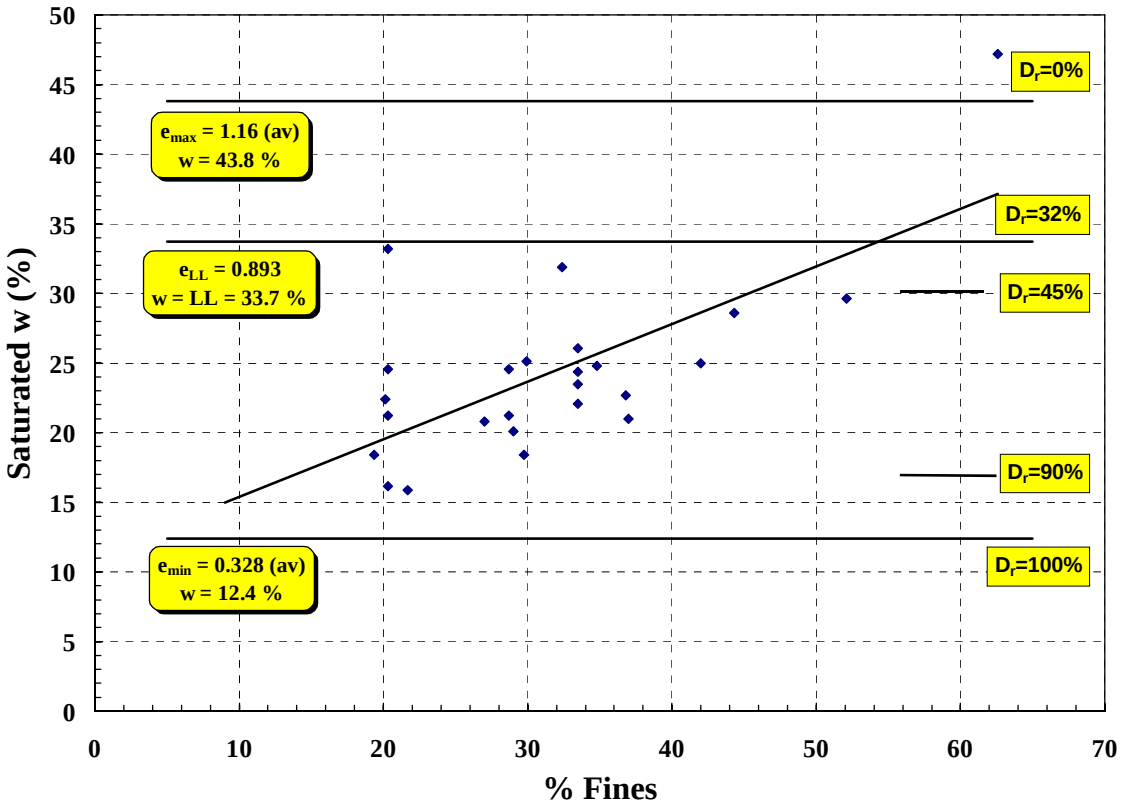

FIGURE 7 Correlation Between Saturated Water Content or Void Ratio and Percent Fines.

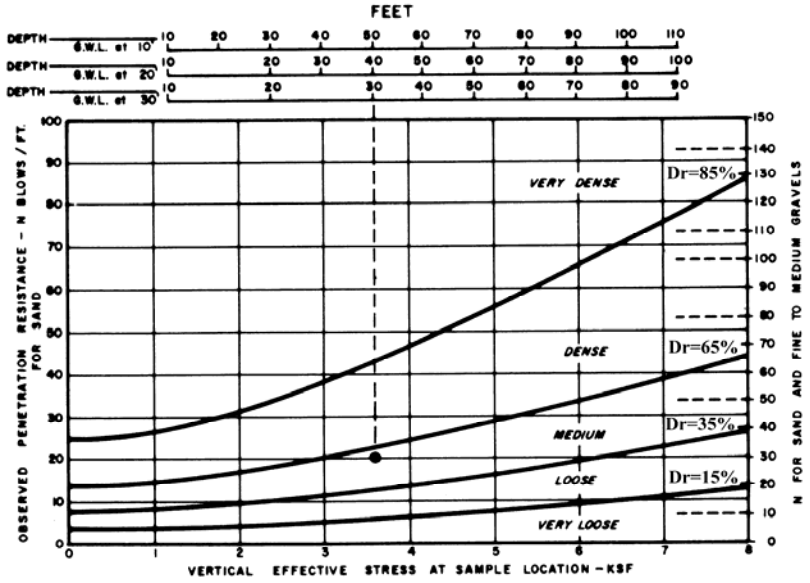

FIGURE 8a Estimated Compactness of Sand From Standard Penetrartion Test (DM-7) (With Terzaghi and Peck D_r Limits Added)

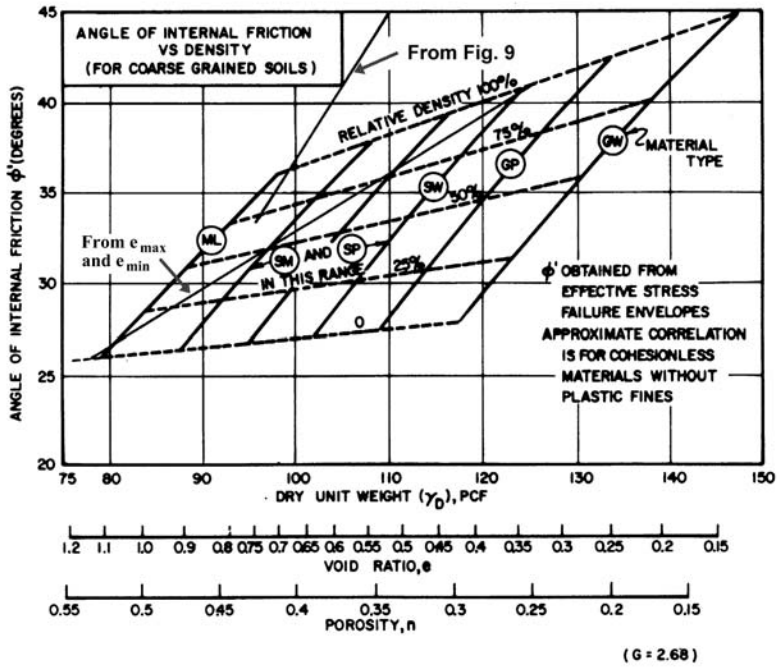

FIGURE 8b Correlations of Strength Characteristics For Granular Soils (DM-7)

FIGURE 8 Correlations for a) D_r and b) ϕ (from DM-7).

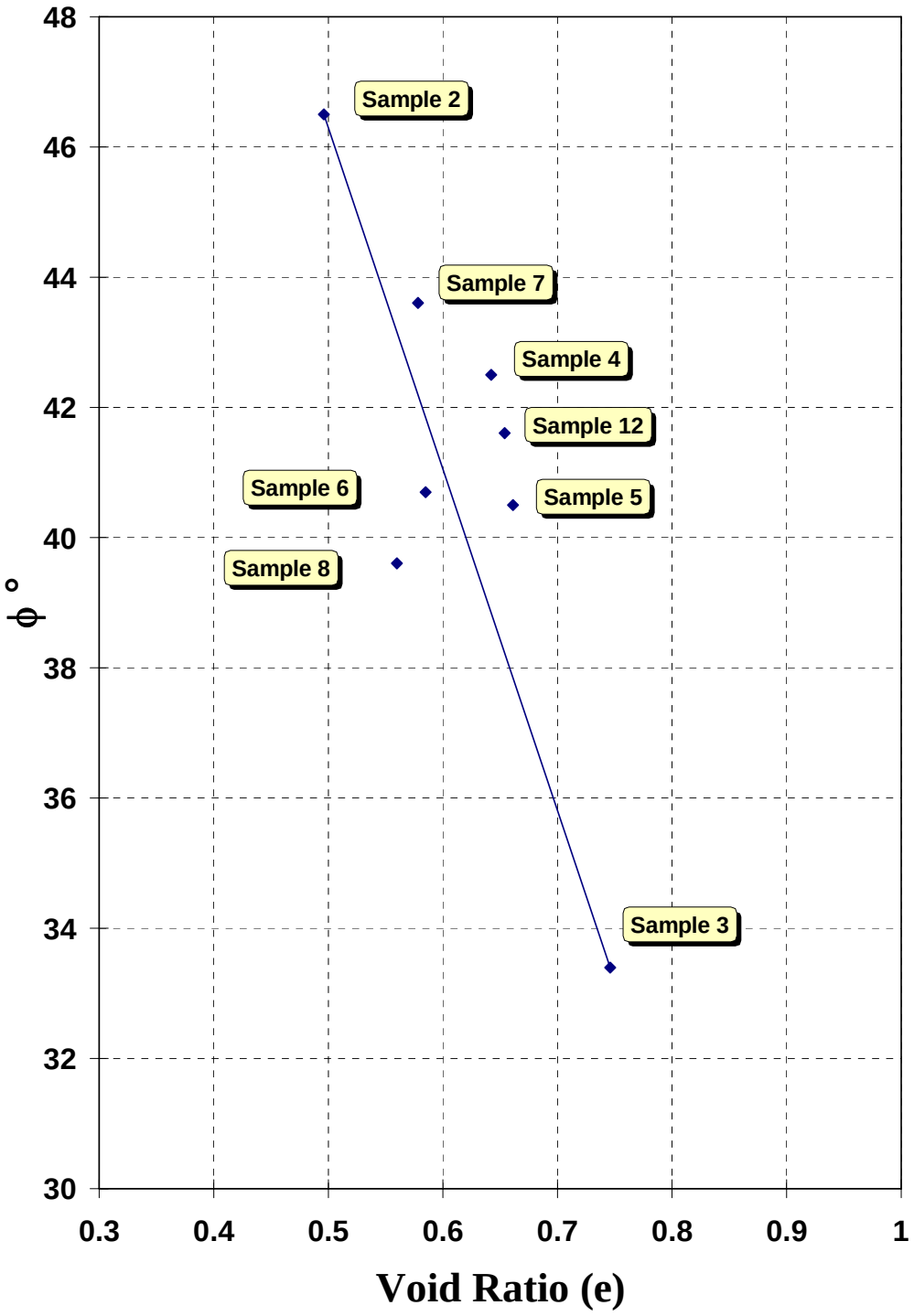

FIGURE 9 Correlation Between Drained or Effective Stress Friction Angle from Standard Triaxial Tests and Void Ratio.

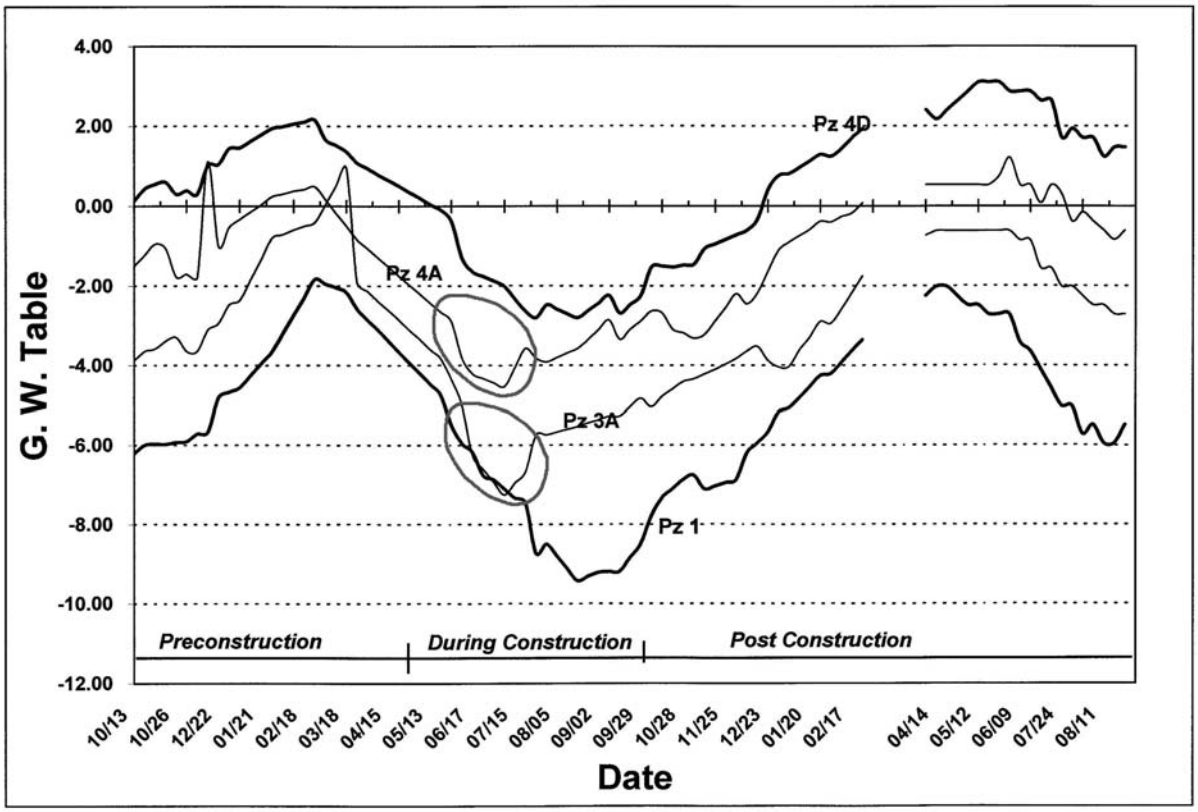

FIGURE 10 Pz 3A and Pz 4A Pore reading Profiles.

Petrography of Coarse Aggregates Used in Design of Stone Matrix Asphalt Pavements in Indiana

Terry R. West, Brandon J. Celaya, and John E. Haddock
550 Stadium Mall Drive, EAS Dept., Purdue University, West Lafayette, IN 47907-2051
Telephone: 765-494-3296; email: trwest@purdue.edu

ABSTRACT

Research was conducted on stone matrix asphalt (SMA) pavements, a replacement for conventional, hot mix asphalt based on the new Superpave design procedure (Celaya, 2005). Six different Indiana coarse aggregates were included: blast furnace slag, three crushed, stream gravels and two crushed dolomites. Aggregate quality tests included: Los Angeles abrasion loss, Micro-Deval loss, aggregate degradation under Superpave Gyratory compaction and particle shape (flat and elongated evaluation). These results were correlated with VMA, voids in mineral aggregate, a measure of asphalt pavement performance. The Micro-Deval test and the compaction degradation test provided the highest correlation with VMA. As a follow up study, the first author performed a detailed megascopic, petrographic analysis on the six aggregates. Specific petrographic data were compared to the VMA correlation results to show how aggregate composition and texture relate to asphalt pavement performance. Results are provided in the paper.

INTRODUCTION

Stone Matrix Asphalt (SMA) originated in Europe about 35 years ago. (Brown and Mallick, 2003) Its original purpose was to yield pavements capable of resisting abrasion due to studded tires. An added benefit of SMA was found, it provided resistance to rutting, a common failure mechanism for asphalt pavements. Maryland and Georgia were the first states to construct SMA pavements. In slightly more than ten years, Maryland has completed more than 85 SMA projects, yielding about 1,300 lane miles of paving (Kuennen, 2003).

Based on the new Superpave design procedure (Celaya, 2005), SMA is a gap-graded hot-mix asphalt (HMA) mixture composed of a coarse aggregate skeleton and a binder-rich mortar. According to a national study (National Asphalt Pavement Association, 1994) a suggested maximum loss in Los Angeles Abrasion of 30% has been proposed for SMA aggregates. This is in contrast to the maximum allowable LA abrasion loss of 40% for hot mix asphalt (HMA) and portland cement concrete pavements (INDOT, 2005, Specifications).

SMA is considered to be a premium paving material with an expected service life of 20 to 30% greater than conventional, dense-graded HMA mixes (Kuennen, 2003). This longer service life is achieved through increased durability and increased resistance to permanent deformation. Increased durability is accomplished by the higher content of binder mortar used to hold the coarse aggregate together. In addition, the increased resistance to permanent deformation is achieved by the stone-on-stone contact between the coarse aggregate pieces. However, the increase in performance by SMA comes at a cost, 20 to 30 percent more than HMA, with the extra cost attributed mainly to production expenses for SMA. Currently this extra cost seems to be warranted, as compared to HMA (Kuennen, 2003) because of the longer life of SMA achieved.

Blast furnace slag has been the preferred coarse aggregate for SMA because of its high strength and durability. However, because of its high density and limited source area in Indiana (mostly the northwest portion of the state), slag is expensive to ship which prevents a wide distribution of the material.

A total of six coarse aggregate sources were considered in the study (Celaya, 2005). The following aggregates were included: blast furnace slag, three crushed gravels and two crushed dolomites. Laboratory testing included Los Angeles abrasion loss, the Micro-Deval loss, flat and elongated measurements, and degradation caused by Superpave Gyratory Compactor testing. These results were correlated with VMA, voids in mineral aggregate, a measure of asphalt pavement performance. This completed the initial study (Celaya, 2005) on SMA for Indiana aggregates. As a follow up analysis, the current research adds the petrographic evaluation of the six aggregates to

determine how their composition and texture relate SMA to performance. This work was accomplished by the first author who has presented several research reports previously on highway aggregates at the Highway Geology Symposium (Bruner et al., 1994; West, 1995; West and Park, 1996; West, 1998; West, 2000; Cho and West, 2001; West and Cho, 2002).

LABORATORY TESTING

Los Angeles Abrasion Loss

The Los Angeles abrasion test was conducted in accordance with ASTM C 131, Degradation of Small Size Coarse Aggregates by LA Abrasion (ASTM C 131, 2003). This familiar test, known as the "LA Rattle Test" involves a drum of graded aggregates and steel spheres rotated for 500 revolutions and the loss in fine particles is determined by sieving the sample over the #12 screen. The test is conducted under dry conditions. A maximum loss of 30% for the SMA aggregates has been proposed for national consideration (National Asphalt Pavement Association, 1994). Five of the six aggregates achieved LA loss values less than 30%, whereas Dolomite B had a loss of 30.7

Micro-Deval Abrasion Loss

The Micro-Deval test is used to determine aggregate abrasion loss in the presence of water, as contrasted to the dry, LA abrasion test. Conducted with wet aggregate, the Micro-Deval test considers the influence of water on aggregate degradation (Meininger, 2004). The test was performed in accordance with ASTM D6928, Standard Test Method for Resistance of Coarse Aggregate to Degradation by Abrasion in the Micro-Deval apparatus (ASTM D6298, 2003).

In the Micro-Deval test, the sample weighing 1500 ± 5g is soaked in 2.0 ± 0.05 liters of tap water for a minimum of one hour (ASTM D6298, 2003). Gradations used for testing were 750g for the fraction from 9.5 to 6.3 mm (3/8 in to 1/4 in) and 750g for the fraction from 6.3 to 4.75 mm (1/4 in to No. 4 sieve). Additionally, 5000 ± 5g steel spheres were added and testing proceeded. The Micro-Deval machine rotated at a rate of 100±5 rpm for 95±1 minutes. Following the test, the steel spheres were removed and the sample was dried. Subsequently, the dry sample was sieved over the No. 16 sieve (1.18 mm). The original weight minus the dry weight, divided by the original weight yields the Micro-Deval abrasion Loss.

Test results for the six samples ranged from 4.2 to 24.7% loss. Typically a maximum loss of 18% is considered for acceptance of concrete and asphalt aggregates. Only Dolomite B, which had a value in excess of 18, fell into the unacceptable category according to this test.

Flat and Elongated.

The flat and elongated test was conducted on the crushed coarse aggregate samples. INDOT (INDOT, 2005) specifications require an evaluation by count for dimensional ratios of 3 to 1 and 5 to 1 with a maximum allowable value of 20% and 5%, respectively for the two dimensional ratios mentioned above. All six crushed aggregates had results that fell within the acceptable amount of flat and elongated particles so that this condition was not an issue for these aggregates. Aggregate shapes that are more equidimensional yield a stronger skeleton which is desirable under the Superpave Design procedure. The lack of flat and elongated pieces in the six aggregates is an assurance that a stronger skeleton is obtained.

Compaction Degradation

Aggregate degradation by the Superpave Gyratory Compactor (SGC) was used to evaluate degradation by the compaction process during construction of stone matrix asphalt pavements (Brown et al., 1997). In order to test the aggregates during SGC compaction, a mix design was completed for each combination of materials according to AASHTO MP8, "Standard Specification for Designing Stone Matrix Asphalt (SMA)". Specimens prepared at the optimum binder content were compacted in the SGC using 100 gyrations. When the specimens had cooled properly, the asphalt binder was extracted according to AASHTO T308 "Determining the Asphalt Binder Content of Hot-Mix Asphalt (HMA) by the Ignition Method". This is the method most applicable to SMA samples. For each specimen, gradations of the remaining aggregates were determined according to AASHTO T11, "Materials Finer Than 75-μm (No.200) Sieve in Material Aggregates by Washing" and T27, "Sieve Analysis of Fine and Coarse Aggregates".

These aggregate gradations from the specimens compacted by the SGC were then compared to gradations from specimens that were mixed, but not compacted. The objective was to determine the amount of aggregate degradation occurring during the SGC compaction process.

Volumetric Properties of SMA

The volumetric properties of interest in SMA samples are voids in the mineral aggregate (VMA) and voids in the total mixture (VTM). VMA is the volume of voids filled by the asphalt binder and air between the coarse mineral aggregates. VTM is the air voids in the specimen. These volumetric properties are determined during the mix design procedure for the SMA samples. The VTM or air voids, as specified by INDOT, must be 4.0% at optimum binder content. The VMA is specified to be a minimum of 17.0% at the optimum binder content.

The laboratory test results for the five samples discussed previously are presented in Table 1. Note that the specifications were not met for VMA of the dolomite aggregates as both have values less than the required 17%. Also note that the compaction loss for both dolomite samples during supercompaction is significantly greater than for the other four samples (Slag, plus Gravels A, B and C). A comparison of values for VMA suggests that a maximum of 3% for the SGC compaction loss delineates acceptable from nonacceptable aggregate materials.

PETROGRAPHIC EVALUATION

A petrographic examination was performed on the three gravel samples. All consisted of crushed gravel particles less than 12.7 mm (1/2 inch) in size. The coarse fraction between 12.7 and 9.5 mm (1/2 to 3/8 inch) was examined. For megascopic evaluation a minimum of 300 pieces must be considered (ASTM C295), Petrographic Examination of Aggregate for Concrete. For the three samples the number of pieces ranged from 506 to 622. A difference in the overall appearance of the three gravel samples was noted. Gravel A consisted of gray, pink, white and some black pieces and Gravel C was similar, but not quite as dark. Gravel B consisted of brown, white and some gray pieces. This is in keeping with the higher carbonate content of Gravel B.

Results of the analysis are presented in Table 2 along with the LA abrasion loss of these aggregates as determined in the current study. The three LA abrasion values are similar, ranging from 18.9 to 20.3% loss, all well below the maximum loss of 30% required for SMA aggregates prescribed by the National Asphalt Association, 1994. Note that the total carbonate percentage of the samples is 27% or less, the total sedimentary rock percentages is 44% or less and the total igneous and metamorphic rock percentages range from 41.8 to 67.1%. In all, this indicates that harder, non-sedimentary portions make up a major part of the samples. Presumably some of the weaker, sedimentary materials i.e. shales and siltstones, were removed by the crushing process.

The two dolomite sources were also evaluated in a previous Indiana aggregate study on frictional resistance of wearing surfaces for asphalt pavements (West and Kuo, 2002). In that study (Table 3) the frictional resistance of aggregate coupons was determined using the British Polishing Wheel and Pendulum Testing Procedures (ASTM D3319-90 and E303-83). In these tests, three values are obtained, IFV, PV and WI. These designate Initial Friction Value; Polish Value, which is the friction value obtained after polishing is completed; and WI, wear index, the difference between IFV and PV, which represents the amount of polishing or loss that occurred during the polishing test.

An interesting comparison can be made between Dolomite A and Dolomite B using the data in Table 3. First, note the dolomite content in the two samples. Dolomite A is nearly a pure dolomite, 94.1%, and the insoluble residue is only 1.7%. This suggests that the remainder, 4.2% is calcite. That portion of the insoluble residue finer than the number 200 sieve size is likely clay (0.48%), whereas the greater than #200 sieve size is mostly quartz. Despite the purity of this dolomite, the friction resistance of the aggregate is only PV = 24.9%. Research on frictional resistance (West and Cho, 2002) indicates that a minimum of 25% PV is a good target for friction resistance of bituminous wearing courses. Obviously Dolomite A barely qualifies as an acceptable aggregate in this regard.

Next examining the data for Dolomite B, Table 3 shows a dolomite content of 85% and a clay content of 4.55% (less than #200 size, insoluble residue portion). This correlates well with the sulfate soundness loss of 13.18% which is quite high as 12% loss is the maximum allowed for Class A stone according to INDOT (use as concrete and asphaltic pavements) (INDOT, 2005). Ironically, however, the PV for this aggregate is 32.00%, well above 25%,

indicating it is perfectly satisfactory as a frictional resistant aggregate for surface wearing courses of asphalt overlays. The absorption for Dolomite B is 4.00% as contrasted to the 0.79% for Dolomite A, which also has a sulphate soundness loss of 0.36%. This also suggests that Dolomite A is considerably more durable than is Dolomite B as an aggregate material.

Returning now to Table 1, Dolomite A has a Micro-Deval loss of 8.9% and a compaction loss of 5.0%, whereas Dolomite B has a Micro-Deval loss of 24.7 and a compaction loss of 7.4%. Clearly Dolomite A is a better quality aggregate for use in stone matrix asphalt than is Dolomite B. Both dolomites, however, fall short of the required VMA value of 17% that is preferred for stone matrix asphalt aggregates.

Finally, a comparison between the gravel composition shown in Table 2 and the results in Table 1 is revealing. Based on Table 1 Gravel B has the highest LA abrasion loss, 20.3%, highest Micro-Deval loss, 8.1% and the greatest compaction loss 2.1%. Also, in Table 2, Gravel B has the greatest percent of sedimentary rock, 44% as compared to 34.7 and 33.4% for Gravels A and C respectively. It also has the highest percentages of limestone, typically a weaker constituent of Indiana gravels. Gravel B contains 14.1% limestone as compared to 7.4 and 8.3% respectively for Gravels A and C. The brownish overall color of the gravel particles as contrasted to darker appearance of Gravels A and C indicates the predominance of sedimentary rocks in Gravel B.

DISCUSSION OF RESULTS AND CONCLUSIONS

Six coarse aggregates were investigated for use in Stone matrix Asphalt construction. Blast furnace slag and the three gravel samples would be acceptable based on compaction loss and VMA values. The two dolomites showed too much degradation due to SGC compaction loss and they also were unable to achieve the 17% requirement for VMA

Four laboratory tests were used in the evaluation: LA Abrasion, Micro-Deval, flat and elongated and compaction degradation by the supercompaction device. With VMA as the controlling factor for acceptance, Micro-Deval loss was found to have the highest correlation. This relationship is preferred over LA abrasion loss as Micro-Deval loss accounts for the presence of water in the degradation process. The flat and elongated analysis did not provide any guidance to the evaluation as all crushed materials met this criteria, showing a lack of platy-shaped pieces in the samples.

The proposed value of 30% maximum LA loss is not a sufficient requirement alone for SMA aggregates, as Dolomite A had a loss of 23.7%, but yielded a VMA value less than the required 17.0% (15.6% obtained). Dolomite B performed the worst, with a high Micro-Deval loss (24.7%), a high SGC compaction loss (7.4%) and a low VMA, less than 17% (15.9%). A maximum loss of 18% for Micro-Deval loss has been suggested for Class A aggregates, but this seems too high for this application. Dolomite A had a Micro-Deval loss of 8.9%, but showed a SGC compaction loss of 5.0% and a VMA of 15.6%. A maximum of 3.0% and minimum of 17% have been suggested for compaction loss and VMA, respectively. Micro-Deval loss and compaction degradation correlated best with VMA.

The petrographic examination showed why Dolomite A performed better than Dolomite B due to its greater durability indicated by a lower sodium sulfate loss, and lower absorption and insoluble residue content. The rock composition data on the three gravel samples also indicated why Gravel Sample B performed somewhat poorer than did Gravel Samples A and C, because it contained more soft rocks, the sedimentary portion. Data on the two dolomite samples also pointed out the paradox that a seemingly lower quality aggregate (Dolomite B) performs better in frictional resistance of bituminous wearing courses than does the better quality aggregate (Dolomite A). This is because the higher clay content in Dolomite B yields an uneven surface on the aggregate pieces, providing a greater resistance to polishing (see West and Cho, 2002).

REFERENCES

AASHTO MP8, Standard Specifications for Designing Stone Matrix Asphalt (SMA).

AASHTO T11, Materials Finer than 75μm (No.200) Sieve in Material Aggregates by Washing.

AASHTO T27, "Sieve Analysis for Fine and Coarse Aggregates".

AASHTO T308, "Determining the Asphalt Binder Content of Hot-Mix Asphalt (HMA) by the Ignition Method".

ASTM, C131, Standard Test Method for Resistance to Degradation of Small-Size Coarse Aggregate by Abrasion and Impact in the Los Angeles Abrasion Machine, Annual Book of Standards, 2003.

ASTM, C295, Standard Practice for Petrographic Examination of Aggregate for Concrete, Annual Book of Standards, 2003.

ASTM, D6928, Standard Test Method for Resistance of Coarse Aggregates to Degradation by Abrasion in the Micro-Deval Apparatus, Annual Book of Standards, 2003.

ASTM, E303, Standard test method for using the British Polishing Wheel and Pendulum Tester, Annual Book of Standards, 2002.

ASTM, D3319, Standard test method for accelerated polishing of aggregates using the British Wheel, Annual Book of Standards, 2002.

Brown, E.R., John E. Haddock, Rajib B. Mallick and Todd A. Lynn, 1997, Development of a Matrix Design Procedure for Stone Matrix Asphalt (SMA), Journal of the Association of Asphalt Paving Technologists, vol. 66, pp. 1-30.

Brown, E.R. and Rajib B. Mallick, 2003, "Experience with Stone Matrix Asphalt in the United States", National Asphalt Pavement Association, NCAT Report No.03-05, December.

Bruner, D.W., J.C. Choi and T.R. West, 1994, "Evaluation of Indiana Aggregates for Use in Bituminous Highway Overlays", Proceedings, 45th Highway Geology Symposium, pp. 201-212, August, Portland, Oregon.

Celaya, Brandon J., 2005, Investigation of Coarse Aggregate Strength for Use in Stone Matrix Asphalt (SMA), M.S. Thesis, Purdue University, School of Civil Engineering, December.

Cho, K.H. and T.R. West, 2001, "Evaluation of Carbonate Aggregates for Bituminous Overlays in Indiana", Proceedings, 52nd Highway Geology Symposium, pp. 81-90, Rocky Gap, MD, May.

Indiana Department of Transportation (INDOT), 2005, Standard Specifications.

Kuennen, Timothy, 2003, Stone Matrix Asphalt is Catching on in the U.S., Better Roads, September.

Meininger, Richard, 2004, "Micro-Deval vs L.A. Abrasion", Rock Products, April 1.

National Asphalt Pavement Association, 1994, "Guidelines for Materials, Production and Placement of Stone Matrix Asphalt (SMA), IS 188, Lanham, MD

West, T.R., 1995, "Evolution of a Technique: Petrography of Aggregates for Concrete and Bituminous Pavements", Proceedings, 46th Highway Geology Symposium, pp. 166-176, Charleston, West Virginia, May.

West, T.R., 1998, "Evaluation of Crushed Stone Used for High Traffic Bituminous Pavement Wearing- Courses in Indiana", Proceedings 49th Highway Geology Symposium, pp. 388-398, Prescott, AZ, Sept.

West, T.R., 2000, "Deleterious Constituents in Indiana Aggregates: A Challenge for Non-Geologists to Identify", Proceedings, 51st Highway Geology Symposium, pp. 61-64, Seattle, WA, August.

West, T.R. and K.H. Cho, 2002, "Petrography of Gravel Aggregates for Indiana Bituminous Pavement Overlays", Proceedings, 53rd Highway Geology Symposium, pp. 316-327, San Luis Obispo, CA, August.

West, T.R. and H.J. Park, 1996, "Rock Durability of Argillaceous Carbonate Rocks in Cut Slopes for Indiana Highways", Proceedings, 47th Highway Geology Symposium, pp. 183-205, Cody, WY, Sept. 6-9.

Table 1. Test Data for Stone Matrix Asphalt Aggregates.

	LA Abrasion Loss, %	Micro Deval. %	Compaction Loss %	VMA	VTM
Slag	15.7	4.2	0.2	17.1	4.2
Gravel A	18.9	7.7	1.3	17.8	4.0
Gravel B	20.3	8.1	2.1	17.4	4.0
Gravel C	19.3	7.8	1.8	17.7	4.1
Dolomite A	23.7	8.9	5.0	15.6	3.9
Dolomite B	30.7	24.7	7.4	15.9	4.0

VMA = Voids in mineral aggregates
VTM = Air voids in specimen

Table 2. Rock Type Content, Crushed Glacial Gravel, 1/2 - 3/8" fraction.

Sample	A	B	C
LA Loss, %	18.9	20.3	19.3
	Percent Present		
Granite	12.4	5.2	9.6
Rhyolite	1.9	1.2	3.0
Diorite	12.8	8.6	18.2
Basalt	23.3	7.8	10.0
Andesite	5.2	6.1	9.6
Quartzite, hard & siliceous siltstone	9.5	24.2	14.2
Quartzite slightly weathered	-	3.7	1.5
Chert, hard	6.3	16.6	15.8
- weathered	1.4	3.2	1.7
Limestone	7.4	14.1	8.3
Dolomite, hard	16.7	9.3	8.1
- weathered	2.0	--	--
- deeply weathered	1.1	--	--
TOTAL	100.0	100.0	100.0
Carbonates	27.2	23.4	16.4
Igneous	55.6	28.9	50.4
Metamorphic	9.5	27.9	15.7
Other Sedimentary	7.7	19.8	17.5
TOTAL	100.0	100.0	100.0

Table 3. Laboratory Testing Data, Dolomite Aggregates for Stone Matrix Asphalt Samples.

Id. No.	IFV	PV	WI	Absorption %	Sp.Gravity	LA Abrasion Loss, %	Sulfate Soundness Loss, %	Mg (%)	Dolomite (%)	Insol Residue (Total)	>#200 %	<#200 %
Dolomite A	40.00	24.90	15.10	0.79	2.732	25.53	0.36	12.40	94.1	1.70	1.22	0.48
Dolomite B	46.70	32.00	14.70	4.00	2.480	30.28	13.18	11.20	85.0	5.27	0.72	4.55

TECHNICAL SESSION V
Hazards

Guess What Dropped in for Breakfast?

Joseph A. Fischer, P.E.
James G. McWhorter, P.G.
Geoscience Services, 3 Morristown Rd., Bernardsville, NJ 07924
(P)908-221-9332; (F)908-221-0406; geoserv@hotmail.com

Andrew Salmaso, VP
Janod Contractors, P.O. Box 2487, Champlain, NY 17919
(P) 518-298-5226; andrew@janod.biz

ABSTRACT

Rock Creek Crossing is a small enclave of some 172 town homes and apartments in Riverdale, New Jersey. Development of the property took place some 12 to 15 years ago by cutting into the Proterozoic gneisses of the New Jersey Highlands. Protection was not afforded to the slopes left behind, which, in several cases were near-vertical and up to 80 feet in height. The majority of the slopes were essentially parallel to strike, with foliation dipping steeply (>60 degrees) out of the faces.

The senior author's firm was retained in the spring of 2004 to perform a reconnaissance level engineering geologic assessment of the site. Subsequent geologic mapping and limit equilibrium analyses of the data collected resulted in factors of safety of the slopes ranging from about 1 to 1.4 in areas of potential failure indicated by stereographic projection plots, suggesting that the slopes were in danger of failure. Initial recommendations consisted of installation of TECCO® Mesh and rock bolts on most of the pre-split faces with tensioned DCP bolts for a number of severe rock overhangs in slopes behind buildings, after scaling. The slopes were "triaged" according to their condition and location, with higher priority given, obviously, where slopes were more likely to impact nearby occupied buildings. Our report sat for several months until the morning of February 24, 2005, when a 35-ton wedge of biotite-quartz-feldspar gneiss dropped out of the access road slope. The road has since remained closed until recently when emergency remedial efforts on the sections deemed most dangerous were completed by Janod Contractors.

INTRODUCTION

In the early spring of 2004, Geoscience Services (GS) was contracted by an architectural/engineering (A/E) firm representing the Home Owner's Association (HOA) of Rock Creek Crossing, a 172-unit townhouse/condominium development in the town of Riverdale in northern New Jersey. The development was constructed by cutting into the side of a till-covered hillside of faulted and fractured metamorphic, crystalline rock. Concerns were voiced by the A/E in regard to a large overhanging "face" of rock near the corner of a three-story residential building. A GS representative visited the site with the A/E.

That visit was enough to engender serious concern for the potential loss of life and property damage from the obvious signs of rock slope instability *throughout the site*. A preliminary analysis of the geotechnical conditions was undertaken under a limited budget. At that time, the HOA was about to take over responsibility for the site from an apparently unknown developer. The site planning and initial site work had started in the early 1990s, moving through the municipal approval system with fits and starts as a number of different engineers and developers worked on or reviewed the work of others for the site. Final design criteria for the rock cuts, essential to developing most portions of the site, were noted as "cut to stable slopes or construct retaining walls". Apparently, the rock slopes were developed both by ripping along foliation and intersecting joints, and a nominal amount of conventional drilling and blasting. The apparent ease of "rippability" of this rock would attest to its overall susceptibility to future movement along fractures. In addition, weathering, likely occasioned by water moving through fractures, was evident to varying degrees in all of the existing slopes.

GEOLOGY

As shown on Figure 1, the various bedrock formations below the site generally differ only in type and proportion of their mineral constituents. Unfortunately, most contain layers of easily weathered amphibolite. Possible failure types expected for the conditions at this site are, planar, wedge (or a combination thereof), toppling, and raveling. In addition, boulders and cobbles in the overlying till soils occasionally rolled down the slopes where development and erosion exposed the till. A total of 3,000 feet of suspect slope was estimated from preliminary slope-stability analyses. Remediations costs were roughly estimated to be in the 2 to 3 million-dollar range.

In addition, some 375 to 400 linear feet of undesigned boulder retaining wall was observed, but not evaluated at this time other than to warn the interested parties of the probable danger of rocks and wall failures

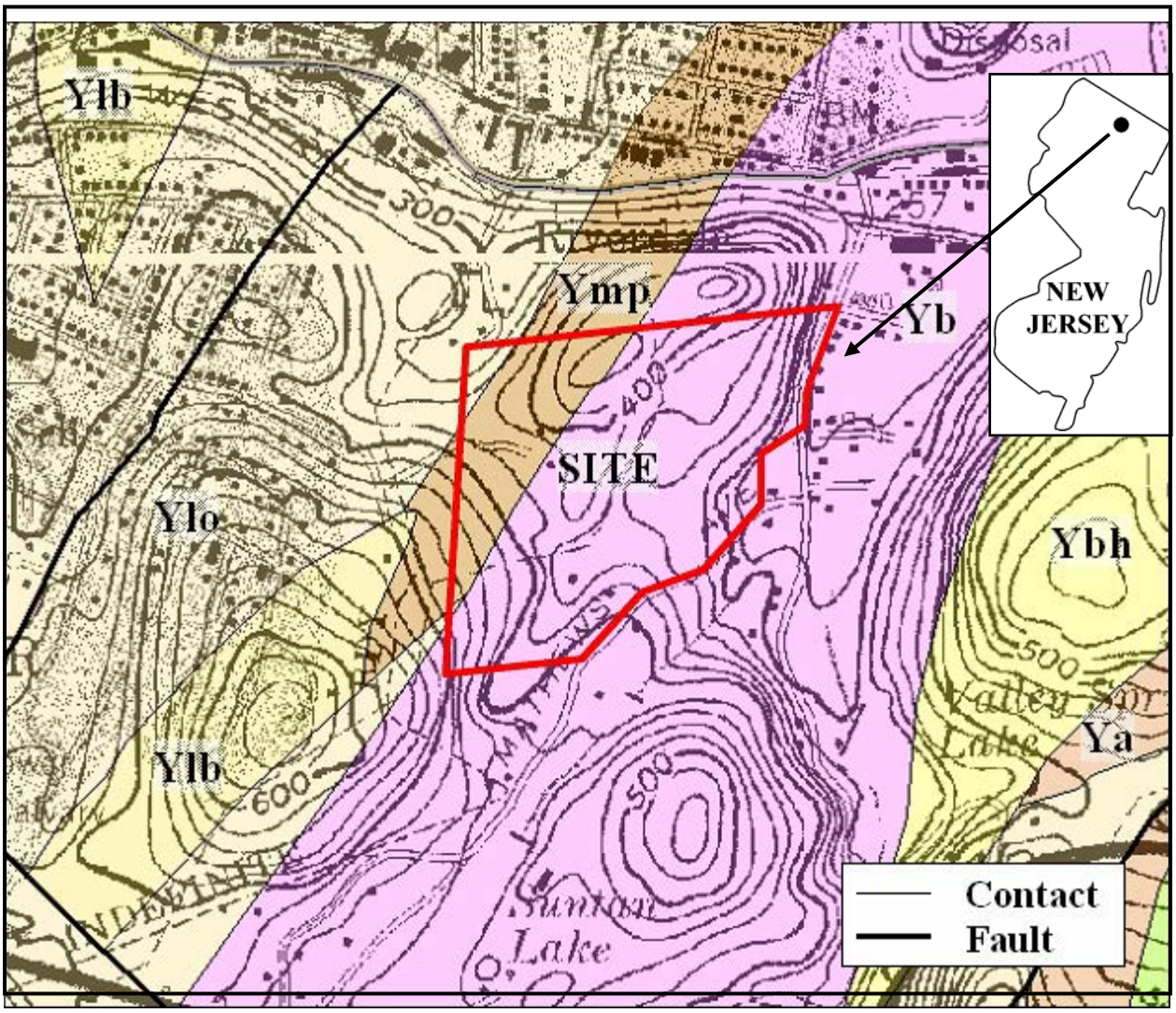

Figure 1 – Geology Map Showing Site

The preliminary report (April 2004) identified the local geology (see Figure 1). The various rock types shown on Figure 1 are:

Yb: Biotite-quartz-feldspar gneiss - Gray-weathering, locally rusty, gray to tan or greenish-gray, fine- to medium-coarse-grained, moderately layered and foliated gneiss that is variable in texture and composition. Composed of

oligoclase, microcline microperthite, quartz, and biotite. Locally contains garnet, graphite, sillimanite, and opaque minerals.

Ymp: Clinopyroxene-quartz-feldspar gneiss - Pinkish-gray- or pinkish-buff-weathering, white to pale pinkish-white or light-gray, fine- to medium-grained, massive to moderately well-layered gneiss composed of microcline, quartz, oligoclase, clinopyroxene, and trace amounts of epidote, biotite, titanite, and opaque minerals. Commonly interlayered with amphibolite or pyroxene amphibolite.

Ylo: Quartz-oligoclase gneiss – White-weathering, light-greenish-gray, medium- to coarse-grained, moderately layered to indistinctly foliated gneiss and lesser amounts of granofels composed of quartz, oligoclase or andesine, and, locally, biotite, hornblende and (or) clinopyroxene. Contains thin amphibolite layers.

Ylb: Biotite-quartz-oligoclase gneiss – White- to light-gray-weathering, light- to medium-gray or greenish-gray, fine- to coarse-grained, massive to moderately well layered, foliated gneiss composed of oligoclase or andesine, quartz, biotite, and, locally, garnet. Commonly interlayered with amphibolite.

Ybh: Hornblende granite – Pinkish-gray- to medium-buff-weathering, pinkish-white or light-pinkish-gray, medium- to coarse-grained, gneissoid to indistinctly foliated granite and sparse granite gneiss composed principally of microcline microperthite, quartz, oligoclase, and hornblende. Some phases are quartz syenite or quartz monzonite.

Ya: Amphibolite – Gray- to grayish-black, medium-grained amphibolite composed of hornblende and andesine. Some phases contain biotite and (or) clinopyroxene. Ubiquitous and associated with almost all other Middle Proterozoic units. Some amphibolite is clearly metavolcanic in origin, some metasedimentary, and some appears to be metagabbro.

SLOPE MAPPING

A proposal for geologic mapping and analyses shortly followed the preliminary report. Mapping started in July and continued into August. A survey line was set-up along the base of the various slopes and the geologic mapping progressed from the ground upward, including the use of a man-lift for the highest and steepest slopes. Slopes up to about 70 feet in height were mapped.

Conventional mapping techniques were used to gather a broad distribution of data regarding the attitude, orientation and condition of discontinuities present in the rock masses comprising the various slopes present at the site. Mapping was accomplished at a scale of 1-inch = 10-feet or 1-inch = 5 feet, vertical and horizontal, depending on the detail required to represent the geologic conditions observed. An articulated boom was used to reach the higher portions of slopes behind Buildings B and C and along Timber Ridge Road. Other slopes, where we physically could not get the boom truck positioned, were climbed and mapped where it was safe to do so. Specific information collected in preparing the geologic section maps included: 1) the type of rock present at that location; 2) the strike and dip of discontinuities mapped; 3) the rock mass rating, where enough diagnostic characteristics were present to make an interpretation; 4) the character and nature of any observed joint-filling material; and 5) the presence of water emanating from the mapped fractures that could affect the stability of the slopes.

A total of some 2,870 linear feet of slopes were mapped.

ANALYSES

The resultant sections of geologic data were evaluated utilizing conventional rock mechanics analytical techniques (e.g., Hoek and Bray, 1994[1]). The techniques included:

[1] Hoek, E. and J.W. Bray, 1994, *Rock Slope Engineering*, E & FN Spon, London; 358 pp.

1. *Stereographic projection of data* on an equal area stereonet, where mapped planar discontinuities are shown as traces of planes on a reference sphere in two dimensions. These traces of planes define the dips and dip directions of the mapped discontinuities as taken from the slopes in the field. This part of the analysis defines the structural fabric present in the various rock slopes at the site and affords the opportunity to evaluate whether a kinematically-possible failure mode is present in the rock mass being evaluated. There are several types of rock mass failure modes that are potentially occurring, including planar, wedge, toppling, and raveling failures. Once it had been identified that a particular failure mode was kinematically possible for a set series of mapped discontinuities for a slope, analyses were performed to evaluate the stability of the rock slope.
2. *Stability Analyses* of the various slopes present at the site employed a limit-equilibrium approach, wherein the shear strength along potential failure surfaces, the effects of pore-water pressure and the influence of external forces were considered. The geologic data gathered and analyzed under the previous item were used as input to a spreadsheet program where the basic stability equations were resolved for each case considered.

3. Assumptions as to strength properties along rock discontinuities were made in our analyses as is conventional for extensive slopes in metamorphic or intrusive rocks. The assumptions made were consistent with analyses for similar rocks in the literature (e.g., Hoek and Bray, 1994). Typically, we used a rock density of 160 pounds per cubic foot (pcf), an internal friction angle (Φ) of 30 degrees and a cohesion ranging from 200 to 400 pounds per square foot along the failure surfaces. With these assumptions as to strength (which are reasonable, not conservative), any solution to a planar or wedge type failure potential that had a factor of safety of less than 1.5 to 2 would be a candidate for some sort of remedial measure to protect the slope from failure under long term environmental conditions. Obviously, calculated safety factors on the order of 1 indicate incipient failure.

The final report was intended both as a design document and as a basis for legal action.

Five areas of greatest concern were defined upon the bases of the areas that posed the greatest risk to the residents and the presumed susceptibility to failure over time. These five areas are listed below in order of perceived importance.

1. Slope behind Building C.
2. Slope behind Building B.
3. Slope behind Building 4 and Club House.
4. Slope behind Buildings 2 and 3.
5. Slope above Timber Ridge Road.

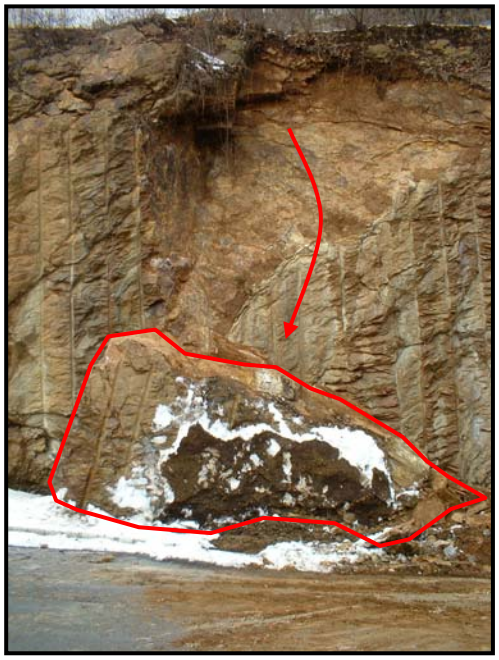

THE FAILURE

The failure in late February of 2005 occurred at Station 68+20 on Timber Ridge Rd. (see Figure 2). A block weighing an estimated 35 tons fell to the base of the slope then rolled into Timber Ridge Rd. Fortunately, it happened very early in the morning and no one was injured. Damage was limited to a collapsed catch basin within the roadway. However, the HOA was galvanized into action. The HOA's legal group was fired and a second group hired managed to locate the developer and initiate legal proceedings. The HOA was forced to obtain a bank loan in order to initiate the emergency remedial measures.

GEOLOGY OF THE SLOPE AT TIMBER RIDGE RD

The rock slopes in this portion of the site are the longest continuous slopes present at the site. Because Timber Ridge Rd. changes orientation along the descent from Mt. View Terrace to Mathews Avenue, the stability conditions along the slope change as the orientation of the rock slope face changes in relation to critical joint orientation and foliation direction.

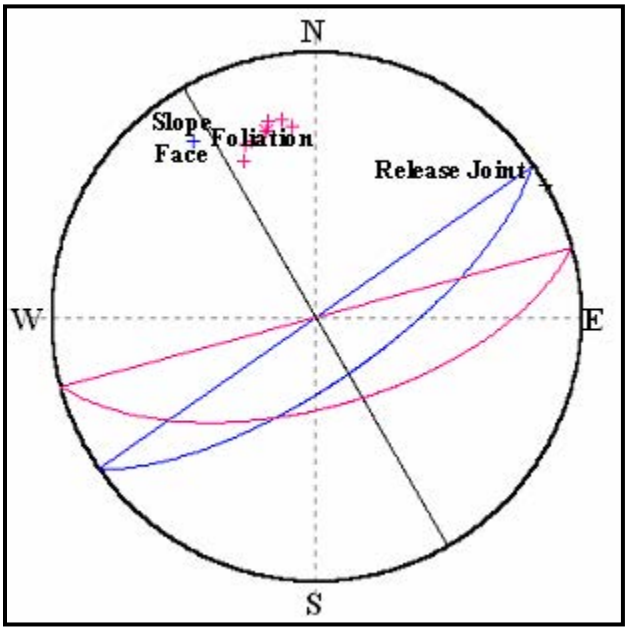

Figure 3 – Failure Surface at Timber Ridge Rd., Sta. 68+20

The general condition of the rock in this area of the site varies from extremely weathered at the northwesterly end of Timber Ridge Rd. to weathered along the rest of the exposure. The rock is biotite-quartz-feldspar gneiss with varying amounts of garnet and sillimanite as accessory minerals. In appearance, it is gray-weathering, locally rusty from the iron-bearing minerals present, gray to tan or greenish-gray, fine- to medium-grained, moderately layered and foliated gneiss.

In our 2004 report, we described the portion of the slope on Timber Ridge Rd that eventually failed as: "Between Stations 67 and 69 the slope face is at a modest angle with the foliation strike and dip, which makes wedge-type failure the favored kinematic model for this area. Potentially large wedge failures were apparent all along this portion of the slope. Several recent rock falls of 800 to 900 pounds in size are on top of the mulch surface adjacent to Station 69. Critical joint and foliation surface orientations were modeled for this portion of the slope and it was found that factors of safety between 1.1 and 1.4 prevailed, suggesting a marginal factor of safety against failure at this location. At Station 68 plus 20 feet, a highly altered and deformed zone occurs in the rock with gouge present on all joint surfaces. This deformed zone is extremely weathered and appears to be a flexural-induced fault zone that occurred during folding of the rock. This is confirmed by its orientation, which is essentially parallel to the foliation. Foliation surfaces within exposed overhangs in the rock slope face here are open up to ¼ inch, which is a very unstable situation, making this area of the slope prone to incipient failure, which will be exacerbated by precipitation and freeze/thaw cycles".

Figure 4 – Failure Location Sta. 68+20

Figure 3 shows a stereographic projection (lower hemisphere) of the failure surfaces involved for the large rock fall on Timber Ridge Rd. As can be seen, the intersection of the release joint, which strikes North 25 degrees West and is near vertical, with the gouge-filled foliation plane falls within the instability region of the diagram. Because we could measure the size of the block that fell, we were able to back-calculate what the equilibrium conditions were just prior to failure. Using a density of 160 pounds per cubic foot for the biotite-quartz-feldspar gneiss, and a measured failure surface of 140 square feet, we estimated that the cohesion along the failure surface at a safety factor of 1 would be about 330 pounds per square foot (if it were dry). However,

there was more than normal precipitation during January and February of 2005, making it likely that water in the slope, coupled with freeze/thaw cycles, contributed greatly to the failure. With water present in the slope along the foliation failure surface, the cohesion would drop off significantly to about 70 pounds per square foot just prior to failure. Figure 4 shows the location of the failure as it was mapped in July 2004 and Figure 2 shows the actual failed surface and block.

Figure 5 – Rock Overhanging Bldg. C

EMERGENCY REMEDIAL MEASURES UNDERTAKEN

With the failure of the slope at the site, the HOA managed to secure a line of credit to enable some emergency remedial measures to be initiated. While the failure on Timber Ridge Rd was important, in the sense that it validated our report and all of its inclusive warnings about the slopes at the site, it was not the most potentially dangerous slope at the site. A large overhang of rock, some 35 to 40 feet above and behind Building C, was the slope with the most serious consequences were it to fail. Figure 5 shows the location described, prior to any remedial measures.

The rock here is a clinopyroxene-quartz-feldspar gneiss, a pinkish-gray to pinkish-buff weathering, white to pale pinkish-white or light gray, fine-to medium-grained, massive to moderately well layered gneiss composed of microcline, quartz, oligoclase, clinopyroxene and trace amounts of epidote, titanite and opaque minerals. Locally rusty, because of the presence of some trace amounts of magnetite, the overall character of the slope behind Building C is one of moderate weathering.

Figure 6 – Bldg. C Overhang Shotcrete Application

Shotcreting of Slope at Building C

Loose rock on the benches above and behind Building C were removed by hand prior to shotcrete being applied to the slopes. Loose soil in the areas where it had accumulated was also swept down to the base of the slope behind Building C. In areas where shotcrete was to be applied as a buttress below overhangs, four-foot long 1-inch diameter deformed galvanized bars were installed first in holes drilled two feet into the rock with a plugger or wagon drill. These dowels act as additional support for the steel-reinforced shotcrete after it cures. The dowels, which were grouted in place, were cut off with a portable saw to just above the surface of the shotcrete.

Drainage fabric was installed along near-vertical joints at what were believed to be key locations prior to shotcrete installation. Typically, the fabric was fastened in place with galvanized nails hammered into a joint in the rock or into a small drilled hole. The drainage fabric allows water and moisture to be wicked away from the rock behind the shotcrete so that it does not exert hydrostatic pressures or freeze and spall off the shotcrete. The drainage fabric was allowed to extend below the bottom of the shotcrete surface to provide an exit point for water.

Figure 7 – Final Appearance of Bldg. C Shotcrete Application

MS-D1 steel fiber-reinforced shotcrete was applied to several overhang areas behind Building C. When cured, this material reaches compressive strengths of about 6500 pounds per square inch at 28 days. The material came in 1,000-kilogram bulk bags, which was run through a hopper/conveyor/ blender apparatus in the dry state. The blended material was then conveyed to the face of the slope by compressed air hose and mixed with water at the nozzle and sprayed onto the cleaned slopes. The shotcrete was applied to the slopes at Building C in layers approximately four to six inches thick at a time. Total thicknesses of shotcrete in any particular area of the slopes behind Building C approached two to three feet in the buttress areas. Figures 6 and 7 provide examples of the shotcrete process used at the site, including what the final appearance of the slopes looks like. A total of forty 1,000-kilogram bags, or slightly over 24 cubic yards, of shotcrete was applied to the slopes behind Building C.

Rock Scaling along Timber Ridge Rd.

Prior to initiating rock bolting of several difficult areas along Timber Ridge Road, rock scaling was performed over 80% of the slope present. Brush and small trees were cut back approximately 10 feet from the edge of the slope. As seen in Figure 8, many of the large pieces of rock scaled off the slope at Timber Ridge Rd were classic incipient wedge failures just waiting to happen. The block scaled off the slope just below and to the left of the technician in the photo was a piece of some 3,800 pounds that required almost no effort to remove. A total of some 125 cubic yards of scaled rock was removed from Timber Ridge Rd.

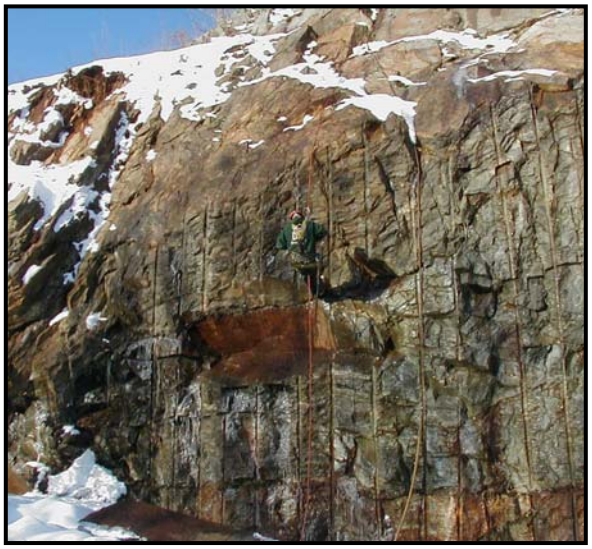

Figure 8 – Wedge of Rock Scaled Before Failure.

Rock Bolting at Building C and Timber Ridge Rd.

After completion of the rock scaling and shotcreting at the two locations at Rock Creek Crossing, rock bolt holes were drilled for both standard No. 8 150 grade galvanized rock bolts and the double corrosion protected (DCP) rock bolts used in the large rock overhang behind Building C. 245 linear feet of DCP bolt holes were drilled behind Building C and 984 linear feet of bolt holes for the standard 150 grade No. 8 galvanized bars were drilled at both Building C and Timber Ridge Rd. The holes were drilled with wagon drills winched into place and secured on the slopes with "come-alongs". Typically, the holes ranged in depth from 8 feet to 20 feet for the galvanized No.8 150 grade bolts

and 35 feet for the specialized DCP bolts. Plastic centralizers were used on the bolts to keep them in the center of the 3½-inch holes. Typically, two centralizers were used on a 20-foot bolt and three on the 35-foot DCP bolts.

The bolts were installed into their respective holes on the slope face by tying the bolt in two places with a separate rope that was then hauled up the slope by the technicians and inserted into the hole. The DCP bolts, because of their greater weight and length, required the use of mechanical assistance in the manner of a guide wire secured to the top of the slope behind Building C at one end and attached at the other end to a large boom truck on the ground at the side of Building C. A system of pulleys, shackles and ropes was then used to hoist the DCP bolts up along the guide wire to their respective bolt holes where technicians then inserted them into the holes.

Grout used to secure the bolts in the holes was Sika 300PT, a high performance, non-shrink ultra-fine grout that was mixed in six-bag batches in a grout mill and pumped under pressure up to the face of the slope where it was injected into the bolt holes via a 3/8 inch grout tube installed with the bolt. Grouting continued on each bolt hole until grout was visible and running out at the surface.

Several of the DCP bolt holes drilled in the large rock overhang behind Building C had significant communication between them as well as with the surface via steeply-dipping fractures as evidenced by the escaping compressed air. When grouting was attempted with the Sika 300PT, the grout emanated from several north-trending and steeply dipping fractures at the base of the large slope behind Building C. This condition necessitated switching to another Sika high performance grout with sand in it, Sika 212. The additional larger-grained solids contained in this grout helped build up a thicker coating in the fractures and helped close them off away from the walls of the bolt hole. This grout was mixed by hand and carried up the slope to the bolt holes via bucket and rope, where it was poured into the bolt hole annulus using a funnel. The grout was placed in this manner until visible at the surface of the rock.

Once the grout had cured in the bolt holes, plates and nuts were then installed on the grade 150 bolts and dogged down tight. The DCP bolts were tensioned using a 10,000 pounds per square inch hydraulic jack and jacking stand. The bolts were locked off at 60% of their ultimate strength at 77,000 pounds. Proof tests were performed on two of the DCP bolts to ascertain their effectiveness in meeting the design criteria. Both bolts tested performed as expected. Figure 9 shows a DCP bolt being installed in the slope behind Building C.

CONCLUDING REMARKS

The emergency remedial measures taken so far are only a partial fix to the most threatening areas of the site. The costs of the required additional remediation will necessitate the completion of the legal proceedings, which have yet to mature.

Additional rock fall can be expected to occur on occasion. It was recommended that periodic (semi-annual) inspection of the slopes be performed and any loose rock observed be removed by scaling. Additionally, it was also recommended that warning signs be installed along Timber Ridge Road alerting passers-by to the potential for falling rock.

NHDOT Response to the Destructive Forces of Nature: Alstead Flood 2005

Richard M. Lane, PG, CPG
New Hampshire Department of Transportation
Bureau of Materials & Research
PO Box 483
Concord, New Hampshire 03302-0483
Tel: (603) 271-3151
Email: dlane@dot.state.nh.us

Marc Fish, PG, CPG
New Hampshire Department of Transportation
Bureau of Materials & Research
PO Box 483
Concord, New Hampshire 03302-0483
Tel: (603) 271-3151
Email: mfish@dot.state.nh.us

ABSTRACT

During a two-day period in October 2005, severe flooding in New Hampshire resulted in the Governor declaring a State of Emergency in five counties. The most severe and widespread damage was in the village of Alstead located in the southwestern section of the state. During a 30-hour period, this area received approximately 12 to 16 inches of rainfall. The most devastating of the flood related events occurred during the early morning hours on October 9th, when water was temporarily impounded behind a roadway embankment. The floodwater breached the embankment fill sending a 30 to 40 foot high wall of water and debris surging down the valley of Warren Brook, toward the center of Alstead. Within minutes, damage from the raging floodwater extended 6.5 miles downstream.

Extensive repairs to private and public properties, and a massive cleanup operation, unprecedented in the history of the state, was immediately undertaken. Interim repairs on some segments of the state roadway system were completed within hours or days, while other sites were repaired within weeks. Short-term repairs were completed prior to the winter season and permanent solutions are currently being designed. It is estimated that damage to state roads and bridges across New Hampshire exceeds $30 million.

Accounts describing the devastation in Alstead provide some insight into the awesome power of flooding as a geological process. These events are also a frightening reminder that even a small brook, under the right circumstances, can become a destructive force as well as a powerful agent of erosion.

INTRODUCTION

The October 2005 flood event was the most destructive flooding to ever occur in the state of New Hampshire. The most severe and widespread damage was in the village of Alstead located in the southwestern corner of the state near the New Hampshire/Vermont border (Figure 1). During a 30-hour period, this area received approximately 12 to 16 inches of rainfall. Destruction from the flood events included: loss of life, damage to private property, loss of homes and businesses, severe damage to public infrastructure (roads, bridges, drainage structures, government facilities, etc.), damage to utilities, extensive erosion, contamination of drinking water, loss of agricultural productivity and psychological trauma. The storm event also triggered mudslides in several areas across the state.

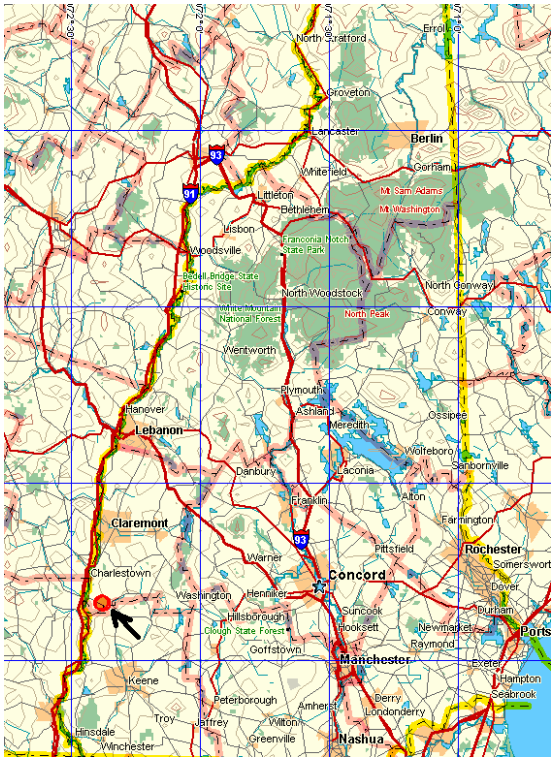

Figure 1. *Location Map*

On October 9, 2005, the storm damage resulted in the closure of 57 miles of state highways. Approximately 8 miles of state roads were destroyed or impassable, which included 4.5 miles of NH Route 123 in the Alstead area (Figure 2). Six bridge structures were severely damaged and one bridge completely destroyed. The restoration of major state routes, the repair and reconstruction of damaged bridges, and the cleanup of massive amounts of debris within an 8-week period are some of the greatest civil engineering accomplishments in New Hampshire.

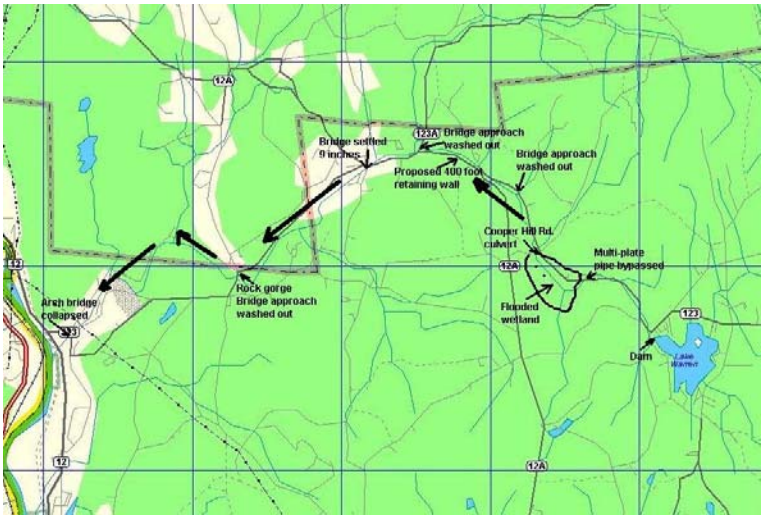

Figure 2. *Alstead flood damage*

ALSTEAD FLOOD

The flooding in Alstead occurred because of the combined effect of heavy rainfall, sheet runoff from the surrounding steep valley slopes, overflow from Lake Warren and a large volume of water becoming impounded behind the roadway embankment at the Cooper Hill Road brook crossing. Warren Brook flowed through a 12-foot diameter multi-plate culvert that extended underneath a 40-foot high embankment at Cooper Hill Road, approximately 2 miles upstream from Alstead Village (Figure 3). During the early morning hours of October 9th, the impounded water breached the Cooper Hill Road embankment, sweeping away the culvert and a large section of the embankment fill. A 30 to 40 foot high wall of water and debris surged down the valley of Warren Brook and Cold River, following the NH Route 123 roadway. The floodwater swept through Alstead Village and continued downstream for 6.5 miles to the Connecticut River. The raging floodwater carved a gorge at the Cooper Hill Road crossing estimated to be 50 feet deep and 110 feet wide. At the culvert location, the floodwater cut deep into the underlying, dense glacial till, lowering the channel of the brook an additional 8 to 10 feet.

Figure 3. *Cooper Hill Road embankment*

Along Warren Brook and the Cold River, acres of farmland were stripped of topsoil and the adjacent flood plain was covered with all types of debris. Cars were carried thousands of feet downstream, some perched in trees and others crushed like aluminum cans (Figure 4). Eroded stream banks undercut foundations and concrete slabs. Buildings were ripped from their foundations (Figure 5), large trees were uprooted, roads were washed out, bridges were carried away and at some locations the overlying soil was stripped to bedrock. Concrete foundations were all that remained of several houses. The only remnants of a gas station were a concrete slab and exposed buried fuel tanks. A total of 36 buildings were completely destroyed and 71 homes sustained varying degrees of damage.

Figure 4. *Vehicle crushed by floodwater and debris*

Figure 5. *House ripped from foundation*

Runoff below the Lake Warren Dam caused severe erosion, washouts of the NH Route 123 roadway (Figure 6) and damage to drainage structures. Hundreds of feet of buried underdrain pipe, installed at a depth of 6 feet along the edge of the road, were plucked from the ground. The rushing water cut narrow trenches with nearly vertical walls into the underlying dense glacial till. The trenches were eroded four feet below the pipe elevation for a total depth of 10 feet (Figure 7). Warren Brook cut deep into its banks, undermining steep side slopes, triggering slides that threatened to undermine segments of Route 123.

Figure 6. *NH Route 123 washed out*

Figure 7. *Vertical trenches eroded into dense glacial till*

Warren Brook bypassed a large multi-plate pipe, wiped out a section of Route 123, cut a new channel in place of the roadway alignment and completely filled a 60-foot long cross pipe with gravel and boulders (Figures 8 and 9). Areas below the dam and Cooper Hill Road were buried under assorted debris and soil deposits with boulders measuring up to 4 feet in diameter. Several bridges below Cooper Hill Road were severely damaged to include loss of the roadway approaches. A 600-foot long section of Route 123, located 1.5 miles upstream from Alstead Village, was completely washed away and the soil stripped to bedrock (Figure 10). In some areas the force of the floodwater was so great that it removed the upper layer of fractured bedrock. The Route 123 bridge over Cold River in the village of Alstead sustained major damage to its abutments and wing walls to include settlement of the southern abutment by approximately 9 inches (Figure 11).

Figure 8. *New brook channel cut into roadway*

Figure 9. *Temporary Bailey bridge over brook*

Figure 10. *Section of Route 123 stripped to bedrock*

Damage and devastation from the floodwater continued further downstream from Alstead Village to include the washout of another bridge over Cold River and the loss of a historic twin arch bridge in Walpole, New Hampshire, approximately 6.5 miles downstream from Cooper Hill Road (Figure 12).

Figure 11. *Bridge wing walls damaged and abutment settled 9 inches*

Figure 12. *Twin arch bridge washed out*

WHY WAS THE IMPACT TO THIS WATERSHED SO SEVERE?

The local geology, weather and manmade features lead to the events that resulted in the most destructive flood in the history of New Hampshire. Remnants of tropical storm Tammy joined with another tropical storm to dump 12 to 16 inches of rainfall in a 30-hour period in the Alstead area. The deluge of rain exceeded the holding capacity of Lake Warren resulting in excess water overflowing the dam at the north end of the lake. Floodwaters from four primary sources (Mill Hollow – 820 cubic feet per second, Cooper Hill Road – 24,900 cubic feet per second, Vilas Pond – 6370 cubic feet per second, Drewsville – 21,800 cubic feet per second) contributed to the flood surge. Most of the area is underlain by very dense, non-permeable glacial till and/or bedrock, which resulted in water being absorbed at a very low rate.

The embankment fill at the Cooper Hill Road crossing of Warren Brook acted as a dam when the 12-foot diameter culvert was partially plugged with debris. Four hundred and twenty acres feet storage of wetland, upstream from the roadway embankment, provided an area for impounded water to collect. When the embankment was breached a 30-40 foot high wall of water and debris rushed down Warren Brook and joined Cold River just upstream from Alstead Village. The US Geological Survey calculated that the flooding was equivalent to 500-year and 100-year events for Warren Brook and Cold River, respectively. Most engineered structures, embankments and drainage systems are designed for a 100-year flood. The heavy rainfall and related events that occurred during October 2005 exceeded the established limits for normal engineering design.

EMERGENCY REPAIRS AND CLEANUP OF DEBRIS

The damage to state roads and bridges across the state is estimated to be in excess of $30 million. Some locations were temporarily repaired within hours or days, while other sites will take weeks to months to be restored. In addition to repairing the highway infrastructure, a massive cleanup operation was undertaken in the Alstead area to remove debris from the stream and adjacent flood plain. Several stream crossings were spanned with temporary Bailey Bridges, while approaches were reconstructed and plans were underway to build new replacement structures. A segment of Route 123 at the Cooper Hill Road intersection was temporarily rerouted while permanent repairs are being designed and constructed. One of the most difficult sites to repair is a 600-foot long segment of Route 123 that hugs the channel of Warren Brook. Temporary repairs at this site involved the placement of stone fill along the northern portion and the construction of a Redi-Rock™ concrete block retaining wall along the southern portion. The stone fill was constructed at a 1.5H:1V slope directly on a steeply dipping bedrock surface with anchorage required along the toe of the embankment. Closely spaced dowels were grouted into bedrock to secure the toe of the stone slope (Figure 13). Only one lane was restored along the northern section because of the limited room between the brook channel and a steep wooded slope. The NHDOT installed temporary traffic lights at this location to maintain the flow of traffic. The southern section consisted of a Redi-Rock™ retaining wall constructed on a concrete sub-footing that was anchored to the underlying bedrock (Figure 14). A 1.5-inch crushed stone was used behind the retaining wall with geogrid at every course (18 inches thick) extending the full width of the excavation. The feasibility and cost of cutting into the steep hillside and moving the road further away from the brook are being studied.

Figure 13. *Toe of stone filled slope secured with grouted dowels*

Figure 14. *Redi-Rock™ concrete block retaining wall*

Approximately 4.5 miles of NH Route 123 were completely reconstructed to include temporary drainage pipes and 7000 linear feet of concrete barrier. Six bridges were repaired to include construction of several wing walls and the demolition of a collapsed stone arch bridge. The scope of the permanent repairs to the Rte 123 bridge in the Village of Alstead will depend on the subsurface conditions and whether voids have developed under the southern abutment. Demolition of the collapsed twin arch bridge has been completed, while plans are underway to replace the historic structure.

The cleanup operation involved disposal of more than 36,575 tons of flood debris consisting of building materials, vehicles, tires, metal, household items, chemicals, septic systems, pipes, etc (Figure 15). The categories of debris and methods of disposal were the following:

- Burned debris – 6,330 tons
- Loam – 25,320 tons
- Concrete/pavement – 600 tons
- Debris to landfills – 5,427 tons
- Tires to recycle centers – 91 tons
- Metals to recycle center – 200 tons
- Wood Chips – 1061 tons
- Logs – 400 tons

Several areas to include the parade field in Alstead Village were utilized as temporary staging and storage areas for flood debris. The flood debris materials were sorted by type into separate piles (Figure 16). Trees were shredded into wood chips, topsoil was recovered by screening the woody debris and some of the recovered wood was burned. The cleanup activities were ongoing from sunrise to sunset, seven days per week. The cost for pickup and disposal of debris averaged $150,000 per day for an estimated total of $ 5 million.

Figure 15. *Flood debris*

Figure 16. *Flood debris sorted by type*

SUCCESSES, SOLUTIONS AND SHORTCOMINGS

The restoration of major state routes, repairs to bridges and the cleanup of flood debris were formidable challenges. The response consisted of a coordinated effort by the Governor, state agencies, town government, law enforcement, rescue organizations, utility companies, private groups and contractors. The keys to success were good communication, team work, knowledge of resources and capabilities, dedicated personnel, cooperation with the New Hampshire Department of Environmental Services (NHDES), commitment of all parties, the Department's previous experience with smaller flood damage repairs and innovative engineering.

Due to safety concerns, seven NHDOT bridge inspection teams were mobilized to inspect over 170 bridge structures across the state. Other NHDOT teams were mobilized to inspect roads, drainage structures and slopes throughout the state.

Construction challenges included working without contracts, plans, survey control and a local field office. The priority was to provide access for search and rescue, utility crews, law enforcement and residents. Storm damage resulted in 57 miles of state roads being closed on October 9, 2005. One day later, 43 miles of road were open for emergency vehicles and local traffic, while 14 miles remained closed. On October 19th only 4.5 miles were closed, 29 miles were open and 23.5 miles were open for emergency vehicles/local traffic. To expedite repairs and open the roads to traffic before winter, some sections were constructed without full compaction and with limited subsurface drainage. Contractors and state crews had to work through sub zero temperatures, frozen ground and double-digit snowfall. Limited time and frost required the installation of over 7,000 linear feet of concrete barrier in lieu of conventional guardrail. In some instances, the channel of Warren Brook had to be reconstructed and/or relocated to its original location. Temporary repairs in the Alstead area included the placement of approximately 40,000 cubic yards of earth fill and 13,000 cubic yards of stone fill.

SUMMARY - GEOLOGY ON FAST FORWARD

Flooding is one of the most common and destructive geological hazards. Water-related events account for over three-quarters of the federal disaster declarations in the United States. These devastating events allow a glimpse at some of the geological forces that shape our planet and continually change the environment. Stream erosion and deposition are ongoing geological processes that can be greatly accelerated during periods of flooding. A flood event is like watching geology on fast forward. What may normally take tens to thousands of years to occur can take place within minutes.

Accounts describing the devastation in Alstead provide some insight into the awesome power of flooding as a geological process. Buildings ripped from foundations, miles of paved roads washed out, bridges destroyed, large trees uprooted and swept away like twigs, vehicles crushed and carried thousands of feet, 3000 pound propane tanks bobbing in the water like corks and extensive erosion of land are examples of the destruction. It was reported that floodwater washed over the bridge in Alstead Village at a height of four feet above the deck. An eyewitness stated that a wreaker truck carried by the floodwater, crashed into the bridge, flipped over the bridge deck and then was swept further downstream. There were strange but true occurrences such as a concession stand that was carried

downstream for a distance of 3.25 miles to where it was deposited undamaged and an outdoor furnance floating downstream with the fire still burning.. These events are a frightening reminder that even a small brook, under the right conditions, can become a destructive force as well as a powerful erosional agent.

Emergency repairs to open the state roads were expedited by a design build approach. Teamwork, innovation and communication were the keys to completing the work in a timely manner. Restoration of the state roads, temporary repairs of bridges and disposal of massive amounts of flood debris within an 8-week period prior to the winter season are one of the greatest civil engineering accomplishments in New Hampshire history.

REFERENCES

Lane, R. M. The Geological Impact of the October Floods, Geology on "fast forward", *New Hampshire Highways*, January/February 2006, pp. 13-15.

Lane, R. M. The Geology of a Flood: "Tens of Thousands of Years in a Few Minutes", *New Hampshire Department of Transportation*, Winter 2005-2006, pp. 6, 7 and 10.

Lane, R.M. Geological Hazard – New Hampshire Flood 2005, *Granite State Geologist*, Issue No. 51, Winter 2005, pp. 6 –10.

Liebowitz, S. Minute by minute, disaster emerged, *Concord Monitor*, October 20, 2005, pp A1 and A10.

Case Study: Monteagle Mountain Rockfall Project

Vanessa Bateman
Tennessee Department of Transportation
6601 Centennial Boulevard
Nashville, Tennessee 37243-0360
615-350-4137
vanessa.bateman@state.tn.us

Len Oliver
Tennessee Department of Transportation
6601 Centennial Boulevard
Nashville, Tennessee 37243-0360
615-350-4137
len.oliver@state.tn.us

ABSTRACT

In February of 2003, a rockfall incident along I-24 East on Monteagle Mountain temporarily closed the interstate. The rock cut which failed had been a continuing problem, shedding smaller rocks and previously closing the interstate in 1988. Because of the deterioration of the cut since the last geotechnical inspection and the threat to the interstate, an emergency contract was let in March of 2003. The presence of a clay shale layer at the bottom of the cut, the presence of numerous solution widened joints trending sub-parallel to the face, cavities in the rock and the large colluvial pile on top of the rock cut all added to the site mitigation challenges. In addition to this, a large volume rock fall occurred during construction. This event closed the interstate and required adjustments to the original design. This incident also destabilized the colluvial pile above the cut, resulting in a slide. Despite these challenges, the original project was completed successfully. The final design makes use of a wide rockfall catchment ditch, a soil berm between the rockfall ditch and the roadway, a “hurricane” type fence to prevent rock splatter from reaching the roadway. A supplementary project was let to put a shotcrete cover on the shale at the site to prevent rapid deterioration of the newly stabilized rock cut. Several rockfalls have occurred at the site since the final catchment ditch and berm was constructed and none have reached the roadway.

INTRODUCTION

Tennessee has a number of problem areas for rockfall, many of which occur along older state routes that were built before presplit blasting was commonly used and before rockfall catchment ditches were regularly designed for TDOT Projects. Like many of our problem sites, this particular area was built with a small catchment ditch that was inadequate to contain the increasingly larger falls that were occurring, though presplit was used at this site. This particular section of I-24 has had several rockfall incidents over the years with some smaller and some larger falls (1). However, the trend at this site was toward increasingly larger volumes of material. Earlier mitigation and clean up was proving to be insufficient and it became apparent in 2003 that there was severe instability in the slope that was going to result in an even larger fall than had been previously seen at the site.

GEOLOGY OF THE SITE

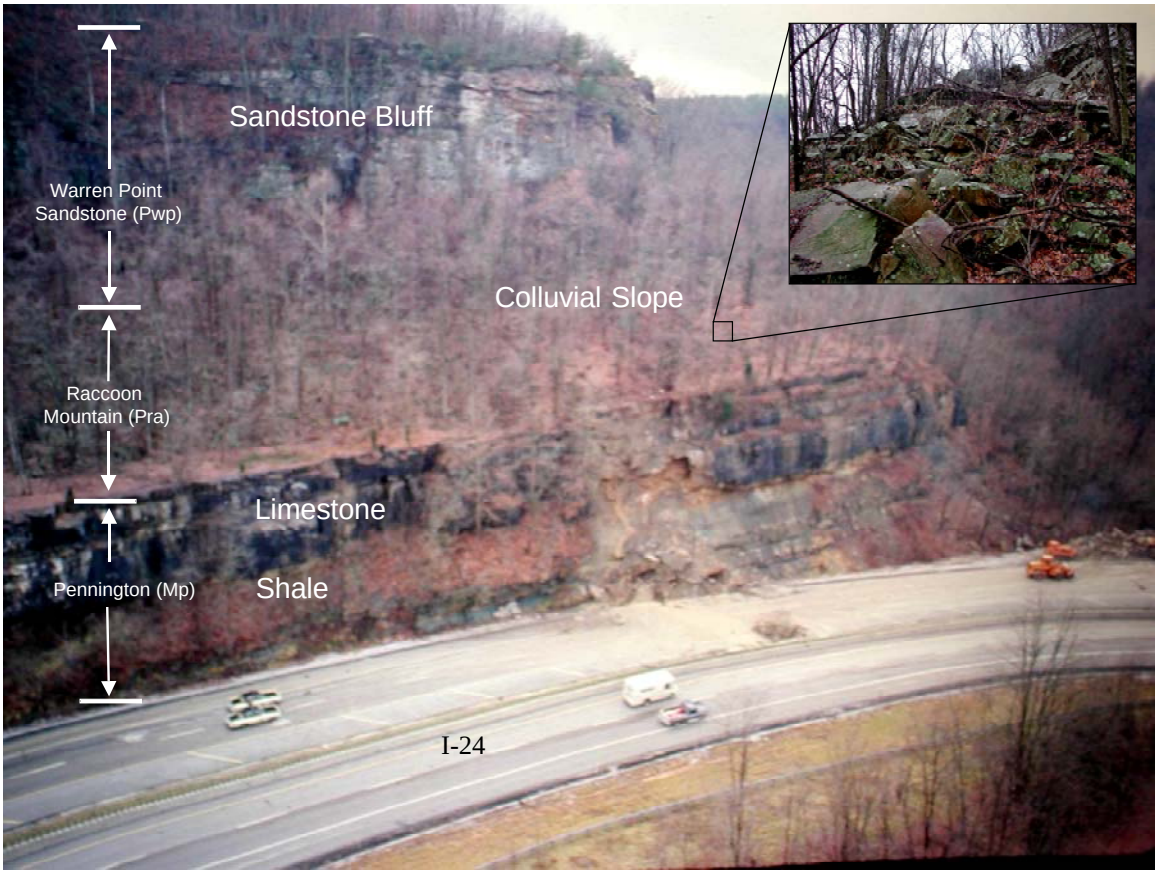

Figure 1. View of Rockfall at site in the 1980's with geology Notes

GEOLOGIC SECTION AND SETTING

The Pennington Shale, located at the base of the cut, is notoriously water sensitive and decomposes readily to a highly plastic clay. It is a known problem formation in Tennessee and has long been associated with rockfall and landslide problems (2). The weathering of this reddish-green shale destabilizes the limestone layers also contained within the Pennington as well as the upper faces. The natural bench on top of the Pennington formation is caused by more rapid weathering in the Raccoon Mountain Shales below the Warren Point Sandstone. Here again we have a much more weathering prone layer destabilizing the more sound overlying material. This leaves an unstable colluvial deposit on top of the Pennington shale that is made up of very large sandstone boulders, clay, shale and mixed organics such as trees and other vegetation have also been incorporated into the deposit.

Complicating the matter are the large solution widened joints run roughly parallel to the face of the rock cut along this section of interstate. The solution widened joints leave tall, thin columns of rock that can be easily destabilized by the weathering out of the Pennington Shale. A cave opening is also located just to the left of the photo in Figure 1, it follows along a solution widened joint and continues back into the mountain. The base of the cave is located on top of one of the Pennington shale layers. The overlying Warren Point sandstone is also jointed, and like the Pennington layers below also parallel to the face.

Figure 2. Views of Cave, water and solution widened joints in rock face and bench.

Water is another problem at the site. Numerous small springs and streams emit from openings in the rock face. During the winter months, the cut face is frequently covered in ice and water on the site does not stop flowing even during the dry summer. The constant flow of water contributes to the rapid deterioration of the Pennington Shale.

ROCKFALLS AND CONTINUED DETERIORATION

There have been several rockfalls at this location that entered the roadway as the shale continued to weather out much faster than the overlying limestone starting very shortly after the original construction. Several falls occurred in the 1980's including the one shown in Figure 1 (3). Numerous smaller falls have occurred at the site since that time, generally affecting the inside lane or paved shoulder.

Figure 3. Unstable Face and Joint Behind the Rock face

Figure 3 shows the continued deterioration of the site as of Feb 2003 after another fall occurred at the site. These photographs, and the investigation requested by TDOT Region 2 Maintenance in 2003, alerted the department that an emergency project was going to be needed. Again, though there have been several falls at the site over the years, this time we started to see something different. The joint shown in the figure above was approximately twice as large as it was during the previous site visit in 2002. Large sections of the face were becoming unstable and were going to topple into the roadway. The catchment ditch at this location was approximately 15 feet in width, completely inadequate to capture the amount of material that we knew would be coming down.

ORIGINAL DESIGN CONCEPT AND PLAN

Because of the continued instability in the site, TDOT decided to let an emergency contract in order to repair the site. A second contract was to be let at a later time in order to cover the shale at the site. Only the currently unstable portion of the rock cut was chosen for repair due to the likely expense of letting an emergency contract. This first contract was for re-cutting the slope and constructing at least a 38 foot rockfall catchment ditch for the site. There were right-of-way and other limitations at the site. These limitations along with the expense of an emergency contract were the constraints that dictated a minimum repair area. Also, we wanted to minimize any disruption of the colluvial slope located above the rock cut. Destabilizing that slope would cause additional problems at the site and risked destabilizing sections of the overlying sandstone bluff.

Current TDOT rockfall charts, the Colorado Rockfall Simulation Program and the Oregon Rockfall Design Guidelines were all used for ditch width design (4,5). We knew that one particular parallel joint face in the rock was unstable, and this repair would remove all of the rock that was in front of that joint face. Approximately 320 feet of slope length was chosen for repair.

However, we did not want to rely solely on rockfall catchment ditch at this location. However, we did not want to rely solely on rockfall catchment ditch at this location. As the deterioration of the shale was the primary cause of rockfall on the site, we decided to cover the shale with a shotcrete and rock dowel wall. A similar treatment had been applied to shale layers along I-24 on Monteagle Mountain in the 1970's (6). It was installed without more modern drainage and had reached the end of its design life. This former cover was failing in numerous locations, but those failures began after 15-20 years of relatively successful service.

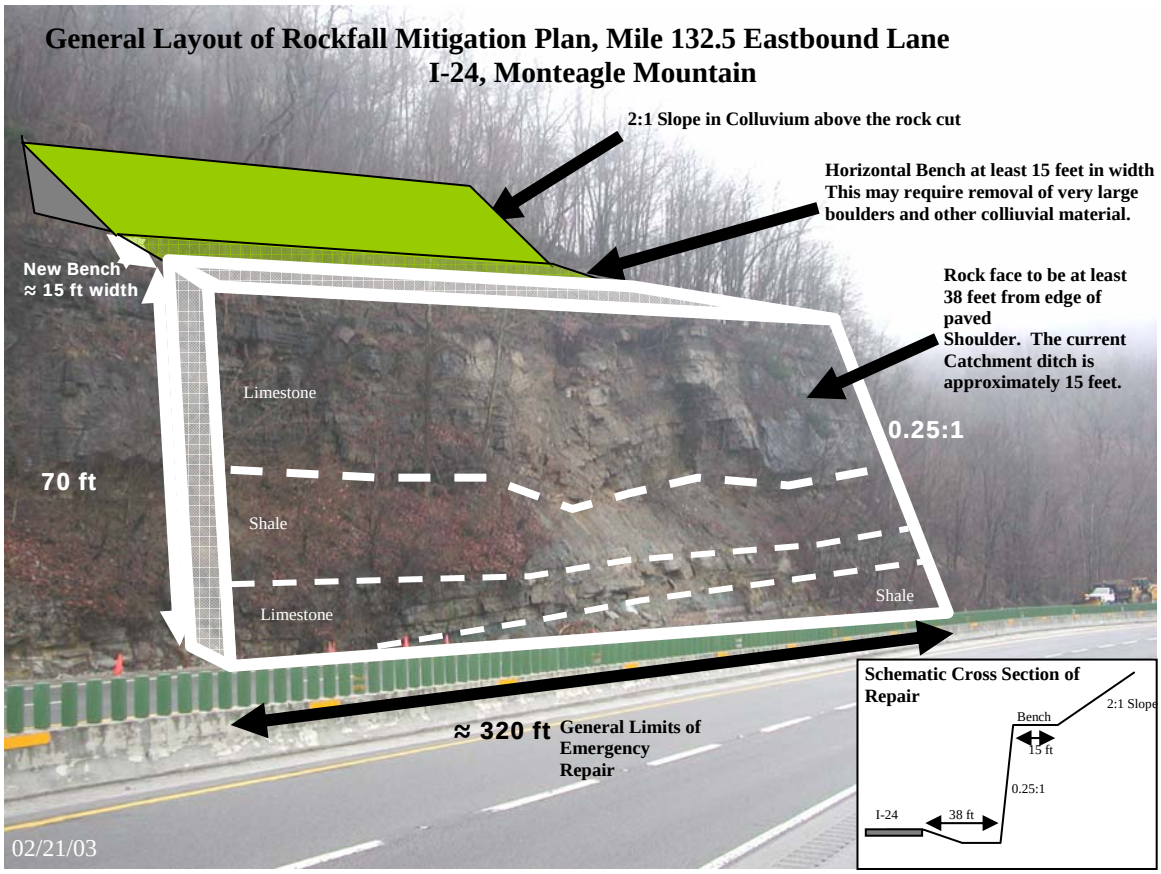

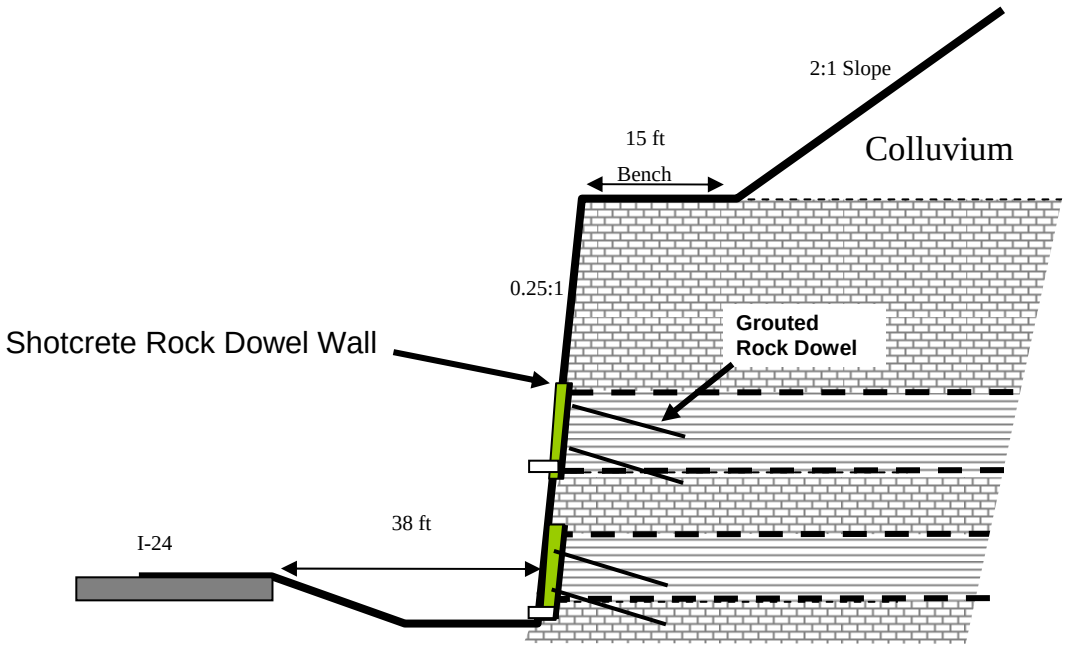

Figure 4. Original Design Concept of Rock Cut including Shale Cover

This time, we designed a shale cover with grouted rock dowels and using geocomposite drain strips (Figure 5 and 6). Rock dowels were to be installed on 5 foot centers and drilled approximately 10 feet into the face. Some drain strips were to be placed along bedding planes on the face that were weeping water and were inclined to drain toward the vertical drain strips.

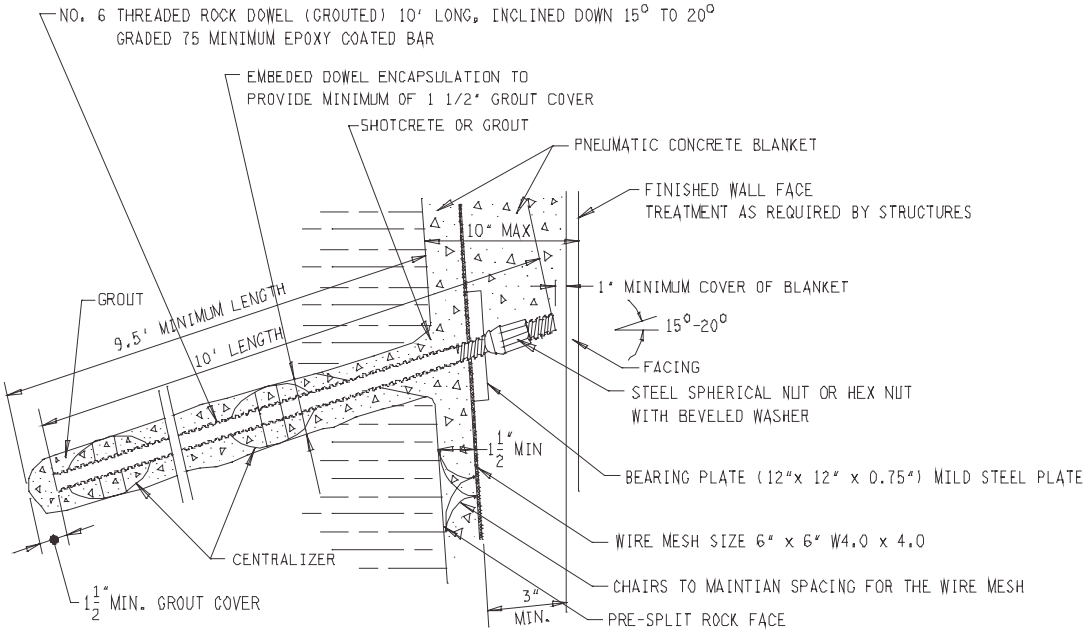

Figure 5. Detail of Grouted Rock Dowel for Shale Cover

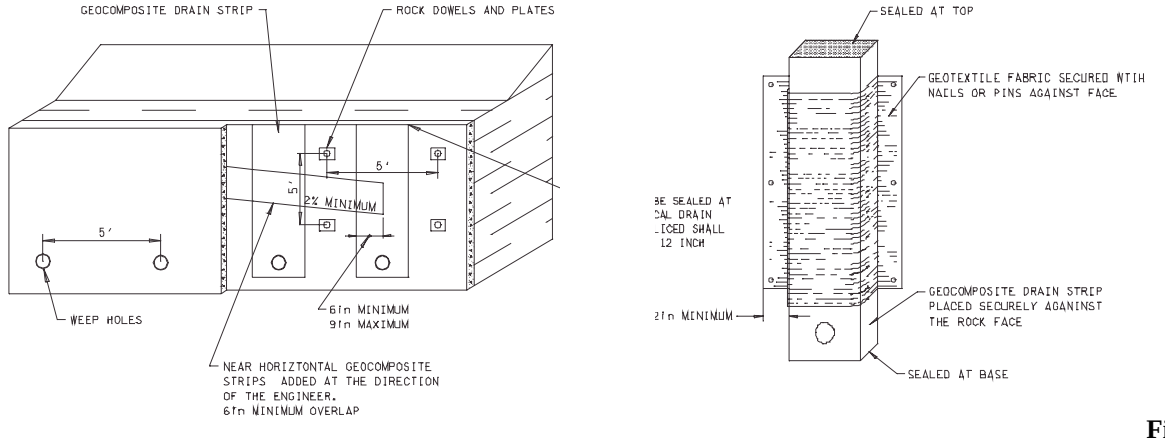

Figure 6. Detail of Drainage Installation

MITIGATION BEGINS AT THE SITE

Highways Construction won the bid for project and got to work re-cutting the slope. The site presented a lot of difficulties for construction, as there was no stable area to install a construction road for equipment to access the top of the limestone cut. A construction road was constructed up the side of the cut; however, it failed several times and was eventually abandoned. Periodic closures were also needed for blasting at the site and Highways had a tight time frame to clear the interstate of debris and get traffic flowing again after every blast.

Figure 7. Construction begins, view of blasting and clean-up at the site

As construction proceeded we started noticing additional problems. We were destabilizing part of the face adjoining the blasted section after each blast. The face had to be inspected by the Geotechnical Engineering Section, the Construction Engineer for the project and the foreman of Highways before the interstate could be re-opened. Figure 8 shows some of the destabilized face and the stress relief fractures noted on the project. These were all near the edge of the excavation. No major shifting was noted in the colluvial slope above our cut and there was no indication of stress fractures further back into the hillside.

Figure 8. Photo of Destabilized Face at top of Limestone

A large fall occurred on the site on July 31, 2003. The previous day's inspection of the site revealed stress relief fractures in the rock just above an area that was blasted near the cut face. Twenty-four hour monitoring was instituted at the site and the next day's planned blast was called off. Additional safety discussions and conditions for work were had between representatives from TDOT and the contractor. No equipment was to be left underneath the face overnight. This alert paid off, as a large fall occurred in the early morning hours of July 31, 2003.

Figure 9. View of the Face before and after large Rockfall, July 30 and 31, 2003

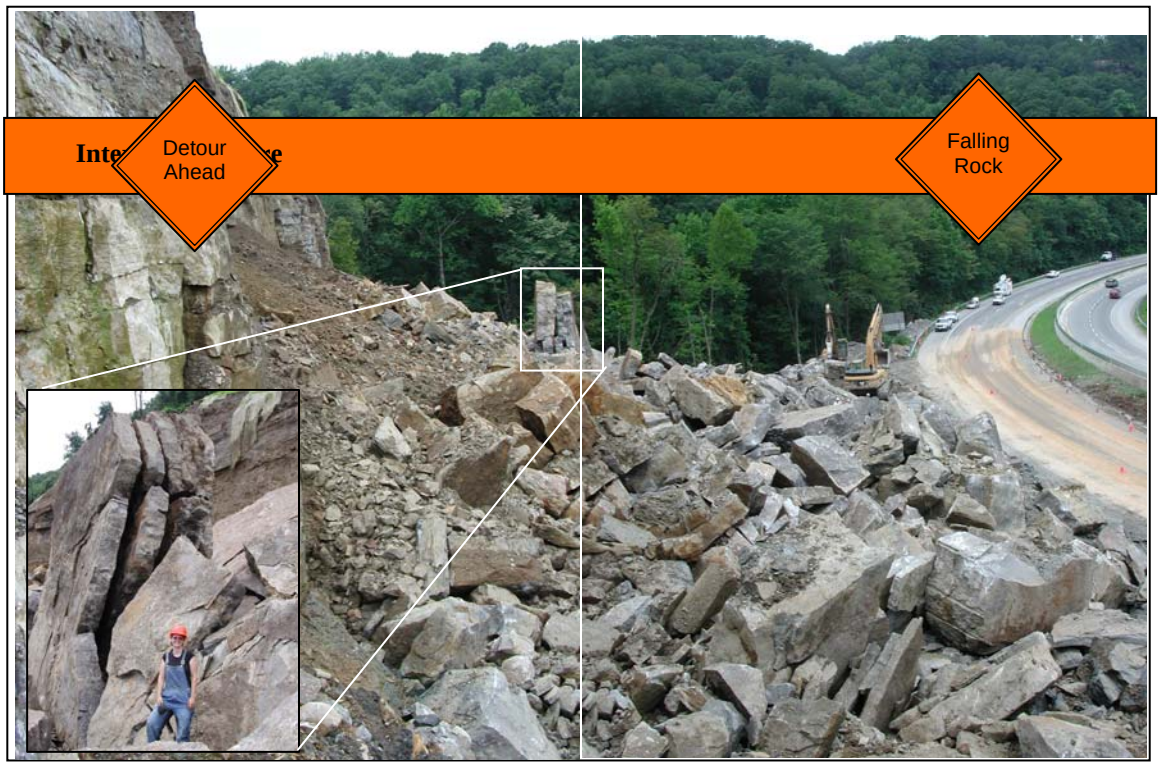

Figure 10. Large Fall after some clean-up July 30, 2003

TDOT Construction and Maintenance forces which were present monitoring the site promptly closed the interstate and there were no injuries or damage to vehicles. Traffic was stopped when some raveling was noted on the slope at the site, very shortly after the raveling from the upper slope was noted, the limestone face toppled over. Approximately 90% of the material that fell was contained in the ditch. However, material did reach the far side of the interstate and traffic was diverted to a narrow 2 lane road which did cause a large impact to traffic flow.

In addition to the need to clean up the additional rock we had not intended to excavate and getting the material out of the interstate, the fall on July 31, 2003 caused another problem. Instead of a 2:1 slope, now the overlying colluvial slope was vertical and perched just above our cut. This started a landslide above the rock cut in the colluvium destabilizing large boulders contained in the colluvial deposit. Large and small boulders, clay and other material began falling over the edge of the cliff into our catchment area. This slope movement continued through the winter of 2003/2004 exposing large material. The large boulder shown in Figure 11 was continuously monitored when it neared the edge of the cut until it finally fell in early Spring 2004 and was contained in the ditch.

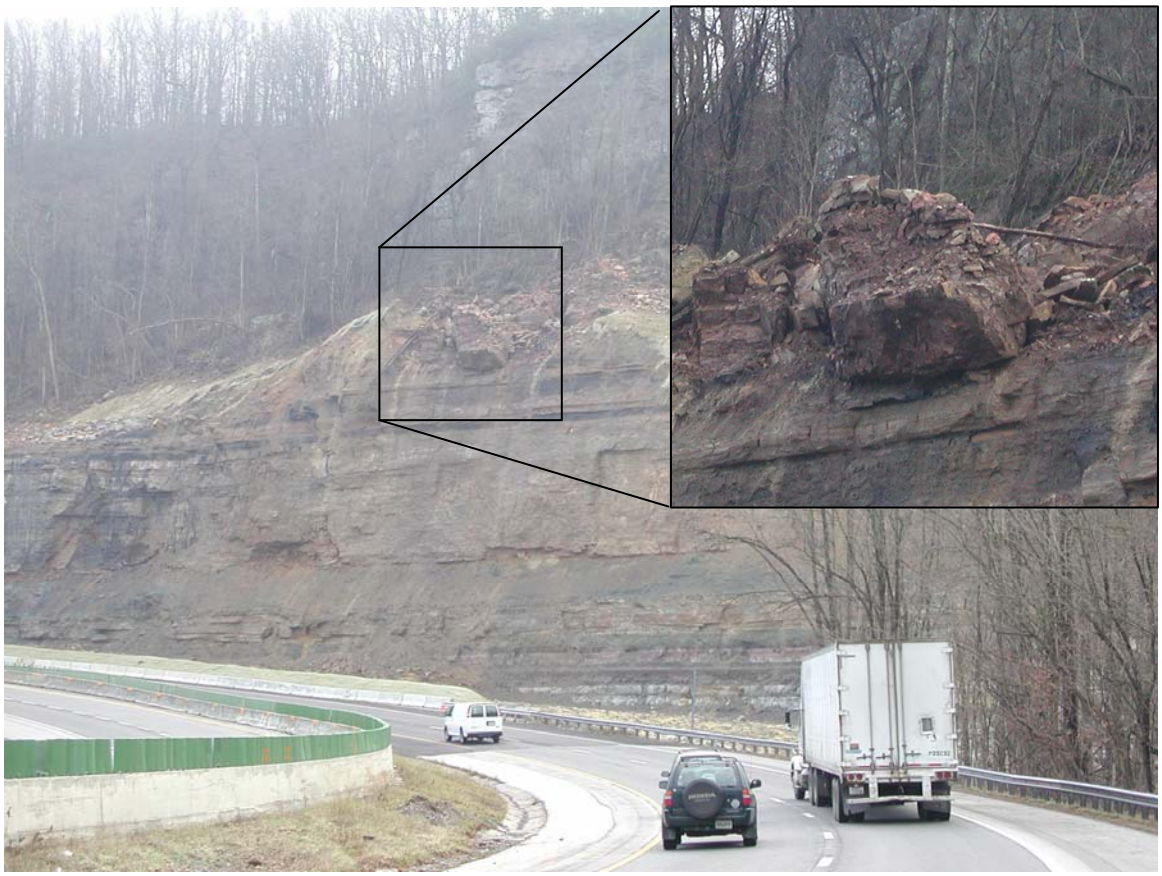

Figure 11. View of unstable slope above rock cut with large boulder, early Spring, 2004

REVISED DESIGN CONCEPT AND FURTHER WORK

Based on the fall, we needed to revise our original design concept. A wider catchment was ditch was needed and all of the unstable material on the face needed to be removed. TDOT Geotechnical, TDOT Construction and Highways, Inc. debated several methods for stabilizing the colluvial slope above the cut. However, after considering our options, and attempting some trim blasting of the larger boulders, we decided to allow the colluvial slope to stabilize itself by allowing the slide material to fall into the ditch. Analysis indicated that the ditch was wide enough to contain any sliding material that might fall and it was safer to remove it once it was at the base of the cut, rather than trying to stabilize an active slide above a rock cut. TDOT Maintenance would then clean up any material that fell after the contract was completed.

Generally, the colluvial slope moved most after rain events and had to be inspected after each event before work could begin and material in the catchment ditch could be removed. The slope was inspected after every blast and a berm was added to the project. Additionally, while it was not ideal from a rock cut design standpoint, an offset was left in the shale for part of the slope in order to make sure that we did not destabilize any further rock. The tall thin columns of rock formed by the face and the joints meant that any further failure of the shale would result in further rock toppling. Figure 12 shows the basic design elements and the revised concept plan.

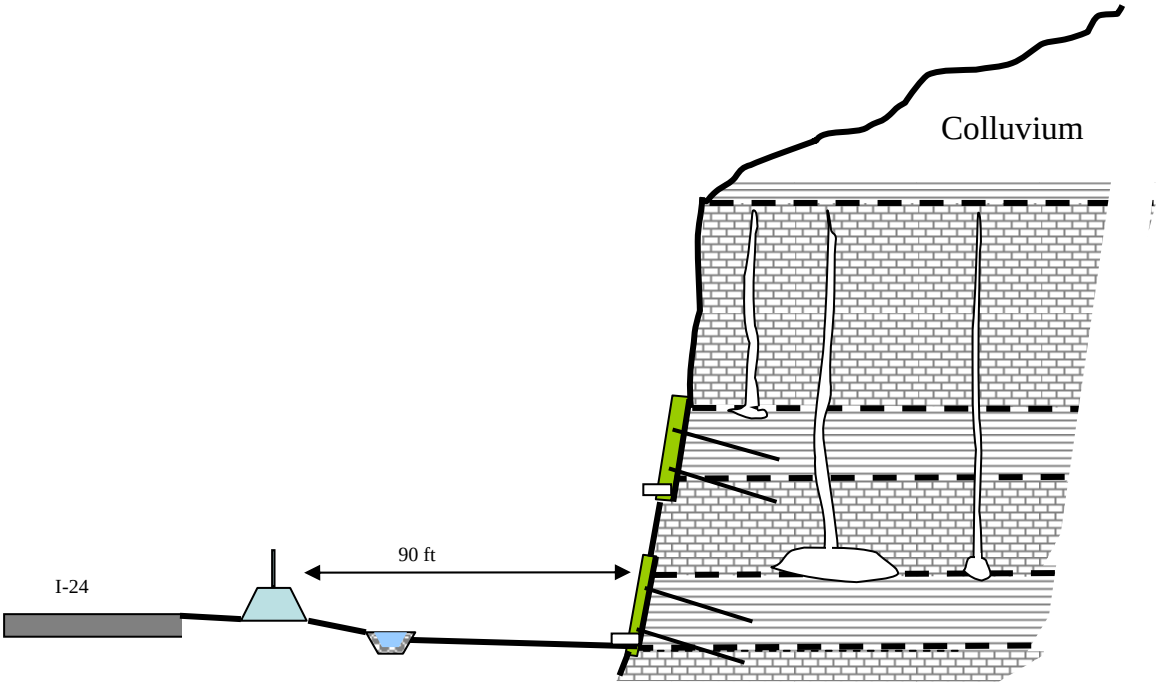

Figure 12. Revised Design Concept with added Berm and Wider Ditch

No work was allowed during and immediately after rain events due to safety concerns. There is a great deal of water that moves through the joints and solution cavities in the rock and through the colluvial slope at the site. Several days after a rain, the movement of the colluvial slide would cease or slow to a barely perceptible creep but it could move rapidly during and immediately after rain. Figure 13 shows slide material contained in the catchment area, notice the large boulders, few of which have made it across the drainage ditch.

Figure 13. View of Slide Material and Large Boulders Contained in Catchment Ditch

The berm was added to the site as an additional safety precaution and the fence was added mainly to keep the general public away from the site. Also, we ended up needing a drainage ditch along our cut as the location of water flow from the cut face shifted during construction and we had to cope with more water than was anticipated. Scaling was performed at the site and all loose material from the face that could be removed was brought down. Because of the dynamic nature of the site and safety concerns an offset was left in the shale layers at one end of the site. While this was not considered to be "ideal" rock cut design, it was a compromise we felt necessary to make sure that we did not destabilize our now more stable rock cut face. Some horizontal blasting was used in one area in order to remove some problem material, but overall the face was cleaned by mechanical scaling and left to fall in the ditch as needed. We judged the risks of continuing with blasting and excavation much greater than rock reaching the road across a 90 ft wide ditch and berm. Monitoring continued all winter and in the spring a second contract was let in order to cover the Pennington Shale layers that caused the initial failure.

INSTALLATION OF ROCK DOWEL SHALE COVER

After the large boulder shown in Figures 11 and 13 fell and further inspections of the site were made to ensure that the colluvial slope was more stable, the second contractor was allowed to get to work. American Shotcrete won the contract for the shale cover using a wire mesh and rock dowel wall as shown in Figures 5 and 6. No decorative shotcrete treatment was used at the site due to cost and the presence of shotcrete with no face treatment near the site. Figure 14 shows layout of the grouted rock dowels, wire mesh and drainage installation. The shotcrete was tied into the more stable limestone above the shale, something that was not consistently done with previous attempts at covering this problem shale layer along I-24.

Figure 14. Installation of Shale Cover

RESULTS AND FINAL CONTRACT COSTS

The final cost of the project was approximately 3.6 million dollars. This included both contracts, removal of additional material due to the fall during construction, the addition of the berm and fence, additional drainage work and installation of the shotcrete and rock dowel wall. Very little rock or soil has reached the berm. No falls have impacted the fence since construction was completed in 2004 and no rock has reached the roadway.

Overall, while we had some significant challenges during construction, the project has proved to be successful at mitigating a dangerous and unstable site. Many thanks and a good deal of the credit are due to an excellent TDOT Construction Team led by Darrell Bost of the Dunlap Construction office. His staff, assisted by TDOT Maintenance staff spent many hours monitoring the site, often with late nights and weekends. Well-informed and vigilant inspectors at the site brought attention to problems at the site as they occurred. It was his staff that made sure traffic on the interstate stopped, just before the large fall that occurred in July 2003.

Decisions and adjustments at the site were made as a team with TDOT Construction, TDOT Geotechnical and the general contractor Highways, Inc. The willingness of Highways, Inc. to adjust construction techniques during the project was a huge factor in completing the project safely. The location and spacing of presplit holes was adjusted several times in order to better accommodate conditions at the site. Both horizontal blasting and trim blasting were used at the site to address problems. This was a dynamic site and conditions could and did change rapidly. The attention paid to the site by Highways and by TDOT Construction and Maintenance led directly to the successful completion of this challenging project with no injuries during or after construction. The site still receives periodic monitoring and inspection by TDOT Geotechnical and TDOT Maintenance. No further problems have been noted at the site, and no rock has reached the roadway or impacted traffic.

REFERENCES:

1. *TDOT Geotechnical Engineering Section Files*, reports, photographs and memoranda
2. *Royster, D.L.* Highway landslide and stability problems in Tennessee, Prepared for presentation at the 46th annual Tennessee Highway Conference, April 9-10, 1964.
3. *TDOT Geotechnical Engineering Section Files*, photographs of site made by George Hornal of TDOT aerial photography.
4. *Jones, C. L., Higgins, J. D., and Andrew, R. D.:* Colorado Rockfall Simulation Program Version 4.0, Colorado Department of Transportation, Denver, CO, 127 pp., 2000. http://www.dot.state.co.us/geotech/crsp.cfm
5. *Pierson, L.A., Gullixson, C.F., Chassie, R.G.*, Rockfall Catchment Area Design Guide, Final Report for Oregon Department of Transportation – Research Group and Federal Highway Administration, December, 2001. *http://www.oregon.gov/ODOT/TD/TP_RES/AbstractsIII.shtml#Rockfall*

Karst Vulnerability Considerations in Highway Route Selection, Juneau Area, Alaska

N. J. Darigo
URS Corporation
2700 Gambell St., Suite 200
Anchorage, Alaska 99503
907-261-6750
nancy_darigo@urscorp.com

ABSTRACT

The protection of caves and karst gained recognition following passage of the Federal Cave Resources Protection Act of 1988 and the development of U.S. Forest Service protection standards in the 1990s. A karst vulnerability assessment was conducted for the Alaska DOT&PF as part of an FHWA-funded Environmental Impact Statement (EIS) to evaluate the effects of highway construction along the east and west sides of Lynn Canal northwest of Juneau. The assessment focused on portions of west Lynn Canal where limestone had previously been mapped.

A classification system originally developed by Tongass National Forest was used to rate impacts based on extent of epikarst development, presence of karst features, and the openness of the system whereby debris and pollutants could affect downstream watersheds. The approach utilized aerial photograph evidence, systematic traverses, and standardized documentation methods to map areas of low, moderate, and high vulnerability karst in GIS. Detailed mapping of structural and stratigraphic trends effectively removed much of the previously suspected karst terrain from vulnerability consideration.

Following route modification to avoid identified caves, the resulting alternative crossed about 0.5 mile of high vulnerability karst (e.g. open sinkholes on glaciomarine benches) and 8 miles of low to moderate vulnerability karst (e.g., hummocky soil-plugged doline terrain). Correlation of watershed mapping with vulnerability ratings identified approximately 100 acres of vulnerable watershed area downgradient of the highway route. Other environmental and socioeconomic factors led to an alternative route in non-karst terrain being preferred in the recently completed Final EIS.

INTRODUCTION

Lynn Canal is the waterway that serves to connect Juneau, Alaska with the cities of Haines and Skagway via the Alaska Marine Highway System. Juneau is the state capital of Alaska. At present, there is no roadway connecting these three cities to one another, or connecting Juneau to the continental highway system. The Juneau Access Improvements Project was undertaken by the Alaska Department of Transportation and Public Facilities (ADOT&PF) to improve the surface transportation link between these cities.

As required by the National Environmental Policy Act (NEPA) of 1969, a Draft EIS begun in the 1990s and a Supplemental Draft EIS conducted for the project between 2002 and 2006 considered a number of highway and ferry route alternatives. One of these, the West Lynn Canal Highway alternative, would have extended the existing highway north of Juneau to a shuttle ferry across Lynn Canal, connecting to a 40-mile long highway along the west side of Lynn Canal through Tongass National Forest lands (Figure 1). Reconnaissance investigations conducted in the 1990s along west Lynn Canal indicated that carbonate rock and potential karst foundation conditions exist along the southern two-thirds of this alternative (*1, 2, 3*), triggering environmental concerns with regard to impacts to karst and cave resources.

Environmental Concerns for Karst Resources

The term “karst’ is used to describe a three-dimensional terrain of limestone where landforms are dominantly solutional in origin, and drainage is underground through enlarged fissures and conduits (*4*). The effects of subsurface karst as a geologic hazard for foundations of engineered structures are well documented. Less recognized is the potential for environmental damage to karst ecological systems from surface development. Beneficial aspects of karst areas typically include well developed forests, highly productive plant and animal

communities, high quality water, extremely productive aquatic communities, well developed subsurface drainage, and unique cave resources.

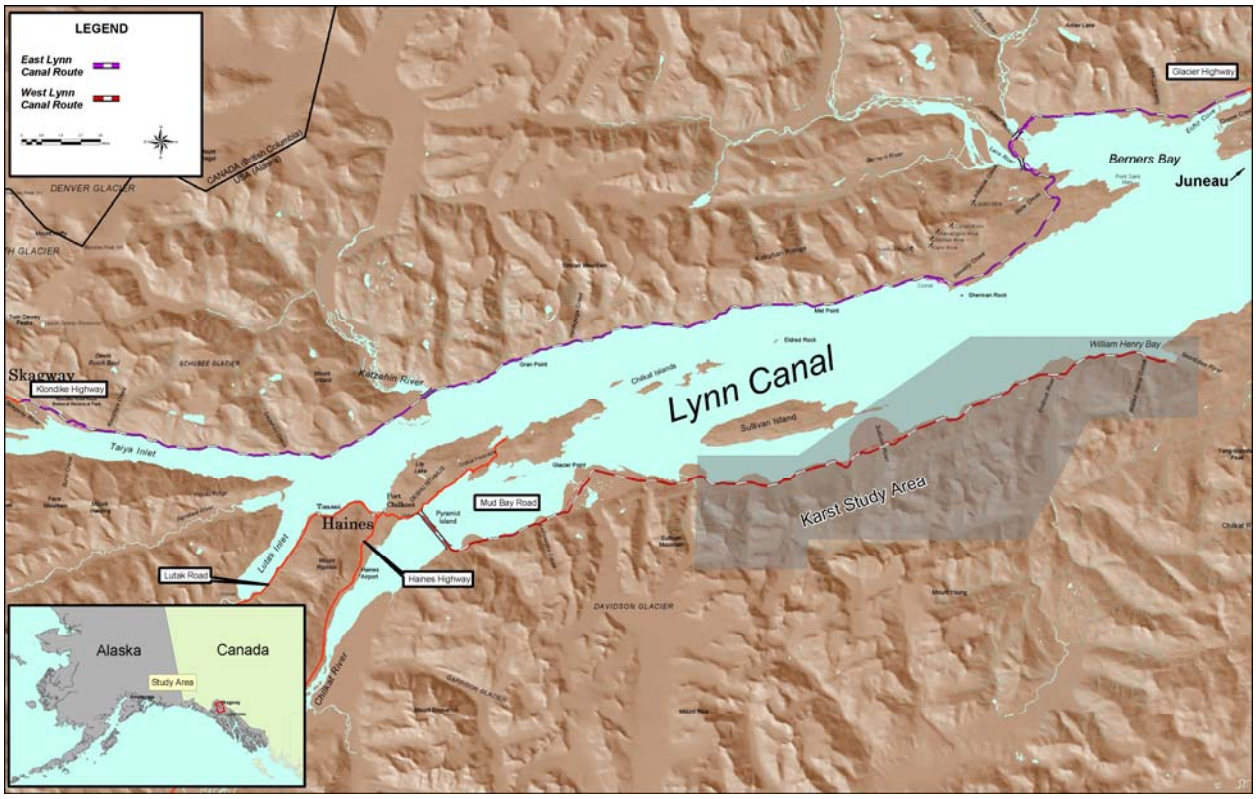

Figure 1. Location of study area in northern part of southeast Alaska.

Impacts to karst from surface disturbing activities have been documented both in the Tongass and worldwide (e.g., *4*, *5*). Increased surface runoff following forest clearing and road building can increase sediment, nutrient, and debris transport into underground drainage networks. Paved road surfaces generate additional runoff that commonly gets diverted into karst features. Because of the direct link between surface water and subsurface drainage, potential impacts to karst hydrologic systems can include changes to drainage patterns and infiltration rates, sediment production, debris and pollutant transport, and introduction of organic materials that increase oxygen demand. Clearing of vegetation can alter the water balance of a watershed. The removal of forest canopy alters both evaporation and transpiration rates, resulting in an increase in water available for surface or subsurface flow. Such effects could involve more frequent exceedance of the capacity of underground conduits, resulting in unexpected surface water flow during major storm events, especially if sediment-laden runoff causes karst pathways to become plugged. Such a transition has ecological implications both above and below ground.

The vulnerability of karst landscapes to ground disturbing activities is largely dependent on the degree of access to the subsurface karst, an idea that forms the basis for the karst vulnerability classification criteria used in this project. Where recharge is diffused through deep soils, the underlying karst is less vulnerable to increased sediment input and other pollutants, than in areas where soils are thin or nearly absent. Where soils are thin or removed during surface activities, exposure of the epikarst results, providing an easy pathway for sediment directly into the subsurface via solution-widened fissures in the rock. Discreet recharge points, such as open sinkholes, are especially vulnerable to ground disturbing activities because flowing surface water can carry sediment and other pollutants directly into the subsurface, sometimes from long distances upstream of the actual sinkhole.

Regulatory Framework

The Federal Cave Resources Protection Act (FCRPA) of 1988 mandates the protection of significant caves on Federal lands, and requires that specific location information for caves not be available to the public. FCRPA defines the term "cave" to mean

> "any naturally occurring void, cavity, recess, or system of interconnected passages which occurs beneath the surface of the earth or within a cliff or ledge (including any cave resource therein, but not including any vug, mine, tunnel, aqueduct, or other manmade excavation) and which is large enough to permit an individual to enter, whether or not the entrance is naturally formed or manmade. Such term shall include any natural pit, sinkhole, or other feature, which is an extension of the entrance."

In 1994, the U. S. Forest Service responded to FCRPA by establishing a final rule (36 CFR Part 290) with the intended effect to fully implement the cave protection regulation on Forest Service lands, ensuring that they are managed in a manner to protect and maintain significant caves. The final rule prohibits the excavation, damage, or removal of cave resources without special use authorization, and presents a number of criteria for determining whether a cave is potentially significant. These include habitat for flora and fauna, cultural features, mineralogic or paleontologic features, hydrologic resources, recreational opportunities, and educational or scientific opportunities. Caves that possess one or more of these features or values are considered potentially significant. Though "non-significant" caves may exist, most meet the criteria for "significant," and until resource values are determined on a case-by-case basis, the Forest Service considers all caves significant.

Although the stated intent of FCRPA is to protect cave resources and not karst resources, the Forest Service recognizes that caves with associated features and resources are an integral part of the karst landscape, and that karst must therefore be managed as an ecological unit to ensure protection of cave resources. To this end, they developed management strategies and a classification system in the 1990s (*6*, *7*) to characterize karst resource sensitivity in the Tongass, resulting in published standards and guidelines in the Tongass Land and Resource Management Plan (TLMP) in 1997 (*8*). TLMP embodies provisions of the National Forest Management Act of 1976 and its implementing regulations.

Because of differing interpretations of the TLMP standards and guidelines since their publication (e.g., *9*, *10*), an attempt was made by the Forest Service in the late 1990s to modify the classification system through a formal process known as a Tongass Plan Implementation Team (TPIT) Clarification Paper. Discontinued in 2001, the purpose of TPIT was to clarify management direction contained in TLMP, and provide consistency in the application of the karst standards and guidelines across different portions of the Tongass. A draft TPIT Clarification Paper dated 1999, together with TLMP and subsequent field applications of the classification system (*11*), provided the basis for the criteria and methodology used for this study.

REGIONAL SETTING

Southeast Alaska is a landscape of intensely glaciated and heavily forested mountains with moderate to steep slopes broken by raised benches and bare rock cliff bands. Drainage patterns typical of areas underlain by non-carbonate rock are characterized by steep, deeply incised (V-notched) streams which feed into wide, braided rivers in the base of glacially-carved valleys. Areas underlain by carbonate rock are generally internally drained with very little surface water flow. Annual precipitation in this maritime climate ranges from 54 to 92 inches, with greater accumulations towards the south. Melting snows and spring rains contribute large amounts of water to the rivers and creeks within the study area. Tidal fluctuations in Lynn Canal are typically in the range of 14 to 16 feet (*2*, *3*).

Structural Geology

The northern part of southeast Alaska is underlain by a complex heterogeneous assemblage of sedimentary, volcanic, metamorphic, and intrusive rocks of Paleozoic through Tertiary age. These rocks were emplaced in the southeastern Alaska archipelago during a series of subductions and accretions by tectonic plates obliquely colliding with the ancient continental margin of western North America during Jurassic to early Tertiary time (*12*, *13*).

The west side of Lynn Canal lies within the Alexander Terrane geologic province, one of five subcontinental blocks of rock in Southeast Alaska. The eastern boundary of Alexander Terrane rocks in the project vicinity is formed by the potentially active Lynn Canal-Chatham Strait fault system, which trends north-northwest beneath Lynn Canal, and is an extension of the active Denali fault system in interior Alaska. Silurian turbidites, shallow marine

carbonates, and conglomerate are the most widespread geologic units within the Alexander Terrane (*13*). These rocks formed near the paleoequator in an oceanic and volcanic island arc environment, prior to northward rafting that resulted in the current structural setting. Deformation during accretion resulted in regional metamorphism and a network of major northwest-trending lineaments and strike-slip faults, with secondary faults trending northeasterly (*5*,*12*). Many of these faults provided preferential pathways for glaciers, which formed deeply carved valleys and fjords throughout southeast Alaska.

Geologic Units

The geology of the study area was previously mapped by several authors (*14, 15, 16*) and locally revised during this study based on aerial photo and field observations (Figure 2). The dominant carbonate and karst-forming bedrock in the study area is a limestone unit within the Silurian Point Augusta Formation ("Stal," shown in solid blue on Figure 2). It outcrops along the coastline in several major exposures totaling about 5 miles long, that are broken by east- and northeast-trending faults and intervening outcrops of non-carbonate rocks. This unit consists of thin- to medium-bedded light gray limestone with minor limestone turbidites. Bedding generally strikes northwesterly and dips steeply to the southwest. The limestone beds contain relatively pure calcium carbonate ($CaCO_3$) (*17*), and are generally unfossiliferous in the site vicinity. Layers of non-carbonate turbidites, graywacke, and schist occur as interbeds with varying frequency and thickness within the limestone.

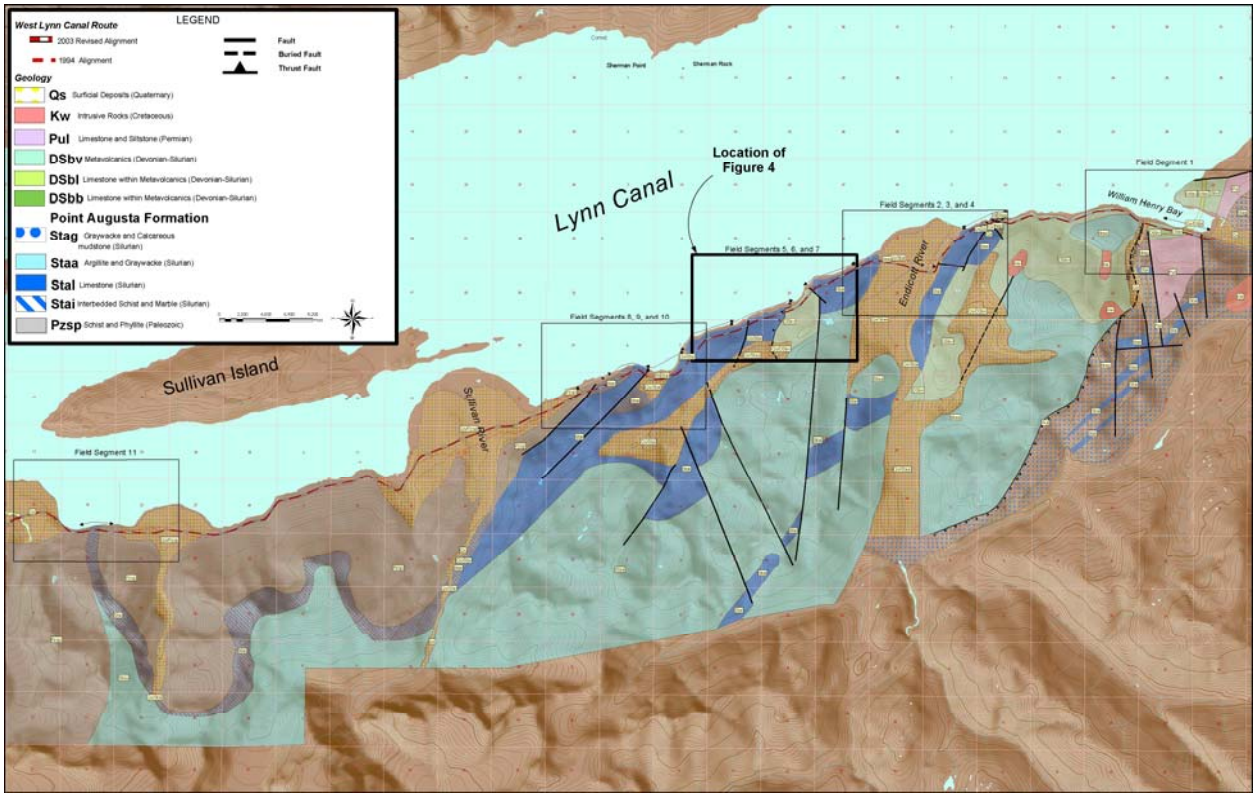

Figure 2. Geologic map of study area. Primary karst-forming unit is the limestone member of the Silurian Point Augusta Formation (solid blue).

Other rock types within the Point Augusta Formation include siliceous argillite, graywacke, limestone clast-bearing conglomerate, and calcareous mudstone above the limestone member (*14, 15*); and interbedded schist and limestone/marble beds beneath the limestone member in the north end of the study area. Where interbedded rocks were observed to be dominated by carbonates during this study, they were assigned to the limestone member of the Point Augusta Formation; where dominated by non-carbonates, they were remapped as the interbedded member

("Stai") to distinguish them from the more karst-forming rocks. The interbedded member exhibits a range of metamorphism from metagraywacke and limestone; to schist, phyllite, and marble. Other bedrock types along the proposed west Lynn Canal route include Permian limestone and siltstone (in a small fault block at the south end of the route), Devonian-Silurian metavolcanics, and Paleozoic schist and phyllite with minor limestone beds (*3, 15*).

Quaternary surficial deposits in the study area include glacial till and outwash alluvium, mass wasting/talus slope deposits, beach gravels, and alluvium and deltaic deposits beneath the major streams. Uplift in response to glacial unloading and Quaternary structural deformation has raised old marine terraces or benches on the lower slopes along the proposed west Lynn Canal highway route (*2, 3*). Pebbly glacial soils with occasional boulder-sized erratics were commonly observed to be mantling these benches and the more gentle slopes. Soil thicknesses in the study area range from a thin mossy cover in areas of exposed limestone bedrock, to tens of feet in the major stream valleys.

Karst Characteristics

Karstlands in southeast Alaska have been characterized as unique ecological units which encompass several components: the forest and forested wetlands on top and adjacent to the karst, recharge areas on adjacent non-carbonate substrata, the karst surface and subsurface interactions, and the groundwater that develops from these systems. Factors influencing the development of karst in this region include:

1. Purity of the carbonate bedrock
2. Extent of faulting, jointing, fractures, and bedding planes
3. Metamorphism altering carbonates and other rock types in a way that may block subsurface flow
4. Proximity of carbonate rocks to muskegs and forested wetlands that generate and drain highly acidic water onto the carbonates
5. Glacially modified surface topography and drainage, and
6. Precipitation and temperature influences on weathering rates and solutional activity (*5*).

Regional fault patterns in southeast Alaska are important to karst development, in that they are mimicked at a very local scale, resulting in zones of weakness that are more subject to chemical weathering than adjacent rock. Linear epikarst and karst features such as collapse channels develop preferentially along sets of fractures, joints, and faults (*4, 8*). Stratigraphic contacts between carbonates and non-carbonates determine the lateral and vertical extent of individual karst features and terranes, subsurface drainage pathways, and the type of features present.

The most favorable climatic environment for karst development occurs in alpine and cold temperate regions with high precipitation and runoff rates (*18*), conditions that are optimal in southeast Alaska, creating one of the most actively developing karst regions in the world. The presence of muskegs and forested wetlands in the study area creates acidic surface water, resulting in aggressive solution activity where it drains onto carbonate rock. Epikarst and subsurface solutional features are developed through this chemical weathering process. Collapse features occur when downward solution, combined with upward stoping of cavity roofs from below, weakens spans of surface bedrock or soil.

Glacial activity during the Pleistocene greatly influenced the character of karst landscapes in southeast Alaska. The extent of this influence is the result of a complex interplay between ice extent, sea level changes, tectonic uplift and deformation, and isostatic rebound. Glaciation has destroyed karst by mechanical erosion, ice plucking, and wrenching of bedrock blocks; and glacial detritus has been introduced into subsurface cavities following ice retreat and sea level rise. During the last glaciation, ice originated in major river valleys located at the north end of Lynn Canal, filling it to an elevation of 2,500 feet (*2*). Glaciation of karst terrain in southeast Alaska has resulted in karst development that varies, in large part, with elevation (e.g., *19*). Karst development is typically more extensive at higher subalpine elevations, than at lower elevations where much of the epikarst has been scoured off and blanketed by glacial till.

METHODOLOGY FOR KARST VULNERABILITY ASSESSMENT

A systematic karst vulnerability field survey of the proposed west Lynn Canal highway route was undertaken in 2003 to determine the extent of karst development, and to evaluate whether the location and design of the highway would be protective of karst resources, based on FCRPA as well as vulnerability criteria and land use objectives established by the Forest Service (*8*).

Classification System

Karst vulnerability mapping is a tool for rating potential effects on karst from surface development. Vulnerability mapping utilizes the fact that some parts of a karst landscape are potentially subject to appreciably greater resource damage and contamination risk than others. These differences are a function of the extent of epikarst development; the presence of beneficial karst resources; and the openness of the karst system whereby sediment, debris, and other pollutants can be introduced and affect downstream resources. Criteria in each of three karst vulnerability categories were used to evaluate the vulnerability of karst in the project area to potential damage from road building activities. The characteristics used to establish vulnerability were organized into forms in an effort to standardize field documentation among geologists (Figure 3).

Low Vulnerability Karstlands

Low vulnerability karstlands are those areas where damage associated with road building is not appreciably greater than damage posed to non-carbonate substrate. These are areas underlain by carbonate bedrock that are commonly internally drained, but surface streams may be present. Generally, these areas of the Tongass have been greatly modified by glaciation, have a deep (>40 inches) covering of glacial till or mineral soil, and little or no epikarst exposed at the surface. The epikarst may be buried or abraded, depending on the intensity of glaciation. These lands pose little or no threat of organic, sediment, debris, or pollutant introduction into the underlying karst hydrologic system. Often these areas exhibit little or no slope (<20 percent) and tend to lie at lower elevations, i.e., <500 feet. No special provisions for the protection of karst values are considered necessary in low vulnerability karstlands. Road building could be conducted in such areas in a similar manner to those normally employed on lands underlain by non-carbonate bedrock.

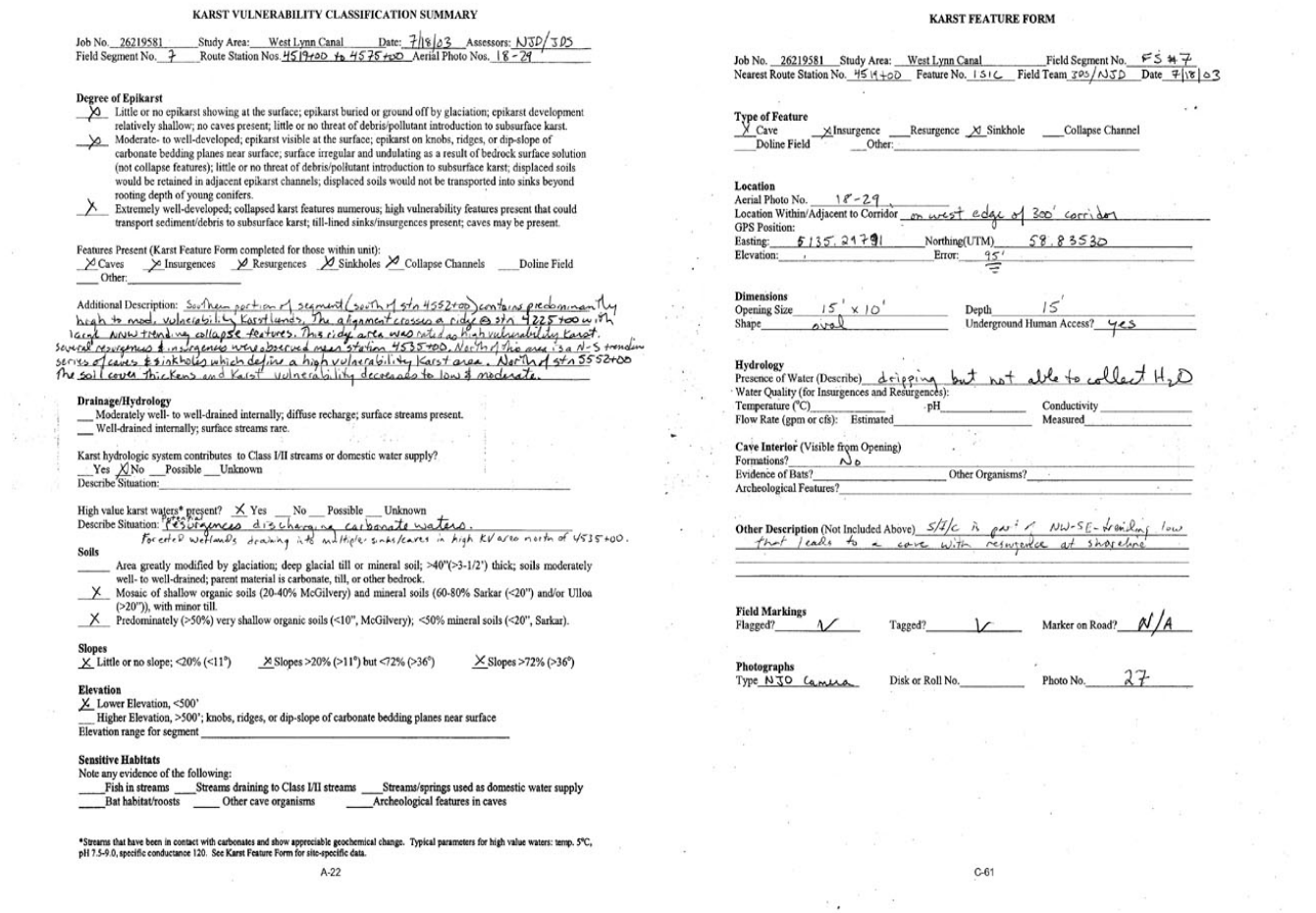

KARST VULNERABILITY CLASSIFICATION SUMMARY

Job No. 26219581 Study Area: West Lynn Canal Date: 7/18/03 Assessors: NJD/JDS
Field Segment No. 7 Route Station Nos. 451900 to 457500 Aerial Photo Nos. 18-29

Degree of Epikarst

X Little or no epikarst showing at the surface; epikarst buried or ground off by glaciation; epikarst development relatively shallow; no caves present; little or no threat of debris/pollutant introduction to subsurface karst.

X Moderate- to well-developed; epikarst visible at the surface; epikarst on knobs, ridges, or dip-slope of carbonate bedding planes near surface; surface irregular and undulating as a result of bedrock surface solution (not collapse features); little or no threat of debris/pollutant introduction to subsurface karst; displaced soils would be retained in adjacent epikarst channels; displaced soils would not be transported into sinks beyond rooting depth of young conifers.

X Extremely well-developed; collapsed karst features numerous; high vulnerability features present that could transport sediment/debris to subsurface karst; till-lined sinks/insurgences present; caves may be present.

Features Present (Karst Feature Form completed for those within unit):
X Caves X Insurgences X Resurgences X Sinkholes X Collapse Channels ___ Doline Field
___ Other:

Additional Description: Southern portion of segment (south of stn 455200) contains predominantly high to mod. vulnerability karstlands. The alignment crosses a ridge @ stn 452500 w/ several large NW trending collapse features. This ridge area was rated as high vulnerability karst. Several resurgences & insurgences were observed near station 453500. North of the area is a N-S trending series of caves & sinkholes which define a high vulnerability karst area. North of stn 455200 the soil cover thickens and karst vulnerability decreases to low & moderate.

Drainage/Hydrology

___ Moderately well- to well-drained internally; diffuse recharge; surface streams present.
___ Well-drained internally; surface streams rare.

Karst hydrologic system contributes to Class I/II streams or domestic water supply?
___ Yes X No ___ Possible ___ Unknown
Describe Situation:

High value karst waters* present? X Yes ___ No ___ Possible ___ Unknown
Describe Situation: Perched resurgences discharging carbonate waters. Forested wetlands draining into multiple sinks/caves in high KV area north of 453500.

Soils

___ Area greatly modified by glaciation; deep glacial till or mineral soil; >40"(>3-1/2') thick; soils moderately well- to well-drained; parent material is carbonate, till, or other bedrock.
X Mosaic of shallow organic soils (20-40% McGilvery) and mineral soils (60-80% Sarkar (<20") and/or Ulloa (>20")), with minor till.
X Predominately (>50%) very shallow organic soils (<10", McGilvery); <50% mineral soils (<20", Sarkar).

Slopes

X Little or no slope; <20% (<11°) X Slopes >20% (>11°) but <72% (>36°) X Slopes >72% (>36°)

Elevation

X Lower Elevation, <500'
___ Higher Elevation, >500'; knobs, ridges, or dip-slope of carbonate bedding planes near surface
Elevation range for segment

Sensitive Habitats

Note any evidence of the following:
___ Fish in streams ___ Streams draining to Class I/II streams ___ Streams/springs used as domestic water supply
___ Bat habitat/roosts ___ Other cave organisms ___ Archeological features in caves

*Streams that have been in contact with carbonates and show appreciable geochemical change. Typical parameters for high value waters: temp. 5°C, pH 7.5-9.0, specific conductance 120. See Karst Feature Form for site-specific data.

A-22

KARST FEATURE FORM

Job No. 26219581 Study Area: West Lynn Canal Field Segment No. FS #7
Nearest Route Station No. 451900 Feature No. 151C Field Team JDS/NJD Date 7/18/03

Type of Feature

X Cave X Insurgence ___ Resurgence X Sinkhole ___ Collapse Channel
___ Doline Field ___ Other:

Location

Aerial Photo No. 18-29
Location Within/Adjacent to Corridor on west edge of 300' corridor
GPS Position:
Easting: 5135.29791 Northing(UTM) 58.83530
Elevation: Error: 95'

Dimensions

Opening Size 15' x 10' Depth 15'
Shape oval Underground Human Access? yes

Hydrology

Presence of Water (Describe) dripping but not able to collect H_2O
Water Quality (for Insurgences and Resurgences):
Temperature (°C) pH Conductivity
Flow Rate (gpm or cfs): Estimated Measured

Cave Interior (Visible from Opening)

Formations? No
Evidence of Bats? Other Organisms?
Archeological Features?

Other Description (Not Included Above) S/H/C in gen'l NW-SE-trending low that leads to a cave with resurgence at shoreline

Field Markings

Flagged? V Tagged? V Marker on Road? N/A

Photographs

Type NJD camera Disk or Roll No. Photo No. 27

C-61

Figure 3. Examples of data forms used during field surveys. The karst classification form provided a mechanism for the standardization of geomorphic data collection and vulnerability criteria application among different field personnel. The karst feature form was used for collecting field data on individual karst features.

Moderate Vulnerability Karstlands

Moderate vulnerability karstlands are those areas where damage from road construction could be appreciably greater than on low vulnerability karstlands. These areas are underlain by carbonate bedrock that is well drained internally. Surface streams are rare. Moderate vulnerability areas often occur on knobs and ridges, and on the dip-slope of carbonate bedding planes. The ground surface of these areas tends to be irregular and undulating, mimicking the epikarst development beneath. Moderate vulnerability features such as grikes and doline fields are often the result of slow, diffuse processes, rather than collapse or major subsidence processes, which typify high vulnerability features. The primary characteristic used to differentiate between moderate and high vulnerability karst is the openness of the system. Moderate vulnerability features are not as open to the subsurface as high vulnerability features, and pose little threat of organics, sediment, and debris introduction into the karst hydrologic systems beneath. Resurgences (springs) could be classified as moderate or high vulnerability depending upon the level of atmospheric connectivity they provide to the underground system. Soils of moderate vulnerability areas are typically a mosaic of shallow organic soils (20-40 percent) and mineral soils (60-80 percent) with minor amounts of glacial till. The epikarst is moderate- to well-developed, and visible at the surface in these areas.

Forest Service management objectives in moderate vulnerability karstlands are to allow certain land uses while protecting the function and biological significance of karst and cave resources. Ideally, roads would not be placed in moderate vulnerability areas exhibiting a high density of features and/or exposed epikarst. Small expanses of these lands, however, could be crossed by roads to access other areas where road building is deemed appropriate. New

roads built across moderate vulnerability areas would avoid individual karst features, and not divert water to or from them. Measures such as sediment traps and revegetation would be taken to reduce erosion and sediment transport from road surfaces and cut slopes.

High Vulnerability Karstlands

High vulnerability karstlands are those areas where potential damage from road construction could have an appreciably greater impact to karst resources than on low or moderate vulnerability karstlands. High vulnerability karstlands include areas contributing to or overlying significant caves; areas containing a high density of karst features; and areas with karst features exhibiting openness to the subsurface, such as collapse channels and basins, sinkholes, caves, losing streams, insurgences, open resurgences, well developed doline fields, and open grikelands. High vulnerability areas are underlain by carbonate bedrock that is well-drained internally. Surface streams are rare. Karst systems and epikarst are extremely well developed, and collapse features may be numerous. The highest vulnerability features are those that could produce and transport the greatest amount of sediment, debris, and/or organics if disturbed, such as till-lined sinkholes and cave entrances accepting a losing stream. Soils in high vulnerability areas consist of predominantly very shallow organic soils (<10 inches), and less predominantly shallow mineral soils (<20 inches).

High vulnerability areas are managed by the Forest Service to ensure conservation of karst values through the implementation of a high level of protection. With rare exceptions, road construction is disallowed on these lands, and every effort is made to reroute road corridors to avoid high vulnerability areas. Forest Service guidelines require the development of site-specific buffer distances around high vulnerability karst features to account for potential tree blowdown. These may range from a minimum 100-foot radius to 400 feet or more. Buffers are also required along losing streams to a distance of one mile upstream of where they sink. If a road must be built across isolated areas of high vulnerability karst to access areas of lower vulnerability where road building is deemed appropriate, and no alternative route is feasible or economic, design and construction restrictions would be required, such as: minimization of clearing limits and grubbing; use of fill-only construction rather than balanced cut-and-fill design; use of bridges or similar structures to span collapse features; use of geotextiles to prevent aggregate from falling into collapse features; use of sediment traps and erosion control measures; same-season revegetation of slopes to minimize sediment production potential; and Forest Service review of proposed road construction plans prior to construction.

Iterative Assessment Process

The west Lynn Canal karst study generally followed a four-part methodology outlined in Forest Service guidance (*8*) with several project-specific modifications. Prior to conducting the study, a draft methodology and scope were submitted for agency review and approval (*25*).

Step 1 – Identification of Potential Karst Areas

This step involved the compilation and review of known karst features and caves in the study area and preliminary characterization of karst geomorphology to identify potential karst terranes and features. The presence or absence of carbonate rocks, watershed information, and known karst features and caves in the study area were identified based on both published and unpublished sources (*1, 2, 3, 12, 14, 15, 16, 17, 20, 21, 22, 23, 24*). Topographic base maps were developed for the project in GIS at 1"=1,000' scale using GPS route coordinates supplied by ADOT&PF and best-available USGS topography at 100-foot contour intervals. Uncontrolled stereographic aerial photographs at 1"=1,000' scale were reviewed in detail for identification of likely karst features, trends, or lineaments. Light Distancing and Ranging (LIDAR) topographic data and orthorectified aerial photographs of the project area flown in late 2003 were unavailable at the time of the field survey.

Step 2 – Field Inventory

A field inventory of karst resources and potential karst features was completed for segments of the proposed west Lynn Canal route determined to be underlain by carbonate bedrock. The objective of this phase was to document karst features, establish initial vulnerability ratings, and identify areas that were deemed highly vulnerable and therefore unacceptable for road building without additional routing or engineering considerations. The inventory documented the degree of epikarst development; the presence and location of potentially significant karst features; the depth and nature of soil; the presence of streams contributing to, or flowing from, the karst hydrologic system; and sensitive habitats and features that might be adversely affected by road construction and land use changes.

The proposed survey area was subdivided into route segments that could potentially be covered during a single field day, designated Field Segments FS-1 through FS-11 from south to north. Survey corridors were at least 300-feet wide in all field segments (150 feet on either side of centerline), and expanded to 500-feet wide in areas of high vulnerability karst (*25*). Field segments were accessed via helicopter from Juneau by two teams of geologists and bear guards. The surveys required rapid deployment of field personnel due to constraints on ADOT&PF's overall project timetable.

The field surveys consisted of systematic split traverses through the route corridors, with a focus on potential karst lineaments and features identified from aerial photographs and previous studies, and trends of features encountered in the field. Potentially significant karst features, or groups (polygons) of similar features, were documented on field maps and forms, flagged and tagged in the field, and assigned an alphanumeric identification number based on feature type. Mapping of initial karst vulnerability classifications was completed on a landscape or geomorphic unit basis while in the field. Vulnerability criteria and individual karst feature data were recorded onto forms (e.g., Figure 3) developed for use in karst field surveys and post-field analysis (*11)*.

Data from exposed bedrock outcrops, particularly along coastal cliffs, were recorded during the field surveys. Soils and slope data were evaluated to the extent that they provided information on the potential for introduction of sediment and debris into the subsurface karst system when disturbed. Hydrologic data collected in conjunction with Step 3 (below) included field measurements of temperature, pH, conductivity, and estimated flow rate from insurgences, resurgences, and selected streams. Forested wetlands were also noted in that they imply the presence of thick soils or low vulnerability karst, or provide a source of acidic water for solutional development downgradient. Sensitive habitats, such as those supporting cave organisms or downgradient streams important to fisheries, were also documented if observed. Following the field effort at each route segment, the data collected were summarized in a Field Summary Reports which highlighted route station numbers crossing high vulnerability karst.

Step 3 – Karst Hydrologic Evaluation

Concurrent with Step 2, hydrologic information was collected and synthesized with other data, in order to define, to the extent necessary and practicable for the proposed land use, the karst hydrologic system and approximate recharge or catchment areas along west Lynn Canal. The objective of this step was to understand the karst hydrologic system well enough to assess and characterize potential impacts to downgradient resources (e.g. fisheries, drinking water supply).

The locations of hydrologic karst features (e.g., resurgences, insurgences, and losing streams), were documented as part of the field surveys. Water quality data, the water volume entering or discharging from the groundwater system, and prevailing weather conditions were estimated at the time of the field efforts. Field data were tabulated and reviewed to identify potential variability between carbonate and non-carbonate waters; that is, potential differences that could result from chemical interaction with carbonate bedrock. Temperatures less than 5^{o}C, pH in the range of 7.5 to 9.0, and specific conductance greater than 120 microSiemens/centimeter (μS/cm) are typically an indication of high value karst waters in the Tongass (*8*).

This step also included a generalized interpretation of apparent catchment area boundaries (similar to watershed boundaries for non-karst areas). The scope of this study did not include tracer dye testing (*25*); however, the Forest Service encourages the use of tracer dye tests to delineate karst catchment area boundaries that may differ significantly from typical surface watershed boundaries (*8*). It is common for subsurface drainage pathways in karst to cross surface topographic divides, particularly at higher elevations in watersheds. In the absence of tracer dye data for the west Lynn Canal area, approximate catchment area boundaries were drawn based primarily on surface topographic data and stream observations in the field. The results of this task can only be considered "apparent"; that is, subsurface flow boundaries likely differ from those inferred from surface data, but may mimic them in a very general sense.

Step 4 – Vulnerability Interpretation

Step 4 involved the processing and synthesizing of data from the previous steps in order to assess karst sensitivity to the proposed land use. Karst data inventoried and mapped during the field surveys were entered into the GIS database, and the following map layers were created or updated based on the results: geology, including contacts, units, faults, and bedding or structural orientations; karst features, including potentially significant caves and other features documented in the field; karst vulnerability classifications resulting from the field surveys; and apparent watershed or catchment area boundaries. This step also included a reassessment of the initial karst vulnerability

classifications mapped in the field, which were based on localized geomorphic observations, to consider the overall boundaries of catchment areas and the position of the proposed highway alignment within the watersheds.

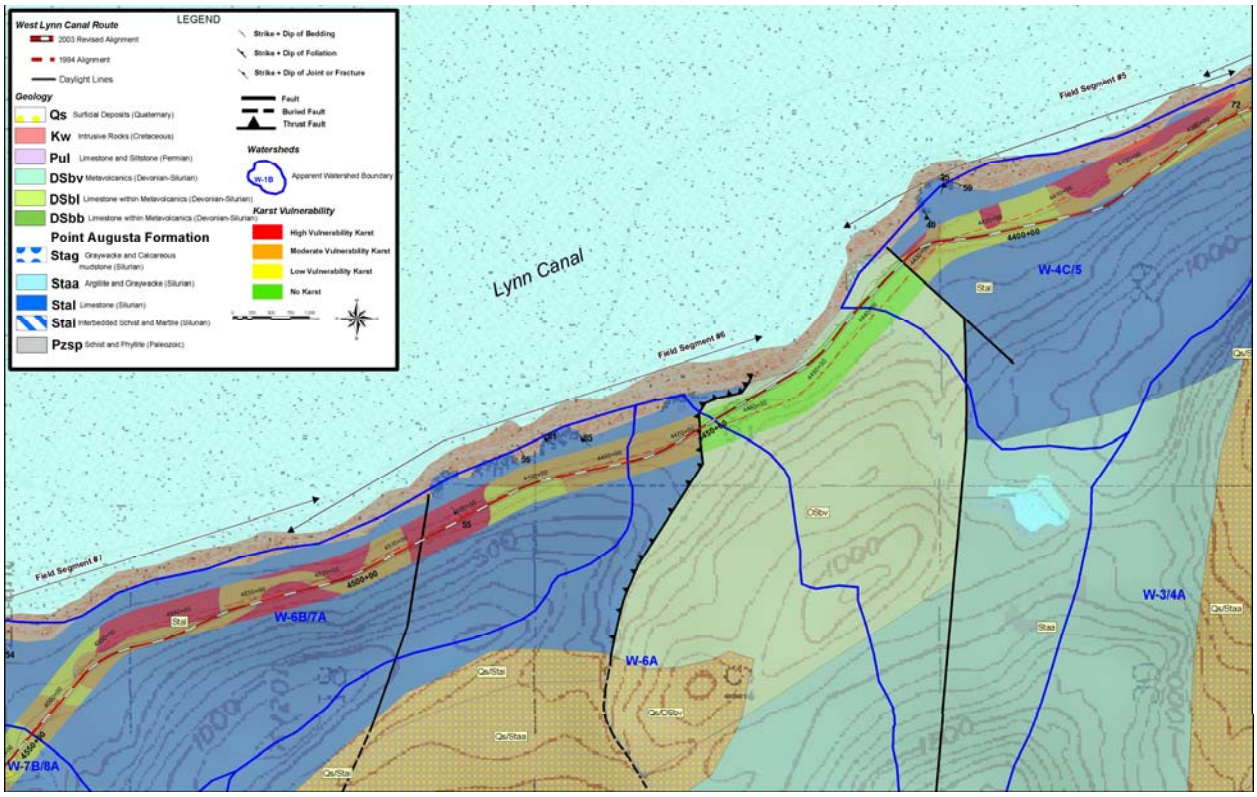

Figure 4. Karst vulnerability results, revised geology, and watershed/catchment area boundaries map. Example is shown for Field Segments FS-5 through FS-7 in central part of study area (location on Figure 2). Approximately 85 individual karst features (including caves, sinkholes, doline fields, vertical pipes, insurgences, resurgences, collapse channels, and linear depressions) were also mapped within and immediately downgradient of these field segments, but are not depicted due to the confidentiality requirements of FCRPA.

RESULTS

Complete sets of maps depicting karst vulnerability, geology, watersheds, and individual karst features were compiled in a *Karst Technical Report* for the Juneau Access Improvements Supplemental Draft EIS (*26*). Figure 4 provides an example of the mapping results for the central portion of the study area.

Karst Vulnerability Characteristics

The following paragraphs summarize characteristics of the karstlands encountered within the west Lynn Canal study area.

No to Low Vulnerability Areas

Areas with underlying non-carbonate bedrock were mapped as having no karst vulnerability. Areas underlain by carbonate-bearing bedrock which is otherwise dominated by non-carbonates, e.g., schist with minor marble interbeds or limestone clast-bearing conglomerate, were given low vulnerability ratings. The landscape over these rocks typically exhibited little to no karst characteristics; however, they were assigned to the low vulnerability category in consideration of potential variability in carbonate concentration. Vugging or other small-scale solutional

features may be present beneath the glacial soil cover in areas with a greater concentration of grain-supported clasts or carbonate interbeds.

Table 1. Characteristics of moderate and high vulnerability karst associated with Field Segments FS-5 through FS-7 (Figure 4).

Station Numbers[1]	Karst Vulnerability Rating	Characteristics of Karst Landscape/Features Within Footprint Daylight Lines[1]
		Field Segment FS-5
4378+00 to 4411+00	Moderate	Ridges and depressions mimicking interlayered non-carbonates, low to moderately developed epikarst on tops and sides of cliff bands, hummocky terrain at base of cliff and talus slope, occasional closed sinkholes. Caves and other high karst features 150 to 450 feet downgradient of footprint.
4428+00 to 4432+00	Moderate	Closed dolines/sinkholes at base of ridge.
4429+00 to 4432+00	High	High vulnerability karst along east edge of footprint due to littoral caves about 100 feet east of footprint.
		Field Segment FS-6
4468+00 to 4492+00	Moderate	Small dolines, closed sinkholes, hummocky terrain, shallow filled grikes, occasional exposed epikarst.
4497+00 to 4508+00	High	Series of resurgences and insurgences in colluvium/till over epikarst.
4508+00 to 4518+00	Moderate	Cliff bands, moderately developed epikarst, thin soils, possible resurgent dry streambed, hummocky well-drained topography.
		Field Segment FS-7
4517+00 to 4520+00	High	Possible resurgence leading to diffuse insurgence; footprint is approx. 200 feet upgradient of sinkhole/cave leading to cave with resurgence at coastline.
4519+00 to 4522+00	Moderate	Hummocky terrain, glacial soils covering epikarst.
4522+00 to 4530+00	High	Series of large linear collapse basins.
4529+00 to 4534+00	Moderate	Cliff bands and ridges, suspect resurgences and diffuse insurgences into soil cover.
4534+00 to 4536+00	High	Possible resurgence leading to series of sinkholes outside downgradient edge of footprint.
4536+00 to 4557+00	Moderate	Hummocky terrain with well-drained soils, cliff bands, occasional closed sinkhole. Series of caves 100-200 feet downgradient of footprint.

1 = 2003 revised alignment footprint.

Low to Moderate Vulnerability Areas

Most of the karst encountered in the study area was of low to moderate vulnerability typical of other low-elevation karstlands around southeast Alaska. These areas were characterized by shallow undulating terrain, thick glacial deposits, and rare bedrock exposures along benches and gentle slopes. Exposed limestone cliffs, ridges, and rock overhangs were characterized as moderate if open fractures were observed that appeared to be soil-filled at shallow depths. Limestone cliffs and ridges with closed fractures were characterized as low vulnerability, as were lower slopes at the base of cliffs where covered by a thick section of colluvium or talus deposits. Karst features identified within areas of moderate vulnerability included shallow soil- and moss-filled doline fields and grikes (up to 5 feet deep), suspect karst resurgences emanating from soil or talus deposits overlying carbonate bedrock, and diffuse insurgences at the lower end of dry streambeds where surface water disappears into the soil cover over a broad area of forest floor. Table 1 summarizes characteristics of moderate vulnerability areas associated with the example map in Figure 4.

High Vulnerability Areas

Several portions of the road corridors were characterized as having high vulnerability karst. These generally fell into one or more of three categories: (1) areas along shoreline cliffs, in which caves or other karst features were observed; (2) areas on flat to gently sloping benches where forested wetlands drain into well-developed sinkholes and caves; and (3) areas exhibiting a series of large U-shaped collapse basins. Table 1 summarizes characteristics of high vulnerability areas associated with the example map in Figure 4.

Linear strips of high vulnerability karst were mapped along coastal cliffs in several areas where the proposed highway route comes close to shore, and caves or other potential karst features were observed in the cliffs. Similar features were also occasionally observed along inland cliffs along what may be raised wave-cut terraces. A number

of the coastal caves which had been previously mapped and named (*1,17, 24*) fall outside of the east edge of the study corridor. Several of the coastal caves exhibited evidence of animal habitat such as porcupine quills and scat.

Figure 5. Example of coastal cave exhibiting origins by cavitation, littoral erosion, and block failure along dip-slope of bedding planes.

Many of the caves or other features observed in the shoreline cliffs in the study area do not appear to be solutional in origin; rather, most appear to have been formed by cavitation and littoral erosion accompanied by block failure. Although solutional connectivity appeared to be lacking in most of these features, the littoral caves were considered high vulnerability because they met the definition of a cave under FCRPA. Many of the coastal caves appear to have formed along the dip-slope of fractures or bedding in the rock (Figure 5). Based on the alignment of many of the coastal caves along north- to northwest-trending lineaments, it is possible that fracturing is being driven by tectonic activity on the similarly aligned Lynn Canal-Chatham Strait fault system, which may be causing block failure to occur at a faster rate than that of solutional denudation. Evidence of water, where present in the littoral features, appears to have aggravated the block failure process, rather than created solutional openings. The coastal caves may also have been formed or aggravated by ice plucking deformation during glaciation. In areas with interbedded schist, swales and pocket beaches have formed along the highly erodable schist, providing preferential drainage over the schist and along schist/limestone bedding planes.

Areas of high vulnerability karst were identified on gently sloping benches in Field Segments FS-3 through FS-7. Typically these areas lie below steep cliffs to the west, where water accumulating at the base of the slopes forms forested wetlands on top of a thick section of glacial till. The high vulnerability features tend to occur abruptly downgradient of the forested wetlands, which often appear to be part of a low vulnerability terrain. A few of the caves encountered in these areas had been previously mapped and named (*1, 17*), including one aptly called Animal House Cave for the presence of porcupine droppings. Other karst features observed within these bench areas included individual sinks with insurgences into open bedrock at the bottom, and multiple sinks or collapse channels along north-northwest-trending lineaments. The presence of these features, combined with nearby littoral caves or other coastal karst features, create the highest vulnerability situation observed along the study area. Glacial soil cover in the bench areas is typically several feet thick, and appears to have plugged most of the open features. In

several of these features, there was evidence of flow and soil transport into the sinks, along resurgent streams emanating from upgradient soil cover.

Based on the general lack of solutional features and resurgences observed in shoreline caves, it is possible that waters draining into the high vulnerability features on the bench areas may resurge below the low tide mark in Lynn Canal. This condition has been suggested to explain losing streams in the karst of southeast Chichagof Island (*27*).

High vulnerability karst was mapped in Field Segment FS-7 in an area of large collapse basins. These features were observed to be on the order of 10 to 75 feet wide, by more than 200 feet long, with sidewalls 5 to 50 feet high. They are typically elongated in a north-northwest direction parallel to the coastline. These features were assigned a high vulnerability rating based on overall landscape appearance and likely underlying solutional connectivity.

Table 2. Watershed/catchment areas associated with Field Segments FS-5 through FS-7 (Figure 4).

Watershed/ Catchment Area Designation[1]	Watershed Description	Fish Habitat	Geology		Karst Vulnerability Along Route	Elevation Range (feet)	Watershed Area		
			Bedrock Type	Amount of Watershed Underlain by Limestone (Stal)			Total Area (acres)	Area Downgradient of Proposed Route[2]	
								Acres	% of Total Area
W-4C/5[3,4]	Drainage to coastline: coastal cliffs northern 2/3rds; Endicott River delta southern 1/3rd.	Yes. Lynn Canal	Limestone along north 2/3rds; surficial deposits along delta.	95%	Mostly Moderate to High.	0 to 1,100	430	117	27
W-6A[3]	"Fault Creek" follows thrust fault between volcanics and limestone.	Yes. Class I	Limestone north side of creek; volcanics south side of creek; mostly graywacke at upper elevations.	Approx. 10% slice along NE side	Moderate north side. None south side.	0 to 3,300	1,600	4	0.2
W-6B/7A[3]	Drainage to coastal cliffs	Yes. Lynn Canal	Limestone	100%	Mostly Moderate to High	0 to 1,200	440	160	36
W-7B/8A[3]	Canyon Creek	Yes. Class I	Limestone NE and central parts of watershed; graywacke in southern and western (higher) parts of watershed.	Approx. 1/3rd, NE and central parts of watershed	Low to Moderate	0 to 4,590	10,300	24	0.2

1 = Corresponds to field segment number.
2 = Based on 2003 revised alignment.
3 = Watershed boundaries previously mapped (*16*).
4 = Subwatershed identified locally based on topography, aerial photos, and field observations.

Catchment Area/Watershed Characteristics

The generalized interpretation of apparent catchment areas was based on previous watershed mapping (*16*), as well as local surface topographic and geologic data, aerial photo evidence, and stream observations in the field. Some of the previously mapped watersheds were subdivided into subwatersheds in an effort to focus on those that are underlain mostly by carbonate rocks. A number of the watersheds are Class I or II stream drainages with anadromous fish habitat (*28*).

Catchment area/watershed boundaries are depicted on the example map in Figure 4 for the central portion of the study area. Characteristics of these watersheds are summarized in Table 2. Catchment areas with the highest vulnerability karst in the study area are W-4B/5 and W-6B/7A, which contain the bench-type high vulnerability karst features described above.

The size of individual watersheds that drain across the proposed highway route, and the amount of carbonate bedrock beneath these watersheds, varies considerably. Small coastal drainages along shore-parallel ridges, and those that drain local V-notch streams, are in the range of 100 to 600 acres. The largest crossed by the study area are the Canyon Creek and the Endicott River watersheds (approximately 10,700 and 100,500 acres, respectively) which are underlain primarily by non-carbonate bedrock. These watersheds rise to elevations of 4,600 to 5,800 feet, while maximum elevations in the smaller coastal catchment areas underlain primarily by limestone are on the order of 1,000 to 2,000 feet.

Water quality data collected during the 2003 field surveys was very limited due to low precipitation, and the lack of flowing insurgences and true karst resurgences encountered. Data were collected for a total of seven resurgences or small streams suspected of emanating from resurgences. Two of these were found in the area depicted on Figure 4 (Field Segment FS-6) seeping from glacial soils at flow rates of <1 to 2 gallons per minute (gpm). Suspected of being karst in origin beneath the soil cover, their measured temperatures and conductivities (4.9 to 5.5 ^{o}C, 189 to 203 µS/cm) were generally in the range of high value karst waters (*8*), while one of the two pH measurements (7.05, 7.65) was slightly below the typical range for karst waters, possibly owing to contact with soils.

Analysis of Potential Environmental Consequences

An analysis of potential environmental effects on karst resources was conducted based on the results of the west Lynn Canal field surveys. Analysis of these types of impacts was not conducted for other alternative routes in the Juneau Access Improvements project, because no carbonate rock is known to underlie the other alternatives.

The evaluation of direct environmental impacts to karst is intrinsic to the vulnerability mapping process, in that the ratings criteria used recognize the parts of the landscape potentially subject to greater resource damage and risk than others. Effects on the karst hydrologic system were evaluated both through field observations, as well as by calculating the approximate portion of carbonate catchment areas that could be potentially affected by the route (Table 2). The analysis of karst effects consisted of two components:

1. Revision of the original highway alignment to avoid caves and as much high vulnerability karst as practicable, and
2. Measurement of the remaining vulnerable karst crossed by the revised alignment, in order to provide quantitative input to the broader comparison of alternatives in the EIS.

Revised Highway Alignment

In response to karst issues identified during the 2003 field survey, ADOT&PF shifted the original highway alignment away from as many high vulnerability karstlands and caves that could be avoided within engineering and constructability constraints (e.g., road curvature, high cliffs, open water). With the exception of one cave located just north of the Endicott River, the footprint of the realigned highway route avoids caves to a minimum distance of 100 feet. Thus, the realigned route has fewer environmental consequences for karst than the original route. The location of the original and revised highway alignments with respect to karst vulnerability identified during the field survey is shown on the example map in Figure 4.

Environmental Effects

A summary of the effects on karst resources as measured by distances along, and areas downgradient from, the revised alignment centerline are presented in Table 3. A total of approximately 2,600 feet (0.5 miles) of high vulnerability karst lies along the centerline of the revised alignment, representing about 1.3 percent of the 38.8-mile long West Lynn Canal alternative. The amount of high vulnerability karst intersected by the entire footprint of the proposed road is slightly greater than that measured along centerline (about 2.1 percent of the total route length), as some high karst areas do not touch centerline. The initial measurement of high karst areas during the field surveys was approximately 7,000 feet along centerline; thus, more than half of the mapped high vulnerability karst was avoided by realigning the route.

Throughout many of the high vulnerability karst areas, the revised alignment appears likely to impact surficial and shallow subsurface landforms and hydrology more than deep interconnected karst hydrologic systems. The presence

of interbedded non-carbonates and soil infilling generally appears to have been a limiting factor in underground solutional development. Glacial soils were observed to be plugging many of the high vulnerability features, and most littoral features do not appear to have open subsurface connections to upgradient areas. It is possible, however, that subsurface connections to subsea resurgences exist downgradient of areas exhibiting high concentrations of open karst features.

Table 3. Summary of potential karst effects as measured by road distance and watershed area.

Karst Survey Data	Direct Effects of West Lynn Canal Alternative[1]					
	Route Distance Along Centerline			Watersheds Crossed by Route		
	Feet	Miles	% of Total Route[2]	Total Watershed Areas[2] (Acres)	Downgradient of Centerline	
					Acres	% of Total Watershed Areas
Bedrock Type						
Carbonate[3]	33,300	6.3	16.3	-	-	-
Predominantly non-carbonate with carbonate component[4]	10,000	1.9	4.9	-	-	-
Non-carbonate	161,700	30.6	78.9	-	-	-
Total[2]	205,000	38.8	100	-	-	-
Karst Vulnerability						
High	2,600	0.5	1.3	-	-	-
Moderate	21,000	4.0	10.3	-	-	-
Low	19,700	3.7	9.6	-	-	-
None[5]	161,700	30.6	78.9	-	-	-
Total[2]	205,000	38.8	100	-	-	-
Watersheds						
>50% Carbonate Substrate[3,6]	30,300	5.7	14.8	1,600	450	28
<50% Carbonate Substrate[3] or Partial Carbonate Substrate[4]	19,700	3.7	9.5	115,000	610	0.5
No Carbonate Substrate	155,000	29.4	75.8	104,000[6]	12,000[6]	11
Total[2]	205,000	38.8	100	220,600	13,100	6

1 = Based on 2003 revised alignment.
2 = Based on total West Lynn Canal route length from William Henry Bay to Haines.
3 = Point Augusta Limestone (Stal).
4 = Includes interbedded schist with minor marble beds, limestone clast-bearing conglomerate, and calcareous graywacke (Stai, Stag, Pul, DSbl).
5 = Areas mapped as "no karst" and unmapped areas underlain by non-carbonate bedrock.
6 = Order-of-magnitude estimates for watersheds outside of karst study area.
- = not applicable

Moderate vulnerability karst underlies approximately 21,000 feet (4.0 miles) of the revised alignment, or about 10.3 percent of the total length of the West Lynn alternative. The amount of moderate vulnerability karst crossed by the revised alignment is about 2,000 feet more than the original route, due to shifts away from high vulnerability areas into moderate vulnerability areas.

Five of the 16 watersheds mapped during this study are underlain by more than 50 percent limestone substrate (e.g., watersheds W-4C/5 and W-6B/7A, Table 2, Figure 4). All of these are relatively small coastal drainages facing Lynn Canal, and represent about 15 percent of the total west Lynn Canal route length. Within these watersheds, the area of karst landscape that lies downgradient of the revised alignment, which could potentially be affected by the proposed project, totals approximately 450 acres. This acreage represents an average of 28 percent of their total watershed areas (Table 3). Watersheds containing partial carbonate substrate are crossed by about 10 percent of the route, and those underlain completely by non-carbonate bedrock represent the remaining 75 percent of the route. These watersheds are typically larger in size; thus, a smaller fraction of their acreage (0.5 to 11 percent) lies below the proposed route.

SUMMARY AND LIMITATIONS

A systematic karst vulnerability assessment was conducted to identify the potential for environmental damage to karst features and hydrologic resources from proposed highway construction along the west side of Lynn Canal in southeast Alaska. The use of vulnerability criteria to map karst areas and caves requiring protection under FCRPA is a relatively recent science. The identification of karst geomorphology in a remote heavily forested field setting required experienced practitioners and a standardized approach based on Forest Service-developed guidance. Although somewhat specific to southeast Alaskan conditions, these criteria could be adapted for use in other karst areas of the world. The results of the survey identified approximately 0.5 mile of high vulnerability karst and 4 miles of moderate vulnerability karst, and required realignment of the highway route to avoid caves and high vulnerability karst.

Following completion of the subject study, environmental and socioeconomic issues other than karst ultimately drove the selection of the preferred alternative in the Final EIS towards a combined highway and ferry route along the east side of Lynn Canal (*29*). Thus, further investigation of karst conditions along the west Lynn Canal route is not necessary at this time. If the west Lynn Canal route had been selected, or if it is ever reconsidered for construction in the future, several areas of further study would be warranted:

- The results of this study should be systematically checked against LIDAR topographic maps and orthorectified aerial photographs. Because of the lack of available LIDAR and often unreliable GPS in the subject study area, the locations of individual karst features identified during the field surveys are considered approximate. Specific karst features that would typically be evident on LIDAR topographic maps may have been missed in the field due to the spacing of split traverses and obscuring forest cover on aerial photos. Confirming the location of features would enhance the reliability of these data for supporting mapped vulnerability boundaries and protecting specific karst features. Newly identified features from LIDAR data that suggest a change in the vulnerability ratings should be field-checked.
- It is possible that additional data or revised maps resulting from review of LIDAR data would indicate that tracer dye tests may be warranted at specific locations or subwatersheds.
- Approximately 6,300 feet of the realigned highway route lies outside of the corridor assessed during the field survey, due to revision of the original alignment to avoid high vulnerability karst and caves. For the purposes of this study, these areas were estimated to contain low to moderate vulnerability karst based on extrapolations of nearby geomorphology. They should be field-checked to confirm the estimated ratings.
- The results of the karst vulnerability assessment are partly a function of the survey corridor widths determined in the scoping process. Features located outside of the survey corridors could have a bearing on the understanding of karst systems within the corridors. For example, resurgent streams originating upgradient of the corridors could insurge within the strip between the east edge of the corridor and the top of the shoreline cliffs, resulting in high karst vulnerability buffer zones being applied to losing streams within the corridors. A detailed review of LIDAR topographic maps would help identify whether there are significant features outside the corridors that would suggest a change in vulnerability rating. All such features should be field-checked.
- The lack of precipitation during the field surveys may have precluded hydrologic features such as resurgences and insurgences from appearing. In the absence of flowing water, the presence of such features was largely inferred from secondary evidence such as the accumulation of gravel along dry drainages. The study area may warrant re-evaluation during rainy periods to further assess hydrologic flow patterns and revisit the need for tracer dye tests.
- The vulnerability criteria used in the study were developed by the Forest Service primarily for timber harvest and gravel road construction. Prescribed design and construction practices associated with each vulnerability category may or may not be protective of karst resources in a highway scenario. Prescriptions specific to highway construction should be developed in the event the west Lynn Canal highway route is reconsidered in the future.
- The presence or absence of surficial material is an important component of vulnerability criteria. As such, the removal of surficial material during road construction may alter the rating. Areas mapped as moderate and high vulnerability should be monitored during road clearing to identify changes to vulnerability that could adversely affect the resource, and to assess compliance with potentially revised vulnerability criteria.

ACKNOWLEDGEMENTS

The author would like to thank the Federal Highway Administration (FHWA) for providing funding for this project as part of the Juneau Access Improvements EIS, and Rueben Yost, project manager with ADOT&PF for permission to publish. Jim Baichtal, Forest Geologist with Tongass National Forest and Bob Burk, geologist with URS provided critical review of the original report. Geologists Bob Burk, Rik Langendoen, Paul Myerchin, and Jamie Schick of URS are appreciated for their insight and fortitude in the field; Timothy King and Luke Boggess of URS for their excellent GIS mapping skills; and Pauline Schulte, Joyce Payne, and Barry Bergdoll of URS for project management and field logistics coordination.

REFERENCES

1. Dames & Moore. *Draft Report, Preliminary Karst Assessment, West Lynn Canal Alternative, Juneau Access Project, Juneau, Alaska.* Report prepared for FRP/Roen-Lochner Joint Venture, D&M Job No. 23696-014-020, October 1994, 9 p.
2. Northern Land Use Research, Inc. *Archeological Survey on the West Coast of Lynn Canal: William Henry Bay to Pyramid Island.* Report prepared for FPE/Roen Engineers, Inc., Fairbanks, Alaska. September 1994, 130 p.
3. Shannon & Wilson, Inc. *Juneau Access Improvement Reconnaissance Engineering Report, Appendix C, Geology Report.* Report prepared for H.W. Lochner, Inc, Bellevue, Washington. February 8, 1994, 62 p. plus App.
4. Drew, D. Karst Waters and Human Activities: an Overview. In D. Drew and H. Hotzl, eds., *Karst Hydrogeology and Human Activities – Impacts, Consequences and Implications.* International Contributions to Hydrogeology 20, International Association of Hydrogeologists, A.A. Balkema Publishers, Brookfield,VT, Part 1, 1999, pp. 3-34.
5. Baichtal, J.F. and D.N. Swanson. *Karst Landscapes and Associated Resources: A Resource Assessment.* U.S. Forest Service, Pacific Northwest Research Station, General Technical Report PNW-GTR-383, 1996.
6. Aley, T., Aley, C., Elliot, W., and Huntoon, P. *Karst and Cave Resource Significance Assessment*. Final Report, prepared for Ketchikan Area of the Tongass National Forest, 1993, 76 p. plus App.
7. U.S. Forest Service. *Draft Karst and Cave Resource Management Forest-Wide Direction and Standards and Guidelines.* Tongass National Forest, 1994.
8. U.S. Forest Service. *Tongass National Forest Land and Resource Management Plan*. R10-MB-338dd, U.S. Forest Service, Alaska Region, 1997.
9. Baichtal, J.F. *Application of a Karst Management Strategy: Two Case Studies from the Tongass National Forest, Southeastern Alaska, The Challenges of Implementation.* Report, National Cave Management Symposium, 1997.
10. Baichtal, J.F. and D.J. Landwehr. *Heceta Sawfly Salvage Sale, Soils, Karst, and Cave Resource Evaluation, Heceta Island, Southeastern Alaska.* Unpublished report, on file with U.S. Forest Service, Region 10, Tongass National Forest, 1997, 13 p.
11. URS Corporation. *Final Report, Karst Vulnerability Assessment, Kosciusko Island, Tongass National Forest, Alaska.* Report prepared for U.S. Forest Service, URS Job No. 53-03619119.00, November 2001, 32 p. plus App.
12. Gehrels, G.E. and H.C. Berg. *Geologic Map of Southeastern Alaska*. USGS Miscellaneous Investigation Series Map I-1867, Scale 1:600,000, 1992.
13. Gehrels, G.E. and H.C. Berg. 1994. *Geology of Southeastern Alaska*. In The Geology of North America, Volume G-1, The Geology of Alaska. The Geological Society of America. Chapter 13, 1994, pp. 451-467.
14. Lathram, E.H., R.A. Loney, W.H. Condon, and H.C. Berg, H.C. *Progress Map of the Geology of the Juneau Quadrangle, Alaska.* U.S. Geological Survey Miscellaneous Investigations Map I-303, Scale 1:250,000, 1959.

15. Brew, D.A., and A.B. Ford. *Preliminary Reconnaissance Geologic Map of the Juneau, Taku River, Atlin, and part of the Skagway 1:250,000 Quadrangles, Southeastern Alaska*. U.S. Geological Survey Open-File Report 85-395, 1985, 23 p. plus 2 plates.

16. Geiselman, J., J. Dunlap, P. Hooge, and D. Albert, eds. *Glacier Bay Ecosystem GIS CD-ROM Set.* U.S. Geological Survey and Interrain Pacific, Anchorage and Juneau, Alaska, 2 vol, 1997.

17. Love, D. West Lynn Canal Karst Inventory. *The Alaskan Caver*, Glacier Grotto, Juneau, Alaska, Vol. 19, No. 2, April 1999, p.11-17.

18. Ford, D.C., and P.W. Williams. *Karst Geomorphology and Hydrology*. Chapman & Hill, London, 1994.

19. U.S. Forest Service. *Central Prince of Wales Final Environmental Impact Statement, Ketchikan Pulp Company Long-term Timber Sale Contract, Vols. I and II*. Tongass National Forest, R 10-MB-229a, July 1993.

20. Gilbert, W.G. *Preliminary Geology of the Northern Chilkat Range, Southeastern Alaska*. Alaska Div. of Geologic and Geophysical Surveys Report of Investigation R1-88-8, 2 maps, scale 1:36,200, 1988.

21. Carl. S., U.S. Geological Survey, Anchorage, Alaska. *Personal communication regarding potential USGS unpublished geologic mapping information along west Lynn Canal.* June 20, 2003.

22. Allred, K. Strawberry Fields Forever. *The Alaskan Caver,* Glacier Grotto, Juneau, Alaska, Vol. 20, No. 5, October 2000, pp. 3-4.

23. Allred, K. Lynn Canal Karst Trip 2001. *The Alaskan Caver*, Glacier Grotto, Juneau, Alaska, Vol. 21, No. 4. October 2001, pp. 2-3.

24. Allred, K. and Allred, S. Broken Motor Cave. *The Alaskan Caver*, Glacier Grotto, Juneau, Alaska, Vol. 15, No. 3, June 1995, pp. 14.

25. Alaska Department of Transportation & Public Facilities (ADOT&PF) and URS Corporation. *Memorandum to file: Minutes from June 25, 2003 meeting regarding methodology and scope of karst technical study*. June 25, 2003, 2 p.

26. URS Corporation. Karst Technical Report. J*uneau Access Improvements Supplemental Draft Environmental Impact Statement,* Prepared for ADOT&PF, State Project No. 71100, Federal Project No. STP-000S(131), March 2004.

27. Baichtal, J.F. *Southeastern Chichagof Karst Resources*. Internal U.S. Forest Service memorandum, Ketchikan, Alaska, File Code 2880/2356 Geology and Karst Resources, February 9, 1997, 4 p.

28. URS Corporation. Anadromous and Resident Fish Streams Technical Report. *Juneau Access Improvements Supplemental Draft Environmental Impact Statement,* Prepared for ADOT&PF, State Project No. 71100, Federal Project no. STP-000S(131), September 2004.

29. Alaska Department of Transportation & Public Facilities (ADOT&PF). *Juneau Access Improvements Final Environmental Impact Statement.* Prepared for Federal Highway Administration, Alaska Division, State Project No. 1100, Federal Project no. STP-000S(131), January 2006.

I-70 Georgetown Incline Rockfall Mitigation Feasibility Study Georgetown, Colorado

Ben Arndt, P.E., P.G. *(Presenter/Author)*
Yeh and Associates, 5700 East Evans Ave
Denver, CO 80222

Ty Ortiz *(Presenter/Author)*
Colorado Department of Transportation
Rockfall Program Manager
4670 Holly Street, Unit A
Denver, CO 80216

Richard Andrew, P.G. *(Co-Author)*
Yeh and Associates, 5700 East Evans Ave
Denver, CO 80222

ABSTRACT

Rockfall is a common hazard along transportation routes in the mountainous terrain in Colorado. Many accidents, injuries, and fatalities resulting from rockfall events have occurred along I-70 specifically along the Georgetown Incline near Georgetown, Colorado. In response to the rockfall potential, Yeh and Associates, Inc. completed a study for the Colorado Department of Transportation (CDOT) to evaluate the feasibility of various mitigation alternatives. The study presented the results of our evaluation of the rockfall potential from rock cuts and natural slopes above I-70 along the Georgetown Incline.

In addition to reviewing CDOT's existing rockfall hazard rating system for sites along the Georgetown Incline, the study reviewed and evaluated data from a previous report conducted by Yeh and Associates, Inc. which included remote mapping of bedrock outcrops and associated rockfall pathways using the Modified Q-system rock mass rating. The previous report also evaluated the rockfall potential at selected locations using the Colorado Rockfall Simulation Program (CRSP) to determine likely impact velocities, energies and bounce heights. Full-scale field demonstrations were also conducted at the site by CDOT to evaluate the effectiveness of various rockfall mitigation fences and attenuators that were installed. The demonstration required temporary closure of I-70 to roll rocks approximately 1,500 vertical feet.

Based on our review, analysis, and consideration of CDOT's long term objectives, the study presented a tiered rating of sections along I-70 with a greater rockfall potential based on previous cut and natural slope rating systems. The study also generated a rockfall mitigation matrix and evaluation flowchart that provided CDOT with a tool to evaluate which sections along I-70 to consider for mitigation and to be incorporated into CDOT's Rockfall Mitigation Project Plan (RMPP).

INTRODUCTION AND BACKGROUND

Rockfall hazards are common along Colorado's Mountain corridors and periodically cause traffic delays, road closures, and in some instances fatal accidents. As population and tourism increases result in larger traffic volumes, the consequence of rockfall incidents will also increase.

A two-mile section of Interstate 70 between the towns of Georgetown and Silver Plume, Colorado known as Georgetown Hill, is one of Colorado's highest rated locations for the potential of rockfall to occur (See Figure 1). Rockfall incidents along this stretch of highway have resulted in four fatalities since 1999.

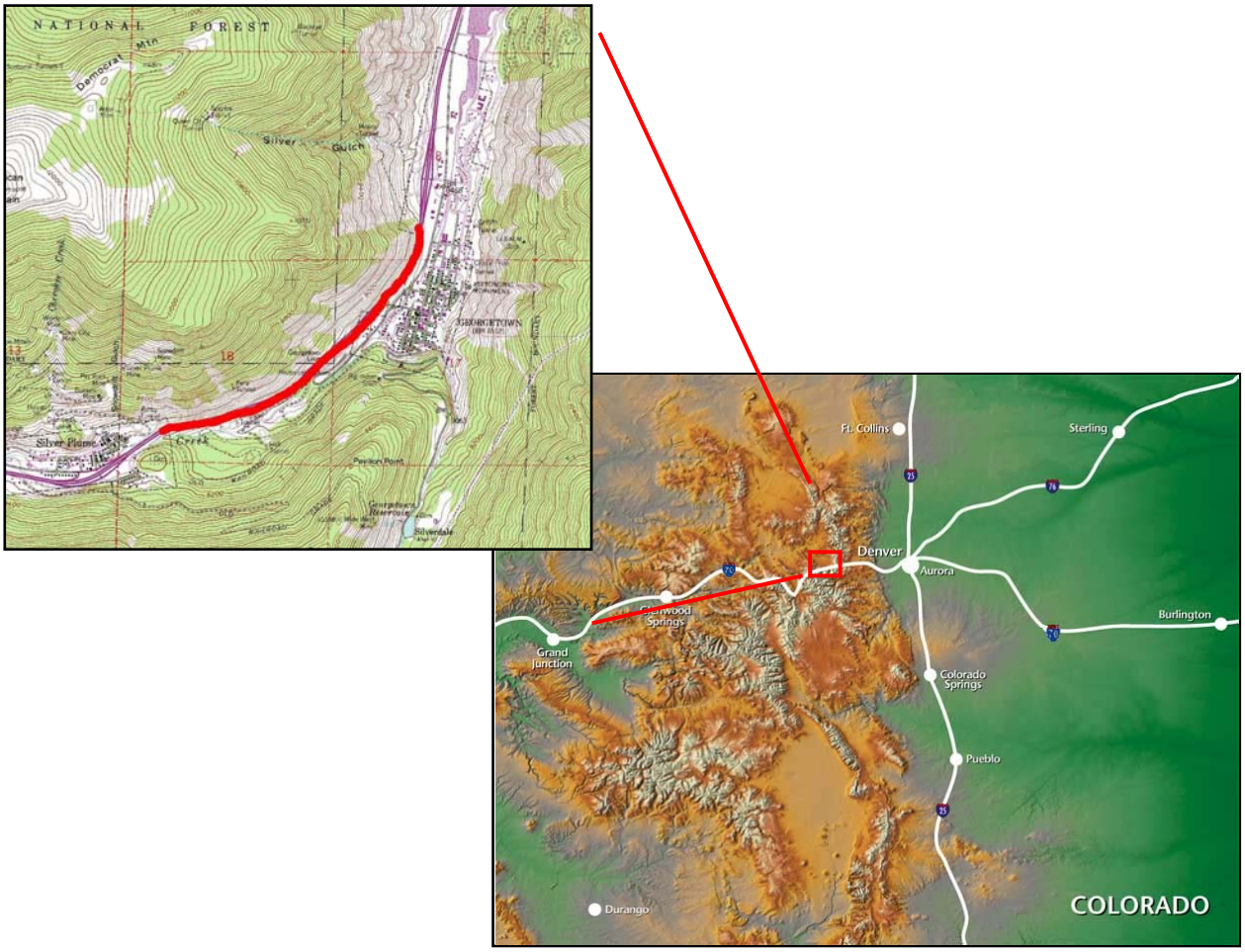

Figure 1: Site location map

The Colorado Department of Transportation contracted with Yeh and Associates to characterize the rockfall potential along Georgetown Hill. This characterization was presented in a report titled I-70 Georgetown Incline Rockfall Evaluation (Evaluation Study), completed in November 2003. The study identified the potential causes of rockfall, several rockfall sources areas and rockfall pathways by use of remote mapping of bedrock outcrops and associated rockfall pathways using the Modified Q-system rock mass rating. In addition, select locations were chosen to simulate likely impact velocities, energies and bounce heights of rockfall using the Colorado Rockfall Simulation Program (CRSP). One outcome of the study indicated that rock outcrops located up to 2,000 feet above the interstate can be the primary source areas for rockfall at Georgetown Hill. The results of this evaluation were presented at the 2002 Highway Geology Symposium in San Luis Obispo, California.

In June 2005, Yeh and Associates submitted an accompaniment to the rockfall evaluation study titled I-70 Georgetown Incline Rockfall Mitigation Feasibility Study (Feasibility Study). The study presented the results of an evaluation of the rockfall potential from rock cuts and natural slopes above I-70 along Georgetown Hill and discussed mitigation alternatives for this area. It is important to note that the Feasibility Study was specific to rockfall. The intent was to provide information to be used for the allocation of CDOT's rockfall resources along Georgetown Hill.

The information provided from the feasibility study was used to prioritize locations for rockfall mitigation and determine appropriate mitigation alternatives. This paper provides an overview of the Feasibility Study, which reviews the mitigation alternatives, and discusses future monitoring and mitigation along this section of interstate.

SITE CONDITIONS

The highway grade at this location ranges between 5% and 8% as the elevation of the roadway rises approximately 500 feet between the towns Georgetown and Silver Plume. Truck traffic comprises about 6.5% of the 30,000 average daily traffic count. The combination of a steep mountain highway and a mix of vehicles and driving speeds contribute to the highly variable driving conditions magnifying the impacts of rockfall to traffic flow. In addition, the town of Georgetown is located directly below the cut slope. Rockfall from past incidents have been known to roll into the less populated sections of town.

At this location, the highway cuts through oversteepened, glacially carved slopes. The natural slopes above the highway cuts primarily consist of colluvium and talus deposits. Mining was once abundant in this area, and several locations are composed of weathered mine-tailing deposits. Rock outcrops above the highway consist of intrusive granites and metamorphic gneisses and schists.

For the Feasibility Study, the slope was divided into two segments; 1) the disturbed slopes which were excavated during construction of I-70 that consist of the rock cuts and the slope immediately above the rock cuts, which were impacted during construction of the interstate; and 2) natural slopes that consist of undisturbed slopes above the disturbed rock cuts. It should be noted that a majority of the rock outcrops that contribute to the rockfall hazard are located on the natural slopes. .

ROCKFALL EVALUATION

Two methods of evaluating the rockfall potential were utilized at Georgetown Hill. The Colorado Rockfall Hazard Rating System (CRHRS) was used to evaluate the cut slopes and disturbed slopes. Sites along Georgetown Hill are among the most significant rockfall hazards of the 756 sites listed statewide. The CRHRS uses a standard combination of slope data, geology and traffic data to develop a rockfall hazard rating for a site. Sites are then categorized from A to D. Category A sites are considered to have the most significant rockfall potential and are prioritized first for mitigation.

In addition, an evaluation of the effectiveness of the existing ditch as a rockfall catchment, utilizing the Oregon Department of Transportation (ODOT) Rockfall Catchment Area Design Guideline, found that rockfall generated from cut slopes steeper than about 45 degrees generally tend to stay within the ditch adjacent to I-70. Rock cuts along this section of highway range between 20 and 150 feet in height.

Rockfall evaluations of the rock outcrops located within the natural slopes above the rock cuts utilized the Modified Q-System, a method of evaluating the rock mass quality adopted from the mining industry. The Modified Q system was utilized since the bedrock outcrops above the highway cannot be accessed directly without the potential for triggering rockfall by traversing the slopes above I-70. The Modified Q-System measures the joint conditions of the rock outcrop. Six factors are used to accomplish this utilizing the following equation:

$$Q = \left[\frac{RQD}{J_n}\right] * \left[\frac{J_r}{J_a}\right] * \left[\frac{J_w}{AF}\right]$$

The factors include:

- Rock Quality Designation (RQD)
- Joint Set Number (Jn)
- Joint Roughness Number (Jr)
- Joint Alteration Number (Ja)
- Joint Water Reduction (Jw)
- Aperture Factor (AF)

Overall, the lower the Q rating the higher the potential of rockfall from bedrock outcrops. The majority of the outcrops identified as rockfall source areas rated between 0.5 and 5. The results were used as part of a decision matrix to determine where to locate rockfall mitigation.

To prioritize locations for mitigation, a decision flowchart, specific to Georgetown Hill was developed. The decision flow chart used the existing CRHRS ratings and the results of the Modified Q-System ratings. Using this process, sites were categorized into a tiered system. The method of categorizing the sites considered the CRHRS classification first and the Modified Q-System rating second. For example, CRHRS Class A sites with source rock outcrops having a Modified Q rating below 1.0 were given the highest priority, Tier 1; CRHRS Class A sites with outcrops having a Modified Q rating above 1.0 were listed as Tier 2 Sites; CRHRS Class B sites with a Modified Q rating below 1.0 were listed at Tier 3; and CRHRS Class B site with a Modified Q rating above 1.0 are listed as Tier 4. The process was repeated until all of the possible conduits for rock to roll onto the highway were prioritized. The system produced eight possible rating tiers for sites to be listed in.

The prioritization resulted in dividing the 2.2 mile section of interstate into 19 rockfall areas to be considered for mitigation. Figure 2 depicts a photo map of the bedrock outcrops, color coded according to Modified Q-System scores, and rockfall pathways beneath these outcrops that appear to be the most likely path for rock from these outcrops to take and potentially roll and bound onto the interstate.

ROCKFALL MITIGATION

Prior to the completion of the Evaluation Report and before the Feasibility Study began, three rockfall barrier systems were constructed on the slopes along Georgetown Hill. The location of these barriers was based on input from Maintenance personnel and the experience of CDOT geologists and engineers. The design capacity and height of the barriers was determined similarly based on the experience of the CDOT staff and conversations with fence manufacturers. The result was one barrier with an 80-foot-ton (220 kJ) capacity and two barriers with a 180-foot-ton (500 kJ) capacity. All three barriers were 11 feet in height.

In April 2004, a large rockfall incident originating as a rock slope failure from an outcrop located between 1,500 feet and 2,000 feet above the highway resulted in significant damage to the interstate. Figure 3 shows the location of the source relative to the interstate. The incident occurred at approximately 1:00 am, consequently traffic volumes were low, only one vehicle was affected, and no significant injuries were reported (Figure 4). The failure occurred above the 80 foot-ton barrier and the ensuing rockfall destroyed the fence system (Figure 5).

Using the Colorado Rockfall Simulation Program (CRSP), energy associated with rocks from this incident was in the 1,000 foot-ton range (3,000 kJ), significantly higher than the existing fence barrier was designed for. Average bounce heights, according to the CRSP modeling, were as high as 40 feet where the fence was located indicating that rockfall from the failure also bounded over the fence.

As a result of the rockfall event, it was evident that the mitigation strategy of attempting to stop rockfall at the bottom of the slope with protection devices was not effective for large incidents. This method is common along many corridors, however, because of the limits of existing property boundaries. At Georgetown Hill, the decision was made to make an effort to mitigate rockfall events originating from outcrops above the highway. To do this will require a significant effort in terms of survey and right-of-way acquisition.

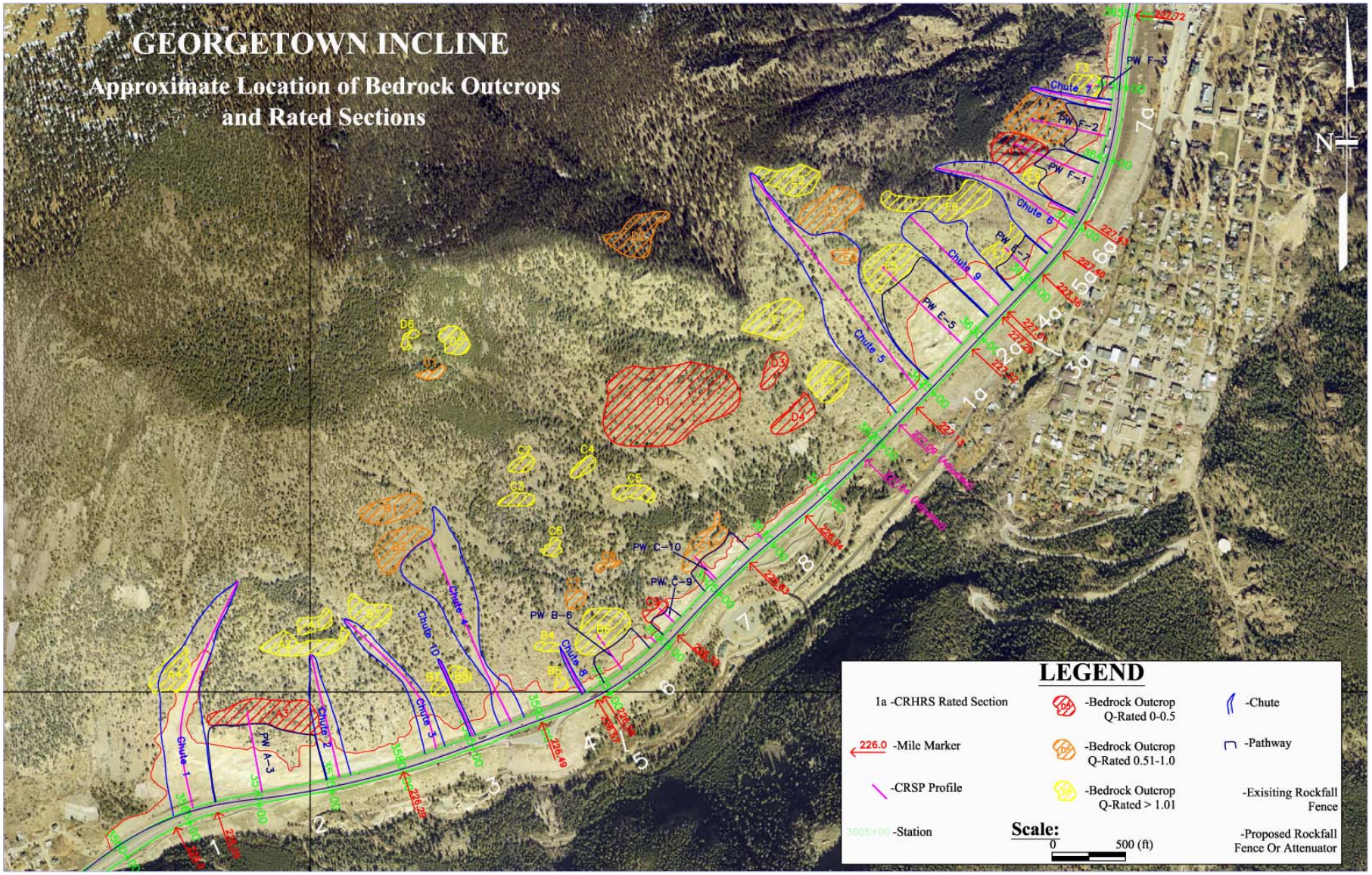

Figure 2: Aerial photograph showing outcrops, and rockfall pathways

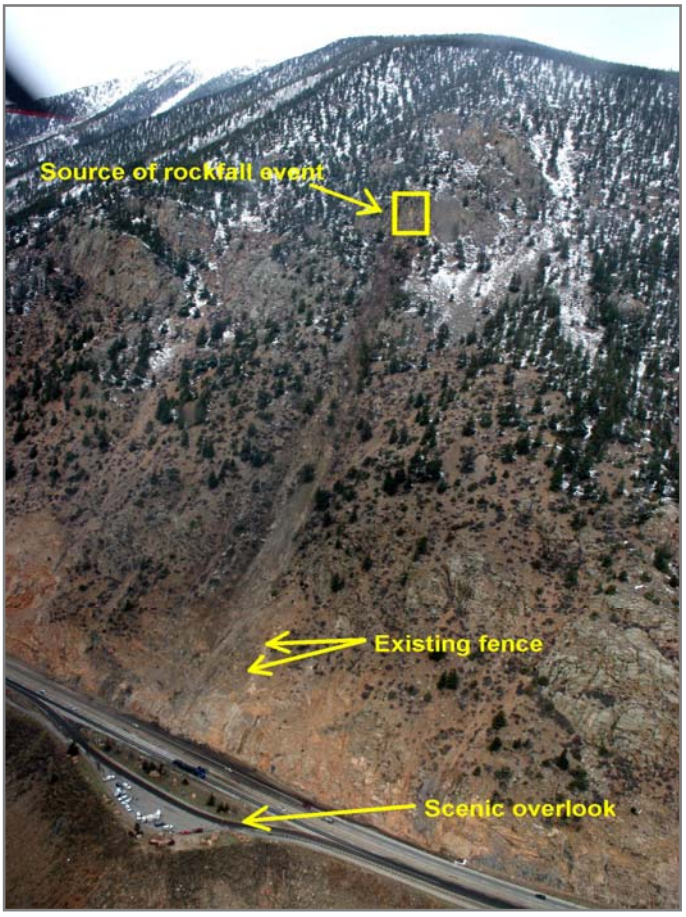

Figure 3: Source location of April 2004 rockfall

Figure 4: Vehicle damage resulting from April 2004

Figure 5: Damage to existing rockfall barrier resulting from April 2004 rockfall incident

In an attempt to understand the behavior of rockfall generated at locations that allow long run out distances, in June 2004 a rock rolling exercise was conducted at the location of the April 2004 rockfall incident. Because it was unsafe to remove rock from the source area of the incident, residual loose rock from below the source outcrop was used in the exercise. The location of this exercise above the interstate necessitated short closures of the interstate during the rock rolling; and with the variability of the slope, controlled data collection of velocities and bounce heights was not possible. Consequently, empirical observations were the basis of the conclusion drawn.

CONCLUSIONS

Observations taken during the rock rolling exercise validated the results of the CRSP modeling, thought to be extraordinary before with relatively high bounce heights. As a result, the natural conclusion to the question of how to meaningfully reduce the rockfall hazard along this section of highway was to prevent the rockfall from gaining the momentum needed to bounce higher than mitigation devices can be constructed. The need to reduce bounce heights was reiterated in the fall of 2005 when a rockfall incident damaged one of the existing 180 foot-ton barriers and rock was observed by residents of Georgetown to bounce over the fence, onto the highway and into the town.

Rockfall barrier technology has advanced such that the capacity of single rockfall incidents with high energies can be mitigated, however, as revealed by the incidents at Georgetown Hill, the necessary heights of these barriers is substantial. An alternative mitigation scheme in the form of rockfall protection is to attenuate rockfall closer to the source. By using a series of attenuating and protection devices, it is believed that bounce heights can be reduced such that the rockfall can be prevented from reaching the roadway. In 2005 and 2006 the process of constructing these devices in series began. Figure 6 shows an example of a typical hybrid barrier used to attenuate rockfall.

Although it is not feasible to stop or prevent all rockfall incidents from affecting the highway, this strategy will reduce the rockfall potential significantly more than single barriers at the base of a slope. This mitigation scheme has been used before with varying degrees of success in Colorado and other DOT's. Other mitigation options of avoidance, stabilization, and other methods of protection were considered but believed to be unrealistic give the existing resources and future improvements along the I-70 corridor through Colorado.

Future work along Georgetown Hill will be located according to the tiered prioritization determined in the Feasibility Study. However, as technology increases and rockfall evaluation methods evolve, changes to the tier system may be appropriate.

Figure 6. Example of a common hybrid protection system

U.S. Highway 6 – Clear Creek Canyon Rockslide: Working to Reopen a Major Road Closure

Kent Pease, P.E.
Lyman Henn, Inc./ Denver, Colorado
110 16th Street, Suite 900, Denver, CO 80202
303.534.1100
kpease@lymanhenn.com

Minal Parekh, P.E.
Lyman Henn, Inc./ Denver, Colorado
110 16th Street, Suite 900, Denver, CO 80202
303.534.1100
mparekh@lymanhenn.com

Ty Ortiz
Colorado Department of Transportation
4340 East Louisiana Avenue
Denver, CO 80246-3482
303.757.9424
Ty.Ortiz@dot.state.co.us

ABSTRACT

Highway 6 through Clear Creek Canyon is a major thoroughfare to the Rocky Mountains from Denver, CO. The corridor is frequented by small rockfall events that deposit rocks on the roadway. On June 21, 2005 approximately 1,300 CY of rock slid from an existing rock cut, pushing two trucks off the road and closing the highway with debris. To address the safety and stability issues with highway use, a strong team headed by CDOT with input from the Colorado Geological Survey, Federal Highways Administration, and local geotechnical consultants developed a design for stabilization. Concurrently, bids were solicited from contractors, and a contractor was hired on an emergency basis.

This paper presents the facts of the incident and the resulting stabilization project. This paper also reviews how the project design and construction team was assembled and how they worked together to stabilize the road cut and reopen the highway. Details presented include a history of incidents at the site, the rockslide, geologic conditions, the engineered stabilization, and construction. The highway was closed to through traffic for 83 days to reconfigure and stabilize the cut—the longest in Colorado state history.

Ground conditions, which led to the rockslide and were key components to the engineered stabilization, consisted of foliated gneiss and schist with two prominent secondary joint sets and pegmatite intrusions. The paper describes how a planar pegmatite intrusion along a secondary joint led to the rockslide, and also how these geologic conditions were used as the basis for the stabilization. Long term cut stabilization consisted of a new slope configuration with an inclination of approximately 1 horizontal to 1 vertical (1H:1V), generally following the pegmatite and jointing, with the removal of 38,000 CY of rock, and rock dowels and bolts spotted in the field. Rockfall wire mesh and a catchment ditch were used to contain future small-scale rockfall.

SETTING

Clear Creek Canyon is situated on the western side of the Denver metropolitan area, as shown in Figure 1. Highway 6, which runs through the canyon, is a major thoroughfare handling approximately 12,000 vehicles per day providing access to the high mountains and the gaming towns of Black Hawk and Central City. The section of Highway 6 through the canyon from Golden to its intersection with Interstate 70 is approximately 14.5 miles long.

At approximately 11.5 miles up canyon, Highway 119 diverges to Black Hawk and Central City. Although Interstate 70 is an alternative route to Black Hawk/Central City, the route is considered inconvenient by some so Highway 6 is preferred.

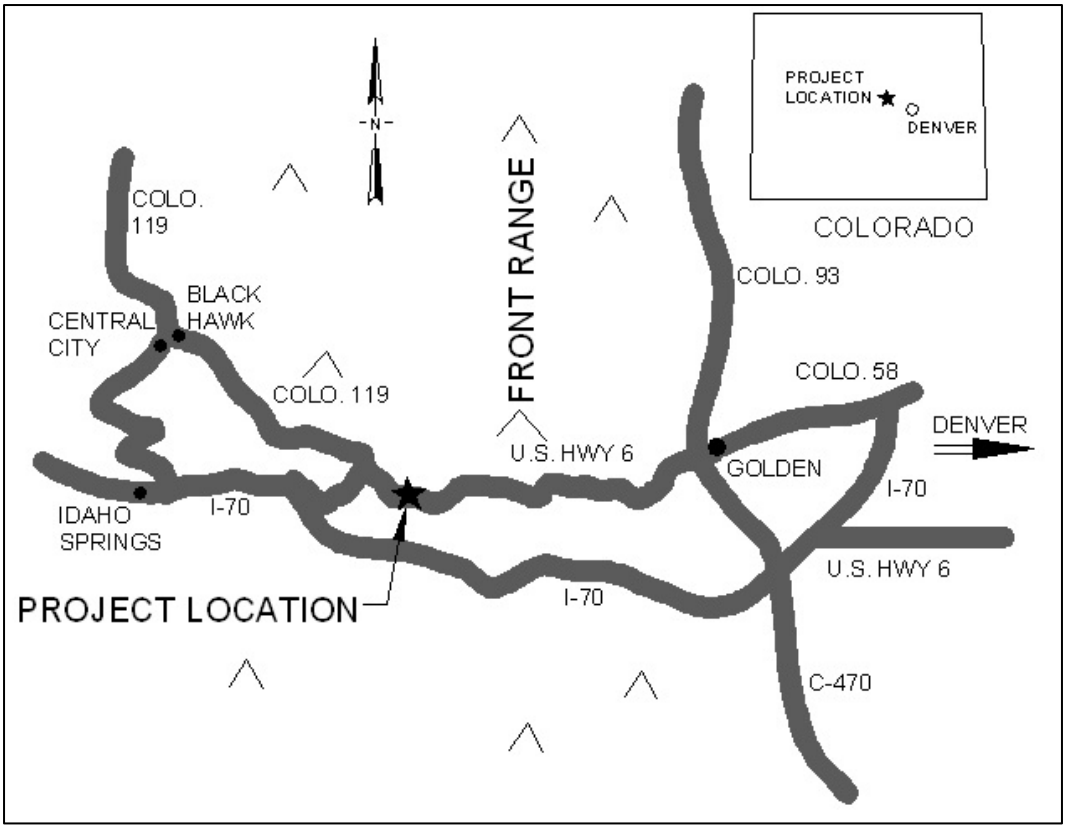

Figure 1 Site Location

The canyon is steep, rugged, and used heavily for recreation including hiking, fishing, boating, rock climbing, and gold panning. Historically the canyon was exploited for gold primarily from placer mining, and at one time a railroad snaked up the canyon. Much of the land, including the site of the slide, is owned by Jefferson County as part of their open space program. The slide location is south-facing and is north of Clear Creek at an 80 degree bend in Highway 6. The original cut was over 120 ft high and 500 ft long at an inclination of approximately 0.5H to 1V, and it wrapped around with the road curve. The slide is located at milepost 261.65.

THE EVENT

At 11:00 AM on June 21, 2005 approximately 1,300 CY of rock (in place volume) was released from the existing rock cut approximately 10 miles up from the mouth of the canyon. This event pushed two trucks off the road and covered the road with 2,200 cubic yards of debris. Figure 2 shows the road immediately after the slide. Fortunately there were no injuries in the event. After the slide, overhangs remained perched over the road, creating a further hazard for highway users.

Figure 2 Rock Slide Debris

THE RESPONSE

Immediately after the slide, the Colorado Department of Transportation (CDOT) initiated a two-pronged response to the situation. First, a team of rockfall and design experts was assembled to evaluate the situation and formulate an emergency response action plan. Second, CDOT initiated emergency contracting procedures to obtain bids and get a contractor on board quickly to implement cleanup and stabilization measures.

The Rockfall Program of the Materials and Geotechnical Branch of CDOT headed by Ty Ortiz visited the site and made a preliminary assessment of the conditions. Based on their initial observations, they developed initial response measures for stabilization, and they prepared contract documents to be used as the basis for contractor selection. This work included removal of slide debris, blasting to remove rock blocks that posed an immediate hazard, rock bolting, and installation of wire mesh.

Figure 3 Initial Cleanup

Within 12 hours of the event, CDOT Region 1 Foothills Residency and the CDOT Rockfall Program prepared contract documents and distributed a construction package to potential contractors. Three bids were received the following day. Ames Construction of Aurora won the contract and began mobilizing within days. Actual site work commenced on June 24, 2005, three days after the rock slide. Ames' first task was to clear the debris from the roadway and create a berm along the south side of the shoulder to protect Clear Creek from construction activity. The initial clean up effort is shown in Figure 3. Simultaneously, CDOT assembled a construction management team and used a general services contract to bring on Parsons Transportation Group for management and oversight, and Lyman Henn, Inc. for geotechnical field engineering services during construction. CDOT also assembled additional geotechnical rock slope expertise from the local engineering practice and academic community to pool the local knowledge in order to come up with a timely solution. The geotechnical review and design team was expanded, ultimately including representatives from CDOT's Rockfall Program, the Federal Highways Administration, the Colorado Geologic Survey, Lyman Henn, and Yeh and Associates.

DESIGN EVOLUTION

From the beginning, the geotechnical review and design team had a concern for the overhangs and the rock remaining on the eastern edge of the slide surface. Although the highway could have been reopened after removal of the slide debris on the highway, the remaining rock face above the highway was not stable and presented a looming hazard. Specifically, a two-stepped rock overhang remained 120 ft above the highway and posed a risk for additional slides, as shown in Figure 4. Stabilization of the first overhang was not considered feasible as a reliable solution because of the condition of the rock and adverse jointing, so the design team agreed that it should be targeted for removal. The initial plan was to remove the first overhang and stabilize the remaining overhang with 60 to 70 foot long tensioned rock bolts extending through the unstable zone and anchored into firm rock behind the slide plane. These blasting and reinforcement measures were the principal parts of the initial response. Although the construction contract included removal of the worst part of the overhangs and intended to use rock bolts for reinforcement of the remaining rock based on the conditions known and observed at the time, it was not clear that these measures would be adequate. The team planned to assess the results of each step of the initial response plan and adjust accordingly. Observations made from ropes and helicopter helped provide perspective on the overall geometry of the slide and remaining rock, but the rock conditions in the immediate vicinity of the overhangs were not clear.

Following the initial evaluations and prior to any blasting, CDOT installed a series of monitoring devices to observe and track movement of the rock face. These were located along the brow of the slope and consisted of four crack gauges installed across key joints and one survey prism. The crack gauges were low tech "tell-tales" consisting of overlapping metal lathes with scales or initial conditions scribed onto the surface. Baseline conditions were recorded for each and observations were taken after the blasting work. These observations indicated movement on one of the tell tales located across an open fracture making up the overhanging features.

Figure 4 Overhangs

Initial construction work consisted of removal of the first overhang by blasting, estimated to consist of between 400 and 600 cubic yards of in place material. During this work, observations of the blast hole drilling and some additional exploratory holes indicated that the rock behind the overhangs was weak and friable in addition to being adversely jointed. The drilling was difficult as a result of the variable rock quality, jointing, and the fact that it was staged from a crane basket. Wind conditions in the canyon limited work time. Additionally, concern arose about the rock remaining on the east of the slide area; the foliation and jointing created a toppling hazard.

After the removal of the first overhang, conditions were more clearly exposed, better revealing the slide mechanism and remaining conditions. The team made up-close observations of the conditions in a crane basket. These observations revealed the rock which would remain was highly fractured and weathered, and it would be exposed in two vertical or overhanging highwalls. Furthermore, a pegmatite intrusion which formed the base of the slide appeared to continue beneath the remaining rock, with the weak, friable schist zone behind it. With these conditions, reinforcement and stabilization of the remaining rock was considered risky; the stabilization could be ineffective if the rock in the anchor zone was weak. Additionally, drilling and installing long bolts through the rock would be time consuming and technically difficult since the work would have to be staged from a crane basket, and since the joints might have a tendency to force the drill holes off alignment.

The extreme difficulties encountered during the drilling of blast holes for the first series of blasts to remove the overhanging rock features highlighted the expected difficulty in performing construction work from a crane or hanging from ropes 150 ft up the rock face. It was apparent to the design team that installation of the reinforcement would have been difficult or impractical, potentially unsafe, and likely ineffective.

Ultimately, following the initial blasting work to remove the first overhang and based on closer observations, the team determined that removal of the hazard under a full road closure was the best approach. This would entail large-scale rock removal and reshaping of the entire slope. Cut reconfiguration was a better long term design that would pose a lower risk for further rockfall events and require less maintenance in the future. This decision was based on observed conditions, likely ineffectiveness of the reinforcement, difficulty in installing the rock bolts, and apparent loosening of the rock mass as described below. Another prime consideration in this decision was the fact that there had been previous instabilities at the site and the team did not want to risk a "third strike." To follow is an overview of geologic conditions and a description of the slide mechanism and remedial measures implemented. Additional information regarding the project is presented by members of the team in Ref 1. *(1)*

GEOLOGIC CONDITIONS

The parent rock is Precambrian (>1.7 million years ago) interlayered gneiss *(2)* of various compositions. Although classified as gneiss, there are frequent schist-rich layers. The rock is strongly foliated and banded with layers varying from an inch to several feet thick. Weathering varies from slight to moderate with minor decomposition of minerals and occasional clay along joints.

Foliations of the gneiss strikes approximately N 80 degrees E with an average dip approximately 45 degrees to the north. For the eastern part of the rock cut (which is the pertinent area for this project) the foliation is sub-parallel to the road and dips into the slope. As the road and cut wrap around to the west, the foliation is perpendicular to the road with a dip parallel to the road.

In addition to the foliation, there are two prominent joint sets plus occasional random joints. The most prominent joint set is perpendicular to the foliation, striking at approximately N 80 deg. E and dipping approximately 45 degrees south which is directly out of the slope. The other persistent joint set strikes at approximately N 10 deg. W and is vertical. The rock mass and jointing are shown in Figure 5.

Pegmatite intrusions are common, taking the form of dikes, lenses and irregularly shaped bodies. The pegmatite is coarse grained and of late Precambrian age (1.4 to 1.7 million years ago). It is less jointed (more massive) than the gneiss and is more resistant to weathering, often forming ridges and outcrops in contrast to the gneiss which is commonly at lower angles.

The pegmatite intrusions are located preferentially along the joint set perpendicular to the foliation, and occasionally along the foliation or at random. The pegmatite appears to be more resistant to weathering than the schist/gneiss and is frequently expressed as steep cliffs and outcrops. The pegmatite appeared to be relatively intact without any persistent or through-going joints. Of particular importance is a three foot thick pegmatite intrusion along the out-dipping joint set, forming a continuous plane through the rock mass in the project area.

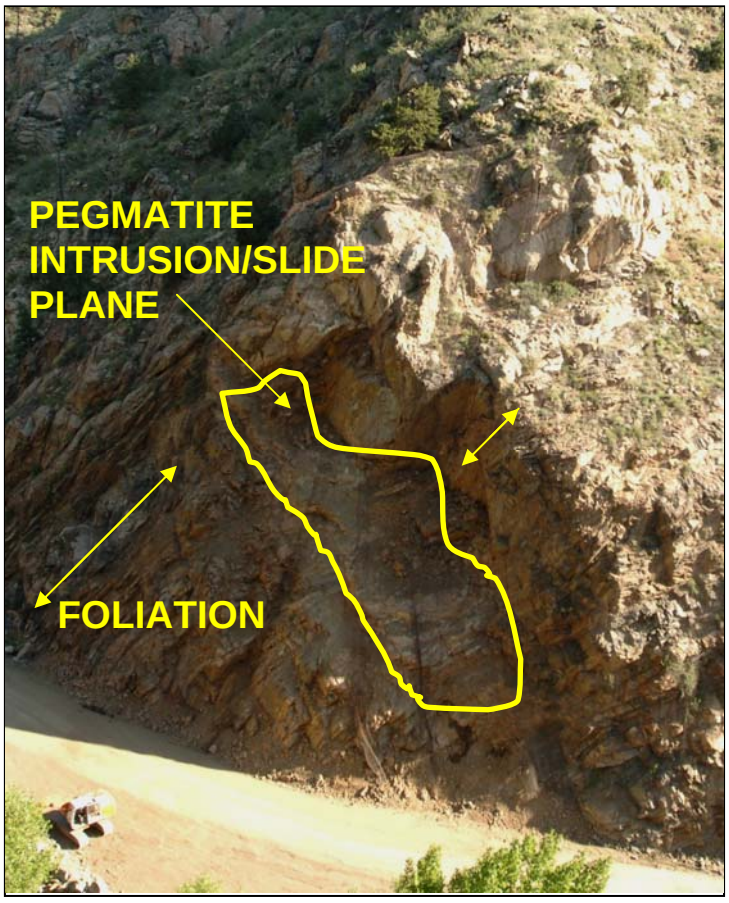

Figure 5 Jointing and Slide Plane

HISTORICAL NOTES

CDOT performed an inventory of rock cuts on Colorado highways in 1994, summarizing the rockfall hazard rating for each rock cut *(3)*. The study was based on historical events and on the likely incidence of rockfall reaching the highway. In this study, the subject rock cut was listed as a hazard rating C on a scale of A to E, in which A represents the highest hazard and E the lowest. Prior to 1994 the accident database *(4)* listed two historical accidents at the site. These are the only recorded accidents between 1986 and 2003.

In subsequent ratings this site has scores of 585 (1998 rating) and 582 (2003 rating) making it a category A site as a result of an updated rating system. Note however, that rockfall incidence for this study (which is predominantly the release of single loose rocks) is a

different phenomenon than large scale rock slides. In general, and at this site in particular, the two phenomena are not necessarily caused by the same underlying mechanisms, other than the broad effects of weathering.

There had been previous rock slide and stabilization activity at the site. In 2003 there was an event releasing approximately 400 cubic yards of rock from the road cut. Soon after this event, CDOT scaled loose rocks from the cut to reduce the incidence of rockfall. Later, in 2004, CDOT installed rock bolts to improve the stability of the cut against rock slides, and draped the cut with rockfall mesh to contain rockfall that would otherwise end up in the travel way. These measures were implanted as maintenance to mitigate potential rockfall and were not designed for a large scale rock slide event.

FAILURE MECHANISM

After the failure, a portion of the pegmatite plane was exposed with a 45 degree overhang approximately 25 ft wide at the top of the exposure bounded on the east by a vertical joint. At this location, the rock overlying the pegmatite plane was approximately 30 ft thick (perpendicular to the plane).

The failure was a slide of gneiss on top of a prominent pegmatite plane perpendicular to the foliation, with the eastern limit of the slide defined by a prominent vertical joint, as depicted in Figure 6. The rock slide in 2003 released rock in a similar but smaller scale event at the base of the pegmatite plane. A clay lens was also present and observed immediately after the 2003 slide. In response to this previous slide, remaining gneiss on top of the pegmatite plane had been reinforced with rock bolts. The subject rock slide overwhelmed the previously placed reinforcement and left several rock bolts nakedly protruding from the failure plane.

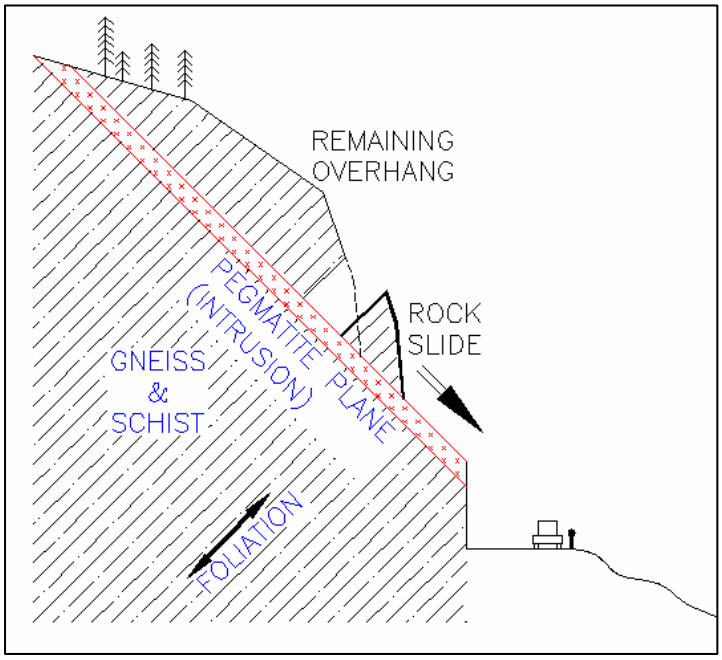

Figure 6 Geologic Cross Section and Failure Mechanism

The pegmatite intrusion is generally a planar feature estimated to extend over a distance of at least 100 ft both vertically and horizontally. The pegmatite is variable and possibly undulating and discontinuous. The exposed top surface of the pegmatite appeared to be relatively fresh. However, later during excavation, one area was exposed revealing a clay lens approximately an inch thick at the pegmatite-gneiss interface. After the failure, no significant water seeps were noted, and the top of the pegmatite was not observed to be wet. However, one very small wet spot was observed a couple weeks after the failure. The foliation of the gneiss possibly facilitated a toppling behavior that loosened the rock and contributed to the event. Also, it is likely that over time, water seeped through joints along foliation in the gneiss. The pegmatite plane formed a barrier to this seepage, directing it along the top of the plane resulting in accelerated weathering along this contact.

Recent rainfall events were not likely the root cause of the slide. Although precipitation is often a trigger, the preceding weather was not unusual, and the failure plane was not observed to be wet after the slide. Thunder storms in the weeks preceding the event were normal for the area. Additionally, the lack of observed water on the slide surface, or seeps from the slide area, suggest that water was not a significant factor.

STABILIZATION DESIGN

Stabilization was initially designed to include removal of the overhangs and installation of long tensioned rock bolts penetrating into the schist zone. However, the position of this mass on top of the pegmatite presented a potential for movement if not stabilized. Following partial removal of the overhangs and with close observations by the design team, the design was altered to include a reconfiguration of the cut.

The reconfigured cut was designed to be at an inclination of between 0.9H to 1V and 1H to 1V, near perpendicular to the foliation to reduce the potential for topping failure. The cut had a conical shape as it wrapped around the cut and was 220 ft high (slope distance of 315 ft) and 300 ft long around the base. This new cut was sub-parallel to the pegmatite plane (and the prominent secondary joint in the gneiss).

The designed cut was estimated to require removal of approximately 35,000 cubic yards of rock. The design included provisions for both tensioned rock bolts and untensioned rock dowels. The purpose of the rock reinforcement was to stabilize individual rock blocks and prevent loosening of the rock mass in key areas. Both the bolts and the dowels were number 10 epoxy coated rebar grouted with epoxy resin cartridges. To stabilize the top of the cut, two rows of 30 ft long tensioned rock bolts were installed along the brow. Additional bolts and dowels from 20 to 30 ft long were located on the face based on observed conditions. Following the reconfiguration, the cut face was designed to be scaled then covered with rock mesh to within 10 to 20 ft of the road surface for the purpose of containing loose rocks and directing them to the roadside ditch rather than into the road.

CONSTRUCTION

Construction was conducted in two phases. The first phase consisted of partial removal of the overhangs and cleanup of slide debris on the highway as discussed previously. This work not only improved the safety and accessibility of the work area, but allowed close observation of conditions by the design team. Phase one work was performed under the original construction contract as bid by the contractor. The second phase consisted of major cut reconfiguration. With the scope of the project significantly changed from the scope that was bid, work in this phase was conducted with negotiated unit prices.

Figure 7 Pioneer Road

Figure 8 Drilling for First Overhang Blast

Phase 1, which was elimination of the first overhang, involved removal of approximately 400 cubic yards of rock down to the pegmatite plane. Because the work area was over 100 ft above the road with no practical access and due to safety concerns, drilling for the blast holes was performed from a crane basket and by hand with personnel secured to the top of the slope with ropes, as shown in Figure 7.

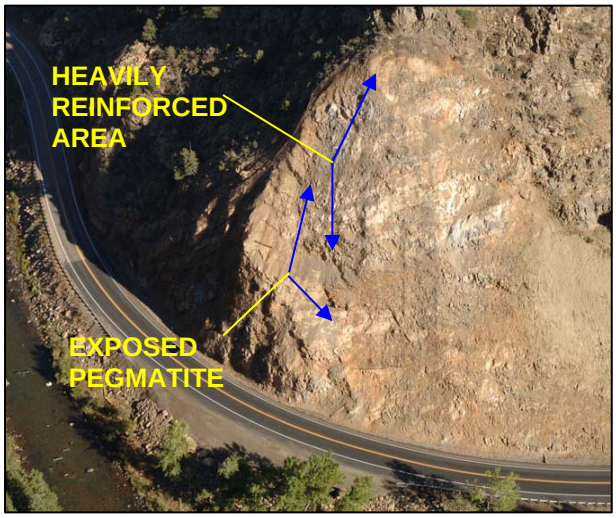

Figure 9 Reinforced Edge

Phase 2, cut reconfiguration, started with construction of a pioneer road to the top of the cut. Construction of the pioneer road was a challenging endeavor requiring two switchbacks and a road inclination as steep as 2H to 1V in some spots. Road construction involved excavation through talus and colluvium, blasting through rock, and construction of a small retained fill area.

Excavation of the cut was performed from the top down, in benches approximately 20 ft thick. Blast holes were drilled vertically on a typical spacing of 4 to 8 ft which were loaded with ANFO and set off with dynamite. The powder factor was commonly around 0.9 (pounds of explosive per cubic yard of rock). Blasted rock was pushed off the bench, typically in two 10-foot lifts per bench to facilitate installation of rock reinforcement. Drilling and blasting, and the installation of rock reinforcement was performed during daylight hours. The blasted rock accumulated on the road below and was loaded into trucks and hauled off predominantly during night shifts. Most of the muck was transported to a rock quarry approximately 4.5 miles up the canyon, and eventually processed into aggregates. The total volume of excavation was 38,000 cubic yards (in place).

Rock reinforcement elements were installed from the working bench in phases as the bench was lowered. Reinforcement was installed based on the rock conditions revealed after blasting, mucking, and scaling. Reinforcement consisted of both tensioned bolts and untensioned dowels from 20 to 30 ft long. Tensioned bolts utilized a combination of fast set cartridges for the anchor zone and slow set for the free zone. A total of 118 reinforcement units were installed with an aggregate length of 2755 ft.

Of particular note is that the strike of the pegmatite intrusion was approximately 15 degrees off of the road alignment. As a result, the pegmatite served as the base of the cut for the western third of the cut, then dove into the mountain for the eastern two-thirds of the cut, as shown in Figure 9. The gneiss overlying the pegmatite near the interface was identified as potentially being unstable and, therefore, was heavily reinforced with rock bolts and dowels, as shown in Figure 10.

Figure 10 Reinforcement at Overlap

Rockfall mesh was installed over the entire reconfigured portion of the cut from the top to within approximately 10 to 20 ft of the road surface. Top anchors and cabling were installed by hand along the top of the rock cut. The mesh was lifted in place in panels with a helicopter. The mesh covered an area of approximately 85,000 square feet. Construction began on June 24, 2005 and was complete by October 12, 2005. The construction cost of the work was approximately three million dollars. The highway was reopened to traffic on September 12, 2005. It was closed to through traffic for 83 days, a closure which is the longest in Colorado state history.

PERFORMANCE

The final cut configuration is shown in Figure 11. As of spring 2006 the cut is performing as expected. Small rocks discharge from the face as a result of the natural weathering process, and there is a small accumulation of debris in the ditch at the toe of the cut.

Figure 11 Final Completed Cut

PROJECT PARTICIPANTS

The project was spearheaded by CDOT with significant support from the Federal Highway Administration. Design was a collaborative effort between CDOT, the Colorado Geological Survey, Lyman Henn, and Yeh and Associates. Construction oversight was managed by CDOT with assistance and construction engineering provided by Parsons Transportation Group and Lyman Henn.

References

1. Parekh, Minal; Pease, Kent; and Ortiz, Ty. U.S. Highway 6 - Clear Creek Canyon Rockslide and Remediation. Proceedings of *Golden Rocks, 2006*. 41st U.S. Symposium on Rock Mechanics, Golden, CO 2006.
2. United States Geologic Survey by Sheridan, Douglas M. and Marsh, Sherman P.; (1976); "Geologic Map of the Squaw Pass Quadrangle, Clear Creek, Jefferson, and Gilpin Counties, Colorado."
3. Colorado Department of Transportation and Colorado Geological Survey by Andrew, Rick; (1994); "The Colorado Rockfall Hazard Rating System."
4. Colorado Department of Transportation, Rockfall Mitigation Project Plan 2005-2010, Appendix B, Colorado Rockfall Hazard Rating System Sites.

TECHNICAL SESSION VI
Hazards, continued

Field Testing and Numerical Modeling of Flexible Debris Flow Barriers

C. Wendeler, B.W. McArdell & D. Rickenmann
WSL Swiss Federal Institute for Forest, Snow and Landscape Research, Birmensdorf, Switzerland

A. Volkwein
WSL Swiss Federal Institute for Snow and Avalanche Research SLF, Davos-Dorf, Switzerland

A. Roth & M. Denk
Fatzer AG Geobrugg Protection Systems, Romanshorn, Switzerland

John Kalejta II - presenter
Geobrugg North America, LLC, Geobrugg Protection Systems

ABSTRACT:

Because it is practically impossible to establish a full scale field test site with controlled event triggering for testing debris flow barriers, the torrent Illgraben in the Central Swiss Alps, with an average of five to six natural debris flows per year, was selected. Instrumentation consists of rain gauges, geophones, radar and laser devices, digital video cameras, a debris flow force plate and a wireless data transmission system. The flexible barrier, in this case a net consisting of interconnected rings, is installed at the downstream end of the torrent channel, where anchors have been drilled in both channel banks and heavy-duty load cells have been installed between the anchors and support ropes. This paper deals with the commissioning of the net-testing part of the Illgraben test site, the first event which was retained by the barrier and the numerical modeling of the interaction between debris flow and barrier using the finite element software FARO which was especially designed to simulate highly flexible system

INTRODUCTION

Flexible wire net and ring net barriers were originally designed to protect villages, highways and railway lines from rockfalls. Their main load-bearing principle is to restrain the falling rocks using a long braking distance and therefore producing a soft stop, reducing the peak loads in the barrier components and the anchors. The same principle also works for a variety of other problems such as snow slides, tree falls, floating woody debris during flooding and debris flows. The latter are gravity driven two phase flows intermediate between intensive bed-load transport and landslides that cause considerable damage in mountain regions. The performance of flexible barriers loaded by debris flows is the topic of this paper.
It is the aim of this research project to improve the knowledge of the loads that act on rigid and flexible debris flow barriers. Contrary to rockfall where the load is clearly defined as one single block that can be typically assumed as rigid, the load from a debris flow cannot easily be determined. Therefore, an extensive experimental program is needed to find suitable load characteristics when designing such barriers.

Since July 2005, a flexible debris flow test barrier has been installed in the Illgraben close to the confluence of the Illgraben and the river Rhone (Fig. 1).

Figure 1. Installed debris flow test barrier.

TEST SITE DESCRIPTION

Field tests are essential for determining the scaling effects that have to be considered when interpreting the results of laboratory tests. However, debris flows in general cannot be predicted in nature because there is little knowledge about the initiating conditions. Therefore, a catchment area with a history of annual debris flow activity was chosen. Together with automatically triggered measurement facilities, it provides an

ideal opportunity to study the interaction between a debris flow and a flexible barrier.

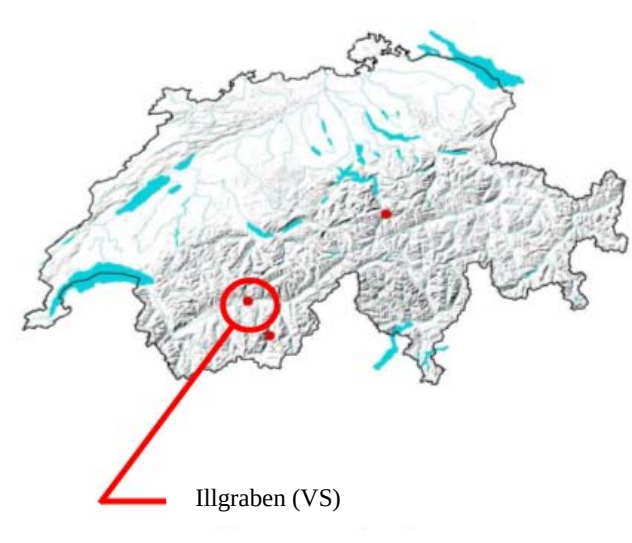

Figure 2. Location of the Illgraben within Switzerland.

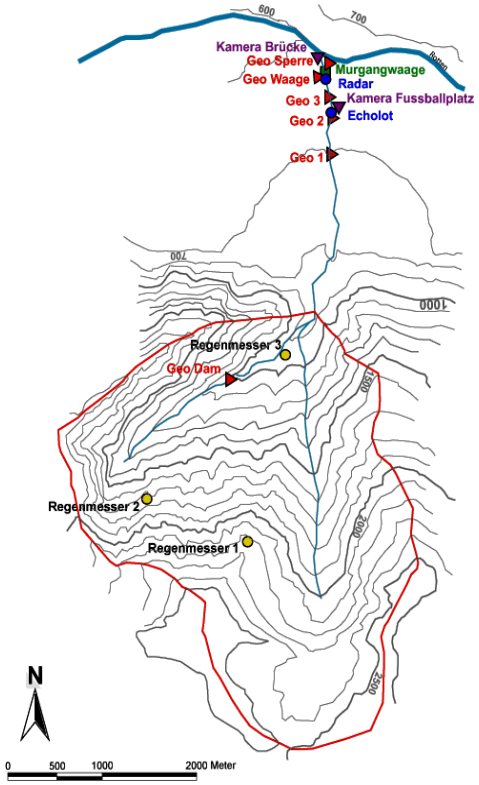

Figure 3. Topographical map and distribution of measurement devices in the catchment area.

Table 1. Parameters of the Illgraben catchment.

Area	10.5 km^2
Ground coverage:	
Rock, loose material	25 %
Forest	30 %
Open vegetation	43 %
Glacier	-
Lake	2 %
Highest point	2790 m ASL
Lowest point	610 m ASL
Exposure	N
Mean slope of torrent	16 %
Mean slope of fan	10 %
Length of main channel	2.6 km

The Illgraben catchment is in the canton of Valais, near Sion, in the Central Swiss Alps (Fig. 2). A topographical map of the Illgraben is shown in Figure 3 and the main characteristics of the Illgraben catchment are listed in Table 1.

Six geophones, one radar device, two ultrasonic devices, two video cameras, a debris flow force plate and three rain gauges are installed in the Illgraben catchment (Fig. 3). The geophones measure the vibrations produced by a passing debris flow and are also used to trigger the other measuring devices. The reach-wise front velocity of debris flows is calculated using the time of travel between the measuring devices.

The most unique device is the debris flow force plate, in use since 2004. With the instantaneous measurement of the debris weight and flow height, the bulk density and the water content of a passing debris flow can be reconstructed.

Historical data on the debris flow activity in the Illbach indicate that it is one of the most active catchments in the Alps. Debris flows have occurred regularly during the last 100 years including many smaller events (volumes less than 75,000 m^3), five events with volumes ranging from 75,000 to 250,000 m^3 and one event in 1961 with a total volume of about 500,000 m^3. An overview of the events in 2005 is shown in Table 2. The highlighted events occurred after the installation of the debris flow barrier was complete.

Table 2. Summary of debris flows recorded at the Illgraben observation station in 2005.

Date	Volume m^3	Qmax m^3/s	Hmax m	Vmax m/s
May 28th	140,000	145	2.25	9.0
June 3rd	30,000	16.1	1.08	2.5
June 3rd	18,000	10.1	1.25	1.3
June 13th	25,000	30.0	1.00	5.3
July 4th	25,000	14.1	1.12	2.4
July 18th	19,000	24.1	1.3	2.3
August 2nd	8700	17.9	1.16	1.4
August 18th	5600	7.5	0.80	0.7

FLEXIBLE DEBRIS FLOW BARRIERS

When using the systems of *Geobrugg Protection Systems*, there are two different setups of flexible debris flow barriers depending on the shape of the torrent. For V-shaped torrents the system illustrated in Figure 4 (VX barrier without posts) is used (also in Illgraben, see Fig. 1). For a wider - mostly U-shaped torrent - a UX-System with supporting posts in the middle of the net is more suitable. For spans of more than 12 – 14 m, UX barriers are advisable. On the top support ropes, special abrasion protection components are attached.

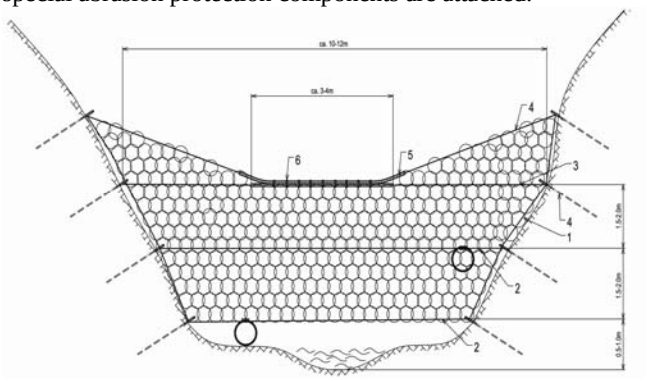

Figure 4. Debris flow barrier (VX-system) used at the Illgraben.

Mode of action

The debris load is transmitted by the ring net to the support ropes anchored in the river banks. The kinetic energy is absorbed by the flexible system and by special brake elements (so-called brake rings) that are integrated into the ropes. These brake rings also damp the impact loads transmitted to the anchors. Furthermore, they act as an overload protection to the ropes.

Water is critical to the efficiency of debris flows. If the water can be extracted from the flow, the solid mass can easily be stopped. Because of the large permeability of the ring net barrier, water drains at the front of the barrier and the granular blocks are retained. A part of the debris flow is then stopped. The newly built dam created by the solid material is strong enough to retain the remaining debris flow volume. This is the main assumption made in this project. Its correctness is proven at the end of this paper.

The maximum retained volume V_{DF} depends on the topographical situation and the width b and height H_0 of the barrier. The tangent of the slope of the deposited material is about 2/3 of the slope gradient S_o of the river bed (Rickenmann 1999).

The height of the barrier after the filling process should be about ¾ of the height before the event (see Fig. 5). The minimum height H_0 of the barrier can therefore be calculated by

$$H_0 = \sqrt{\frac{32}{9} \cdot \frac{V_{DF}}{b} \cdot \tan[\arctan(S_0) - \arctan(\frac{2}{3} \cdot S_0)]} \qquad (1)$$

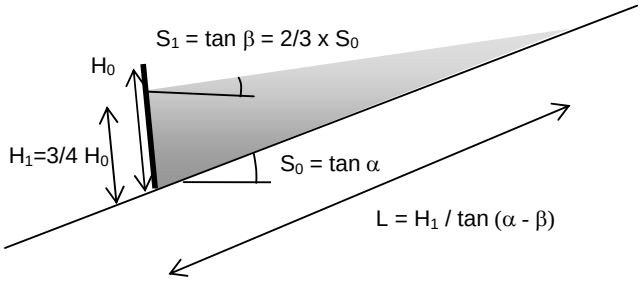

Figure 5. Deposited material behind the barrier.

Instrumentation at the Illgraben test barrier

The barrier is monitored by a video camera with an additional lighting system for night recording. A laser measurement device is situated above the barrier to measure the rate of filling of the barrier and the height of the debris overflowing the filled barrier. The video as well as the light and the laser measurement are triggered by a signal from a geophone upstream. Hence, the observation of the barrier and the debris flows infilling upstream of the barrier are nearly guaranteed.

In the steel wire ropes of the barrier, heavy duty load cells with 50 tons capacity are installed. The overview of the load cell arrangement is shown in Figure 6. The data logging of the force sensors is also initiated by the previously described trigger signal.

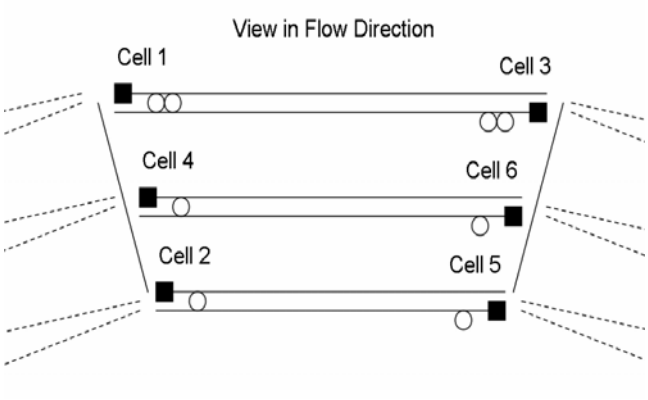

Figure 6. Arrangement of the load cells.

Measurement results

The first test period of the barrier in summer 2005 was quite successful because all of the measurement systems functioned and the barrier captured the front of a flow and was overtopped by subsequent flows, providing a chance to evaluate the behavior under severe field conditions. Three debris flows passing the barrier were measured (Tab. 2). The tension forces of the support ropes of the debris flow event from 2 August 2005 are shown in Figure 7.

The event of 18 July 2005 filled and overtopped the barrier. Due to an initially too soft trigger level it was not possible to obtain video and load values from the actual filling process of the barrier. This event was characterized by relatively small initial vibrations. Therefore, the geophone set off the trigger signal too late and the load cell measurements started when the barrier was already full. The triggering values have since been adjusted to increase the likelihood of capturing the barrier filling process in 2006. Fortunately the events recorded in 2005 still provide valuable data for the model calculations, which are described in the following section.

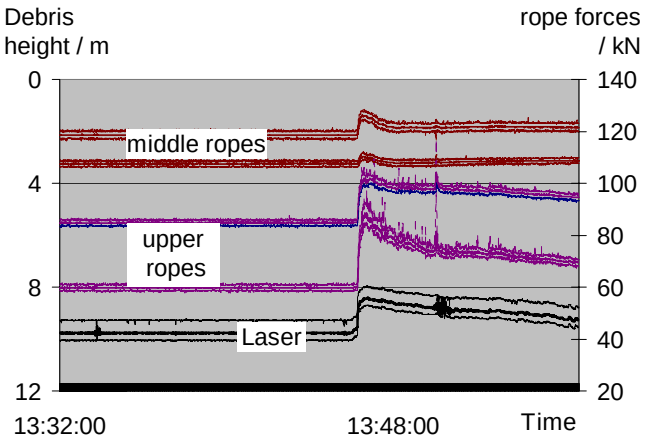

Figure 7: Tension forces in the load cells on Aug. 2nd 2005.

During the 2 August 2005 event, the debris flow front arrived at 13:48 when the flow height measured by the laser increased. The initial load cell level at the top ropes lay between 60 and 80 kN for the completely filled barrier. For the middle ropes, the initial tension force was about 110 to 120 kN. The bottom rope was only initially loaded with 40 kN. When the flow height increased, the barrier was overtopped and the tension forces in the ropes increased by 40 kN. The largest increase of the tension force was in the rope at the top because it was most directly affected when the flow passed over the barrier. The increase of the laser level showed a flow height of about 2 m at the barrier. Figure 8 shows the filled barrier.

Figure 8. Filled barrier after debris flow event.

CALCULATION METHODS

Parameters for characterizing debris flows and dimensioning barriers are rather poorly constrained and in some cases not yet fully investigated, yet they are required for engineering work. The deficit originates on one hand from the complex mechanics of two phase flows and on the other hand from the difficulties

in measuring typical debris flow parameters such as shear or impact forces.
Several mechanical and rheological models have been proposed to route debris flows but they have not yet been generally verified with field experience. A simplified approach was taken for the first calculation of the barriers (Rickenmann 1999, Roth et al. 2004) and is described below.
First, it is necessary to determine the volume V_{DF} of the debris flow at the construction location. This is an imprecise exercise because the relations are generally empirical. The best approach at the moment is to use events in the catchment of interest (Tab. 1 for the Illgraben) and make a geomorphologic assessment of the expected volume.
The volume of the material that will potentially be retained by a flexible protection barrier lies between 100 m^3 and up to 1000 m^3 (Fig. 5). It is clear that the debris flow volume V_{DF} is related to the peak discharge Q_p (beside the amount of debris available, of course). Therefore one has to distinguish between granular or muddy debris flow types.
Mizuyama et al. (1992) present the following equation for a granular debris flow

$$Q_p = 0.135 \cdot V_{DF}^{0.78} \quad (Q_{p,d} = 5\ m^3/s - 30\ m^3/s) \qquad (2)$$

The empirical relation for a muddy debris flow is

$$Q_p = 0.0188 \cdot V_{DF}^{0.79} \quad (Q_p = 1\ m^3/s - 5\ m^3/s) \qquad (3)$$

Using the peak discharge, the mean flow velocity v_d can be calculated. Rickenmann (1999) gives the following equation, which also depends on the inclination S of the river bed:

$$v = 2.1 \cdot Q_P^{0.33} \cdot S^{0.33} \quad (v = 2\ m/s - 6\ m/s) \qquad (4)$$

In Japan (PWRI 1988), calculating the mean velocity using a Manning Strickler equation is recommended. They take a pseudo Manning value n_d in a range of 0.05 $s/m^{1/3}$ and 0.18 $s/m^{1/3}$. For a granular debris flow n_d should lie between 0.1 $s/m^{1/3}$ and 0.18 $s/m^{1/3}$

$$v = \frac{1}{n_d} \cdot h^{0.67} \cdot S^{0.5} \quad (v = 1\ m/s - 6\ m/s) \qquad (5)$$

The recommended solution for determining the maximum load on a barrier is to compare the maximum velocities calculated using the two different methods described above (Roth et al. 2004).
The flow height can then be calculated with the cross-sectional width b and the peak discharge.

$$h = \frac{Q_p}{v \cdot b} \quad (h = 0.1\ m - 1\ m) \qquad (6)$$

The density of the material depends on a range of factors but typically ranges from $_d = 1800\ kg/m^3$ to 2300 kg/m^3. In the Illgraben, a bulk density of about 2100 kg/m^3 has been measured.

One of the most unknown processes is the barrier filling process, which depends on the impact and filling time at the barrier. At the moment we assume that only a part of the debris flow has to be stopped; this stopped mass is assumed to be capable of retaining the remaining debris. Therefore, the mass of the debris directly stopped by the barrier has to be estimated. Together with the mean flow velocity calculated above, the kinetic energy the barrier is loaded with can be estimated. The mass which is acting on the barrier is

$$M = \rho_d \cdot Q_P \cdot T_{imp} \quad (M = 10{,}000 - 200{,}000\ kg) \qquad (7)$$

and the kinetic energy is then

$$E_{kin} = \frac{1}{2} \cdot M \cdot v^2 \quad (E_{kin} = 100 - 3000\ kJ) \qquad (8)$$

Ring net barriers were originally used as rockfall barriers, where their behavior is comparatively well-known. The required design for a debris flow can be deduced by comparing the kinetic energies between an expected debris flow and an equivalent rockfall barrier. However, the loading differences between rockfalls and debris flows must be considered. A comparison of loads in these two cases can be found in Table 3. By considering these factors, one can assume a relation between debris flow and rockfall energies. The energy capacity of debris flow barriers is also dependent on multiple acting sections (in contrary to rockfall barriers where a falling rock generally only affects one section).

Table 3. Comparison of the load transmitted by rockfall or debris flow onto a ring net barrier.

	Rockfall	Debris flow	Influence on debris flow design
Load form	single load	area load	Positive: No local load peaks
Impact time	0.2 - 0.5s	1 – 4s	Positive: smaller peak loads
Impact style	single impact	wave shaped impact	Negative: Already loaded but still additional loads
Brake distance	5 – 8m	2-3m	Negative: Increased dynamic loads

NUMERICAL MODELING

To improve the design process for flexible debris flow barriers, a finite element software package FARO, originally developed to simulate rockfall protection barriers (Volkwein 2005), was

modified. FARO was calibrated in field and laboratory tests. This program is being adapted to consider the area load of a debris flow impact. At the moment, there are two different approaches:

1. The impact is modeled using a kind of "inertial load". The impacting mass is distributed onto the single net nodes. Every single mass point then is assigned an initial velocity. The barrier then has to restrain this inertia load. The problem with this approach is a collapse of the barrier model upon itself when the debris flow is stopped and the mass points follow their gravitational loading.

2. The area load is distributed onto the net nodes as single forces. The application of the forces over the barrier height is time dependent corresponding to the filling process of the barrier (Fig. 9). After the stopping process the barrier stays in the deformed condition.

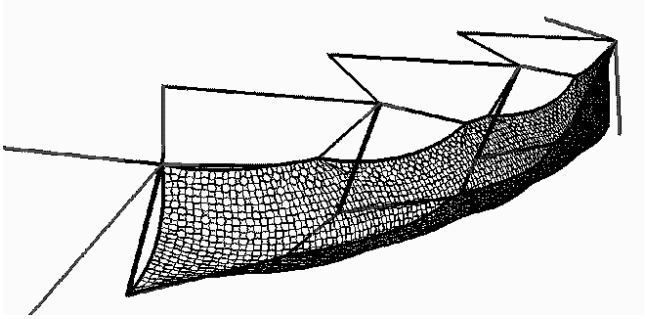

Figure 9. Simulated debris flow barrier with three sections loaded by an area load distributed into single net node forces.

The second approach produces a more realistic shape of the deformed barrier and is – at the moment - the preferred load application for a debris flow barrier. In Figure 10, a qualitative comparison between the loaded full scale barrier and the corresponding simulation model is shown. Measured and simulated rope forces after the barrier has been filled by the debris flow event from July, 18th 2005 are shown in Table 4. For this first simulation a maximum difference of 20 % to the measured field values seems to be quite good. As the project is developing further in the next years, better load models for the debris flow impact will improve the results.

The results also prove that the main assumption made in section 0 is correct. The load model described in section 0 has been built using the theory that a small part of the debris flow builds a small dam that is capable to retain the rest of the debris flow. The obtained simulated forces compared to the measured ones confirm this assumption.

Table 4. Rope forces after impact: measured and simulated.

	Measured	Simulated	Difference
Upper ropes	120 kN	110 kN	16 %
Middle ropes	160 kN	210 kN	20 %

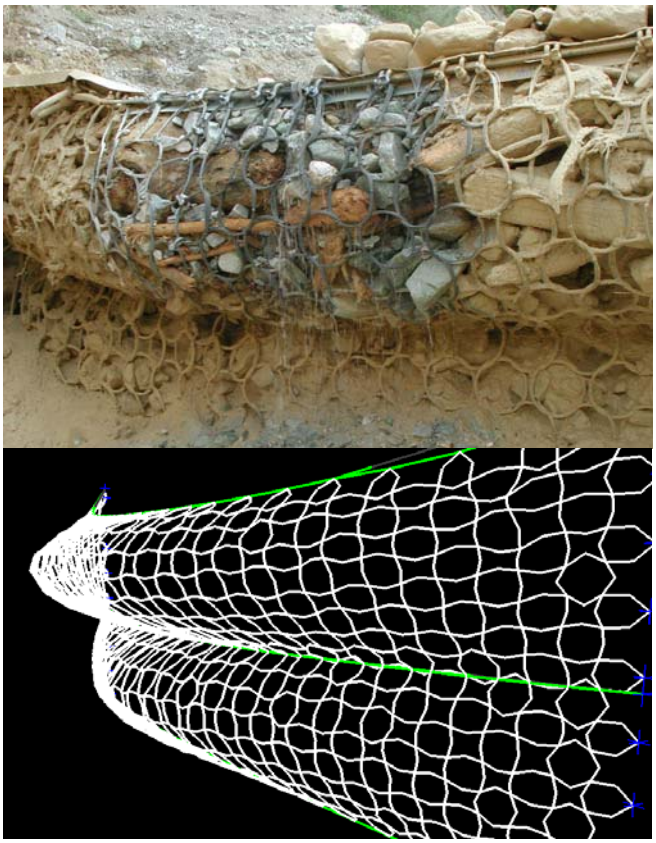

Figure 10. Deformed barrier in the Illgraben and the corresponding simulation.

CONCLUSIONS AND OUTLOOK

A new research project dealing with flexible barriers against debris flows has been introduced. The combination of full-scale field experiments together with the corresponding simulations will result in a physical approach to designing flexible barriers. In addition, the results can be used to transfer the knowledge to rigid barriers and to verify or to improve existing models.

After the work of DeNatale et al. (1996) who were testing net panels in a debris flow test channel and the work of Imai et al. (2005) who were instrumenting a wire net dam, the here presented project is a further step ahead with a test site where different types of flexible debris flow barriers can be installed and full-scale tested by natural debris flows

.

However, the impact of a debris flow is still inadequately known. Furthermore, it is difficult to predict debris flow events. Even at the same location, flows have a wide range of volumes, velocities and consistencies. However, these parameters are very important for the design of protection barriers. It is therefore the aim of this project to treat such questions for the design purpose.

One of the next steps is to run laboratory tests with small debris flows impacting into different kinds of barriers. The variation of the barrier stiffness will then give information about the stopping process depending on the flexibility of the structure as also treated in Horii et al. (2002). Additionally, it will be possible to describe the scale effects comparing the field tests with the laboratory experiments.

REFERENCES

DeNatale, J. S., Gregg, G. L. & Fisher, G.D. 1996. *Response of the Geobrugg cable net system to debris flow loading*. San Luis Obispo: California Polytechnic State University.

Horii, N., Toyosawa, Y. & Hashizume, H. 2002. Influence of particle size and structure rigidity on impact stress in simulated debris flow. *Proc. ICPMG, 2002*: 399-404.

Imai, K., Higuchi, J., Kasai, S., Momma, K. & Shimojo, K. 2005. Survey regarding the transformation and design of Kamikami-horisawa improved wire net dam. *Journal of the Japan Society of Erosion Control Engineering*, Vol.58 (4).

Mizuyama, T., Kobashi, S. & Ou, G. 1992. Prediction of debris flow peak discharge. *Proc. Int. Symp. Interpraevent*. 4: 99-108.

Public Works Research Institute. 1988. *Technical Standard for measures against debris flows* (draft). Japan: Ministry of Construction.

Rickenmann, D. 1999. Empirical relationships for debris flows. *Natural Hazards*. 19(1): 47-77.

Roth, A., Kästli, A. & Frenez, Th. 2004. Debris Flow Mitigation by Means of Flexible Barriers, *Proc. Int. Symp. Interpraevent*. Riva del Garda, Italy. Klagenfurt: Interpraevent.

Volkwein A. 2005. Numerical Simulation of flexible rockfall protection systems, *Proc. Computing in civil engineering.* Cancun: ASCE.

ACKNOWLEDGEMENTS

This project is partly funded by the Swiss KTI/CTI (Federal Commission for Technology and Innovation). Many thanks also to Bruno Fritschi for his assistance in the design and construction of the Illgraben debris flow observation station. The authors gratefully acknowledge the work of Francois Dufour (Antenne ENA Valais), Alexandre Badoux (Antenne ENA Valais), Andreas Koeppel, Bruno Koeppel and Marco Marty.

Rolling Rocks in a Peruvian Mine for Calibration of the CRSP Model

Nancy C. Dessenberger, P.E., P.G.
Golder Associates Inc.,
44 Union Blvd, Suite 300
Lakewood, Colorado 80228

Michael G. Skurski, P.E.
Newmont Mining, Minera Yanacocha S. R. L.
Peru

ABSTRACT

The Colorado Rockfall Simulation Program (CRSP) has become a standard tool for analysis of rockfall in the transportation industry. It is also well suited for application in other venues where rockfall is of concern, as it was for the development of a geomembrane-lined reservoir beneath 340 to 564-foot (104 to 172 meter) high mine pit highwalls in Peru. In any application of software derived models, the chance to conduct a field test for model calibration is advantageous. Using CRSP for design of rockfall mitigation after a site-specific calibration provides greater confidence in the results. This paper describes such a field test and how the results were applied to the CRSP model to obtain increased confidence in model predictions.

PROJECT SITE AND CONDITIONS

The project site is the Yanacocha Mine complex in northeastern Peru, operated by Minera Yanacocha S.R.L. (MYSRL). Yanacocha is a gold mine situated in the central Andes mountains with site elevations ranging from 11,800 to 13,500 feet (3,600 to 4,120 meters). The location of this study was the San Jose Sur Pit, which was actively mined from 1997 to 2000 and has been in care and maintenance since. This was a small mine pit that is ideally suited for conversion to a water storage reservoir due to its shape and location high on a ridgeline to allow for gravity drainage to community canals. The project was designed to improve the management of treated process water and the creation of water storage capacity also provides an opportunity to use the stored water to mitigate base flow reductions which result from site-wide pit dewatering activities. At mine closure the reservoir will continue to be used for management of treated water which creates a sustainable benefit to local communities. Currently the project is in the construction phase of building flatter reservoir slopes (compared to the existing mine pit slopes) to allow for placement of an HDPE geomembrane lining. Therefore one of the principal concerns was rockfall from the pit highwall above the reservoir crest that could potentially damage the geomembrane lining, thereby reducing the reservoirs' water retention effectiveness. The West and Northeast pit walls extend to elevations of 104 and172 meters above the reservoir dike crest, respectively and represent the largest risk of rockfall. Since one possibility is for MYSRL to ultimately transfer reservoir operation responsibility to local communities this study took a long-term view of rockfall potential, well beyond the active mining period at Yanacocha. This extended time frame has particular significance because mine pit high walls age over time.

The maximum height of the Northeast Wall is approximately 172 meters. Wall (inter-ramp or between mine haul ramps) angles range from about 38° to 51°. The upper portion of the wall has a flatter angle than the lower portion of the wall, with slope angles ranging from about 39° to 43° compared to lower wall angles of about 49° to 51°. The pit was mined with single 8-meter high benches down to about the middle third of the slope. At this point the conditions were conducive to allow for limits excavation in a double bench configuration resulting in catch benches separated by 16-meter high bench faces. The resident rock type in the pit is andesite which presents itself in various alterations in the Northeast Wall such as massive silica, argillic, and advanced argillic rock types.

Three areas of existing failures are present on the Northeast Wall. An assessment of slope stability for the highwalls was included in the study, but is not discussed herein. However, existing failure areas on the Northeast Wall were of concern for rockfall, where failures in argillic rock were undercutting more competent layers capable of producing relatively large block falls.

The maximum height of the West Wall is approximately 104 meters. It has an overall slope angle of about 48°. The rock mass within the West Wall, comprised predominantly of massive and vuggy silica alteration types of andesite, is highly shattered from blasting damage which is more common in mine pit slopes than in road cut slopes. However, there is no apparent evidence of multi-bench failures present in the West Wall. The slopes of the West Wall are covered with debris where benches were filled in after mining, and this had a significant effect on rockfall behaviour.

FIELD INVESTIGATION

Data on rock slope condition, potential rockfall size, and observations pertinent to selection of CRSP parameters (such as tangential and normal coefficients), were gathered in field studies. Access to highwall benches was severely limited, in part due to existing conditions of loose rock and debris filled benches, but mostly because steep slopes surrounding the walls did not allow safe access under MYSRL's stringent safety requirements for highwall work. Some work was done using rock climbing techniques to access the slopes, but safe access was still very limited. However, between data gathered during this study and information gathered during active mining, a total of 415 measurements of bedding, joint, and fault surfaces in the Northeast Wall and 181 measurements on the West Wall were collected. More important to the CRSP analyses, the field investigation for the study included observations of surface irregularity, block sizes from previous rockfall, and surface conditions pertinent to the selection of parameters for the CRSP model.

CRSP'S CONTEXT IN THE ROCKFALL MITIGATION STUDY

The purpose of the rockfall study for the proposed reservoir construction was to apply CRSP as a tool for optimizing the dike crest width and developing alternative strategies for catchment, to satisfy the intent of maximizing rockfall capture and mitigating rockfall damage to the reservoirs' interior lining. Minimum acceptable dike crest width was variable depending on the nature and effectiveness of the various rockfall catchment strategies examined.

MYSRL initially specified 100 % retention as a target criteria for design of rockfall catchment. While design tools such as CRSP can report results at a theoretical 100 percent retention, variations in the size and number of rocks, and in field conditions beyond the assumptions incorporated in a model render the simulation results an approximation. As such, even with 100% calculated retention, it was recognized that an element of residual risk remains. Therefore, for most of the cases analyzed in this study, a calculated rockfall retention of 99% or better was considered to provide a suitable degree of protection to the reservoirs' geomembrane lining.

Analyses of the pit wall slopes, including the geometry of catchment alternatives, were undertaken using CRSP (Colorado Geological Survey, 2000). CRSP is a computer model for examining rockfall behavior on slopes developed primarily for use in highway design and evaluation, but was deemed applicable for MYSRL's project as a means of evaluating the potential for rockfall to impact the proposed reservoir. Rockfall models within CRSP are defined in terms of slope profile geometry, and include a series of input parameters such as rock size and shape, rockfall source, slope surface roughness, and tangential and normal coefficients of restitution. There are aspects of rockfall behavior that are not modeled by CRSP, such as the effect of larger rocks breaking apart during rolling or impacts, and thus some judgment regarding the potential for multiple rockfalls, large rock mass rockfalls and shattering boulders must to be exercised during evaluation.

One of the most challenging aspects of utilizing the CRSP model is the assignment of parameters which characterize the nature of the slope along which the rockfall bounces, rolls, or comes to rest. The CRSP manual provides some guidance and ranges of typical values to be used for the coefficients of restitution parameters (tangential and normal coefficients), which are the most difficult to define, since they are not readily measured. This range of parameters has been defined based on calibration to various rockfall tests, by comparison to observed velocity and energy.

However, where practical a rock rolling field test conducted on the actual slopes to be modeled provides a much higher level of confidence in the parameters used in the model for analysis of a given site.

During the development of the reservoir design and initial construction, we were permitted to conduct a rock rolling test. Observations of the behavior of the rocks made during the test, and measurements of rollout distances of the individual rocks, were used to "back calculate" parameters for use in modeling a series of alternatives for rockfall mitigation.

TEST SITE CONDITIONS

The two highwalls with concern for rockfall are quite different in character. The Northeast Wall is a maximum of 172 meters high. Catch bench widths average about 8 meters, but infilling in some areas have reduced bench width effectiveness to 3 meters or less. Rock types vary within the Northeast Wall, but much of the rock tends to produce blocky structure. In most areas, the existing benches appear to be capturing most rockfall, which is a function of flatter overall slopes producing wider catch benches, except where benches are highly infilled. Field mapping of the wall included delineating zones of rock type and associated rockfall character, (such as degree of bench filling, block size ranges, rock structure/condition pertinent to generating rockfall). Figure 1 shows a photo of the Northeast Wall, and how zones were defined based on alteration rock type.
The West Wall is predominantly characterized by a relatively shattered rock mass of brittle massive silica rock.

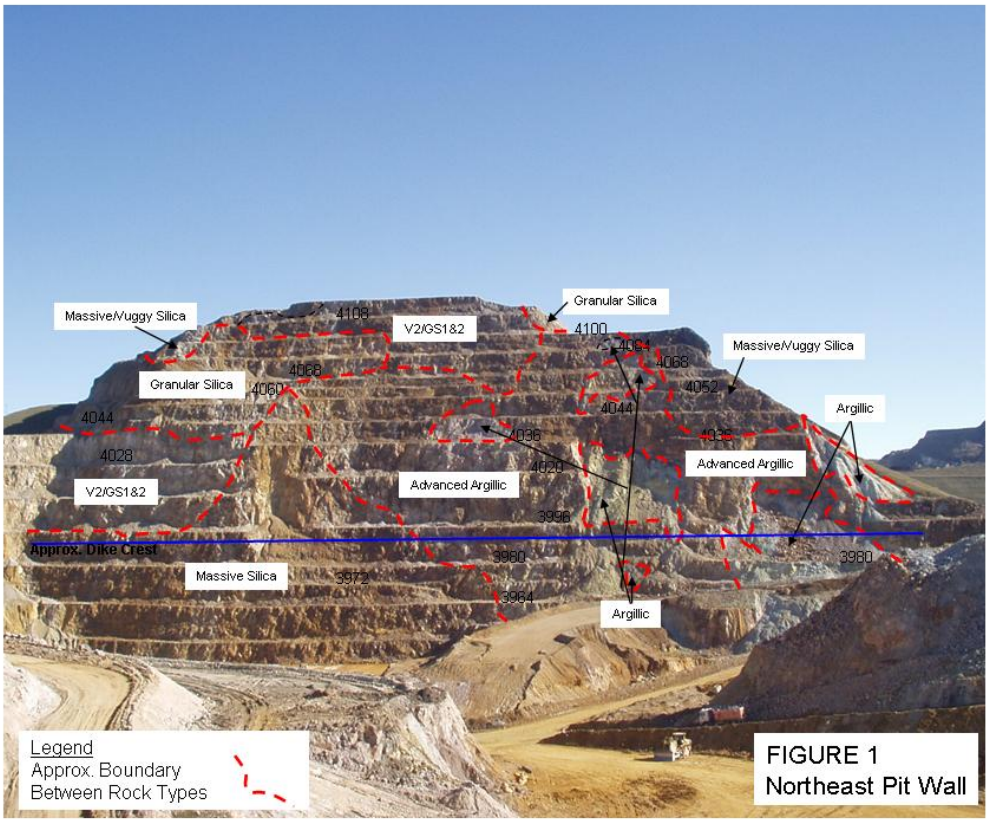

As a result, actual block sizes generated from the West Wall (0.6 m) were estimated to be smaller than for the Northeast Wall (0.8m). Also, benches on the West Wall were almost completely filled, thereby reducing catch bench effectiveness for rockfall capture to practically zero. Figure 2 shows a photo of the West Wall.

FIGURE 2
West Pit Wall

Due to the greater height and larger face area, our first choice would have been to roll rocks from the top of the Northeast Wall. However, this was considered impractical due to both poor access and geometry of the wall itself. Although the top of the Northeast Wall was readily accessible, the upper benches were relatively wide and it seemed unlikely that rocks rolled from the top of the wall would make it past the first few benches. Lower benches on the steeper portions of the wall were not safely accessible. A bulldozer was used to cut access to one of the upper benches in the north corner of the wall, but again the benches immediately below were too wide to likely permit rockfall to reach the pit floor, and rockfall from the accessible locations would have been subject to atypical slope geometry at the pit corner.

The rock rolling test was performed on the West Wall, near the highest point of the wall where a bench had been cleaned to facilitate geologic mapping efforts during the project. The selected location provided the maximum practical slope height, reasonable access for equipment, and a suitable location from which to obtain video records. Below the selected "launch pad", the pit wall slopes were steep, and the benches were mostly filled with debris. Near the bottom of the wall was a very wide bench, approximately 20 meters wide at elevation 3964 m (3964 bench) where an old haul road was left in the highwall during mining. This bench was the lowest bench above the pit floor, and due to its width, captured most of the test rocks, as well as "natural" rockfall from the West Wall. This was beneficial as it was accessible on foot to allow for roll out measurements.

Due to the lack of access, actual slope surveying was not practical. The cross-section used for the CRSP model calibration analysis was constructed from a cross-section incorporating data used in the reservoir construction drawings, modified to reflect observed configuration of the "launching pad" platform and slopes below, filled benches, and actual reservoir bottom elevation at the time of the test. At the time of the test, the pit floor was being backfilled with random fill in thin, compacted layers to provide a gentle sloping floor for the reservoir to facilitate liner installation and water drainage in the lower reservoir elevations. This was an ideal situation as the floor simulated well the proposed reservoir crest where rockfall mitigation items such as rock fall capture fences and ditches were being contemplated for inclusion in the design. The portion of the West Wall used to model this cross-section is shown in Figure 3.

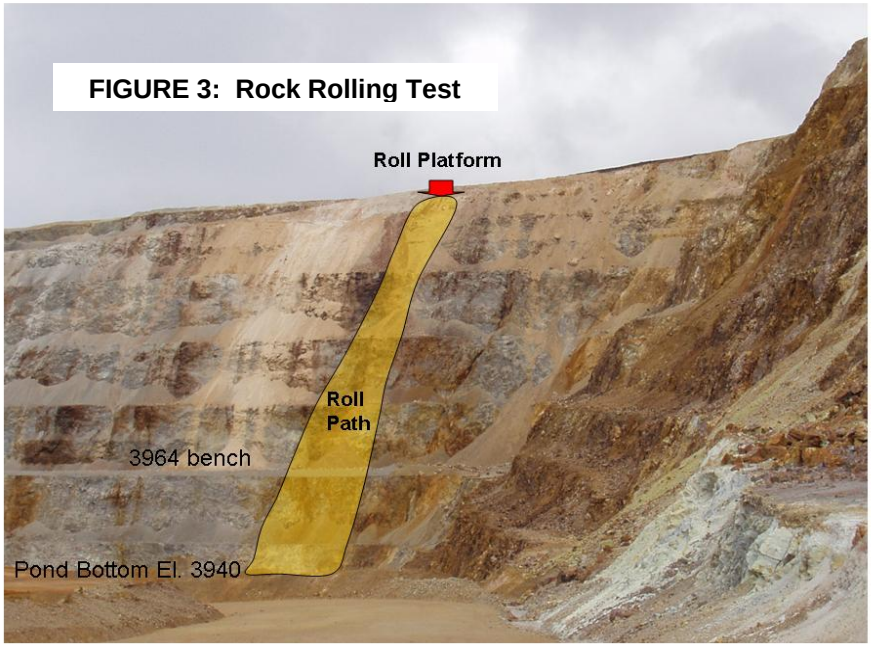

FIGURE 3: Rock Rolling Test

The calibration of the CRSP model for use in the overall study recognized the differences between the West Wall, upon which the rock rolling test was conducted, and the Northeast Wall, which had the potential to generate larger rockfall events. Due to the differing character of bench infill conditions and surface rock types, parameter calibrations determined through the field testing are less direct for the northeast wall. Still, comparison of values selected to characterize the West Wall, based on the results of the rock rolling test, to published guidelines (CRSP, 2000) provided useful guidance in adjusting the presumptive values to site-specific values for the Northeast Wall. This was done by examining the differences between the pre-test, presumptive values estimated for the West Wall and the corresponding revised values based on the rock rolling test results, and applying similar modifications to the final values used to model the Northeast Wall.

METHODOLOGY

A total of 46 boulders was selected for roll testing. Boulders were selected from durable materials, and included massive and vuggy silica andesite from another portion of the San Jose Sur pit. The boulders were not intended to necessarily be representative of rocks from the West Wall, but to be durable enough that most would survive the rolling test.

The boulders were selected to represent two general size categories. Boulders from about 0.3 to 0.5 meters average diameter were painted green, and boulders from about 0.6 to 0.8 meters average diameter were painted orange. All boulders were numbered for identification. Approximate dimensions were measured in three axes and averaged to obtain an average diameter for each boulder.

The boulders were transported to the rolling platform using a small front end loader. Little damage from transport was observed. The boulders were set in motion by the bucket of an excavator. Two methods of rolling initiation were employed; first by gently nudging the boulders to the platform edge past their limit equilibrium point, and secondly by dropping the boulders from the excavator bucket at an elevation equivalent to the launching platform. While the former method was used for most of the trials, the two methods of rolling initiation were considered equivalent in terms of rockfall starting velocities. As each boulder was pushed over the edge, the camera crew was notified and video taping of the rock was completed by conventional means as well as with highs speed video. Although not all of the trials were recorded on film, those that were provided insight into boulder rolling and bouncing behavior. Notes were taken during each rock roll regarding rollout distance and behavior during the roll. Table 1 presents an example of how these observations were tabulated.

Following the test, measurements were taken on the final distances from the slope where boulders came to rest, also shown in Table 1. All boulders were accounted for and only 6 of the 46 rocks rolled made it past the 3964 bench and continued to the reservoir floor that was being constructed.

TABLE 1
Example Observations/Results of Rock Rolling Test

Rock Roll No.	Rock Inventory No.	Rock Avg. Dim. (m)	"Good push" or drop?	Roll or hop on slope	Hit bench-level debris cone?	Estimated Land Distance from Toe at 3964 Bench Level	Estimated Stop Distance from Toe at 3964 Bench Level	Estimated Land Distance from Toe at 3940 Floor Level	Estimated Stop Distance from Toe at 3940 Floor Level	Comments
1	Orange 17	0.77				8	berm toe (17)			
2	Orange 19	0.67	yes	hop		past	past	4	23	barely rolled over bench berm
3	Green 18	0.43	yes	hop	yes	in debris cone	9.3			
4	Orange 14	0.77			yes	10	16.3			
5	Green 12	0.5	yes		rolled		8.7			broken
6	Green 21	0.43					12.2			
7	Green 13	0.33		roll	yes		10			momentum stalled in upper debrus cones
8	Orange 16	0.57		hop	no	6	6.7			cleared 3980 bench and landed on 3964 bench without rolling
9	Orange 2	0.73	yes				berm toe (17.3)			
10	Green 4	0.43	yes	roll	rolled		berm toe (17)			
11	Green 14	0.4	no	roll	rolled		11.3			
12	Green 8	0.37			no		11.6			clean fall from 3980 bench
13	Green 25	0.37					16.3			
14	Green 5	0.43			no		10			
15	Orange 1	0.67		hop		past	past	3.5	3.5	
16	Orange 8	0.63			yes	in debris cone	6			

TEST RESULTS

Test observations and measurements for each rock were tabulated (Table 1 example). The following general observations were also made:

- Rocks that fell at a steep trajectory onto debris cones significantly reduced their energy on impact. Many rocks initially struck the larger debris cone just above the 3964 bench after launching from the benches above.
- Rocks that rolled onto debris cones (or hit obliquely) often gathered speed rolling down the cone face(s).
- The small berm at the outside edge of the 20-meter bench seemed quite effective in trapping rocks that made it that far. However, rocks which made it over the top regained considerable momentum on the slope below.
- Rocks landing on the 3964 bench either stopped close to where they first landed (if having a steep trajectory), or rolled a considerable distance. Rocks which rolled (rather than bounced) down the lower slope rolled out the farthest. A similar effect was observed for rocks making it to the reservoir floor.
- A number of rocks launched from the second bench above the 3964 bench in an airborne trajectory before impacting on the 3964 bench. There did not appear to be any distinct launch feature at this point. It may be a function of momentum gained after rolling that far, combined with a minor launch feature.
- Most rocks seemed to have their initial impact location on the 3964 bench within the first 10m (first ½ of the bench width).
- In general, it seemed that the smaller (green) rocks were more likely to roll, and the larger rock (orange) more likely to hop down the slope. Shape difference (deviation of average dimensions) was not significant between green and orange rocks.

CRSP CALIBRATION

A cross-section for analysis of the rock rolling test was constructed from the same cross-section as the section used in rockfall analysis for the West Wall (Figure 3). However, for the calibration, this section was modified to reflect the slope geometry at the time of the rockfall test, including the current location of the pit floor, the location of the rock rolling platform, and the 3964 bench. Initial values for CRSP parameters were selected from the tables of recommended values (CRSP, 2000). Rock size was designated as the average rock size for each of the two size categories, 0.4 meters for the smaller (green) rocks, and 0.64 for the larger (orange) rocks.

First the model was run and calibrated to the rollout distances for the larger rocks. Since a greater number of the large rocks rolled beyond the 3964 bench and onto the reservoir floor, the percentage of large rocks passing the outer edge of the 3964 bench was used as a criterion for calibration. The model input parameters of slope surface roughness, and normal and tangential coefficients are generally the most difficult parameters to quantify and were thus the primary objective of site-specific calibration. These parameters were adjusted in the model within the reasonable range of values until the rollout behavior indicated by the model mimicked that recorded from the rock rolling test. After model calibration, the number of rocks rolling to the pit floor was calculated to be 18%, which compares favorably with the actual percentage observed in the test of 17%. The rockfall trajectories displayed in the CRSP model also were checked against the field observations, and in fact the model indicated that a significant number of rocks "cleared" the bench above the 3964 bench as described above in the test observations. (Figure 4).

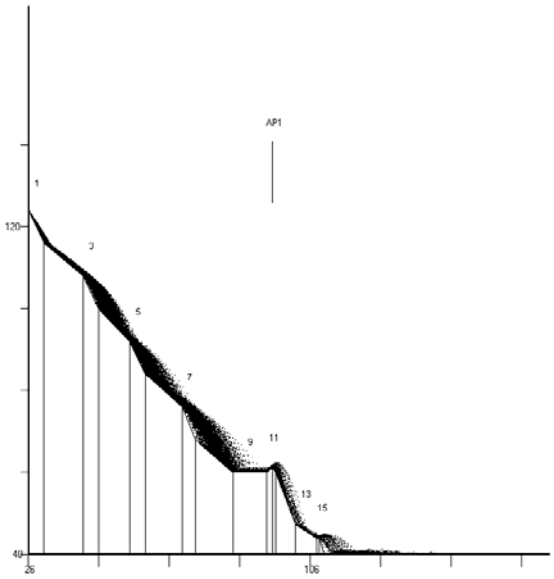

FIGURE 4: CRSP Plot of Rock Rolling Test

After the CRSP parameters were calibrated using the large rock test results, the model was run for the smaller rock size range. Approximately 8% of the smaller rocks rolled to the reservoir floor in the rock rolling test. The calibrated CRSP model calculated that about 9% of the smaller rocks would roll to the pit floor.

Rollout distances calculated by the CRSP models slightly exceeded those observed in the testing. This is appropriate, since actual samples population from the rock rolling test was significantly less than the 1,000 trial calculations used in the CRSP models, and thus is biased toward conservatism.

Table 2 presents the calibration parameters derived from the rock rolling tests, and compares them to the presumptive values selected from the CRSP (2000) manual. Most values changed only a small degree from presumptive estimates, and some did not change at all.

However, CRSP can be highly sensitive to small changes in parameter values. An example is that estimated rollout distances were dramatically sensitive to the assumptions for tangential and normal coefficients. In addition actual rollout distances were found to be less than predicted using presumptive values.

CONCLUSION

By utilizing the values obtained from the actual field testing, we believe that inappropriate conservatism was removed from the mitigation design process. Note that this particular finding is site specific and should not be blindly applied at other sites! In the absence of site-specific data, we would still tend to rely on judgment-tempered application of the presumptive values. Conservatism must be accepted when a design is based on non-site-specific, assumed parameters. Hence, where a project can significantly benefit from a more refined design basis, such as a large capital project or where potential risk justifies the additional effort and expense, field testing to obtain site-

specific modeling parameters is highly recommended. In the case of MYSRL's San Jose reservoir, field calibration of the CRSP model has proven to be an effective means for optimizing the crest design, therefore project economics. It has also resulted in mitigating long term risk of rockfall from the large pit slopes above the reservoir crest such that rockfall is not expected to have an adverse impact on the reservoir's lining system, and therefore benefits the design by ensuring the lining system's storage effectiveness.

TABLE 2: COMPARISON OF ROCK ROLLING TEST PARAMETERS TO PRESUMPTIVE VALUES

CALIBRATED VALUES DERIVED FROM ROCK ROLLING TEST

Parameter	Rock faces and clear bench surfaces	Debris cones in finer materials (granular silica, argillic rock, and shattered silica of the West Wall)	Debris cones from structural failures (all other rock types)	Compacted fill surfaces (reservoir dike)
Slope Roughness (for rock sizes of 0.6 and 0.8m, SR=0.4 used for 2m rocks)	**0.2**	0.1	**0.2**	0.2
Tangential Coefficient	0.9	0.75	0.9	**0.8**
Normal Coefficient	0.3	**0.2**	0.3	**0.6**

Note: Bold Values differ from presumptive values shown below.

PRESUMPTIVE VALUES FROM CRSP (2000) MANUAL

Parameter	Rock faces and clear bench surfaces	Debris cones in finer materials (granular silica, argillic rock, and shattered silica of the West Wall)	Debris cones from structural failures (all other rock types)	Compacted fill surfaces (reservoir dike)
Slope Roughness (for rock sizes of 0.6 and 0.8m, SR=0.4 used for 2m rocks)	**0.3**	0.1	**0.3**	0.2
Tangential Coefficient	**0.9**	0.75	0.9	**0.9**
Normal Coefficient	**0.3**	**0.17**	0.3	**0.8**

Note: Bold values differ from calibrated values shown above.

REFERENCES

Colorado Geological Survey. Colorado Rockfall Simulation Program (CRSP), Version 4.0. March 2000.

Golder Associates Ltd. Letter report: Review Visit – September 1997. October 30, 1997.

Golder Assosciates, Ltd. Pit Slope Design Review for Yanacocha Norte Pit. January 2001.

Golder Associates, Inc. Project files for Minera Yanacocha, 1998, 1999, 2000.

Minera Yanacocha S.R.L., Mine Engineering. Memo: Wedge Failure, San Jose Northeast Wall. December 6, 2000.

Zamora, Percy, MYSRL Mine Geologist. Personal conversations and review of work in progress regarding geology at San Jose Pit. November, 2005.

British Columbia Provincial Highway Tsunami Hazard Evaluation

Donald R. Lister, M.Sc., P.Eng.
Golder Associates Ltd., 2640 Douglas Street, Victoria, BC, Canada, V8T 4M1, 250-881-7372
dlister@golder.com

Rowland J. Atkins, M.Sc., P.Geo.
Golder Associates Ltd., 2640 Douglas Street, Victoria, BC, Canada, V8T 4M1, 250-881-7372
ratkins@golder.com

Jason McNamee, B.Sc.
Golder Associates Ltd., 2640 Douglas Street, Victoria, BC, Canada, V8T 4M1, 250-881-7372
jmcnamee@golder.com

Rob Buchanan, P.Eng.
British Columbia Ministry of Transportation, Geotechnical Materials & Pavement Engineering Section
P.O. Box 9850, Stn. Prov. Govt., BC, V8W 9T5, Canada, (250) 387-7702
now with Golder Associates Ltd.
2640 Douglas Street, Victoria, BC, Canada, V8T 4M1, 250-881-7372
rbuchanan@golder.com

ABSTRACT

How do you evaluate the potential hazard that a Tsunami represents to a highway network? Video footage of the effects of the 2004 earthquake in Indonesia brought into sharp focus the fact that cars on coastal roads essentially became entrained as bedload as the Tsunami wave surged ashore. In addition, the volume of graphic imagery collected resulted in the focusing of public attention on the hazards associated with Tsunamis and the need to identify the potential for exposure to tsunami impacts. As a result of this heightened awareness of the effects of Tsunamis, the BC Ministry of Transportation required an evaluation of Tsunami hazard for the Provincial Highway network.

A simple analytical model to assess Tsunami hazard was developed for the British Columbia coast. The analytical model includes consideration of potential Tsunami wave height, wave run-up height at the shoreline and the slope of the coastal terrain. The analytical model was applied to those segments of the highway system managed by the Provincial Government. The analytical model enabled highway segments to be classified for exposure to potential Tsunami hazard. Segments of highway on Vancouver Island and the Queen Charlotte Islands were field inspected to calibrate the analytical model predictions. Although the results are preliminary, the analytical model provides a step forward in assessing Tsunami hazard related to highways.

INTRODUCTION

The large magnitude earthquake which occurred near Bande Aceh, Indonesia on December 26, 2004 resulted in a tsunami which caused widespread damage around the margins of the Indian Ocean. The tsunami from the Bande Aceh earthquake propagated across the Indian Ocean within hours and caused terrible and tragic destruction to coastal communities and infrastructure and resulted in a large loss of life.

Unlike many historic tsunami events, the tsunami impacted coastal areas frequented by tourists from western countries. Many of these tourists were able, through modern capabilities in recording technology such as digital cameras, camcorders and video-phones, to capture graphic, live footage of the tsunami making landfall. Video footage collected included images of large, 20-25 m (50-75 ft) high breaking waves rushing inland through built up areas uprooting trees and smashing buildings, rapidly and steadily rising sea surface elevations overwhelming and inundating coastal communities, and surging flows of debris and water moving inland along roadways entraining vehicles and people (ref. 1). Following the abatement of the tsunami, photographic and video images from the aftermath showed bridges, roads and other structures completely wiped from the face of the earth. These images,

broadcast round the world by the news media, focused world attention on the hazards associated with living on coastal margins subject to tsunami events.

As a consequence of the images broadcast from around the Indian Ocean, many coastal communities and governments around the Pacific Ocean wanted to know the extent of their exposure to the effects of a tsunami. Large tsunamis have occurred within historic memory in the Pacific Ocean (ref. 2). They have also occurred within living memory but not with the same destructive impact as the Indonesian earthquake. The Alaska quake in 1964 generated a tsunami which impacted the coastal community of Port Alberni on the west coast of British Columbia, Canada. "Could a similar impact happen here?" was a common question (ref. 3).

In response to the heightened awareness of the effects of a tsunami, the British Columbia Ministry of Transportation undertook an evaluation of the Provincial Highway network. The scope of the project was to assess the exposure of the Provincial Highway network to impacts from tsunamis. The principal objective of the project was to identify those segments of Provincial Highways which could be considered susceptible to impacts from tsunamis. The data collected by the project could be used to enable consideration of tsunami impacts in road design and engineering for those areas deemed vulnerable and as input into disaster response scenarios to highlight road sections which could likely be impassable and the identification of those segments to be avoided in the event of a major earthquake of at least Magnitude 7 on the Richter Earthquake Magnitude Scale (M_R).

The project included evaluation of existing modeled wave heights for tsunamis for the British Columbia coast, assessment of tsunami wave run-up heights and distances in coastal areas and mapping of areas susceptible to tsunami impacts.

TSUNAMI GENERATION AND CHARACTERISTICS

Unlike common or ordinary waves which are generated by wind blowing over the ocean surface, a tsunami is a wave generated by the displacement of rock or sediment on the sea floor (refs. 4,5) or by the introduction of landslide material into the water (ref. 6). The displacement of rock or sediments may be caused by a seismically (earthquake) induced rupture of the sea floor or by a seismically induced landslide on the sea floor. Similarly, seismic, volcanic or slope failure activity may generate a landslide in terrestrial environments which may reach the ocean. When the movement of rock or sediments displaces an equivalent volume of water the result is a change in the elevation of the water at the sea surface. This change in elevation generates the tsunami.

A tsunami does not typically occur as a solitary wave but typically as a group of large waves. The group of tsunamis propagates across the ocean from the source of displacement much as ripples spread across a pond when a stone is tossed into the water. In general, the larger the displacement of water, the larger the resulting tsunami. In the case of the Indonesian earthquake tsunami, the vertical rupture was very large (of the order of 10-20 m (30-60 ft) vertical displacement extending greater than 1000 km (600 miles) along the seafloor (ref. 7)) thus the tsunami was also large.

A tsunami in deep water typically has a low amplitude (of the order of tens of centimeters/tenths of feet) and a very long (of the order of 100's of km/miles) wave length. Due to the low amplitude and long wave length, tsunami waves travel very quickly. The tsunami from the Indonesian earthquake was observed by the Jason 1 satellite as it crossed the Indian Ocean. Sea surface measurements gave a deep-water wave amplitude of approximately 0.5 m (1.5 ft) and a wavelength of approximately 500 km (300 miles). The wave was determined to have a velocity of approximately 700 km/hr (440 mph). The first tsunami crossed the Indian Ocean to impact the coastline of India and Sri Lanka approximately 1.5 to 2 hours following the impacts in Indonesia and Thailand (ref. 7).

Tsunamis on the west coast of North America, including British Columbia, may potentially be generated anywhere within the Pacific Basin although historic records suggest only earthquakes in the Gulf of Alaska and around the Aleutian Islands appear able to result in a damage causing tsunami. The Cascadia Subduction Zone offshore of the BC coast has the potential to create large magnitude earthquakes (> 7 M_R) which have the potential to result in a damage causing tsunami. Numerical modeling of tsunami propagation from such a large magnitude earthquake indicates that tsunami impacts may reach the North American coast within 30 minutes of the earthquake and will propagate to the BC inner coastal regions on Juan de Fuca Strait within 1.5 hours and the Strait of Georgia within 3 hours (ref. 3).

POTENTIAL TSUNAMI IMPACTS ON THE COAST

Graphic photographic evidence from the tsunami associated with the Indonesian earthquake indicated that potential tsunami impacts to highways and infrastructure can be severe (ref. 1). Tsunamis arrive onshore in a variety of forms including breaking waves, rapidly and steadily rising water levels, and surging waves. Additionally multiple crests are typical with periods between crest of the order of hours.

Run-up, or the elevation to which tsunami waters rise onshore, may be highly variable. At least one location in Indonesia experienced run-up of the tsunami to elevations of the order of 35 m (105 ft) above mean sea level and several locations experienced inundation several kilometers inland from the shoreline.

Based on visual observations of the 2004 Indonesian earthquake and tsunami typical potential impacts to road networks include:

- Impact by entrained debris;
- Entrainment of cars and highway infrastructure by the tsunami;
- Undermining of highway embankments and sideslopes making highway unsafe;
- Washing out and erosion of highway surface, culverts, bridges, and other infrastructure, and;
- Debris litter on highway alignment.

These impacts may occur both during the onrush of the initial wave and during the drainage of the waters back to the sea.

TSUNAMI WAVE HEIGHTS – BC COAST

Modeled wave heights for tsunamis on the British Columbia coast were reviewed. These modeled tsunami wave heights assumed the occurrence of a large (> 7 M_R) earthquake near the Aleutian Islands, in the Gulf of Alaska or in the Cascadia Subduction Zone. Therefore the maximum tsunami wave heights used in this study may be considered representative of the waves generated by large (> 7 M_R) earthquakes such as may occur in the Pacific Ocean and impact the BC Coast. Inclusion of local modifications of wave height related to the magnitude and displacement of the rupture associated with the earthquake and to refraction and diffraction of the tsunami by complex bathymetry was beyond the scope of the study and not included in the analysis.

Modeled potential tsunami wave heights were compiled from published literature sources (refs. 8,9,10) and through dialogue with staff from the Pacific GeoScience Centre[2] and Simon Fraser University[3]. A compilation of available wave model results is presented in Table 1 grouped by general geographic regions on the British Columbia coast.

Table 1. Modeled Tsunami Wave Heights

Geographic Location	Height (m)	Geographic Location	Height (m)
North & Central Coast and Queen Charlotte Islands		**West Coast Vancouver Island**	
Bella Bella	2.8	Ahousat	1.1
Bella Coola *(inlet)*	2.2	Bamfield	3.5
Cape St. James	1.0	Barkley Sound *(inlet)*	5.0
Dawsons Landing	2.8	Barkley Sound (near Bamfield)	3.0
Johnstone Strait *(inlet)*	1.0	Barkley Sound (Toquart Bay) *(inlet)*	7.6
Kelsey Bay	1.0	Gold River *(inlet)*	10.8
Kincolith *(inlet)*	1.7	Holberg	3.4
Kitimat *(inlet)*	1.9	Nootka (Yuquot)	3.6

[2] Dr. Fred Stephenson, Canadian Hydrographic Services, pers comm., May-September, 2005.
[3] Dr. John Clague, Department of Earth Sciences, pers comm., May-September, 2005.

Klemtu *(inlet)*	4.3	Port Alberni *(inlet)*	8.3, 16
Namu	1.3	Port Alice *(inlet)*	9.1
Ocean Falls *(inlet)*	4.2	Port Angeles	2.25
Port Essington (Skeena River)	1.2	Quatsino Sound *(inlet)*	4 to 7
Port Hardy	1.5	Tahsis *(inlet)*	3.1
Prince Rupert (Seal Cove) *(inlet)*	2.7	Tofino	3.5
Queen Charlotte City	1.25	Winter Harbour *(inlet)*	9.6
Rennel Sound	1.25	Zeballos *(inlet)*	6.1
Rivers Inlet *(inlet)*	5.0	**Strait of Georgia**	
Stewart *(inlet)*	4.1	Burrard Inlet *(inlet)*	1.0
Tasu Sound *(inlet)*	2.4	Comox	0.5
Juan de Fuca Strait		Delta/ Richmond	0.75
Port Renfrew *(inlet)*	2.0, 2.5	Discovery Passage *(inlet)*	1.0
Sooke	2.0	Nanaimo	0.5
Victoria	2.0	Point Atkinson N. Vancouver	0.5
Bellingham (USA, Rosario Strait)	2.0	White Rock	1.0
Sidney (Haro Strait)	1.75		

Examination of Table 1 indicates that tsunami wave heights within each broad geographic region are generally higher at the heads of inlets than out on the exposed coast. Additionally, the data in Table 1 suggests that tsunami wave heights may be considered reasonably consistent across each geographic region. The scope of this study did not enable a detailed evaluation of the variability in wave heights and highly localized amplifications or reductions in wave heights. From this existing information four potential Tsunami hazard zone areas were developed for the British Columbia coast including:

- Region 1: The north and central coasts, and the Queen Charlotte Islands and Inlets;
- Region 2: The west coast of Vancouver Island and Inlets;
- Region 3: The Strait of Georgia and Inlets, and;
- Region 4: The Juan de Fuca Strait and Haro Strait and Inlets

Based on the data in Table 1, generally anticipated maximum wave heights for tsunamis generated by a large (> 7 M_R) earthquake were established for each region. These estimated maximum wave heights are presented in Table 2.

Table 2. Maximum Tsunami Wave Height Used for Hazard Evaluation

Hazard Zone Area	Maximum Wave Height	Maximum Wave Run-up Elevation
Coastal Areas not Including Fjord-like Inlets		
Region 1: North Coast and Queen Charlotte Islands	3 m (9 ft)	6 m ASL (18 ft)
Region 2: West Coast of Vancouver Island	4 m (12 ft)	8 m ASL (24 ft)
Region 3: Strait of Georgia	1 m (3 ft)	2 m ASL (6 ft)
Region 4: Juan de Fuca Strait	2.5 m (7.5 ft)	5 m ASL (15 ft)
Fjord-like Inlet Areas		
Region 1a: North Coast and Queen Charlotte Islands Inlets	6 m (18 ft)	12 m ASL (36 ft)
Region 2a: West Coast of Vancouver Island Inlets	10 m (30 ft)	20 m ASL (60 ft)
Region 3a: Strait of Georgia Inlets	2 m (6 ft)	4 m ASL (12 ft)
Region 4a: Juan de Fuca Strait Inlets	5 m (15 ft)	10 m ASL (30 ft)

HAZARD EVALUATION

To establish the hazard to Provincial Highways, estimates of anticipated maximum run-up associated with the tsunami were considered. Review of available wave run-up literature indicated that standard calculation methods to estimate wave run-up were not generally appropriate for use with tsunami events. Based on our review of available wave run-up methods, we estimated that a maximum run-up elevation equivalent to twice the maximum wave height would be suitable and provide a conservative estimate. Discussion with staff from the Pacific GeoScience Centre[4] indicated that the assumed maximum tsunami wave run–up elevations would provide a reasonable estimate. These maximum wave run-up estimates are summarized in Table 2.

Following this, the extent of low-lying land near the coast was established by querying British Columbia Terrain and Resources Inventory Mapping (TRIM) data, mapped at a scale of 1:20,000, using GIS software. The GIS analysis highlighted all Provincial Highway segments below 20 m (60 ft) elevation ASL. The elevation of 20 m (60 ft) was selected as it is generally the lowest contour elevation on TRIM maps. Coincidentally, 20 m (60 ft) ASL was also the maximum estimated wave run-up elevation derived from the assessment of modeled tsunami wave data.

Each TRIM sheet was reviewed by Golder Associates staff to determine the potential tsunami hazard impact zone for each mapsheet (Appendix IV). Potential tsunami run-up distances were calculated using trigonometry and the average nearshore slope gradient. Slope gradients were verified in the field, derived from prior knowledge of the highway system, or assigned a default value of 1 degree. Wave run-up elevations, Table 2, were divided by the tangent of the beach slope to determine wave run–up distances. Hazard impact zones were determined by measuring the map distance from the shoreline to the highway segment. If the distance was determined to be less then the calculated wave run-up distance the road segment was determined to be susceptible to tsunami impact.

The effects of friction on the wave crossing the beach and inundating the terrestrial area were ignored. Potential tsunami run–up distances may be reduced by loss of wave energy due to friction with the beach, lowland areas and roughness elements (e.g. trees, boulders, buildings). To calculate beach friction site specific information such as beach substrate, detailed lowland topography, vegetation (species and size), anthropogenic structures, type and roughness of bedrock would be required to estimate the frictional losses to the wave and corresponding reductions in run-up distance. This information was beyond the scope of this study, therefore friction was ignored in the calculations resulting in a more conservative run–up estimate.

MAPPING RESULTS

For the purposes of this study, all coastal TRIM mapsheets with segments of a Provincial Highway on them were examined for potential tsunami hazard. A total of 147 mapsheets were reviewed, consisting of approximately 1,240 km (775 miles) of Provincial Highway. Of the reviewed mapsheets, 91 TRIM mapsheets had low elevation of segments of coastal Provincial Highway below 20 m (60 ft) ASL. Provincial Highway segments on 40 of the 91 mapsheets with low elevation coastal road were evaluated to have no tsunami hazard. The remaining 51 mapsheets were evaluated to have Provincial Highway segments with susceptibility to tsunami hazard. These mapsheets included approximately 384 km (240 miles) of Provincial Highway of which only approximately 155 km (97 miles) were evaluated to be susceptible to tsunami hazard.

Examples are presented below for each of the four geographic regions. In each figure, Provincial Highway segments susceptible to impacts by tsunamis are shown in yellow. Provincial Highway segments below 20 m (60 ft) ASL which were deemed to be beyond the zone of tsunami impact are shown in red. Provincial Highway segments above 20 m (60 ft) ASL which were also deemed to be beyond the zone of tsunami impact are shown in dark grey. Terrain areas highlighted in pink are those areas assessed to be below 20 m elevation ASL based on the GIS analysis. Only in inlet areas on the West Coast of Vancouver Island are the pink-shaded areas within the tsunami impact zone. Other roads marked in the figures are not managed by the Ministry of Transportation and were not part of the study.

[4] See Footnote 2

Region 1: North & Central BC Coast and Queen Charlotte Islands

On the north and central coasts and Queen Charlotte Islands, which are generally directly exposed to the Pacific Ocean, the maximum tsunami wave height was estimated to be approximately 3 m (9 ft). The estimated maximum wave run-up elevation was 6 m (18 ft) ASL. In inlet areas, the estimated maximum tsunami wave height increases to 6 m (18 ft) while the estimated maximum wave run-up elevation increases to 12 m (36 ft).

Applying the estimated maximum run-up in non-inlet areas and assuming a ground slope of one degree, water associated with the estimated maximum tsunami wave could reach up to approximately 350 m (1,050 ft) inland. On similar slopes in inlets, water associated with the estimated maximum tsunami wave could reach up to approximately 700 m (2,100 ft) inland.

Figure 1 illustrates the typical exposure to tsunami hazard in the Queen Charlotte Islands. The Provincial Highway (Hwy. 16) approaching Masset, shown in yellow, is located in low-lying coastal areas and is subject to inundation by a tsunami at various locations. Similar hazard segments are present on the segment of Provincial Highway from Tlell towards Queen Charlotte City. The pink-shaded area is the terrain situated below 20 m (60 ft) ASL and not all of it is subject to tsunami impacts.

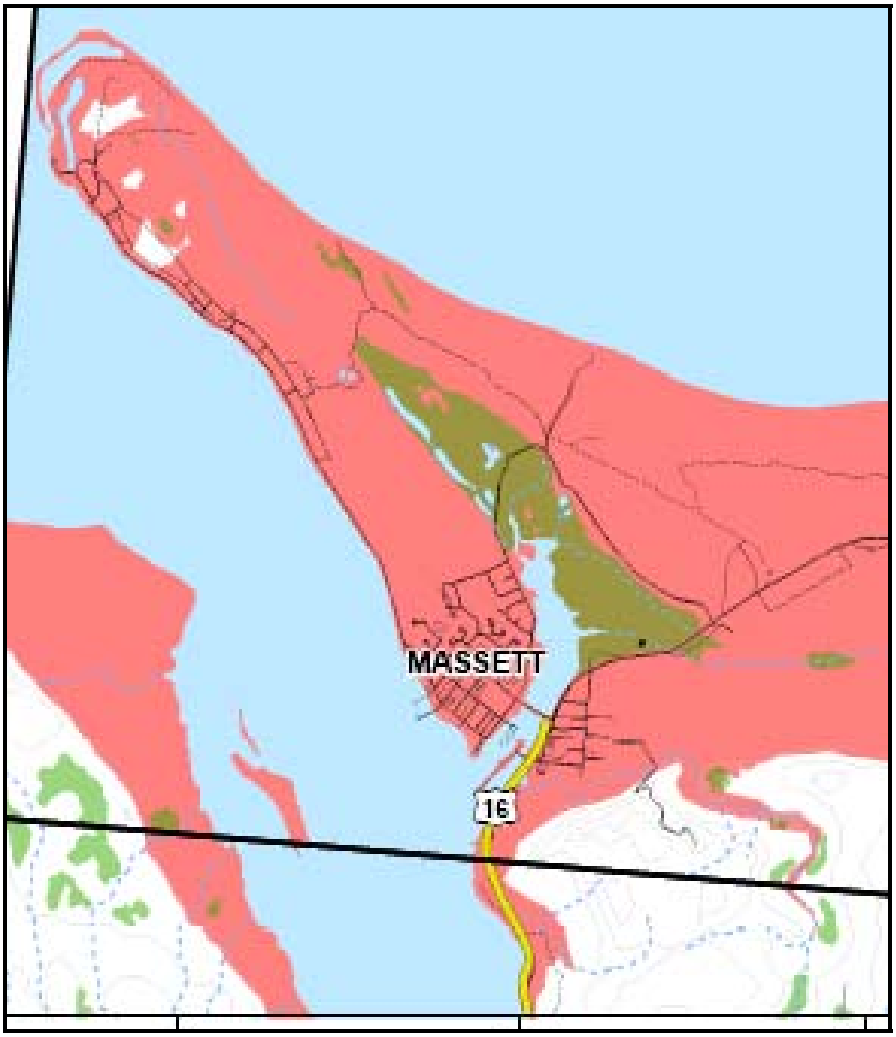

Figure 1: Provincial Highway segments susceptible to impact by tsunami from large magnitude earthquake near Masset, BC.

Region 2: West Coast of Vancouver Island

On the west coast of Vancouver Island, which is directly exposed to the Pacific Ocean, the maximum tsunami wave height was estimated to be approximately 4 m (12 ft). The estimated maximum wave run-up elevation was 8 m (24 ft) ASL. In inlet areas, the estimated maximum tsunami wave height increases to 10 m (30 ft) while the estimated maximum wave run-up elevation increases to 20 m (60 ft).

Applying the estimated maximum run-up in non-inlet areas and assuming a beach slope of one degree, water associated with the estimated maximum tsunami wave could reach approximately 460 m (1,380 ft) inland. On similar slopes in inlets, water associated with the estimated maximum tsunami wave could reach up to approximately 1,150 m (3,450 ft) inland.

Figure 2 illustrates the typical exposure to tsunami hazard on the west coast of Vancouver Island. Tsunami impacts are generally limited to a narrow band along the coast due to steep terrain with impacts reaching further inland associated with low-lying and less steeply sloped terrain. The town of Tofino is situated on a rise that is generally above the elevation or far enough inland from where a tsunami could be expected to reach. However, the coastal Provincial Highway (Hwy. 4) is susceptible to tsunami hazard to the south of Tofino. Similar low-lying Provincial Highway segments are present near Ucluelet. As can be seen by the red segment of Provincial Highway, not all of the Provincial Highway segments below 20 m (60 ft) ASL are susceptible to tsunamis.

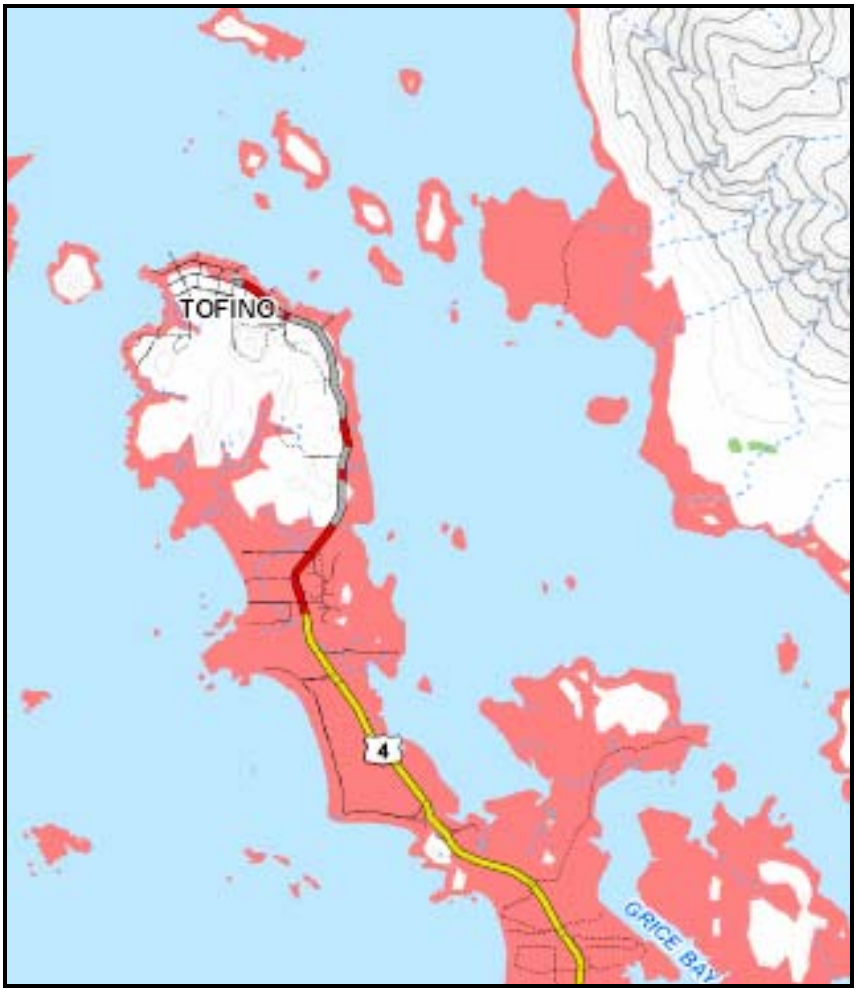

Figure 2: Provincial Highway segments susceptible to impact by tsunami from large magnitude earthquake near Tofino, BC.

Region 2a: West Coast of Vancouver Island – Inlet Area
Many inlet areas on the west coast of Vancouver Island have inlet entrances which are directly exposed to the Pacific Ocean. In these inlet areas, the maximum tsunami wave height was estimated to be 10 m (30 ft) with maximum wave run-up elevations estimated to be 20 m (60 ft). Applying the estimated maximum run-up and assuming a ground slope of one degree, water associated with the estimated maximum tsunami wave could reach up to approximately 1,150 m (3,450 ft) inland.

Figure 3 illustrates the typical exposure to tsunami hazard on an inlet on the West Coast of Vancouver Island. Port Alberni, situated at the head of a long inlet was affected by a tsunami associated with the 1964 Alaskan earthquake. The Provincial Highway (Hwy. 4) through town descends from higher ground into the valley at the head of Alberni Inlet. The segment of Provincial Highway crossing the valley is susceptible to impacts from tsunamis since the wave will be amplified in height as it traverses Alberni Inlet from the sea. Based on the estimated maximum wave run-up elevation, all land shown in pink in Figure 3 is generally exposed to tsunami hazard.

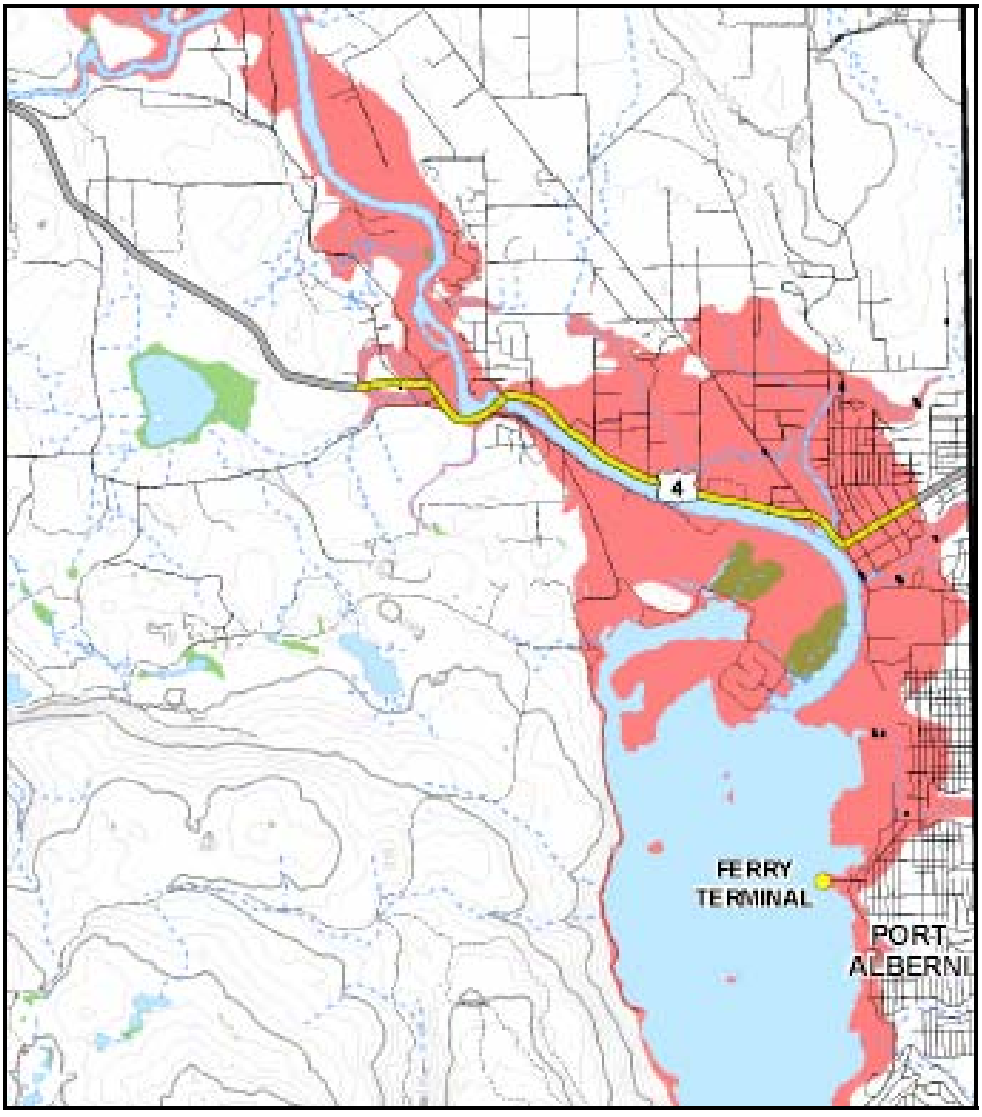

Figure 3: Provincial Highway segments susceptible to tsunami impact from large magnitude earthquake near Port Alberni, BC.

Region 3: Strait of Georgia

In the Strait of Georgia, between Vancouver Island and the southern mainland of British Columbia, the maximum tsunami wave height was estimated to be approximately 1 m (3 ft). The estimated maximum wave run-up elevation was 2 m (6 ft) ASL. In inlet areas, the estimated maximum tsunami wave height increases to 2 m (6 ft) while the estimated maximum wave run-up elevation increases to 4 m (12 ft). Unlike the North Coast of the Province (Region 1) and the West Coast of Vancouver Island (Region 2), this area is generally protected from large tsunamis by the geometry of the basin and the presence of bedrock sills at the entrances which limit the passage of large, long-period waves like tsunamis.

Applying the estimated maximum run-up in non-inlet areas and assuming a ground slope of one degree, water associated with the estimated maximum tsunami wave could reach up to approximately 120 m (360 ft) inland. On similar slopes in inlets, water associated with the estimated maximum tsunami wave could reach up to approximately 230 m (690 ft) inland.

Figure 2 illustrates the typical exposure to tsunami hazard on the Strait of Georgia. Although much of Vancouver is situated close to the shoreline, a large part of the city is not deemed to be susceptible to impact by an earthquake-generated tsunami due to the small amplitude of the tsunami and generally low elevation to which wave run-up is anticipated. In the downtown core of Vancouver (shown), the only segment of Provincial Highway susceptible to tsunami impacts is the short segment leading past Lost Lagoon on the approach to Stanley Park (top left of Figure). The presence of red segments of Provincial Highways (e.g. Hwy. 99) through Vancouver indicates that much of the city, although below 20 m (60 ft) ASL, is not susceptible to the impacts of a tsunami.

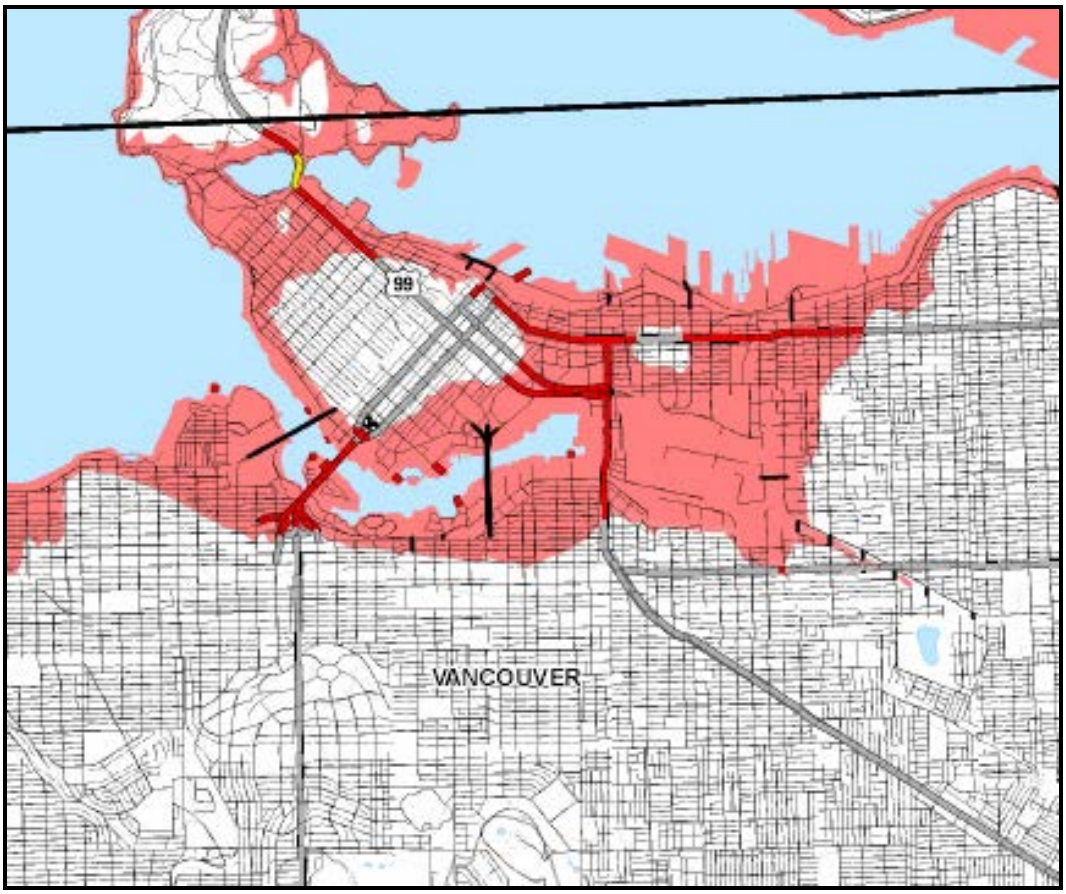

Figure 4: Provincial Highway segments susceptible to impact by tsunami from large magnitude earthquake in Vancouver, BC.

Region 4: Juan de Fuca Strait - Victoria

In Juan de Fuca Strait, on the south coast of Vancouver Island, the maximum tsunami wave height was estimated to be approximately 2.5 m (7.5 ft). The estimated maximum wave run-up elevation was 5 m (15 ft) ASL. In inlet areas, the estimated maximum tsunami wave height increases to 5 m (15 ft) while the estimated maximum wave run-up elevation increases to 10 m (30 ft).

Applying the estimated maximum run-up in non-inlet areas and assuming a ground slope of one degree, water associated with the estimated maximum tsunami wave could reach up to approximately 290 m (870 ft) inland. On similar slopes in inlets, water associated with the estimated maximum tsunami wave could reach up to approximately 580 m (1,740 ft) inland.

Figure 5 illustrates the typical exposure to tsunami hazard along Juan de Fuca Strait near the Provincial Capital of Victoria. Provincial Highway segments (e.g. Hwy. 1A) leading into the city, shown in red and dark grey, are either too far from the water (red) to be susceptible to tsunami impact or too high above sea level (dark grey). The notable exception includes the segment of Provincial Highway, shown in yellow, along the margins of Victoria Harbour near the Ferry Terminal for the Ferry to Port Angeles, WA. Coastal sections of the city around the harbour and in low lying bay areas are generally exposed to tsunami hazard. However, the presence of red-shaded Provincial Highway segments in the pink-shaded areas indicate that much of the city, although below 20 m (60 ft) ASL, is not within the zone that is generally susceptible to impact by a tsunami.

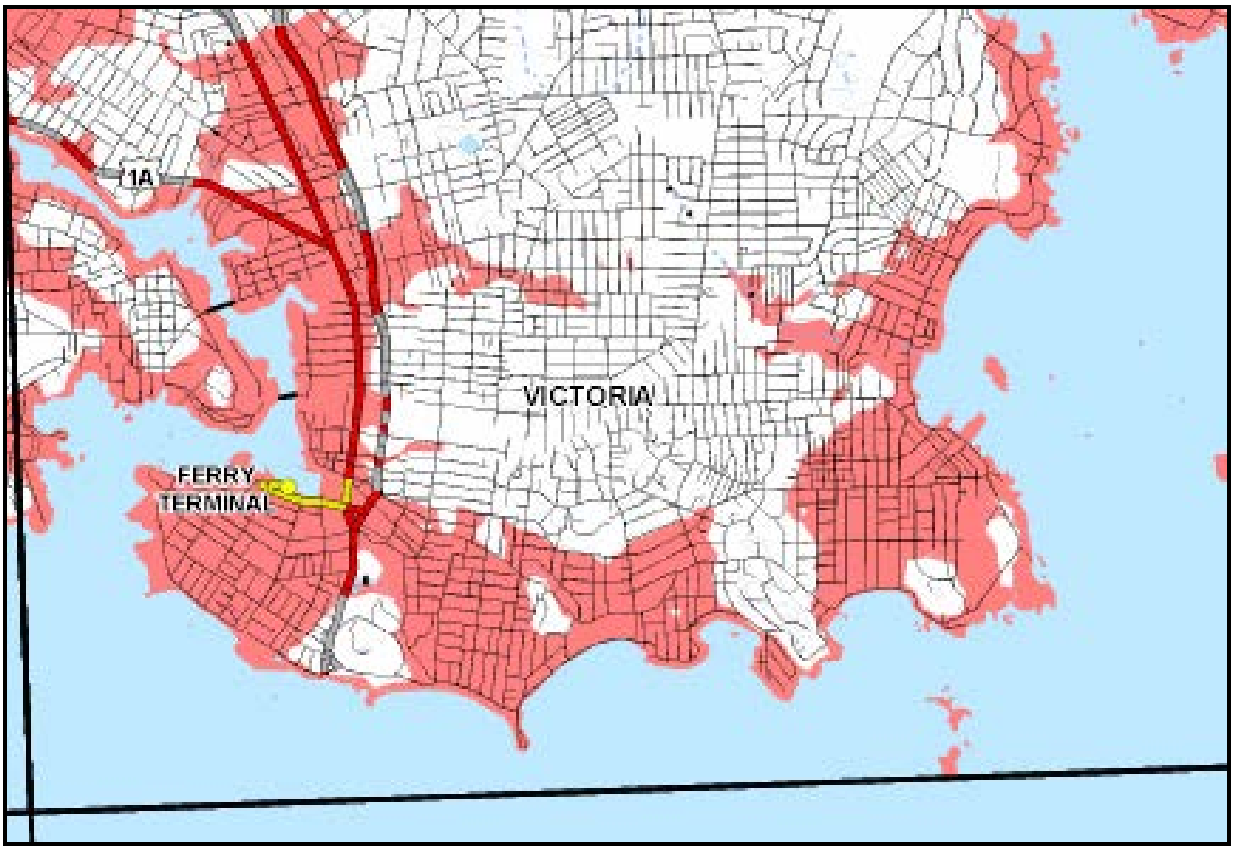

Figure 5: Provincial Highway segments susceptible to impact by tsunami from large magnitude earthquake in Victoria, BC.

CONCLUSION

The December 26, 2004 Indonesian earthquake focused world attention on the hazards of living in areas susceptible to tsunamis. In response to the heightened awareness of the effects of a tsunami, the British Columbia Ministry of Transportation undertook an evaluation of the Provincial Highway network. Preliminary tsunami hazard maps for highways were developed by evaluating modeled tsunami wave heights, estimating maximum wave heights and comparing estimated maximum wave run-up values with topographic data. This study evaluated the tsunami hazard for the Provincial Highway network in British Columbia. Approximately 1,240 km (775 miles) of Provincial Highway were reviewed and approximately 155 km (97 miles) were identified as being exposed to hazards from tsunamis associated with the occurrence of a large (> 7 M_R) earthquake in the Aleutian Islands, the Gulf of Alaska, or in the Cascadia Subduction Zone.

Hazard areas were mapped at a scale of 1:20,000 to provide a preliminary evaluation of the extent of tsunami impact susceptibility. Hazard zones were estimated based on available modeled data on tsunami wave heights, estimates of maximum wave height and maximum wave run-up, and on GIS analysis of topographic data. Additional work is required to refine the estimates of maximum wave height, maximum wave run-up and to include local variations in these key factors. This study highlights those areas where additional investigations should be focused.

ACKNOWLEDGEMENTS

The authors would like to acknowledge the Golder staff that worked on this project and assisted in the preparation of this paper and staff at the BC Ministry of Transportation who helped to guide the study.

REFERENCES

1. www.waveofdestruction.com accessed January-September 2005.

2. Satake, K., K. Wang and B. Atwater. Fault Slip and Seismic Moment of the 1700 Cascadia Earthquake Inferred from Japanese Tsunami Descriptions, *Journal of Geophysical Research*, vol. 108(7), 2003, pp. 1 – 17.

3. Clague, J. Could it Happen in BC? Implications of the South Asian Tsunami. In Innovation, Journal of the Association of Professional Engineers and Geoscientists of BC, vol 9(2), 2005, pp. 22-26.

4. Clague, J., P. Bobrowsky and I. Hutchinson. A Review of Geological Records of Large Tsunamis at Vancouver Island, British Columbia, and Implications for Hazard, *Quaternary Science Reviews*, vol. 19, 2000, pp. 849 – 863.

5. Clague, J., A. Munro, and T. Murty. Tsunami Hazard and Risk in Canada, *Natural Hazards*, vol. 28, 2003, pp. 433 – 461.

6. Bornhold, B., R. Thomson, A. Rabinovich, E. Kulikov, and I. Fine. Risk of Landslide Generated Tsunamis for the Coast of British Columbia and Alaska. In *2001 An Earth Odyssey edited by the Canadian Geotechnical Society*, 2001, pp. 1450 – 1454.

7. Wilson, M. Modeling the Sumatra-Andaman Earthquake Reveals Complex, Nonuniform Rupture. In *Physics Today*, American Institute of Physics, vol. 58(6), 2005, pp. 19-21.

8. Ng, M., P. LeBlond and T. Murty. Numerical Simulation of Tsunami Amplitudes on the Coast of British Columbia, *Science of Tsunami Hazards*, vol. 8, 1990, pp. 97 – 127.

9. Ng, M., P. LeBlond and T. Murty. Simulation of Tsunamis from Great Earthquakes on the Cascadia Subduction Zone, *Science*, vol. 250, 1991, pp. 1248 – 1251.

10. Dunbar, D., P. LeBlond and T. Murty. Maximum Tsunami Amplitudes and Associated Currents on the Coast of British Columbia, *Science of Tsunami Hazards*, vol. 7, 1989, pp. 3 – 44.

How Wide is a River? Bridge Design and Applied Geomorphology

Rowland J Atkins, M.Sc., P.Geo.
Golder Associates Ltd.
2640 Douglas Street
Victoria BC V8T 4M1
Canada
Phone: (250) 414-6414
E-mail: ratkins@golder.com

Peter W Morgan, M.Sc., P.Eng.
Golder Associates Ltd.
#202 – 2790 Gladwin Road
Abbotsford BC V2T 4S8
Canada
Phone: (604) 850-8786
Email: pmorgan@golder.com

All highways, being linear features, ultimately have to cross other linear features including rivers and streams. Typically we define the width of the channel and the volume of flow in the channel and then design a bridge to span the river. However, once we've built a span, we have defined an opening for the river through which the river must run from now on. Yet rivers are not static entities, they change and shift over geologic time such that our bridge may become an impediment to the natural form of the river and be eroded, outflanked, undermined, washed out.

All rivers have an active corridor in which river bends move and realign through erosion and deposition. This corridor is more often than not much wider than the wetted width of the river, yet functionally this active corridor is part of the river over geologic time. The active corridor or geomorphic width of the channel is generally equal to or less than the active floodplain width. Applied geomorphology enables us to identify potential future alterations in the channel alignment through erosion and deposition and alter the design accordingly so that in addition to the 200-year flood elevation we can also accommodate the 100-year or 200-year channel migration forecast. Examples from failed river crossings on the Alaska Highway are used to illustrate the lesson of why ignoring applied geomorphology is only done to our long term cost, peril and disruption of traffic.

The Role of Engineering Geology on Rehabilitation of the Likelike Highway Wilson Tunnel, Oahu, Hawaii

Victor S. Romero, PE CEG
Jacobs Associates
465 California Street, Suite 1000
San Francisco, CA 94104
Tel (415) 434-1822
Fax (415) 956-8502
romero@jacobssf.com

Clayton Mimura, PE
Geolabs, Inc.
2006 Kalihi Street
Honolulu, HI 96819
Tel (808) 841-5064
Fax (808) 847-1749
clayton@geolabs.net

ABSTRACT

One of the major highway crossings of the Koolau Mountains between Honolulu and the windward coast of Oahu, the Wilson Tunnel is comprised of one-half mile long twin tunnels, each carrying 2-lanes of traffic. Leakage into the tunnel has been persistent since construction. The recent rehabilitation consisted of remediating tunnel lining cracks and leakage, as well as improve wall finishes.

During construction of the first tunnel in 1954, full-face excavation transitioned from competent volcanic rock to extremely weathered rock and soil, which ultimately led to sinkholes and tunnel collapses that killed five construction workers. This incident is one of the more famous tunnel failure case histories, and was investigated by notable figures such as Karl Terzaghi, Ralph Peck and Donovan Jacobs. Tunnel construction was successfully completed between 1956 and 1960 using the "stacked drift" tunneling method.

Tunnel inspection and evaluation efforts began in 2002. The tunnel inspection, combined with as-built and historical information on construction and engineering geology, was the basis for evaluations of alternative rehabilitation methods. A challenging aspect of rehabilitation was that leaks through the lining were severe in the ventilation plenum where space is minimal and access difficult. A unique solution was to seal major leaks with polyurethane grout and manage the remaining leaks with a panning system and drainage improvements. The rehabilitation was successfully completed in 2005, with traffic maintained during construction.

PROJECT HISTORY AND BACKGROUND

The Wilson Tunnel consists of two tunnels along the Likelike Highway (Route 63) in the Districts of Honolulu and Koolaupoko on the Island of Oahu, Hawaii. The general location and vicinity of the project site are shown on Figure 3. Bore 1, previously named the Kalihi Tunnel, carries 2 lanes of traffic up an approximately six percent grade in the direction of Honolulu. Bore 2 is parallel and to the south of Bore 1, with a center-to-center distance of 119 feet, and carries 2 lanes of traffic down an approximately six percent grade in the opposite direction towards Kaneohe. Both tunnels are similar in length, with Bore 1 being 2,780 feet long and Bore 2 being 2,813 feet long. The western portals of both tunnels are identified as the Kalihi Portals, while both eastern portals are designated as the Kaneohe Portals. Maximum ground cover above both tunnels is approximately 870 feet, located about 2,100 feet east of the Kalihi Portals. A common ventilation shaft that is partitioned serves both tunnels and is located approximately 935 feet east of the Kalihi Portals. There is approximately 180 feet of ground cover above the tunnel at the shaft. The tunnel operates in a semi-transverse mode for ventilation. Fresh air enters the tunnels through the portals, travels through the tunnel and is drawn through ceiling air vents into the plenum and from there into the ventilation shaft and exhausted at ground level at the top of the

shaft. Water leakage near the Kalihi Portal and extending approximately 1,200 feet east into the tunnels has posed maintenance and aesthetic problems for a number of years.

Geology

The Wilson Tunnel project site is located at the upper head of Kalihi Valley along the Koolau Pali. In general, the Koolau Mountain Range and the Koolau Pali are composed of layered volcanic rocks that consist of alternating sequences of thin flows of basaltic a'a and pahoehoe lavas that were erupted from rift zone vents of the Koolau Volcano. Regionally, the bedding inclination of the lava flows dip gently seaward toward the south and southwest from the summit region of the Koolau Pali. The individual lava flows range from less than about 5 feet thick to about 30 feet in thickness.

Typically, the basalt rock grades with depth from extremely weathered and weak rock (saprolitic) near the surface to progressively less weathered and harder rock materials. The weathering gradation may occur over intervals of tens of feet to hundreds of feet in depth depending on the degree of chemical and physical decomposition the rock has experienced. The lavas of the summit of the Koolau Volcano are typically deeply weathered due to the high rainfall and extensive groundwater aquifers encompassed by the volcano.

The layered basaltic rock is considered to be very porous due to the presence of closely spaced rock joints, rubbly clinker seams, lava tubes and voids, and other irregular contacts that occur between the individual lava flow layers. Rainfall that does not runoff as stream flow percolates downward through the porous volcanic layers.

Intrusive seams of fine-grained, dense, basaltic rock, referred to as volcanic dikes, transect the layered and porous basaltic rock, which compose the mass of the Koolau Volcano. The fine-grained, dense rock character of the volcanic dikes emplaced within the surrounding porous, layered volcanic rock acts to retard the free percolation of groundwater in localized zones.

Kalihi Valley is a large erosional U-shaped valley formed by the incision of flowing streams and mass wasting (landslide collapse) of the adjacent valley walls. As a result, the valley floor has been partially filled with thick accumulations of alluvial and colluvial materials that represent the eroded and transported products of the volcanic mountain range. Since the valley filling processes occurred over very long periods of time, the deeper alluvial and colluvial materials are more weathered and are typically semi-consolidated due to burial beneath thick overburden layers of more recent alluvial and colluvial deposits. The older alluvial/colluvial materials are referred to as Quaternary Age Older Alluvium (Qa). The Qa deposits generally consist of decomposed basaltic cobbles and boulders in a tight matrix of clayey and fine sandy soil. The deposits may be so decomposed that the original rocky materials may be crushed to form finer soil constituents such as clay, silt, sand, and gravel.

The ground surfaces of the Kalihi Valley floor, especially along the existing stream drainages and other topographic depressions, may be mantled with some Recent Alluvium (Ra) of Holocene and Recent geologic time. These deposits are generally unconsolidated and consist of various eroded and transported earth materials consisting of soft/loose sediments (clays, silts, sands, and gravels) with some cobbles and boulders. The recent alluvial deposits typically mantle the older alluvial deposits and other underlying in-situ volcanic products.

Based on a review of available boring logs completed for the Bore 1 design, descriptions of materials encountered during Bore 1 excavation, and regional geologic information pertaining to the Wilson Tunnel site, it appears that the tunnels penetrate older alluvial/colluvial deposits (Qa) and some saprolitic/residual soils at the Kalihi end of the tunnels. Less weathered basalt rock associated with the Koolau Volcanic Series (Tkb) were encountered approximately midway and through the Kaneohe end of the tunnels. The saprolitic/residual soils encountered by the tunnels represent a gradational zone of extremely to completely weathered basalt rock located at the margin of the less weathered basalt rock penetrated by the bores. The saprolitic and residual soils deposits represent the in situ, deeply weathered product of the basaltic rock. Therefore, the deposits resemble soil that includes silt, sand, and decomposed rock. The existing tunnel alignment and the interpreted soil/rock profile are shown on Figure 4.

The location of the more significant cracks in the tunnel lining, groundwater leaks, and mineral deposits on the tunnel walls appear to correlate well with the segment of tunnel that was constructed within the clayey alluvial/colluvial (Qa) deposits. Severe problems were encountered with the construction of Bore 1 within the Qa and saprolitic/residual soil deposits, as described below.

Engineering Geology Reconnaissance

Prior to tunnel inspections, a general site reconnaissance was performed by a geologist to observe the existing ground surface conditions and geology in the vicinity of the tunnel portals and ventilation building located on the Kalihi side of the tunnels. The purpose of the site reconnaissance was to evaluate the existing surface conditions in an attempt to identify possible causes of the groundwater infiltration experienced within the tunnel structures. The weather conditions during the site visit were generally dry with some passing light showers. The weather conditions for the week preceding the site reconnaissance was generally normal in terms of rainfall with only light to moderate rainfall recorded at the Wilson Tunnel rain gauge.

A road provides vehicular access to the existing Wilson Tunnel ventilation building, which is located above the tunnels on the Kalihi side of the Koolau Pali. The access road crosses the main concrete diversion channel of Kalihi Stream and a concrete spur drainage diversion ditch (Spur No. 7). Much of the low gradient, sinuous topography surrounding the elevated access road appears to be related to the abandoned stream channel meanders of Kalihi Stream and other small stream tributaries that traverse the area.

The near surface soils observed between the Kalihi portals and the ventilation building consist of brown and tan colored, stiff, clayey and silty soils with embedded decomposed gravel, cobbles, and boulders that are representative of Recent Alluvium (Ra) and Older Alluvium/Colluvium (Qa) deposits. The Qa deposits were observed in slope exposures and along the existing drainage ditch sidewalls. The soils were noted to be very wet with widespread groundwater seepage emanating from steep slopes that border the existing drainages. Basalt rock was not observed at the ground surface between the Kalihi tunnel portals and the ventilation building.

The Wilson Tunnel is located in an elevated region of very high rainfall at the summit of the Koolau Pali. Average annual rainfall is on the order of about 150 to 200 inches per year. Rainfall may occur on a near daily basis, thus the ground surfaces are typically wet. The tunnels are located at the amphitheatre-shaped head of Kalihi Valley where drainage from the surrounding ridgelines and slopes is directed toward the valley axis from a multitude of tributary drainage channels and ditches. The Kalihi side of the tunnels penetrates this wet region of drainage convergence.

Based on the available tunnel construction plans, prior to the construction of the tunnel and related drainage improvements, the original (natural) Kalihi Stream alignment had established channel meanders that traversed the low gradient ground surface located above the tunnel structures. Kalihi Stream is a perennial stream that appears to have sustained flow throughout the year and is fed by spring discharges located at higher elevations. Based on the size of the source watershed and channel width, it appears that the stream may experience some very large flows during periods of heavy rainfall. As part of the tunnel construction, the natural Kalihi Stream channel was realigned and a concrete diversion channel was constructed to divert the stream flow away from the tunnels.

Based on the site reconnaissance, it appears that the original ravine topography of the abandoned Kalihi Stream channel remains in place above the tunnels. The ravine and other smaller feeding tributaries are bounded by a complex system of hillslopes and inter-stream divides. The abandoned channel and tributaries were observed to contain no flowing water; however, the ground was observed to be soft and wet with some evidence of areas that may have contained standing water. Based on the reconnaissance, it would appear that during moderate to heavy rainfall and subsequent periods of runoff that the low gradient topographic depressions associated with the abandoned stream channel and feeding tributaries may collect surface water and harbor localized areas of ponded water. This evaluation is based on the observation of some mucky bog-like conditions that were noted in several of the low topographic gradient basin areas.

Furthermore, since this area was once traversed by Kalihi Stream and other stream tributaries, it is possible that the streams have deposited Recent Alluvium (Ra) consisting of more granular soils and stream cobbles and boulders within their channel alignments. These Ra deposits (if actually present) may act as a buried permeable conduit through which ponded surface water would percolate into, rather than flow through, the low gradient basin areas. In other words, the abandoned Kalihi Stream channel and adjacent tributary channels may be introducing additional surface runoff into the subsurface in areas that are located directly above or adjacent to the tunnel alignments. In addition, other localized topographic basins and depressed areas situated above the tunnel alignment may allow ponded surface water to infiltrate into the buried more permeable Qa and Ra deposits located in the subsurface.

Based on the available construction drawings for the tunnel projects, it appears that the main channel of Kalihi Stream located above the tunnels was realigned and a concrete channel of about 14 feet in height was constructed to contain and divert the stream flow from the pre-existing natural channel. A reconnaissance of the lined diversion channel was also conducted. A slight, continuous flow of water was observed in the upper reaches of the main diversion channel. Approximately 120 feet downstream of the main channel box culvert, the stream flow was observed to flow into a gap separation in the concrete channel. It is not precisely known where the leak is located in relation to the tunnel alignment but a cursory review indicates that the channel leak may be located above the outbound tunnel alignment.

In summary, the site reconnaissance above the Kalihi portals of the Wilson Tunnel indicated:

Depressions associated with the sinkholes experienced during the construction of Bore 1 (see below), along with poorly drained remnants of the old Kalihi Stream, form areas of poor surface drainage above the tunnels.

The Access Road complicates drainage in the area.

The Kalihi Stream diversion channel parallel to the Access Road has a gap which permits flows to infiltrate into the ground.

The Kalihi Stream diversion channel has significant debris accumulation.

History of Construction

The history of the tunnels, from design through construction and operation, was considered valuable in providing insight into the present day tunnel condition. As a supplement to the inspection, this historical knowledge of the tunnel structure was also considered to be potentially valuable in the later assessment of alternatives for remediation.

Bore 1 Construction (Honolulu Bound)

Drawings for City and County of Honolulu Department of Public Works Construction Contract 26-53 constitute the design record for Bore 1. Design drawings show this bore as the "Kalihi Tunnel," which eventually became one of the two tunnels comprising the Wilson Tunnel. The record of construction for Bore 1 is based on a published article by Peck (*1*) and unpublished reports by Terzaghi (*2*), Peck (*3,4,5,6*), and Hirota (*7*), which were prepared as a result of the tunnel collapse during construction. In addition, drawing revisions for Contract 26-53 appear to document the as-built condition of Bore 1.

Construction bids for Bore 1 were received October 20, 1953, and the contract was awarded to a Joint Venture of Gibbons & Read from Salt Lake City and E.E. Black Ltd. from Honolulu. Bids were on a unit price basis, which included prices of steel tunnel support, timber lagging, and backpacking.

Tunnel excavation commenced on January 8, 1954 from the Kaneohe Portal at the eastern end in rock and was driven full face with little support. Near the end of May 1954 tunnel excavation transitioned from rock to "earth," which ranged from highly weathered rock, extremely weathered rock (saprolite), residual soil, and transported soil deposits. Full face excavation was employed with horseshoe-shaped steel sets (structural steel) on approximately 3-foot centers until difficulties were encountered in the earth (soft-ground) section. Excavation was by drill-and-blast in rock and hand-mining in earth.

As the tunnel was advanced from sound rock into weathered "earth" like conditions, progressive sloughing and spalling was experienced in the upper part of the tunnel face. In the summer of 1954, several tunnel collapses and subsequent surface sinkholes were experienced on July 10, 27 and 28, ultimately leading to a large collapse on August 14, which killed five construction workers. The largest sinkhole was recorded at the ground surface to be about 75 feet in diameter and 30 feet deep. Initial ground cover at that location was approximately 100 feet. "A continuous zone of disturbed material extended from the bottom of the tunnel to the ground surface" as noted by Peck (*1*).

Following the collapse on August 14 construction ceased while consideration was given to alternative methods of completion. Tunnel excavation restarted in February 1956 using a different approach for the excavation sequence. In principle, soft-ground tunneling techniques were implemented. This approach was distinctly different from that of classical hard-rock tunneling. Small-

sized tunnels (drifts) were used to excavate the overall tunnel in stable increments, in a method that is known as the "stacked drift." Details of execution varied, but generally proceeded as follows:

First a small exploration drift in the top heading was mined from both ends of the tunnel (collapsed section and undisturbed ground from Kalihi Portal) to facilitate drainage and to explore the geology.

Two footing drifts were then excavated and filled with concrete to form footings and part of the sidewalls.

Excavation of arch drifts then proceeded in top-down sequence to the footing drifts. The drifts were excavated in short longitudinal sections and supported by steel sets.

Tunnel concreting varied, which appears to have ranged from just concreting between steel sets initially to cast the full thickness of concrete lining as the tunnel heading advanced. Detailed records are not known.

New tunnel lining sections were designed with substantially thicker walls, and very wide footings that in the extreme were a full-width flat structural invert, and in some cases a curved structural invert. The concrete lining was completed in June 1957 and the tunnel was opened to two-way traffic in October 1958.

Initially the design included three separate lining sections which ranged in thickness from 1 foot to 1 foot-6 inches. Various invert slabs and footing widths were indicated for ground conditions ranging from "soft-ground" to rock. However, due to the extraordinary difficulties encountered during tunneling, five additional variations of the tunnel lining for "soft-ground" conditions were developed, with selection based on the conditions encountered in an 8 foot by 9 foot top drift, which was an the first exploratory drift. These variations consisted of lining thicknesses ranging from 2 foot-8 inches to 5 feet, as well as various curved invert slab and footing geometries.

Bore 2 Construction (Kaneohe Bound)

Drawings for City and County of Honolulu Department of Public Works Construction Contract 13-57 constitute the design record for Bore 2. Design drawings show this as "Wilson Tunnel 2nd Bore." Lining configurations are similar to Bore 1. Unfortunately, construction records for Bore 2 are very limited. According to Peck (*8*), the same Joint Venture that constructed Bore 1 also constructed Bore 2. Peck (*8*) also notes that Bore 2 was constructed using similar excavation and support methods as Bore 1, and that Bore 2 was completed without major incident as a result of experience gained during construction of Bore 1. The construction for Bore 2 began in 1957. In November 1960 both tunnels were opened to traffic in the present configuration.

Based upon experience with Bore 1, four separate lining sections were designed for Bore 2. These lining sections range in thickness from 1 foot-2 inches to 3 feet, with curved invert slab and footing geometries similar to Bore 1.

Work Subsequent to Construction

Since the opening of Bores 1 and 2, many remediation and upgrade projects have been performed. Based on a review of Highways Division files, at least 21 maintenance and/or improvement contracts were completed between 1958 and 1992. These various efforts ranged from routine cleaning of the tunnels to replacement of lighting, repairing cracks in the tunnel linings, ventilation equipment replacement, and various other safety improvements. In 1998, management and maintenance of the Wilson Tunnel was transferred from the City and County of Honolulu to the State of Hawaii Department of Transportation, Highways Division.

RECENT INSPECTIONS

Since the Wilson Tunnel forms a critical transportation link between Kaneohe and Honolulu, closure of the tunnels for extended periods to implement an improvement program was undesirable. However, with completion of the H-3 highway tunnels approximately 2 miles to the north in 1997, it is now be possible to close portions of the Wilson Tunnel for improvements. However, since the Wilson Tunnel is still a busy commuter corridor, even after the opening of the H-3 Tunnel, is was the goal of

the Highways Division to implement an improvements program with minimal disruption to traffic. The first phase of this improvements program was to assess the tunnel condition and gather data for rehabilitation through an inspection.

Tunnel Inspection

Prior to the main inspection, a preliminary inspection was made into the plenum of Bore 1 on June 28, 2002. The purpose of this preliminary inspection was to observe typical conditions in the tunnel and determine the best format for recording data during the detailed inspections. A "test section" was mapped in the plenum to determine the desired scale for inspection mapping and to estimate the amount of time required for the detailed mapping.

The preliminary inspection indicated a structurally sound lining but with significant leakage, mainly through shrinkage cracks or construction joints. Rebound (Schmidt) Hammer soundings and concrete cores were determined to be necessary in addition to the detailed inspection mapping. Other tests as recommended by the American Concrete Institute (*9*), such as petrographic analysis, chemical analysis, Windsor probe, pulse velocity, or other geophysical tests, were determined to be unnecessary for the tunnel evaluation.

The detailed inspections for Bore 2 were conducted between July 8 and July 11, 2002, while detailed inspections for Bore 1 were conducted between July 15 and July 18, 2002. The inspections and mapping were carried out by personnel from R. M. Towill Corporation, Geolabs, Inc., and Jacobs Associates.

The tunnels were inspected following the methodology given in the then-draft Federal Highway Administration Highway and Rail Transit Tunnel Inspection Manual (*10*) and by the American Concrete Institute (*9*). Map sheets, each showing a developed plan of 75 feet of the tunnel, were used to record inspection observations. Data recorded on the map sheets followed the classification system shown on Figure 5 and Figure 6. Each 25 foot section of tunnels was given an Overall Condition Rating per Federal Highway Administration guidelines. And example map sheet from the inspection is shown on Figure 7.

Rebound Hammer tests were performed to determine the relative hardness and approximate unconfined compressive strength of the concrete in the tunnel linings. A total of 20 locations were selected in Bore 2 and 16 locations were selected in Bore 1 to perform Rebound Hammer tests. Ten Rebound Hammer tests were performed at each test location.

A total of eight horizontal cores (4 in each tunnel) were drilled through the tunnel walls to determine the thickness and integrity of the concrete. The cores were drilled using a portable drill rig with rotary coring tools. Three-inch diameter concrete core samples were retrieved during the drilling operations and were tested to determine the compressive strength of the concrete.

Condition of Tunnel Lining

The inspected reaches of the tunnels exhibited a regular pattern of circumferential cracking in the tunnel lining – some at construction joints (also termed expansion joints) and others due to shrinkage. No significant longitudinal cracks were observed in the tunnel lining. Similar transverse cracking was observed on the underside of the plenum slab, along with limited longitudinal cracking. Fairly large areas of map cracking (also termed pattern cracking) were also recorded, but these cracks appeared to be shrinkage cracks. The numerous shrinkage cracks observed as circumferential or map cracking in the tunnel lining likely formed at an early age (i.e., during construction) and is restricted to the concrete surface and with no evidence of structural distress.

The majority of circumferential cracks in the tunnel lining showed varying amounts of water leakage with an accompanying amount of efflorescence and staining. Efflorescence was also observed along construction joints in the tunnel lining, and in some cases where no cracks were observed. On overhead surfaces, the efflorescence formed stalactites and stalagmites, with typical lengths ranging from 3 to 6 inches (Figure 8).

A limited number of minor concrete spalls, exposed reinforcement, scaling, honeycombing and hollow areas were observed in the tunnel lining and plenum slab. Spalling and scaling was approximately ½ inches deep. The exposed reinforcement was moderately corroded with some scales and flaking. Certain spalling exposed iron pipes that were heavily corroded. Extensive staining to the walls, ceiling of the tunnel and of the plenum was recorded, mainly black due to traffic soot.

The Rebound Hammer tests and Unconfined Compressive Strength test on the concrete cores indicated that the strength and quality of the concrete lining is qualitatively good. Rebound Hammer test results indicated that the approximate compressive strength of the concrete in Bores 1 and 2 is a minimum of 8,200 psi and 8,700 psi respectively, with many locations testing in excess of 10,000 psi. Testing of the lining cores (two from each tunnel) yielded similar results, with compressive strengths ranging from 6,329 psi to 8,218 psi.

It was observed that patches to some of the cracks in the lining walls and crown had been performed, but with limited success. Some cracks have opened up again and many of the joint spalls that were repaired have failed. The majority of the patch failures observed were along construction joints.

The walls of the tunnel had been painted previously, but due to the leakage and traffic soot, the walls are a dull gray color and do not reflect light very well (Figure 9). The tiled areas are generally intact with cracks in some locations.

The concrete roadway has a longitudinal construction joint down the center of the road, which was severely spalling in certain areas. Transverse cracks were also present in the roadway, some of which were spalling. Failed repairs to these spalled joints and cracks were recorded. Based on historical information, it was understood that the original pavement section consisted of asphaltic concrete underlain by portland cement concrete. Because the asphaltic concrete did not provide adequate skid resistance for vehicular traffic, the asphaltic concrete was cold-planed to expose the underlying portland cement concrete. Based on inspection observations, the roadway elevation was up to 1 inch below the existing gutter level.

The overall condition rating for Bore 2 ranged from 4 to 8, where a rating of 4 can be considered poor to fair condition and a rating of 8 can be considered excellent condition. The overall condition rating for Bore 1 ranged from 5 to 7, where a rating of 5 can be considered fair condition and a rating of 7 can be considered good condition.

Leakage

Leakage, especially into the plenum spaces, has been ongoing in the tunnels for some time. Leakage through the concrete lining in both tunnels was observed during the inspection. Leakage was typically through cracks in the lining and construction joints (Figure 10). Major leaks appeared to be from point sources near the intersection of the plenum arch and the plenum slab. It is unclear if these major leaks were through cracks or through pre-existing remedial plenum “ceiling drains” which were back flowing as a result of being connected to the weeper assemblies.

The leakage, although unsightly, did not appear to have significantly impaired the structural service condition of the tunnels. In addition, leakage occurs regardless of the tunnel lining thickness. Leakage in the soil/saprolite sections was higher than in the rock section of the tunnels. This is likely the result of geologic conditions, construction history (including the sinkholes), topography, and unfavorable surface drainage.

Extensive efflorescence and staining of the tunnel lining was observed due to the leakage. Neither the efflorescence nor the staining were rust colored, which indicates that the water is not aggressive and that minimal corrosion of reinforcing steel has occurred. Reinforcing bars encountered in the lining cores had little to no corrosion.

Prior Tunnel Drainage System & Leak Management

In certain areas, and especially in the plenum, persistent leakage through the tunnel lining has been occurring. To prevent the water leaking into the plenum space from making its way into the tunnels through the vent slots, a number of curbs, probably constructed in 1976, were installed on top of the plenum slab. The water from these areas was intended to be collected into drainpipes penetrating the plenum slab and discharging into the roadway gutter. A few of the drainpipes through the plenum slab down to the roadway were functioning, but most were damaged. Many of the curbs installed on top of the plenum slab were being overtopped due to large flows or "silting up" from soot deposits. Stalagmites near the edge of the plenum floors were also creating barriers that allowed water to pond in localized areas. In some cases, water on the plenum slab was draining through vent slots through the plenum or longitudinal cracks near the edge of the plenum slab.

The roadway drainage itself was not functioning properly since some the roadway inlets were covered with debris. In addition, cold-planning of the roadway resulted in a surface that was up to 1 inch below the gutter level. This resulted in most of the water leaking from the plenum to pond on or run down the roadway, but not necessarily into the drains.

PROPOSED IMPROVEMENTS

Remediation efforts fell into 2 categories: structural defects and leakage. The following criteria were adopted for the improvement recommendations:

Repair defects that impact the structural integrity of the tunnels.

Repair defects to arrest progressive deterioration that might ultimately affect structural integrity.

Either reduce or manage leaks to prevent lining degradation, and to improve the appearance of the tunnels to the public.

Either reduce or manage leaks to prevent flow on the roadway or drips onto passing vehicles.

A challenging aspect of rehabilitation was that leaks through the lining were most severe in the ventilation plenum where space is minimal and access difficult. It was therefore not economical to install a traditional waterproof membrane and a new inner lining without reconstructing the plenum, which would result in closing the heavily used tunnels for an extended period.

Structural/Architectural Remediation

All significant spalls were recommended for repair to avoid further rusting of the reinforcing and prevent any additional deterioration of the lining.

From a structural viewpoint the cracks in the lining do not need to be repaired since they are generally shrinkage cracks and do not affect the structural integrity of the concrete lining. However, some cracks should be repaired as part of the leakage remediation (see below).

To improve tunnel appearance and reflectivity of light, tile was extended from the portal sections to the entire length of the tunnels. Architectural wall panels were not selected to improve appearance since such panels require an installation clearance which would reduce the limited space available for the emergency safety walk.

Leakage Remediation

The recommended method for leak remediation was to use HDPE panning in combination with crack sealing (
Figure **11**). Major leaks are being sealed with polyurethane grout. Although this grouting will not completely eliminate leakage from these locations, it did reduce the overall amount of leakage. The balance of the leaks and potential leaks (as indicated by the presence of stains or efflorescence) in the plenum were either sealed with polyurethane grout or covered with panning. In areas were it is not possible to install panning due to interference with conduits, actively leaking cracks were sealed with polyurethane grout. It should be noted that this approach will not result in achieving "zero" leaks, as it is impractical to eliminate or capture and

divert all leaks from the plenum arch. In addition, leakage is sensitive to rainfall conditions, with flows fluctuating with different amounts of precipitation.

It was also recommended to direct panning discharge water into a trough along the corners of the plenum. At certain intervals in the plenum trough (6 to 8 per tunnel), water flows down through a new drain drilled through the slab. From the plenum drains water is carried in 2-inch HDPE pipes mounted on the tunnel walls in recessed pockets created by breaking out the concrete. At the safety walk, the circular wall pipes connect into flat HDPE pipes mounted in recessed pockets. The entire plenum drain/wall pipe/safety walk pipes are located such that discharge of water at the roadway gutter level is at a roadway drain inlet. In order to promote drainage into the roadway inlets, the entire road surface will be resurfaced and sloped into the inlets.

The as-built configuration of the leak remediation is shown in Figure **12**.

Surface Drainage Remediation

It appears that the existing ground surface topographic conditions may contribute to the convergence of surface runoff and potential ponding of water above the tunnels between the Kalihi tunnel portals and the ventilation building. At this location the tunnels have generally thinner overburden composed of alluvial and colluvial soils found in this region. Thus, it is believed that surface water infiltration from the myriad of stream channels and drainage ditches in the area may be passing through the alluvial and colluvial deposits to reach the tunnel structures. The position of the access road embankment may be contributing to the potential ponding of surface runoff within low gradient topography overlying the tunnel alignment. A drainage study was recommended to evaluate the stream flow and the runoff characteristics of the area. Improvements may be needed to facilitate the surface drainage of the area, reduce the occurrence of ponded water and improve the transmittal of surface water through the area.

In addition, the existing lined drainage channels above the tunnel were recommended to be cleared of accumulated earth and vegetation debris to improve the flow in the channels and reduce the possibility of channel blockage and overflow. A gap in the concrete between the wall and invert of the main Kalihi Stream diversion channel lining was recommended for repair to prevent the stream flow leakage into the subsurface. Constructing new GRP lined drainage inlets leading to the existing diversion ditches should also reduce the erosion and deposition of undesired soil and rock materials in the channels.

Maintenance

It was also recommended that the current maintenance procedures be augmented with a scheduled maintenance regimen that includes the following:

Cleaning of tunnel walls once a year with truck-mounted power brushes.

Cleaning of roadway drain inlets and laterals once a year.

Maintenance of the plenum panning system to seal any leaks around the edges of the panning; replace damaged panning sheets; clean or repair the trough in the plenum corners; and clean or repair drain pipes in the tunnel walls and safety walks.

Inspection of tunnels, similar in scope to that documented in the Inspection Report, every 2 to 5 years as recommended by Federal Highway guidelines (2002). Such inspections should also include the roadway drain system.

STATUS OF IMPROVEMENTS

A $13.8 million contract for the recommended improvements was awarded to Kiewit Pacific Co., and work commenced in March 2004. Most of the work was carried out at night, with intermittent closures of one tunnel at a time so as to minimize traffic disruptions. In August 2005, work on the Kaneohe-bound tunnel was completed 1 day ahead of schedule. Later in October 2005, work on the Honolulu-bound tunnel was complete 4 days ahead of schedule.

ACKNOWLEDGEMENTS

The authors would like to acknowledge the kind support of R.M. Towill as the prime consultant for the project, particularly Craig Luke (Project Manager) and Michael Okamoto. The authors would also like to thank the Hawaii Department of Transportation, notably Rodney Haraga (Director), Christine Yamasaki (Project Manager) and Lana Murashiges.

REFERENCES

Peck, R. B. (1981). "Weathered-rock portion of the Wilson Tunnel, Honolulu," Soft-Ground Tunneling, Failures and Displacements, Conference Proceedings, D. Reséndiz & M. Romo eds., Instituto de Ingeniería, National University of Mexico, A. A. Balkema, pp. 13-22.

Terzaghi, K. (1955). Report on the reconstruction of the caved-in section of the Wilson Tunnel, City and County of Honolulu, 26 p.

Peck, R.B. (1954). Report on Kalihi Tunnel, City and County of Honolulu, 15 p.

Peck, R.B. (1954). Report on soil conditions at Kalihi End Wilson Tunnel, City and County of Honolulu, 57 p.

Peck, R.B. (1955). Report on field observations to be carried out during the completion of the Wilson Tunnel, City and County of Honolulu, 8 p.

Peck, R.B. (1956). Supplementary report on field observations Kalihi End Wilson Tunnel, City and County of Honolulu, 4 p.

Hirota, S.O. (1954). Brief progress report on construction of Kalihi Tunnel bore from January 8 to August 15, 1954, City and County of Honolulu, 19 p.

Peck, R.B. (2002). Personal communication.

American Concrete Institute (1979). "Practices for Evaluation of Concrete in Existing Massive Structures for Service Conditions," ACI Manual of Practice, ACI 207.3R-79, pp. 207.3R-1 to 207.3R-15.

U.S. Department of Transportation, Federal Highway Administration (2002), Highway and Rail Transit Tunnel Inspection Manual, Final Draft, 98 p.

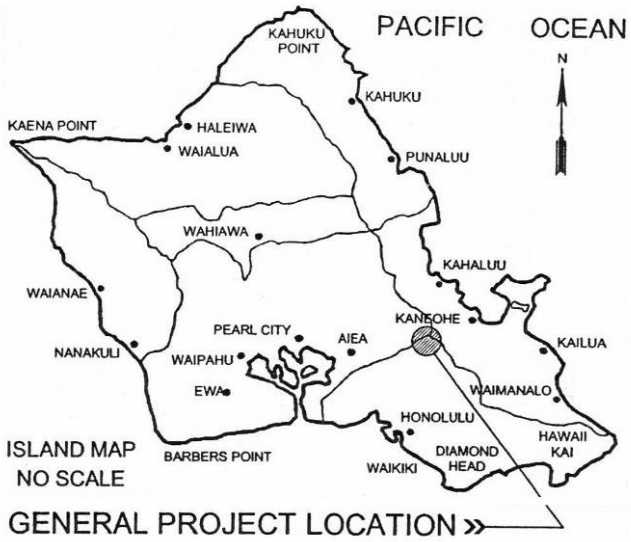

Figure 3. Project Location

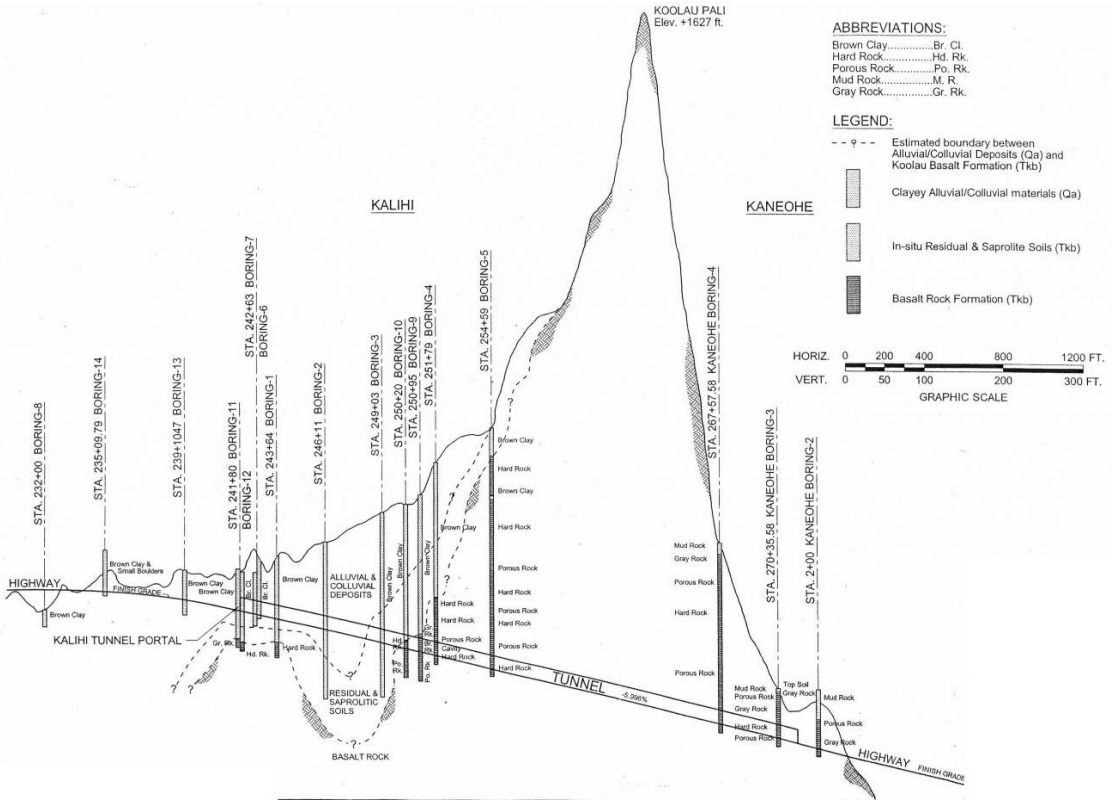

Figure 4. Geologic Profile

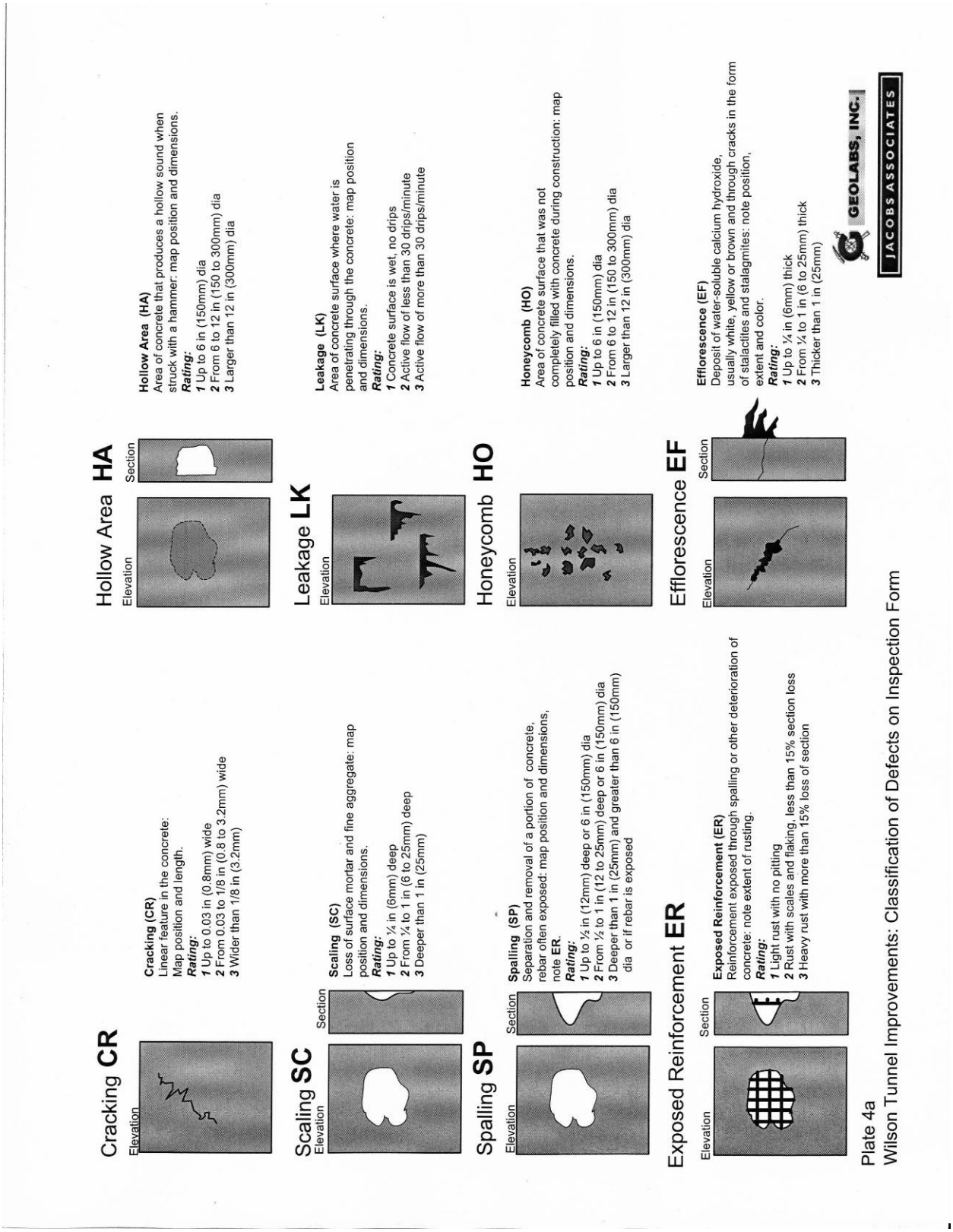

Figure 5. Inspection Classification (Page 1)

Patch Failure **PF**

Elevation Section

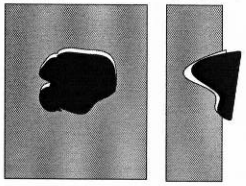

Patch Failure (PF)
Previously installed concrete patch showing signs of separation, cracking or any other distress: map position and dimensions.

Staining **ST**

Elevation

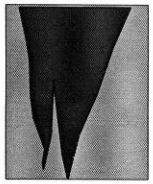

Staining (ST)
Discoloration of the concrete surface caused by dissolved materials being passed through cracks and deposited when water evaporates: map position and dimensions, note color.

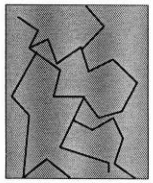

Map Cracking (MCR)

CJ Construction Joint

EJ Expansion Joint

Overall Condition Code Summary

Overall Lining Rating	Cast –in-Place Concrete
9	Newly completed construction.
8	**Excellent condition**- No defects found.
7	**Good condition**- No repairs are necessary although certain elements contain isolated minor deficiencies and minor presence of efflorescence. No delaminations or spalls are present.
6	Shading between "5" and "7".
5	**Fair condition**- Minor repairs required but element is functioning as originally designed. Concrete elements contain moderate cracks at 1.5m (5ft.) to 3m (10ft.) intervals with moderate presence of efflorescence and minor to moderate active leakage. Minor delaminations, spalls, map cracking, and staining exist on the concrete but no reinforcement steel is exposed.
4	Shading between "3" and "5".
3	**Poor condition**- Major repairs are required and element not functioning as originally designed. Concrete elements contain numerous moderate cracks with extensive efflorescence, severe leakage, and staining. Delaminations and spalls are present over 50% of the concrete surface and exposed reinforcement steel has up to 15% section loss.
2	**Serious condition**- Major repairs required to keep structure open to highway or rail transit traffic. Concrete elements contain extensive severe cracks, delaminations, spalls and leakage. Exposed reinforcement steel has up to 40% section loss.
1	**Critical condition**- Immediate closure required. Study should be performed to determine the feasibility of repairing the structure.
0	**Critical condition**- Structure is closed beyond repair.

Figure 6. Inspection Classification (Page 2)

Plate 4b
Wilson Tunnel Improvements: Classification of Defects on Inspection Form

GEOLABS, INC.
JACOBS ASSOCIATES

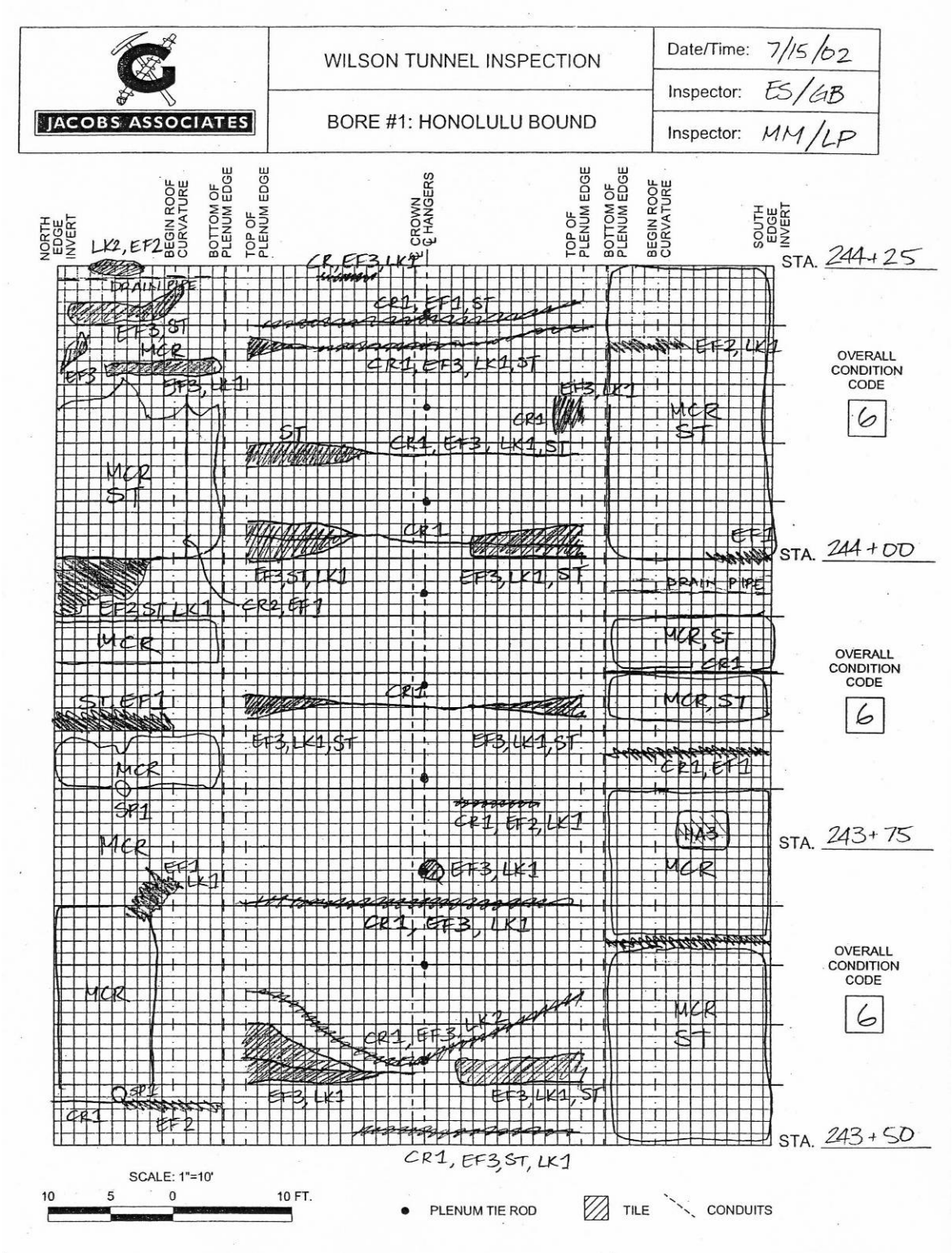

Figure 7. Tunnel Inspection Map Sheet

Figure 8. Leakage in Ventilation Plenum

Figure 9. Bore 2 Prior to Improvements

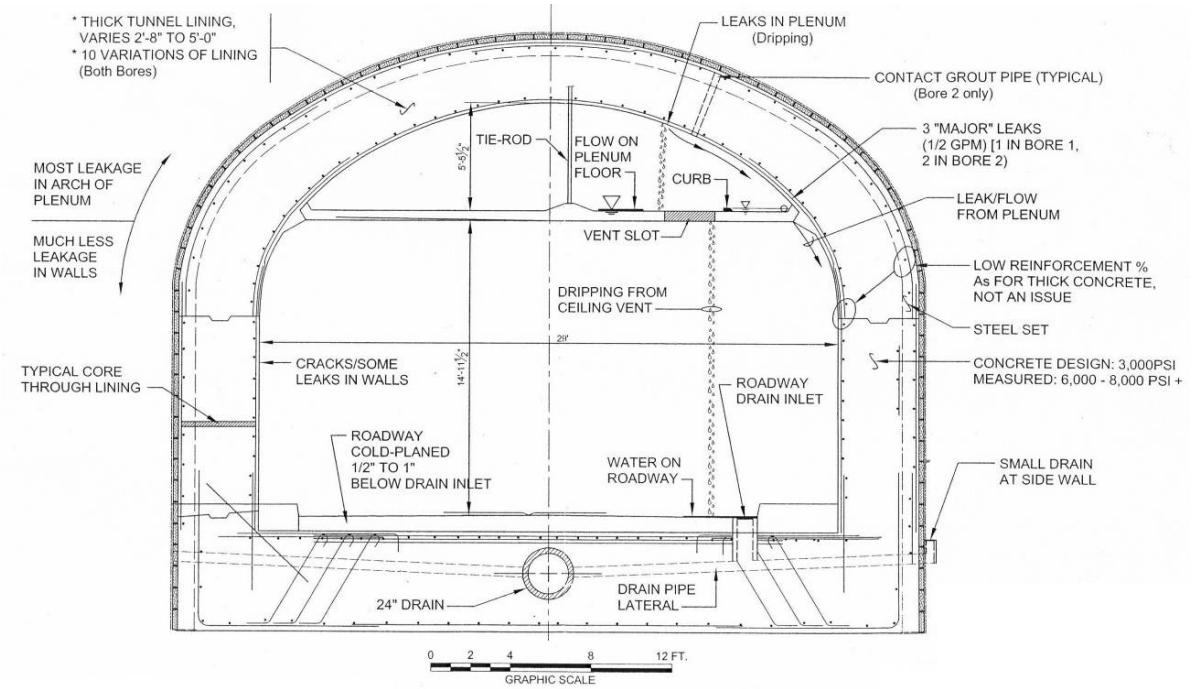

Figure 10. Summary of Tunnel Conditions Prior to Improvements

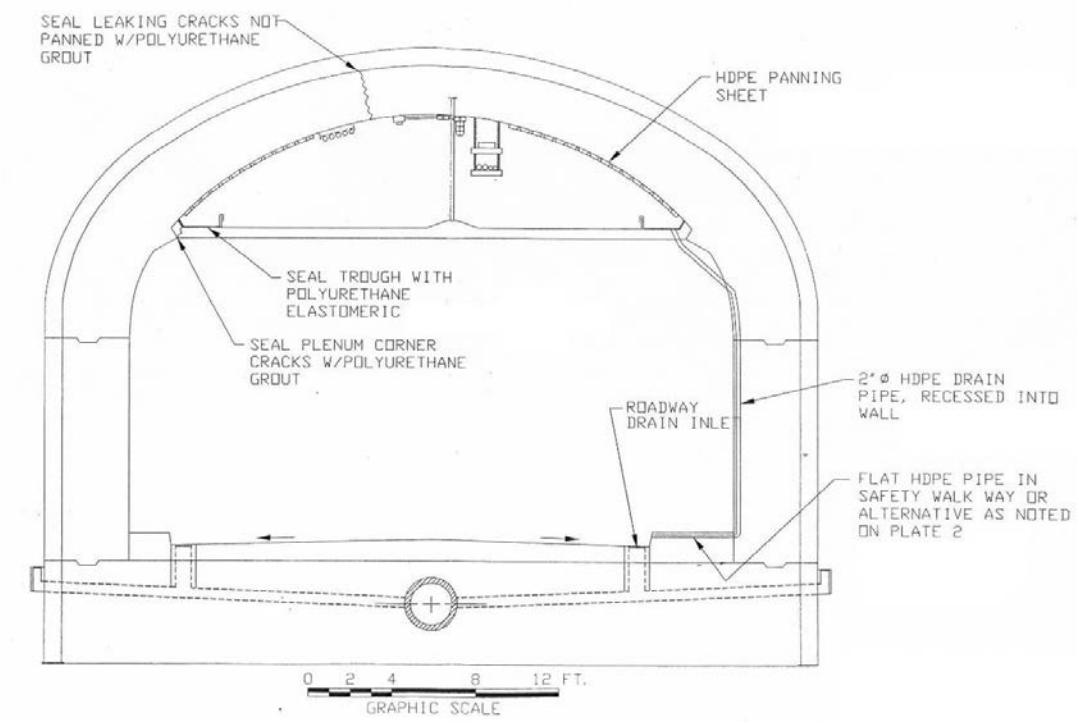

Figure 11. Schematic of Leakage Improvements

Figure 12. Completed Panning & Drainage Trough

POSTERS

The Influence of Rock Geometry on the Tangential Coefficient of Restitution in Rockfall Analysis Based on Rigid Body Impact Mechanics

Parham. **Ashayer**, *Ph.D. Candidate*
Lassonde Institute, Dept. of Civil Engineering, University of Toronto,
170 College St., Mining Building, Room 78, Toronto, Ontario, Canada, M5S 3E3
E-mail: ashayer@ecf.utoronto.ca, Phone: 416-946-0800.x16, Fax: 416-978-4820

John H. Curran, *Robert M. Smith Professor*,
University of Toronto and
Founder & Director, Rocscience Inc.
170 College St., Mining Building, Room 121, Toronto, Ontario, Canada, M5S 3E3
E-mail: john.curran@utoronto.ca, Phone: 416-946-4027, Fax: 416-978-4820

ABSTRACT

A rockfall occurs when a rock or boulder detaches from the rock mass and tumbles down a slope. Rockfalls can pose significant hazards to infrastructure such as highways, buildings, and mine open pits and, sometimes, result in personal injury or death. Prediction of rockfalls is a difficult task. Slopes that are at risk of rockfall have highly variable geometry. The location and mass of the rocks that will, eventually, become the rockfall are uncertain. The materials that make up the slope can vary considerably from one section of the slope to another and the relevant material properties are usually not well known. Performing probabilistic simulation of rockfalls, combined with a proper statistical analysis has proven to be an effective and acceptable method for dealing with these difficulties. A rockfall model is evaluated on its ability to efficiently predict the velocity, frequency, height of bounce and run-out distance of the falling rocks. Most of the existing rockfall simulators are based on particle models that consider the falling rock as an infinitesimal particle with a mass [1] [2].

In this study, a more sophisticated rigid body theory has been developed in which the movement of the falling rock consists mainly of bouncing, sliding and rolling. In this application, contact is categorised in two different modes; impact and rolling while in each mode sliding might occur. In the impact mode rigid body impact mechanics (RBIM) is utilised, in which the variations are a continuous function of the normal component of the impulse at the contact point [3, 4]. This theory results from considering that the coincident points of contact on two colliding bodies are separated by an infinitesimal deformable particle – a particle that represents local deformation around the small area of contact.

In RBIM, the falling rock can have the shape of a superellipse (including a cylinder and an ellipse) or a polygon. The impact material parameters are the energetic coefficient of restitution, ε^*, and the friction coefficient, *f*, for the rock/slope contact. Both of these parameters can be determined through laboratory experiments or by back analysis of rockfall field studies. The static friction coefficient is utilized because the dynamic friction is only slightly smaller than the static one. It is observed that ε^* depends on the impact velocity, decreasing significantly at high velocities. To model this behaviour, the nonlinear function introduced by Pfeifer [1] has been implemented. It produces the same trend as nonlinear viscoelastic damping which incorporates velocity dependence [5].

Lumped-mass models use normal and tangential coefficients of restitution to correlate the incident and outgoing velocities. RBIM shows that the outgoing velocity is also a function of falling object's geometry. Thus the tangential coefficient of restitution is not a constant but depends on the shape of the falling rock. Unlike lumped-mass models, RBIM is able to model all categories of impact response including continuous slip, continuous stick, slip-stick or slip-reversal [4]. This shape dependent behaviour can be observed in the other shape-inclusive but much more computationally intensive techniques such as discrete element methods.

It is the authors' opinion that once the robust rockfall algorithm based on rigid body impact mechanics has been thoroughly tested and verified against a wide range of field data sets, it will replace the conventional particle impact model currently used in commercial rockfall software [6, 7, 8, 9, 10].

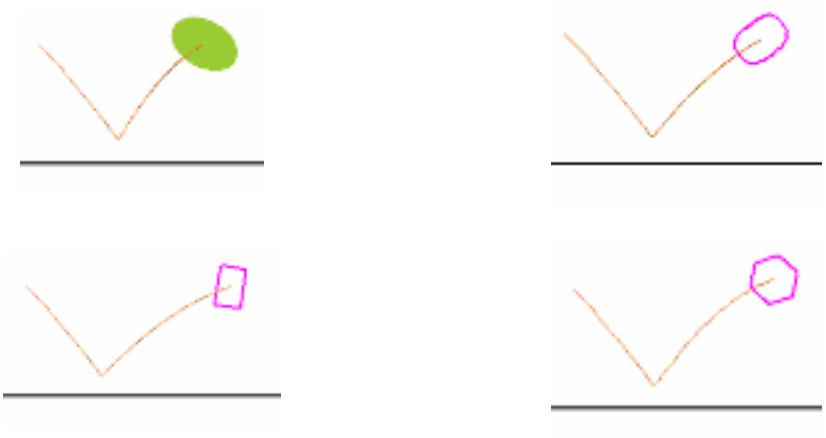

Figure-1 Impact of different types of the objects on a horizontal surface

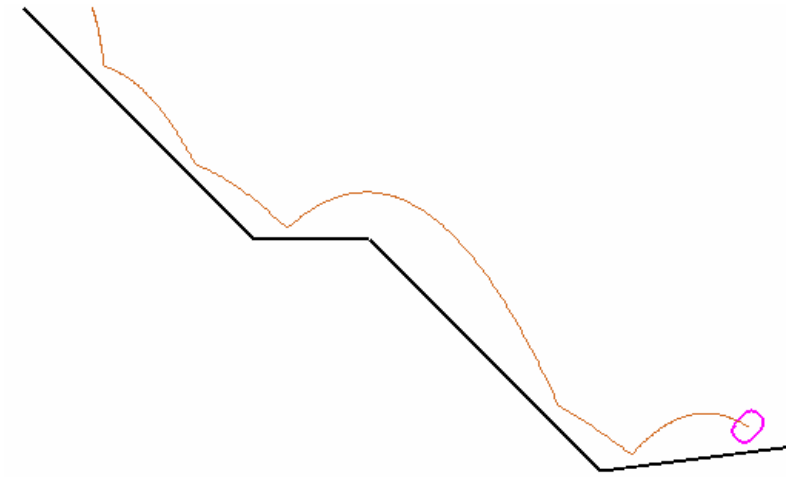

Figure-2 Motion of a super-ellipsoidal (power four) object on a slope

REFERENCES

1. Pfeiffer T.J. and T.D. Bowen, 1989. *Computer simulations of rockfalls*. Bull. Assoc. Eng. Geol. 26(1): 135-146.
2. Hoek E. 1986. *Rockfall- a program in Basic for the analysis of rockfalls from the slopes*. Golder Associates/University of Toronto, Unpublished notes.
3. Brach R.M., 1988. *Impact dynamics with applications to solid particle erosion*. Int. J. Impact Eng. 7 (1) 37-53.
4. Strong W.J., 2000, *Impact Mechanics*. Cambridge University Press.
5. Chatterjee A. 1997. *Rigid body collisions: some general considerations, new collision laws and some experimental data*, PhD Dissertation, Cornell Uni., Ithaca, NY.
6. Pierson L.A., C.F. Gullixson and R. Chassie, 2001. *Rockfall catchment area design guide – Final report*, Oregon Department of Transportation.
7. Ashayer P., Curran J., 2006. *Rockfall analysis using rigid body impact mechanics*, to be published in ARMA 2006.

8. Azzoni A., G.L. Barbera and A. Zaninetti, 1995. *Analysis and prediction of rockfalls using a mathematical model.* Int. J. Rock. Mech. Min. Sci. Geomech. Abstr. 32(7): 709-724.

9. Wu S.S. 1985. *Rockfall evaluation by computer simulation.* Transp. Res. Rec. 1031:1-5.

10. Chau, K.T., R.H.C. Wong and J.J. Wu. 2002. *Coefficient of restitution and rotational motions of rockfall impacts*. Int. J. Rock Mech. Min. Sci. 39: 69–77.

Improved p-y Curve Response Based on Strain Wedge Model Analysis

Mohamed Ashour[1], Gary Norris[2] and Sherif Elfass[3]

[1]Assistant Professor, Civil Engineering Dept, WVU Tech, Montgomery, WV 25136, Phone: (304) 442-3913 Mohamed.ashour@mail.wvu.edu
[2]Professor, Civil Engineering Dept., University of Nevada, Reno, NV 89557, Phone: (775) 784-6835, norris@unr.edu
[3]Research Assistant Professor, Civil Engineering Dept., University of Nevada, Reno, NV 89557, Phone: (775) 784-6664 elfass@unr.edu

ABSTRACT

The traditional p-y curve approach of analyzing laterally loaded pile response based on empirical curves developed from a few but well documented field tests has given the profession the confidence and desire to employ such beam-on-elastic foundation (BEF) analysis in preference to available finite element and elastic continuum solutions. Such longevity can be explained by the profession's desire to have a method that is simple and straightforward to apply and has been calibrated (albeit back-calculated) against full scale behavior over a reasonable range of response (i.e. pile head deflection). To prolong the useful life of such analysis procedure requires the development of more and more correction factors (so-called p-multipliers) to account for effects never envisioned in the original work. However, there is another BEF approach that compliments the p-y curve methodology that will provide for evaluation of such effects more logically. The strain wedge model (SWM) incorporates the nonlinear stress-strain behavior of the layered soils in combination with the nonlinear behavior of pile material at larger load, the depth dependent interaction of the developing passive wedge as it fans out and grows deeper with increasing load, the end condition of a short or intermediate length member and the vertical side shear of a larger diameter shaft. Such methodology relates the stress and lateral side shear in the soil to the line load p, the deflection pattern with depth to the horizontal strain of the soil in the developing wedge , and consequently, the BEF subgrade modulus (Es = p/y) to the Young's modulus (E= ˜ .) of the soil. This paper reviews the status of the SW model.

INTRODUCTION

The problem of a laterally loaded pile is often solved as a beam on an elastic foundation (BEF) involving nonlinear modeling of the soil-pile interaction response (p-y curve). See Fig. 1. Currently employed p-y curve models were established/back-calculated based on the results of field tests in uniform soils such as the Mustang Island (Reese et al. 1974), Sabine River (Matlock 1970) and Houston (Reese and Welch 1975) tests, and adjusted mathematically using empirical parameters to extrapolate beyond the soil's specific field test conditions. The traditional p-y curve models developed by Matlock (1970) and Reese et al. (1974) are semi-empirical models in which soil response is characterized as independent nonlinear springs (Winkler springs) at discrete locations. Therefore, the effect of a change in soil type of one layer on the response (p-y curve) of another is not considered. In addition, the formulations for these p-y curve models do not account for a change in pile properties such as pile bending stiffness, pile cross-sectional shape, pile-head fixity and pile-head embedment below the ground surface. Soil-pile interaction or p-y curve behavior is not unique but a function of both soil and pile properties. It would be prohibitively expensive to systematically evaluate all such effects through additional field tests; hence it behooves us to consider such influences based on available theoretical means (SW model formulation, Norris 1986 and Ashour et al. 1998) that allows transformation of envisioned three-dimensional soil-pile interaction response to one-dimensional BEF parameters.

EFFECT OF PILE BENDING STIFFNESS ON THE p-y CURVE

As Terzaghi (1955) and Vesic (1961) stated, the subgrade modulus, E_s (and , therefore, the p-y curve), is not just a soil but, rather, a soil-pile interaction (and, therefore, a pile property dependent) response (Figs. 1 and 2). Figure 3 shows the effect of the bending stiffness of a free-head pile on the behavior of the SW model predicted p-y curves in the loose and dense sand at a given depth of 1.22 m below ground surface. As seen, pile stiffness has a significant effect on the p-y response in the dense sand and a moderate effect on that in the loose sand. Traditional p-y's do not account for pile stiffness (EI) on the p-y curves; they are a function of soil properties and pile diameter only.

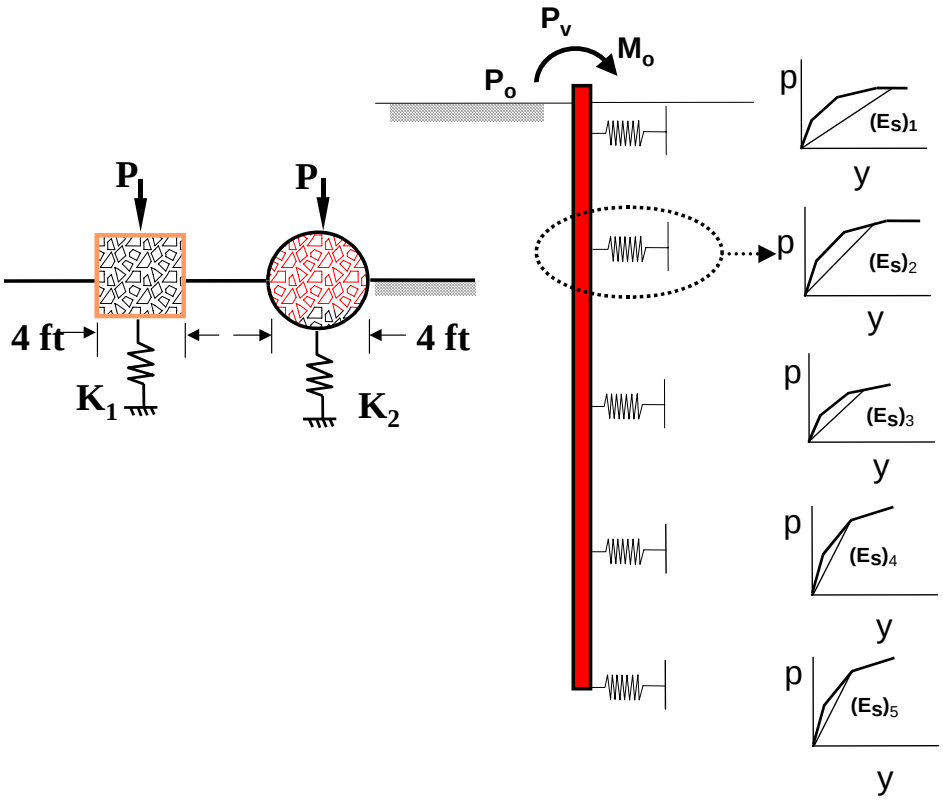

Fig. 1 One-Dimensional Beam-on- Elastic Foundation (BEF) or Winkler Springs Characterization

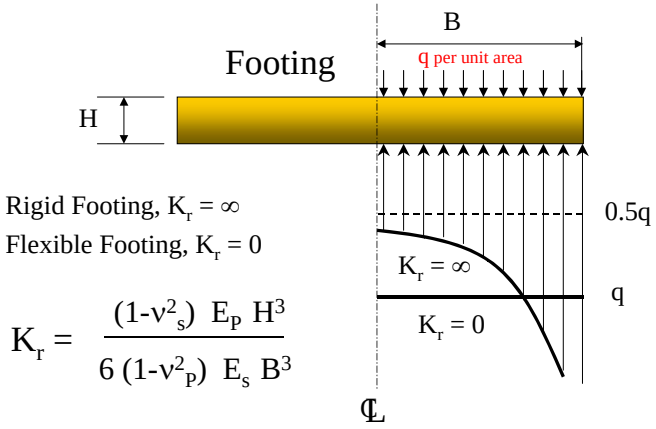

$$K_r = \frac{(1-\nu_s^2)\ E_p\ H^3}{6\ (1-\nu_p^2)\ E_s\ B^3}$$

Fig. 2 Effect Flexural Rigidity (EI) of a Footing on the Variation of the Soil Reaction (Terzaghi 1955)

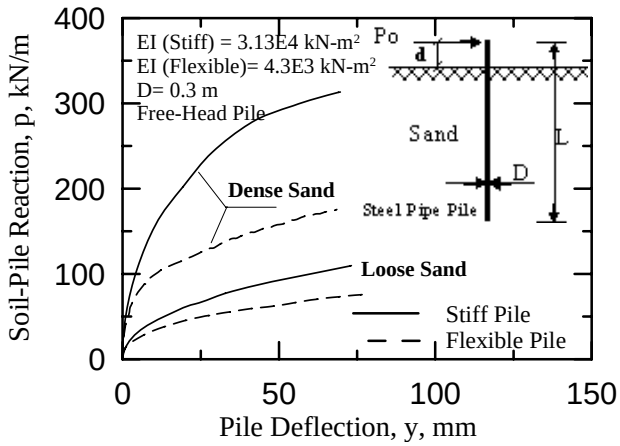

Fig. 3 Effect of Bending Stiffness (EI) of the Pile on the p-y Curve in Sand at 1.22 m Depth from SW Model Analysis

EFFECT OF PILE CROSS SECTION SHAPE ON THE p-y CURVE

The SW model considers the effect of the pile cross-sectional shape (Fig. 1) via shape factors (Briaud et al. 1984). The SW model was used to assess the p-y curves at a 1.22-m depth in sand of two reinforced concrete piles which are assumed to have the same bending stiffness. The first pile has a square cross-section of 0.305-m width, while the second pile has a circular cross-section of 0.305-m diameter. The only difference between the two piles is their cross-sectional shapes. As shown in Fig. 4, the square pile in loose and dense sand exhibits a soil-pile resistance higher than that of the circular pile. Traditional p-y's do not account for pile shape on the p-y curves; they are a function of only the pile's diameter.

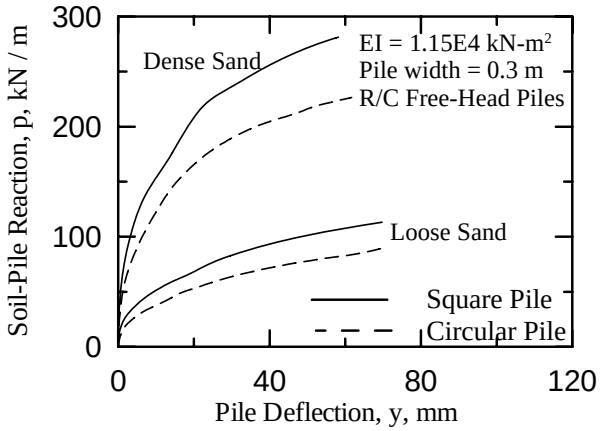

Fig. 4 Effect of Pile Cross-Section Shape on the p-y Curve at 1.22 m Depth

EFFECT OF PILE-HEAD FIXITY ON THE p-y CURVE

The effect of pile-head conditions (free or fixed-head) is one of the significant factors that determines the depth of the developing passive wedge and, therefore, the shape of the p-y curve as shown in Fig. 5 for the given soil. Note that the fixed head p-y curve in sand (Fig. 5) reaches a greater ultimate p value than that of the free head p-y curve. This is the result of the development of a larger passive wedge (due to a deeper zero deflection crossing) for the fixed head case at the same value of soil strain. As shown in Fig. 6, Kim et al. (2003) have proven experimentally the distinctive effect of the pile-head conditions on the associated p-y curve. The traditional p-y curves do not consider this effect.

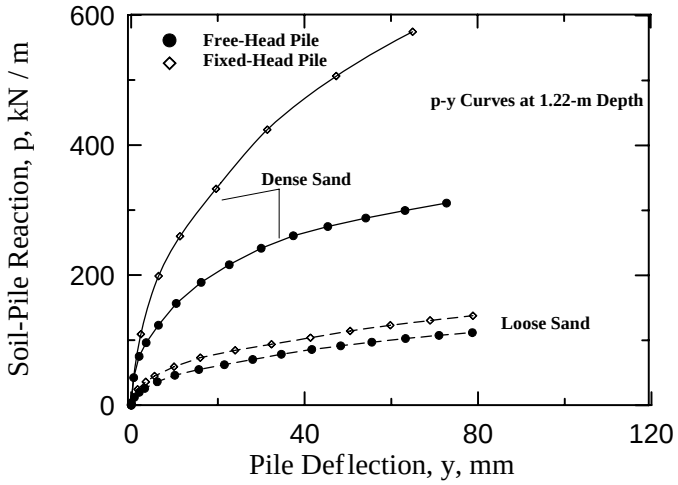

Fig. 5 Effect of Pile-Head Fixity (Fixed/Free) from the SW Model on the p-y Curve in Dense and Loose Sand at 1.22 m Depth

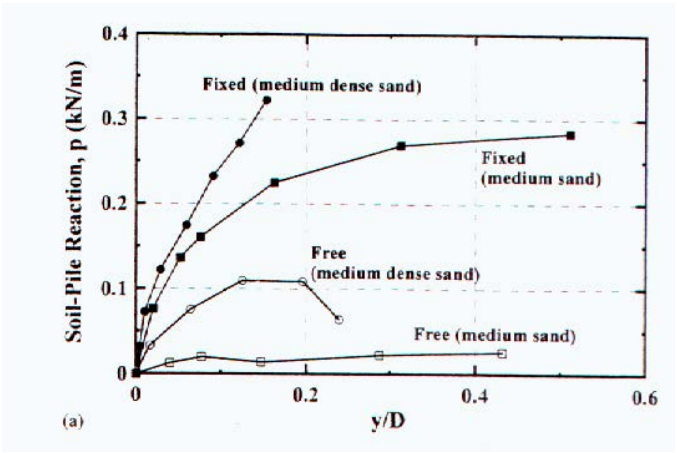

Fig. 6 Effect of Pile-Head Fixity (Fixed/Free) on the p-y Curve in Dense and Medium Dense Sand from Experiment (Kim et al. 2003)

EFFECT OF SOIL ABOVE AND BELOW ON THE p-y CURVE

Changing the soil immediately above or below the soil in which the p-y curve is sought will affect the nature of the p-y curve. Figure 7 shows the SW model predicted effect of doing just that. As seen by the insert, changing the type of the lower layer of soil (from 1.83 m down) in Fig. 7 has some effect on the p-y curve in loose sand (upper layer) at a depth of 1.22 m. The same is true for the p-y curves in a lower layer where the soil of the overlying layer is changed (not shown here). Therefore, SW model p-y curves
derived from fundamental soil behavior reflect a relation to soils on either side (above and below) of that in question (soil continuity), they are not independent Winker springs, as are traditional p-y curves that are a function of only the soil layer in question. SW model p-y curves are not unique to one soil (or, as mentioned above, independent of pile properties of EI, shape and head fixity).

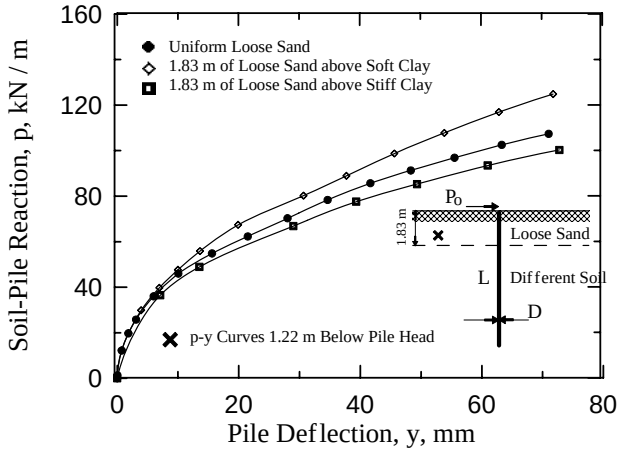

Fig. 7. Effect of Soil Continuity (Differing Layers) on the p-y Curve in Loose Sand at 1.22 m Depth

EFFECT OF PILE GROUP INTERACTIO ON THE p-y CURVE

The pile group analysis procedure commonly used today is the p-y multiplier technique (Brown et al. 1988). Such a procedure is based on reducing the stiffness of the traditional (Matlock-Reese and others) p-y curve by using a multiplier ($f_m < 1$). Brown et al. 1988 presented the overlap among the adjacent passive wedges (Fig. 8) to explain the reasoning behind the adoption of a multiplier (f_m). The value of the p-y curve multiplier is assumed based on the data collected from full-scale field tests on pile groups which are few in number (Brown et al. 1988). Consequently, a full-scale field test is strongly recommended in order to determine the value of the multiplier (f_m) appropriate for the soil profile under consideration. Moreover, the suggested value of the multiplier (f_m) is taken to be the same at all depths and over the full range of deflection (and, therefore, all levels of loading). Such characterization is pictured in Fig. 9.

As seen in Fig. 8, the overlap of the wedges among the piles in a group varies with depth, even in the same uniform soil, and will increase with the level of pile head loading as the wedges grow deeper and fan out farther (the concept behind the strain wedge model). Therefore, the use of a single multiplier that is both constant with depth and constant over the full range of load/deflection would seem to involve significant compromise.

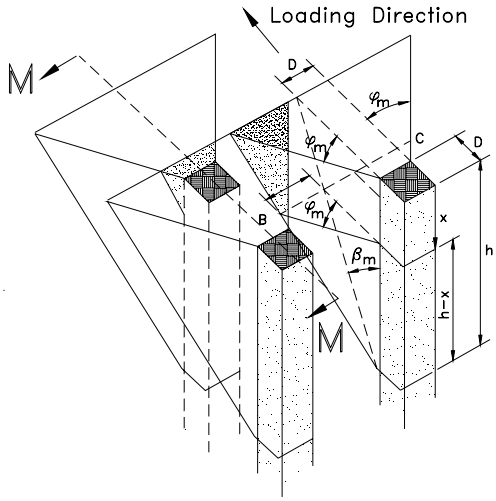

Fig. 8. Pile Group Interaction in the SW Model and as Suggested by Brown et al. (1988)

Figure 10 shows a comparison between the field data by Morrison and Reese (1986) and the results obtained using the SWM program. As seen in Fig. 10, the observed and computed responses of an average pile in the tested pile group are in good agreement. The good match of the calculated and observed behavior of the single pile carries over to the imagined average pile in the group.

Figure 10 shows the corresponding variation of the p-multiplier 0.9 m below pile head for different piles in the group constructed using SW model results. Note that the multiplier varies with both pile position (type) and level of loading beyond 1 mm deflection. Compared to the single pile, a significant reduction in the p-y curves of the various piles in the group can be observed. It should be noted that the value of the p-multiplier at a given pile head load increases with increasing depth. Figure 10 suggests that the p-multipliers derived at working load levels vary only moderately over reasonable levels of deflection. However, such working level values would significantly underestimate soil-pile resistance (p) and foundation stiffness at low deflection levels (e.g. seismic). However, such multipliers are more than just a function of pile position: they are a function of soil and pile properties, i.e. anything that influences the depth and fan angle of the wedges.

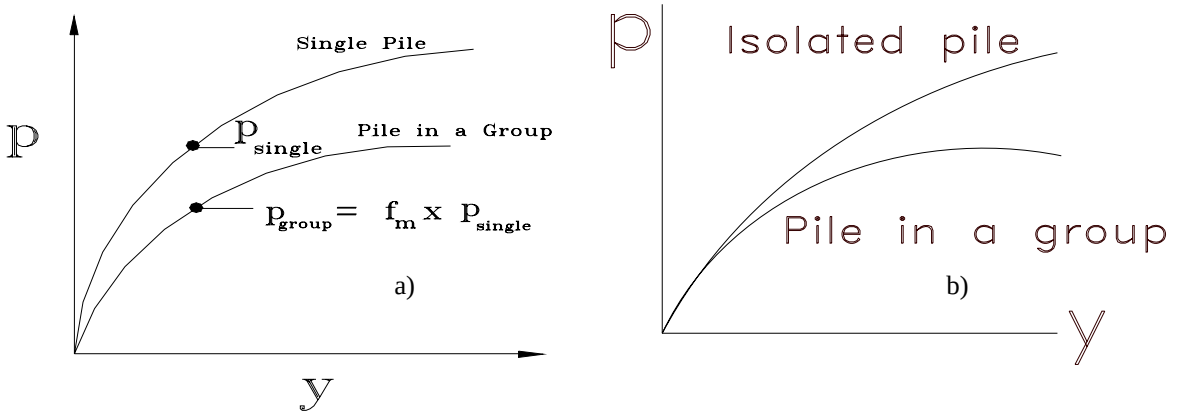

Fig. 9. Modification of the Traditional p-y Curve for Group Effect using a Multiplier (a) versus Anticipated Difference in p-y Response (b)

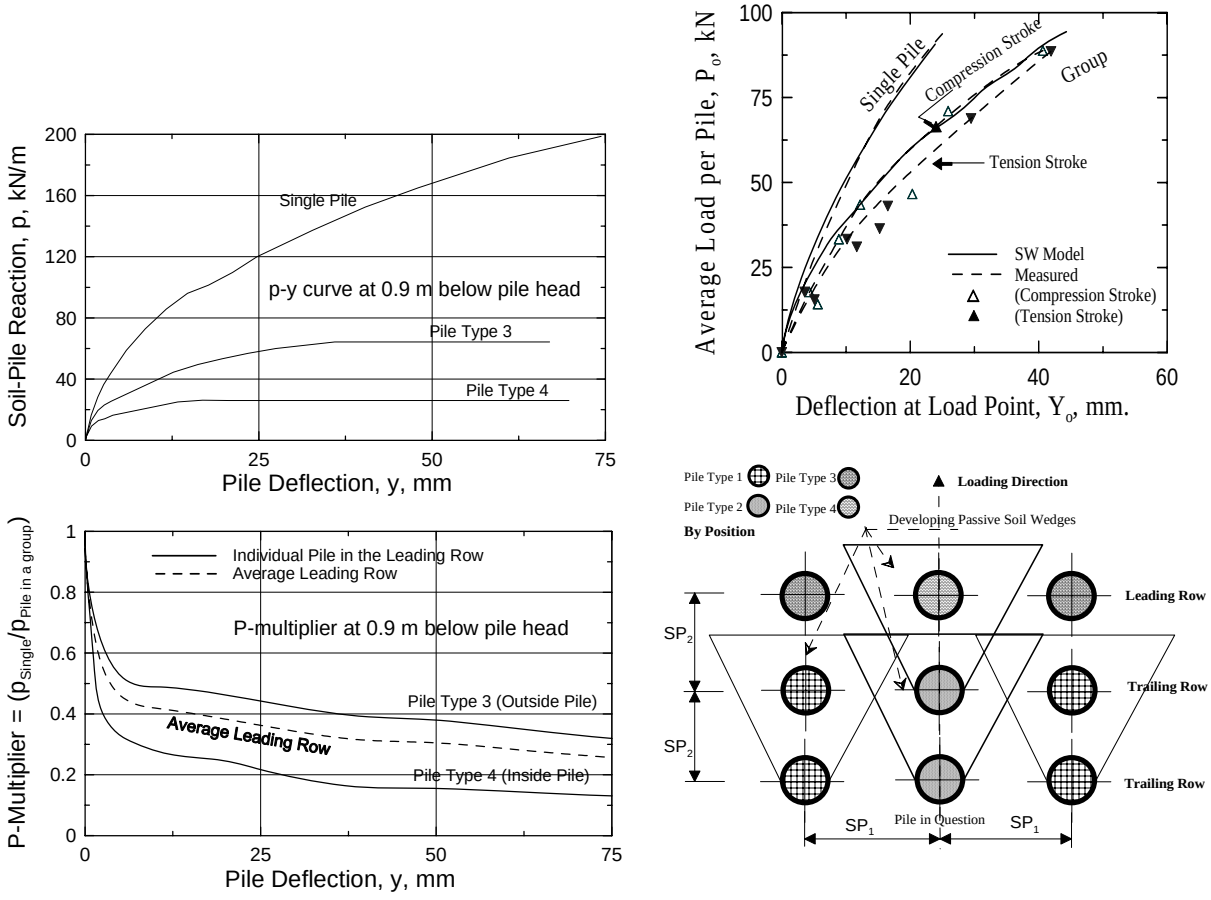

Fig.10. Variation of p-Multiplier and p-y Curves Assessed Using the SW Model at 0.9 m Depth for Piles in 3 x 3 Pile Group Tested in Sand by Morrison and Reese (1986)

EFFECT OF SOIL LIQUEFACTION ON THE p-y CURVE

Due to the shaking from an earthquake and the associated lateral load from the superstructure, excess pore water pressure in the free- and near-field develops and reduces the strength of loose to medium dense sand around a pile. In the SW model, the degradation in soil resistance and the induced excess pore water pressure in the free-field ($u_{xs,ff}$) is based on the procedures proposed by Seed et al. 1983. This requires input as to the magnitude of the earthquake to be considered as well as the peak ground surface acceleration at the site. Accordingly, a reduced vertical effective stress is evaluated along the pile length in potentially liquefiable layers. This is followed by the assessment of the additional excess pore water pressure ($u_{xs,nf}$) generated in the near-field soil region (the wedge) induced by the lateral load from the superstructure. The variation in soil resistance (i.e. the undrained stress-strain-strength behavior and stress path in susceptible layers) in this near-field zone is evaluated based on effective stress analysis using drained triaxial test results for saturated sand as demonstrated by Norris et al. (1997). The undrained behavior due to the inertial load from the superstructure is assessed based on effective stress (i.e. drained triaxial test) stress-strain formulation (Ashour and Norris 1999) that is part of the SW model software (Ashour and Norris 2003). Thus, the procedure accounts for both $u_{xs,ff}$ and $u_{xs,nf}$.

It should be noted that the aforementioned procedures incorporate the whole undrained stress-strain curve (at any level of loading, Fig. 11) not just the residual strength of the sand. The SW model analysis characterizes the reduction in subgrade modulus E_s (of the p-y curve, Fig.1) and pile response due to the drop in sand strength and Young=s modulus E as a result of developing liquefaction in associated sand layers. The full-scale load tests on the post-liquefaction lateral response of piles that were performed at Treasure Island (Weaver et al. 2005 and Rollins et al. 2005) addressed the severe limitations of provisional techniques used to correct traditional p-y curves for liquefaction (Fig. 12). Figure 13 shows a comparison between the back-calculated p-y curves from the Treasure Island test results (liquefied soil) and the predicted curves obtained using the SW model analysis (the 0.61-m-diamter CISS pile). The excellent agreement between “measured” and SW model computed pile-head load response (not shown), p-y curves (Fig. 13), and the moment, deflection and shear force distribution along the pile (not shown here) demonstrates the validity and reliability of SW model analysis.

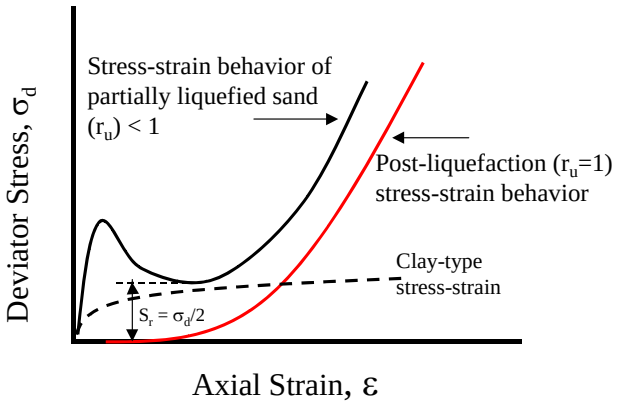

Fig. 11. Undrained Stress-Strain Behavior of Completely and Partially Liquefied

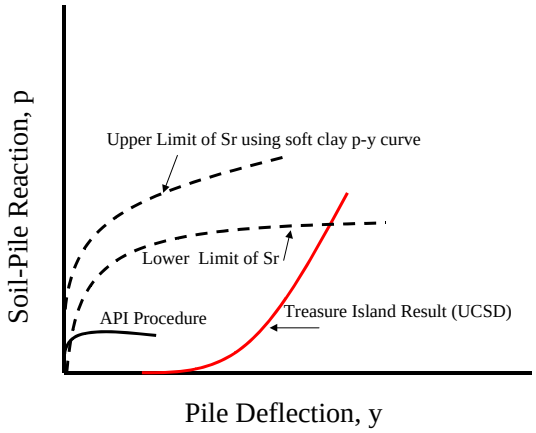

Fig. 12. Back-calculated or “Measured” p-y Curve in Fully Liquefied Soil Compared to Suggested Corrections to Traditional p-y Curves

Soil

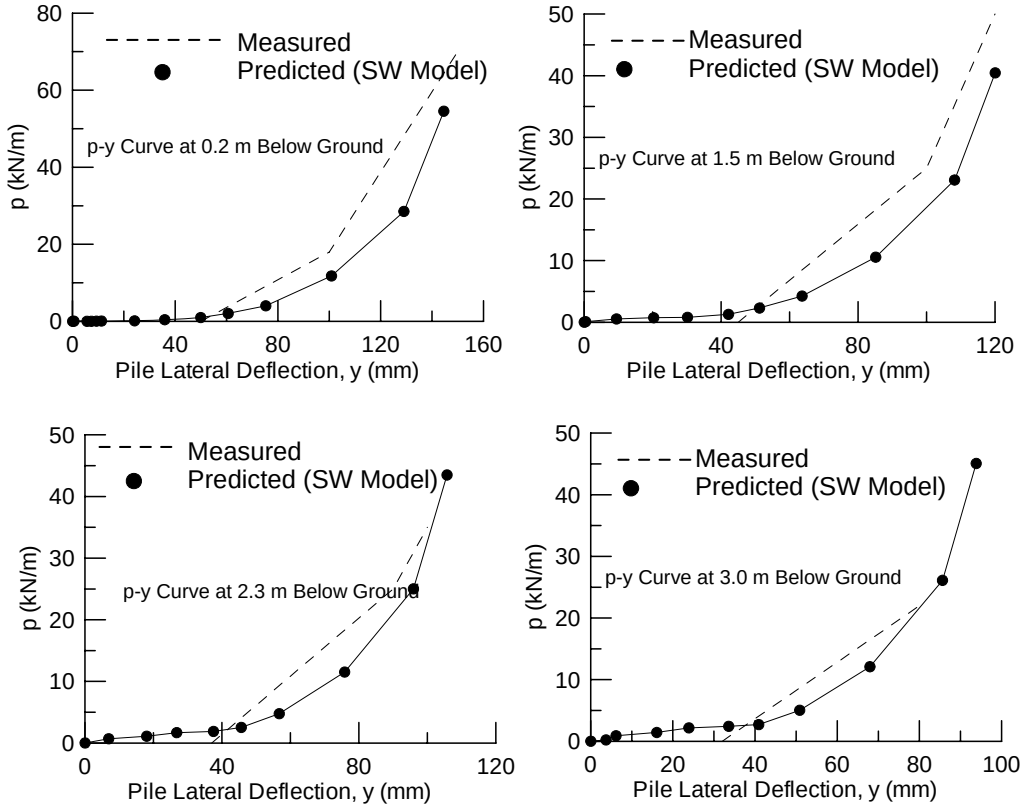

Fig. 13. SW Model p-y Curves vs. Observed (Back-Calculated) Curves from Treasure Island Test (0.61-m-CISS)

CONCLUSIONS

One-dimensional beam-on-elastic foundation (BEF) analysis for analyzing laterally loaded pile analysis is viewed by the profession as a simple and straightforward approach that is backed up by back-calculated nonlinear p-y curves from a few well-instrumented field tests for the basic soil types. It is unlikely that such an analysis technique will be supplanted by three-dimensional elastic continuum or finite element approaches which have not been calibrated against field test data. Furthermore, the input to BEF analysis requires only basic soil information. However, to prolong the useful life of such an analysis procedure, requires the development of more and more correction factors (so-called p-multipliers) to account for effects never envisioned in the original work. There are currently correction factors for group interference and liquefaction effects, but there should be more to account for a varying/changing pile bending stiffness with depth and load, head fixity (pinned or fixed), pile shape (round vs. square), the effect of layers of soil above and below that in question, bottom shear and moment contributions of short and intermediate pile lengths, and the contribution of vertical side shear to the lateral resistance of larger and larger diameter members. Unfortunately the interaction of such correction factors that are derived on the basis of only the variation of one complicating factor at a time will never be known.

There is another BEF approach that compliments the p-y curve methodology that will provide for evaluation of the above mentioned effects. The Strain Wedge (SW) model provides the means for evaluating soil-pile interaction based on such factors as pile size, shape, bending stiffness (an EI that varies with moment/curvature as a function of depth and load level, including the development of a plastic hinge), pile head fixity and group interference effects in addition to the nonlinear soil response of a layered system of soils (and hence, continuity). The effect of such variables has been demonstrated herein. The resulting p-y curves are a product of, not the input to, the SW model. The SW model approach incorporates a simplified three-dimensional analysis (Ashour et al. 1998, 2002 and 2004) that is linked to the needed one-dimensional BEF parameters (notably the nonlinear variation in the subgrade modulus) from which p-y curves can be evaluated. SW model results have been generated for comparison/validation against more than 40 case studies reported in the literature, all yielding very pleasing matches.

While the work presented herein demonstrates the need for (accompanied by the likely difficulty of) establishing corrections to the traditional p-y curves for a number of heretofore neglected effects, there are others that should be mentioned. The traditional p-y curves are for a long pile; what logical way would you account for bottom moment and bottom shear for a short or intermediate length pile in traditional analysis? That has already been incorporated in current SW model programming. Furthermore, traditional p-y curves are for piles and drilled shafts of smaller diameter; how do you account for vertical side shear acting as an equivalent backwardly applied moment at each depth as a larger diameter pile or shaft deflects/rotates under increasing pile head load? Such added resistance is not accounted for in the traditional p-y curves, but is considered in the SW model.

Most importantly, p-y curves are not unique but depend upon a number of variables a function of both the soil and pile. To continue using the current curves and apply empirically derived correction factors is a task that cannot be satisfactorily mastered. Instead, once sufficient confidence develops for the SW model, it should become the well used method of analysis. Best of all, it requires the same basic soil information that is needed for current/traditional p-y curve evaluation and the public domain program is very easy to use.

ACKNOWLEDGEMENTS

The interest and financial support of Caltrans and WSDOT in the development of the Strain Wedge model are gratefully acknowledged.

REFERENCES

1. Ashour, M. Post Liquefaction Response of Liquefied Soils. *Proc. 37th Engineering Geology and Geotechnical Engineering Symposium*, Boise, Idaho, 2002, pp. 11-26.
2. Ashour, M., G. Norris and P. Pilling. Lateral Loading of a Pile in Layered Soil Using the Strain Wedge Model. *J. of Geotech. Engg, ASCE* vol. 124 (4) 1998, pp. 303-315.
3. Ashour, M. and G. Norris. Liquefaction and Undrained Response Evaluation of Sands from Drained Formulation. *J. of Geotech. Engg, ASCE* vol. 125 (8), 1999, pp. 649-658.
4. Ashour, M., G. Norris and P. Pilling. Strain Wedge Model Capability of Analyzing Behavior of Laterally Loaded Isolated Piles, Drilled Shafts and Pile Groups. *J of Bridge Engineering, ASCE*, vol. 7 (4), 2002, pp. 245-253.
5. Ashour, M., and G. Norris. Lateral Load Pile Response in Liquefied Soil. *J of Geotechnical and Geoenvironmental Engineering, ASCE*, vol. 129 (6), 2003, pp. 404-414.
6. Ashour, M., P. Pilling and G. Norris. Lateral Behavior of Pile Groups in Layered Soil. *J of Geotechnical and Geoenvironmental Engineering, ASCE*, vol. 130 (6), 2004, pp. 580-592.
7. Briaud, J.L., T. Smith and B. Mayer. Laterally Loaded Piles and the Pressuremeter: Comparison of Existing Methods. *Laterally Loaded Deep Foundations, ASTM, STP 835*, 1984, pp. 97-111.
8. Brown, D. A., C. Morrison and L.C. Reese. Lateral Load Behavior of Pile Group in Sand. *J. of Geotechnical Engineering, ASCE*, vol. 114 (11), 1988, pp. 1261-1276.
9. Kim, B.T., N.K. Kim and W.J. Lee. Experimental Load-Transfer Curves of Laterally Loaded Pile in Nak-Dong River Sand." *J. of Geotechnical and Geoenvironmental Engineering, ASCE*, vol. 130 (4), 2003, pp. 416-425.
10. Matlock, H. Correlations for Design of Laterally Loaded Piles in Soft Clay. *Proc 2nd Annual Offshore Technology Conference*, Houston, Texas, OTC 1204, 1970, pp. 577-607.
11. Morrison, C. and L.C. Reese. *Lateral-Load Test of a Full-Scale Pile Group in Sand*. Report to US Department of Interior, Federal Highway Administration, and U. S. Army Engineer, Waterways Experiment Station, Vicksburg, Mississippi. 1986.
12. Norris, G. Theoretically Based BEF Laterally Loaded Pile Analysis. *Proc 3rd International Conference on Numerical Methods in Offshore Piling*, Nantes, France, 1986, pp. 361-386.
13. Norris, G., R. Siddharthan, Z. Zafir, and R. Madhu. Liquefaction and Residual Strength of Sands from Drained Triaxial Tests. *J. of Geotech. Engg, ASCE*, vol. 123 (3), 1997, pp. 220-228.
14. Reese, L.C., W.R. Cox and F.D. Koop. Analysis of Laterally Loaded Piles in Sand. *Proc. 6th Annual Offshore Technology Conference*, Houston, Texas, OTC 2080, 1974, pp. 473-483.
15. Reese, L.C., and R.C. Welch. Lateral Loading of Deep Foundations in Stiff Clay. *J. of Geotech. Engg, ASCE*, vol. 101 (7), 1975, pp. 633-649.

16. Rollins, K.M., T.M. Gerber, J.D. Lane and S. Ashford. Lateral Resistance of a Full-Scale Pile Group in Liquefied Sand. *J. of Geotechnical and Geoenvironmental Engineering, ASCE* , vol. 131 (1), 2005, pp. 115-125.
17. Terzaghi, K. Evaluation of Coefficients of Subgrade Reaction. *Geotechnique*, vol. 5 (4), 1955, pp. 297-326.
18. Vesic, A. (1961) "Bending of Beams Resting on Isotropic Elastic Solid. *J. Engineering Mechanics , ASCE,* vol. 87 (2), 1961, pp. 35-53.
19. Weaver, T. J., S. Ashford and K.M. Rollins Response of 0.6 m Cast-in-Steel-Shell Pile in Liquefied Soil under Lateral Loading. *J. of Geotechnical and Geoenvironmental Engineering, ASCE* , vol. 131 (1), 2005, pp. 94-102.

Laterally Loaded Pile/Shaft Response in Liquefying and Lateral Spreading Soil

Mohamed Ashour[1], Gary Norris[2] and JP Singh[3]

[1]Assistant Professor, Civil Engineering Dept, WVU Tech, Montgomery, WV 25136, Phone: (304) 442-3913
Mohamed.ashour@mail.wvu.edu
[2]Professor, Civil Engineering Dept., University of Nevada, Reno, NV 89557, Phone: (775) 784-6835, norris@unr.edu
[3]JP Singh and Associates, 23 Red Arrow Ct., Richmond, CA 94803, Phone: (510) 569-1400, JPSASSOC@aol.com

ABSTRACT

This paper provides an analysis procedure for assessing the lateral response of an isolated pile or drilled shaft in saturated sands as liquefaction and lateral soil spread develop in response to dynamic loading such as generated during earthquake shaking. The phenomenon of lateral soil spreading and its impact on deep foundations is under intense investigation via lab and field testing by a number of researchers. The analysis of piles and shafts in liquefied soils with lateral soil spread involves a number of challenging issues such as the evaluation of the driving force exerted by crust layer(s), the continuously varying mobilized strength of the liquefied soil, and the amount of lateral soil displacement developed during lateral spread. The analytical and empirical concepts employed in the Strain Wedge (SW) model technique allow for extension to handle the complex phenomenon of lateral soil spreading that could accompany or follow the occurrence of a seismic event. As a result, the p-y curve for liquefied soil with lateral spreading can be assessed based on fundamental behavior associated with basic soil and pile properties and the characteristics of the seismic event. The amount of lateral soil spread is used to provide a representative p-y curve (i.e. a realistic pile/shaft lateral response) without the need for introducing very limiting, empirical corrections.

INTRODUCTION

The procedure presented predicts the post-liquefaction behavior of laterally loaded piles and drilled shafts in sand under developing or fully liquefied conditions. Due to the shaking from the earthquake and the associated lateral load from the superstructure, the developing free-field ($u_{xs,ff}$) and near-field ($u_{xs,nf}$) excess pore water pressures reduce the strength of loose to medium dense sand around the pile. The soil is considered partially liquefied or experiencing developing liquefaction if the excess pore water pressure ratio (r_u) induced by the earthquake shaking (i.e. $u_{xs,ff}$) is less than 1, and fully liquefied if $r_u = 1$. The undrained response due to the inertial load from the superstructure can be assessed at the end of strong shaking based on the full magnitude (M) of the earthquake considered, or during shaking, by assessing a reduce magnitude in which the equivalent uniform number of cycles reflects that time in the full record at which such response is desired. (For example, an assigned M = 7 corresponds to 12 equivalent cycles into an M = 7.5 earthquake of 15 total cycles.) The resulting stress-strain response of the soil in front of the pile/shaft due to the subsequent lateral push from the pile or shaft as the result of the superstructure load (and $u_{xs,nf}$) is of the form shown in Fig. 1.

The full-scale load tests on the post-liquefaction response of isolated piles and a pile group, performed at Treasure Island (Rollins et al. 2005 and Weaver et al. 2005), are the most significant related tests with which to validate the Strain Wedge model capabilities.

The most common practice employed heretofore is that presented by Wang and Reese (1998) in which the traditional p-y curve for clay is used but modified to reflect undrained residual strength (S_r) of the liquefied sand. As seen in Fig. 2 (Seed and Harder 1990), S_r can be related to the equivalent clean sand standard penetration test (SPT) corrected blow count, $(N_1)_{60}$. However, a very large difference between values at the upper and lower limits at a particular $(N_1)_{60}$ value affects the assessment of S_r tremendously. Even if an accurate value of S_{ir} is available, S_{ir} occurs at a large value of soil strain (and, hence, pile deflection). In addition, a higher peak of undrained resistance is ignored in the case of the partially liquefied sand, while greater resistance at lower strain is attributed to the sand in the case of complete liquefaction. As seen in Fig. 1, such clay-type modeling can, therefore, be either too conservative (if $r_u < 1$) or unsafe (if $r_u = 1$). Furthermore, realistic p-y curve response reflects soil-pile-interaction, not just soil behavior. Therefore, the effect of soil liquefaction (i.e. degradation in soil resistance) does not reflect a one-to-one change in soil-pile or p-y curve response. Wang and Reese (1998) shift the p-y curve resistance in the crust layer, that is overlying the fully liquefied soil, by a lateral displacement (Δy) that is assessed from the relationship developed by Bartlett and Youd (1995) (see Fig. 3).

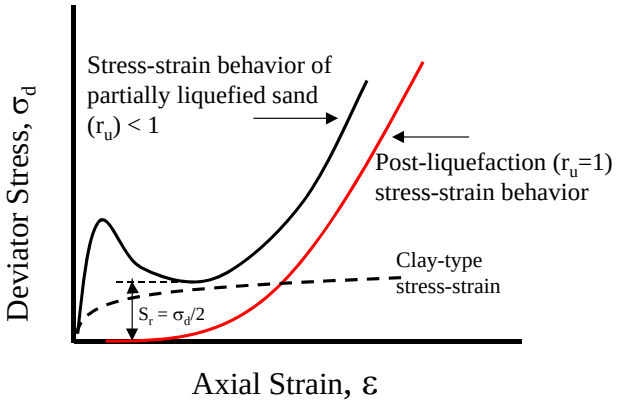

Figure 1. Subsequent undrained stress-strain behavior of sand that has experienced partial (r_u <1) or complete (r_u =1) liquefaction

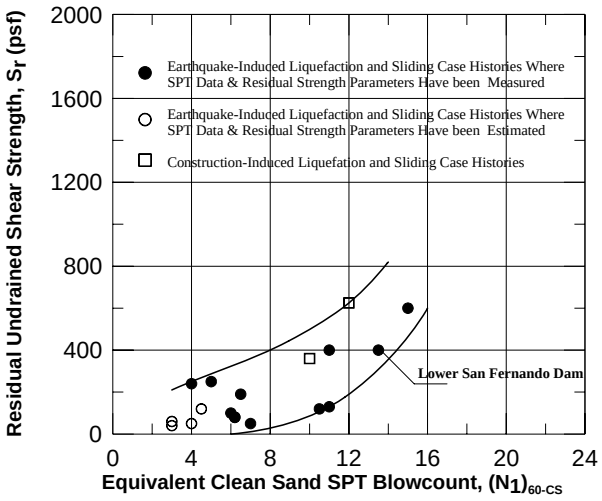

Figure 2. Corrected blow count vs. residual strength (Seed and Harder 1990)

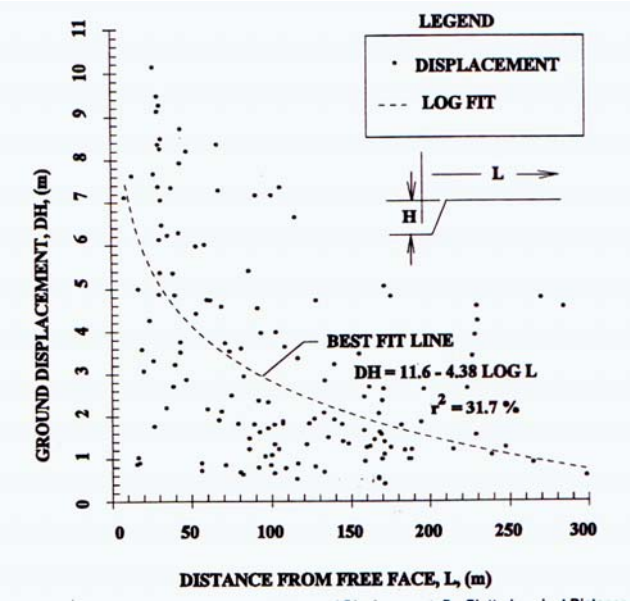

Figure 3. Lateral soil spread based on field data (Bartlett and Youd 1995)

SOIL LIQUEFACTION

The post-liquefaction stress-strain characterization of a fully or partially liquefied soil is still under investigation. There is considerable uncertainty relative to the current assessment of the resistance of a liquefied soil. With lateral loading from the superstructure following full or partial liquefaction (with significant drop in the effective confining pressure in the latter case), the sand responds in a dilative fashion due to the imposed deviatoric stress (horizontal stress increase in the SW) from the pile/shaft load. Alternatively, with a small drop in confining pressure, partially liquefied sand may first experience contractive behavior followed by dilative behavior under subsequent compressive monotonic loading. The post cyclic response of sand, particularly after full liquefaction, reflects a stiffening response, regardless of its initial conditions (density or confining pressure).

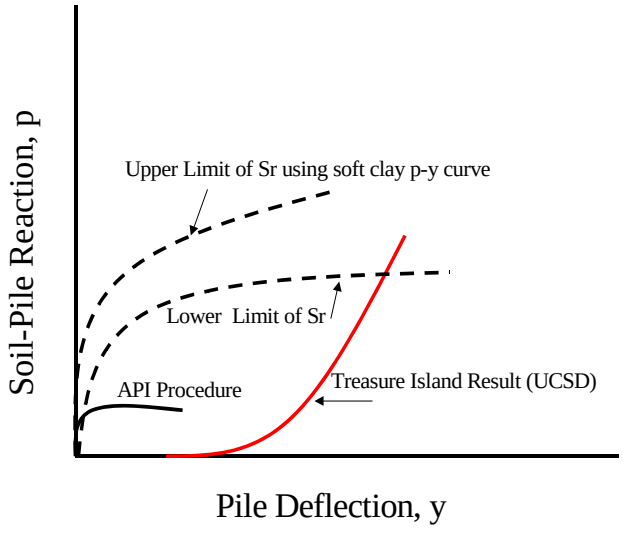

Figure 4. Undrained p-y curve in fully liquefied soil (Rollins et al. 2001)

As seen in Fig. 4, there is no particular empirical technique that allows the assessment of the p-y curve and its varying pattern in partially or fully liquefied sand. Instead, the soil's undrained stress-strain relationship should be used in a true soil-pile interaction model to assess the corresponding p-y curve behavior. Because the traditional p-y curve is based on field data, a very large number of field tests for different pile types in liquefying sand would be required to develop a realistic, empirically based, p-y characterization. In the technique proposed here, the degradation in soil resistance due to earthquake shaking and the induced pore water pressure in the free-field ($u_{xs,ff}$) is based on the procedures proposed by Seed et al. 1983. This $u_{xs,ff}$ reduces the effective stress of the soil. Thereafter, the lateral load (from the superstructure) is applied at the pile head that generates additional pore water pressure ($u_{xs,\ nf}$) in the near-field soil immediately around the pile causing an additional degradation in soil strength already reduced by $u_{xs,\ ff}$.

Note that $u_{xs,\ ff}$ is taken to reduce the vertical effective stress from its pre-earthquake state $'_{vo}$ to $'_{v} = '_{vo}(1-r_u)$. Thereafter, the undrained behavior due to an induced inertial lateral load is assessed using undrained stress-strain formulation (Ashour and Norris 1999 and Ashour 2002) in the extended SW model. This procedure incorporates the whole undrained stress-strain curve (at any level of loading) and associated effective stress path, not just the residual strength of the sand (Ashour and Norris 2003).

LATERAL SOIL SPREADING

The major challenges in the analysis of piles/shafts in liquefied soil undergoing lateral spreading are 1) how far the crust layer moves; 2) the undrained behavior (the varying strain based, effective stress strength) of the liquefied soil layer in the near-field; and 3) the amount of driving (inertial) force on the piles. The technique suggested allows the assessment of the undrained stress-strain-strength relationship of a fully ($r_u = 1$) or partially ($r_u < 1$) liquefied soil as seen in Fig. 1 and proven via the comparisons with the Treasure Island Test results. Therefore, the mobilized strength of the liquefied soil can be assessed according to the level of soil strain and restrained dilation. The lateral soil spreading analysis implemented assumes that the crust layer keeps applying an increasing lateral driving force on the piles as long as the underlying soil layer(s) is fully liquefied (Phase I in Fig. 5). Once the fully liquefied soil layer starts gaining some strength (i.e. $r_u < 1$) due to progressive deformation, the overlying crust layer switches from applying driving force to providing passive resistance to the pile's lateral deflection (Phase 2 in Fig. 5).

Figure 5 shows the modeling (characterization) of a pile in liquefied soil undergoing spreading and the shape of the associated p-y curves in the liquefied and nonliquefied soil layers. The suggested technique allows the evaluation of the lateral displacement of the liquefied soil (Δy_s) [i.e. the associated displacement of the upper nonliquefied soil(s), Δy_{sl}] before the shear strength of the liquefied soil starts picking up (rebounding). In addition, the varying driving force exerted by the crust on the pile during the lateral spreading (Phase I) can be determined based on the interaction between the pile and the surrounding soil. Therefore, the resulting p-y curve in the crust will account for the displacement caused by lateral spreading of the underlying soils as seen in Fig. 5. In addition, the p-y response assessed for the liquefied soil will account for the varying strength of the soil and the continuous changes in the water pressure at any level of loading. The lateral displacement (lateral spread) of the crust layer ($X_o = \Delta y_{sl}$, Fig. 6) is evaluated based on the approach presented by Ashour and Norris (2000) and Ashour (2002).

COMPARISON WITH FIELD AND MODEL TEST RESULTS

Full-Scale Load Test of an Isolated Pile (0.61 m CISS) in Liquefied Soil at Treasure Island

Full-scale load tests of the post-liquefaction response of long isolated piles performed at the Treasure Island site (Weaver et al. 2005) provide the data with which to evaluate the capability of the SW model (Ashour et. 1998 and Ashour and Norris 2003) to predict laterally loaded pile response in liquefied soil. The soil properties employed in the SW model analysis of Table 1 are based on the data reported by Weaver et al. (2005). The sand is assumed to contain 10% fines. The soil was liquefied by carrying out controlled blasts that did not densify the soil in the test area. Drained and undrained lateral load tests were performed on an isolated CISS (cast in steel shell) pile of 0.61 m diameter. The pile exhibited free-head conditions and was loaded laterally 1.0 m above the ground surface.

The predicted and observed drained responses of the pile compare favorably as seen in Fig. 7. The assessed undrained post-liquefaction behavior of the pile considers both the free- and near-field pore water pressures. The pile was cyclically loaded after the first blast. The good agreement between the measured and predicted undrained response of Fig. 7 is based on peak ground acceleration, a_{max}, of 0.1g and an earthquake of magnitude 6.5 in the SW model analysis. This free-field value of a_{max} generates high pore water pressures ($u_{xs,\ ff}$) of $r_u \approx 0.9$ in most of the upper sand layers that best matches the measured free-field pore water pressure pattern induced in the field test.

Figure 5. SW model pile/shaft response in liquefied soil undergoing lateral spreading

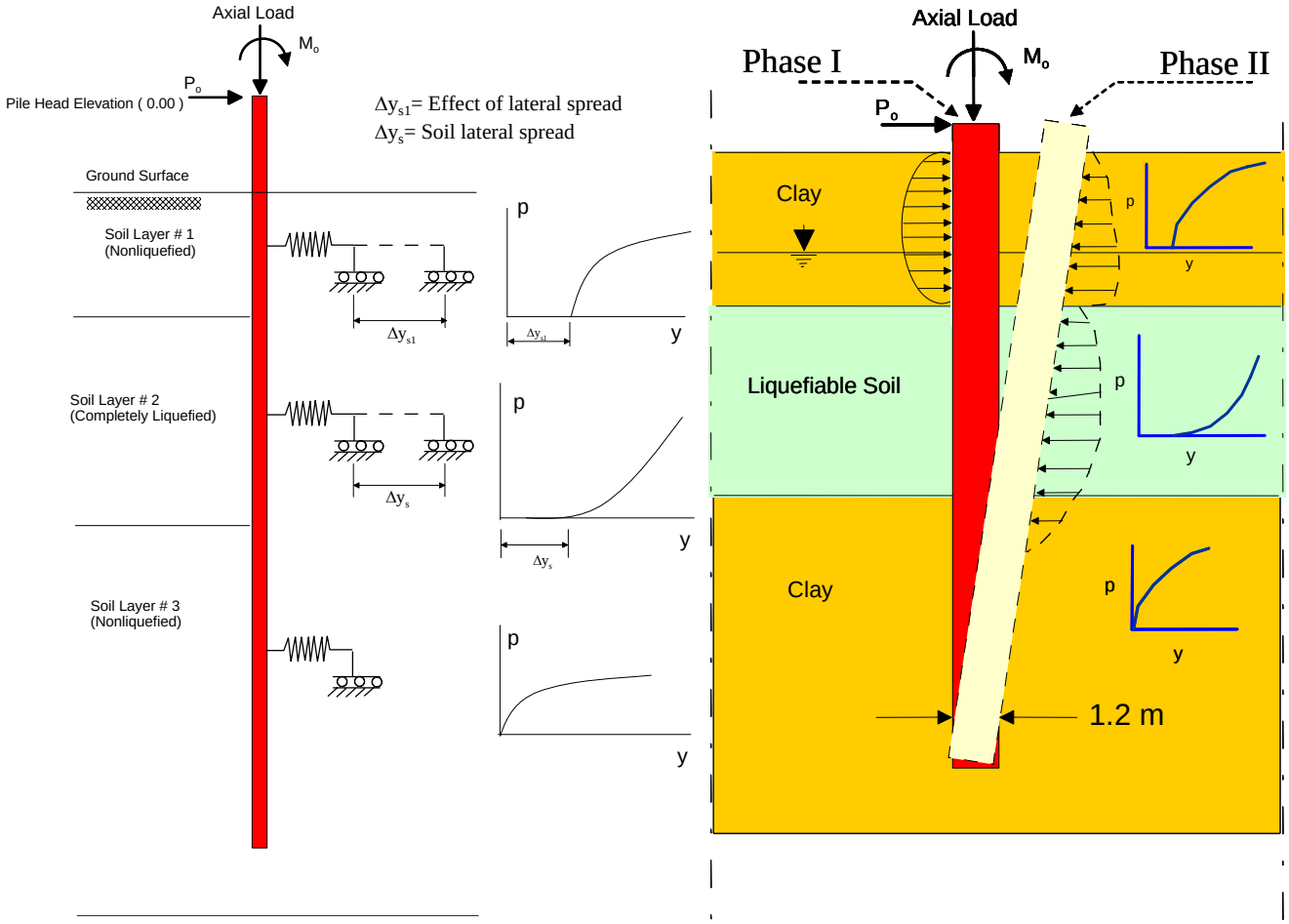

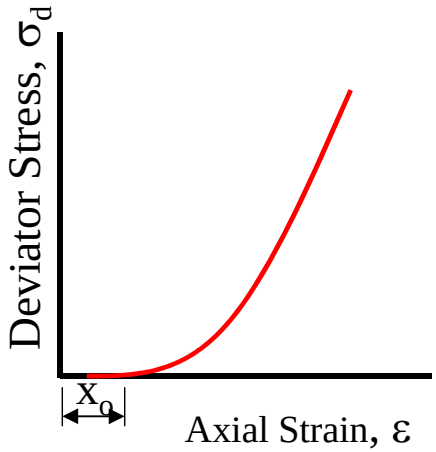

Figure 6. Rebound response of fully liquefied soil (Ashour 2002)

Table I. SOIL PROPERTIES EMPLOYED WITH TREASURE ISLAND TEST (WEAVER ET AL. 2005)

Soil Layer Thick. (m)	Soil Type	Unit Weight, $\bar{\gamma}$ (kN/m^3)	$(N_1)_{60}$	Φ (degree)	~ %	*S_u kN/m^2
0.5	Brown, loose sand (SP)	18.0	16	33	0.45	
4.0	Brown, loose sand (SP)	8.0	11	31	0.6	
3.7	Gray clay (CL)	7.0	4		1.5	20
4.5	Gray, loose sand (SP)	7.0	5	28	1.0	
5.5	Gray clay (CL)	7.0	4		1.5	20

* Undrained shear strength

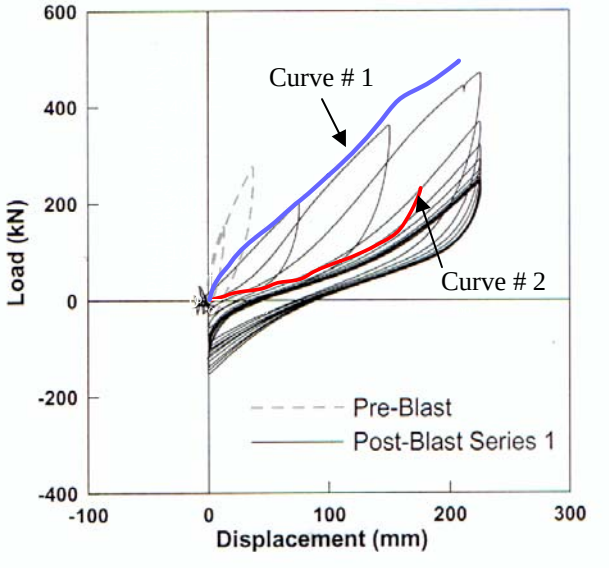

Figure. 7. Post-liquefaction pile-head response at Treasure Island (0.61 m CISS pile)

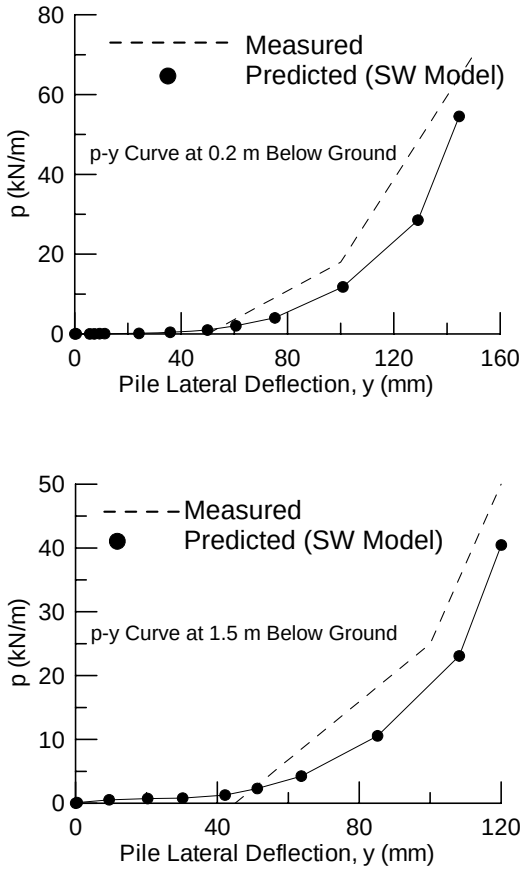

Figure 8. Computed vs. observed p-y curves for Treasure Island (0.61 m CISS pile)

The computed result represented by Curve # 1 in Fig. 7 is in good agreement with the data collected during the first 4 cycles of loading. However, by the seventh cycle of loading, the rising water generated by liquefaction covered the ground surface and, as a result, the pile-head load response took a concave-up pattern due to progressive soil liquefaction around the pile (Curve # 2 in Fig. 7). The computed pile-head response takes the shape of Curve # 2 based on the updated soil profile, i.e. the water surface is taken at soil surface and the uppermost).5 m is reassigned a buoyant unit weight. As mentioned by Weaver et al. (2005) and Rollins

et al. (2005), the concave-up p-y curves shown in Fig. 8 were back-calculated at the seventh cycle of loading. Excellent agreement between SW model computed and back-calculated ("measured") p-y curves can be seen in Fig. 8.

Full-Scale Load Test on a Long Isolated Pile (0.324 m Diameter) and Pile Group at Treasure Island

The 3 x 3 0.324 m diameter steel pipe pile group at Treasure Island was tested under drained conditions. The group was retested in the soil liquefied by controlled blasting as addressed by Rollins et al. (2005). An earthquake event with a magnitude of 6.5 and peak ground acceleration (a_{max}) of 0.1 g was employed in SW model analysis. The soil profile presented in Table 2 (Rollins et al. 2005) was employed in that analysis. The data shown in Fig. 9 for the isolated pile and pile group were computed for the first 4 cycles of loading (Curve #1) and at the seventh cycle of loading (Curve # 2) when the soil profile reached peak liquefaction conditions and the rising water generated by liquefaction covered the ground surface (the upper 0.5 m soil layer again becomes submerged below water level).

Table II. SOIL PROPERTIES USED IN THE ANALYSIS OF TREASURE ISLAND TEST (ROLLINS ET AL. 2005)

Soil Layer Thick. (m)	Soil Type	Unit Weight, $\bar{\gamma}$ (kN/m^3)	$(N_1)_{60}$	Φ (degree)	˜ %	*S_u kN/m^2
0.5	Sand	19.5	16	38	0.4	
2.5	Sand	10.3	12	38	0.4	
1	Sand	10.3	10	36	0.5	
2	Sand	10.3	6	33	0.8	
1.5	Sand	10.3	7	34	0.7	
1.75	Clay	9.5	3	0	2.0	20
1	Sand	10.3	8	33	0.8	
1.7	Clay	9.5	3	0	2	20

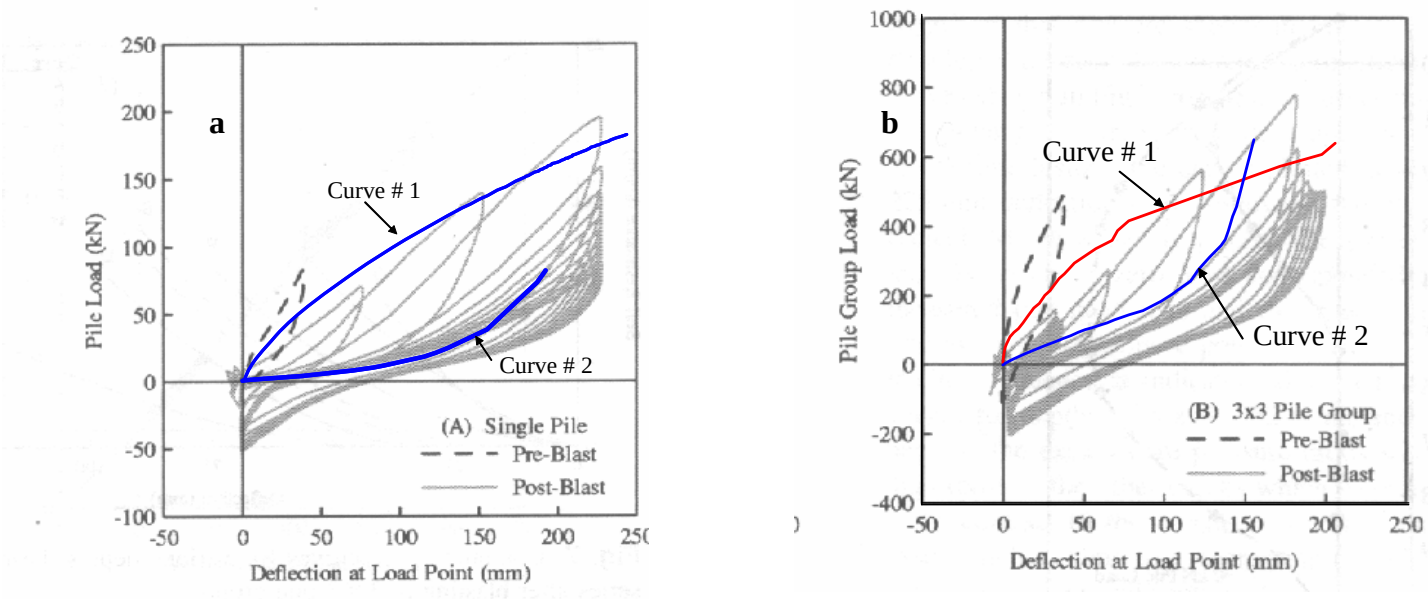

Figure 9. Computed vs. measured response of (a) an isolated and (b) a 3 x 3 group of 0.324 m CISS piles in the liquefied soil at Treasure Island (after Rollins 2005)

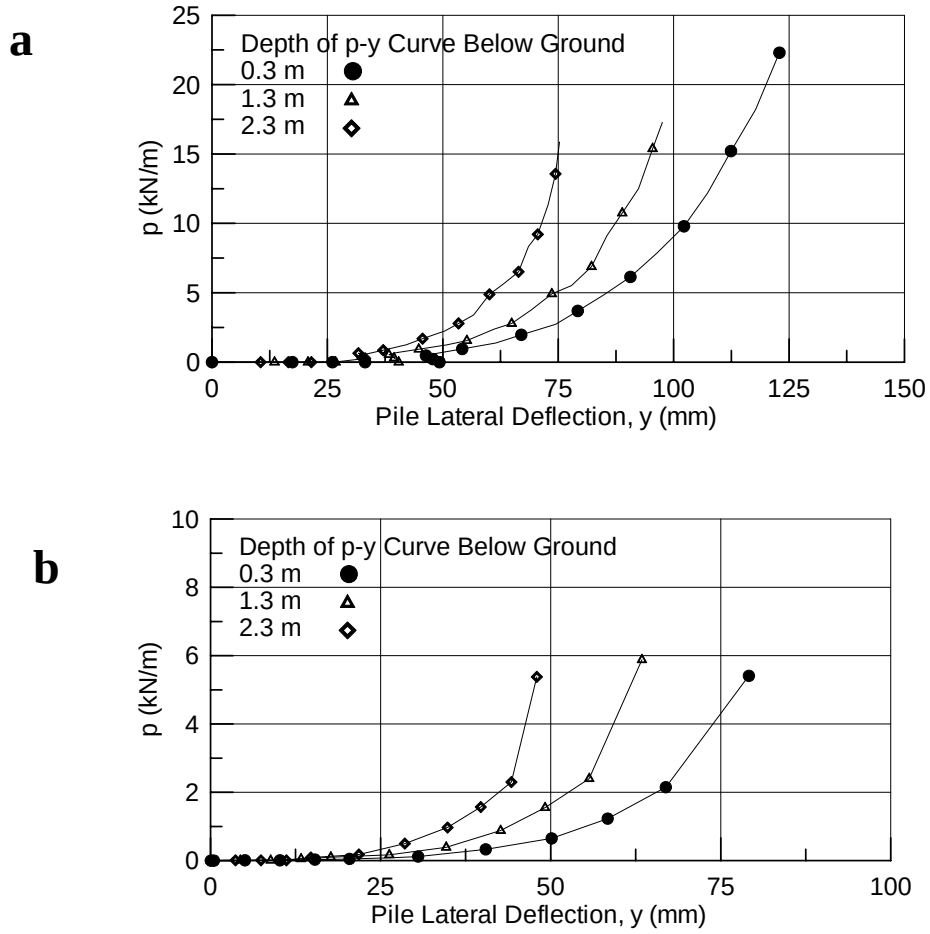

Figure 10. SW model p-y curves for (a) an isolated and
(b) a 3 x 3 group
of 0.324 m CISS piles at different depths in the liquefied soil at Treasure Island

The assessed post-liquefaction behavior of the pile group is based on consideration of both free- and near-field pore water pressures and group interaction. The SW model calculated p-y curves shown in Figs. 10a and 10b for an isolated pile and a pile in the group are in good agreement with the back-calculated ones presented by Rollins et al. (2005). It should be noted that because of the fully achieved liquefaction condition, the group effect on the p-y curves shown in Fig. 10 is very limited. However, with partial instead of complete liquefaction, the group effect becomes much more pronounced relative to curves at these same depths.

University of California (UC) Davis Centrifuge Test Involving Lateral Spreading (Barndenberg and Boulanger, 2004)

Centrifuge tests were performed on the 9-m radius centrifuge at UC Davis. All tests were performed in a flexible shear beam container with centrifugal accelerations ranging from 36 to 57 g. The soil profile consisted of a nonlinear crust (San Francisco Bay mud) overlying loose sand (Dr = 21 – 35%) overlying dense sand (Dr = 69 – 83%). The Bay mud was mechanically consolidated using a large hydraulic press and subsequently carved to the desired slope. The properties of the components of the soil profile are presented in Table III.

The 2 x 3 model pile group seen in Fig. 11 consisted of 1.17-m prototype diameter piles with a large pile cap embedded in the nonliquefied crust. The pile cap provided fixed pile-head conditions. The properties of the pile group and pile cap are presented in Table IV. The top of the pile cap was located near ground surface. The pile group had no superstructure but was tested under conditions that led to lateral spreading of the soil. Three scaled Kobe earthquake motions were applied to the base of the model with a_{max} ranging from 0.1g to 0.67g.

TABLE III. SOIL PROPERTIES EMPLOYED IN THE SIL-SHORT PROGRAM FOR THE UC DAVIS LATERAL SOIL SPREADING TEST

Soil Layer Thick. (m)	Soil Type	Unit Weight, $\bar{\gamma}$ (kN/m^3)	$(N_1)_{60}$	φ (degree)	ε_{50} %	*S_u kN/m^2
3	Clay	6	0	0	0.015	44
7	Loose Nevada Sand	6	10	30	0.01	
20	Coarse Monterey Sand	17	30	36	0.004	

TABLE IV. PILES, PILE GROUP AND PILE CAP GEOMETRY

Pile Length (m)	Diameter (m)	Wall Thick. (m)	Pile Spacing (m)	Pile Cap Height (m)	Pile Cap Width (m)	Pile Cap Length (m)
23.5	1.17	0.051	4.6	2.2	9.2	14.3

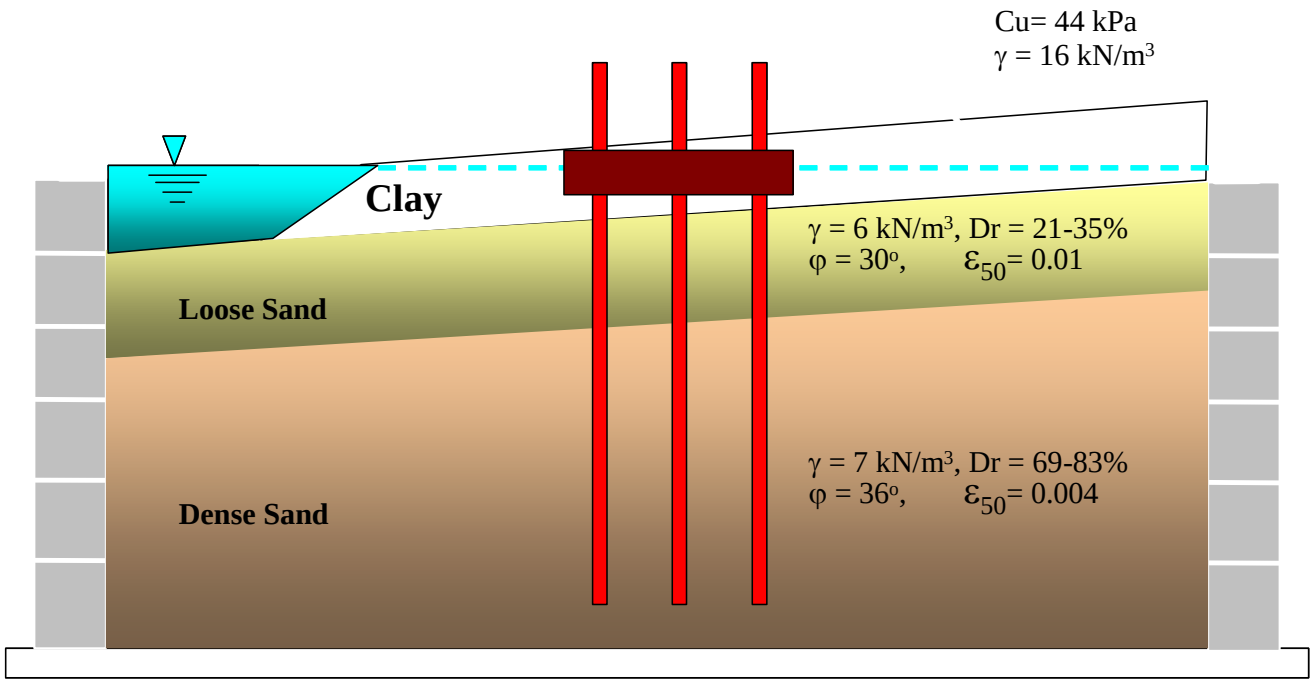

Figure 11. Schematic layout of the UC Davis centrifuge model (Barndenberg and Boulanger, 2004)

The aluminum model pile properties were converted to those of a steel pile with the same bending stiffness (EI) and diameter. The suggested large event a_{max}= 0.67g created full liquefaction along the loose sand layer (r_u = 1.0) and partial liquefaction in the dense sand layer. Figures 12 and 13 show a comparison between measured and SW model computed pile group deflection at the end of seismic shaking and the development of lateral spreading. It should be noted that the lateral soil spreading assessed using the SW

model is triggered in conjunction with development of complete liquefaction and ceases when the fully liquefied soil starts gaining strength (stiffens). The SW model computed pore water pressure ratio and shear force distribution along the length of the pile in the group are shown in Fig. 14.

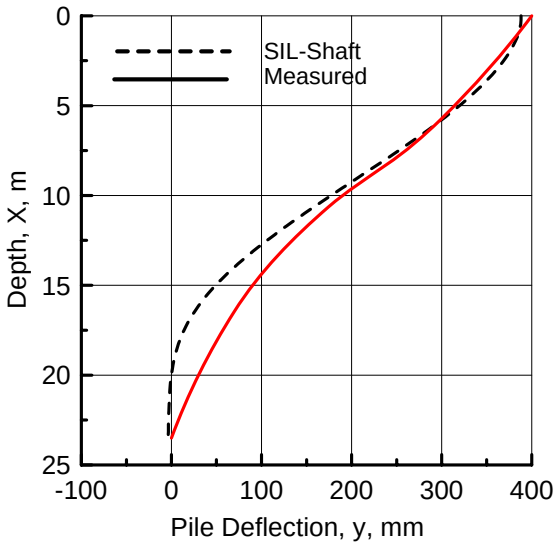

Figure 12. Back-calculated and computed pile deflection under lateral spread triggered by a_{max} = 0.67g

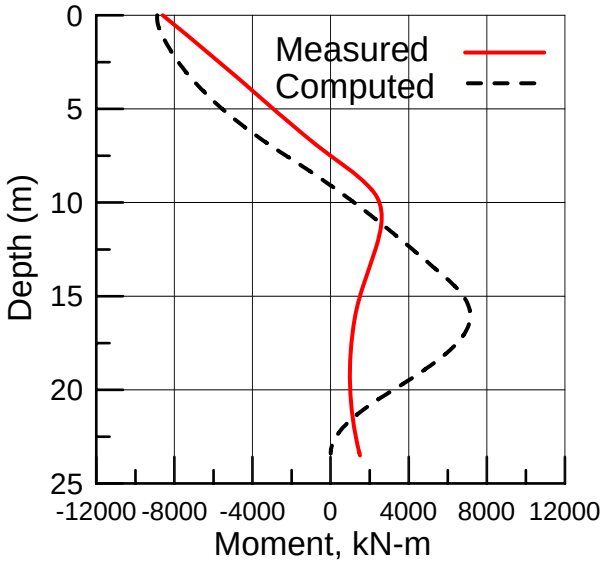

Figure 13. Back-calculated and computed pile deflection under lateral spread triggered by a_{max} = 0.67g

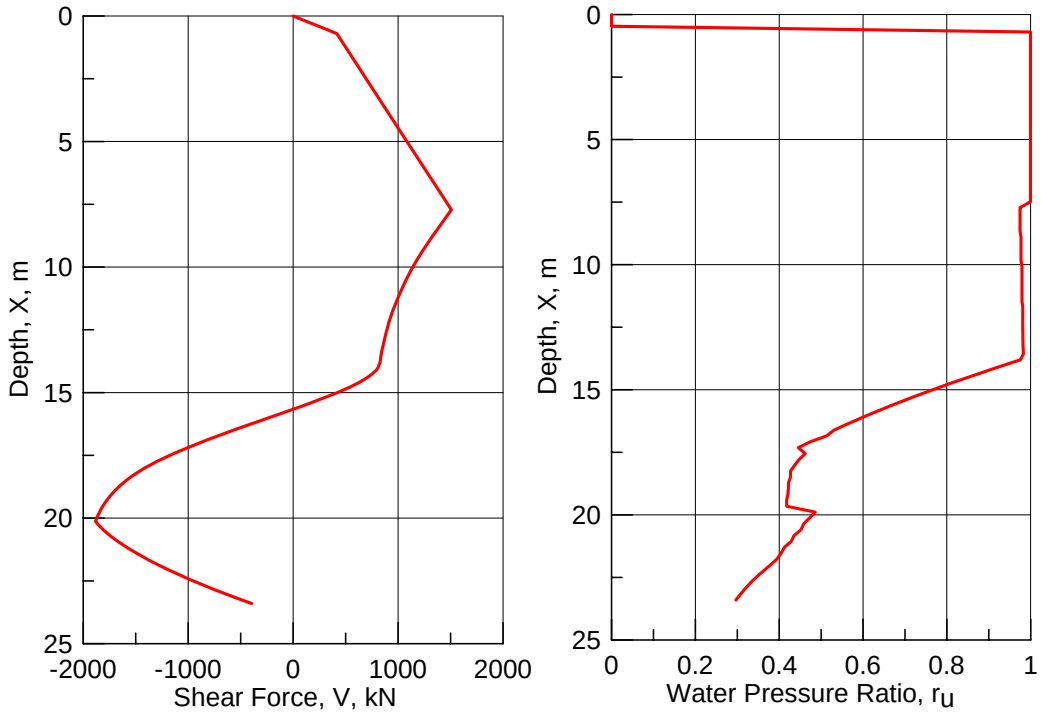

Figure 14. Shear force and pore water pressure ratio along the length of a pile in the group from the UC Davis test computed using SW model

CONCLUSIONS

Strain Wedge (SW) model analysis of laterally loaded pile and drilled shaft behavior has been extended to include consideration of the undrained response to inertial superstructure loading from earthquake shaking under developing or fully liquefied conditions in one or more soil layers along the pile/shaft length. Since the SW model is based upon an envisioned three-dimensional characterization of the one-dimensional beam-on-elastic-foundation (BEF) parameters and the associated p-y curves (with due consideration of the effect of both soil and pile properties), no additional empirical corrections factors are necessary for the abovementioned undrained analysis. The validity of the SW model approach to liquefied behavior has been demonstrated with respect to full-scale tests at Treasure Island for both isolated and pile group response. The SW model has also been upgraded to evaluate lateral spreading and results from such computation are compared with available centrifuge test data from tests undertaken at UC Davis.

ACKNOWLEDGEMENTS

The interest and financial support of both Caltrans and WSDOT in the development of the Strain Wedge Model are gratefully acknowledged.

REFERENCES

1. Ashour, M., G. Norris and P. Pilling. Lateral Loading of a Pile in Layered Soil using the Strain Wedge Model.. *J. of Geotech. Engg, ASCE* vol. 124 (4), 1998, pp. 303-315.
2. Ashour, M. and G. Norris. Liquefaction and Undrained Response Evaluation of Sands from Drained Formulation." *J. of Geotech. Engg, ASCE* vol. 125 (8), 1999, pp. 649-658.
3. Ashour, M. Post Liquefaction Response of Liquefied Soils. *Proc. 37th Engineering Geology and Geotechnical Engineering Symposium*, Boise, Idaho, 2002, pp. 11-26.
4. Ashour, M., and G. Norris. Lateral Load Pile Response in Liquefied Soil. *J of Geotechnical and Geoenvironmental Engineering, ASCE*, vol. 129 (6), 2003, pp. 404-414.

5. Bartlett, S.F. and T.L.Youd. Empirical Prediction of Liquefaction-Induced Lateral Spread. *J. of Geotechnical Engineering, ASCE*, vol. 121 (4), 1995, pp. 316-329.
6. Brandenberg S.J. and B.W. Bollinger. OpenSees Beam on Nonlinear Winkler Foundation Modeling of Pile Groups in Liquefied and Laterally Spreading Ground in Centrifuge Tests. *Proc. ANCER Annual Meeting*, Honolulu, Hawaii, 2004.
7. Norris, G., R. Siddharthan, Z. Zafir, and R. Madhu. Liquefaction and Residual Strength of Sands from Drained Triaxial Tests." *J. of Geotech. Engg, ASCE*, vol. 123 (3), 1997, pp. 220-228.
8. Rollins, K.M., T.M Gerber, J.D. Lane, and S. Ashford. Lateral Resistance of a Full-Scale Pile Group in Liquefied Sand. *J. of Geotechnical and Geoenvironmental Engineering, ASCE*, vol. 131 (1), 2005, pp. 115-125.
9. Seed, R.B. and L.F. Harder. SPT-based Analysis of Cyclic Pore Pressure Generation and Undrained Residual Strength. vol. 2, *BiTech Publishers Ltd*, Vancouver, B.C., Canada, 1990, pp 351-376.
10. Seed, H. B., I.M. Iris and I. Arrange. Evaluation of Liquefaction Potential using Field Performance Data. *J. of Geotechnical Division, ASCE*. vol. 109 (3), 1983, pp. 458-482.
11. Wang, T. and L.C. Reese. Design of Pile Foundations in Liquefied Soil. *Pub. No. 75, ASCE, Geotech. Earthquake Engg. and Soil Dynamics Conf.*, vol. 2, ASCE, Seattle, WA, 1998, pp. 1331-1343.
12. Weaver, T.J., S. Ashford, and K.M. Rollins. Response of 0.6 m Cast-in-Steel-Shell Pile in Liquefied Soil under Lateral Loading. *J. of Geotechnical and Geoenvironmental Engineering, ASCE*, vol. 131 (1), pp. 94-102.

The Maple Ridge Wind Farm Access Road

Martin P. Derby, P.G., CPG
Malcolm Pirnie, Inc.
(formally with Contech Construction Products, Inc.)

Patrick O'Rourke
Contech Construction Products, Inc.

ABSTRACT

The Maple Ridge Windmill Farm is located on the Tug Hill plateau in the Town of Lowville, New York. The site consists of 120 windmills, and when fully constructed will produce approximately 200MW of electricity – enough to power 59,400 homes. The Maple Ridge project ($320M) is the largest windmill project east of the Mississippi River. Approximately 23 miles of access roads were required for the windmill project.

During the initial stages of the access road construction (May 2005), the general contractor (Blattner), and the excavation contractor (Delaney) encountered unstable soil conditions. Engineers from Contech Construction Products, Inc. (Contech) were contacted to assess the soil conditions, and to provide an access road design/solution capable to withstanding 300 ton crane loadings. The original access road design included an undercut of approximately ten inches, inclusion of a geotextile, and the installation of 10 inches of 3 to 4 inch aggregate.

Contech performed an inspection on two of the completed access roads and observed several areas were the soil (primarily silt) had day-lighted at the surface (indicating the geotextile had ruptured or failed) due to rutting. Soft to medium soils were encountered with an estimated CBR of approximately 0.8 to 1.6 based on observed rutting depths of vehicle tracks.

Contech reviewed the available boring logs, and utilized the SpectraPave2 software to determine the amount of aggregate material that would be required for both the average and "worst case" CBR scenarios. The results indicated that utilizing Tensar's BX1200 geogrid, a minimum of 14 inches of Type 2 aggregate would be required for the access roads. The aggregate thickness could be increased to 22 inches where softer subgrades were encountered.

To date approximately 453,000 square yards of Tensar BX1200 have been installed.
Tensar BX geogrids were successfully used at the Maple Ridge Wind Power site to improve the bearing capacity of the soils, reduce the amount of aggregate required to stabilize the soils underlying the tower access roads and provide ease of construction.

Landslide Mitigation, Arterial Highway Stabilization with Multi-Agency Interaction El Toro Road, Mission Viejo, California

William Goodman
CEG, Principal Geologist
NMG Geotechnical, Inc.
17991 Fitch, Irvine, CA 92614
WGoodman@nmggeotechnical.com

ABSTRACT

El Toro Road (ETR), located west of the Upper Oso Reservoir in Mission Viejo, California, was realigned by the County of Orange in 1981 to avoid flooding and erosion impacts from Aliso Creek. However, the new alignment was built over the lower portions of several landslides in a west-facing natural slope, approximately 200' high. The bedrock in this hillside area consists of west-dipping siltstone and claystone of the Monterey Formation. Grading for ETR consisted of excavation of 2:1 cut slopes into the hillside and filling the natural drainages. Remedial grading was not performed to mitigate potential landslide impact to the new highway. During the 1980s to early 1990s, numerous debris topple and slump-type landslides occurred on the west side of ETR due to stream erosion and undercutting of the existing landslide mass. In the winter of 1995, a portion of one of the landslides reactivated and undermined a 200' section of the road, which was closed for 3± months during the slope/road repair. In 1998, the City of Mission Viejo, having jurisdiction over this portion of El Toro Road, commissioned a study to evaluate the existing stability of the road from the Foothill Transportation Corridor (FTC) to Glenn Ranch Road (GRR). The results of this study provided mitigation recommendations to stabilize the portions of the landslides that could have an adverse impact on ETR. The mitigation consisted of remedial grading in steep, sloping terrain adjacent to protected natural habitat and an existing creek. Interaction with numerous public agencies and public utilities required coordination and permits to complete the project. ETR was closed from the FTC to GRR for one year during remedial grading and road reconstruction. The project involved temporary creek diversion, dewatering, excavation of a shear key 15 to 20 feet below the groundwater table, select grading, geogrid slope construction, stream scour protection, grading setbacks from sensitive environmental habitat, temporary realignment of existing utility mains and monitoring temporary slopes during remedial grading operations.

Application of the Block Theory for Rock Slope Stability Analysis at Highway Semenyih-Sg.Long, Selangor State in Malaysia

Hswanto
Geology Department
Faculty of Science & Technology
National University of Malaysia
43600 Bangi, Selangor
MALAYSIA
haswanto_wa@yahoo.com

Rafek A. Ghani
Department of Geology,
UKM, Bangi, Malaysia.

ABSTRACT

The granitic rock mass which exist along the highway Semenyih-Sg.Long, Selangor state in Malaysia contains a number of major discontinuities, and several sets of minor discontinuities. Therefore, the rock engineering problems of high steep rock slopes are somewhat complicated. The major discontinuities were determined and used to perform a block theory based analysis of the rock slope stability.

The orientations of the major discontinuities that occur in the researched area have been considered in this analysis. The orientation of the major discontinuities were as follows (dip-direction/dip-angle) : J1:360/660; J2:1520/600; J3:790/880; J4:1170/660 and the free-face is ff5:1050/700. The block theory analysis was used to determine : 1. The key blocks type I that are finite, removable, unstable without support and potential key blocks type II that are finite, removable, stable with sufficient friction of the rock slope. 2. A safe angle for the rock cut slope at highway Semenyih-Sg.Long.

Based on the data analysis, the following types of key blocks were determined: type I (keyblock) is the JPs 0000, and type II (potential keyblock) is JPs 0100. The result showed that the maximum safe slope angle (MSSA) is 450 for the type I (keyblock) and MSSA is 630 for the type II (potential keyblock). The cut slope along the highway Semenyih-Sg.Long are greater than 700 within fresh to slightly weathered granite, and contains these discontinuities, therefore there is a need for installation of a proper support system in order to maintain the long term stability of this rock slope.

Key-word : Block Theory, Rock Slope Stability, MSSA, Highway Semenyih-Sg.Long Selangor state, Malaysia.

Overview of 2005 Storm Damage to Lower Mount Wilson Road, San Gabriel Mountains, Los Angeles County, California

Jeffrey R. Keaton
Engineering Geologist
MACTEC Engineering and Consulting
Los Angeles, CA 90040
(323-889-5316;
jrkeaton@mactec.com

ABSTRACT

Extensive winter storm damage in 2005 rendered the Mount Wilson Road impassable. The lower 2.63 miles of this road provides vehicle access to Los Angeles County fire lookout facilities at Henninger Flats in the San Gabriel Mountains above Pasadena. Storm damage consisted of 1) sloughing of debris onto the roadway from above, 2) sliding of material down slope from the roadway, and 3) 'double-whammy' slopes at switchbacks where slope failures simultaneously slough onto the lower roadway and encroach on the upper roadway. Several vintages of drainage devices and retaining walls exist along the road, which was built originally in the late 1800s. A fiber optics cable buried along the up-slope shoulder of the road to provide communication to Mount Wilson is still in use.

Los Angeles County Fire Department wanted to restore vehicle access to Henninger Flats facilities and asked for repair alternatives at a conceptual level. Results of an engineering geologic reconnaissance were compiled onto a 1:1200 photogrammetric topographic map prepared for the study. Any efforts to restore vehicle access were considered to be very expensive and have some level of risk of future damage. The typical 1.5 factor of safety required for County projects could not be achieved with reasonable cost. Bridge alternatives were identified at three locations but probably are not practical. Reasonable repair strategies consisted of rock-fall and slough barriers on upslope sides, and soldier-pile-and-lagging retaining walls on down slope sides. Two areas require more extensive treatment and welded-wire steepened slope systems were considered.

Nightmare on Elm Street – Urban Rockfall Case History

Thomas McArdle
Assistant Public Works Director,
39 Main Street
Montpelier, Vermont.

Tom Eliassen
Transportation Engineering Geologist,
Vermont Agency of Transportation.

Daniel Journeaux
President, Janod Contractors, Inc,
Champlain New York.

Jay Smerekanicz
[1] Senior Consultant and Associate,
Golder Associates Inc.,
N 540 Commercial St.,
Manchester, NH

Peter Ingraham
[1] Senior Consultant and Associate,
Golder Associates Inc.,
N 540 Commercial St.
Manchester, NH

ABSTRACT

On December 26, 2005 a rockslide occurred in Montpelier, along the crest of a slope adjacent to Cliff Street and within sight of the State Capital Building. The rockslide occurred during a rainfall and thawing event, following a month of consistent subfreezing temperatures. Rocks, soil and debris fell over 100 feet downslope and onto Elm Street, with several large rocks striking power poles and narrowly missing an apartment building across Elm Street from the slope. A section of Cliff street 5 feet wide and 50 feet long was lost to the slide and Elm and Cliff Streets were closed until repairs could be completed. Past landslide activity on the hillside damaged a house in 1998 and the house was subsequently removed. The slide mechanisms were a combination of flexural toppling of steeply dipping (56 to 76 degrees) rock strata that dip into the hillside slope and chevron toppling in lower reaches of the slope.

The upper slide scarp was repaired with a soil/rock nail wall, thickened to restore up to 4 feet of roadway width along Cliff Street, installation of a Tecco mesh soil slope stabilization, rock bolting and scaling of loose rock and soil from the slope. The design of repairs and slope stabilization were completed concurrently with a “design on the fly” approach involving close communication between the City, engineer and contractor. This approach saved time and restored services rapidly to the residents affected by the rockslide.

Effect of Rock Types on Slope Failures Along Selected Problematic Parts of a Mountain Road, Al-Baha, Saudi Arabia

Bahaaeldin H. Sadagah
Engineering and Environmental Geology Department,
Faculty of Earth Sciences, King Abdulaziz University,
P.O.Box 80206, Jeddah 21589, Saudi Arabia. Email: bsadagah@kau.edu.sa

ABSTRACT

Al-Baha descent road of 32 km long lies at one of the harshest terrains in western Saudi Arabia. The rock masses consists of Precambrian and metamorphic rocks. Sharp cliffs are characterizing the morphology of the descent area. The maximum elevation of the descent cliff is 2300 m a.s.l., and the elevation difference range from 1400 m to 100 m above the valley bottom.

The natural and man-made rock slopes along the road has been divided into stations characterized by similar geotechnical properties. The descent road is suffering from continuous landslides and rockfalls especially at the rainy season. The allocated igneous rocks have a wide variety of technical properties. Landslides and rockfalls consist of very large to small igneous rock blocks. Landslides at the areas formed of metamorphic rocks are mainly plane and toppling failures.

The study resulted in classifying the remedial measures according to the rock type and technical properties of the rock blocks. It also shows that the bedrock technical characteristics are the main reason for increasing various modes of failure. Dimensions of the landslide are related to the moving earth material. In addition, the trajectories of rockfalls simulated by computer software are greatly related to the rock
strength, slope height, cliff elevation, block size and discontinuities orientations of the
rock masses.

Key words: mountain roads, rock slopes, rock types, modes of failure, GSI.

INTRODUCTION

Roads projects play a vital role in the developing countries. Rugged terrains are major obstacles to build roads in mountainous terrains due to the possible and frequent occurrence of landslides across the road. Landslides occur in a form of a circular, plane, wedge, toppling and combinations of failures. These types of rock slope failures frequently take place especially in roads running along high relief descent areas located in the western part of Saudi Arabia. One of the most difficult terrains is Al-Baha descent where high elevations reach above 2000 m above sea level. Along the slopes of the sharp cliffs, the descent road is connecting the high-rising mountains with the Red Sea coastal plain.

Al-Baha descent lies between longitudes 41° 25" E and 41° 29" E and latitudes 19° 47" N and 20° 01" N; see (Fig. 1). Al-Baha escarpment road starts southwest of Al-Baha city, and runs through Al-Baha descent. The total length of 50 km-escarpment road connects the highlands where Al-Baha city is located at north with the lowlands where Al-Mukhwah town is located further south. Along this distance, a large number of man-made and natural slope cuts, in addition to numerous engineering structures were studied along 32 km only.

Al-Baha city is located within the southwestern Asir Province of Saudi Arabia, a region known for its rugged and highest mountainous terrain in the country. It encompasses three distinct geomorphologic terrains: i) a dissected upper plateau of low mountains and hills, ii) a precipitous escarpment, and iii) a low-lying coastal plain (Fig. 1). The most prominent of these features is the northwesterly trending Asir or Tihama escarpment, a structure, which is traceable for some 1500 km long between Yemen in the south and Medina in the north. The escarpment resulted from a 3000 m lowering of the Tihama Coastal Plain during the Tertiary opening of the Red Sea. Post tectonic erosion of the Precambrian rocks that underlies the Asir Escarpment has produced a rugged mountainous topography where elevations reach 2000m or more.

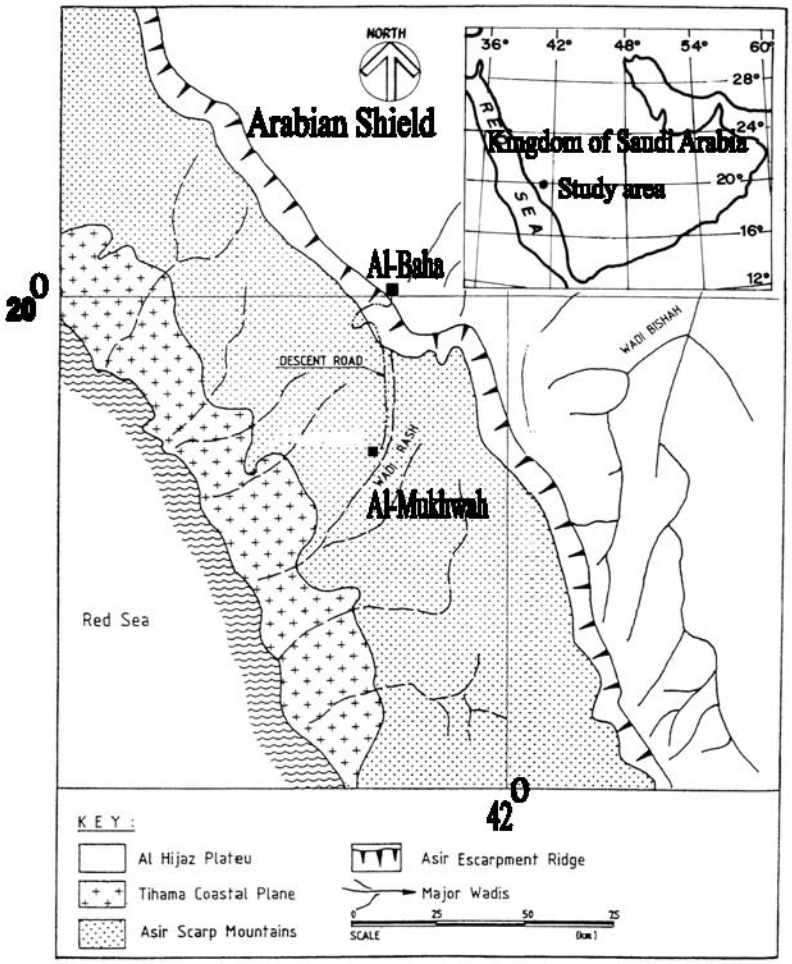

Fig. 1. Location of the study area.

Wadis flow away from the Asir escarpment, either eastward across the Al-Hijaz Plateau or westward towards the Red Sea. The westerly flowing wadis deeply cut into the escarpment face. The Al-Baha descent's road is contained almost within a narrow valley, called Wadi Rash, striking south-south east direction away from the escarpment ridge. Steep tributaries start from the escarpment ridge, and radiate out from the wadi head and cut deeply into the valley sides and escarpment face. Several small native forests grow at the edge of the escarpment near the township of Al-Baha.

Al-Baha region is underlain predominantly by a north-south trending belt of Precambrian schistose rocks comprised predominantly of fine grained mafic to intermediate extrusives, intrusives and pyroclastics with minor intercalations from clastics and metasediments (Prinz, 1983). The majority of the rocks have been subjected to greenschist facies metamorphism. Metamorphic grades may increase up to the chlorite and amphibolite facies within the igneous intrusions. Intrusives of plutonic rocks have been intruded into the metamorphosed rocks and are represented mainly by orthogneiss, alkali granite, granodiorite, microgranite, quartz diorite, pegmatite-aplite veins and mafic sills and dykes. The tectonic cycles resulted in a very complex and disturbed basement with a dominant northwesterly to northeasterly trending faults and folds.

GENERAL GEOLOGY

Al-Baha city and its vicinities occupy a small part of the Precambrian Arabian Shield. It lies at the central western part of the shield (Brown and Jackson, 1958; Brown, et al., 1963; Carter, 1977; Carter and Jackson, 1986; Hadley and Fleck, 1980; Greenwood, 1975a, b, and c; and Greene and Gonzalez, 1980). The region is located at Al-Qunfudah quadrangle, underlain by

north-south trending belt of schistosed Baish Greenstone suite.

The rocks are fine grained-mafic to intermediate intrusive, extrusive and pyroclastics rocks.

Posttectonic plutonic rocks have been intruded into the basement rocks. The intrusives consists of orthogneiss, alkali granite, granodiorite, quartz diorite, microgranite, pegmatite-aplite veins and mafic dykes and sills, see (Fig. 2).

The Baish greenstone is the oldest rock group exposed in Al-Baha descent area. Overlying the greenstone is a suite of younger sedimentary Precambrian rocks, formed of metasediments and metapyroclastics rocks tentatively related to the chronologically younger Baha group. The younger Baha group underlies the older Baish group as a result of thrust faulting. In Al-Qunfudah quadrangle, Jeddah and Ablah groups are younger in age than Baha group; all of these groups are related to Proterozoic age (Prinz, 1983).

The major orogenic cycles, with periods of folding, faulting and igneous activation resulted in a complex basement. Details are given by Prinz (1983), Greenwood, et el. (1982).

Local Geology

The majority of the rocks are metamorphosed to the greenschist facies, of low-grade metamorphism of regional alteration. In some places the degree of metamorphism increases to higher grades such as chlorite and amphibolite facies.

Detailed geological mapping encountered during the field trips and engineering geological study includes a few regions of rocks; see (Fig. 2). The regions of rock types encountered are as follows: Fig. 2: Geology of the study area.

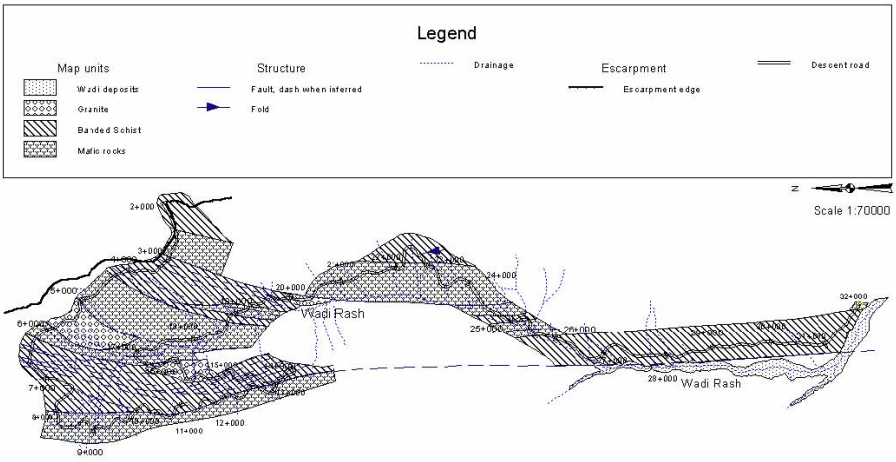

Figure 2. Geological map of the study area.

1 Mafic rocks: intermediate to basic igneous rocks belonging to Baish Group includes basic lithologies such as fine to medium grained intermediate to basic lithologies. Tuffs, diorite, dacite, basalt, gabbro, and andesite. Locally cataclastically metamorphosed to greenschist facies increased in degree of metamorphism to produce chlorite schist and amphibolite schist, and greenstones.

2 Banded schist: Thick sequence of schistosed sediments of Baha Group, formed of metamorphosed sedimentary rocks, medium grained arkose greywacke, tuffs, greywacke, cherts, and marble. These units are mafic to intermediate schist and pyroclastics metamorphosed to greenschist and amphibolite facies. This unit is an undivided banded mix between Baish and Baha groups.

3 Posttectonic plutons: formed mainly of granite intrusive acidic rocks, microgranite, quartz diorite, and dikes of pegmatite and aplite.

Wadi Rash is running through the study area from north to south, and continues further south, off the map, towards Al-Mukhwah town. Wadi Rash and its tributaries contains quaternary deposits of the broken and weathered rock fragments coming from mainly the surrounding rocks allocated at the descent area, and probably from the rocks on the plateau uphill behind the escarpment. The deposits are formed of sediments range in size from boulders to sand size and very small ratio of silt size. Terraces formed of gravel and flood-plain silt deposits are located at the banks of the main wadi course.

Geology of the Descent

Rocks of leucocratic granite around the major fault at km 5+900 are sheared; small bodies of gabbro dikes are altered in the shear zone of leucocratic granite. Shear zone extends from almost km 5+400 to 6+000. The whole body of leucocratic granite (km 5+000-6+000) contains fragments of diorite and gabbro, and dikes of gabbro.

Dikes of diorite are cutting the country rocks of schist and granite in the location km 6+000 to 8+000. At locations km 7+300 to 7+650 plagioclase and sericite increase in the rock matrix. This indicates that in case of rainfall, the rock mass produce clay which in turn form mud going from uphill down through the wadi tributaries.

Rock fragments of basalt, dacite, and rhyolite are rich in schist at km 8+500 to 8+700 increase towards km 8+700.

Andesitic tuffs of volcanic origin are extending from km 8+850 to southwards, include volcanic fragments and lithic fragments (greywacke), and change in grain size from fine grained at km 8+850 to coarse grained towards south. The layered sequence is formed of andesite (at km 8+580, volcanic flow of andesite, dacite, and basalt), tuff, lapilli tuff (at km 12+000), and andesite again. At location km 13+600-13+800 and km 13+800-14+000 (at tuff rocks), the pyrites are altered to goethite, and present as pseudomorph. When goethite mixed with water it will form sulphuric acid, which is corrosive to the rocks and engineering structures at this location. Wadi Rash represents the contact between the tuffs at the west side of the wadi and the sheared diorite at the east side of the wadi. Tuff extends from location km 14+000 to 15+700, where a small granitic body is intruded. At the east of this granite body banded, very fine tuff rocks extends to km 16+860; where the major fault is located at Wadi Rash.

Metamorphosed diorites to the amphibole facies forming schistosed amphibolite are located at the eastern side of Wadi Rash. The diorite is sheared and banded, the schistosity intensity increase eastwards up to km 18+200 where the maximum fragmentation of diorites occur. The result of metamorphism and high-pressure zone is shown in very fine-grained texture, and alteration of diorite. This zone extends to km 19+050 where schistosity increase and the mafic minerals content increase.

Mixed undivided rock units (Baish and Baha groups) formed of banded chlorite sericite schist starts from km 19+300 up to 20+050.

Small posttectonic granite intrusions are located at km 20+050-20+300, granite is mylonitized and highly deformed.

Highly deformed, banded, sheared diorite, highly metamorphosed metadiorite starts from km 20+300 to km 20+600. In addition to the foliated and banded quartz chlorite and sericite schist, hornblende schist is also shown from km 22+200 to km 22+800. These groups of rocks are located east of Wadi Rash, extends eastwards towards the escarpment line (off map). The strike of the foliation is roughly parallel to the strike of Wadi Rash, dipping towards west. The gabbro, granite and andesite intrusions bodies from km 22+900-24+400 are sheared and highly crushed.

The group of rocks form banded schist and tuffs starts from km 24+800 up to km 25+200, followed by 1) mafic rocks extends from km 24+800 to km 25+900 formed of highly sheared gabbro and basalt, and 2) sheared calcite marble extends from km 26+000 to km 26+300.

Quartz schist, calcite quartz schist, biotite schist, plagioclase schist, banded schist, and greywacke are predominant in the area from km 26+300 up to the end of the geological map and the area of study at km 32+000.

STRUCTURE

The structure is dominated by i) westward dipping schistosity, see (Figs. 3 and 4), and ii) north-north-east to northeast trend faults and folds, see (Figs. 5 and 6). The observed faults are steeply dipping where the folds are tightly compressed isoclinal folds; see (Fig. 6 and 7).

Faults

The predominant structures at the area are north to northeast and northwest trending faults and folds. Northwest-trending faults located at the western part of the study area are related to Red Sea rifting during Tertiary (Prinz, 1983). All types of faults are steeply dipping; see (Figs. 5 and 6). Thrust faults are located between the banded schistosed rocks of Baish and Baha groups. Therefore, Wadi Rash is initiated due to major fault, and it could be classified as a structurally controlled valley, as indicated earlier. The major faults in the study area are formed in post Baha group, in accordance with Prinz (1983) who suggested after Ablah time.

Folds

The schistosed rocks are folded along north- to northeast-trending axes. Small-scale folds are observed along the road cut; see (Fig. 7). Large-scale folds are observed off the study area, and off the geological map. Due to tectonic movements, the rocks layers are dipping towards west, as shown in (Figs. 3 and 4).

Fig. 3: Westward dipping schistosity dominated along the descent road. Fig. 4: Schistosity (arrows) dipping westward in the western part of the descent.

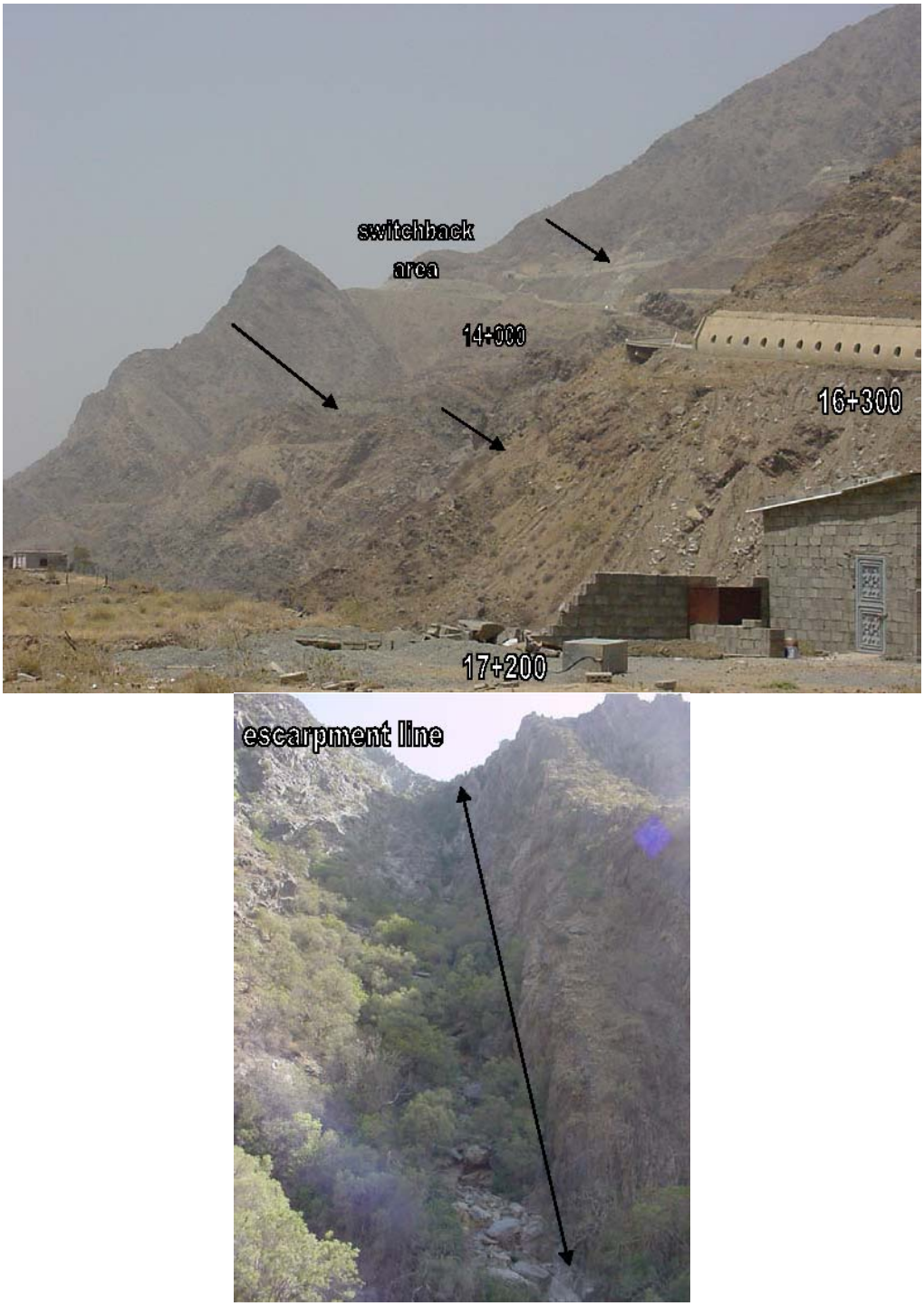

Fig. 5: Fault plane (double arrow) at location about 8+000-8+500, reach up to the descent escarpment line and extend on the plateau, nearby some houses build very close to the edge (upper right corner).

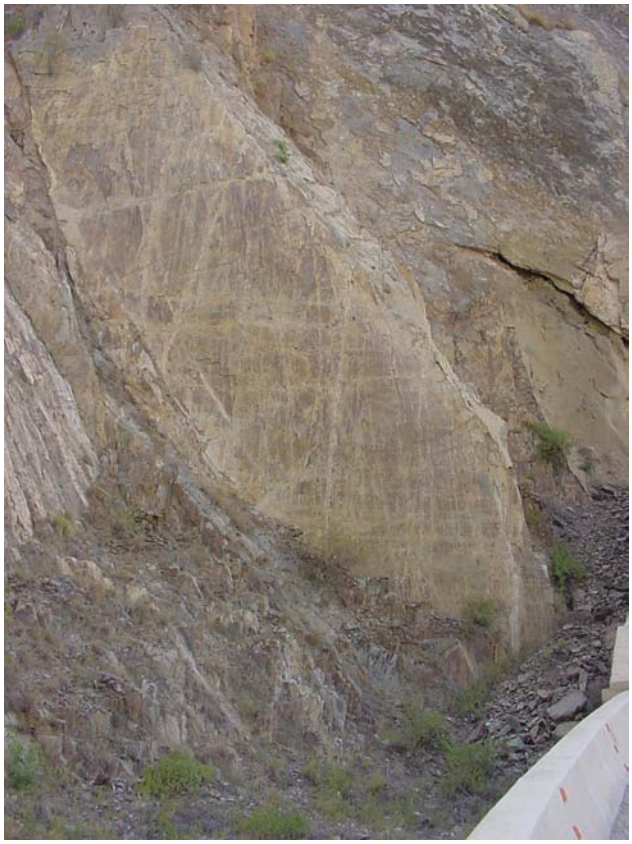

Fig. 6: Striations along the fault plane.

Fig. 7: Folding (single arrow) associated with faulting (double arrow) in the lower part of the descent road, km 22+500-23+000.

ROCK SLOPES STABILITY CONDITIONS

Along Al-Baha descent road the rock slope failures are i) rock slope slides formed of plane, wedge, toppling and combination of them, and ii) rockfalls due to toppling and loose rock blocks resting in a critical balance on the rock slope surface. Many of these slopes are dangerous and unsafe due to rockfalls, and rockslides especially during rainstorms. Rainy seasons are usually at autumn and winter (September to March).

This research is concerned only with the rock slope failures. Sadagah (2004) and Sadagah et al. (2005) discussed rockfalls in the study area.

Stability Analysis of the Studied Area

Landslides and rockfalls are numerous throughout the whole study area. These failures are invariably governed by the geometry of discontinuities. In an attempt to calculate the required engineering properties for commencing the rock slope stability analyses, the shear strength parameters of discontinuities were obtained using portable Hoek shear box PHI-10. The roughness of the exposed failure surfaces was measured using roughness gauge.

The rock slopes along the descent road were divided into stations, each station include homogenous rock mass with a prevailing joint sets, rock type and weathering conditions. The joint roughness coefficient (JRC) of each rock type for each station was determined according to the procedure described by Barton and Choubey (1977). The values of inclination angle, i, were obtained from the relationship proposed by Barton (1973).

$$i = JRC \cdot \log_{10} \frac{JCS}{\sigma_n} \quad \text{.....} \quad (1)$$

Where JCS denotes joint wall compressive strength and σ_n represents the value of normal stress acting on the planes of discontinuity. Based on the above relationship, it was found that the value of i ranges from 8° to 20°. For each rock type at each station, the residual friction angle, φr, was determined by the tilt test that was carried out in the laboratory on saw-cut rock cores. The values of peak friction angle, φp = φr +i for the above-mentioned area ranges from 23° to 41°. This procedure was followed at all stations. Rock slope stability analyses were carried out using the value of φp along with 100 readings of the attitudes of planes of discontinuities, and natural slopes, at each station (Sadagah, 2006).

Field investigation shows no evidence of the presence of complete infillings between discontinuity surfaces and in the view of the low normal stresses, the value of cohesive component in these discontinuities can therefore be considered as negligible. This assumption brings one to conclude that the failure of the slopes in the area is largely governed by the mobilization of frictional resistance along the planes of discontinuity (Sadagah, 2006).

The stability analysis of natural and man-made rock slopes was carried out to define the stable and unstable regions in the area utilizing the stereographic projection technique based on Hoek and Bray (1981) using DIPS/W Version 4.0 computer software produced by ROCKSCIENCE Co. Ltd., and the Geographic Information System, ArcView Version 3.2 GIS computer software program.

ROCK TYPES AND SLOPE FAILURES

Field investigations prove that the igneous and metamorphic rocks have different technical characteristics along the descent area. Igneous rocks had a wide variety of technical characteristics, while metamorphic rocks had a closer variety of properties. Landslides and rockfalls at the igneous rocks consist of rock fragments range from small to very large blocks. In case of metamorphic rocks the landslides are mainly plane and toppling failures. The fracture system at both types of rocks plays a role in the size and height of the rock slope cut. In case of igneous, as the rocks are blockier the rock slope height is higher, while at the metamorphic rocks if not that high. Table 1: Effect of rock type on the rock slope height and support measures.

Location, km	Rock type	Block size	Rock slope heights above the road, m	Rock mass structure*	Supports #
2000-2500,	Banded schist	Small	8-20	Laminated, sheared	0, 5
2500-3000	Mafic rocks	Medium	10-20	Disintegrated	1, 4, 5
3200-4200	Banded schist	Small to medium	20-30	Laminated	1, 3, 5
4200-5000	Mafic rocks	Medium	25-40	Blocky	1, 2, 3, 5
5000-6000	Granite	Medium to v. large	25-50	Blocky	1, 3-5
6000-8000	Banded schist and granites	Small to large	30-40	Blocky, disturbed	1, 3-5
8000-10000	Mafic rocks	Medium to v. large	50-100	Blocky, laminated	1, 3-5
10000-13000	Mafic rocks, banded schist	Medium to large	30-80	Blocky, laminated	1, 3-5
13000-15000	Mafic rocks	Small to large	10-30	Blocky, laminated, disintegrated	2, 3
15000-15700	Granite	Medium to v. large	25-50	Blocky	1, 3,5
16000-18000	Mafic rocks	Small to large	20-30	Disintegrated	1, 3-5
18000-20000	Mafic rocks, banded schist	Medium to large	30-40	Blocky, disturbed	1, 3-5
20000-22900	Banded schist	Small	15-25	Laminated	3, 5
22900-24400	Mafic rocks	Small to medium	10-25	Laminated, sheared	1-5
24400-25200	Banded schist	Small	15-25	Laminated	1, 3-5
25200-26300	Mafic rocks, banded schist	Small to medium	10-20	Blocky, laminated, disintegrated	0, 5
26300-32000	Banded schist	Small to medium	7-15	Blocky, laminated, disintegrated	0, 5

* Terminology of GSI is used.
# 0=no support, 1=rock bolts, 2=steel mesh, 3=Heavy-duty rock fence, 4=shotcrete, 5=benches.

The nature of failures along the descent is changing along the road according to the rock types. Failures are 1) at the north side of the descent road, the rocks are dominantly blocky (Fig. 5), this nature reflect of the type of the failure. The wedge, plane and toppling failures are dominant. 2) at the western side of the road (west bank of Wadi Rash), where the schistosity of the banded mafic rocks and schists are dipping towards the west inside the rock mass (Fig. 4), the types of failures are predominantly toppling and rockfalls. At the eastern side of the road (east bank of Wadi Rash), see Fig. 3, failures are mainly plane failure with minor cases of wedge failures. According to the types of experienced types of failures, the support measures are different. Table 1 shows the various types of taken measures. Furthermore, the GSI system of Hoek and Marinos (2004) was used to describe the rock mass structures.

In accordance, the trajectories of experienced rockfalls greatly related to the rock strength, slope height, cliff elevation, block size and discontinuities orientations of the rock masses, using computer software Rockfall.

CONCLUSIONS

The present study showed that the rock type and structural setting of the rock masses could play a decision-making tool for the engineering design process especially of the mountain roads.

Dipping direction of the metamorphic rocks is a key factor for expecting the type of failure, and hence choosing the suitable remedial measure.

Rock structures condition associated with the height of the natural and/or man-made rock cut could give an indication of the size and extent of failure.

ACKNOWLEDGEMENT

The author would like to express his gratitude to King Abdulaziz City for Science and Technology (KACST), Riyadh, for supporting and funding this research project (grant No. ARP-19-33), which made this work possible.

REFERENCES

Barton, N. (1973) Review of a new shear-strength criterion for rock joints. Engineering Geology, 7: 287-332.

Barton, N.R. and Choubey, V. (1977) The shear strength of rock joints in theory and practice. Rock Mechanics, 10: 1-54.

Benjamin, J.R. and Cornell, C.A. (1970) Probability, statistics, and decision for civil engineers. McGraw-Hill Book Co., 684p.

Brown, G.F., and Jackson, R.0. (1958) Geologic map of the Tihamat ash Sham quadrangle. Kingdom of Saudi Arabia: U.S. Geological Survey Miscellaneous Geologic Investigations Map I-216-A. Scale 1:500,000.

Brown, G.F., Jackson, R.0., Bogue, R.G., and MacLean, W.H. (1963) Geologic map of the southern Hijaz quadrangle. Kingdom of Saudi Arabia: U.S. Geological Survey Miscellaneous Geologic Investigations Map I-210-A. Scale 1:500,000.

Cater, F.W. (1977) Reconnaissance geology of the Wadi Salibah quadrangle, sheet 20/40 B. Kingdom of Saudi Arabia: Saudi Arabian Directorate General of Mineral Resources Geologic Map GM-27, scale 1:100,000.

Cater, F.W., and Jackson, P.R. (1986) Geologic map of the Jabal Ibrahim quadrangle, sheet 20E, Kingdom of Saudi Arabia: Saudi Arabian Directorate General of Mineral Resources Geologic Map GM-96C, scale 1:100,000.

Greene, R.C., and Gonzalez, L. (1980) Reconnaissance geology of the Wadi Shuqub quadrangle, sheet 20/41 A, Kingdom of Saudi Arabia: Saudi Arabian Directorate General of Mineral Resources Geologic Map GM-54, scale 1:100.000.

Greenwood, W.R. (1975a) Geology of the Al 'Aqiq quadrangle, sheet 20/41 D, Kingdom of Saudi Arabia: Saudi Arabian Directorate General of Mineral Resources Geologic Map GM-23, scale 1:100,000.

Greenwood, W.R. (1975b) Geology of the Biljurshi quadrangle, sheet 19/41 B. Kingdom of Saudi Arabia: Saudi Arabian Directorate General of Mineral Resources Geologic Map GM-25, scale 1:100,000.

Greenwood, W.R. (1975c) Geology of the Jabal Shada quadrangle, sheet 19/41 A, Kingdom of Saudi Arabia: Saudi Arabian Directorate General of Mineral Resources Geologic Map GM-20, 10p., scale 1:100,000.

Greenwood, W.R., Stoeser, D.B., Fleck, R.J., and Stacey, J.S. (1982) Late Proterozoic island-arc complexes and tectonic belts in the southern part of the Arabian Shield, Kingdom of Saudi Arabia: Saudi Arabian Deputy Ministry for Mineral Resources Open-File Report USGS-OF-02-8, 46p.

Hadley, D.G., and Fleck, R.J. (1980) Reconnaissance geologic map of Jabal ‘Afaf quadrangle, sheet 20/40 D, Kingdom of Saudi Arabia: Saudi Arabian Directorate of Mineral Resources Geologic Map GM-33, Scale 1:100,000.

Hoek, E. and Bray, J.W. (1981) Rock slope engineering. Institution of Mining and Metallurgy, 358P.

Hoek, E. (2001) Rock engineering. Internet edition. 313p.

Hoek, E. and Marinos, P. (2000) Predicting tunnel squeezing problems for weak heterogeneous rock masses. Tunnels and Tunnelling November and December issues, pp. 45-51 and pp. 33-36.

Ko Ko, C., Flentje, P. and Chowdhury, R. (2003) Quantitative landslide hazard and risk assessment: a case study. Quarterly J. of Engineering Geology and Hydrogeology, 36: 261-272.

Montgomery, D.C. and Runger, G.C. (2002) Applied statistics and probability for engineers. John Wiley & Sons, 706p.

Prinz, W.C. (1983) Geologic map of the Al Qunfuhah quadrangle, sheet 19E, Kingdom of Saudi Arabia. Ministry of Petroleum and minerals Resources, Deputy Ministry for Mineral Resources. Geologic Map GM-70C, scale 1:100,000. 19p.

Sadagah, B.H. (2004) Application of the rockfall hazard rating system at parts along a mountain road, Al-Baha, Saudi Arabia. International Conference of the Geology of the Arabian World (GAW-7), 16-19 Feb. 2004, Cairo University, Cairo, Egypt. pp. 527-532.

Sadagah, B.H. (2006) The probabilities of rock slope failures along parts of a mountain road, Al-Baha, Saudi Arabia. 4th Asian Rock Mechanics Symposium, Singapore, 8-10 Nov. Accepted for publication.

Sadagah, B.H., Gouth-Ali, A.R., Qari, M.H., Abo-Seadah, Y.E., and Aazam, M.S. (2005) Landslides: investigation, mitigation, monitoring and safety measures of Al-Baha descent. Project No. AT-19-33. Final technical report 1458p.

Şen, Z. (2005) Istanbul Technical University, Istanbul, Turkey. Personal communications.

Rockfall Hazard Inventory Development and Maintenance – A 20-Year Perspective

Michael Vierling, Engineering Geologist
New York State Thruway Authority
200 Southern Blvd.
Albany, New York

Richard Cross, Senior Consultant
Golder Associates Inc.
540 Commercial St. Suite 250
Manchester, NH.

Peter Ingraham
Senior Consultant and Associate
Golder Associates Inc.
540 Commercial St.
Manchester, NH

ABSTRACT

The New York State DOT and Thruway Authority began developing rockfall hazard assessment tools in 1988 patterned after early rockfall hazard rating systems for railways. Following a fatal rock strike in 1988, a statewide rockfall hazard rating system was developed and implemented in 1988 and 1996. Data developed from the ratings of system-wide slopes was initially stored in file folders and oracle data files. With the advent of more user-friendly data management systems, rock slope inventories and data associated with rockfall hazard ratings, maintenance, and repairs such as rock bolts, drapes, rockfall catchment fences and retaining walls were incorporated into the Thruway's Oracle database and more recently a GIS database. Early development of the rock slope inventory included involvement by maintenance personnel to ensure that the personnel responsible for maintaining slopes and slope repairs would recognize the need and usefulness of the inventory and provide data pertaining to minor rockfalls and degradation of slope conditions as observed and keep the inventory an actively updated database. Thruway Design and management personnel were also involved in rock slope inventory development and a review of rock slope conditions and design of repairs/improvements included in improvement and widening projects. The rockfall hazard rating system generally follows FHWA RHRS guidelines and has evolved to include system-specific rating categories to reflect the nature of the Thruway system. The evolution of the rockfall hazard rating system and dynamic nature of the rock slope inventory have made them valuable tools in managing the rock slopes along the Thruway system, and an integral part of prioritizing rock slopes for the Thruway's 15-year rock slope improvement program.

AUTHOR INDEX

AUTHOR INDEX